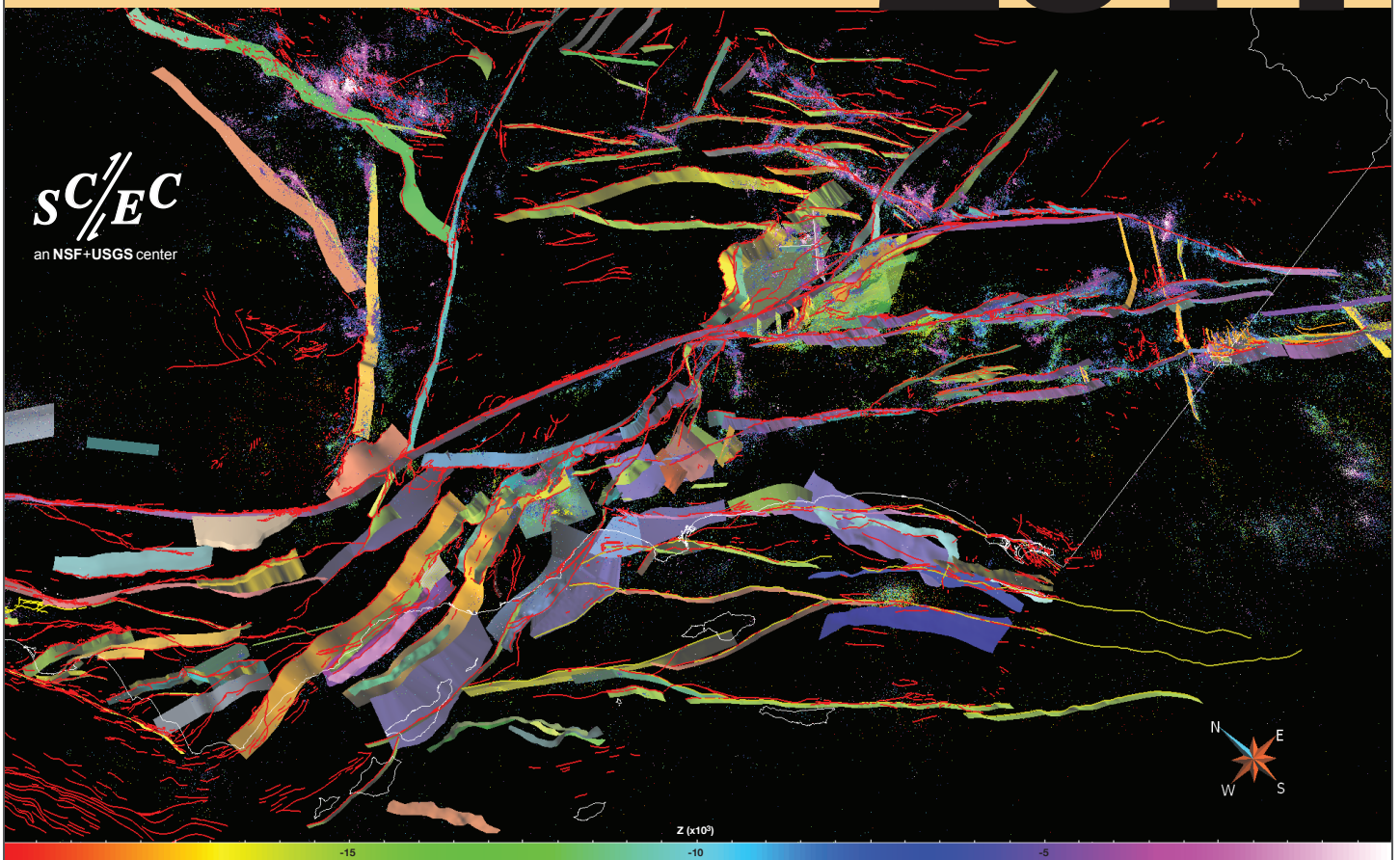


Southern California Earthquake Center
ANNUAL MEETING

2014

SC/EC
an NSF+USGS center



SCEC Community Fault Model Version 5.0 and Revised 3D Fault Set for Southern California

PROCEEDINGS VOLUME XXIV

September 6-10, 2014

SCEC LEADERSHIP

The Board of Directors (BoD) is the primary decision-making body of SCEC; it meets three times annually to approve the annual science plan, management plan, and budget, and deal with major business items. The Center Director acts as Chair of the Board. The liaison members from the U.S. Geological Survey are non-voting members.

Core Institutions and Board of Directors (BoD)

USC Tom Jordan*	Harvard Jim Rice	UC Los Angeles Peter Bird	UC Santa Cruz Emily Brodsky	USGS Pasadena Rob Graves
Caltech Nadia Lapusta**	MIT Tom Herring	UC Riverside David Oglesby	UNR Glenn Biasi	At-Large Member Roland Bürgmann
CGS Chris Wills	SDSU Steve Day	UC San Diego Yuri Fialko	USGS Golden Jill McCarthy	At-Large Member Judi Chester
Columbia Bruce Shaw	Stanford Paul Segall	UC Santa Barbara Ralph Archuleta	USGS Menlo Park Ruth Harris	* Chair ** Vice-Chair

The leaders of the Disciplinary Committees and Interdisciplinary Focus Groups serve on the Planning Committee (PC) for three-year terms. The PC develops the annual Science Collaboration Plan, coordinates activities relevant to SCEC science priorities, and is responsible for generating annual reports for the Center. Leaders of SCEC Special Projects (i.e., projects with funding outside the core science program) also serve on the Planning Committee. They ensure the activities of the Special Projects are built into the annual science plans.

Science Working Groups & Planning Committee (PC)

	Disciplinary Committee			
PC Chair Greg Beroza*	Seismology Egill Hauksson* Elizabeth Cochran	Tectonic Geodesy Jessica Murray* Dave Sandwell	EQ Geology Mike Oskin* Whitney Behr	Computational Sci Yifeng Cui* Eric Dunham
	Interdisciplinary Focus Groups			
* PC Members	USR John Shaw* Brad Aagaard	SoSAFE Kate Scharer* Ramon Arrowsmith	EFP Jeanne Hardebeck* Ilya Zaliapin	EEII Jack Baker* Jacobo Bielak
	FARM Greg Hirth* Pablo Ampuero	SDOT Kaj Johnson* Thorsten Becker	GMP Kim Olsen* Christine Goulet	
	Special Projects			
	CME Phil Maechling*	CSEP Max Werner* Danijel Schorlemmer	WGCEP Ned Field*	
	Technical Activity Groups			
	Code Verification Ruth Harris	SIV Martin Mai	EQ Simulators Terry Tullis	Transient Detection Rowena Lohman
	GMSV Nico Luco Sanaz Rezaeian			

The external Advisory Council (AC) provides guidance in all aspects of Center activities, including basic and applied earthquake research and related technical disciplines, formal and informal education, and public outreach. Members of the AC are elected by the Board for three-year terms and may be re-elected. The Council meets annually to review Center programs and plans, and prepares a report for the Center.

Advisory Council (AC)

Gail Atkinson , Chair Western U	Donna Eberhart-Phillips UC Davis	M. Meghan Miller UNAVCO	John Vidale U Washington
Norm Abrahamson PG&E	Kate Long CalOES	Farzad Naeim John A Martin	Andrew Whittaker MCEER/Buffalo
Roger Bilham U Colorado	Warner Marzocchi INGV Rome	Tim Sellnow U Kentucky	

Center Management

	Center Administration	Communication, Education & Outreach	Information Technology
Center Director Tom Jordan	Associate Director John McRaney	Associate Director Mark Benthien	Associate Director Phil Maechling
Deputy Director Greg Beroza	Special Projects/Events Tran Huynh	Education Programs Bob de Groot	Research Programmer Scott Callaghan
	Contracts & Grants Karen Young	Digital Products John Marquis	David Gill Masha Liukis Kevin Milner Fabio Silva
	Admin Coordinator Deborah Gormley	Web Developer David Gill	Systems Programmer John Yu
		Communications Jason Ballmann	

Table of Contents

SCEC Leadership	2
Table of Contents	3
State of SCEC, 2014	4
2013 Report of the Advisory Council	12
Communication, Education, and Outreach Highlights	18
Research Accomplishments	31
SCEC4 Science Milestones	73
Draft 2015 Science Plan	78
Meeting Agenda	102
Meeting Presentations	111
Meeting Abstracts	124
Meeting Participants	191
SCEC Institutions	197

State of SCEC, 2014

Thomas H. Jordan, SCEC Director

Welcome to the 2014 Annual Meeting!

This week in Palm Springs both the weather and science promise to be hot! The SCEC community will gather here from across the country and around the world to share our recent research accomplishments and review our ambitious science plans. 573 people have pre-registered for the meeting (Figure 1), and 286 poster abstracts have been submitted—the largest numbers ever. The pre-registrants include more than 155 first-time attendees and almost two hundred undergraduate and graduate students.

The goals of this 24th Annual Meeting are threefold. We are more than halfway through the SCEC4 cycle, so we need to assess our research accomplishments and plan our research for the remaining two years of SCEC4. We also need to gear up for the SCEC5 proposal, which will be submitted to the National Science Foundation (NSF) and U.S. Geological Survey (USGS) about one year from now. But our main goal is scientific: to learn all we can about earthquakes from the formal presentations and posters, and especially from the informal discussions with our scientific colleagues.

Many of those discussions will concern the M6 South Napa earthquake of two weeks ago. This destructive event is a potent reminder of why we are here. Californians and other residents of U.S. earthquake country have been lucky to live in seismically quiescent times, but this good fortune cannot be sustained indefinitely. While we have the time, we must do all we can to understand earthquake phenomena in California and elsewhere, working with our many partners towards the goal of reducing seismic risk and improving the resilience of our communities. As a long-term resident of Hotel California, I remain committed to our multi-decade project, and at this meeting I will ask you to join me in continuing our deep collaboration into SCEC5.

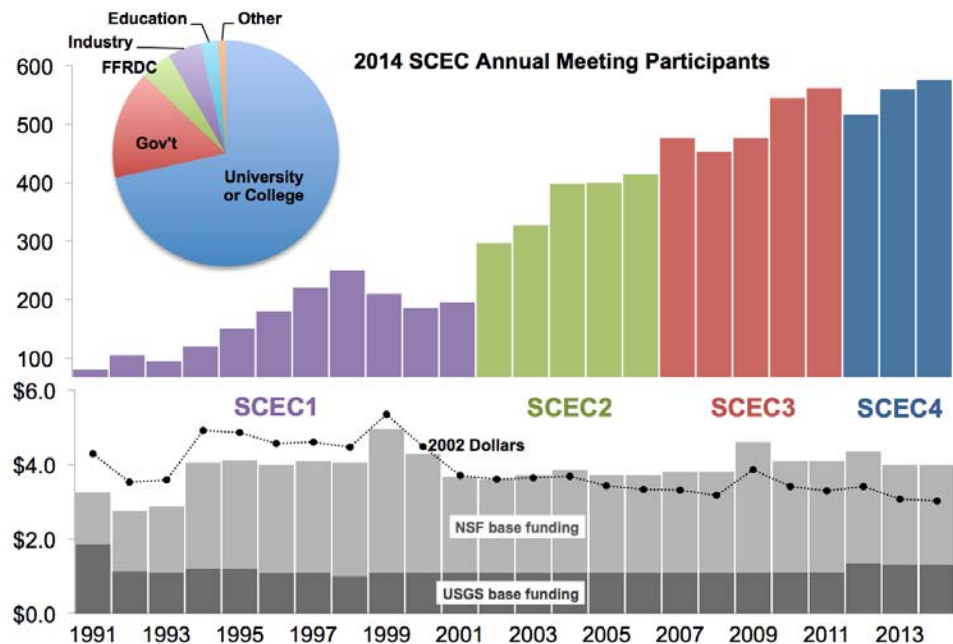


Figure 1. Registrants at SCEC Annual Meetings 1991-2014. Number for 2014 (573) is pre-registrants, with 155 first-time attendees. Pie chart shows the demographic profile for 2014 pre-registrants. The lower bar chart is the history of SCEC base funding in as-spent dollars; the connected dots are the base-funding totals in 2002 dollars. Funding for 2014 is current authorization.

In the next few days, we'll all be standing in the hot spray of a scientific firehose. As always, the Planning Committee has put together a blazing program. Saturday and Sunday feature workshops on six worthy topics:

- San Geronio Pass Special Fault Study Area
- Testing Operational Earthquake Forecasts and Seismic Hazard Models
- Community Geodetic Model Workshop
- Source Inversion Validation
- Earthquake Ground Motion Simulation and Validation
- Post-Earthquake Rapid Scientific Response

At 6 pm Sunday evening, this year's Distinguished Speaker, Dr. Norm Abrahamson of the Pacific Gas & Electric Company, will kick off the main meeting with a challenge-posing talk on "Reducing Epistemic Uncertainty in Seismic Risk Estimation."

Over the next three days, the agenda will feature keynote speakers addressing fundamental problems, discussions of major science themes, poster sessions on research results, earthquake response exercises, technical demonstrations, education and outreach activities, and some lively social gatherings.

Assessing SCEC Accomplishments

Last year, we requested an assessment of the key SCEC4 activities from our external Advisory Council (AC), and they responded with a detailed and thoughtful evaluation, narrated in terms of the “six fundamental problems of earthquake science” posed in the SCEC4 science plan (Table 1). They noted how these system-level problems are interrelated and require the type of interdisciplinary, multi-institutional research at which the SCEC community excels. The 2013 AC report, which is reproduced in this meeting volume, highlights the considerable progress we have made in addressing these problems, as well as the remaining challenges.

The AC assessment will inform scientific discussions at this meeting, and we will use it as a baseline evaluation to evaluate the scientific progress during the past year. From my perspective as SCEC director, we are on target for a successful completion of SCEC4, but I urge you to inform the members of the AC of your own assessment.

Table 1. Fundamental Problems of Earthquake Science for SCEC4

-
1. Stress transfer from plate motion to crustal faults: long-term fault slip rates
 2. Stress-mediated fault interactions and earthquake clustering: evaluation of mechanisms
 3. Evolution of fault resistance during seismic slip: scale-appropriate laws for rupture modeling
 4. Structure and evolution of fault zones and systems: relation to earthquake physics
 5. Causes and effects of transient deformations: slow slip events and tectonic tremor
 6. Seismic wave generation and scattering: prediction of strong ground motions
-

Each year, SCEC Deputy Director Greg Beroza and the Planning Committee (PC) assemble an annual report on research accomplishments, which is submitted in November as part of a full report on SCEC activities to our primary sponsoring agencies, the National Science Foundation and U. S. Geological Survey. The PC’s 2014 report is included in these Proceedings. Greg will summarize the research results, with an emphasis on our more recent accomplishments, in his plenary address on Monday morning. This meeting volume also contains a report by Mark Benthien, the SCEC Associate Director for Communication, Education, and Outreach (CEO), on the remarkable accomplishments of the CEO program, some of which are highlighted below.

The five poster sessions scheduled between Sunday evening and Tuesday evening will show off the entire spectrum of SCEC accomplishments. In a very popular change, brought back two years ago, posters will stay up for the entire meeting to allow more face-to-face interactions on the nitty-gritty aspects of SCEC scientific research.

Onward to SCEC5!

Based on NSF and USGS guidance, we are preparing to submit the SCEC5 proposal circa October 1, 2015, which is half a year later in SCEC’s 5-year funding cycle than previous core-program proposals. According to this plan, the site review for the proposal would likely be scheduled for January, 2016, and the funding decision would probably be made by the agencies about six months before the end of SCEC4 (January 31, 2017).

At the SCEC Leadership Retreat in early June, ten “tiger teams” were organized to develop potential SCEC5 themes for discussion at the Annual Meeting. The six themes that emerged are listed in Table 2. Each theme will be the topic of a special session at this meeting. From the discussion captured in those sessions, the team leaders will develop a short white paper for input into the proposal process, and they will summarize the conclusions near the close of the meeting on Wednesday. We hope you will participate in these discussions and comment on which of

Table 2. SCEC5 Theme Sessions at the 2014 Annual Meeting

-
- A. *How do we deal with known unknowns and unknown unknowns?***
 1. Reducing epistemic uncertainty and characterizing aleatory variability
 - B. *What properties of the Earth and the faults within it are important for understanding system behavior?***
 2. Simulators
 3. Beyond elasticity
 - C. *How can the hazard from simulated earthquakes effectively reduce risk in the real world?***
 4. Ground motion simulations
 5. Infrastructure system risk
 - D. *What aspects of earthquake behavior are predictable?***
 6. Science of operational earthquake forecasting
 7. "Atectonic" seismicity
 - E. *Here it comes! What just happened? How can SCEC better prepare to respond to future earthquakes?***
 8. Earthquake early warning research
 9. Earthquake response
 - F. *How can we communicate more effectively what we know and what we don't?***
 10. Risk communication and new technologies
-

STATE OF SCEC

the theme areas you find most compelling for development in the SCEC5 plan.

The themes hit many of the exciting topics in earthquake science, both basic and applied, but they are hardly exhaustive of the SCEC5 possibilities. We are also looking for interesting focus areas not covered by these themes.

Organization and Leadership

SCEC is an institution-based center, governed by a Board of Directors, who represent its members. The Center is an open consortium, available to all qualified individuals and institutions seeking to collaborate on earthquake science in Southern California, and its membership continues to evolve. The institutional membership currently stands at 67, comprising 17 core institutions and 50 participating institutions, which are listed on the inside back cover of the meeting program. As you can see from the list, SCEC institutions are not limited to universities, nor to U.S. organizations. The three USGS offices in Menlo Park, Pasadena, and Golden and the California Geological Survey are core institutions, and URS Corporation is a participating institution. Ten foreign institutions are recognized as partners with SCEC through a set of international cooperative agreements.

For attendees who don't see your institution on this list, please note that it's really easy to apply; all we need is a letter from a cognizant official (e.g., your department chair or dean) that requests participating-institution status and appoints an institutional representative who will act as the point-of-contact with SCEC.

SCEC currently involves more than 600 scientists and other experts in active SCEC projects. A key measure of the size of the SCEC community—registrants at our Annual Meetings—is shown for the entire history of the Center in Figure 1. For the last five years, more than 500 people have attended each of the Annual Meetings.

Board of Directors. Under the SCEC4 by-laws, each core institution appoints one member to the Board of Directors, and two at-large members are elected by the Board from the participating institutions. The Board of Directors is the primary decision-making body of SCEC; it meets three times annually to approve the annual science plan, management plan, and budget, and deal with major business items. The liaison members from the U.S. Geological Survey are non-voting members. As Center Director, I chair the Board and also serve as the USC representative. Nadia Lapusta of Caltech serves as its Vice-Chair.

We also elect two people from our participating institutions as at-large members of the Board. These positions are currently filled by Judi Chester of Texas A&M and Roland Bürgmann of UC-Berkeley. The complete Board of Directors is listed on the inside front cover of the meeting program.

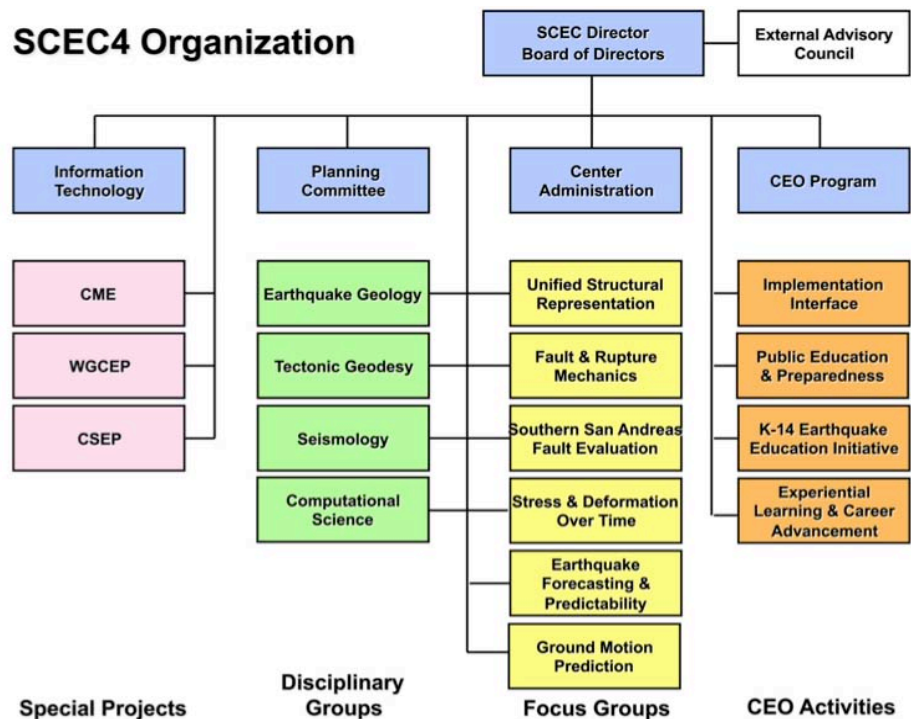


Figure 3. The SCEC4 organization chart, showing the disciplinary committees (green), focus groups (yellow), special projects (pink), CEO activities (orange), management offices (blue), and the external advisory council (white).

External Advisory Council. The External Advisory Council is charged with developing an overview of SCEC operations and advising the Director and the Board. Since the inception of SCEC in 1991, the AC has played a major role in maintaining the vitality of the SCEC and helping its leadership chart new directions. The Center has always provided its sponsoring agencies and participants, with verbatim copies of the yearly AC reports. The full 2013 AC report is included in this volume.

There have been several changes to the AC membership since last year. Gail Atkinson (Western University, Canada) has taken over from Jeff Freymueller (U. Alaska) as the AC chair, and we look forward to her leadership of the Council. Bob Lillie (Oregon State) and Susan Cutter (U. South Carolina) have rotated off the AC, and, at this meeting, we welcome three new members: Norm Abrahamson (PG&E), Warner Marzocchi (INGV, Italy), and Tim Sellnow (U. Kentucky). The current AC membership can be found on page 2.

Planning Committee. The SCEC Planning Committee is chaired by the SCEC Deputy Director, Greg Beroza, and comprises the leaders of the SCEC science working groups—disciplinary committees, focus groups, and special project groups—who, together with the working group co-leaders, guide SCEC’s research program. The PC is responsible for formulating the Center’s science plan, conducting proposal reviews, and recommending projects to the Board for SCEC support. Its members will play key roles in formulating the SCEC5 proposal. I urge you to use the opportunity of the Annual Meeting to communicate your thoughts about future research plans to them.

Working Groups. The SCEC organization comprises a number of disciplinary committees, focus groups, special project teams, and technical activity groups (TAGs). These working groups have been our engines of success, and many of the discussions at this meeting will feed into their plans. The current working group structure of SCEC4 is shown in Figure 3, and a complete listing of the working group leaders is on the inside cover of the meeting program.

The Center supports disciplinary science through standing committees in Seismology, Tectonic Geodesy, and Earthquake Geology. A new disciplinary committee in Computational Science was added for SCEC4. These groups (green boxes of Figure 3) are responsible for disciplinary activities relevant to the SCEC Science Plan, and they make recommendations to the Planning Committee regarding the support of disciplinary research and infrastructure. Mike Oskin of UC Davis is replacing Lisa Grant as the leader of the Earthquake Geology Disciplinary Group, and Whitney Behr of the University of Texas will be joining the group as co-leader.

SCEC coordinates earthquake system science through six interdisciplinary focus groups (yellow boxes): Unified Structural Representation (USR), Fault & Rupture Mechanics (FARM), Earthquake Forecasting & Predictability (EFP), Southern San Andreas Fault Evaluation (SoSAFE), Stress and Deformation Through Time (SDOT), and Ground Motion (GMP). A seventh interdisciplinary group, the Earthquake Engineering Implementation Interface (EII, an orange box), is coordinating educational as well as research partnerships with practicing engineers, geotechnical consultants, building officials, emergency managers, financial institutions, and insurers.

Technical Activity Groups are self-organized to develop and test critical methodologies for solving specific problems. TAGs have formed to verify the complex computer calculations needed for wave propagation and dynamic rupture problems, to assess the accuracy and resolving power of source inversions, and to develop geodetic transient detectors and earthquake simulators. TAGs share a *modus operandi*: the posing of well-defined “standard problems”, solution of these problems by different researchers using alternative algorithms or codes, a common cyberspace for comparing solutions, and meetings to discuss discrepancies and potential improvements. This year we welcome Sanaz Rezaeian as co-leader of the Ground Motion Simulation Validation TAG.

Special Projects

The Special Project teams (pink boxes in Figure 3) are organized around large-scale projects funded through special grants outside the NSF-USGS cooperative agreements that support the SCEC4 base program. This has been an exceptionally productive year for all three of our special projects. The UCERF3 project, sponsored by the California Earthquake Authority (CEA), was completed in March, and the UCERF3 long-term model was incorporated as the California component of the 2014 revisions to the U. S. National Seismic Hazard Model, released in July. Congratulations are in order to Ned Field and his colleagues on the Working Group for California Earthquake Probabilities (WGCEP), who labored long and hard on this groundbreaking project. Work on the short-term forecasting component of UCERF3 continues, and new results will be presented at the CSEP workshop on Saturday.

The Collaboratory for the Study of Earthquake Predictability (CSEP), which began at SCEC in 2006, has expanded into an international program for the prospective and retrospective testing of earthquake forecasting models in natural laboratories around the world, including California, New Zealand, Italy, Japan, and China. Currently, more than 400 forecasting models and their variations are under prospective testing at CSEP centers in Los Angeles, Wellington, Zürich, and Tokyo. CSEP’s importance to the development of operational earthquake forecasting is underlined in a paper just published by Warner Marzocchi and his colleagues in *Seismological Research Letters*, which describes a new OEF system developed for Italy (Figure 3). Plans for the testing of OEF models and deployment of OEF systems will be discussed at the Saturday CSEP workshop.

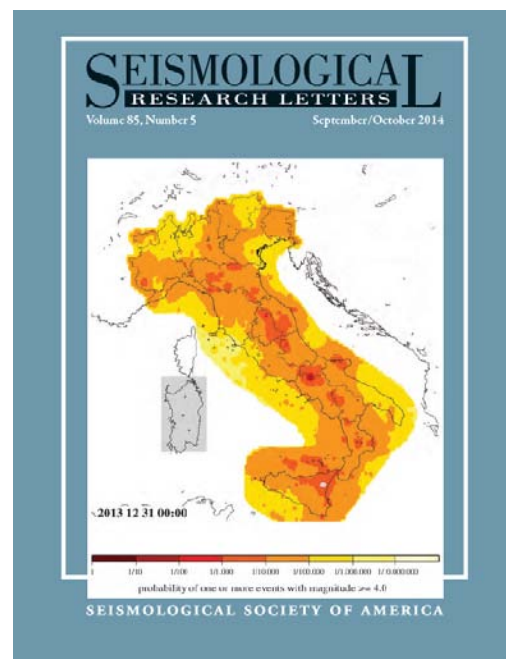


Figure 3. Cover of the Sept-Oct issue of *Seismological Research Letters*, showing an earthquake probability map for Italy from INGV’s new operational earthquake forecasting system.

STATE OF SCEC

SCEC's program in high-performance computing, managed through its Community Modeling Environment (CME) collaboration, has been very active in developing new capabilities for earthquake simulation, including validated software for engineering-oriented simulations (the Broadband Platform), the use of large ensembles of simulations for complete probabilistic seismic hazard analysis (the CyberShake project), the extensions of simulations to high frequencies (the High-F project), and the assimilation of earthquake and ambient-field data into 3D velocity structures using full-3D tomography (the F3DT project). CME has become one of the most well-recognized collaborations in high-performance computing, bringing together world-leading geoscientists, computational scientists, earthquake engineers, and software engineers to develop new large-scale computational capabilities for earthquake system science. Substantial new results will be described at the Workshop on Earthquake Ground Motion Simulation and Validation on Sunday.

Center Budget and Project Funding

The SCEC base program has been more-or-less flat funded since the beginning of SCEC2, when I took over as director (Figure 1). In 2013 NSF/EAR cut our base budget by 10%, from the \$3.0M received in 2012 to \$2.7M. The USGS cuts were proportionately smaller (3%), from \$1.34M to \$1.30M. The cuts, a result of the federal sequester law, continued in the SCEC funding from both agencies in 2014. Supplementing the \$4.0M in base funding was \$328K from Pacific Gas & Electric, the Keck Foundation, the NSF SAVI supplement, and the geodesy royalty fund. In total, SCEC core funding for 2014 is \$4,328K, down from \$4,494K in 2013.

Our 2014 funding was not finalized until early June, which caused delays in the 2014 funding for some investigators. The continuing budget cuts are painful, but we were able to preserve most of the research projects approved by the PC and Board in February, though some at lower funding levels.

The base budget approved by the Board of Directors for this year allocated \$2.968M for science activities managed by the SCEC Planning Committee; \$420K for communication, education, and outreach activities, managed by the CEO Associate Director, Mark Benthien; \$175K for information technology, managed by Associate Director for Information Technology, Phil Maechling; \$320K for administration and \$270K for meetings, managed by the Associate Director for Administration, John McRaney; and \$100K for the Director's reserve account.

Structuring of the SCEC program for 2014 began with the working-group discussions at our last Annual Meeting in September, 2013. An RFP was issued in October, 2013, and 184 proposals requesting a total of \$5.53M were submitted in November, 2013. Both the number of proposals and the total funds requested were records for the SCEC science program.. Including collaborative proposals, there were more than 250 individual budget requests. All proposals were independently reviewed by the Director and Deputy Director. Each proposal was also independently reviewed by the leaders and/or co-leaders of three relevant focus groups or disciplinary committees. (Reviewers were required to recuse themselves when they had a conflict of interest.) The Planning Committee met on January 22-23, 2014, and spent two days discussing every proposal. The objective was to formulate a coherent, budget-balanced science program consistent with SCEC's basic mission, short-term objectives, long-term goals, and institutional composition. Proposals were evaluated according to the following criteria:

1. Scientific merit of the proposed research
2. Competence and performance of the investigators, especially in regard to past SCEC-sponsored research
3. Priority of the proposed project for short-term SCEC objectives as stated in the RFP
4. Promise of the proposed project for contributing to long-term SCEC goals as reflected in the SCEC3 science plan
5. Commitment of the P.I. and institution to the SCEC mission
6. Value of the proposed research relative to its cost
7. Ability to leverage the cost of the proposed research through other funding sources
8. Involvement of students and junior investigators
9. Involvement of women and underrepresented groups
10. Innovative or "risky" ideas that have a reasonable chance of leading to new insights or advances in earthquake physics and/or seismic hazard analysis.
11. The need to achieve a balanced budget while maintaining a reasonable level of scientific continuity

The recommendations of the PC were reviewed by the SCEC Board of Directors. The Board voted unanimously to accept the PC's recommendations. After minor adjustments and a review of the proposed program by the NSF and USGS, I approved the final program in March 2014.

We still have some hope at this point in time, more than seven months into the SCEC fiscal year, that additional funding might become available to augment our science budget for 2014.

Communication, Education, and Outreach

The success of SCEC's CEO program matches that of its science program. CEO offers a wide range of student research experiences, web-based education tools, classroom curricula, museum displays, public information brochures, online newsletters, workshops, and technical publications. Highlights of CEO activities for the past year are reported in these Proceedings by the Associate Director for CEO, Mark Benthien, who will present an oral summary on Monday morning.

SCEC has led the development of the Earthquake Country Alliance (ECA), an umbrella organization, now statewide, that includes earthquake scientists and engineers, preparedness experts, response and recovery officials, news media representatives, community leaders, and education specialists. Mark acts as the ECA Executive Director. The ECA has become our primary framework for developing partnerships, products, and services for the general public. SCEC maintains the ECA web portal (www.earthquakecountry.org), which provides multimedia information about living in earthquake country, answers to frequently asked questions, and descriptions of other resources and services provided by ECA members. This past year, a special "Northridge Earthquake Virtual Exhibit" was added to the site with "Northridge Near You" animations created by SCEC UseIT interns, and interviews with people who experienced the Northridge earthquake across southern California. Similar "Near You" animations are being made for the Loma Prieta anniversary.

A major focus of the CEO program since 2008 has been organizing the *Great California ShakeOut* and coordinating *Great ShakeOut Earthquake Drills* in many other states and countries. The purpose of the Shakeout is to motivate everyone, everywhere to practice earthquake safety ("Drop, Cover, and Hold On"), and to get prepared at work, school, and home. More than 9.6 million people participated in the 2013 California ShakeOut. Recruitment is well underway for the 2014 ShakeOut, with over 9.1 million participants registered as of August 29.

Beginning in 2010, additional states, territories, and countries began to join the ShakeOut movement, with websites replicated by SCEC in partnership with government agencies who recruited participants. As part of activities for the New Madrid earthquake bicentennial, the Central U.S. Earthquake Consortium (CUSEC) organized the first multi-state drill in April 2011, with 3 million participations across eleven states. CUSEC also now coordinates the SouthEast ShakeOut. As of August, 2014, 25 Official ShakeOut Regions (each with their own website) now span 45 states and territories, three Canadian provinces, New Zealand, Southern Italy (U.S. Naval bases), and a rapidly growing number of Japanese cities and prefectures. All of these areas are holding ShakeOut drills annually (see the global homepage at www.shakeout.org), except New Zealand (which will participate again in 2015). In addition, people and organizations in any other state or country can now register to be counted in the overall global total each year. In 2013 more than 24.9 million people participated worldwide. Many millions more see or hear about the ShakeOut via social media and extensive news coverage. ShakeOut sites now exist in Spanish (Puerto Rico and globally), Italian, and French (for Canada), such that our ability to engage additional countries, especially in Latin America, will likely expand ShakeOut participation further.

I would like to encourage the SCEC community to register for a *Great ShakeOut Earthquake Drill* (www.shakeout.org) and to encourage their institutions to join USC and others that are already registered. Resources for college faculty to lead a simple earthquake drill are available at www.ShakeOut.org/colleges.



Figure 4. Undergraduate students from around the country who participated in the 2014 UseIT summer program at USC. Several of them will be attending the SCEC Annual Meeting to present posters, demos, and animations.

SCEC CEO staff continue to work with museums and other informal education venues to develop content and programs for earthquake education and to distribute SCEC resources, such as the extensive set of publications that has grown out of *Putting Down Roots in Earthquake Country*. In 2008, SCEC and the San Bernardino County Museum (SBCM) organized a group of museums and other locations interested in earthquake education into a network of *Earthquake Education and Public Information Centers* (Earthquake EPIcenters), which has since been expanded to over 70 venues throughout the US. Recent expansion of the Network in Oregon, Washington, and Alaska has gained momentum from a partnership with EarthScope's Interpretive Program and the Cascadia EarthScope Earthquake and Tsunami Education Program (CEETEP). The EPIcenters are essential partners in the ShakeOut, as many hold public events on drill day, help promote participation, and

STATE OF SCEC

build capacity. SCEC is collaborating with the CGS to conduct tsunami and earthquake education workshops at EPICenters (focusing on aquaria) in California. In 2015 SCEC, EarthScope, and Humboldt State University will host the final CEETEP workshop. The USGS, SBCM, Stanford, NEES, EarthScope, and SCEC have facilitated the installation of over 100 Quake Catcher Network seismometers in K-12 schools and informal learning venues throughout California, Oregon, Washington, and Alaska.

SCEC is very active in the Earth science education community, participating in organizations such as the National Association of Geoscience Teachers, the Coalition for Earth System Education, and statewide and national science educator organizations (e.g. CSTA). SCEC Education Program Manager Robert de Groot leads these efforts and runs the SCEC Teacher Workshops and K-12 partnerships. Since 2009, SCEC has been collaborating with EarthScope, UNAVCO, and California State University, San Bernardino to conduct a campaign GPS research program involving both high school teachers and their students. Since 2013 SCEC has had a leading role in the Education and Public Outreach program for InSight (Interior Exploration using Seismic Investigations, Geodesy, and Heat Transport), a NASA Discovery Program mission that will place a single geophysical lander on Mars to study its deep interior in 2016. SCEC developed the ‘Vital Signs of the Planet’ (VSP) Professional Development Program a standards-based middle and high school research experience and curriculum development program offering strong connections to STEM research. This program provides educator fellows with authentic experiences in scientific inquiry, encourages instructional improvement in schools, and fosters deep engagement with local underserved communities. In 2013, ten science educators and four students participated in the Vital Signs program and their posters are on display at this meeting. SCEC worked with the Sherman Indian High School in Riverside, CA, to develop earthquake awareness and preparedness messaging, including the development of the Turtle Story (a Native American account of plate tectonics) lesson package and the second version of a poster featuring translation of “Drop, Cover, and Hold On” into many Native American languages.

Robert de Groot is also skillfully leading SCEC’s Office for Experiential Learning and Career Development (ELCA). His office manages two SCEC intern programs: Summer Undergraduate Research Experience (SURE, 268 interns since 1994), Undergraduate Studies in Earthquake Information Technology (USEIT, 264 interns since 2002), and in 2014 two high school InSight VSP interns from Etiwanda High School. The ELCA office promotes diversity in the scientific workforce and the professional development of early-career scientists (Figure 3). As someone very involved in these intern programs, I really enjoy seeing the students grapple with the tough but engaging problems of cutting-edge earthquake science. For example, the “grand challenge” for this year’s USEIT program was to *develop SCEC-VDO and GIS tools for exploring and evaluating the aftershock hazards implied by the new Uniform California Earthquake Rupture Forecast (UCERF3). These evaluations were guided by using M7 rupture scenarios developed for the 25th Anniversary of the 1989 Loma Prieta earthquake.* Many of the summer interns will be presenting their work at this meeting, and I hope you’ll have the opportunity to check out their posters and demos.

Figure 5. The SCEC Staff, a special group of individuals with exceptional skills and tremendous dedication to the Center and its participants.

Center Administration	Communication, Education and Outreach	Information Technology
 Associate Director John McRaney	 Associate Director Mark Benthien	 Associate Director Phil Maechling
 Special Projects and Events Tran Huynh	 Education Programs Bob de Groot	 Research Programmer Scott Callaghan
 Contracts and Grants Karen Young	 Digital Products John Marquis	 Research Programmer David Gill
 Admin Coordinator Deborah Gormley	 Communications Specialist Jason Ballmann	 Research Programmer Masha Liukis
		 Research Programmer Kevin Milner
		 Research Programmer Fabio Silva
		 Systems Programmer John Yu

A Special Word of Thanks

SCEC has been successful because of the collaborative efforts of many people over many years. As SCEC Director, I want to express my deep appreciation to all of you for your attendance at the Annual Meeting and your sustained commitment to the collaboration. Greg Beroza and the PC have developed another outstanding program, so the entire meeting should be a very pleasant experience.

Special recognition is in order for SCEC staff, which comprises individuals of remarkable skills and dedication (Figure 5). We all benefit immensely from the financial wizardry and personal empathy of John “The Chaplain” McRaney, the organizational skills of Mark “Mr. ShakeOut” Benthien, and the innovative expertise of Phil “Big-Iron” Maechling.

And we all owe a very special *thank you!* to Tran Huynh and Deborah Gormley, the SCEC Meetings Team, and their diligent associates, Karen Young, John Marquis, David Gill, and Jason Ballmann, for their exceptional efforts in organizing this meeting and arranging its many moving parts. Please do not hesitate to contact me, Greg, Tran, or other members of the SCEC team if you have questions or comments about our meeting activities and future plans. Now please enjoy the sessions, the meals, and the pool in the spectacular, though perhaps a bit toasty, setting of Palm Springs!

2013 Report of the Advisory Council

Jeff Freymueller, *SCEC Advisory Council Chair*

November 18, 2013

Introduction

The SCEC Advisory Council (AC) met several times at the SCEC Annual Meeting in Palm Springs, September 8-11, 2013. The AC met with SCEC leadership, including representatives of the SCEC Board of Directors, with representatives of the funding agencies, and in informal settings with individual SCEC scientists and students. Prior to meeting, following the usual custom, we received a confidential letter from SCEC Director Tom Jordan that summarized SCEC's response to last year's Advisory Council recommendations and highlighted some new and continuing issues to solicit the Council's opinion this year. The AC also received copies of the draft SCEC science plan for 2014, copies of major proposals and reports submitted, and other relevant material. The AC set its agenda for discussion based on a combination of issues raised in the SCEC4 proposal reviews, those raised by the Director, and unresolved issues from previous AC reports.

The discussion in the AC meetings mostly fell into the following categories:

- How is SCEC4 doing? We chose to take a look at progress to date on the 6 fundamental questions that SCEC posed for itself in SCEC4.
- CEO-AC, the SCEC CEO advisory committee
- The SCEC Director Succession
- Budget Challenges

As in past years, the AC is deeply impressed by the SCEC organization and community. SCEC is viewed positively by the broader earthquake science community and by its funding agencies, and this impression has been well earned. The SCEC collaboration remains vibrant, with enthusiastic participation across many disciplines. As the section of this report on SCEC4 progress indicates, SCEC has made progress on all of the main goals that it set for SCEC 4, although considerable work remains to be done. In our opinion, SCEC is on the right track and should continue in its present directions.

Membership

Nine members of the Advisory Council attended the SCEC Annual Meeting and participated in all discussions of the AC at that venue. This report is a collaborative product of these AC members. The members who attended are:

Jeffrey T. Freymueller, *Chair* (University of Alaska Fairbanks)
Gail Atkinson (University of Western Ontario)
Roger Bilham (University of Colorado)
Donna Eberhart-Phillips (UC Davis)
Bob Lillie (Oregon State University, Emeritus)
M. Meghan Miller (UNAVCO)
Kate Long (California Office of Emergency Services)
John Vidale (University of Washington)
Andrew Whittaker (University of Buffalo; Director, MCEER)

Two additional members of the Advisory Council were not able to attend the meeting, but they participated in a session by phone:

Farzad Naeim (John A. Martin and Associates)
Susan Cutter (University of South Carolina)

The Future SCEC Director Transition

Tom Jordan, the current Director, intends to step down before the start of SCEC5, should it be funded, and he has made it clear that he will do so. This imposes a tight timeline for the search for the next SCEC Director, as the new Director will need to be in place at USC in time to prepare the SCEC5 proposal. The SCEC Board has developed a good plan for a search and orderly succession to the next Director, with a realistic timeline and process; that process is now well under way. We were pleased to see that the Chair of the search committee was at the SCEC meeting to learn more about SCEC and the SCEC community. This is a positive step, and we hope that there will be a strong candidate identified soon for this critical position.

Facing Budgetary Challenges

Like most scientific and engineering enterprises today, SCEC is facing serious budgetary challenges. The cuts to the SCEC core funding are significant, but not unprecedented and not a worst-case scenario; it is not hard to find organizations or projects that are faring much worse. If the cuts continue, there will be no choice but to scale back some SCEC activities, which will compromise progress toward important SCEC goals.

The actions taken by SCEC to date to deal with the budgetary shortfalls represent the most sensible options available. We agree that the budget cuts taken this year are not sustainable long-term, and some of the cuts taken this year will need to be restored (at the cost of some other SCEC activities) if the current budget levels continue. The key budgetary decisions in Congress have been out of the scientific community's control, and all SCEC can do is roll with the punches until our country has a stable and functioning budgetary process again. SCEC needs to be prepared for further budgetary turmoil in the future, in case the present situation continues indefinitely.

Communication, Education and Outreach (CEO) Advisory Structure and Goals

The 2010–2012 Advisory Council Reports recommended that advisory oversight for the SCEC CEO program be provided through a CEO-focused advisory subcommittee of the Advisory Council that reports to SCEC through the AC. This would allow a small, focused group to give full attention to the needs and opportunities for SCEC CEO, and also ensure that the full Advisory Council is informed about and supportive of the advice for SCEC.

An ad-hoc SCEC AC-CEO subcommittee had an initial meeting on April 9, 2013 at the SCEC offices at USC. Advisory Council members attending the meeting included Susan Cutter, Jim Goltz, Kate Long, Bob Lillie, and Farzad Naeim. Mark Benthien, the SCEC Associate Director for CEO, facilitated the meeting. The meeting also included phone conversations with Greg Anderson (NSF Program Manager for EarthScope and SCEC) and Jeff Freymueller (Advisory Council Chair). Participants reviewed SCEC-CEO Strategic Plan metrics and milestones and recommended:

- Removing, adding or simplifying metrics to focus on activities and achievable results,
- Extending some milestones, and
- Developing a statement of how metrics and milestones will be used as a management tool to improve programs, not just a reporting process.

At the 2013 SCEC Annual Meeting the Advisory Council formally established the CEO Subcommittee membership as follows:

Four (voting) Advisory Council Members

- Farzad Naeim, John A Martin & Associates
- Susan Cutter, University of South Carolina
- Kate Long, California Governor's Office of Emergency Services
- Bob Lillie, Oregon State University

Four (non-voting) Subject Matter Advisors, each representing one of the CEO Strategic Plan "Thrust Areas"

- Implementation Interface
- Public Education and Preparedness
- K-14 Earthquake Education Initiative
- Experimental Learning and Career Advancement

Farzad Naeim was offered and accepted the position of Chair of the CEO Subcommittee.

The AC-CEO Subcommittee members attending the 2013 SCEC Annual Meeting (Kate Long and Bob Lillie) met with Mark Benthien to discuss the structure for CEO Strategic Planning for the next eight years. Susan Cutter and Farzad Naeim also attended via phone. The subcommittee agreed to the following plan over the next few months to initially examine SCEC-CEO needs and consider ways to address them.

CEO subject matter experts will present semi-monthly webinars from the broader community representing various disciplines. Examples include social psychology, public health, risk communication, natural history interpretation, marketing, advertising, and emergency management.

The webinar presentations will address "How can earth science communication be improved?" from the viewpoint of the various disciplines.

The webinars will be open to the entire SCEC Community as well as the broader communications, education and outreach community. This will allow the CEO Subcommittee to hear feedback from a wider stakeholder base, and the webinars themselves will serve an outreach purpose.

REPORT OF THE ADVISORY COUNCIL

The CEO Subcommittee will consider these presentations in making ongoing recommendations to the Advisory Council for improvements in the SCEC-CEO program and the SCEC 5 proposal.

An Assessment of SCEC4 Progress

The AC chose to focus its assessment of SCEC4 progress on the 6 fundamental questions that SCEC posed for itself in the SCEC4 proposal. Members of the AC divided up the questions and brought back information to the full AC, which then produced a summary for each question. These follow here, with the key question or challenge given in bold type as a sub-heading.

1. Stress transfer from plate motion to crustal faults; long-term fault slip rates

Highlights. Fault slip rates determine the long-term slip budget over multiple earthquake cycles, making them particularly important inputs to earthquake hazard assessments. SCEC has supported an impressive set of estimates of geological slip rates on important faults across Southern California. For many faults there are now enough slip-rate estimates to measure with high resolution variations in slip rates in both time and space with high resolution. This is important because slip rates may vary in space across complex fault systems and could vary in time if the fault systems are changing with time; given too few data, it would be easy to confuse spatial variation with time variation, or vice versa. One key result of all this work is that geological and geodetic estimates of fault slip rates are increasingly in agreement. This suggests that many if not most of the previously noted disagreements were the result of problems with the data or with modeling slip rates. The most recent work now suggests that changes in fault slip rates over time are not large for the major faults. That suggests that the present fault system geometry and stressing pattern has remained largely stable for hundreds of thousands of years. Agreement between geologic and geodetic slip rates is not limited to the major faults; even for many smaller faults with slower slip rates the two datasets are now in agreement within uncertainties.

Geodetic estimates of fault slip rates are not measured directly, but rather are inferred from models of fault slip rates and deformation due to the earthquake cycle. We know that postseismic deformation in the years after an earthquake can be very large, but how profound are the changes in deformation rates over longer times? Evidence from deformation before some earthquakes has suggested that deformation over much of the earthquake cycle may be relatively stable and similar to that predicted by simple elastic models, but other observations have suggested otherwise. This problem has not yet been fully resolved, but SCEC has supported significant new work that is shedding light on these questions. The answer may be different for larger and smaller earthquakes, depending on whether they cause significant stress changes in viscoelastic materials with a long relaxation time. Recent work has focused on the impact of very large events such as the 1857 Fort Tejon earthquake on geodetic estimates of present-day fault slip rates, and suggests that the discrepancy between geologic and geodetic slip rate estimates there may be explained by lingering postseismic deformation. Reducing such discrepancies will decrease the uncertainties in future hazard estimations, in addition to providing a more coherent model for tectonic stressing of Southern California faults. If so, then this earthquake has also affected the state of stress on numerous faults for more than a century.

Remaining Challenges. The Garlock fault remains an exception to the general trend of increasing agreement between geologic and geodetic slip rates. The cause of this remains unclear. It may reflect a real time-dependence in fault motions, or problems with current data or models. After the Garlock fault, the Mojave segment of the San Andreas may be the next most significant discrepancy, and it might be no coincidence that these are adjacent and in a conjugate geometry. Disagreements for the Mojave segment may be due to postseismic deformation from the 1857 Fort Tejon earthquake, depending on the rheological model assumed (Hearn et al., 2013). However, significant uncertainty remains about the rheological models.

Fully accounting for all slip on the San Andreas Fault system through the complex geometric bend at San Geronio Pass remains difficult, although progress has been made recently. This region has been designated a Special Fault Study Area, and this seems like a ripe area for further study.

Finally, improving time resolution of fault slip rate estimates opens up the opportunity to study the effects of earthquake clustering in the past through its impact on geologic slip rate estimates. If slip rates are really constant in time but earthquake recurrence is not, then the amount of variability in slip as a function of time reflects the real variability in earthquake occurrence. The opportunity to study this may just be opening up in Southern California as the amount of data increases.

2. Stress-modulated fault interactions and earthquake clustering

Highlights. SCEC continues to perform the ultimate test of earthquake interaction models, namely, whether real earthquakes obey the models. Catalogs continue to accumulate with the critical pre-condition that the models have already been formulated. The model testing underway is unparalleled in rigor and transparency.

The development of the Community Stress Model continues; this is an extremely challenging yet critical measure for both scientific ideas and practical assessment of hazard. It would represent the most comprehensive regional compilation of the state of stress. Its long-term scientific value will come in combination with similarly comprehensive data on stressing rates and fault system modeling to relate the two.

Remaining Challenges. As is widely recognized, many questions about big earthquakes will not find a definitive answer just relying on the few observations in California, and consideration of global catalogs will be necessary. Collaborative efforts with scientists in Japan, New Zealand should be continued, and other international partnerships begun where there are clear benefits to understanding Southern California.

Fundamental questions remain in estimating the magnitude and direction of stresses in the ground. Assessing the changes in stress over time is more tractable, but not trivial.

Better understanding of the state of stress and earthquake interaction may also assist in earthquake early warning. SCEC can contribute to some of the numerous fundamental science problems in this timely and societally useful effort. Salient issues include whether the full extent of a fault rupture can be predicted from just observing its start, whether the state of stress (relative to strength) can be mapped out precisely enough to make useful predictions of fault systems' response to stress changes, proper messaging for the public and emergency managers, and more reliable assessment of fault rates, segmentation, and regularity of recurrence.

3. Evolution of fault resistance during seismic slip

Highlights. Dynamic rupture simulations are becoming more realistic. Simulations are using scales < 100 m, complex roughness and off-fault plasticity, which produce varied rupture including occasional rupture up through velocity-strengthening materials near surface. Past simulations were limited to long-period ground motions only, which limited their usefulness. New simulations are pushing these limits towards higher frequencies; predicting high frequency ground motions accurately would allow simulations to be compared to strong ground motion records and used in more engineering applications.

Numerical models are incorporating more realistic heterogeneity that varies with depth, allows broad gouge-filled shear zones, and includes inelastic deformation. These factors influence thermal pressurization and dynamic rupture, the simulations show that the deforming zone may migrate across the shear zone during rupture.

Observations are finding a wider range of slip models between end members of "aseismic" and "seismic" slip. They are also imaging deformation filling volumes rather than only on 2D faults. Seismic and field-based observations of afterslip and slip below the brittle/ductile transition may reveal evolving fault properties.

New insights due to lab experiments continue to emerge from investigations of temperature effects, pore pressure, fault gouge and fault roughness. Cross-disciplinary collaboration within the SCEC community has been successful in bringing new discoveries in rock mechanics into dynamic rupture simulations, and this is important to continue.

Remaining Challenges. Future dynamic rupture simulations will need to incorporate the realistic velocity models that are being developed elsewhere in SCEC. Increased comparison of the dynamic rupture simulations to seismic observations is important. A goal of improving agreement with strong ground motion observations will enhance utilization of the rupture model results.

4. Structure and evolution of fault zones and systems: relation to earthquake physics

Highlights. SCEC scientists have played key roles in several studies, such as JFAST and studies of fault zone chemistry, that are chasing the elusive goal of measuring the heat generated in earthquakes, and thus the stress state during faulting.

Numerical simulations of elastic, plastic, and viscous models of faults in the crust and mantle are advancing. SCEC scientists are increasingly able to distinguish the deformation signature of mantle viscous flow from that of slip concentrated on creeping faults, thus allowing us to better assign the correct amount of motion on the parallel strands of the San Andreas system.

Laboratory experiments are isolating the special frictional properties of fault zone materials, moving toward explaining the low apparent friction, slow earthquakes, and distribution of strength in the crust and mantle.

Paleoseismology is adjudicating the periodicity, clustering, and oscillating patterns of earthquake recurrence. More trenches and more precise dating techniques are contributing both to basic understanding and hazard assessment.

Improved numerical models run on ever-faster computers are allowing ideas about influence of geometry, friction, and scattering to be evaluated, and facilitating ever more realistic models of the crust and crustal faults.

There is continuing progress in constraining fault zone low-velocity zones, their relation to flower structures, and thus the short- and long-term damage and healing due to earthquakes.

Remaining Challenges. The subsurface geometry of fault systems is only dimly perceived in many locations, and the effectiveness of segmentation is a critical property and remains hotly debated.

REPORT OF THE ADVISORY COUNCIL

The postulated danger of coastal thrust faults and the brutal tsunamis they could generate is not yet well established and needs investigation.

The development of fault zones deserves more attention, and the details controlling velocity-strengthening versus velocity-weakening behavior are so far not clear. Forecasting of earthquake hazards would benefit from a better understanding of these factors.

5. Causes and effects of transient deformations; slow slip events and tectonic tremor

Highlights. Transient deformation offers an exciting opportunity to study the dynamics of fault systems. In addition to postseismic transients, which have been recognized for a long time, transient creep events, slow slip events and tectonic tremor all represent transient slip phenomena or its effects. Understanding the occurrence of these events, their capacity for being triggered or for triggering other events, scaling laws and so on are important for a deep understanding of physics of fault slip.

SCEC has led a multi-year transient detection exercise aimed at detection of transients deformation signals in geodetic data. This exercise, now mature, has been successful in prompting the development of algorithms to detect and model transients. Beyond the exercise, a rich array of geodetic transients has been detected and there has been good progress in characterizing the kinematics of these events.

Tectonic tremor has been detected on an increasing number of faults, including the San Andreas fault system. Tectonic tremor is clearly not restricted only to subduction zones, but can potentially occur on any fault. Both SCEC-funded research and related research by members of the SCEC community have had a leading role in the discovery and description of tectonic tremor on Southern California faults.

More generally, any kind of transient creep acts as an amplifier of stress changes. Creep on a patch of a fault reduces the shear stress on the creeping patch but increases it substantially on its margins. Transient fault creep will temporarily increase the stressing rate on adjacent parts of the fault, potentially increasing the seismicity rate. Some prominent seismic swarms clearly have a causal relation to fault creep, such as the recent Brawley swarm.

Remaining Challenges. The causality of these transient events remains puzzling. Seismic swarms or swarm-like sequences have been identified for a long time, and it remains to be seen whether most or all of these can be explained in terms of creep processes, or if other factors that may also vary with time (such as fluid pressure to change the effective normal stress) are also responsible.

In addition to possible failure in earthquake swarms, transient events may affect the occurrence of earthquakes on nearby faults. Stress changes caused by fault creep may bring neighboring faults closer to failure. The magnitude of this stress change depends on the magnitude of the transient, but in general the magnitude of stress changes will fall in between the size of coseismic stress changes and the size of the long-term tectonic stressing rate. In addition to short-term transients, seasonal hydrological loading also cycles the stress state of faults and may play a role in the timing of earthquakes. Seasonal triggering of events is not common (or else there would be more obvious seasonal variations in seismicity), but individual transient events or transient loads may be large enough to have an impact.

6. Seismic wave generation and scattering: prediction of strong ground motion

Highlights. Under this challenge, SCEC aims to understand the generation and propagation of seismic waves, including scattering effects, particularly within the context of prediction of strong ground motion. Highlights in this area that were evident at the 2013 meeting include the following:

1. Development of broadband simulation platform. A major collaborative effort has been the development of a common and testable computing platform for simulation of ground motions across a broad band of frequencies. Intense activity in this area over the last year has led to a suite of programs that can generate in a common format many ground motion simulations, from a standard set of general input parameters. The vibrant activity in this area was showcased in a well-attended and lively workshop at the 2013 meeting. There are also other exciting developments in ground-motion simulation that were highlighted during the 2013 meeting, in particular the insights gained from dynamic rupture modeling.
2. Development of metrics to evaluate ground motions. A parallel effort to the development of the broadband platform has been progress in developing a common set of objective metrics with which to evaluate the performance of simulated motions. This set of metrics is modest at present, but the framework is in place that will allow the catalogue of metrics to continue to grow and become more useful. This sets the stage for objective validation of ground-motion simulation methods.
3. Coordination with earthquake engineering in the use of simulations. There has been substantial progress in bringing the results of SCEC research closer to use in engineering practice, through the work of a technical activity group to address

uses of simulations in evaluating structural performance. This holds the promise of transforming the role of SCEC and broadening its reach. The progress in this area is particularly significant. Engineers are increasingly recognizing the potential for simulations to address important problems in earthquake engineering, including filling gaps in available time-history datasets, and facilitating investigations of a range of engineering problems (soil-structure interaction, and structure-soil-structure interaction, for example). Moreover, engineers are becoming more positive about the potential applications of simulations to critical infrastructure and tall buildings.

Remaining Challenges.

1. Understanding the physics of wave propagation at higher frequencies and its practical implications remains a challenge, despite substantial progress in codes to simulate such motions. This is an ongoing task for SCEC ground-motion modelers and researchers.
2. There is a need to make the degree of complexity in building modeling commensurate with the level of complexity in simulations. Overly simplified building models are being used, which makes conclusions drawn from simulations of limited value. This is partly a matter of continuing seismology-engineering interface efforts such that the overall framework of the simulations and their use in engineering is understood on both sides. If engineers and seismologist both understand the basics of what is being generated, and how the products are to be used, there will be continued improvement in both the utility of the simulation tools being developed, and in the appropriateness of their application.
3. There is a potential to integrate simulations with engineering effects at local scales, offering both new challenges and new opportunities. Simulations can play a role in understanding complex effects in the upper soil column that can be highly nonlinear, and of importance when inputting motions to a structural system. How to use simulations to explore such issues, and others such as liquefaction and landslide potential, remains a challenging opportunity.
4. SCEC scientists need to continue the excellent progress in working with engineers to build acceptance of simulations as a useful tool of practice in the engineering community. We note that there is a tendency in the engineering community to have a misplaced faith in GMPEs (ground-motion prediction equations) as providing a reliable prediction of ground motions for engineering applications. This is really a matter of educating engineers as to what they are getting - with both the GMPEs and simulations - and illustrating the connection between the two. We think that this topic is mature enough (and important enough) to engage a broader engineering community (i.e., the much larger community that uses codes of practice for analysis and design) through a wide-audience webinar. Such a webinar could be delivered by an engineer and advertised through websites and newsletters that reach much of the earthquake engineering community across North America.
5. A logistical challenge will be to deliver the simulation products (as they become ready) in a format that is useful for practicing engineers. For example, many engineers are familiar and comfortable with USGS-type webtools that deliver PSHA-based ground-motion parameters and deaggregations for building code applications. Further links/tools could allow results of selected simulations that meet identified criteria to be downloaded in a standard format for engineering use.
6. The treatment of site effects in simulations is a challenging task that requires further work, particularly with regards to the level of detail that should be attempted when providing generic simulations for broad-based applications. This issue has not yet been addressed in the broadband platform.
7. There is a need to integrate lessons learned and products obtained across the range of simulation technologies being explored in SCEC. This includes those being developed on the broadband simulation platform, CyberShake, and dynamic simulations. These methodologies differ in their level of detail, maturity of development, and readiness for practical application. It remains a challenge to weave these strands into a coherent simulation cloth.

Communication, Education, and Outreach Highlights

Mark Benthien, *SCEC Associate Director for CEO*

Robert de Groot, *SCEC Manager of Experiential Learning and Career Advancement*

SCEC's Communication, Education, and Outreach (CEO) program complements the SCEC Science Plan, fostering new research opportunities and ensuring the delivery of research and educational products to the general public, government agencies, the broader geoscience community, engineers, students, businesses, and the media. SCEC CEO addresses the third element of SCEC's mission: *Communicate understanding of earthquake phenomena to the world at large as useful knowledge for reducing earthquake risk and improving community resilience.*

The theme of the CEO program during SCEC4 is *Creating an Earthquake and Tsunami Resilient California*. This includes: increased levels of preparedness and mitigation; expanded partnerships with research and practicing engineers, building officials, and others; routine training and drills; financial preparedness; and other ways to speed recovery and enhance future resilience. Each of these activities benefit from advances in earthquake science, by SCEC scientists and others (while tsunami research is not be a focus of SCEC, tsunami education and preparedness is an element of the CEO program and the ECA). The goal is to prepare individuals and organizations for making decisions (split-second through long-term) about how to respond appropriately to changing seismic and related hazards, including tsunami warnings and new technologies such as operational earthquake forecasts and earthquake early warning.

SCEC's Communication, Education, and Outreach (CEO) program is organized to facilitate learning, teaching, and application of earthquake research. SCEC CEO is integrated within the overall SCEC enterprise, and engages in a number of partnership-based programs with overarching goals of improving knowledge of earthquake science and encouraging actions to prevent, mitigate, respond to, and recover from earthquake losses. CEO programs seek to improve the knowledge and competencies of the general public, "gatekeepers" of knowledge (such as teachers and museums), and technical partners such as engineers and policy makers.

SCEC CEO is organized into four interconnected thrust areas:

- **Implementation Interface** connects SCEC scientists with partners in earthquake engineering research, and communicates with and trains practicing engineers and other professionals;
- **Public Education and Preparedness** thrust area educates people of all ages about earthquakes, and motivates them to become prepared;
- **K-14 Earthquake Education Initiative** seeks to improve earth science education and school earthquake safety;
- **Experiential Learning and Career Advancement** provides research opportunities, networking, and more to encourage and sustain careers in science and engineering.

SCEC CEO is led by SCEC's associate director for CEO Mark Benthien, with Bob deGroot managing Experiential Learning and Career Advancement programs, John Marquis as digital products manager and webmaster, Jason Ballman as Communications Specialist, David Gill as web developer, several contractors for ECA and ShakeOut activities, and a legion of USC student assistants and interns each year. The Earthquake Engineering Implementation Interface between SCEC and its research engineering partners is led by Jack Baker (Stanford) (who serves on the Planning Committee) and Jacobo Bielak (Carnegie Mellon). Several other SCEC scientists also are regularly involved in program development, intern mentorship, and other roles. A new subcommittee of the SCEC Advisory Council now reviews the CEO program each year.

SCEC also continues to expand its CEO activities through partnerships with groups in academia and practice. The Earthquake Country Alliance (ECA), created and managed by SCEC, continues to grow and serve as a model for multi-organizational partnerships that we plan to establish within education and among practicing and research engineers.

SCEC CEO has been very successful in leveraging its base funding with support from the California Earthquake Authority (CEA), FEMA, CalEMA, USGS, additional NSF grants, corporate sponsorships, and other sources. For example, for its Putting Down Roots in Earthquake Country publication SCEC CEO has leveraged an additional \$4.4 million for advertising and printing since 2004. Since 2010 FEMA has provided SCEC and its Earthquake Country Alliance partners nearly \$1.5 million for ECA activities and national ShakeOut coordination. The CEA has spent several million dollars on radio, TV, print, and online advertising which features ShakeOut promotion each year. SCEC's intern programs have also been supported with more than \$1.3 million in additional support from several NSF programs and a private donor, and NASA supports SCEC's "Vital Signs of the Planet" teacher development program via a subcontract through JPL

SCEC Implementation Interface

The implementation of SCEC research for practical purposes depends on effective interactions with engineering researchers and organizations, and with practicing engineers, building officials, insurers, utilities, emergency managers, and other technical users of earthquake information. These are most effective as partnerships towards common objectives, although trainings, tools, and other resources are also needed.

Research Engineering Partnerships

SCEC produces a large body of knowledge about the seismic hazard in California that enhance seismic hazard maps, datasets, and models used in building codes and engineering risk assessments. The Earthquake Engineering Implementation Interface led by Jack Baker and Jacobo Bielak provides the organizational structure for creating and maintaining collaborations with research engineers, in order to ensure SCEC's research activities are aligned with their needs. These activities include rupture-to-rafter simulations of building response as well as the end-to-end analysis of large-scale, distributed risk (e.g., ShakeOut-type scenarios). Analysis of the performance of very tall buildings in Los Angeles using end-to-end simulation remains a continuing task that requires collaboration with both research and practicing engineers through PEER and other organizations. An important Technical Activity Group in SCEC4 is the Ground Motion Simulation Validation (GMSV) group, led by Nico Luco, which is developing procedures for the validation of numerical earthquake simulations that are consistent with earthquake engineering practice. Our goal of impacting engineering practice and large-scale risk assessments require even broader partnerships with the engineering and risk-modeling communities, which motivates the activities described next.

Activities with Technical Audiences

The Implementation Interface also develops mechanisms for interacting with technical audiences that make decisions based on understanding of earthquake hazards and risk, including practicing engineers, geotechnical consultants, building officials, emergency managers, financial institutions, and insurers. This will soon include expansion of the Earthquake Country Alliance to include members focused on mitigation, policy, and other technical issues. SCEC is also planning training sessions and seminars for practicing engineers and building officials to introduce new technologies (including time-dependent earthquake forecasts), discuss interpretation and application of simulation records, and provide a forum for SCEC scientists to learn what professionals need to improve their practice. An example is the annual SEAOSC *Buildings at Risk Summits* which SCEC has co-organized since 2011 in both Los Angeles and San Francisco (with SEAONC). The 2014 conference is titled "Strengthening our Cities" and will be held on October 20 in Los Angeles. Also on September 18 SCEC/ECA is supporting the "Earthquake 2014 Business Preparedness Summit" with FLASH, Safe-T-Proof, Simpson Strongtie, and several other partners, an event which will launch a new FEMA QuakeSmart recognition program for businesses that demonstrate mitigation they have implemented. We are also collaborating with EERI, NEES, PEER, and others. These activities will increasingly be online, with frequent webinars and presentations and discussions recorded and available for viewing online.

To understand SCEC's effectiveness in this area, we will track and document use of our technical resources and information, and their impact on practice and codes, guidelines, and standards. Those who utilize SCEC products and information may be asked to notify us, especially partners who understand the value to both SCEC and themselves.

Public Education and Preparedness

This thrust area spans a suite of partnerships, activities, and products for educating the public about earthquake science and motivating them to become prepared for earthquakes and tsunamis. To work towards these goals, we will increase the application of social science, with sociologists and other experts.

Earthquake Country Alliance

The ECA is a public-private partnership of people, organizations, and regional alliances, each of which are committed to improving preparedness, mitigation, and resiliency. People, organizations, and regional alliances of the ECA collaborate in many ways: sharing resources; committing funds; and volunteering significant time towards common activities. ECA's mission is to support and coordinate efforts that improve earthquake and tsunami resilience. The Earthquake Country Alliance is now the primary SCEC mechanism for maintaining partnerships and developing new products and services for the

COMMUNICATION, EDUCATION, AND OUTREACH HIGHLIGHTS

general public. SCEC Associate Director for CEO Mark Benthien serves as Executive Director of the ECA. To participate, visit www.earthquakecountry.org/alliance.



SCEC created the Earthquake Country Alliance (ECA) in 2003 and continues to play a pivotal role in developing and sustaining this statewide (as of 2009) coalition with similar groups in the Bay Area and North Coast. Participants develop and disseminate common earthquake-related messages for the public, share or promote existing resources, and develop new activities and products. SCEC develops and maintains all ECA websites (www.earthquakecountry.org, www.shakeout.org, www.dropcoverholdon.org, and www.terremotos.org), and has managed the printing of the “Putting Down Roots” publication series throughout the state. This past year a special “Northridge Earthquake Virtual Exhibit” was added to the ECA site with “Northridge Near You” animations created by SCEC UseIt interns, and interviews with people who experienced the Northridge earthquake across southern California. Similar “Near You” animations are being made for the Loma Prieta 25th anniversary.

An additional new website, www.tsunamizone.org was also created in 2014 for National Tsunami Preparedness Week in March, with support from NOAA via CalOES. The site is essentially a clone of the ShakeOut model, allowing registration

of tsunami preparedness activities, educational content including inundation maps, and much more. The initial site was created for California but the plan is to expand the site to be national if not international. For now this is considered an ECA activity but when expanded nationally its “home” in the ECA will be reevaluated (this is similar to other activities where ECA is reaching out beyond California.)

Feedback from selected ECA members collected through key informant interviews, indicate that the foundation and development of the ECA very much rests upon SCEC leadership and its credibility and reputation as a trusted science and research consortium. SCEC is viewed as a ‘neutral’ and trusted leader, who employs a collaborative model to organizing stakeholders around a common cause and event. SCEC’s “culture of collaboration” has provided for a bottom-up rather than a top down approach to building the ECA community.

ECA Associates benefit from their participation by coordinating their programs with larger activities to multiply their impact; being recognized for their commitment to earthquake and tsunami risk reduction; having access to a variety of resources on earthquake and tsunami preparedness; networking with earthquake professionals, emergency managers, government officials, business and community leaders, public educators, and many others; and connecting with the following ECA sector-based committees to develop customized materials and activities:

- Businesses
- Communications
- EPIcenters (museums, parks, libraries, etc.)
- Evaluation
- Fire Advisory Cmte. (2013 subtheme)
- Public Sector
- Healthcare
- K-12 Schools
- Non-Profits and Faith-Based Organizations
- Seniors and People with Disabilities
- Speakers Bureau (Southern California)

The ECA public-private partnership is the primary organizational structure within the Public Education and Preparedness thrust area. Due to the success of the ShakeOut, the ECA is now statewide and includes three established regional alliances. In September, 2011 the relationship between SCEC and the ECA (managed by SCEC since its inception in Southern California in 2003) was cemented via a Memorandum of Understanding specifying SCEC as the administration headquarters of the statewide alliance and SCEC’S Associate Director for CEO as ECA’s Executive Director. The MOU describes SCEC’s roles and responsibilities in managing the ECA under the direction of a Steering Committee comprised of three representatives of the three regional alliances in Southern California, the Bay Area, and the North Coast. The Great California ShakeOut has been the primary collaborative activity so far, but additional activities with measurable outcomes are also managed or planned by the ECA. This planning builds on a California Office of Emergency Services earthquake communications plan developed in 2009 that emphasizes the value of a statewide collaboration.

Each ECA organization, including SCEC, independently determines the commitment of their own resources, including human, technical, and financial resources, as they carry out the fundamental actions of this voluntary, non-binding Agreement. As the home of ECA, SCEC allocates appropriate staff and administrative resources (phones, mailing, etc.) and may seek additional funding for these resources in partnership with the ECA. SCEC provides mechanisms for managing

ECA-specific funding and resources that are not co-mingled with other SCEC funding, and works with ECA leadership to ensure that such resources are allocated appropriately.

ECA 5-year goals (2012-2017):

- Further develop the awareness of, engagement in, and support for the ECA among internal audiences
- Cultivate collaboration among stakeholder Alliance members
- Build and maintain a community of earthquake / tsunami-ready Californians who, by demonstrating their readiness activities within their social circles, can help foster earthquake readiness as a social movement as well as all-hazard preparedness
- Expand the community of earthquake / tsunami-ready Californians by reaching out to those who are not yet engaged in earthquake/tsunami readiness activities

The Earthquake Country Alliance (ECA) has coordinated outreach and recruitment for the California ShakeOut since 2008. Because of the creation and growth of the ShakeOut, and other activities and products, ECA has received national recognition. In 2011 ECA was recognized by FEMA with the “Awareness to Action” award, which resulted in SCEC’s Mark Benthien being named a “Champion of Change” by the White House. In April 2012 ECA also received the “Overall National Award in Excellence” at the quadrennial National Earthquake Conference held in Memphis.

Great ShakeOut Earthquake Drills

Great ShakeOut Earthquake Drills began in southern California in 2008, to involve the general public in a large-scale emergency management exercise based on an earthquake on the San Andreas fault (the USGS “ShakeOut Scenario” developed by a team of more than 300 experts led by Dr. Lucy Jones). ShakeOut communicates scientific and preparedness information based on 30 years of research about why people choose to get prepared. Its purpose is to motivate everyone, everywhere to practice earthquake safety (“Drop, Cover, and Hold On”), and to get prepared at work, school, and home.

For the ShakeOut Scenario SCEC developed advanced simulations of this earthquake used for loss estimation and to visualize shaking throughout the region. In addition, SCEC also hosted the ShakeOut website (www.ShakeOut.org) and created a registration system where participants could be counted in the overall total. In 2008 more than 5.4 million Californians participated. While intended to be held only once, requests from ShakeOut participants prompted partners and state agencies to expand the event statewide as an annual ShakeOut drill on the third Thursday of October. More than 6.9 million Californians participated in October, 2009. This date is ideal for schools and follows National Preparedness Month in September, allowing for significant media exposure prior to the drill. While K-12 and college students and staff comprise the largest number of participants, the ShakeOut has also been successful at recruiting participation of businesses, non-profit organizations, government offices, neighborhoods, and individuals. Each year participants are encouraged to incorporate additional elements of their emergency plans into their ShakeOut drill.

In addition to its lead role in organizing the California ShakeOut, SCEC manages a growing network of ShakeOut Regions across the country and around the world (see www.shakeout.org). In order to develop and maintain the ShakeOut brand and reduce potential confusion between the different drills, SCEC works with officials in these regions and for most hosts the website for their drill. This approach serves to standardize earthquake messaging nationally and internationally, and allow groups to share best practices for recruiting participation, such as the use of social networking sites. Some ShakeOuts rely more heavily on SCEC, while some are managing more of their content, reviewing registrations, and more actively communicating with participants. For example, as part of activities for the New Madrid earthquake bicentennial, the Central U.S. Earthquake Consortium (CUSEC) organized the first multi-state drill in April 2011, with 3 million participations across eleven states. CUSEC also now coordinates the SouthEast ShakeOut which had its kick-off event at the damaged Washington Monument on the one-year anniversary of the 2011 Mineral, VA, earthquake.

▫ **Growth of ShakeOut Drills**
2008: 5.4 million
 Southern California
2009: 6.9 million
 California, New Zealand West Coast
2010: 7.9 million
 California, Nevada, Guam
2011: 12.5+ million
 CA, NV, GU, OR, ID, BC, and Central US (AL, AR, GA, IN, IL, KY, MI, MO, OK, SC, TN)
2012: 19.4 million
 All above plus:
 AK, AZ, Southeast (DC, GA, MD, NC, SC, VA), UT, WA, Puerto Rico, Japan (central Tokyo), New Zealand, Southern Italy (US naval bases and surrounding areas), and a new “Global” site for all other areas.
2013: 24.9 million
 All above except New Zealand, plus:
 Rocky Mountain region (CO, WY, MT), HI, OH (now in the Central U.S.), WV & DE (now in the Southeast region), Northeast region (CT, PA, MA, ME, NH, NJ, NY, PA, RI), American Samoa, U.S. Virgin Islands, Commonwealth of Northern Marianas Islands. Charlevoix region of Quebec, and expansion across Japan.
2014: 25+ million?
 All above plus New Mexico, Yukon, all Quebec, and participation in 30+ countries via coordination of Aga Khan Development Network

COMMUNICATION, EDUCATION, AND OUTREACH HIGHLIGHTS



As of September, 2014, 25 Official ShakeOut Regions (each with their own website managed by SCEC) now span 45 states and territories, three Canadian provinces, New Zealand, Southern Italy (U.S. Naval bases), and a rapidly growing number of Japanese cities and prefectures. All of these areas are holding ShakeOut drills annually (see the global homepage at www.shakeout.org), except New Zealand (every few years). In addition, people and organizations in any other state or country can now register to be counted in the overall global total each year. ShakeOut websites are now online in English, Spanish, French, Italian, and Japanese. We are developing outreach materials to encourage other countries to participate, including Iran (which has annual earthquake drills in its schools involving several million people).

Recruitment is well underway for the 2014 ShakeOut on October 16 at 10:16 a.m., with over 9.1 million participants registered in California and more than 13.7 million worldwide as of September 1. Including drills held earlier in 2013, already more than 17.5 million people worldwide have registered in 2014. Our goal is to exceed 30 million participants.

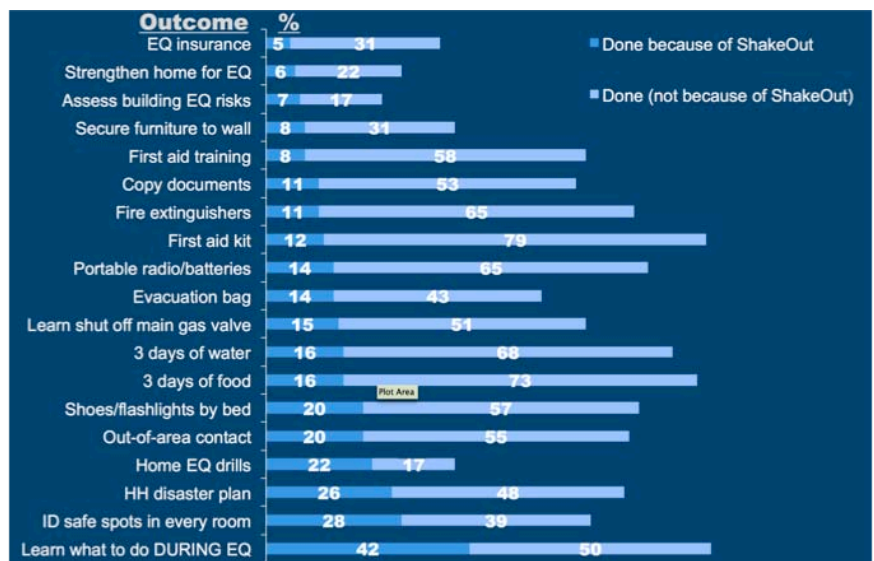
FEMA provides support to SCEC to manage each region’s ShakeOut website, create materials, and provide other assistance. However, each ShakeOut is only successful when state or regional public and private partners work together to recruit participation. One reason for ShakeOut’s success has been its practice

of localizing content for each region, so that organizers and participants take ownership of their ShakeOut (even though all websites and materials are centrally managed). FEMA’s multidisciplinary “Whole Community” approach is essential, with customized information provided for more than 20 audience categories (schools, families, businesses, government, nonprofit organizations, museums, etc.). Each registered participant receives e-mail reminders as well as drill instructions, preparedness and mitigation information, and access to a variety of resources available on their region’s ShakeOut website. These include comprehensive drill manuals, an audio file to play during the drill, and downloadable posters, flyers, and artwork.

The ShakeOut has been the focus of significant media attention and has gone a long way to encourage dialogue about earthquake preparedness in California. Through the ShakeOut, the ECA does more than simply inform Californians about their earthquake risk; it has become an infrastructure for providing earthquake information to the public and involving them in community resiliency, teaching people a life-saving response behavior while fostering a sense of community that facilitates further dialogue. In addition to registered participants, millions more see or hear about ShakeOut via broad news media coverage. ShakeOut generates thousands of news stories worldwide each year and has been featured on the front page of the *New York Times*, on many national and local morning television programs, and even in late-night talk shows. This media attention encourages dialogue about earthquake preparedness.

While assessing participation via registration and showcasing ShakeOut activities have been essential from the start, surveys are providing insights into what participants are learning and improving in terms of preparedness and mitigation. A state-sponsored survey of California household earthquake preparedness in 2008 will hopefully be repeated regularly so that the ShakeOut effort can be continually improved. The ECA Evaluation Committee conducts and encourages additional social science research specific to the ShakeOut.

In the future, operational earthquake forecasts should create additional interest for the ShakeOut drills and increase participation and preparedness in general (as well as interest in earthquake science). The ShakeOut drills are also an excellent structure to prepare Californians to respond to earthquake early warnings. For the warnings to be effective, individuals, organizations, and governments must be trained in how to respond appropriately given their situation. Also, the Shakeout drills continue to be an annual exercise of SCEC's post-earthquake response plan. The slogan of the ECA is “we’re all in this together” and as far as ShakeOut goes, “we’ve only just begun.”



Putting Down Roots in Earthquake Country publication series

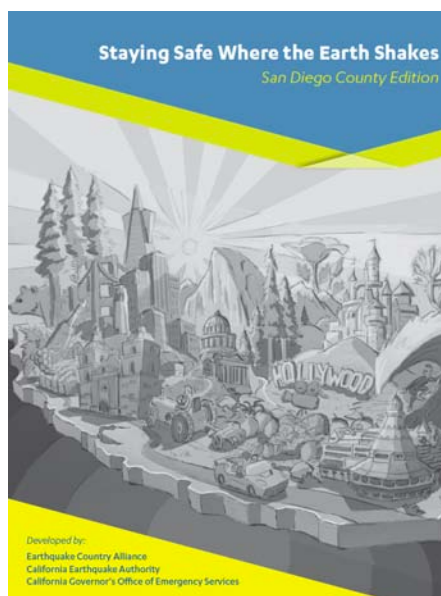
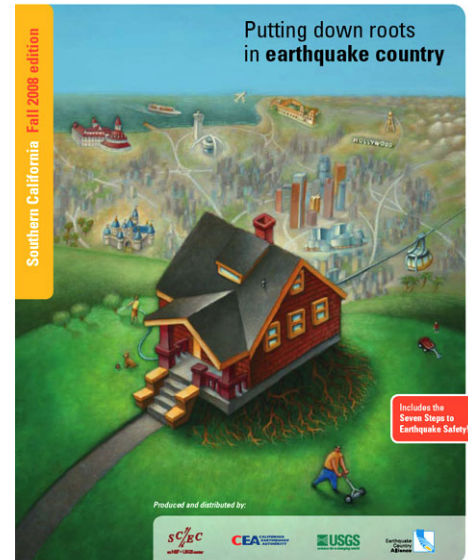
Putting Down Roots in Earthquake Country, a 32-page handbook, has provided earthquake science, mitigation, and preparedness information to the public since 1995. *Roots* was first updated in 2004, including the creation of the *Seven Steps to Earthquake Safety* to organize the preparedness content. Since then the handbook has undergone five additional revisions and printings totaling 3.5 million copies. The first Spanish version of *Roots* was produced in 2006. The Fall, 2008 version added overviews of the ShakeOut Earthquake Scenario and the Uniform California Earthquake Rupture Forecast study (*Field et al., 2009*). The 2011 version included new tsunami science and preparedness content.

As part of the CEO evaluation, an online survey was conducted of people who recently ordered the southern California version of *Roots*, and compared to data collected when copies of the handbooks are requested. The survey indicates a clear increase in levels of household earthquake preparedness from the time they ordered the handbook to the time of the survey.

The *Putting Down Roots* framework (including the *Seven Steps to Earthquake Safety*) extends beyond the distribution of printed brochures and online versions. For example, the Birch Aquarium in San Diego and Fingerprints Youth Museum in Hemet both based earthquake exhibits on the booklet, and the Los Angeles County Emergency Survival Program based its 2006 and 2009 campaigns on the *Seven Steps*. Bogota, Colombia adapted the *Seven Steps* as the basis of the city's brilliant "Con Los Pies en la Tierra" (With Feet on the Ground) campaign (www.conlospiesenlatierra.gov.co). This partnership resulted from SCEC CEO's involvement in the *Earthquakes and Megacities initiative*.

The booklet has spawned the development of region specific versions for the San Francisco Bay Area, California's North Coast, Nevada, Utah, Idaho, and the Central U.S. (totaling an additional 4 million copies). In Fall 2008, SCEC and its partners developed a new supplement to *Putting Down Roots* titled *The Seven Steps to an Earthquake Resilient Business*, a 16-page guide for businesses to develop comprehensive earthquake plans. It and other *Roots* handbooks can be downloaded and ordered from the main ECA website (www.earthquakecountry.org).

This print and online publication series remains very popular and likely will be replicated in additional regions during SCEC4, similar to new versions produced since 2005. The existing versions will continue to be updated and improved with new science and preparedness information. For example, tsunami content was added in 2011 to the Southern California version of the handbook, based on content created for the 2009 version of *Living on Shaky Ground*. This is a similar document published by the Redwood Coast Tsunami Workgroup that now also includes the SCEC/ECA *Seven Steps to Earthquake Safety*.



Research results related to earthquake forecasting are already included in the handbook, and this information will be updated as operational earthquake forecasts and earthquake early warning become a reality in California.

Beyond updates focusing on content, new versions or translations of the publication will expand the reach of *Roots* with particular emphasis on underserved communities. This will involve partners that specialize in communicating in multiple languages and via culturally appropriate channels. Additionally, versions for low-literate or visually impaired audiences, and perhaps for children and seniors will be pursued.

For example, in 2013 the California Earthquake Authority and California Office of Emergency Services supported the development of the latest booklet in the *Putting Down Roots* series, *Staying Safe Where the Earth Shakes*. Subject matter experts from ECA organizations worked together to simplify the *Seven Steps to Earthquake Safety* and local earthquake and tsunami hazard descriptions into a booklet with half the number of pages of other booklets, which can be more easily translated into multiple languages and was produced for 8-10 regions of the state. In Fall 2014 all versions will be available from the ECA website, and CEA will provide support to SCEC for customizing booklets (logos, text) for government agencies or organizations who will then print booklets for their own distribution.

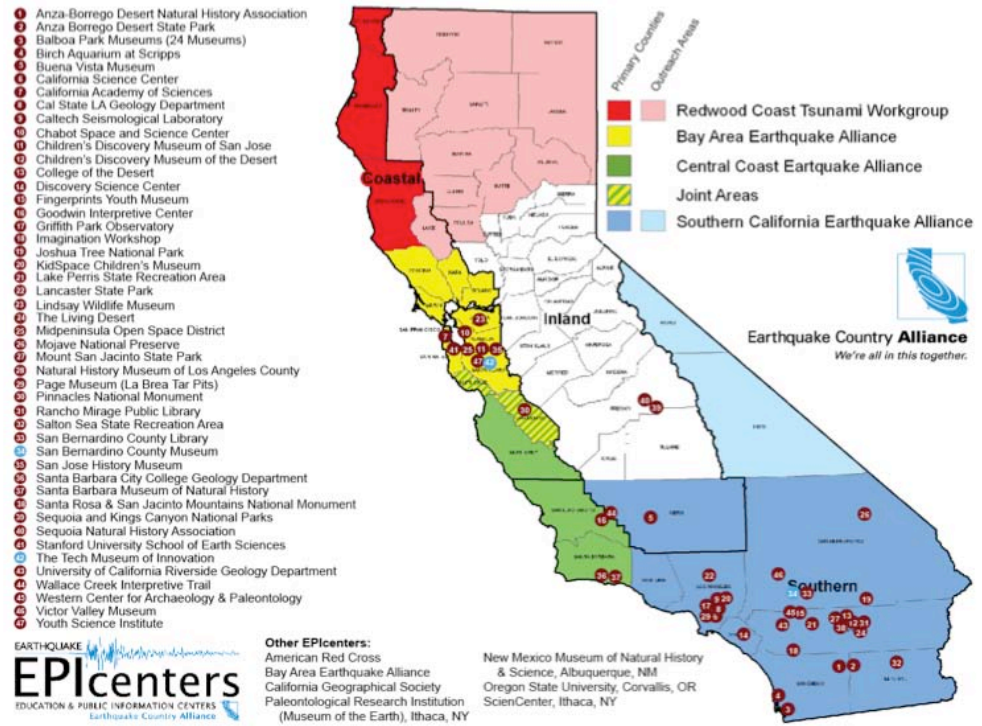
COMMUNICATION, EDUCATION, AND OUTREACH HIGHLIGHTS

Earthquake and Tsunami Education and Public Information Centers (EPIcenters)

SCEC CEO has developed exhibits and partnered with information education venues for many years, including an interpretive trail on the San Andreas fault at Wallace Creek, a permanent earthquake exhibit at a youth museum in Hemet, CA, a temporary earthquake exhibit at the UCSD Birch Aquarium, and most recently with the San Bernardino County Museum (SBCM) we are developing an interpretive site at Pallett Creek. The expansion of these partnerships, especially with the SBCM in 2007, led SCEC to create the Earthquake and Tsunami *Education and Public Information Center* (EPIcenter) Network in 2008. EPIcenters include museums, science centers, libraries, universities, parks, and other places visited by a variety of audiences including families, seniors, and school groups. Each implements a variety of activities including displays and talks related to the ShakeOut and other activities year round. The California network of more than 60 institutions is coordinated by SCEC’s Robert de Groot with Kathleen Springer (San Bernardino County Museum, Redlands) and Candace Brooks (The Tech Museum, San Jose) coordinating Network activities in Southern and Northern California respectively. Kathleen is also a member of the statewide Steering Committee of the Earthquake Country Alliance.

These partners share a commitment to encouraging earthquake and tsunami preparedness. They help coordinate Earthquake Country Alliance activities in their county or region (including ShakeOut), lead presentations or organize events in their communities, develop educational displays, or in other ways provide leadership in earthquake and tsunami education and risk reduction.

Through key informant interviews, EPIcenter members have indicated that the EPIcenter model produces institutional and professional benefits which support collaboration among partners, such as a) access to innovative, cutting-edge earthquake science findings, educational materials, visualizations and other means of presenting information, b) technical assistance with exhibit and/or gallery design, c) earthquake science education training for educators and interpreters, d) resource-sharing for enhanced patron experiences and efficient use of funds, e) increased capacity for partnership development, f) enhanced ability to apply disaster preparedness training, g) increased credibility as perceived by institutional leadership and patrons, and h) opportunities to showcase achievements at professional meetings and EPIcenter meetings.



SCEC CEO has also established relationships with institutional partners in other states (2 in Oregon, 2 in Alaska, 1 in Arizona, and 3 in New England) Growth has been enhanced through the collaboration with the Cascadia EarthScope Earthquake Education and Tsunami Education Program (CEETEP) and the EarthScope Interpreters workshops in Oregon, Washington, and Alaska (see K-12 Education Initiative below for more details). Recently the Network has been collaborating with the Central United States Earthquake Consortium to create an EPIcenter network for the Central U.S.

Activity Highlights

San Bernardino County Museum (SBCM). In 2006 SCEC embarked on a long-term collaboration with SBCM in Redlands, California, beginning with the development and implementation of the *Living on the Edge Exhibit*. This exhibit explains and highlights natural hazards in San Bernardino County (e.g. fire, floods, and earthquakes). SCEC provided resources in the development phase of the project and continues to supply the exhibit with copies of *Putting Down Roots in Earthquake Country*. Then in 2009 the EPIcenter network collaborated with EarthScope in hosting an interpretive workshop at SBCM. This activity broadened participation and brought a new and diverse community to the network. SCEC is now serving as a regional coordinator for EarthScope’s program as well as building membership among EPIcenters.



Community members are greeted by Shakeout banners as they enter the San Bernardino County Museum to participate in the ShakeOut

As a result of the successful collaboration on *Living on the Edge*, SCEC was asked to participate in the development of SBCM's *Hall of Geological Wonders*. The Hall is a major expansion of this important cultural attraction and center of science education in the Inland Empire. One of the main objectives of the Hall is to teach about the region from a geologic perspective. The museum is devoting a large space to the story of Southern California's landscape, its evolution and dynamic nature. SCEC has played an ongoing advisory role, provided resources for the development of the earthquake sections of the exhibit, and will have an ongoing role in the implementation of educational programming. The cornerstone of this new informal learning framework is the creation of the Hall of Geological Wonders Learning Treks Program (GeoTrek). The model outlines a K-12 field trip to the SBCM. A long-term goal of the program is to establish individual GeoTrek for different ages of school groups and Hall of Geological Wonders exhibits. The GeoTrek activity is based on Lesson Study, an educational approach using observations of student learning to inform small, incremental improvements to the lesson. Lesson

Study focuses on a specific, observable learning goal, determined prior to the activity chosen to address the particular aspect of learning.

The SBCM/SCEC collaboration continues to evolve with the development of an innovative approach in museum exhibit experiences. The visitor is invited to stand on the San Andreas fault at Pallett Creek. Over the last two years SBCM and SCEC interns created the prototype of a field guide series, *The San Bernardino County Museum Discover Your Backyard Field Guides*, which interprets Pallett Creek in Valyermo, CA, widely known as "the Rosetta Stone of Paleoseismology". A re-excavated "trenchcrop" at Pallett Creek provides the basis for the field guide, which includes basic geological background as well as lithologic and chronologic data about earthquake events as revealed at the outcrop. This is a unique approach to informal learning, whereby visitors gain information both in a museum setting, then firsthand in the field, making their own discoveries and connections.

Quake Catcher-EPIcenter Network. SCEC has enhanced earthquake programming and resources through working with institutions to enhance programs aimed at floor facilitation, live interactions, and the professional development of educators at all levels. For example SCEC has expanded the Quake Catcher Network of low-cost seismic sensors with installations at over 26 EPIcenter locations in California and Oregon, and more than 100 at schools in each west coast state including Alaska. Sensors have been installed at all high schools in the Lake Elsinore Unified School District. Installation of sensors in the Chaffey Joint Union High School District started in October 2013. The goal is to establish several K-12 sensor stations around a given EPIcenter as a means to build long-term educational partnerships around the ShakeOut, citizen science, and an opportunity to enrich standards-based K-12 curriculum. We have found that free-choice learning institutions are hungry for new programming that will engage science educators and their students in "citizen science" projects. SCEC is collaborating with the USGS, Stanford, NEES, and the California Geological Survey, and various members of the EPIcenter network to establish a QCN professional development program for science educators to be administered by free-choice learning institutions across the Network. Once the teachers are trained to use QCN as research and classroom learning tool, we will build a "citizen science" community among those teachers (and their students) using the local EPIcenter as a hub. The first hub has been established at the San Bernardino County Museum in Redlands.

"Native California is Earthquake Country!" Initiative. SCEC has worked with the Sherman Indian High School (SIHS) in Riverside, CA, to develop earthquake awareness and preparedness messaging, beginning with translation of "Drop, Cover, and Hold On" into many Native American languages. The translations were then featured in two posters; one for the school with languages of tribes from across the U.S. with students attending the school (displayed in classrooms and dormitories at the school) and a "Native California is Earthquake Country" poster which will be distributed to Native American cultural centers, administrative buildings, and schools throughout California. In 2014 SCEC also worked with SIHS to film "The Turtle Story," a Native American accounting of how earthquakes occur, told by storyteller and USC alumna Jacque Tahuka-Nunez (tribal descendant of the Acjachemen Nation). The story comes from the Gabriellino-Tongva Tribe, a California Indian Tribe also known as the San Gabriel Band of Mission Indians.

Other Activities. Recent EPIcenter activities include completion of the Science Spectacular Earthquake Program (co-developed with the California Science Center) and San Andreas fault content for the IRIS "Active Earth" display, and an earthquake and tsunami workshop for Southern California educators was hosted by the Cabrillo Marine Aquarium in Spring, 2014. New EPIcenter exhibits have also recently been completed at the California Academy of Sciences, San Francisco, and the earthquake themed highway reststop in Marston, MO. Ongoing projects include the Hatfield Marine Science Center in Newport, OR and San Diego Mesa College.

Now that the EPIcenter network is maturing, clear agreements for use of materials and participation will be developed. A set of collateral (materials) and memoranda of understanding for their use will be created to outline the costs and benefits of

COMMUNICATION, EDUCATION, AND OUTREACH HIGHLIGHTS

being a partner, along with responsibilities. A rigorous evaluation process will also be developed, including surveys that members can conduct of their visitors.

Media Relations

SCEC scientists are increasingly called upon for interviews by local, national, and international reporters and documentary producers. This is especially true after earthquakes, even those in other countries. As a result the demand on SCEC scientists after a large California earthquake will be even greater than in previous earthquakes. In 2014 SCEC staff developed new procedures for post-earthquake media coordination. In addition, the breadth of SCEC's research, including its information technology programs and the development of time-dependent earthquake forecasting, is also increasing the need for expanded media relations. New strategies and technologies are being developed to meet these demands.

For example, SCEC is implementing use of a media relations service for identifying and connecting with reporters nationwide. The service maintains current contact information for reporters and assignment editors and allows us to distribute and track news releases (rather than relying on USC or other partners). SCEC has used a companion service from the same provider for tracking coverage of SCEC and ShakeOut news.

Social media capabilities have also been expanded in SCEC4 (*twitter.com/scec* now has 517 followers, and *facebook.com/scec* has 2,124 "likes") under the management of SCEC's new Communication Specialist Jason Ballmann (whose hiring is the result of increased support from FEMA). The SCEC Youtube Channel (*youtube.com/scec*) is now regularly supplemented with new content. will soon include the use of podcasts, webinars and other virtual news conferences, and other technologies. SCEC and the ECA are increasing the availability of multi-lingual resources (materials, news releases, experts, etc.) to more effectively engage all media, including foreign media. Summer and school-year internships for journalism or communications students assist CEO staff in developing these technologies and resources.

An important component to our media relations strategy will be media and risk communication training for the SCEC Community. Training will likely be held each year at the SCEC Annual Meeting (the first was in 2012). New content management software for SCEC's web pages will allow members of the community to create online summaries of their research, along with video recordings of presentations, as part of a new experts directory. SCEC will partner with USGS, Caltech, and other partners to offer annual programs that educate the media on how to report earthquake science, including available resources, appropriate experts, etc. The first two were held in January 2014 as part of the 20th Anniversary of the Northridge Earthquake (a media training workshop at Caltech and a press conference at USC).

K-14 Earthquake Education Initiative

The primary goal of this Initiative is to educate and prepare California students for living in earthquake country. This includes improved standards-based earth science education as well as broadened preparedness training. The science of earthquakes provides the context for understanding why certain preparedness actions are recommended and for making appropriate decisions; however earthquake science and preparedness instructions are usually taught in a manner that lacks this context. For example, earthquake science is mostly taught in the context of plate tectonics and not in terms of local hazards. Large distant earthquakes are something that happened "over there" and local connections that are both contextual and "place-based" (such as materials specific to a school's geographic region) are not often made.

SCEC's position is that knowledge of science content and how to reduce earthquake risk may be best achieved through an event-based (teachable-moment) approach to the topic. In other words, even if most earthquake content remains in California's sixth grade and secondary curriculum, earthquake science and preparedness education should be encouraged in all grades when real-world events increase relevance and therefore interest. While we cannot plan when earthquakes will happen, the annual ShakeOut drill provides teachers a new type of teachable moment for teaching earthquake science.

In addition to event-based education opportunities such as the ShakeOut (which is integrated within all SCEC educational activities), educational materials must also be improved or supplemented to provide better information about local earthquake hazards and increase relevance for learning about earthquakes (place-based education). SCEC's role as a content provider is its ability to convey current understanding of earthquake science, explain how this understanding is developed, and provide local examples. The SCEC4 focus on time-dependent earthquake forecasting may take many years to appear in textbooks, yet SCEC can develop resources now.

SCEC's approach is as follows. First, we facilitate learning experiences and materials for use with real earthquakes and the ShakeOut drill. This will include online resources and activities, appropriate for various subjects (science, math, geography, etc.) for teachers to download immediately after large earthquakes and prior to the ShakeOut, to be hosted on SCEC's website and also shared with IRIS, UNAVCO, USGS and others for their similar teachable moment resource webpages (similarly as our coordination with IRIS and EarthScope on the Active Earth display). Second, SCEC and our education partners will develop learning materials that complement traditional standards-based instruction with regional and current earthquake information. Teacher workshops will be offered to introduce these resources to educators at all levels, and will

include follow-up activities over the long-term to help implement the content. Evaluation will be conducted across all activities, perhaps involving education departments at SCEC institutions. These activities are described below.

Partnerships with Science Education Advocacy Groups and Organizations with Similar Missions

SCEC is an active participant in the broader earth science education community including participation and leadership in organizations such as the National Association of Geoscience Teachers, the Coalition for Earth System Education, and local and national science educator organizations such as the California Science Teachers Association (CSTA). Improvement in the teaching and learning about earthquake science hinges on improvement in Earth science education in general. Hence, SCEC contributes to the science education community through participation on outreach committees and work groups wherever possible, co-hosting meetings, workshops, and building long-term sustained partnerships.

National Science Teachers Association and California Science Teachers Association (CSTA). Earthquake concepts are found in national and state standards documents and SCEC is on the leading edge of engaging education professionals as the New Generation Science Standards and Common Core State Standards are implemented SCEC participates in national and statewide science educator conferences to promote innovative earthquake education and communicate earthquake science and preparedness to educators in all states. In 2011 and 2013 SCEC participated in the planning committee for the annual California Science Education Conference hosted by CSTA. For the 2013 conference SCEC sponsored a keynote talk given by 2007 USEIT intern alumnus Emmett McQuinn. McQuinn and his team at IBM won first place in the Illustration Category in the 2012 International Science & Engineering Visualization Challenge for the image *The Connectivity of a Cognitive Computer Based on the Macaque Brain*. Since 2009 SCEC has hosted a field trip for the conference and in 2013, SCEC and the San Bernardino County Museum hosted a field trip along the San Andreas fault. This will be conducted again in December, 2014 as part of the combined NSTA/CSTA meeting in Long Beach. The trip will be co-hosted by SCEC and the InSight Vital Signs of the Planet Program.

EarthScope Partnership. SCEC has collaborated with EarthScope since 2009, when the two organizations co-hosted a San Andreas Fault workshop for park and museum interpreters at the San Bernardino County Museum. SCEC continues to collaborate with the EarthScope workshops for Interpreters by providing educational expertise and capitalizing on the synergism of the ShakeOut drills throughout the United States (SCEC participated in the Fall 2013 EarthScope Interpreters workshop being held at Acadia National Park in advance of Maine's participation in the ShakeOut). In summer 2013 SCEC participated in the first Cascadia EarthScope Earthquake and Tsunami Education Program (CEETEP) program held at the Hatfield Marine Science Center in Newport, OR. At these workshops SCEC provides resources and information about SCEC science, ShakeOut resources, and the Quake Catcher Network. Workshop convenors have found that the ShakeOut is an important event that helps promote their program and vice versa. For example, a group of teachers from the Oregon coast (Lincoln County) worked with education staff at Hatfield to host a 2013 ShakeOut day which included visiting tsunami exhibits, a drop, cover and hold on drill, and a talk about the science of the Cascadia subduction zone. In 2014 SCEC participated in additional workshops in Aberdeen and Forks (Washington), and in Alaska. The final CEETEP workshop will be hosted by SCEC, EarthScope, and Humboldt State University in Arcata in summer, 2015.

CGS Workshops. SCEC is collaborating with the California Geological Survey to conduct education workshops at ECA EPIcenters (focusing on aquaria) in California. Cabrillo Marine Aquarium in San Pedro, CA, hosted the first Earthquake and Tsunami workshop in spring, 2014, and more are being planned. SCEC and CGS also regularly co-host a booth at the California Science Teachers Association annual meetings.

Teacher Professional Development

InSight Vital Signs of the Planet (VSP) Program. Starting in 2013 the partnership with Sally McGill expanded as part of SCEC's lead role in the Education and Public Outreach program for *InSight* (Interior Exploration using Seismic Investigations, Geodesy, and Heat Transport), a NASA Discovery Program mission that will place a geophysical lander on Mars to study its deep interior in 2016. For this mission SCEC developed the '*Vital Signs of the Planet*' professional development program, a standards-based middle and high school research experience and curriculum development program offering strong connections to STEM research.

VSP expands on a collaboration that began in 2009 between SCEC and the Cal State San Bernardino/EarthScope RET program led by Dr. Sally McGill. During the course of each summer 7-10 high school teachers and their students conducted campaign GPS research along the San Andreas and San Jacinto faults. SCEC facilitated the education portion of the project through the implementation of the professional development model called Lesson Study. This allowed for interaction with the teachers for an entire year following their research. In their second year teachers and students participated in the SCEC Annual Meeting by participating in meeting activities and presenting their research at one of the evening poster sessions.

COMMUNICATION, EDUCATION, AND OUTREACH HIGHLIGHTS



2014 InSight Vital Signs of the Planet participants on a field trip to the Jet Propulsion Laboratory.

VSP is now a three-week summer institute that provides 10-15 educator fellows with authentic experiences in scientific inquiry, encourages instructional improvement in schools, and fosters deep engagement with local underserved communities. The Summer Institute is 3 weeks long which includes seminars, field research, field trips, and curriculum development. The program is centered around a 5-day field research component in partnership with California State University, San Bernardino using survey mode GPS to monitor tectonic deformation in Southern California, and are installing QCN sensors in their classrooms. In 2014, ten science educators and four students participated and their posters are displayed at the 2014 SCEC Annual meeting. Teacher participants also help plan and implement the workshop for science

educators held in conjunction with the SCEC Annual Meeting, where they share the research lessons they developed. During the fall these lessons are test taught at the schools and revised. Each lesson will also be developed into a lending kit that can be shared among all current participants and alumni of the program.

Other Activities

Plate Tectonics Kit. This teaching tool was created to make plate tectonics activities more accessible for science educators and their students. SCEC developed a user-friendly version of the *This Dynamic Earth* map, which is used by many educators in a jigsaw-puzzle activity to learn about plate tectonics, hot spots, and other topics. At SCEC's teacher workshops, educators often suggested that lines showing the location of plate boundary on the back of the maps would make it easier for them to correctly cut the map, so SCEC designed a new (two-sided) map and developed an educator kit.

ShakeOut Curricula. With the advent of the Great Southern California ShakeOut in 2008, SCEC CEO developed a suite of classroom materials focused primarily on preparedness to be used in conjunction with the drill. An important result of the ShakeOut is that it has enhanced and expanded SCEC's reach into schools at all levels from county administrators to individual classroom educators.

Experiential Learning and Career Advancement

The SCEC Experiential Learning and Career Advancement (ELCA) program seeks to enhance the competency and diversity of the STEM workforce by facilitating career advancement pathways that (1) engage students in STEM-based research experiences at each stage of their academic careers, and (2) provide exposure and leadership opportunities to students and early career scientists that engage them in the SCEC Community and support them across key transitions (undergraduate to graduate school, etc.).

Undergraduate Internships

The ELCA program in SCEC4 is built on the foundation of our long-established USEIT and SURE internship programs that challenge undergraduates with real-world problems that require collaborative, interdisciplinary solutions. Each summer they involve over 30 students (including students at minority-serving colleges and universities and local community colleges). The interns experience how their skills can be applied to societal issues, and benefit from interactions with professionals in earth science, engineering, computer science, and policy. Some interns continue their research during the academic year (especially USC students).

- The **Summer Undergraduate Research Experience (SURE)** internship places undergraduate students in research projects with SCEC scientists. Internships are supported from base SCEC funding and funding from internship mentors. 268 interns have been supported since 1994. SCEC/SURE has supported students working on numerous projects in earthquake science, including the history of earthquakes on faults, risk mitigation, seismic velocity modeling, science education, and earthquake engineering.

- The ***Undergraduate Studies in Earthquake Information Technology (USEIT)*** internship brings together undergraduates from many majors and from across the country in an NSF Research Experience for Undergraduates Site at USC. The eight-week program develops and enhances computer science skills while teaching the critical importance of collaboration for successful learning, scientific research and product development. Since 2002, 264 students have participated. UseIT interns tackle a scientific “Grand Challenge” that varies each year but always entails developing software and resources for use by earthquake scientists or outreach professionals, including SCEC-VDO (visualization software developed and refined each summer by UseIT interns). The Grand Challenge for the 2014 USEIT program was to *develop SCEC-VDO and GIS tools for exploring and evaluating the aftershock hazards implied by the new Uniform California Earthquake Rupture Forecast (UCERF3)*. These evaluations were guided by using M7 rupture scenarios developed for the 25th Anniversary of the 1989 Loma Prieta earthquake.

These internship opportunities are connected into an intellectual pipeline that encourages students to choose STEM (Science, Technology, Engineering, and Math) careers and is improving the diversity of the scientific workforce. These programs are the principal framework for undergraduate student participation in SCEC, and have common goals of increasing diversity and retention. In addition to their research projects, participants come together several times during their internship for orientations, field trips, and to present posters at the SCEC Annual meeting.

Since 2002, over 1500 eligible applications for SCEC internship programs were submitted (at www.scec.org/internships), with more than 450 internships awarded in current and past programs. Leveraging of additional funding has allowed SCEC to double the number of internships offered each year (38 in 2014). On average 30% of interns were underrepresented minority students, with some years near 50%. A 22% gender gap in 2002 has effectively been erased with near-parity since 2005. First generation college attendees have also increased from 24% in 2004 to more than 30% in recent years. Much of the success in increasing diversity has come from increased efforts to recruit students from other states and also from community colleges, making the internship programs an educational resource that is available to a broader range of students.



These students from colleges and universities across the country participated in the 2014 UseIT summer program at USC. Several will be attending the Annual Meeting to present posters, demos, and animations.

Past interns report that their internship made lasting impacts on their course of study and career plans, often influencing students to pursue or continue to pursue earthquake science degrees and careers. By observing and participating in the daily activities of earth science research, interns reported having an increased knowledge about what it's like to work in research and education. When interns developed good relationships with their mentors, they reported an increased ability to work independently, which coupled with networking at the SCEC annual meeting, gave them the inspiration and confidence to pursue earth science and career options within the field. Interns also report that their experience with the SCEC network (fellow interns, students and mentors) has been rewarding in terms of community building and networking, and a key component in creating and retaining student interest in earthquake science and related fields.

Additional Programs

These undergraduate internship programs are the centerpiece of a high school to graduate school career pathway for recruiting the best students, providing them with high-quality research, education, and outreach experiences, and offering career mentoring and networking opportunities.

At the high school level, this effort is closely linked with SCEC's K-14 Earthquake Initiative and its programs such as *InSight Vital Signs of the Planet*. The goal is to provide activities that expose high school students to earthquake research, inquiry-based curricula, and interactions with SCEC scientists. Students who have participated in SCEC research experiences during high school that have now advanced to college are now beginning to participate in USEIT or a SURE. Two high school students participated in the 2014 InSight VSP program.

COMMUNICATION, EDUCATION, AND OUTREACH HIGHLIGHTS

For graduate students, we are considering how to provide support for master's level (including new Ph.D. students) internships that provide unique opportunities. This will include support for cross-disciplinary computer science research by master's students similar to the SCEC ACCESS program (which completed in 2010). Students may participate in the USEIT program as mentors, conduct research with scientists at other SCEC institutions than their own school, and participate in CEO activities such as media relations, curricula development, and program evaluation.

For graduate students and post-docs, the effort being considered will be focused on collaboration, networking, and employment opportunities, as most are supported by their institution, or with SCEC research funding. Social networking will allow interaction across institutions and research projects. Students will be encouraged to interact within the SCEC "collaboratory" regardless if they or their advisor has received SCEC research funding. In addition to research and education/outreach opportunities, mentoring will be offered to help ELCA participants consider career possibilities, and longitudinal tracking of alumni will provide data on how students are progressing.

The final element of the ELCA program is career advancement opportunities for early-career researchers, including post-docs, young faculty, and research staff. We will highlight employment opportunities via SCEC's email list and on the SCEC website, and perhaps also post CVs of early career researchers seeking positions. We may also provide travel support for early career researchers to give presentations at conferences and department lectures nationwide, and provide presentation materials so that they can highlight their role in SCEC. Also, SCEC leadership positions, especially the planning committee, provide opportunities for exposure and career advancement. See the CEO Metrics and Milestones chart for current demographic

Research Accomplishments

Greg Beroza, SCEC Science Planning Committee Chair

The fundamental research goal of SCEC4 is understanding how seismic hazards change across all time scales of scientific and societal interest, from millennia to seconds. The SCEC4 science plan was developed by the Center's Board of Directors and Planning Committee with broad input from the SCEC community in support of this goal. Through that process we identified six fundamental problems in earthquake physics:

Table 3.1 Fundamental Problems of Earthquake Physics

- I. Stress transfer from plate motion to crustal faults: long-term slip rates.
- II. Stress-mediated fault interactions and earthquake clustering: evaluation of mechanisms.
- III. Evolution of fault resistance during seismic slip: scale-appropriate laws for rupture modeling.
- IV. Structure and evolution of fault zones and systems: relation to earthquake physics.
- V. Causes and effects of transient deformations: slow slip events and tectonic tremor.
- VI. Seismic wave generation and scattering: prediction of strong ground motions

These six fundamental problems define the focus of the SCEC4 research program. They are interrelated and require an interdisciplinary, multi-institutional approach. During the transition to SCEC4, we developed four interdisciplinary research initiatives and reformulated our working group structure in accordance with the overall research plan. We have also formalized Technical Activity Groups (TAGs) in which groups of investigators develop and test critical methods for solving specific forward and inverse problems.

Seismology

The Seismology Group gathers data on the range of seismic phenomena observed in southern California and integrates these data into seismotectonic interpretations as well as physics-based models of fault slip. This past year's accomplishments include: Archival and distribution of seismic waveforms through the Southern California Earthquake Data Center; Refinement and updating of catalogs of earthquake locations and focal mechanisms and application of refined catalogs to the Community Fault Model; Analysis of foreshocks, aftershocks, and triggered events to examine changes in focal mechanism scatter, seismicity rates, and stress drops; Application of new tremor detection techniques and analysis of crustal structure in regions where tremor is observed; Development of new techniques to investigate scattering, site response, and attenuation using very dense array data.

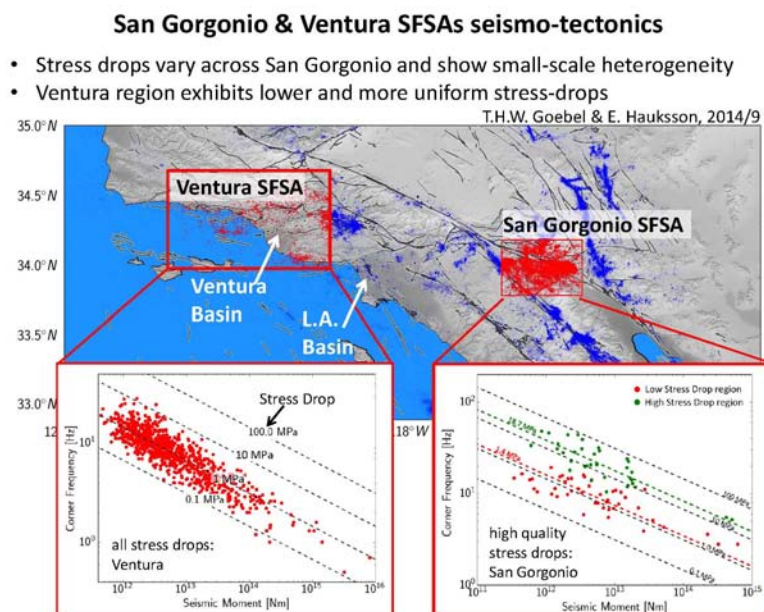


Figure 1. Stress drop comparison for Ventura basin region and selected areas in San Gorgonio Pass (from Goebel et al., in review, 2014).

RESEARCH ACCOMPLISHMENTS

Earthquake Locations, Focal Mechanisms, and Fault Representation Refinements

Revised earthquake location catalogs and focal mechanisms have been produced for the period from 1981–2013 and made available to the scientific community. The archived seismic waveforms, improved catalog, and focal mechanism are routinely used by SCEC researchers to investigate earthquakes and fault processes. Refined catalogs were used in the updated, revised 3D faults in the Community Fault Model, including within the San Geronio Pass and Ventura Area Special Fault Study Areas. Revised 3D fault representations for the major active, through-going faults in the Mojave, Transverse Ranges, Coast Ranges and offshore Borderland areas have been added. Goebel et al. (2014b) also used to investigate stress drop and other source properties in the SFSAs (Figure 1).

Seismic amplification in sedimentary basins from the ambient seismic field

The cities of Tokyo and Los Angeles are both located in sedimentary basin that have the potential to trap and amplify seismic waves. Denolle et al. (2014a&b) studied the basin amplification for both cities by analyzing the ambient seismic field. For the Tokyo study, they use data from Hi-Net deep borehole seismometers distributed across central Honshu as virtual sources. In addition they used seismic stations of the MeSO-Network of shallow-borehole seismometers in the basin as receivers to map the basin impulse response. For the Los Angeles study they used data from the Caltech/USGS Southern California Seismic Network as well as from a portable deployment. They found 3D basin effects that could be developed for ground motion prediction equations, but that the strength of basin amplification depends strongly on the direction of illumination by seismic waves. The ambient seismic noise approach is promising because it can be used to estimate expected long-period ground motions even though strong ground motion from earthquakes that would excite that shaking have not yet been recorded instrumentally.

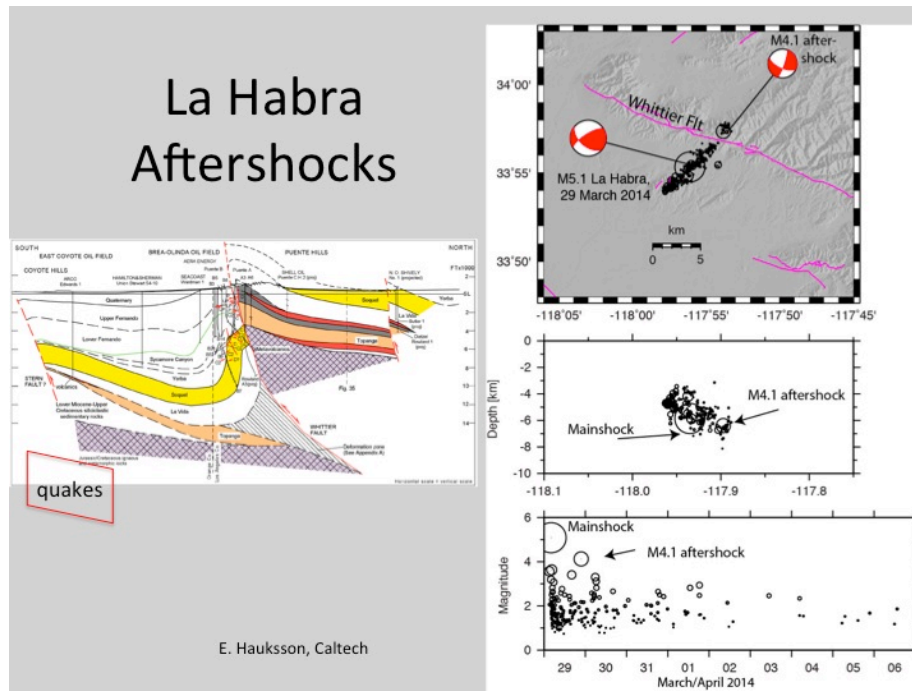


Figure 2. Overview of the La Habra earthquake sequence. (Left) Cross-section showing the location of the sequence relative to nearby fault structures. (Right top) Map view of the sequence (circles scaled by magnitude), focal mechanisms for the mainshock and largest aftershock, and major fault structures (pink lines). (Right middle) Cross-sectional view of sequence. (Right bottom) Evolution of the sequence through time. (From Hauksson, unpublished).

Seismicity and Earthquake Physics

Several seismicity studies to improve both the catalog as well as interpretation of seismicity patterns are underway. Researchers are examining data from several recent moderate earthquakes that occurred in 2014 in the Los Angeles Basin region including the M4.4 Encino and M5.1 La Habra sequences (Figure 2). Meng and Peng (2014) analyzed continuous waveforms recorded by the Southern California Seismic Network and applied template matching to detect small events. They observed a clear seismicity increase in southern California following the 2010 Mw7.2 El Mayor Cucupah earthquake. They suggested that dynamic triggering caused seismicity increases over short time scales while static triggering caused increases in seismicity over a longer time scale. In a different study Chen and Shearer (2013) applied the refined southern California earthquake catalog to study earthquake triggering models and how they apply to swarms and foreshock sequences. They suggested that most small earthquake clustering is likely driven by fluid or slow slip, rather than inter-event stress triggering. In particular, foreshock sequences may be driven by an aseismic processes rather than by static stress

triggering. Using a combined laboratory and seismicity catalog analysis, Sammis et al. developed a fully dynamic micromechanical damage model, which they used to simulate earthquake ruptures. Fault zone damage and propagation appear to be highly asymmetric. Their most recent efforts are directed towards generating spontaneous ruptures in very brittle material. Goebel et al. (2014a) also studied off-fault damage under laboratory conditions.

Select Publications

- Baltay, A. S., T. C. Hanks and G. C. Beroza, 'Stable Stress Drop Measurements and their Variability: Implications for Ground-Motion Prediction', *Bulletin of the Seismological Society of America*, 103, 1, (2013).
- Chen, X., and P. M. Shearer, California foreshock sequences suggest aseismic triggering process, *Geophys. Res. Lett.*, 40, doi:10.1002/grl.50444, 2013.
- Denolle, M. A., E. M. Dunham, G. A. Prieto, and G. C. Beroza, 'Strong Ground Motion Prediction using Virtual Earthquakes', *Science*, 343, 6169, (2014a): 399-403.
- Denolle, M. A., E. M. Dunham, G. A. Prieto, G. C. Beroza, (2014b) Strong Ground Motion Prediction Using Virtual Earthquakes, *Science*, vol. 343 no. 6169 pp. 399-403 DOI: 10.1126/science.1245678
- Gabriel, A. A., J.-P. Ampuero, L. A. Dalguer, and P. M. Mai, 'Source Properties of Dynamic Rupture Pulses with Off-fault Plasticity', *Journal of Geophysical Research*, 118, 8, 4117-4126 (2013).
- Goebel, T. H. W., T. Candela, C. G. Sammis, T. W. Becker, and G. Dresen, 'Seismic event distributions and off-fault damage during frictional sliding of saw-cut surfaces with predefined roughness', *Geophysical Journal International*, (2014a).
- Goebel, T. H. W., E. Hauksson, P. M. Shearer, and J. P. Ampuero, Stress drop heterogeneity within tectonically complex regions: A case study of the San Geronio Pass, southern California, *EPSL*, in review, (2014b).
- Huang, Y., L. Meng and J.-P. Ampuero, 'A dynamic model of the frequency-dependent rupture process of the 2011 Tohoku-Oki Earthquake', *Earth, Planets and Space*, 64, 12, (2013): 1061-1066.
- Kaneko, Y., and P. M. Shearer, 'Seismic source spectra and estimated stress drop derived from cohesive-zone models of circular subshear rupture', *Geophysical Journal International*, (2014).
- Li, Y. G., Z. Q. Xu, and H. B. Li, 'Rock Damage Structure of the South Longmen-Shan Fault in the 2008 M8 Wenchuan Earthquake Viewed with Fault-Zone Trapped Waves and Scientific Drilling', *ACTA Geological Sinica (English Edition)*, *China Academy of Geological Science*, 88, 2, (2014): 444-467.
- Li, Y.-G., G. P. De Pascale, M. C. Quigley, and D. M. Gravley, 'Fault Damage Zones of the M7.1 Darfield and M6.3 Christchurch Earthquakes Characterized by Fault-Zone Trapped Waves', *Tectonophysics*, Elsevier, 611-614, February 18 2014, (2014): 35.
- Meng, L., J.-P. Ampuero, Y. Luo, W. Wu and S. Ni, 'Mitigating artifacts in back-projection source imaging with implications on frequency-dependent properties of the Tohoku-Oki earthquake', *Earth, Planets and Space*, 64, 12, (2013): 1101-1109.
- Meng, X. and Z. Peng (2014), Seismicity rate changes in the San Jacinto Fault Zone and the Salton Sea Geothermal Field following the 2010 Mw7.2 El Mayor-Cucapah Earthquake, *Geophys. J. Int.*, 197(3), 1750-1762, doi: 10.1093/gji/ggu085.
- Sammis, C.G., Smith, S.W., Triggered tremor, phase-locking, and the global clustering of great earthquakes, *Tectonophysics* (2013), <http://dx.doi.org/10.1016/j.tecto.2012.12.021>
- Shi, Z. and S. M. Day, 'Rupture dynamics and ground motion from 3-D rough-fault simulations', *Journal of Geophysical Research*, 118, 3, (2013): 1122-1141.
- Taborda, R. and J. Bielak, 'Ground-Motion Simulation and Validation of the 2008 Chino Hills, California, Earthquake', *Bulletin of the Seismological Society of America*, SSA, 103, 1, (2013): 131-156.

Tectonic Geodesy

Tectonic Geodesy activities in SCEC4 are focusing on data collection and analysis that contribute to improved earthquake response and to a better understanding of fault loading and stress transfer, the causes and effects of transient deformation, and the structure and evolution of fault zones and systems.

Work by the SCEC community in the area of Tectonic Geodesy this year has focused on three areas: development of a Community Geodetic Model (CGM), earthquake early warning, and automated transient detection algorithms, and the analysis of high resolution geodetic data.

Community Geodetic Model

Densification of GPS arrays as part of Earthscope, the rapidly growing volumes of InSAR data from various satellites, and the development of time series analysis for InSAR data all motivated the development of a Community Geodetic Model (CGM), and we report here on progress in meeting science milestone 4. The CGM should improve geodetic studies of non-secular strain phenomena observed in Southern California, including post-seismic deformation. It will be distinct from the past SCEC Crustal Motion Map (CMM) because it will be time dependent and will incorporate InSAR data to constrain both the vertical deformation field and small-scale details of the regional deformation. This will lead to refined and improved tectonic geodesy data products for use in modeling. The CGM would be used in combination with other SCEC community models to infer the evolution of sub-surface processes. It will also provide a time-dependent reference frame for transient detection algorithms, as well as models of interseismic loading to evaluate stress changes and update rupture forecast models as tectonic conditions evolve in California. The challenge of the CGM is to exploit the spatially sparse, temporally dense 3D GPS time

RESEARCH ACCOMPLISHMENTS

series and spatially dense, temporally sparse InSAR line-of-site time series consistent with GPS time series in an appropriate projection. We note that the recent launch of two new InSAR satellites will greatly facilitate the development of InSAR time series by providing more accurate and frequent observations from multiple look directions at both C-band and L-band.

SCEC funded research in support of this effort is taking many forms including data collection to fill gaps in coverage, assessment of modeling approaches appropriate for our needs, and exploration of ways to mitigate noise and merge datasets.

California State University San Bernardino and University of Arizona researchers have teamed up to continue a field program started in 2002 that involves undergraduates and local teachers in collecting and interpreting GPS data in the San Bernardino mountains and surrounding area where previous data coverage was sparse. In addition, researchers at UC Riverside and MIT are using a dataset that combines campaign GPS data from their own field surveys with data from continuous networks and archives, to investigate the degree to which the San Jacinto Fault (SJF) slip rate varies along-strike. Continued efforts by MIT scientists to merge PBO and USGS continuous GPS solutions for southern California will prove vital in development of the CGM (Figure 3).

InSAR observations complement GPS by providing spatially dense deformation measurements. Ongoing work by this group aims to improve InSAR processing methods in order to mitigate decorrelation in areas that have experienced large coseismic offsets. Current research at Cornell is focused on integrating InSAR and GPS data into time varying deformation maps by mitigating the effects of atmospheric noise as well as using synthetic tests to explore the optimal ways to combine InSAR and GPS data. Scientists at NASA's Jet Propulsion Laboratory are currently applying InSAR time series analysis techniques to 18 years of SAR data from southern California to produce a line-of-sight velocity map constrained by GPS in order to investigate time-varying deformation (Figure 4). Modeling of dense GPS and InSAR velocity transects crossing the Southern San Andreas Fault (SAF) by investigators at SIO and San Diego State University has revealed evidence for along-strike variations in the width and depth of the creeping segment (Figure 5).

The 2010 El Mayor Cucupah earthquake has provided opportunities to investigate crust and upper mantle rheology using geodetic observations of postseismic deformation. Data collection conducted through a collaboration between Scripps Institution of Oceanography (SIO), UC Riverside, and CISESE has resulted in an improved understanding of the afterslip following the El Mayor Cucupah earthquake (Figure 6).

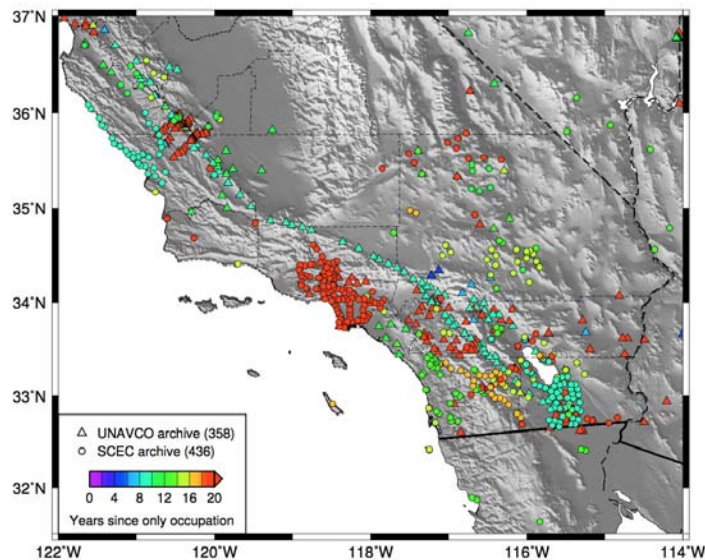


Figure 3. Densification of GPS data. GPS marks that have been occupied multiple times and may therefore provide spatial dense geodetic velocities. A primary goal of future CGM work is to identify such sites and archive or process the available data [Herring and Floyd, personal communication, 2014].

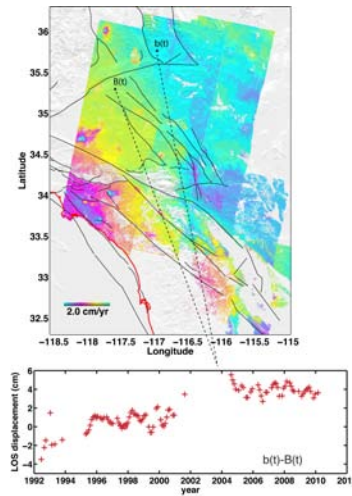


Figure 4. InSAR time series. Mosaic view of the mean LOS velocity map of descending tracks 170, 399, 127, 356, and 84 from combining ERS-1/2 and Envisat data. Note that certain tracks are displayed with ERS LOS map only to not show coseismic deformation signals of the Hector Mine earthquake. Differential LOS time series between $b(t)$ and $B(t)$ across East California Shear Zone show long term transient that is likely related to postseismic relaxation of Lander and Hector Mine earthquakes.

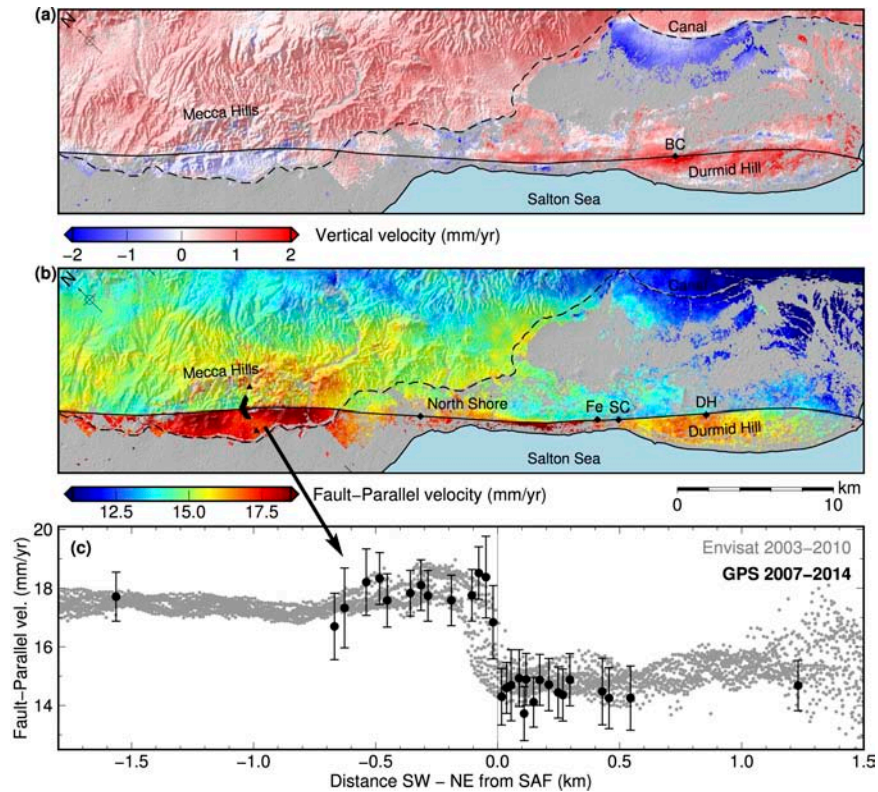


Figure 5. Refined near-fault creep measurements. Envisat InSAR and survey-mode GPS observations reveal the pattern of uplift and shallow fault creep along the southernmost San Andreas Fault. (a) Vertical ground velocity from Envisat, using a combination of ascending (Track 77) and descending (Track 356) InSAR observations. BC denotes the Bat Caves Buttes leveling line, which recorded a similar rate of uplift [Sylvester et al., 1993]. Note also areas of subsidence related to hydrologic processes. (b) Fault-parallel ground velocity from Envisat. Diamonds indicate creepmeters at North shore, Ferrum (Fe), Salt Creek (SC), and Durmid Hill (DH), operated by Univ. Colorado at Boulder. Triangles show locations of GPS monuments at Painted Canyon. (c) Comparison of InSAR velocities with GPS at Painted Canyon. The InSAR data are in good agreement with ground-based observations, and reveal that creep occurs along the entire fault segment. Creep is localized on the fault trace only at Durmid Hill and Mecca Hills, where the local fault strike leads to transpression and a high fault-normal stress. At Bombay Beach and North Shore, decreased normal stress may lead to distributed yielding — in these areas creep is distributed across a 1-2 km wide zone. (Lindsey et al., J. Geophys. Res., in review).

RESEARCH ACCOMPLISHMENTS

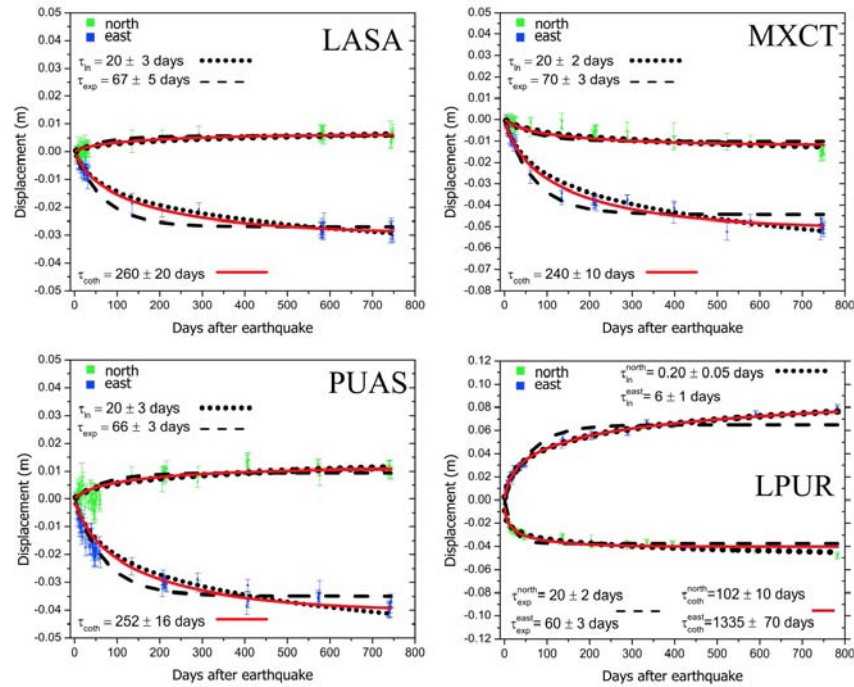


Figure 6. Collaborative surveys of El Major Cucapah postseismic deformation. Within one day of the rupture scientists from CICESE, UCSD and UCR began campaign surveys in the near field of the EMC rupture zone and have continued these measurements for more than 3 years to capture these postseismic transients. [Gonzales-Ortega et al., 2014] Daily GPS positions for the four sites closest to the earthquake rupture. The north and east components of the displacement vector are denoted by the green and blue symbols, respectively. The best fitting exponential, logarithmic, and hyperbolic cotangent functions are indicated by the black dashed, black dotted, and solid red lines, respectively. Also shown are the corresponding relaxation times (τ).

Scientists at Appalachian State University, UC Riverside, JPL, and Harvard have coordinated efforts to better constrain fault slip rates and patterns of interseismic deformation in the western Transverse Ranges of southern California with a particular focus on the Ventura Special Fault Study Area. This has involved the combined analysis of GPS and InSAR data into a mechanical dislocation model to better constrain fault slip rates.

Ongoing collaborative activities of the CGM include:

- First SCEC Community Geodetic Model (CGM) workshop (Menlo Park, CA, 30-31 May, 2013): This workshop (presentations available at: <http://www.scec.org/workshops/2013/cgm>) addressed the major problems and paths forwards towards generation of a joint GPS-InSAR 3-dimensional deformation field product. The workshop was summarized in a Meeting report in EOS, Volume 94, Number 35, 2013.
- Focus Groups: We formed GPS and InSAR focus groups that will assess and validate potential time series generation approaches for the individual data types.
- InSAR exercise: We initiated an exercise within the InSAR community to process data for a particular frame in Southern California, for the purposes of comparison of the result of different approaches, validation against GPS data and data from overlapping tracks, and assessment of the appropriate errors to use in joint GPS-InSAR efforts.
- Second SCEC Community Geodetic Model (CGM) workshop – A second GPS/InSAR workshop will be held prior to the 2014 SCEC Annual Meeting and will include 20 participants. The workshop report will be available in October 2014.

Transient Detection and Early Warning

Scientists at UCSD have made progress in estimating the magnitude of an emergent earthquake by combining seismometers and GPS sensors to measure the full spectrum of the near-field strong motions. GPS-seismometer units will be deployed at several CRTN stations in southern California during the project period.

Scientists at MIT are refining a transient detection algorithm and have submitted our algorithms to the Colaboratory for the Study of Earthquake Predictability (CSEP) and they are now running operationally. A transient detection algorithm based time-dependent displacement gradient fields and statistical analysis of measured strain anomalies has been developed at Stony Brook University and is now implemented in the CSEP testing system. Scientists at Woods Hole Oceanographic institution are studying the 22 year history of aseismic creep transients on the Superstition Hills Fault. They found that models

which included significant heterogeneity in the shallow frictional properties of the fault, can be consistent with both the afterslip and interseismic creep events observed on the Superstition Hills Fault.

Scientists at Stanford University are continuing to refine their transient detection algorithm through an improved understanding of the network noise processes. They have selected a set of 20 GPS stations over stable North America where the glacial isostatic signal provides a known, large scale secular signal. A better characterization of the noise in this stable environment will help to refine the network-based transient detection algorithms being deployed in Southern California.

High-resolution Geodetic Measurements

PBO borehole strainmeters in the Anza region and the laser strainmeters at the Pinon Flat Observatory continue to provide high-resolution observations of transient behavior associated with southern California earthquakes. Triggered aseismic slip on the San Jacinto fault has been inferred from these data to have occurred following the 2005 Anza earthquake and again after the El Mayor Cucapah earthquake at the southern end of the Anza gap. Transient deformation consistent with aseismic slip during 2010 – 2011 at the location of the 2005 earthquake has also been observed. A March 2013 M4.7 event on the San Jacinto fault near Anza triggered strain rate changes indicative of fault parallel shear with short duration (1 – 2 hour) slip accelerations. Further analysis and modeling will be required to investigate causes of observed variability in the occurrence and timing of strain recorded at different locations following the same events.

Select Publications

- Arrowsmith, R., C. Crosby, E. Kleber, E. Nissen, and P. Gold, (2013), Imaging and Analyzing Southern California's Active Faults with Lidar, November 4-6, 2013 San Diego Supercomputer Center (SDSC), UCSD, La Jolla, CA.
- Arrowsmith, R., K. Okumura, E. Nissen, T. Maruyama, C. Crosby, M. Oskin, S. Toda (2013), VISES SCEC Workshop on High Resolution Topography Applied to Earthquake Studies, September 18-20, 2013 Earthquake Research Institute (ERI), The University of Tokyo, Japan; September 21, 2013, Center for Spatial Information Science, The University of Tokyo, Japan.
- Agnew, D. C. (2014). Variable Star Symbols for Seismicity Plots, *Seismol. Res. Lett.*, v. 85, p. 775-780.
- Agnew, D. C. and F. K. Wyatt (2014). Dynamic Strains at Regional and Teleseismic Distances, *Bull. Seismol. Soc. Amer.*, in revision.
- Crowell, B. W., Y. Bock, D. T. Sandwell, and Y. Fialko (2013), Geodetic investigation into the deformation of the Salton Trough, *J. Geophys. Res. Solid Earth*, 118, 5030–5039, doi:10.1002/jgrb.50347.
- Dmitrieva, K., and P. Segall (2014), Network-based estimator of time-dependent GPS noise, in preparation.
- Gonzalez-Ortega, A., Y. Fialko, D. Sandwell, F. A. Nava-Pichardo, J. Fletcher, J. Gonzalez-Garcia, B. Lipovsky, M. Floyd, G. Funning (2014), El Mayor-Cucapah (Mw 7.2) earthquake: Early near-field postseismic deformation from InSAR and GPS observations, *J. Geophys. Res.*, doi:10.1002/2013JB010193.
- Ji, K. H. and T. A. Herring, Testing Kalman Smoothing/PCA Transient Signal Detection Using Synthetic Data, *Seismol. Res. Letters*, May/June 2013, 84, 433-443, doi:10.1785/0220120155, 2013.
- Johnson, K., Nissen, E., Saripalli, S., Arrowsmith, J R., McGarey, P., Scharer, K., Williams, P., and Blisniuk, K., in review. Rapid mapping of ultra-fine fault zone topography with Structure from Motion, submitted to *Geosphere*, December 2013.
- Lindsey, E., V. Sahakian, Y. Fialko, Y. Bock, S. Barbot, and T. Rockwell (2013), Interseismic Strain Localization in the San Jacinto Fault Zone, *Pure and Appl. Geophys.*, doi:10.1007/s00024-013- 0753-z.
- Liu, Z., P. Lundgren, Z. K. Shen, 2014, Improved imaging of Southern California crustal deformation using InSAR and GPS, SCEC Annual Meeting, Palm Springs, California
- McGill, S. F., Spinler, J.C., McGill, J.D., Bennett, R.A., Floyd, M., Fryxell, J. and Funning, G., (in prep.), One-dimensional modeling of fault slip rates using new geodetic velocities from a transect across the plate boundary through the San Bernardino Mountains, in preparation for submission to *Journal of Geophysical Research* in Spring 2014.
- Marshall, S. T., G. J. Funning, and S. E. Owen (2013), Fault slip rates and interseismic deformation in the western Transverse Ranges, CA, *Journal of Geophysical Research*, 118, 4511-4534. doi: 10.1002/jgrb.50312.
- Melgar, D. and Y. Bock (2013), Near-Field Tsunami Models with Rapid Earthquake Source Inversions from Land and Ocean Based Observations: The Potential for Forecast and Warning, *J. Geophys. Res.*, 118, doi:10.1102/2013JB010506.
- Melgar, D., B. W. Crowell, Y. Bock, and J. S. Haase (2013), Rapid modeling of the 2011 Mw 9.0 Tohoku-oki earthquake with seismogeodesy, *Geophys. Res. Lett.*, 40, 1-6, doi:10.1002/grl.50590.
- Melgar, D., Y. Bock, D. Sanchez and B. W. Crowell (2013b), On robust and reliable automated baseline corrections for strong motion seismology, *J. Geophys. Res.*, 118, doi:10.1029/2012JB009937.
- Murray, J. R., R. Lohman and D. Sandwell (2013), Combining GPS and remotely sensed data to characterize time-varying crustal motion, *EOS Trans. AGU*, 94.
- Spinler, J.C., Bennett, R.A., Anderson, M.L., McGill, S.F., Hreinsdottir, S., and McCallister, A., (2010), Present-day strain accumulation and slip rates associated with southern San Andreas and Eastern California shear zone faults: *Journal of Geophysical Research*, v. 115, B11407, doi:10.1029/2010JB007424, 29 p.
- Thatcher, W., Y. Fialko, E. Hearn, and G. Hirth, Report on a 2013 Workshop on Ductile Rheology of the Southern California Lithosphere: Constraints from Deformation Modeling, Rock Mechanics, and Field Observations, May 1-2, 2013, USGS, Menlo Park, CA.
- Tong, X., B. Smith-Konter, and D. T. Sandwell (2014), Is there a discrepancy between geological and geodetic slip rates along the San Andreas Fault System?, *J. Geophys. Res. Solid Earth*, 119, doi:10.1002/2013JB010765.

Earthquake Geology

The earthquake geology disciplinary group coordinates diverse field-based investigations of the Southern California natural laboratory. Geology contributes to earthquake response efforts and supports field observations related to many other focus-groups. Among the goals of earthquake geology are the determination of long-term slip rates and long, multi-event paleoseismologic records that have a high impact on seismic hazard assessments. In support of these efforts the Geology group coordinates geochronology infrastructure resources that are shared among SCEC-sponsored projects.

Ventura Special Fault Study Area

The Ventura SFSA project is beginning to reveal a self-consistent history of large uplift events of the Ventura anticline, likely as part of large (>M7.5) reverse-fault ruptures along the northern margin of the Ventura basin. Rockwell et al. have identified four Holocene emergent terraces formed in the past 6000 years. Each terrace records uplift of the fold crest by 4 to 6 meters. Grenader, Dolan, et al. have similarly identified similar magnitudes of coseismic folding above the propagating tip of the Ventura fault (Figure 7). Timing of the last event is consistent between sites, circa 800 years ago. However, the penultimate event timing is demonstrably older at the Ventura Day Road site than at Pitas point, which suggests that a hiatus in deposition could obscure an event at the former. New work, in progress, at the Brookshire Avenue site along Ventura fault (Figure 7) will reveal slip-rate and additional incremental slip information that should help to resolve this issue.

Coseismic uplifts of the Ventura anticline imply at least 5.5m of slip per event on the underlying Ventura-Pitas Point reverse fault (Figure 7). This slip magnitude implies that the Ventura fault ruptured together with adjacent structures. Newly published structural models based on seismic reflection, mapping, and petroleum well data (Hubbard et al., 2014) reveal how structures underlying the Ventura anticline link to a larger, and more continuous reverse fault system bounding the northern margin of the Ventura basin. An earthquake near M8 is possible on this system, which accommodates at least half of the ~1 cm/yr shortening rate across this portion of the Transverse Ranges. Large events likely involve significant deformation offshore in the Santa Barbara basin as well. Evidence for this is being revealed from paleo-tsunami deposits and sudden submergence of the Carpenteria marsh documented by Simms, Rockwell, et al.. Tsunamis may also arise from other regional sources and from distant earthquakes. New work by Berelson et al. hypothesizes that some grey (terrigenous) layers in the Santa Barbara basin could represent scour of the shallow shelf and shoreline due to tsunami run-up. The finely laminated sediments of this basin could thus preserve a long (ca. 100kyr) integrated record of tsunamis in coastal California.

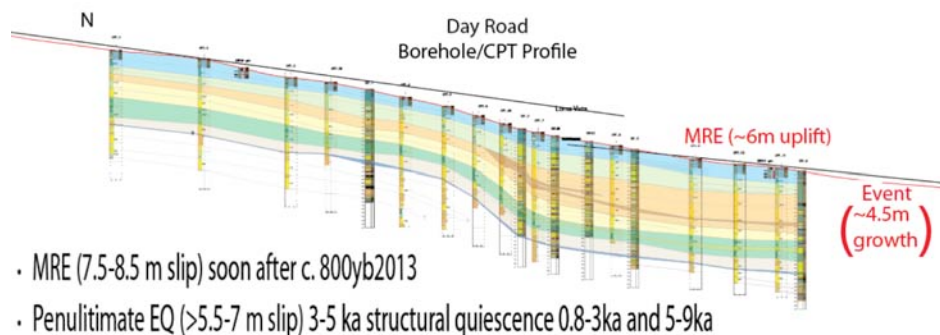


Figure 7. Comparison of growth strata above tip of Ventura fault at Day Road and Brookshire Avenue, from Grenader, Dolan et al.

High-Resolution Topography

Efforts within the SCEC Geology group continue to advance exciting frontiers of high-resolution topography. The VISES-SCEC Workshop on High-Resolution Topography held in Tokyo, Japan in September, 2013, led to a fruitful collaboration and analysis of two Japanese dip-slip earthquakes with pre- and post-event airborne lidar scans. Nissen et al. (in press) describes three-dimensional displacement fields from these events that are quite smooth within 100m of the surface rupture (Figure 8). Structure from Motion (SfM) is a low-cost three-dimensional imaging technique using photographs of the features taken from multiple distances and orientations ("the motion"). The scene "structure" is computed from the matched features in the images and is the best 3D model explaining their relative positions. Newly published results from Johnson et al. (2014) show that SfM topography compares well to terrestrial lidar scans of the 1992 Landers earthquake rupture. The low cost and ease of collection of SfM data will revolutionize post-earthquake geologic studies by digitally preserving ephemeral offset features as 3D models.

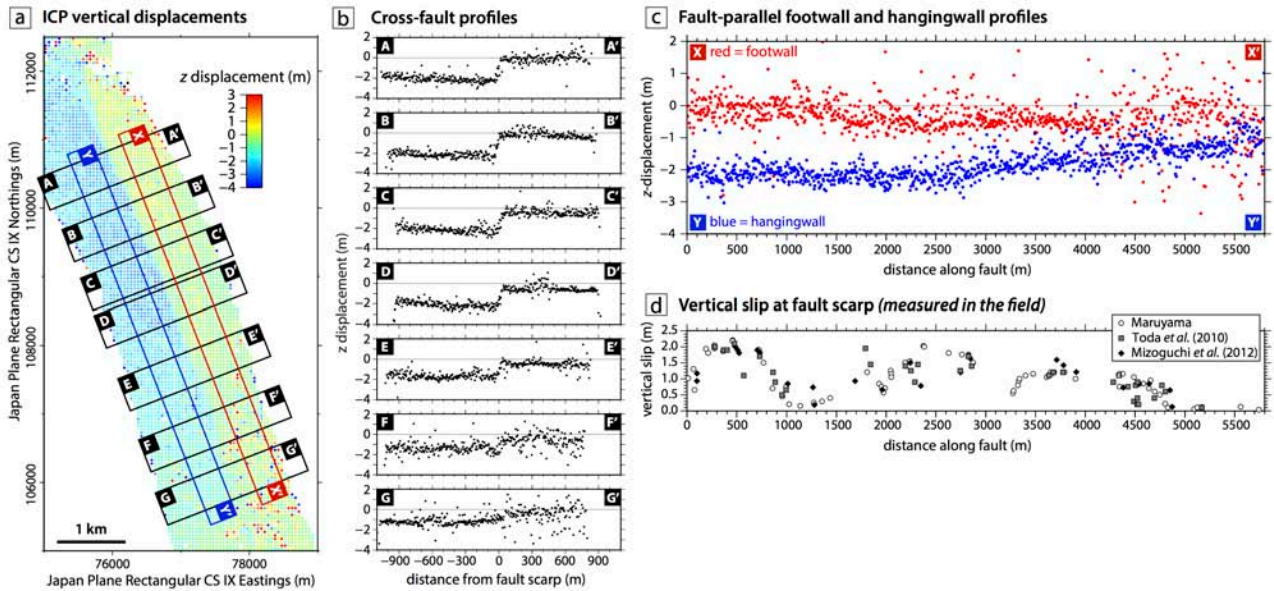


Figure 8. Differential lidar results from the 2011 Fukushima (normal-faulting) earthquake, from Nissen et al. in press.

High-Resolution Topography

SCEC-sponsored research in the eastern California shear zone and the Garlock fault continues to press forward on the related problems of geologic-geodetic slip-rate discrepancy and temporal variation of strain release across fault systems. Fieldwork by Dolan, McAuliffe, et al., coupled with advances in optically stimulated luminescence dating by Rhodes et al., clearly reveal slip-rate variation via earthquake clustering on the Garlock fault. Similar clustering behavior has been inferred for the dextral faults of the eastern California shear zone, although new results from the Panamint Valley fault by McAuliffe et al. (2013) suggest this behavior is more complex than simple alternation with the activity of the Garlock fault. An important component of this problem is the discrepancy between geologic and geodetic slip rates in eastern California, which may be in large part due to unaccounted distributed deformation surrounding active faults (e.g. Dolan and Haravitch, 2014). Modeling of the eastern California shear zone by Herbert et al. (2014a) suggests that substantial slip is lost to distributed deformation around fault tips embedded within the Mojave block (see also Herbert et al., 2014b). Figure 9 shows new modeling by Grette and Cooke, using structural data from Selander and Oskin, that shows how newly documented active reverse faulting in the eastern California shear zone contributes to this distributed deformation by causing uplift and focussing strain at fault intersections and terminations.

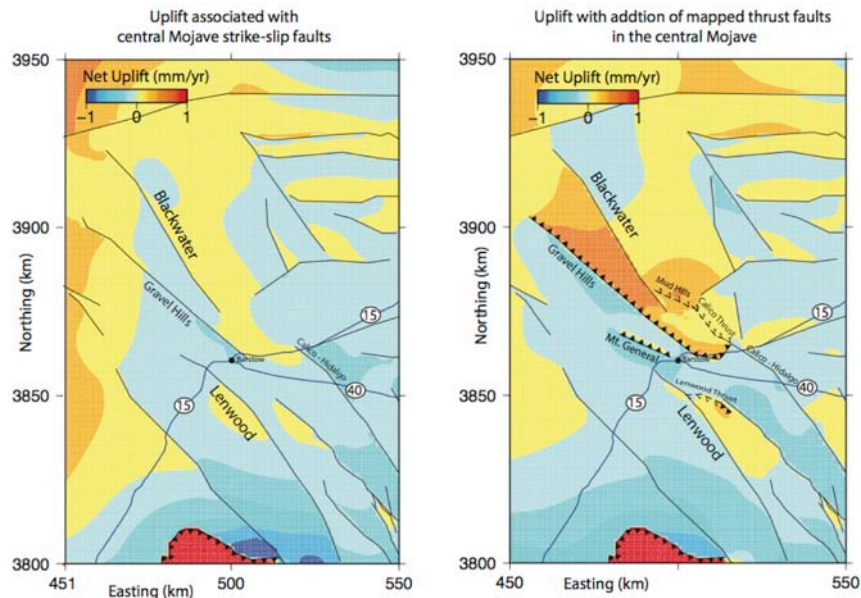


Figure 9. Distributed deformation model of the eastern California shear zone predicts zones of uplift and subsidence, from Grette and Cooke. Select Publications

RESEARCH ACCOMPLISHMENTS

Select Publications

- Dolan, James F., and Ben D. Haravitch., 2014 “How Well Do Surface Slip Measurements Track Slip at Depth in Large Strike-Slip Earthquakes? The Importance of Fault Structural Maturity in Controlling on-Fault Slip versus off-Fault Surface Deformation.” *Earth and Planetary Science Letters* 388 (February 15, 2014): 38–47. doi:10.1016/j.epsl.2013.11.043.
- Herbert, J. W., M. L. Cooke, M. Oskin, and O. Difo., 2014a, “How Much Can off-Fault Deformation Contribute to the Slip Rate Discrepancy within the Eastern California Shear Zone?” *Geology* 42, no. 1 (January 1, 2014): 71–75. doi:10.1130/G34738.1.
- Herbert, Justin W., Michele L. Cooke, and Scott T. Marshall., 2014b, “Influence of Fault Connectivity on Slip Rates in Southern California: Potential Impact on Discrepancies between Geodetic Derived and Geologic Slip Rates: Slip Rate Discrepancies in Southern CA.” *Journal of Geophysical Research: Solid Earth* 119, no. 3 (March 2014): 2342–61. doi:10.1002/2013JB010472.
- Hubbard, J., J. H. Shaw, J. Dolan, T. L. Pratt, L. McAuliffe, and T. K. Rockwell., 2014, “Structure and Seismic Hazard of the Ventura Avenue Anticline and Ventura Fault, California: Prospect for Large, Multisegment Ruptures in the Western Transverse Ranges.” *Bulletin of the Seismological Society of America*, May 6, 2014. doi:10.1785/0120130125.
- Johnson, K., Nissen, E., Saripalli, S., Arrowsmith, J R., McGarey, P., Scharer, K., Williams, P., Blisniuk, K. (2014). Rapid mapping of ultra-fine fault zone topography with Structure from Motion, *Geosphere*, 10 (5), 1–18, doi:10.1130/GES01017.1.
- McAuliffe, Lee J., James F. Dolan, Eric Kirby, Chris Rollins, Ben Haravitch, Steve Alm, and Tammy M. Rittenour., 2013, “Paleoseismology of the Southern Panamint Valley Fault: Implications for Regional Earthquake Occurrence and Seismic Hazard in Southern California” *Journal of Geophysical Research: Solid Earth* 118, no. 9 (September 2013): 5126–46. doi:10.1002/jgrb.50359.
- Nissen, E., Maruyama, T., Arrowsmith, J R., Elliott, J. R., Krishnan, A. K., Oskin, M. E., Saripalli, S. (in press). Coseismic fault zone deformation revealed with differential LiDAR: examples from Japanese Mw 7 intraplate earthquakes. *Earth and Planetary Science Letters*, in press.

Computational Science

The Computational Science Disciplinary Group promotes the use of advanced numerical modeling techniques and high performance computing (HPC) to address the emerging needs of SCEC users and application community on HPC platforms.

This past year’s accomplishments include:

1. Incorporation of new physics into SCEC HPC codes (near-fault and near-surface plasticity and frequency dependent attenuation), and novel user-driven validation studies.
2. Integration of the CyberShake, High-F, and F3DT platforms, as well as a community IO library, into the SEISM framework.
3. Enabling CyberShake workflow automation on NCSA Blue Waters that reduced the makespan of a CyberShake14.2 study from 1467 to 342 hours.
4. Updated basin structures in CVM-S4.26 that correlate strongly with gravity anomalies and major faults in southern California, and validation of the 3D CVMs up to 4 Hz for the M5.4 2008 Chino Hills earthquake, and the M5.1 2014 La Habra earthquake.
5. Development of the Broadband and Unified Community Velocity Model (UCVM) platforms.
6. Development and optimization of GPU-based HPC codes, including AWP-ODC (6.5x speedup on XK7 node compared to XE6), Hercules-GPU, and a matched filter technique to perform massive scale earthquake detections in Southern California.
7. Development of computationally efficient boundary element solvers for quasi-dynamic earthquake simulations.

Advanced Physics of Earthquake Processes

Producing realistic seismograms at high frequencies will require several improvements in anelastic wave propagation engines, including the implementation of nonlinear material behavior. Nonlinear material behavior has been implemented in both CPU- and GPU-based versions of AWP-ODC. Our results on its effect of the 2008 M 7.8 ShakeOut earthquake scenario have shown that nonlinear material behavior could reduce these predictions by as much as 70% compared to the linear viscoelastic solutions. The computational work carried out this year suggests that improvements in the modeling of the physics of the source and wave propagation, together with a more accurate definition of the crustal seismic velocity and geotechnical models, leads us to accurately reproduce earthquake effects at higher frequencies.

Recent earthquake simulations suggest that the shorter wavelengths at high frequencies will require significant changes to existing 3D velocity models. Although we have fine-scale local measures of velocities (down to meter scales) at boreholes, there is not sufficient density of such samples to facilitate the development of a deterministic regional model at the resolution levels required for high-frequency simulations. In order to better resolve near-surface small-scale amplification effect -- typical of soft-soil deposits in sedimentary basins -- material heterogeneities in the models can be incorporating as spatially

correlated random perturbations into velocity models and their effects on regional-scale simulations analyzed. Results in this area by Withers et al. (2013) show that material fine-scale heterogeneities may have a significant effect on the ground motion, especially at high frequencies (> 2 Hz), but also at low frequencies. They are currently pursuing various alternatives to incorporate fine-scale irregularities into material models based on statistical characteristics observed in the raw data extracted from well logs.

The quality of ground motion simulations at higher frequencies depends more strongly on the attenuation structure of the medium than previous, lower-frequency, simulations. In past simulations, SCEC researchers have used different (viscoelastic) models to represent the internal friction of the material. These models are typically expressed in terms of the inverse quality factor, $1/Q$, defined at a certain reference frequency, f_0 . Measurements of $1/Q$ in California and elsewhere show that $1/Q$ is roughly constant below about 1 Hz, but decreases rapidly at higher frequencies. The value of $1/Q$ has usually been expressed as functionals of the local S- and P-wave velocities using empirical rules. The attenuation structure of the upper crust, however, is highly heterogeneous and poorly known. Furthermore, recent investigations (Wang & Jordan, 2014) show that we will need to develop attenuation models that are also depth-dependent. We have investigated these issues and improved existing new attenuation models using simulations with various Q models, independently or in association with the seismic velocity models (CVMs), including adjustments of the attenuation structure when the small-scale heterogeneities are incorporated (Withers et al., 2013).

Development of SEISM Framework

High-level and middle-level scientific software elements developed by SCEC have been integrated into the SEISM framework, a software ecosystem for physics-based seismic hazard analysis. The components include CyberShake, High-F, F3DT, Broadband platforms, and a community IO library. SEISM support the use of petascale computers to generate and manage the large suites of earthquake simulations needed for physics-based PSHA, as well as advanced basic research on rupture dynamics, anelastic wave scattering, and Earth structure.

We have implemented algorithms that allow us to generate large-scale heterogeneous 3D models using SCEC's Unified Community Velocity Model (UCVM) software. We have used SCEC's Broadband Platform tools to validate simulation results against actual data, such as from the La Habra earthquake, and calibrate these perturbations for use in realistic earthquake simulation.

A test version of SEISM-IO has been developed to manage the IO requirements of the petascale earthquake simulations. SEISM-IO is built on top of the available high-performance IO libraries consisting of MPI-IO, ADIOS, HDF5 and PnetCDF. The users only need to determine and communicate with API through the abstract data space. Both Fortran and interfaces have been completed and tested using the wave propagation AWP-ODC solver against validated modeling results and observed data on multiple systems, including Blue Waters and XSEDE Stampede systems. SEISM-IO demonstrated a comparable I/O rate to manually optimized I/O performance of AWP-ODC up to 32,768 cores on Blue Waters XE6 nodes (Poyraz et al., 2014).

Development of accelerated HPC codes

We have developed Hercules-GPU, an octree-based parallel finite element (FE) earthquake simulator, using CUDA/MPI. The stiffness contributions, attenuation contributions of the BKT model, and the displacement updates have been implemented entirely on the accelerator using the CUDA SDK. Hercules-GPU computes, at runtime, the optimum kernel launch parameter configuration for the current compute capability. The software also supports an arbitrary number of GPU devices per compute node, and utilizes a simple load balancing scheme to assign each host CPU to a GPU device on the compute node. The GPU implementation has been validated against well observed earthquakes that combines Broadband platform, UCVM and High-F platforms. The Hercules GPU was validated against the La Habra earthquake using multiple velocity models including CVM-S4.26 on Titan. The largest production problem size tested thus far was a 1 Hz simulation of the 2008 Chino Hills earthquake, with attenuation (BKT damping) enabled, using 128 Titan XK7 GPU nodes. This represents a high level of agreement and validates the GPU approach. The acceleration ratio of the GPU implementation with respect to the CPU is of a factor of about 2.5x.

Another development of GPU-based code is to perform massive scale earthquake detections in Southern California following the 2010 Mw7.2 El Mayor-Cucapah earthquake.

Computationally efficient boundary element solvers for quasi-dynamic earthquake simulations

Andrew Bradley developed two open-source software packages (available at [1]) that greatly improve the efficiency of quasi-dynamic earthquake simulations. H-matrix compression permits Boundary Element calculations relating fault slip and traction on N elements in $O(N)$, rather than $O(N^2)$, time. The second package allows the same speed-up with non-uniform meshing, as required when frictional properties or fault normal stress are non-uniform, without sacrificing accuracy. As an illustration of the power of the numerical methods a simulation is given at [2]. One snapshot in time is shown in Figure 15. The simulation shows a slow slip event propagating bilaterally through a field of randomly distributed circular asperities, providing a possible explanation for tremor that accompanies slow slip events. Each asperity is resolved with about 14 elements along the diameter. The entire simulation includes roughly one million elements, and was run on a single desktop computer.

RESEARCH ACCOMPLISHMENTS

Numerical methods for seismic wave propagation and rupture dynamics in complex geometries

Future SCEC activities will require simulation of dynamic ruptures on geometrically complex, branching fault networks in 3D. This can be done most readily using unstructured meshes. Yet within the same simulation framework it is desirable to accurately capture wave propagation to far-field stations; this is best done with structured meshes. To simultaneously meet both objectives, Kozdon and Wilcox have developed a provably stable and high-order-accurate mesh coupling strategy for both finite difference and discontinuous Galerkin methods. Examples of coupled meshes are shown in Figure 16. Additionally, Kozdon and Wilcox are exploring the use of various local time stepping methodologies as well as emerging many-core (GPU) technologies to improve time-to-solution for large dynamic rupture simulations.

Supercomputing Activities

In 2014 SCEC was granted a record allocation of 500 million core-hours (SUs) on NSF and DOE supercomputers including NCSA Blue Waters, XSEDE and DOE INCITE systems. These allocations support 1) Improvement of the resolution of dynamic rupture simulations by an order of magnitude and investigation of the effects of realistic friction laws, geologic heterogeneity, and near-fault stress states on seismic radiation; 2) Extending deterministic simulations of strong ground motions to 10 Hz for investigating the upper frequency limit of deterministic ground-motion prediction; and 3) Computing PSHA maps and validate those using seismic and paleo-seismic data.

A significant accomplishment this year was to enable the CyberShake14.2 calculations on Blue Waters at NCSA. The reduced makespan of this CyberShake study, from 1467 to 342 hours, was a notable performance enhancement for the calculation of the hazard maps using four models, including the new community velocity model CVM-S4.26. The CyberShake workflow software stack, including the Pegasus Workflow Management System (Pegasus-WMS, which includes Condor DAGMan), HTCondor, and Globus GRAM, with Pegasus-MPI-Cluster successfully mitigated to Blue Waters this year. The advanced workflow tools handle data management efficiently, and automatically transfer many terabytes of data from supercomputer centers to SCEC storage. Furthermore, the SGT computing efficiency enhancement has made possible to increase the CyberShake simulation frequency up to 1.0 Hz, a few sites of such calculations have been successfully completed on OLCF Titan recently.

Select Publications

- Taborda, R. and Bielak, J. (2014). Ground-Motion Simulation and Validation of the 2008 Chino Hills, California, Earthquake Using Different Velocity Models. *Bulletin of the Seismological Society of America*. Submitted for publication.
- Roten, D., K.B. Olsen, S.M. Day, Y. Cui and D. Faeh, Expected seismic shaking in Los Angeles reduced by San Andreas fault zone plasticity, *Geophysical Research Letters*, 41, No. 8, 2769-2777, doi:10.1002/2014GL059411, 2014.
- Xu, H., Y. Cui, J.H. Dieterich, K. Richards-Dinger, E. Poyraz, D.J. Choi (2014), Aftershock sequence simulations using synthetic earthquakes and rate-state seismicity formulation, *Earthquake Science*, pp. 1-10, July, 2014.
- Poyraz, E., H. Xu, and Y. Cui (2014), Application-specific I/O optimizations on petascale supercomputers, *Procedia Computer Science* vol. 29, pp. 910-923, 2014.
- Cui, Y., E. Poyraz, K.B. Olsen, J. Zhou, K. Withers, S. Callaghan, J. Larkin, C. Guest, D. Choi, A. Chourasia, Z. Shi, S.M. Day, P.J. Maechling, T.H. Jordan (2013), Physics-based seismic hazard analysis on petascale heterogeneous supercomputers, SC13, Denver, CO, November 18-21, 2013.
- Chourasia, A., Cui, Y., Poyraz, E., Olsen, K., Zhou, J., Withers, K., Callaghan, S., Larkin, J., Guest, C., Choi, D., A., Shi, Z., Day, S., Maechling, P. and Jordan, Visualization Of Deterministic High-Frequency Ground Motions From Simulations Of Dynamic Rupture Along Rough Faults With And Without Medium Heterogeneity Using Petascale Heterogeneous Supercomputers, SC2013 Visualization Showcase, Denver, Nov 17-22, 2013.
- Scheitlin, T., Domingo, P., Olsen, K., Sarvan, W., Cui, Y., Poyraz, E., Maechling, P. and Jordan, T., Simulated Wave Propagation for the Mw5.4 Chino Hills, CA, Earthquake, Including a Statistical Model of Small-Scale Heterogeneities, SC2013 Visualization Showcase, Denver, Nov 17-22, 2013.
- Isbiliroglu, Y., Taborda, R., and Bielak, J. (2013). Coupled soil-structure interaction effects of building clusters during earthquakes. *Earthquake Spectra*. In review.
- Cui, Y., Poyraz, E., Olsen, K., Zhou, J., Withers, K., Callaghan, S., Larkin, J., Guest, C., Choi, D., Chourasia, A., Shi, Z., Day, S., Maechling, P. and Jordan, T. (2013), Physics-based Seismic Hazard Analysis on Petascale Heterogeneous Supercomputers, SC13, Denver, Nov 17-22.
- Shi, Z., and S.M. Day (2013), Rupture dynamics and ground motion from 3-D rough-fault simulations, *J. of Geophys. Res.: Solid Earth*, Vol, 118, 1-20, doi:10.1002/jgrb.50094.
- Cui, Y., Poyraz, E., Callaghan, S., Maechling, P., Chen, P. and Jordan, T. (2013), Accelerating CyberShake Calculations on XE6/XX7 Platforms of Blue Waters, *Extreme Scaling Workshop 2013*, August 15-16, Boulder, 2013.
- Zhou, J., Y. Cui, E. Poyraz, D. Choi, and C. Guest (2013), Multi-GPU implementation of a 3D finite difference time domain earthquake code on heterogeneous supercomputers, *Proceedings of International Conference on Computational Science*, Vol. 18, 1255-1264, Elsevier, ICCS 2013, Barcelona, June 5-7.
- Callaghan, S., P. Maechling, K. Vahi, G., Juve, E. Deelman, Y. Cui, E. Poyraz, T. H. Jordan (2013), Running A Seismic Workflow Application on Distributed Resources, SC13, Poster, Denver, Nov 17-22.

Lee, E., H. Huang, J. M. Dennis, P. Chen and L. Wang (2013), An optimized parallel LSQR algorithm for seismic tomography. *Computers & Geosciences*, 61, 184-197.

Lee, E. and P. Chen (2013), Automating seismic waveform analysis for full 3-D waveform inversions, *Geophysical Journal International*, doi: 10.1093/gji/ggt124.

Meng, X. and Z. Peng (2014), Seismicity rate changes in the San Jacinto Fault Zone and the Salton Sea Geothermal Field following the 2010 Mw7.2 El Mayor-Cucapah Earthquake, *Geophys. J. Int.*, 197(3), 1750-1762, doi: 10.1093/gji/ggu085.

Bradley, A. M. (2014), Software for efficient static dislocation-traction calculations in fault simulators, *Seismological Research Letters*, in press.

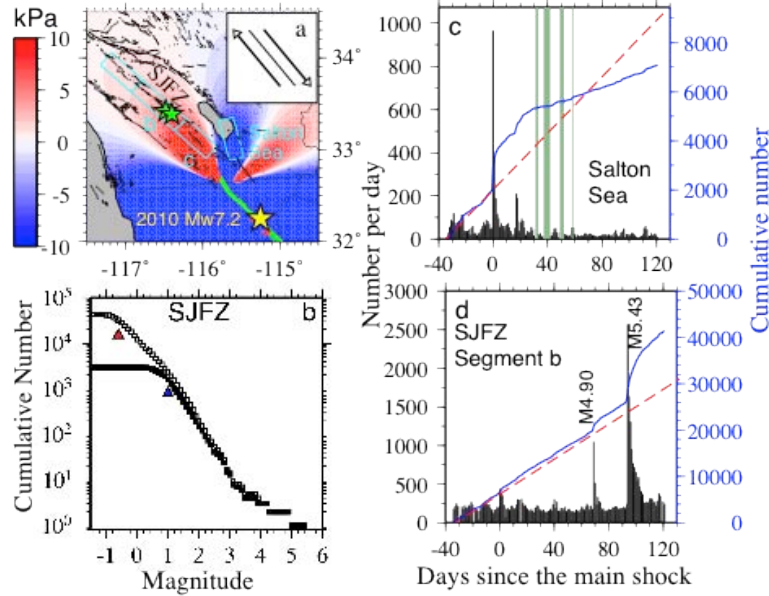


Figure 10. (a) Static Coulomb stress changes in southern California following the 2010 Mw7.2 El Mayor-Cucapah earthquake. (b) The frequency-magnitude relationships in the San Jacinto Fault Zone (SJFZ). The open and black squares denote the newly detected events and those in the original SCEC catalog, respectively. The triangles denote the magnitude of completeness M_c . (c) The seismicity rate changes in Salton Sea showing a short-time increase and long-term decrease following the main shock. (d) The seismicity rate changes in Segment b of the SJFZ showing both short-term and long-term increase following the main shock. After Meng and Peng (2014).

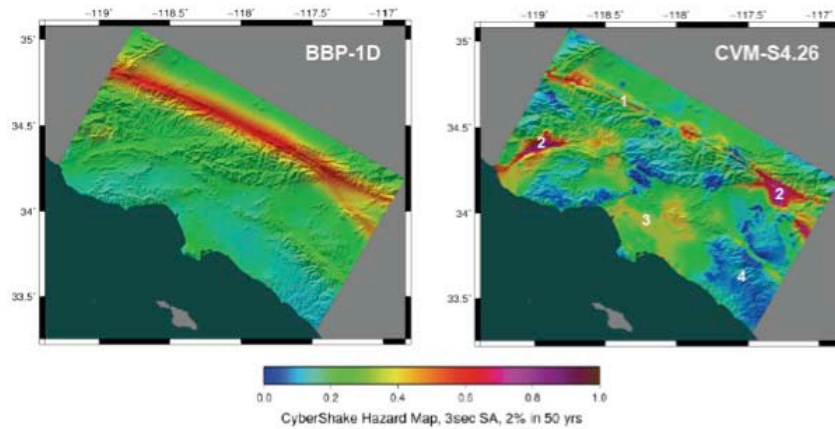


Figure 11. Comparison of two seismic hazard models for the Los Angeles region from CyberShake Study 14.2, completed in early March, 2014. The left panel is based on an average 1D model, and the right panel is based on the F3dT-refined structure CVM-S4.26. The 3D model shows important amplitude differences from the 1D model, several of which are annotated on the right panel: (1) lower near-fault intensities due to 3D scattering; (2) much higher intensities in near-fault basins due to directivity-basin coupling; (3) higher intensities in the Los Angeles basins; and (4) lower intensities in hard-rock areas. The maps are computed for 3-s response spectra at an exceedance probability of 2% in 50 years. Both models include all fault ruptures in the Uniform California Earthquake Rupture Forecast, version 2 (UCERF2), and each comprises about 240 million seismograms.

RESEARCH ACCOMPLISHMENTS

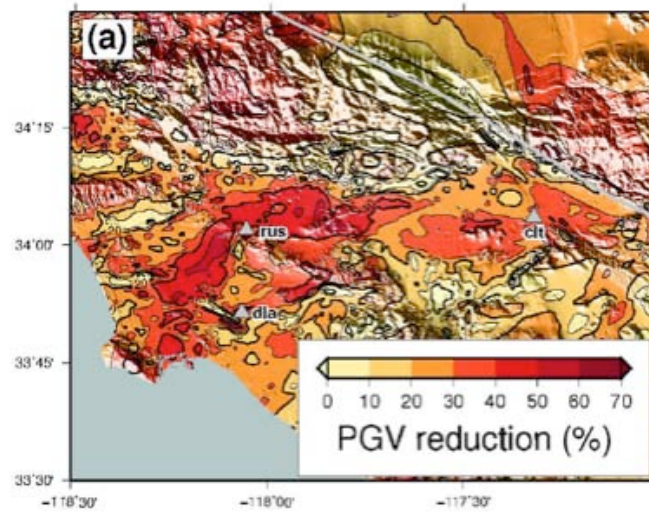


Figure 12. Reduction in horizontal peak ground velocities (%) obtained for one nonlinear simulation of the ShakeOut scenario by Roten et al. (2014). The comparison is relative to a linear anelastic solution, which shows reductions up to 70% in peak ground velocity (PGV).

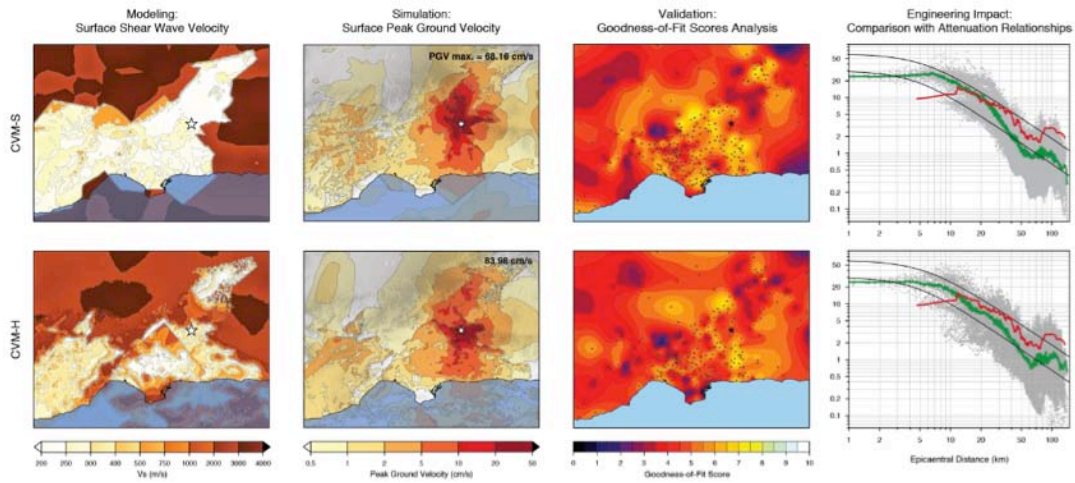


Figure 13. Summary results for simulations for the Mw 5.4 2008 Chino Hills earthquake (star) using different velocity models, CVM-S (top row) and CVM-H (bottom row), that connects geoscience modeling to engineering applications. Columns show (1) surface shear wave velocities for each model; (2) peak horizontal ground velocities; (3) goodness-of-fit metrics comparing synthetics with data at >300 recording stations (lighter colors indicate better fit); and (4) comparison with attenuation relationships used by engineers to estimate peak ground velocity. Red line is the average observed value from Chino Hills; two black lines are upper and lower bound of then empirical relationships, and the green line shows the average surface values from the simulation (gray point cloud). Simulations were done using the Hercules code by Taborda and Bielak (2013, 2014).

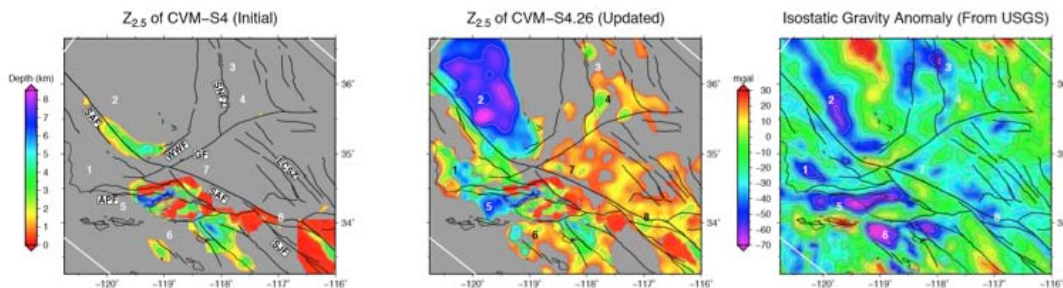


Figure 14. The imaged basins in CVM-S4.26 highly consistent with independent isostatic gravity anomaly. The figure shows the Z_{2.5}, which refers to the depth of Vs=2.5 km/s, maps for CVM-S4 and CVM-S4.26 and the isostatic gravity anomaly - strong correlation with active faults that separate the basins in Southern California. The basin structures, which were not well represented in the initial model of CVM-S4, are numbered as: (1) Santa Maria Basin, (2) Southern San Joaquin Basin (SSJB), (3) Owens Valley (OV), (4) Indian Wells Valley (IWV), (5) Santa Barbara Channel (SBC), (6) Santa Monica Basin, (7) Antelope Valley (AV), and (8) San Bernardino Basin (SBB).

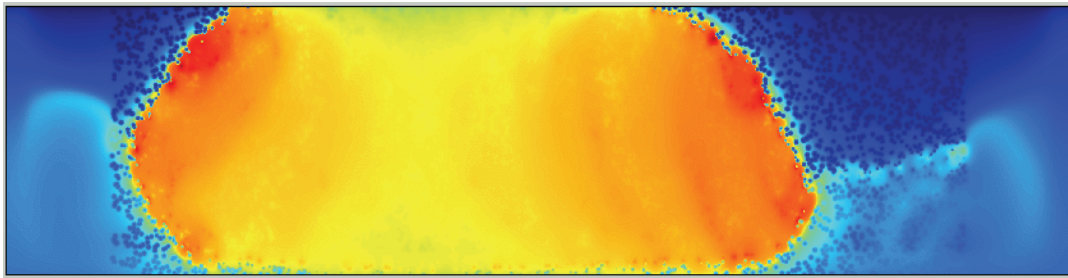


Figure 15. Bradley and Segall quasi-dynamic boundary element simulation of slow slip event, with tremor and low frequency earthquakes occurring as small, randomly distributed asperities rupture. Computational advances permit such simulations, involving roughly one million elements, to be run on a single desktop computer. Plot shows $\log_{10}(\text{slip speed})$ on a fault plane. In addition to generating tremor, the asperity failures produce coherent, back-propagating creep waves. We will be exploring this before more in the future to test ideas relevant to propagating episodic tremor and slip.

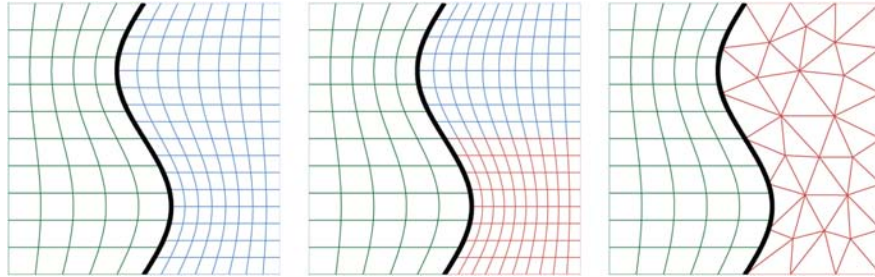


Figure 16. Three examples of new mesh couplings supported by a provably stable method developed by Kozdon and Wilcox. (While illustrated here in 2D, the method is implemented in 3D.) In addition to allowing the coupling of arbitrary finite difference meshes, their coupling supports the connection of high-order finite difference methods and unstructured discontinuous Galerkin methods. These developments will help support the dynamic rupture simulation of realistic networks of faults with unstructured grid methods being used around the complex geometry and structured grids being used to propagate waves for long distances.

Unified Structural Representation (USR)

The Unified Structural Representation (USR) Focus Area develops models of crust and upper mantle structure in California for use in a wide range of SCEC science, including strong ground-motion prediction, earthquake hazards assessment, and fault systems analysis. These efforts include the development of Community Velocity Models (CVM-S, CVM-SI, & CVM-H) and Community Fault Models (CFM, CFM-R, SCFM), which together comprise a USR. In partnership with other working groups in SCEC, the USR Focus Area also helps support the evaluation and improvement of these models through ground motions simulations, 3D waveform tomography, earthquake relocations, and fault systems modeling.

This past year's accomplishments include:

1. Release of CFM (5.0) that includes additional sources and refined segmentation with more precise segment linkages based on Qfault traces and relocated earthquake and focal mechanism catalogs (e.g., Yang et al., 2012; Hauksson et al., 2012), and updated 3D geometry for the San Geronio Pass and Ventura SFSA regions;
2. Modeler-ready fault meshes for the Ventura SFSA with improvements to the Oak Ridge and Ventura faults, consistent topology at fault intersections, and a uniform 2 km resolution;
3. Further development of a new version of the SCEC Community Velocity Model (CVM-SI), following 26 perturbations to the existing model (CVM-S) as a result of iterative inversion simulations by Lee et al (2014);
4. a new 3-D seismic velocity model for the San Joaquin basin with plans to develop a Sacramento basin model, thereby providing a complete representation of the Central Valley structure in CVM-H; and
5. analysis of variations in ground motions for M7.8 ShakeOut simulations in alternative 3-D seismic velocity models (CVM-S4, CVM-SI23, and CMV-H11.9.0).

CFM 5.0

This past year SCEC developed a new release of the Community Fault Model (CFM) for southern California. CFM version 5.0 includes a number of major improvements, including the refinement of fault geometries using the USGS Quaternary Fault and Fold Database (Qfault) traces and relocated seismicity catalogs (Yang et al., 2012; Hauksson et al., 2012), as well as the addition of new fault representations. CFM 5.0 provides a comprehensive suite of improved fault representations in the Santa Maria and Ventura basins, Santa Barbara Channel, Inner Continental Borderlands, Eastern Transverse Ranges, Peninsular Ranges, San Geronio Pass area, and the Mojave Desert region. New fault representations were generated using Qfault

RESEARCH ACCOMPLISHMENTS

traces, relocated hypocenters, and focal mechanisms, as well as seismic reflection and well data, where available. This resulted in fault representations that more precise, and often more highly segmented than in previous model versions. In addition, CFM 5.0 includes the addition of several faults that were not represented in previous model versions. CFM 5 also features a revised naming system that is compatible with the USGS Qfault database, and a selection of preferred fault alternatives based on measures such as fit to Qfault traces or earthquake locations as well as structural and tectonic considerations. In related efforts, Scott Marshall and the USR development team have generated a suite of simplified, more regular meshes for CFM faults that are intended to help modelers more readily incorporate these representations into their studies.

3.5.2 CVM's

SCEC has made strides in improving the Community Velocity Models for southern California, both through 3D tomographic inversions and the development of new basin models. Lee et al., (2014) applied full-3-D tomography (F3DT) based on a combination of the scattering-integral method (SI-F3DT) and the adjoint-wavefield method (AW-F3DT) to CVM version 4.0 (CVM-S4). More than half-a-million misfit measurements made on about 38,000 earthquake seismograms and 12,000 ambient-noise correlograms have been assimilated into our inversion. After 26 F3DT iterations, synthetic seismograms computed using our latest model, CVM-S4.26, show substantially better fit to observed seismograms at frequencies below 0.2 Hz than those computed using our 3-D starting model CVM-S4. CVM-S4.26 has also revealed strong crustal heterogeneities throughout Southern California that are not represented in previous model versions. These improvements provide insights into the crustal structure of southern California, and will help to improve earthquake simulations at low frequencies.

In addition, we developed a new structural velocity model for the San Joaquin basin in California using tens of thousands of direct velocity measurements from well logs, seismic reflection, and geologic constraints. Carl Tape has incorporated this model into SCEC CVM-H 11.9, and generated simulations for San Andreas ruptures that show strong amplification and resonance in the new basin structure. This basin model will be embedded into future versions of the SCEC CVM's, helping to enhance wave propagation simulations.

ShakeOut Simulations in Alternative CVMs

Robert Graves is conducting an analysis of the ground motions for the M7.8 ShakeOut scenario earthquake using three SCEC CVMs (CVM-S4, CVM-Si23, and CVM-H11.9.0). Along the San Andreas fault, the general pattern is similar for all three models with strong rupture directivity towards the northwest. Other features are present in some models but not all. For example, both CVM-S4 and CVM-Si23 show strong amplification in San Bernardino, whereas CVM-H11.9.0 shows only modest amplification. On the other hand, both CVM-Si23 and CVM-H11.9.0 show strong amplification in the area north of San Fernando (Santa Clarita-Fillmore basin), but this feature is not present in CVM-S4. The Los Angeles basin region shows very strong amplification for CVM-S4 with PGV exceeding 50 cm/s throughout most of the basin, and reaching nearly 200 cm/s in the Whitter-Narrows region connecting the San Gabriel and LA basins. The level of amplification is noticeably lower in CVM-Si23, and it is significantly lower in CVM-H11.9.0.

Select Publications

- Lee, E.-J., P. Chen, T. H. Jordan, P. B. Maechling, M. A. M. Denolle, and G. C. Beroza (2014), Full-3-D tomography for crustal structure in Southern California based on the scattering-integral and the adjoint-wavefield methods, *J. Geophys. Res. Solid Earth*, 119, doi:10.1002/2014JB011346.
- Shaw, J. H., A. Plesch, C. Tape, M. P. Suess, T. Jordan, G. Ely, E. Hauksson, J. Tromp, T. Tanimoto, R. Graves, K. Olsen, C. Nicholson, P. Maechling, C. Rivero, P. Lovely, C. M. Brankman, and J. Munster, 2014, Unified Structural Representation of the southern California crust and upper mantle, *Earth & Planetary Science Letters*, (in review).

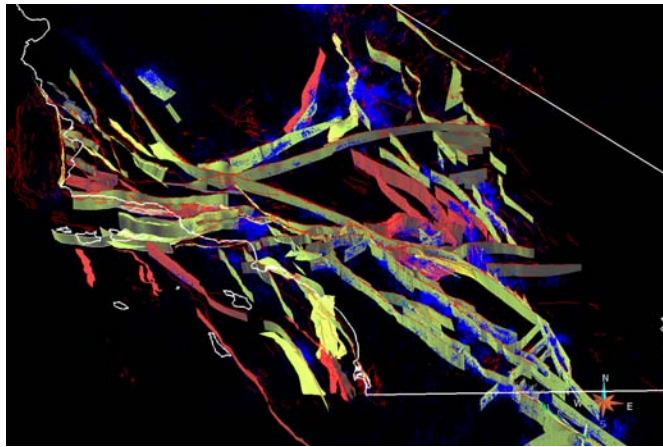


Figure 17. New release of CFM (5.0) that includes additional sources and refined versions of faults based on Qfault traces and relocated earthquake and focal mechanism catalogs (e.g., Yang et al., 2012; Hauksson et al., 2012). Faults in red are new representations; others are refined using Qfault traces and seismicity.

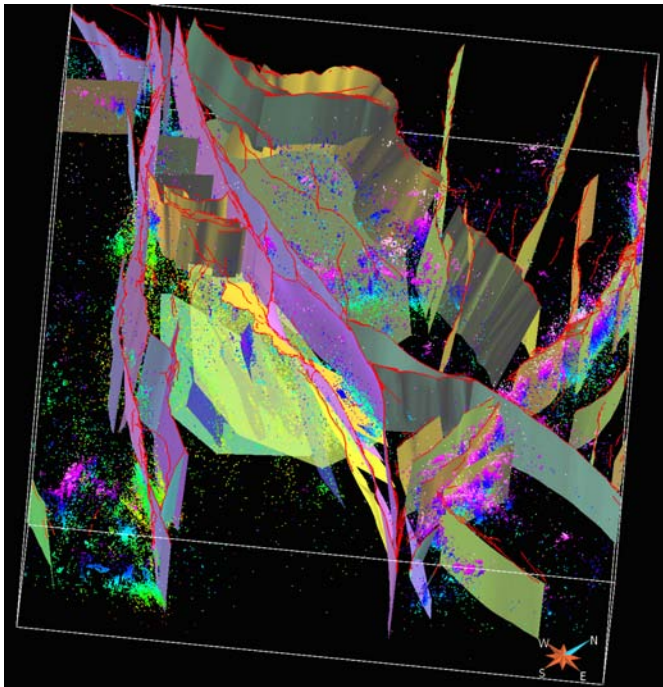


Figure 18. USR CFM5.0 San Geronio Pass Updated fault geometry in CFM5.0 for the San Geronio Pass SFSA region.

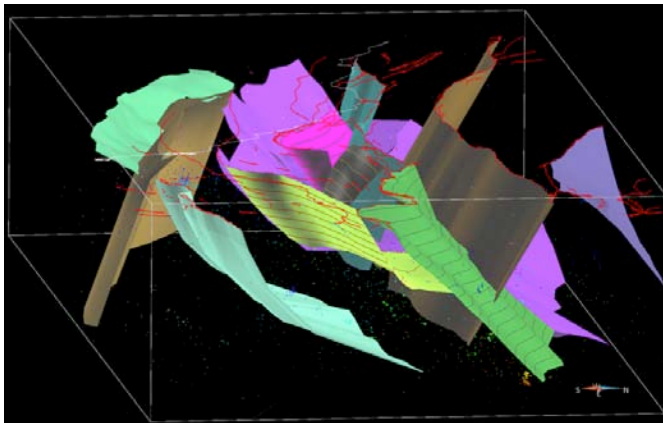


Figure 19. USR CFM5.0 Ventura Updated fault geometry in CFM5.0 for the Ventura SFSA region.

RESEARCH ACCOMPLISHMENTS

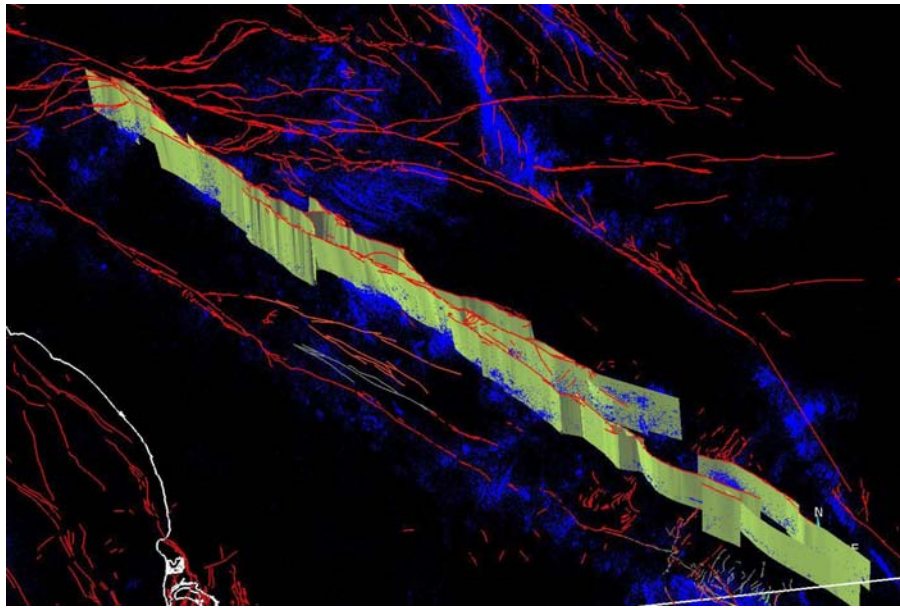


Figure 20. USR CFM5.0 San Jacinto Fault Updated San Jacinto in CFM5.0 illustrating refined geometry with more precise segment linkages based on Qfault traces and seismicity.

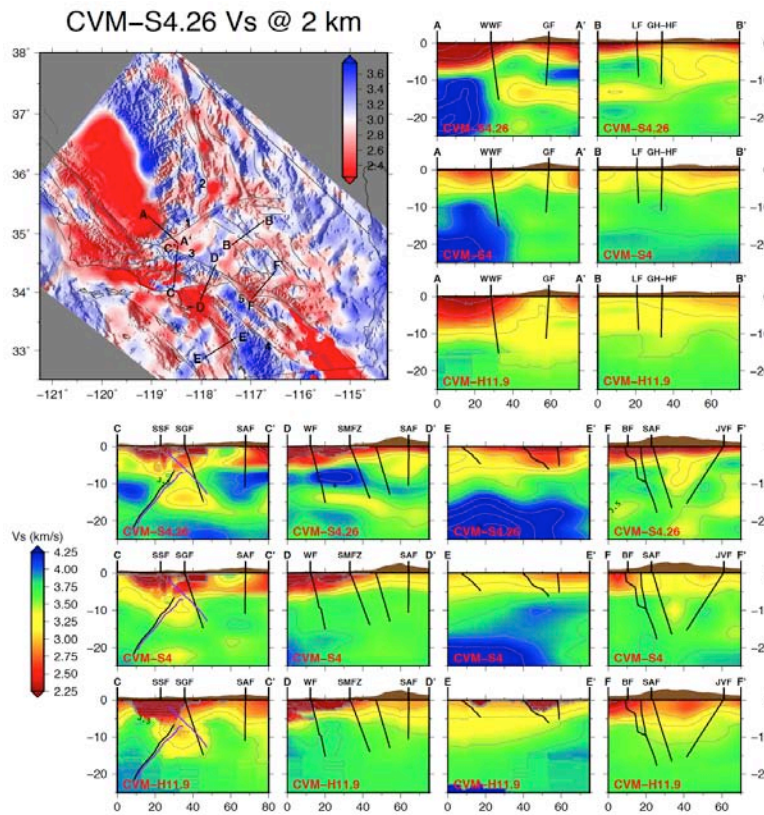


Figure 21. USR CVMSI-4.26 Vs at 2 km depth in CVMSI-4.26 and comparison of cross-sections across various faults from CVM-S4, CVM-H11.9, and CVM-SI4.26.

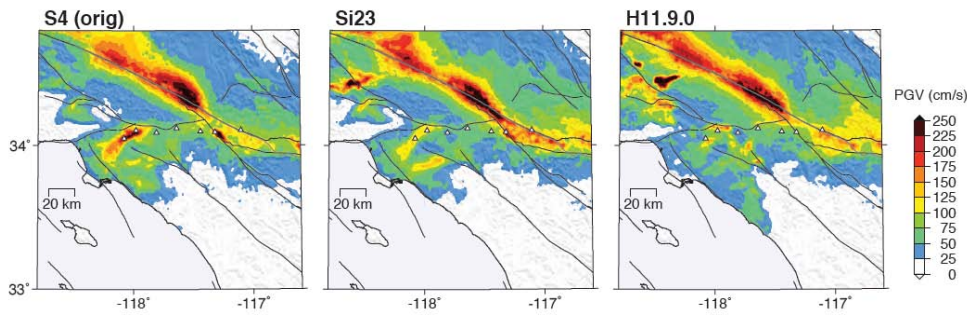


Figure 22. USR ShakeOut ground motion comparison Panels below show peak ground velocity simulated for the three alternative CVMs. The plot at left (CVM-S4) is the original ShakeOut result from Graves et al (2008). The middle panel uses the CVM-Si23 update to CVM-S4 and the right panel is from CVM-H11.9.0. The Los Angeles basin region shows very strong amplification for CVM-S4 with PGV exceeding 50 cm/s throughout most of the basin, and reaching nearly 200 cm/s in the Whittier-Narrows region connecting the San Gabriel and LA basins. The level of amplification is noticeably lower in CVM-Si23, and it is significantly lower in CVM-H11.9.0.

Fault and Rupture Mechanics (FARM)

The Fault and Rupture Mechanics (FARM) interdisciplinary group focuses on understanding earthquake rupture mechanics through a combination of theoretical modeling, laboratory experiments and field observations. The results from research in FARM are closely linked to efforts in the SDOT, UCERF, and CSM programs (among others) in SCEC4. Improvements in computational capabilities are making it possible to more properly model dynamic rupture propagation on geometrically realistic fault structures. Similarly, technical advances in experimental and analytical equipment are opening up new opportunities for investigating the earthquake deformation processes during quasi-static and dynamic conditions in both laboratory and natural fault samples. Progress in this area remains diverse and projects are numerous; however, several themes remain at the forefront as we look forward to SCEC5

Material and Geometrical Heterogeneity

Considerable effort has been focused on how heterogeneous fault stress and fault structure (e.g., roughness and larger scale fault segmentation) influence seismicity and rupture propagation. Several studies have explored the role of fault roughness on earthquake processes. For example, new calculations indicate that supershear ruptures are actually more likely on rough faults than smooth faults (Bruhat, Fang and Dunham), an effect opposite of conventional wisdom (Figure 23). The role of fault roughness on the distribution of seismicity has been investigated in laboratory experiments by Becker, Sammis and Dresen, who found that the power-law exponent that describes the decay of AE density with distance from the primary slip surface depends on fault roughness, as well as normal stress. Similar studies have explored the origin and effect of off-fault damage on dynamic rupture; Ben-Zion and colleagues investigated the links between the dynamic generation of a low-velocity damage zone and rupture dynamics – including the effects of bi-material interfaces. The role of fault structure on inelastic, “off-fault” deformation has been studied in idealized scenarios (e.g., Kang and Duan), in addition to focused regional studies of the San Jacinto fault zone (Ben-Zion). New models also show the limitations of modeling multi-strand fault surfaces with a single fault surface (Shaw et al.).

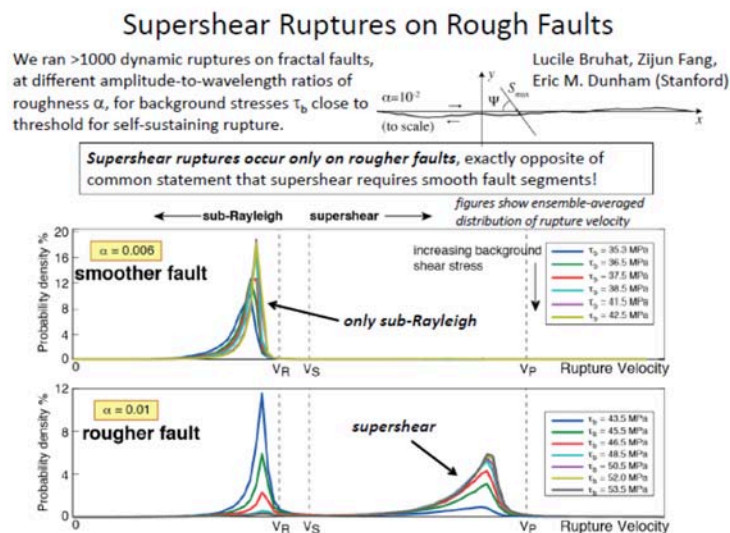


Figure 23. Supershear rupture on rough faults.

RESEARCH ACCOMPLISHMENTS

Stress Heterogeneity

The level of background stress, stress heterogeneity, and heterogeneity of fault zone properties influence both rupture propagation and the distribution of aftershocks. For example, Shi has illustrated through 3D modeling of the San Gorgonio Pass fault system that a through-going rupture is more likely for a non-uniform/stochastic initial fault stress than if the regional stress is uniform (Figure 24). The spatial distribution of frictional properties on the fault zone have been explored to understand the earthquake nucleation process (Viesca and Ray), the depth and timing of seismicity and creep on the Superstition Hills Fault (Wei et al.), and the mechanics of repeating earthquake sequences (Liu and Lapusta). These studies illustrate how observations of seismicity can be used to constrain the frictional properties of faults, which can then be included into integrative earthquake cycle and rupture models and relationships between seismicity and geodetic data.

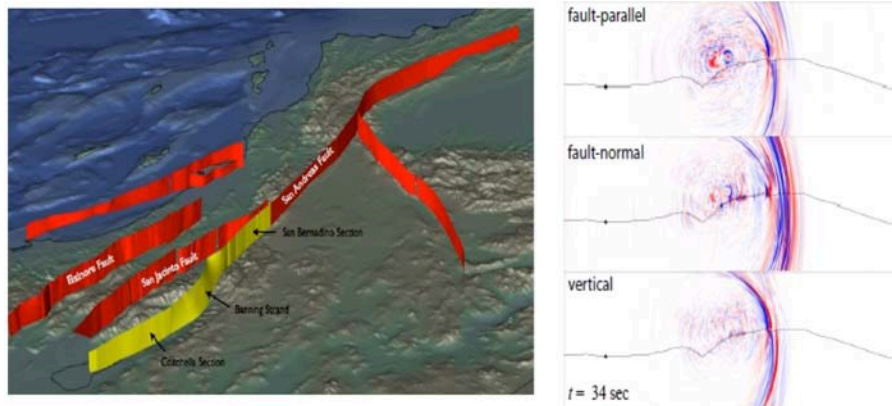


Figure 24. 3D numerical modeling of dynamic rupture along the San Gorgonio Pass section of the San Andreas Fault, to assess the plausibility of through-going ruptures. The dynamic rupture scenarios based on CFM-v4 fault geometry. Through-going rupture is more likely with stochastically variable, rather than uniform, initial stress.

The Deep Roots of Faults

Understanding rupture processes at the base of the seismogenic zone remains critical for evaluating the potential for large events in Southern California. These properties have been studied by incorporating more realistic (i.e., thermally activated power law creep) lower crustal fault rheologies into earthquake cycle models. Lapusta and Jiang illustrate how the history of such ruptures may be identified by a lack of microseismicity at the base of the seismogenic zone (Figure 25). Physically realistic models of lower crustal viscous deformation have also been used to constrain the spatial and temporal evolution of post-seismic creep; these models provide a way to estimate stress magnitudes at the base of the seismogenic zone and the mechanics of stress transfer from plate motion to mature fault zones (Fialko). New experimental data on viscous creep behavior at conditions appropriate for the base of the seismogenic zone provide new insights into the mechanisms responsible for strain localization and potentially slow earthquake instability (Rogers-Martinez, Sammis et al.). In addition, several studies have continued to investigate the slip and deformation behavior of the deeper and/or higher temperature regions of fault zones based on a combination of geodetic (San Jacinto Fault; Lindsey et al), and analyses of seismic velocity (Brawley sequence, Helmberger; Parkfield, Thurber).

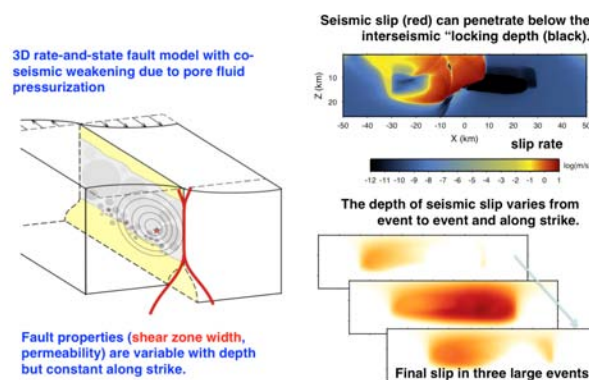


Figure 25. The seismogenic depth is typically defined based on microseismicity or inferences of the locking depth. These simulations show that seismic slip in large events can penetrate deeper. They consider a 3D elastic bulk with 2D rate-and-state fault in which a rate-weakening region is surrounded by rate-strengthening fault areas. The fault has depth-variable shear zone width (shown in red) and permeability that increases with depth. The extent of seismic slip in the model is determined by where thermal pressurization stops being efficient, and not by the rate-and-state transition between weakening and strengthening. The efficiency of thermal pressurization depends on the competition between the shear-zone width and permeability as well as on the slip rate and slip of dynamic rupture itself. As a result, seismic slip can penetrate below the traditionally defined seismogenic depth. The depth extent of large seismic events varies both along the strike and in time, from one event to another.

Mechanisms of Dynamic Weakening

Dynamic weakening mechanisms continue to be the focus of experimental, theoretical and geological studies. Platt, Viesca and Garagash solved for steady slip pulses propagating at a constant rupture velocity with dynamic weakening driven by thermal pressurization and thermal decomposition. When the reaction is accounted for there can be multiple ways to propagate a rupture; slip pulses dominated by thermal decomposition have a distinctive slip rate profile, with peak slip rates near the trailing edge of the rupture. Schmitt and Segall compare how flash heating and thermal pressurization influence earthquake nucleation and rupture on faults with low background stress. Both dynamic weakening mechanisms are capable of propelling dynamic rupture, which nucleate within regions with either high shear stress or low effective normal stress, into regions of low shear stress. These calculations also suggest that thermal pressurization is required to explain the observed relationship between fracture energy and slip. New laboratory experiments have also been performed to characterize the processes responsible for flash weakening in gouge (Proctor et al.) and thermal pressurization (Figure 26, Goldsby & Tullis). SCEC activities have provided synergy between analysis of these new data and the physical models for dynamic weakening (Platt et al.). In addition, the role of thermally activated contact processes has now been included into STZ models of gouge deformation (Carlson and colleagues). These theoretical studies provide new insights into the physical processes responsible for dynamic weakening, and rationale for their inclusion into earthquake cycle and rupture models. Further tests on the impact of dynamic weakening on natural faults is presaged by the calibration of new fault slip thermometers and wattmeters (Figure 27) that incorporate analyses of thermally induced changes in organic compounds within fault gouge (Savage and Polissar).

FARM continues to provide a platform for the incorporation of these processes into earthquake rupture models – and motivate analyses to improve models of earthquake physics and ground motion.

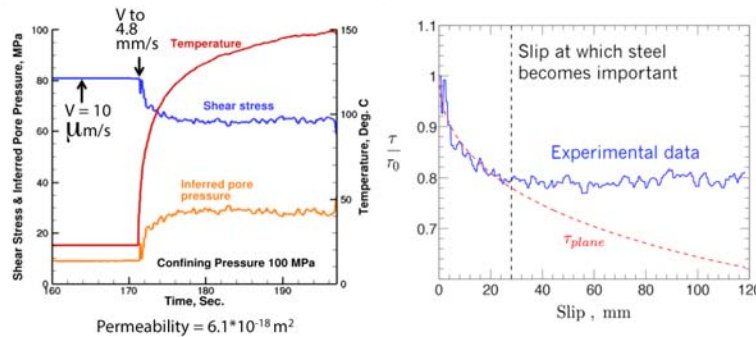


Figure 26. Left, from Goldsby and Tullis, shows observed reduction in strength and of inferred increase in pore-fluid pressure for diabase experiment upon a velocity step increase, assuming that all changes of shear stress were due to changes in fluid pressure, i.e., assuming the effective stress law holds for the experiment and friction coefficient is unchanged. (The permeability is too low to measure pore pressure directly.) Inferred temperatures calculated using our FEM model are also shown in the data plot. Right shows fit of the initial part of the shear stress decay to equation B19 of Rice [2006] that predicts the decay of shear stress τ from its initial value τ_0 in the case of slip on a plane. Although the theoretical prediction continues to decline, after about 28 mm of slip the experimental data level out, which we infer is due to the steel sample grip preventing the temperature from rising as it would for the rock half-space assumed by the analysis of Rice [2006]. The right half of the figure is courtesy of John Platt of Harvard, and shows estimate of the slip at which the steel becomes important, estimated from diabase thermal properties and the distance from the fault to the steel.

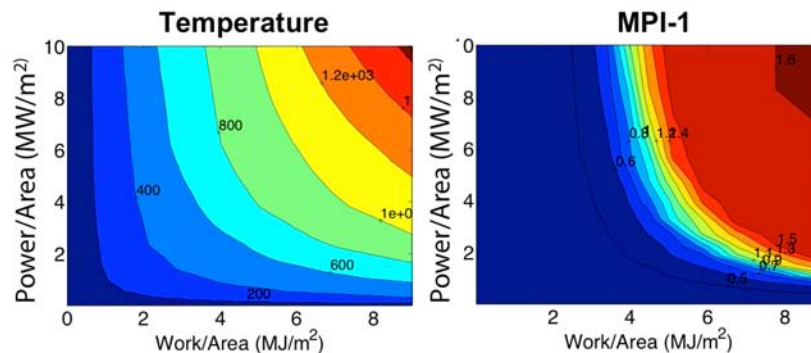


Figure 27. Calibration of organic maturation to temperature in fault zones. The plot on the left is temperature rise during fault slip on a 1 mm thick fault surface as a function of power and work. The plot on the right is the change in the methylphenanthrene maturity index (MPI-1) for the same conditions. We see that the MPI-1 index is a powerful tool for determining temperature rise on faults within the range of about 500-800 C. Calibration of MPI-1 under earthquake conditions was accomplished through a suite of rapid heating experiments at the LDEO rock mechanics lab.

RESEARCH ACCOMPLISHMENTS

Southern San Andreas Fault Evaluation (SoSAFE)

In 2014, advances in SoSAFE research objectives were achieved in the publication of important papers on San Andreas and San Jacinto paleoseismology and development of new paleoseismic studies on these faults. Several new geologic studies in San Gorgonio Pass are fomenting new investigation into strain patterns across this complex system.

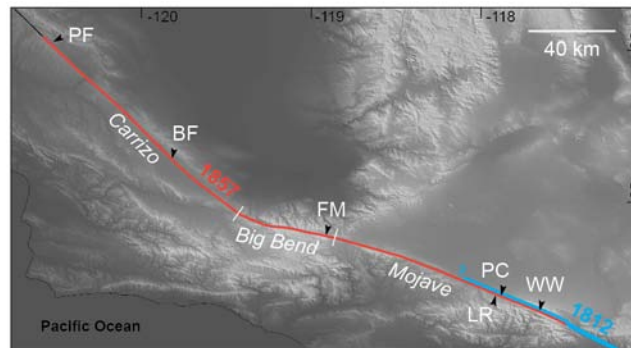


Figure 28. Paleoseismic sites on the 1857 rupture of the San Andreas Fault.

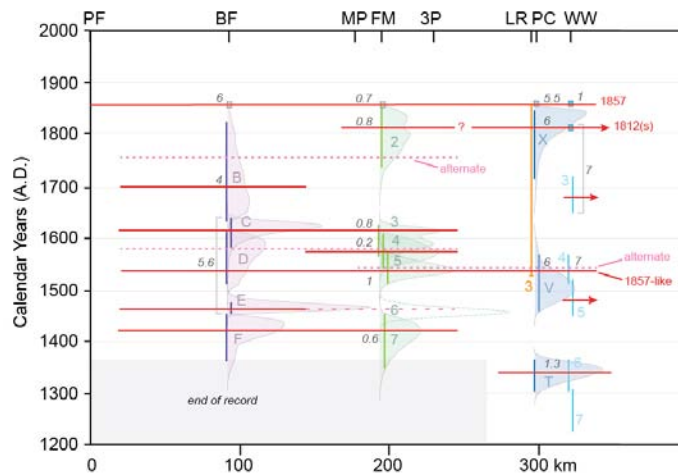


Figure 29. Rupture history on 1857 stretch of SAF.

Paleoseismic Studies

Work published on the Frazier Mountain paleoseismic site (Scharer et al., 2014; see Figures 28 and 29) proposes that ruptures as large as the M7.7-7.9 historic earthquake in 1857 are not the norm across the Carrizo, Big Bend and Mojave sections of the San Andreas Fault. Combining earthquake ages and paleo-displacements where available, at most 75% of the ruptures are less than 300 km long. Tests of this result are already underway at two paleoseismic sites located 50 km to either side of Frazier Mountain. The first is a new site at the southern end of the Carrizo (Akciz et al., 2014). Trenching there revealed active faulting is restricted to the east side of a wide sag pond, and dating of three paleoearthquakes is underway. The second is the Elizabeth Lake paleoseismic site, where work in 2014 established that four to five earthquakes have occurred there since 1200 A.D. (Bemis et al., 2014) In combination with excavations elsewhere at the site, the Elizabeth Lake paleoseismic record will provide important constraints on paleo-ruptures on the Mojave section for the last 1500 years.

On the San Jacinto fault, the Mystic Lake site now comprises a 2000 year record of paleoearthquakes. Onderdonk et al. (2014) show that large earthquakes in this period recur every 160-190 years on the Claremont fault, and that the longest interval was ~200 years. In comparison to the work by Rockwell et al. (2014) at the Hog Lake site on the Clark fault, it appears that most of the earthquakes are not correlative in time, suggesting that most ruptures do not jump the 4 km step between these strands.

Slip Rate Studies and Deformation in San Gorgonio Pass

Several slip rate studies focused in the San Gorgonio Pass Special Fault Study Area are leading to a possible revision of strain patterns across this complex region. On the Banning strand of the southern SAF, two new slip rate sites suggest a dramatic increase in slip rate, from <1.5 mm/yr at the eastern end (Blisniuk et al., 2013) to 11.1 +3.1/-3.3 mm/yr nearer to San Gorgonio Pass (Gold et al., 2014). This increase in the horizontal slip rate on the Banning strand is mirrored by an increase in

the vertical slip rate, which is being investigated with ^{10}Be catchment averaged erosion rates and slip rates across uplifted fans in the Indio Hills (Scharer et al., 2014). On the Mission Creek strand, new estimates from the Pushawalla location in the central Indio Hills overlap with the upper end of published estimates from Biskra Palms oasis (12-22 mm/yr, Behr et al., 2010), furthering interest in the location and amount of strain transferred across the Indio Hills.

In San Gorgonio Pass, several groups are investigating the rate of vertical uplift at several time scales. In trench exposures, slip per event across a narrow aperture of the fault is <1 m (Wolff et al., 2014), leading to a ~ 6000 year slip rate of only ~ 2 mm/yr. By contrast the rates from Millard Canyon appear to be much higher: a Holocene terrace is offset by two fault splays by ~ 4 m, and Plesitocene terrace surfaces are offset hundreds of meters (Heermance et al., 2014); new dating of these surfaces and resultant slip rates will be a major focus of the San Gorgonio Pass Workshop in 2014.

Improvements to the subsurface faults in the CFM in San Gorgonio Pass are also underway, including: blind, sub-parallel, en echelon oblique faults beneath SGP, a new model for the San Gorgonio Pass thrust and its relation to the North Palm Springs fault, new fault models for the Crafton Hills complex and other secondary cross faults, revised Pinto Mountain and Morongo Valley faults and their relation to the Mission Creek and Mill Creek faults, and newly defined detachment surfaces at mid and deep crustal levels beneath the San Jacinto and San Bernardino Mountains that dip towards and interact with the San Andreas fault in SGP (Nicholson et al., 2013; Plesch et al., 2014). This expanded CFM 3D fault set helps characterize a more complex fault geometry and pattern of fault interactions at depth than previously inferred from projecting near-surface data down-dip, or modeling GPS and potential field data alone.

Work is also ongoing to investigate dynamic rupture models in the Pass region and in parallel, developing an approach for estimating absolute stress from stressing rates produced by forward models. Using assumptions about recurrence interval and stress drop on ground-rupturing earthquakes, (i.e., those that would be observable in the paleoseismic record), it appears that fault interaction contributes to loading on faults through the San Gorgonio Pass (Cooke et al., 2014). Consequently, this approach may provide different initial conditions for dynamic rupture models than that derived by resolving the tectonic load on the fault surface.

Workshops

Two related workshops on high resolution topography were partially supported by SoSAFE (and by UNAVCO and OpenTopography). The first (also in collaboration with the VISES activity) was the VISES SCEC Workshop on High Resolution Topography Applied to Earthquake Studies (www.opentopography.org/index.php/resources/VISES_JPN13). It occurred mostly at ERI in Tokyo and had good participation from numerous Japanese colleagues. Several recommendations came from the workshop (see more at <http://activetectonics.blogspot.com/2013/11/workshop-on-high-resolution-topography.html>). Of relevance for SoSAFE, these include: a) There has been an interesting evolution of methodology for study of active faulting and topography. LiDAR has revolutionized many tasks and our ability to measure surface features at the fine scale at which the surface processes and earthquake deformation operate. b) Once faults are identified, reconstructing offset and deformed features is necessary. A combination of field and virtual approaches was advocated. Uncertainty assessment in the reconstructions is an active research area. c) A substantial emphasis has been on surface rupture characterization in high resolution topography acquired shortly after an earthquake. This effort includes airborne and terrestrial laser scanning data integration. Examination of tilted trees in the vegetation (Yoshimi) was a clever use of the three dimensional data to characterize surface deformation along the earthquake rupture. d) Topographic differencing along Japanese and the El Mayor Cucupah earthquake ruptures is yielding exciting results that seem to document variable continuity of slip along fault surfaces in the upper several hundred meters below the Earth surface. These results are complementary with the wide aperture INSAR results typically coming from earthquake studies. The various approaches for differencing (iterative closest point, image correlation, pixel matching, particle image velocimetry, etc.) should be systematically compared.

The second workshop (held in San Diego) was the third of a series supported by SCEC over the years: Imaging and Analyzing Southern California's Active Faults with Lidar (www.opentopography.org/index.php/resources/short_courses/13scec_course/ and activetectonics.blogspot.com/2013/11/imaging-and-analyzing-southern.html). It was well attended by SCEC scientists and many useful tutorials persist on the workshop web site.

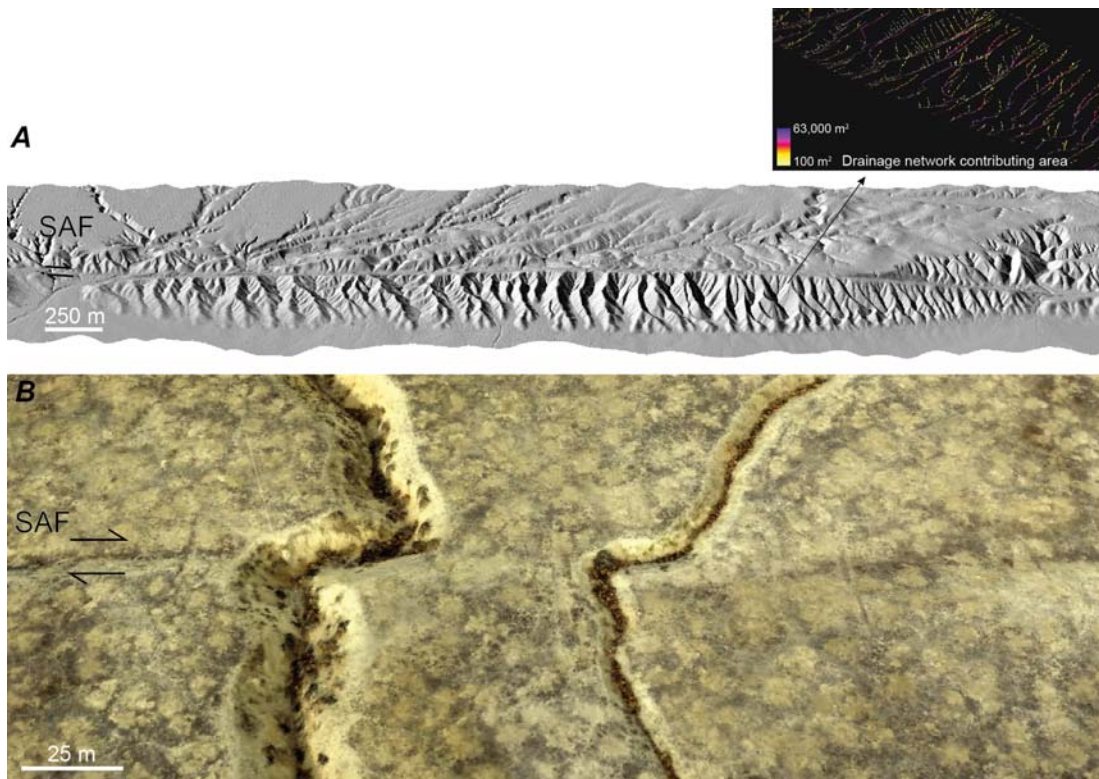


Figure 30. High resolution topography and evidence of recent activity along the south-central San Andreas Fault (SAF): methodology demonstrated at the SoSAFE/SCEC workshops (Arrowsmith, 2014). A) The Dragon's Back pressure ridge shows progressive landscape response to rock uplift and offset relative to a fixed uplift zone in the SE (Hilley and Arrowsmith, 2008). Inset shows drainage network in uplift zone. B) LiDAR topography processed at www.opentopography.org. B) Recent offsets along the SAF at Phelan Creeks. Image is from balloon aerial photography texture-mapped onto topographic model from Structure from Motion (Johnson, et al., 2014).

Select Publications

- Arrowsmith, J R., High resolution topography and active faulting, 2014, Conference paper for PATA Days 2014 - 5th International INQUA Meeting on Paleoseismology, Active Tectonics and Archeoseismology, Busan, Korea.
- Johnson, K., Nissen, E., Saripalli, S., Arrowsmith, J R., McGarey, P., Scharer, K., Williams, P., Blisniuk, K., 2014, Rapid mapping of ultra-fine fault zone topography with Structure from Motion, *Geosphere*, v. 10; no. 5; p. 1–18; doi:10.1130/GES01017.1.
- Rockwell, T., Dawson, T., Ben-Horin, J. Y., and Seitz, G., in press, A 21 event, 4,000-year history of surface ruptures in the Anza Seismic Gap, San Jacinto Fault: Implications for long-term earthquake production on a major plate boundary fault. Submitted to *Pure and Applied Geophysics*.
- Scharer, K., Weldon, R., Streig, A., Fumal, T., 2014, Paleoeathquakes at Frazier Mountain, California delimit extent and frequency of past San Andreas Fault ruptures along 1857 trace, *Geophysical Research Letters*, 41, 4527-4534.

Stress and Deformation Over Time (SDOT)

SDOT's focus is our understanding of the mechanical behavior and structure of the southern California lithosphere and mantle on interseismic and geological timescales to understand fault loading and the time-evolution and formation of plate boundary systems.

This past year's accomplishments include:

- Updating InSAR and GPS based geodetic data for the Ventura basin (Figure 31).
- Providing modeler-ready versions of the CFM fault meshes.
- Modeling long term slip rates on the Ventura fault system taking into account proposed fault geometry alternatives (Figure 32).
- Constructing a comprehensive mechanical model of crustal shortening, uplift, and fault slip rates for the Ventura basin (Figures 33 and 34).
- Improving fault slip rate estimates on the San Andreas and Eastern California Shear Zone faults based on new GPS velocity estimates from the San Bernardino Mountains and San Geronio Pass (Figures 35 and 36).

- Establishing and exploring a workflow for fault slip inversions based on geodesy in the presence of material heterogeneity (Figure 37).
- Estimating uncertainties in moment release and recurrence time estimates given geodetic data and mechanical models (Figure 38).
- Holding successful workshops for the Crustal Deformation and Community Stress Model communities.
- Joint analysis of stress inferred from focal mechanisms and seismic anisotropy from surface and body wave models (Figure 40).
- Coupling of a high resolution, lithospheric finite element model with traction estimates from global mantle circulation.

Ventura Basin Studies

As part of the Ventura SFSA effort, Scott Marshall and others have updated their work on geodetic data in the Ventura Basin area (Figure 31). This includes improved GPS error analysis and more complete InSAR coverage. Also Marshall et al. have tested new fault geometries for the Ventura fault using boundary element codes. They find that the assumed geometry for the fault has a significant influence on the inferred long-term fault slip rate (Figure 32). Kaj Johnson has constructed a kinematic plate flexure model for the western Transverse Ranges to estimate crustal shortening rates, interseismic and long-term uplift rates, and fault slip rates (Figures 33 and 34). This work shows that dipping faults in the western Transverse Ranges accommodate at least 12 mm/yr of reverse slip. The model shows 1-3 mm/yr of subsidence in the Ventura Basin and 1-3 mm/yr of present-day uplift of the Santa Ynez mountains, consistent with GPS observations (Figures 34).

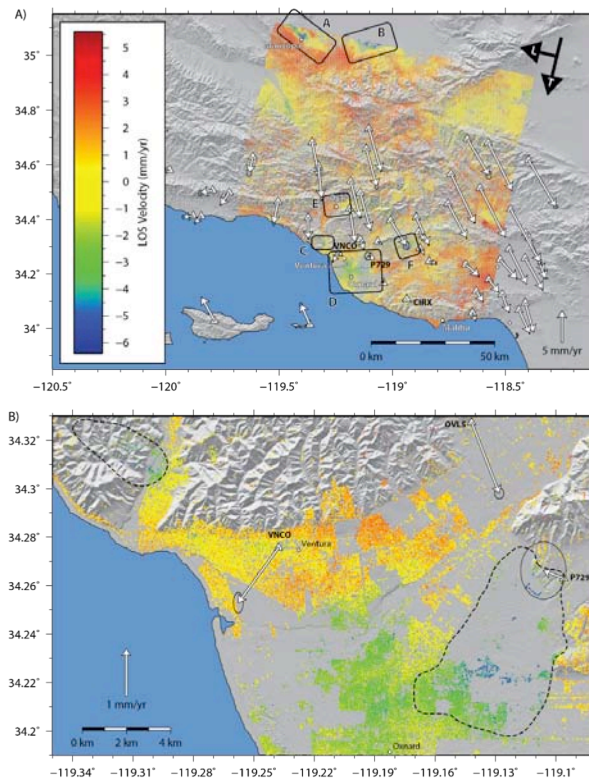


Figure 31. Improved, joint geodetic constraints from GPS and InSAR. Localized anthropogenic deformation is labeled (from work by Scott Marshall et al.).

RESEARCH ACCOMPLISHMENTS

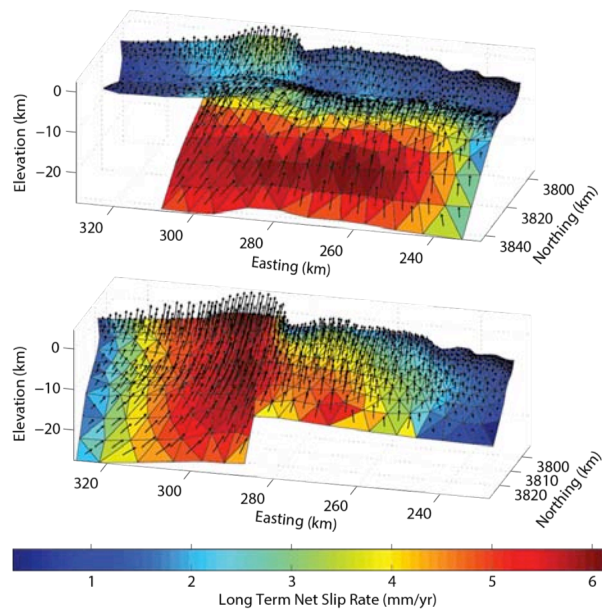


Figure 32. Long term slip rates on the Ventura Fault as predicted by mechanical models. Top shows a fault geometry including a ramp, bottom the Ventura fault with constant dip (from work by Scott Marshall et al.)

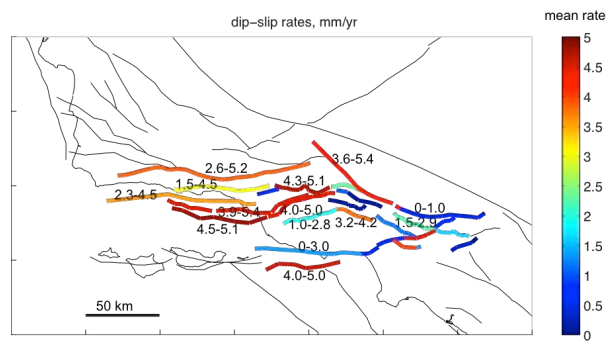


Figure 33. Estimated dip-slip rates on reverse faults in the western Transverse Ranges (from work by Kaj Johnson et al.)

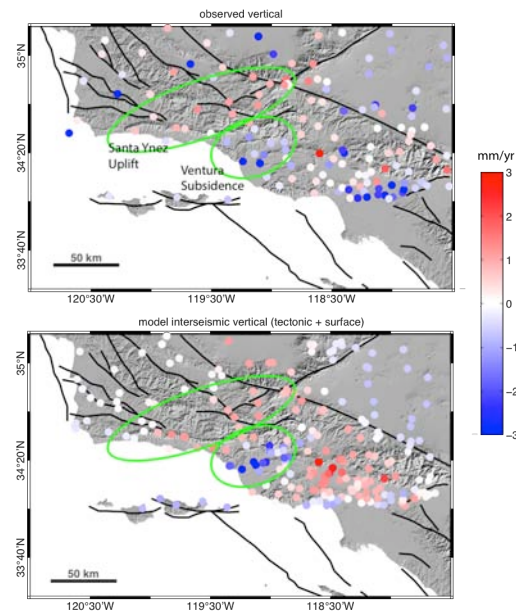


Figure 34. (Top) Observed vertical GPS velocities at continuous sites with long (>7 year) records. (Bottom) Model vertical rates. The model and observations both show 1-2 mm/yr of uplift in the Santa Ynez Mountains and north to the San Andreas fault. The model and observations show 1-3 mm/yr of subsidence of the Ventura Basin (from work by Kaj Johnson et al.)

Fault Slip Estimates from Geodetic Data

Sally McGill, Josh Spinler, and Rick Bennett have new GPS site velocities from the San Bernardino Mountains and San Gorgonio Pass areas (Figure 35) as well as results of 1D elastic modeling (Figure 36) across the plate boundary through the San Bernardino Mountains. They find from 1D modeling that the San Andreas is inferred to slip slower, and the Eastern California Shear Zone inferred to slip faster geodetically than geologic estimates.

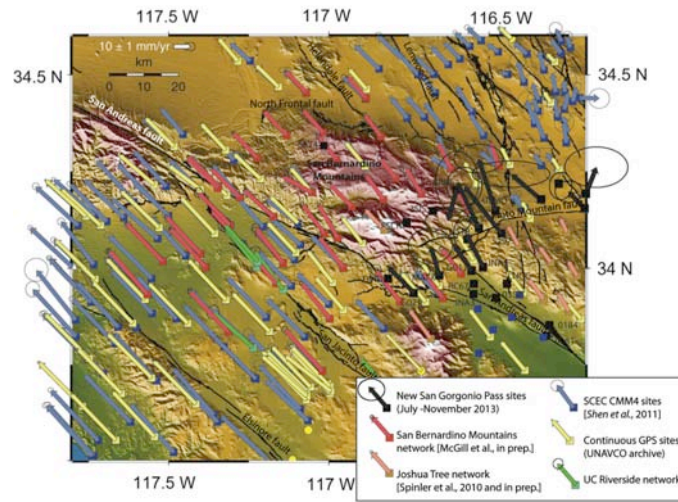


Figure 35. New GPS velocities from the San Bernardino Mountains and San Gorgonio Pass (from work by McGill et al.).

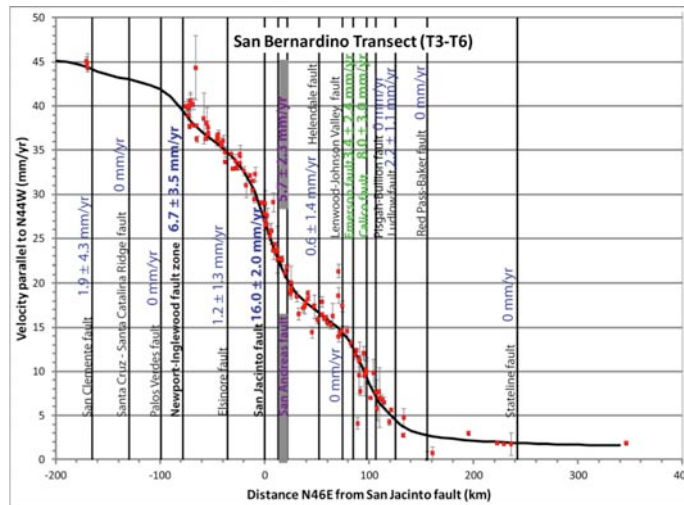


Figure 36. 1.5D elastic modeling inferred fault slip rates. Note how the San Andreas is inferred to slip slower, and the Eastern California Shear Zone inferred to slip faster geodetically than when inferred from geology (from work by McGill et al.).

Charles Williams is developing a framework to allow scientists to easily use FEM-generated Green’s functions for geodetic slip inversions. He has developed a workflow that allows scientists to use PyLith-generated GF with Rob McCaffrey’s DEFNODE inversion code. Figure 37 shows what happens when we include material properties from the New Zealand-wide seismic velocity model (Eberhart-Phillips et al., 2010) when inverting for slow slip along the Hikurangi subduction margin (the Manawatu event from September-December, 2010). Figure shows the difference in predicted slip between homogeneous and heterogeneous models. The homogeneous model requires about 40 mm more slip to match the observations, compared to the heterogeneous model and the seismic potency for the homogeneous model is about 23% larger than that for the heterogeneous model, which has important implications when trying to infer the portion of the slip budget accommodated by slow slip events.

Tom Herring and Mike Floyd have examined comparisons of modeled earthquake recurrence intervals and geodetic estimates based on balancing moment release rates obtained from synthetic experiments that use 1D elastic models. They find that the way in which we interpret and discuss locking depth estimated from geodetic data using a simple elastic dislocation model must be more carefully considered and, regardless of a debate over appropriate physical interpretation, a straightforward inversion and direct interpretation may introduce an error of up to about a factor of 2 on the estimate of recurrence interval (Figure 38).

RESEARCH ACCOMPLISHMENTS

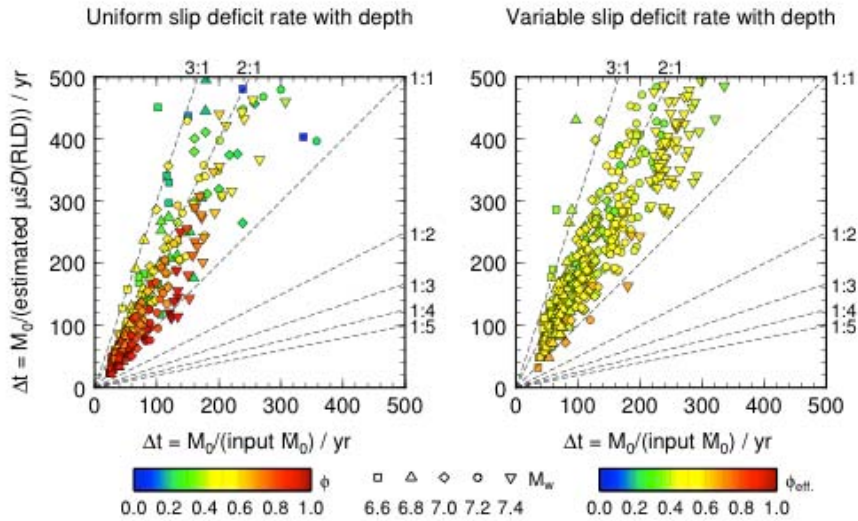


Figure 37. Difference between the inferred slip when using homogeneous or heterogeneous material properties from the New Zealand-wide seismic velocity model (Eberhart-Phillips et al., 2010) when inverting for slow slip along the Hikurangi subduction margin (Manawatu event from September-December, 2010). From work by Charles Williams et al.

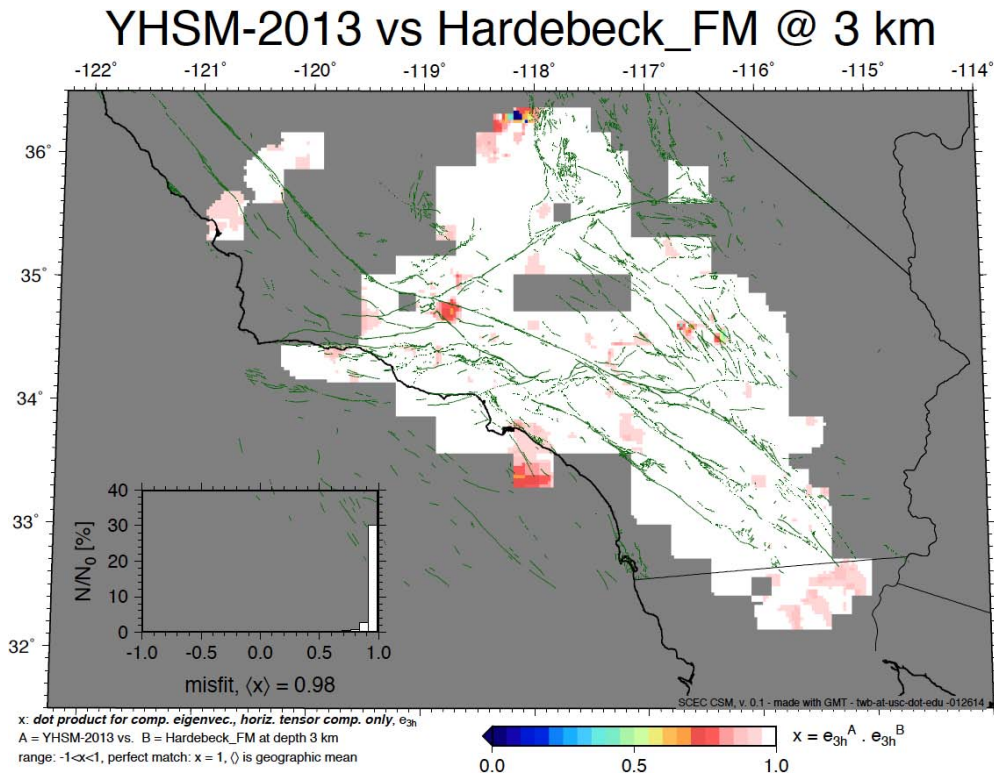


Figure 38. Estimated versus input recurrence times for various magnitudes of earthquake (symbol shape) and effective coupling coefficients (symbol color). The input recurrence time is the seismic moment of a given magnitude earthquake divided by the input moment deficit rate. The estimated recurrence time is the seismic moment divided by the moment deficit rate using the estimated fault slip rate and estimated locking.

Community Stress Model

The Community Stress Model community now has a completed web site with tools for inter-model comparisons and validation (Figure 39). A candidate release for a stress model based on focal mechanisms has been picked, the Yang and Hauksson (2013) model. See this [link to the SCEC CSM web page sceczero.usc.edu/projects/CSM]

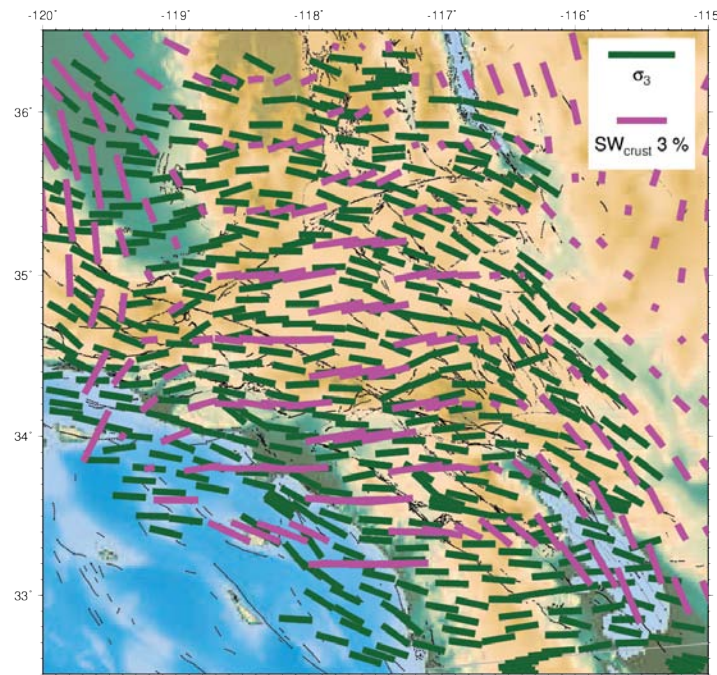


Figure 39. Most extensional stress from the model by Yang and Hauksson (2013) and fast seismic anisotropy orientations within the crust from Lin et al. (2011). From work by Meghan Miller and Thorsten Becker.

Select Publications

- Yang, W. and E. Hauksson, The tectonic crustal stress field and style of faulting along the Pacific North America Plate boundary in Southern California, *Geophys. J. Int.* (July, 2013) 194 (1): 100-117
- McGill et al., Improved GPS velocities for the San Bernardino Mountains and fault slip-rate modeling, Submitted to *JGR*, July 2014.
- Aagaard, B. T., M. G. Knepley, C. A. Williams, 'A Domain Decomposition Approach to Implementing Fault Slip in Finite-Element Models of Quasi-static and Dynamic Crustal Deformation', *Journal of Geophysical Research: Solid Earth*, 118, (2013): 3059–3079
- Crowell, B. W., Y. Bock, D. T. Sandwell, and Y. Fialko, 'Geodetic Investigation into the Deformation of the Salton Trough', *Journal of Geophysical Research: Solid Earth*, 118, (2013): 5030–5039
- Gonzalez-Ortega A., Sandwell D., Fialko Y., Nava A., Fletcher J., Gonzalez-Garcia J., Lipovsky B., Floyd M. and Funning G., 'El Mayor-Cucapah (Mw 7.2) earthquake: Early postseismic deformation from InSAR and GPS observations', *Journal of Geophysical Research*, 119, (2014):

Earthquake Forecasting and Predictability (EFP)

The Earthquake Forecasting and Predictability (EFP) group facilitates a range of studies aimed at improved data and methods for developing earthquake forecasting techniques and assessing earthquake predictability.

This past year's accomplishments include:

1. Development and analysis of high-quality earthquake catalogs with improved locations, magnitudes, focal mechanism, and stress drop information in southern California
2. A range of regional studies focused on the variability of the slip rate, improved estimations of stress drop and its spatio-temporal distribution, and fragile geologic features
3. Focused analysis of predictability in geothermal fields
4. In-depth analysis of seismic patterns with focus on aftershock/foreshock/swarm activity
5. Further development and validation of hybrid earthquake forecasting models within CSEP
6. Continuing work on comparison, validation, and verification of earthquake simulators

Earthquake Catalogs

Earthquake catalogs are the foundation for retrospective and prospective testing of earthquake forecast models, an integral part of forecast models based on spatial-temporal seismicity patterns, and an invaluable resource for hypothesis development. The instrumental earthquake catalog for southern California, which dates back to 1932, provides an important

RESEARCH ACCOMPLISHMENTS

basis for many forecasting and predictability studies. This year's work on the southern California instrumental catalog included study of the December 2012 M6.3 offshore earthquake. This earthquake occurred in the oceanic lithosphere, west of the continental shelf. This area was previously considered to be aseismic, and the occurrence of the 2012 earthquake suggests that the Pacific- North America plate boundary possibly extends 400-500 km to the west of the San Andreas fault system, including plate boundary deformation across the entire Continental Borderland and into the eastern edge of the oceanic Pacific plate (Hauksson et al, 2014).

Focused Regional Studies

Earthquake recurrence models, used in forecasts like the UCERF time-dependent model, usually assume uniform slip rate of a fault, although some work has pointed to slip rate variations through time. McAuliffe et al (2013 SCEC poster) investigated slip rate variations on the Garlock Fault, by dating offset features using the newly-developed K-feldspar single grain "post-infrared IRSL" dating protocol. They found evidence for increased slip rate for the central Garlock fault over the last 2600 years, compared to the Holocene average rate, with minimum slip rates of 8.1-12.4 mm/yr. This supports the model that the Garlock fault exhibits transient strain accumulation with periods of increased slip and frequent earthquakes, separated by periods of little or no slip and few accompanying seismic events.

Geothermal fields provide an intriguing location for earthquake predictability studies because one of the possible drivers of earthquake rate, the time history of the fluid volume, is known. Weiser et al (2013 SCEC poster) studied 11 geothermal fields across California, looking for correlations between Benioff strain and geothermal field injection and production rates. Their results suggest that there is often increased seismicity when a new geothermal field begins pumping, reduction when pumping ceases, and in general a relation between net pumping rate and earthquake rate. Increased seismicity generally follows a surplus in fluid volume, but in the Salton Sea, an increase in seismicity has also occurred following negative volume change.

Constraining the level of predictability of earthquake stress drop is an important problem with implications for earthquake physics and for the predictability and uncertainty of strong ground motions. Hauksson (2014) investigated the distribution of median stress drop in southern California and discovered spatially coherent patterns with similarities to the patterns of stress orientations observed by Yang and Hauksson (2013). A region of low stress drop extends from the Salton Trough north through the Eastern California Shear Zone, spatially coincident with a clockwise rotation in the regional stress field. Another region of low median stress drop and clockwise stress rotation is located to the west of the San Andreas fault, extending across the edges of the Los Angeles and Ventura basins. Medium to high stress drops occur along the major late Quaternary faults, and coincide with geometrical complexities, such as San Geronio Pass (Goebel et al., 2014).

The predictability of strong ground motions is also investigated through the study of fragile geologic features. Stirling and Rood (2013 SCEC poster) considered the hypothesis that the few fragile geologic features observed ~20 km from the San Andreas fault at Lovejoy Buttes may be statistical outliers that do not represent the typical ground motions experienced at this proximity to the San Andreas. They found that less fragile features are more abundant at Lovejoy Buttes. Their initial observations indicate that 0.35-0.6g may be a more realistic estimate of maximum PGA at Lovejoy Buttes. While this is still considerably less than the 10,000 year return period PGA estimates for the site from the US national seismic hazard model (~1g), the discrepancy is less than that indicated from previous interpretations of the rare fragile geologic features.

Seismicity Patterns

The SCEC community continued analysis of recently developed high-quality earthquake catalogs with improved locations, magnitudes, focal mechanism, and stress drop information. The studies performed during this year combine novel approaches to earthquake cluster identification/classification and high quality earthquake catalogs toward improved understanding of seismicity in relation to large events, improved comparative analysis of foreshock/aftershock activity, swarms, and seismic migration. The developed tools and results can have transformative impact on analysis of seismic hazard in active tectonic environments.

The UCSD group led by P. Shearer has studied earthquake triggering models and their relationship to swarms and foreshock sequences. The analysis identified several aspects of the space/time clustering of seismicity that cannot be explained with standard (i.e., ETAS) triggering models, including details of the foreshock and aftershock behavior for small earthquake (Chen and Shearer, 2013). The results support previous work that has suggested that major California foreshock sequences are not caused by static stress triggering and may be driven by aseismic processes. Ongoing results of this work include a more detailed understanding of earthquake source properties and seismicity patterns.

A continuing collaborative research between USC and UNR led by Y. Ben-Zion and I. Zaliapin focused on spatio-temporal evolution of earthquake clustering and its relation to large earthquakes. The analysis included data from southern California, Turkey, and Midwestern US. The project results demonstrate increase of seismic clustering in the spatio-temporal vicinity of large events ($M \geq 6.5$) in southern California during 1981-2011 and the Duzce, M7.1, 1999 earthquake in Turkey. The results contribute to studies of earthquake predictability and to better understanding of the detailed structure of seismic catalogs in relation to physical properties of the crust.

Collaboratory for the Study of Earthquake Predictability (CSEP)

The EFP group continued research towards improving the earthquake forecast methods within the CSEP project. Particular attention has been paid to further development and validation of hybrid earthquake forecasting models. For instance, a set of rigorous statistical procedures were applied to the investigation of hybrid earthquake forecasting models in New Zealand and California (Rhoades et al., 2014). These studies consistently demonstrated the superiority of hybrid models, based on a range of different ideas or data inputs, over individual models, based on a single idea and data input. The developed ideas and approaches will be further substantiated by independent prospective testing of the hybrid models in the CSEP testing centers in New Zealand and California.

Earthquake Simulators

A multi-institutional collaborative project led by T. Tullis has focused on comparison, validation, and verification of earthquake simulators. This project offers understanding of the interaction between earthquakes in a large system of faults through physics-based simulations of long series of earthquakes in all of California. The results offer the possibility of understanding what are the most important factors determining the temporal and spatial pattern of seismicity.

Workshop

A half-day sixth workshop was held on Sunday afternoon, September 8, prior to the 2013 SCEC Annual Meeting. The workshop intended both for those who are participating in the SCEC Collaborative Project on Comparison, Verification, and Validation of Earthquake Simulators and for those with general interest in the topic. The participants discussed the problems of fault-to-fault rupture jumping, multi-fault simulations based on the UCERF3 deformation models, as well as the plans for the future work. The workshop presentations can be found at <http://www.scec.org/workshops/2013/simulators/index.html>

Select Publications

- Chen, X., and P. M. Shearer (2013) California foreshock sequences suggest aseismic triggering process, *Geophys. Res. Lett.*, 40, doi:10.1002/grl.50444
- Goebel, T. H. W., E. Hauksson, P. M. Shearer, and J. P. Ampuero, Stress drop heterogeneity within tectonically complex regions: A case study of the San Geronio Pass, southern California, submitted to *EPSL*, March 2014.
- Hauksson, E., Median Earthquake Stress Drops of Local Earthquakes in Southern California in the Context of Crustal Geophysics: Implications for Fault Zone Healing. submitted to: Special Pageoph volumes I and II on processes and properties of fault zones; Edited by A. Rovelli and Y. Ben-Zion; March 2014.
- Hauksson, E., H. Kanamori, J. Stock, M.-H. Cormier, and M. Legg, Active Pacific North America plate boundary tectonics as evidenced by seismicity in the oceanic lithosphere offshore Baja California, Mexico, *Geophys. J. Int.* (March, 2014) 196 (3): 1619-1630 doi:10.1093/gji/ggt467.
- Kaneko, Y., and P. M. Shearer (2014) Seismic source spectra and estimated stress drop from cohesive-zone models of circular subshear rupture, *Geophys. J. Int.*, doi: 10.1093/gji/ggu030
- Rhoades, D. A., M. C. Gerstenberger, A. Christophersen, J. D. Zecher, D.Schorlemmer, M. J. Werner and T.H. Jordan (2014) Regional earthquake likelihood models: Information gains of multiplicative hybrids. *Bulletin of the Seismological Society of America*, In review.
- Tullis, T. E., et al. (2012), Generic earthquake simulator, *Seis. Res. Lett.*, 83, 959-963, doi:910.1785/0220120093
- Yang, W. and E. Hauksson, The tectonic crustal stress field and style of faulting along the Pacific North America Plate boundary in Southern California, *Geophys. J. Int.* (July, 2013) 194 (1): 100- 117 doi:10.1093/gji/ggt113.
- Zaliapin, I. and Y. Ben-Zion (2013) Earthquake clusters in southern California, II: Classification and relation to physical properties of lithosphere. *J. Geophys. Res.*, 118, 2865-2877. doi: 10.1002/jgrb.50178

RESEARCH ACCOMPLISHMENTS

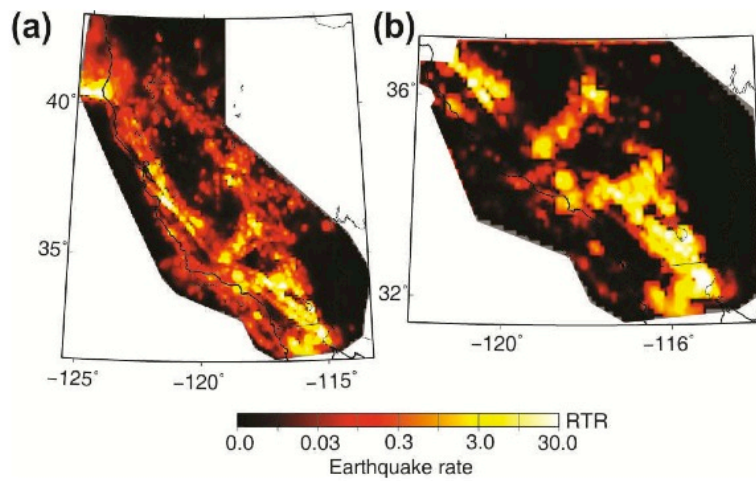


Figure 40. Map of earthquake rates, relative to reference (RTR), in the best three-model hybrids from the RELM experiment for (a) the whole of California; and (b) southern California. In the reference model, one earthquake per year is expected to exceed any magnitude m in an area of 10^m km². From Rhoades et al. (2014).

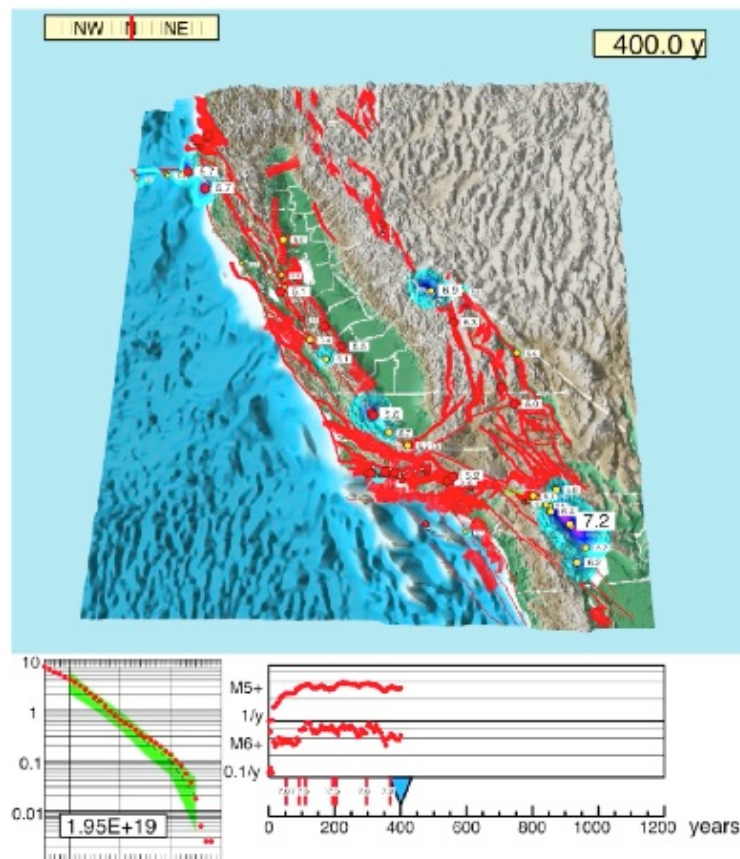


Figure 41. Last frame from a 400-yr movie of earthquakes simulated by ALLCAL for deformation model WCERF3 by Steve Ward. The top figure shows the faults used and the earthquakes that occurred near the end of the movie. The lower left is a frequency-magnitude plot, in events per year, from M4.5 to 8.0, and the lower right shows the frequency of M6+ and M5+ events, from 0.1/yr to 10/yr, the horizontal lines being 1/4 of an order of magnitude apart.

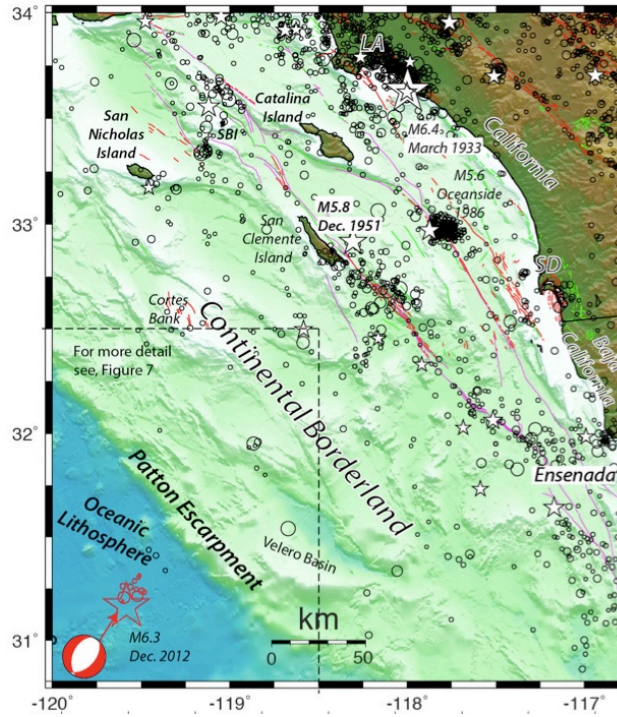


Figure 42. Map showing the bathymetry and topography from NGDC and GeoMapApp, SCSN $M \geq 3.0$ earthquake locations (1930 to 2013), (Hutton et al., 2010); and the 2012 W-phase moment tensor and relocated mainshock (red star) and aftershocks (red circles) of the December 2012 M6.3 offshore earthquake. LA – Los Angeles; SBI – Santa Barbara Island; SD – San Diego. Map courtesy of Egill Hauksson, Caltech.

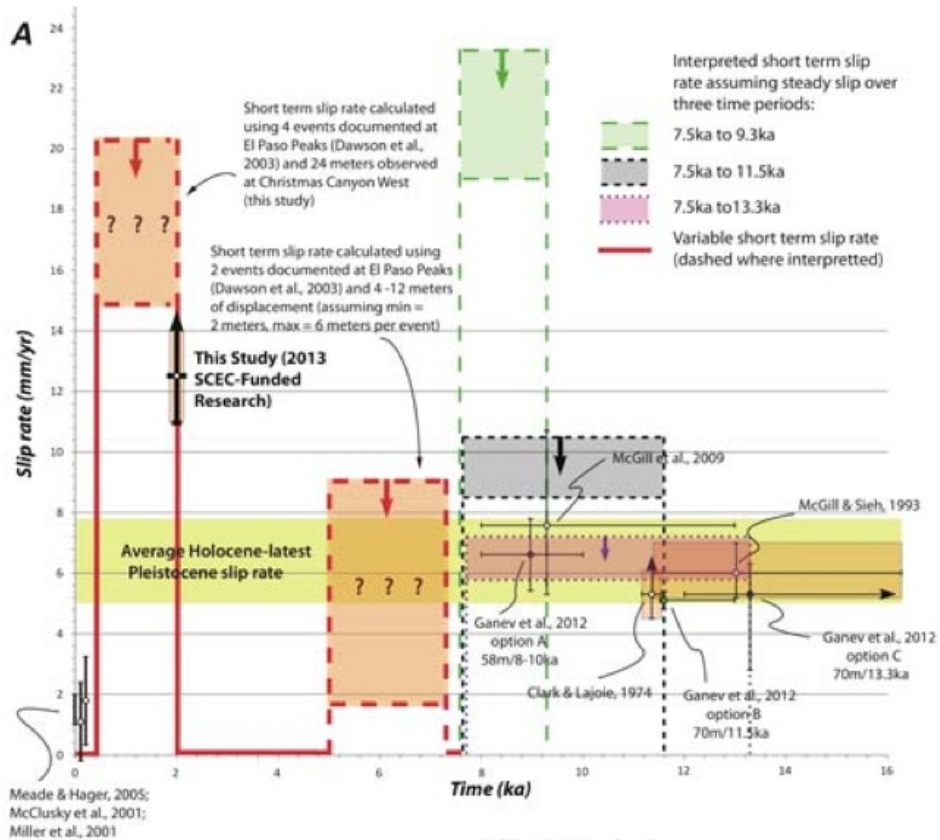


Figure 43. Available slip rate and paleo-earthquake age data from the central Garlock fault. Incremental fault slip rate plotted vs. time. Yellow horizontal band encompasses range of preferred average latest Pleistocene-Holocene rates, solid red line shows known rates. Figure courtesy of Edward Rhodes, UCLA.

RESEARCH ACCOMPLISHMENTS

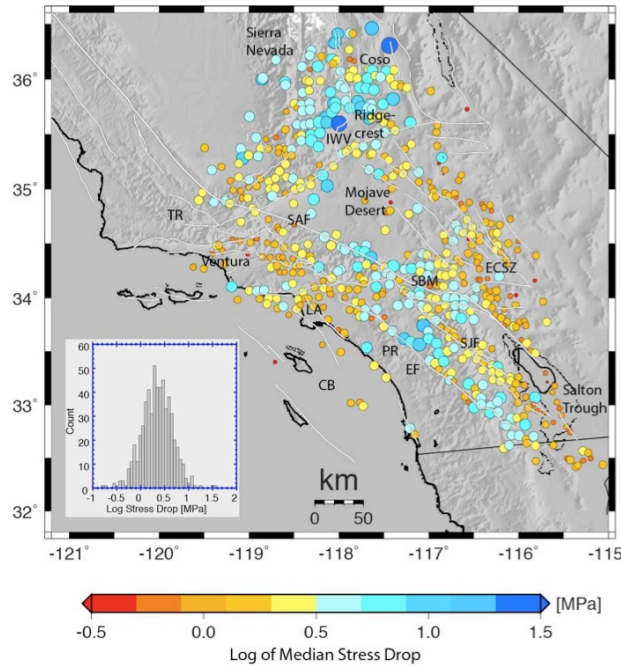


Figure 44. Map of the gridded median stress drops that were corrected for VS(z). The color and size of the symbols are proportional to the size of the logarithm of median stress drops. The (lower left) histogram shows the distribution of the logarithm of the median stress drops plotted on the map. CB – Continental Borderland; ECSZ – Easter California Shear Zone; EF – Elsinore fault; IWV – Indian Wells Valley; LA – Los Angeles; PR – Peninsular Ranges; SAF – San Andreas fault; SBM – San Bernardino Mountains; SJF – San Jacinto fault; TR- Transverse Ranges. Figure courtesy of Egill Hauksson, Caltech.

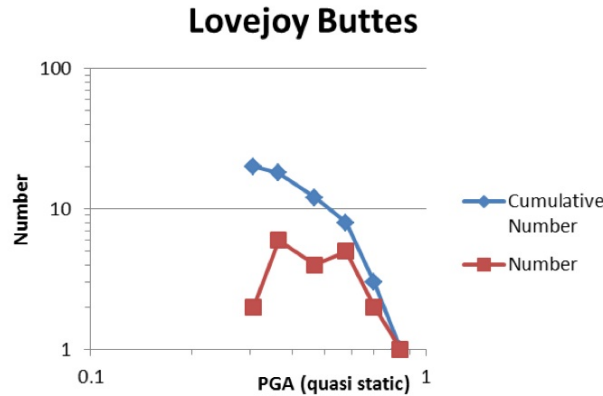


Figure 45. Graph of the number of semi FGFs plotted as a function of the quasi-static estimate of PGA required to topple the FGF (fragility) at Lovejoy Buttes. Note that the 0.3g estimates are based on the two known FGFs at the site, and therefore define the lower limit of fragility. The upper limit of fragility is based on features that still give the overall appearance of fragility, rather than being (e.g.) resistant outcrops which would provide meaninglessly high fragility estimates. Figure courtesy of Mark Stirling, GNS Science.

Ground-Motion Prediction (GMP)

The primary goal of the Ground-Motion Prediction focus group is to develop and implement physics-based simulation methodologies that can predict earthquake strong-motion waveforms over the frequency range 0-10 Hz. Both media and source characterization play a vital role in ground-motion prediction and are important topics for GMP.

This past year’s accomplishments include:

1. Song has developed a statistical framework for earthquake rupture process for physics-based ground motion simulation, including a stochastic model that governs the finite source process with 1-point and 2-point statistics of kinematic source parameters and a pseudo-dynamic rupture model generator (SongRMG, Ver 1.0).
2. Shi and Day have simulated 3D dynamic rupture along the San Gorgonio Pass section of the San Andreas Fault. They find that the fault geometry can play distinctly different roles regarding the plausibility of through-going

ruptures in the SGP region depending on the initial fault traction condition. With homogeneous volume stress input and off-fault plasticity, rupture fails to break through the SGP section regardless of propagation direction or speed. However, with heterogeneous fault tractions and pure elasticity, rupture properties do not seem to be affected much by the relatively long-wavelength geometric irregularities of the Banning fault as is represented in the CFM-v4. In this case, fault geometry has little effect on rupture dynamics, and the SGP section is the determining factor in the likelihood of large through-going ruptures.

3. Archuleta and co-workers have worked on incorporating roughness and supershear ruptures into a kinematic framework to be used by the UCSB Broadband Platform module.
4. Assinaki has validated nonlinear site response prediction methodologies for SCEC Broadband Ground Motion Simulations.
5. Bradley has generated broadband ground motion simulations for the Canterbury earthquakes with nonlinear effective-stress modelling of surficial soils.
6. Sleep studied nonlinear attenuation in the uppermost few hundred meters and ambient intact rock and regolith as fragile geological features. He inferred past shaking from strong Love waves (expressed as peak ground velocity) from the shear wave velocity as a function of depth within the sedimentary basins of Greater Los Angeles. The results include a framework for connecting failure, damage, and nonlinear attenuation when dynamic stress exceeds frictional strength. Also, lowering the ground water levels below the Los Angeles by pumping decreases the nonlinear attenuation, doubling the amplitude of large surface waves impinging from the San Andreas fault.
7. Modeling frequency-dependent anelastic attenuation in southern California. Withers et al. have implemented frequency-dependent Q in the finite-difference code AWP-ODC, and has shown that a power-law formulation of Q as Q^n with $n=0.6-0.8$ provides a much closer fit to short-period ground motion intensities in southern California, as opposed to constant- Q formulations.

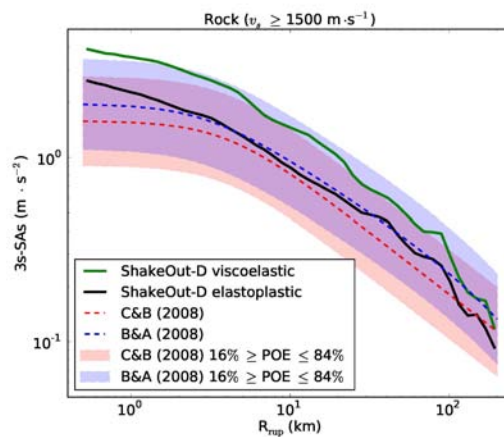


Figure 46. Comparison of spectral accelerations at a period of 3 sec from a 0-1 Hz dynamic simulation of M7.8 Shakeout, with (viscoelastic, black) and without (elastoplastic, green) off-fault nonlinear effects to leading GMPEs, for rock sites. Notice how the elastoplastic results are much closer to the GMPE medians, as compared to the viscoelastic results. This is in agreement with the results by Roten et al. (2014), suggesting that long-period ground motions for large earthquakes may be significantly affected by nonlinear effects. Results from Roten, Olsen and Day.

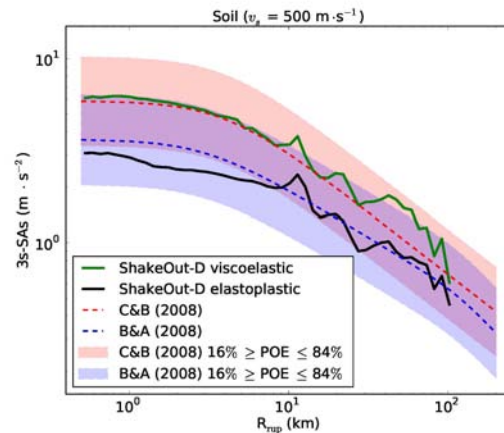


Figure 47. Same as Figure 46, but for soil sites. A similar reduction of the viscoelastic results is found.

RESEARCH ACCOMPLISHMENTS

Wave Propagation in Complex, Nonlinear Media

Roten et al. (2014) and additional recent results on viscoelastic and viscoplastic simulations of the M7.8 ShakeOut scenario on the southern San Andreas fault show that off-fault plasticity can significantly reduce peak ground motions for both rock and soil sites. The results are robust for end-member cohesion models. As compared to the viscoelastic results, elastoplastic simulations generate long-period peak motions much closer to leading GMPEs (see Figures 46 and 47).

Stochastic Descriptions of Basin Velocity Structure

Shaw et al. (Harvard) and Olsen and Savran (SDSU) have constrained the parameters needed to generate statistical distributions of small-scale heterogeneities in the crust using sonic log data from the Los Angeles basin. Both studies find standard deviations from the mean depth trends of 5-10% and vertical correlation lengths of 50-150 m. Horizontal correlations lengths are less constrained by data but tend to be much longer (hundreds of meters to kilometers). Assuming a von Karman distribution, Hurst numbers of 0.0-0.1 best characterize the distributions; however, there are indications that the statistical distribution may be markedly non-Gaussian. Statistical distributions of small-scale heterogeneities with these parameters can amplify or de-amplify ground motions by up to a factor of two; however, small-scale scattering included in the wave propagation for the 2008 Mw 5.4 Chino Hills, CA, earthquake, improves the goodness-of-fit (GOF) between data and synthetics by only 5-10%. On the other hand, we find that shallow sources located on the boundary of a sedimentary basin can generate bands of strong amplification aligned in the direction of the ray paths. The nature of these bands depends strongly on the incidence angle of the waves into the sediments. Moreover, this banded amplification pattern is absent for sources deeper than 1-2 km, consistent with the results for the Chino Hills earthquake. The majority of the scattering recorded in ground motions appears to originate as path effects as waves propagate through the basins, as compared to local site-specific scattering. Lower-velocity sediments and the deep crust contribute approximately equally to the strength of the scattering recorded in ground motion records.

Long-period Effects on the BBP

Efforts are underway to explore why the (1D) broadband platform simulations often obtain relatively poor fit to data for the long-period ground motions (>1s). Preliminary results for hybrid simulations of the M5.4 Chino Hills earthquake show improved fits long-period PSAs when 3D velocity structure is used (R. Taborda, J. Bielak, D. Gill, F. Silva, P. Small, P. Maechling, see Figure 48). The results suggest that including 3D basin crustal amplification effects into the long-period ground motions computed by the platform is important and should be explored further.

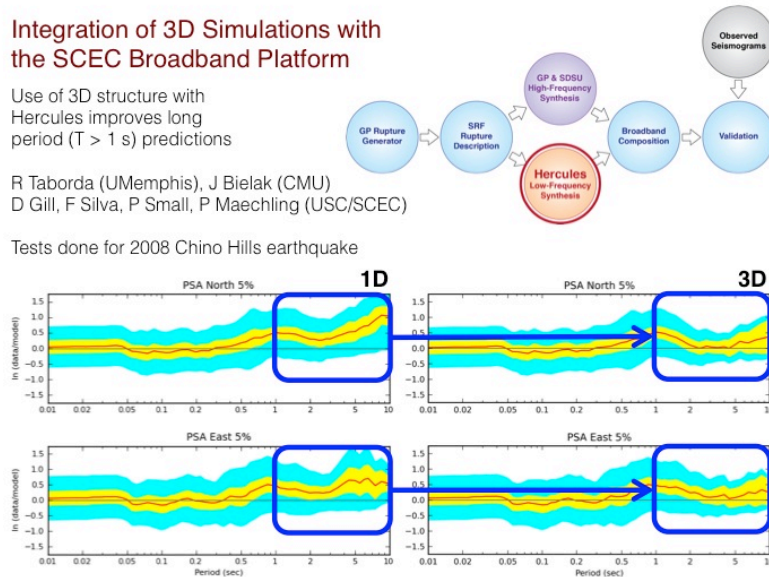


Figure 48. Efforts are underway to explore why the (1D) broadband platform simulations often obtain relatively poor fit to data for the long-period ground motions (>1s). An interface is being built to incorporate 3D low-frequency synthetics into the BBP. Preliminary results for hybrid simulations of the M5.4 Chino Hills earthquake show improved fits long-period PSAs when 3D velocity structure is used (Taborda et al., 2014).

Exploring Basin Amplification Sensitivity Using the Ambient Seismic Field

Denolle et al. have studied Kanto Basin amplification by exploiting the information carried by the ambient seismic field. They used 375 Hi-Net deep borehole seismometers across central Honshu as virtual sources and 296 seismic stations of the MeSO-Net work shallow-borehole seismometers within the basin as receivers to map the basin impulse response. They find a linear relationship between vertical ground motion and basin depth at periods of 2 – 10 seconds that could be used to

represent 3D basin effects in ground motion prediction equations. Moreover, they find that the strength of basin amplification depends strongly on the direction of illumination by seismic waves.

Select Publications

- Roten, D., K.B. Olsen, S.M. Day, Y. Cui, and D. Fah (2014). Expected seismic shaking in Los Angeles reduced by San Andreas fault zone plasticity, *Geophys. Res. Lett.* 2769-2777, DOI: 10.1002/2014GL059411.
- Plesch, A., J. H. Shaw, T. H. Jordan, and X. Song (2014). Stochastic Descriptions of Basin Velocity Structure from Analyses of Sonic Logs and the SCEC Community Velocity Model (CVM-H), *Seism. Res. Lett.* 85:2, 431.
- Savran, W., and K.B. Olsen (2014). Deterministic simulation of the Mw5.4 Chino Hills event with frequency-dependent attenuation, heterogeneous velocity structure and realistic source model, *Seism. Res. Lett.* 85:2, 498.
- Withers, K.B., K.B. Olsen, S.M. Day, and Z. Shi (2014). High-complexity deterministic Q(f) simulation of the 1994 Northridge Mw6.7 earthquake, *Seism. Res. Lett.* 82:2, 471.
- Assimaki, D., and R. Taborada (2014). Site-specific response in validation studies of physics-based earthquake simulations, *Seism. Res. Lett.* 85:2, 470.
- Denolle, M., H. Miyake, S. Nakagawa, N. Hirata, and G. C. Beroza (2014) Long- Period Seismic Amplification in the Kanto Basin Using the Ambient Seismic Field, *Geophys. Res. Lett.*, DOI: 10.1002/2014GL059425.
- Sleep, N. H., and D. R. Lowe (2014). Physics of crustal fracturing and chert dike formation triggered by asteroid impact, ~3.26 Ga, Barberton greenstone belt, South Africa, *Geochem. Geophys. Geosyst.*, 15, doi:10.1002/2014GC005229. SECC contribution number 1915.
- Sleep, N. H., and B. Erickson (2014). Nonlinear attenuation of S-waves and Love waves within ambient rock. Submitted to *G³*
- Restrepo, D., and J. Bielak (2014). Virtual topography - a fictitious domain approach for analyzing free-surface irregularities in large-scale earthquake ground motion simulation, *International Journal for Numerical Methods in Engineering* (accepted for publication).

Earthquake Engineering Implementation Interface (EII)

The implementation of SCEC research for practical purposes depends on interactions with engineering researchers and organizations, and with practicing engineers, building officials, insurers, emergency managers, and other technical users of our information.

This past year's accomplishments include:

1. Refinement of approaches for validating ground motion simulations, including the use of inelastic response spectra, elastic spectral correlations, and polarization of multicomponent motions;
2. Validation of durations from ground motion simulations, to enable use of simulations for geotechnical engineering applications where duration of shaking is an important parameter;
3. Development of a tutorial seminar on ground motion simulations, and presentation of the content at a special session of the 10th National Conference on Earthquake Engineering.

Gauntlets for Validating Ground Motion Simulations

This area of accomplishment relates to validation "gauntlets" that simulations should pass through to be considered viable for use in specific engineering applications, such as building-code analysis (simulations) of nonlinear building or site response. An important goal is to demonstrate how tailored to particular engineering applications such gauntlets must be, and the extent to which some validation gauntlets can cover a wide range of engineering applications. Burks and Baker (2014) have developed a validation gauntlet for the use of simulated ground motions in nonlinear response history analysis of 3D multi-degree-of-freedom buildings. This gauntlet consists of three validation tests that compare simple ground motion "proxy" parameters from simulated ground motions with corresponding empirical models. The simple parameters serve as proxies for the more complicated building response of interest, and the corresponding empirical models are robust against (or insensitive to) differences between the earthquake characteristics (e.g., magnitude) of simulated and historical ground motions. The three ground motion parameters are: (i) correlations of elastic spectral acceleration across multiple pair of spectral periods, (ii) ratios of maximum to median elastic spectral response acceleration across all horizontal ground motion orientations, and (iii) ratios of inelastic to elastic spectral displacement. This gauntlet of validation tests has been demonstrated for sample ground motions simulated by three different methods via the SCEC Broadband Platform.

Simulation Validation for Geotechnical Engineering Applications

A validation gauntlet for the use of simulated ground motions in geotechnical analysis of slope displacements and soil liquefaction is under development. These geotechnical responses are sensitive to ground motion duration--a property of simulated ground motions that has not previously been well studied. Thus, durations from simulated ground motions have been compared with a corresponding empirical model. This work has identified bias in the most recent available empirical model for duration, with respect to more-recently recorded ground motions. This has further led to development of an

RESEARCH ACCOMPLISHMENTS

updated empirical model for duration that is now beginning to be compared with simulated ground motions (Stewart & Afshari, 2014).

Tutorial Session for Earthquake Engineering Outreach

To broaden the impact of SCEC's Ground Motion Prediction work, we developed and delivered a special session on Simulations at the 10th National Conference on Earthquake Engineering on July 22nd in Anchorage. Attended by approximately 100 academic and practicing engineers, the session presented an overview of SCEC's simulation approaches, computational infrastructure, and validation efforts. A lively panel discussion followed the presentations, where the audience had a chance to probe the SCEC speakers more deeply. Norm Abrahamson, Jack Baker, Nico Luco, Rob Graves, Phil Maechling and Kim Olsen were the SCEC scientists presenting at this session, and they also developed an overview paper summarizing the content presented at the session (Baker et al. 2014).

Select Publications

- Baker, J. W., Luco, N., Abrahamson, N. A., Graves, R. W., Maechling, P. J., and Olsen, K. B. (2014). "Engineering uses of physics-based ground motion simulations." Proceedings of the Tenth U.S. National Conference on Earthquake Engineering, Anchorage, Alaska, 10p.
- Bijelic, N., Lin, T., and Deierlein, G. (2014). Seismic response of a tall building to recorded and simulated ground motions. Proceedings of the Tenth National Conference on Earthquake Engineering, Anchorage, Alaska, 10p.
- Burks, L. S., and Baker, J. W. (2014). "Validation of ground motion simulations through simple proxies for the response of engineered systems." Bulletin of the Seismological Society of America, (in press).
- Dreger, D., Beroza, G. C., Day, S. M., Goulet, C. A., Jordan, T. H., Spudich, P., and Stewart, J. P. (2013). Evaluation of SCEC Broadband Platform Phase 1 Ground Motion Simulation Results. Southern California Earthquake Center Report, Los Angeles, California, USA.
- Stewart, J. and Afshari, K. (2014). Validation of simulated ground motions relative to seismic geotechnical engineering demand parameters. Southern California Earthquake Center Annual Report (http://sceccore2.usc.edu/proposalfiles/2012reports/Stewart_12121_report.pdf).

Working Group on California Earthquake Probabilities (WGCEP)

The Working Group on California Earthquake Probabilities (WGCEP) is charged with developing official, consensus, and time-dependent earthquake forecast models for California. The effort builds on a long tradition of previous WGCEPs (e.g., models published in 1988, 1990, 1995, 2003, and 2008), and involves explicit collaboration between SCEC, the USGS, and CGS, with considerable funding from the California Earthquake Authority (<http://www.earthquakeauthority.com>). The last WGCEP model was the Uniform California Earthquake Rupture Forecast version 2 (UCERF2, <http://www.scec.org/ucrf2/>), which was published in 2008. Since that time we have been working on the next model, UCERF3, for which the main goals have been to: 1) relax segmentation and include multi-fault ruptures; 2) develop an algorithm for computing more self-consistent long-term elastic-rebound-based probabilities; and 3) include spatiotemporal clustering effects in acknowledgement that aftershocks and triggered events can be large and damaging. The latter (spatiotemporal clustering) will bring us into the realm of Operational Earthquake Forecasting (OEF). The need for these enhancements has been exemplified by several recent earthquakes, including the 2011 M9 Tohoku earthquake with respect to segmentation, both the 2010 M7.2 El Mayor-Cucapah and 2012 M8.6 Sumatra earthquakes in regard to multi-fault ruptures, and the 2011 M6.3 Christchurch earthquake in terms of spatiotemporal clustering. Progress on each of these goals is given below.

UCERF3-TI, The Time-Independent Model

The backbone of UCERF3 is the long-term, time-independent model (UCERF3-TI), which was published as a USGS Open-File Report on Nov. 5, 2013, and includes a main report, 20 appendices, and various supplements (<http://pubs.usgs.gov/of/2013/1165/>). The main report and one of the appendices have also been published in a peer-reviewed journal (as Field et al. (2014) and Page et al. (2014), respectively). The primary achievement for this model component was relaxing fault segmentation and including multi-fault ruptures, both limitations of UCERF2. The rates of all earthquakes were solved for simultaneously, and from a broader range of data, using a system-level "grand inversion" that is both conceptually simple and extensible. The inverse problem is large and underdetermined, so a range of models was sampled using an efficient simulated annealing algorithm. The approach is more derivative than prescriptive (e.g., magnitude-frequency distributions are no longer assumed), so new analysis tools were developed for exploring solutions. Epistemic uncertainties were also accounted for using 1440 alternative logic tree branches, necessitating access to supercomputers. The most influential uncertainties include alternative deformation models (fault slip rates), a new smoothed seismicity algorithm, alternative values for the total rate of $M \geq 5$ events, and different scaling relationships, virtually all of which are new. As a notable first, three deformation models are based on kinematically consistent inversions of geodetic and geologic data, also providing slip-rate constraints on faults previously excluded due to lack of geologic data. The grand inversion constitutes a system-level framework for testing hypotheses and balancing the influence of different experts. For example, we have demonstrated serious challenges with the Gutenberg-Richter hypothesis for individual faults. UCERF3-TI is still an approximation of the system, however, and the range of models is limited (e.g., constrained to stay close to UCERF2).

Nevertheless, UCERF3-TI removes the apparent UCERF2 over-prediction of M6.5-7 earthquake rates and also includes types of multi-fault ruptures seen in nature. Although UCERF3-TI fits the data better than UCERF2 overall, there may be areas that warrant further site-specific investigation. Finally, the supporting products may be of general interest, and we listed key assumptions and avenues for future model improvements in the report.

UCERF3-TD, The Long-Term, Time-Dependent Model

This model, which builds on UCERF-TI, includes long-term, time-dependent probabilities based on Reid's elastic-rebound hypothesis, which posits that rupture likelihood drops on a fault after experiencing a large rupture and then builds back up as tectonic stresses re-accumulate with time. A new methodology has been developed that solves applicability issues in the previous approach for un-segmented models. The new methodology also supports magnitude-dependent aperiodicity and accounts for the historic open interval on faults that lack a date-of-last-event constraint. Epistemic uncertainties are represented with a logic tree, producing 5,760 different forecasts. Results for a variety of evaluation metrics are presented, including logic-tree sensitivity analyses and comparisons to the previous model (UCERF2). For 30-year $M \geq 6.7$ probabilities, the most significant changes from UCERF2 are a threefold increase on the Calaveras fault and a threefold decrease on the San Jacinto fault. Such changes are due mostly to differences in the time-independent models (e.g., fault slip rates), with relaxation of segmentation and inclusion of multi-fault ruptures being particularly influential. In fact, some UCERF2 segments were simply too long to produce M 6.7 sized events. Probability model differences are also influential, with the implied gains (relative to a Poisson model) being generally higher in UCERF3. Accounting for the historic open interval is one reason. Another is an effective 27% increase in the total elastic-rebound-model weight. The exact factors influencing differences between UCERF2 and UCERF3, as well as the relative importance of logic-tree branches, vary throughout the region, and they depend on the hazard metric of interest (e.g., $M \geq 6.7$ probability changes may not translate to hazard). This sensitivity, coupled with the approximate nature of the model, as well as known limitations, means the applicability of UCERF3 should be evaluated on a case-by-case basis. Overall, UCERF3 represents the best model currently available for forecasting California earthquakes. As listed below, three papers describing UCERF-TD have been reviewed by our Scientific Review Panel and submitted to the Bulletin of the Seismological Society of America for publication. Figure 49 below shows the probability that each area in California will participate in $M \geq 6.7$ earthquakes over the next 30 years.

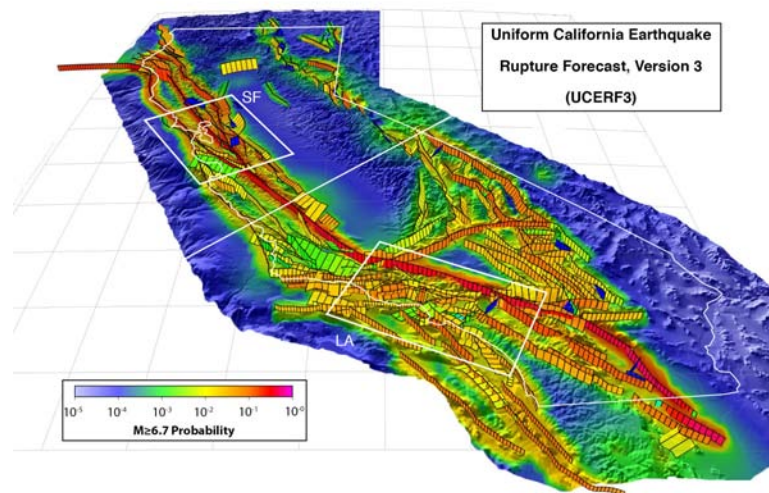


Figure 49. 3D perspective view of UCERF3-TD, where colors depict the mean “participation probability” – the likelihood that each point will experience one or more $M \geq 6.7$ earthquakes in the 30 years following 2014, where participation means that some point on the rupture surface is within about 5 km. The small black rectangular elements represent the 2,606 fault subsections used in the forecast (for one of the two fault models, FM3.1). The influence of the Cascadia megathrust is not shown on this map.

UCERF3-ETAS, Spatiotemporal Clustering for OEF

With the time-independent model published, which relaxes segmentation and includes multi-fault ruptures, and the long-term time-dependent model in review, which incorporates elastic rebound, we have now turned our attention to including spatiotemporal clustering. In recognition that triggered events can be large and damaging, the ultimate goal is to deploy an Operational Earthquake Forecast (OEF) for California, now listed as one of the USGS's strategic-action priorities (<http://pubs.usgs.gov/of/2012/1088>; page 32). To this end, we have added an Epidemic Type Aftershock Sequence (ETAS) component to UCERF3 (UCERF3-ETAS). Most notably, our model represents a merging of ETAS with finite-fault based forecasts, as well as the inclusion of elastic rebound (both firsts, as far as we are aware). In fact, inclusion of elastic-rebound turns out to be critical in terms of getting spatiotemporal clustering statistic correct (otherwise ~85% of large triggered events simply re-rupture the same fault, which we don't see in nature). UCERF3-ETAS is currently being “test-driven”. Our intent is to document the model and subject it to more rigorous testing (e.g., via CSEP) over the next year.

RESEARCH ACCOMPLISHMENTS

Select Publications

UCERF3-TI Open-File Report, including 20 appendices: <http://pubs.usgs.gov/of/2013/1165/>

Field, E. H., R. J. Arrowsmith, G. P. Biasi, P. Bird, T. E. Dawson, K. R. Felzer, D. D. Jackson, K. M. Johnson, T. H. Jordan, C. Madden, A. J. Michael, K. R. Milner, M. T. Page, T. Parsons, P. M. Powers, B. E. Shaw, W. R. Thatcher, R. J. Weldon, and Y. Zeng (2014). Uniform California Earthquake Rupture Forecast, version 3 (UCERF3)—The time-independent model, *Bull. Seism. Soc. Am.*, Vol. 104, No. 3, pp. 1122–1180, June 2014, doi: 10.1785/0120130164

Page, M. T., E. H. Field, K. R. Milner, and P. M. Powers (2014). The UCERF3 Grand Inversion: Solving for the Long-Term Rate of Ruptures in a Fault System, *Bull. Seism. Soc. Am.*, v. 104, p. 1181-1204, doi:10.1785/0120130180.

Field, E. H., G. P. Biasi, P. Bird, T. E. Dawson, K. R. Felzer, D. D. Jackson, K. M. Johnson, T. H. Jordan, C. Madden, A. J. Michael, K. R. Milner, M. T. Page, T. Parsons, P. M. Powers, B. E. Shaw, W. R. Thatcher, R. J. Weldon, and Y. Zeng (2014). Long-Term, Time-Dependent Probabilities for the Third Uniform California Earthquake Rupture Forecast (UCERF3), *Bull. Seism. Soc. Am.*, Submitted

Field, E. H. (2014). Computing elastic-rebound-motivated earthquake probabilities in un-segmented fault models – A new methodology supported by physics-based simulators, *Bull. Seism. Soc. Am.*, Submitted.

Field, E. H., and T. H. Jordan (2014). Time-Dependent renewal-model probabilities when date of last earthquake is unknown, *Bull. Seism. Soc. Am.*, Submitted.

Collaboratory for the Study of Earthquake Predictability (CSEP)

The Collaboratory for the Study of Earthquake Predictability (CSEP) provides a controlled and transparent research infrastructure for the prospective and blind evaluation of earthquake forecasting and prediction methods.

Construction of Optimal Multiplicative Hybrid Models

Rhoades et al. (accepted) conducted a study of the performance of multiplicative hybrid models based on the suite of five-year forecasting models submitted to the Regional Earthquake Likelihood Models (RELM) experiment. They constructed optimal multiplicative hybrids involving the best individual model (the Helmstetter et al. smoothed seismicity model) as a baseline and one or more conjugate models. Many two-model and three-model hybrids show an appreciable information gain (log probability gain) per earthquake relative to the best individual model. The information gains of the best multiplicative hybrids are greater than those of additive hybrids (including Bayesian ensemble models) constructed from the same set of models. The gains tend to be larger when the contributing models involve markedly different concepts or data. Multiplicative hybrids will be useful for assimilating other earthquake-related observations into forecasting models and for combining forecasting models at all time-scales.

Evaluation of 3-month Forecasting Models for California

Schneider et al. (2014) evaluated seven 3-month models for California, consisting of contrasting versions of the Every Earthquake a Precursor According to Scale (EEPAS) and Proximity to Past Earthquakes (PPE) modeling approaches. Besides the standard CSEP tests, the study was complemented by several residual-based methods, which provide detailed spatial information. The testing period covered June 2009-September 2012, when California experienced 23 earthquakes above the magnitude threshold and a significant earthquake sequence. Though all models fail to capture seismicity during an earthquake sequence, spatio-temporal differences between models also emerge. The overall best-performing model has strong time- and magnitude-dependence, weights all earthquakes equally as medium-term precursors of larger events and has a full set of fitted parameters. Models with this time- and magnitude-dependence offer a statistically significant advantage over simpler baseline models. In addition, models that down-weight aftershocks when forecasting larger events have a desirable feature in that they do not overpredict following an observed earthquake sequence.

Extending CSEP to Testing of Ground-Motion Predictions and Hazard

The team at GFZ has continued to work on the integration of ground-motion testing into the CSEP software system. The component for testing intensity-prediction equations is almost complete. As a case study to show the potential of this kind of testing, Mak et al. (in revision) have presented a concise and detailed evaluation of Italian intensity-prediction equations. A case study on ground-motion prediction equations in Japan is in preparation. Testing the USGS hazard map against Did You Feel It?-data and shakemaps is underway.

Collaboration with the Global Earthquake Model

CSEP has worked together with the Global Earthquake Model (GEM) project in the field of testing ground-motion prediction equations and hazard. These studies are well underway. In particular, the testing of the USGS hazard model is a direct result of the Powell Group meeting in September 2013. This meeting was held by the USGS and GEM and targeted the testability of hazard models. With the development of the GEAR seismicity model for GEM at UCLA, CSEP will continue this collaboration by testing the GEAR model.

Prototype Experiments to evaluate External Forecasts and Predictions (EFPs)

Two prototype experiments are in development to import and evaluate external forecasts and predictions (EFPs) that are generated outside of CSEP and may be based on seismic, electromagnetic or any other data sets that CSEP cannot provide internally. The first experiment involves the QuakeFinder group led by Tom Bleier, where progress is being made to define a machine-readable xml-based template to register predictions within CSEP for evaluation. The second experiment involves the import and evaluation of the earthquake prediction algorithm M8: The ETH Zurich group (M. Rierola and J. Zechar) is collaborating with V. Kossobokov (Moscow & IPG Paris) to register and evaluate M8 predictions retrospectively and prospectively within CSEP. M8 predictions starting in 1985 were evaluated retrospectively against the PDE earthquake catalog using the gambling score of Zhuang (2010). Preliminary results using the gambling score showed undesirable features of the score: an entirely pessimist strategy (always declaring alarms) would have outperformed the reference (Poisson) model as well as M8 predictions, most likely as a result of skewed returns (wins are unlimited, losses are limited to the ante). An improved method, the parimutuel gambling score by Zechar and Zhuang (2014), is now being investigated for the purpose of evaluating M8.

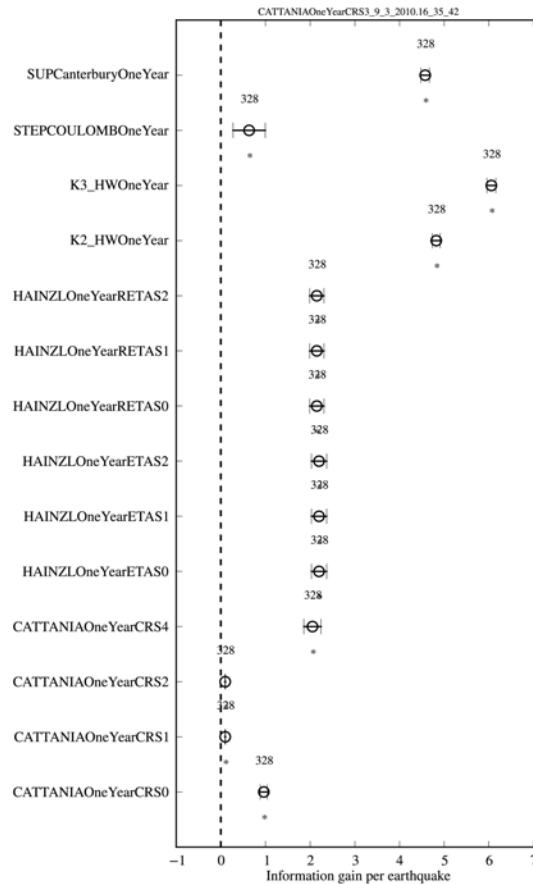


Figure 50. Information gain of a 1-year forecast by a Coulomb/Rate-State model by Cattania et al. against other statistical and physics-based forecasts starting right after the 2010 Darfield earthquake. For the considered 1-year period, the Coulomb model outperforms all other forecasts, including those of a hybrid STEP/Coulomb model, ETAS models with various spatial triggering kernels and various other Coulomb models. The gain shown is calculated with the model on the left as the reference model, i.e. positive gains show superior performance by the Coulomb model named in the title.

Retrospective Canterbury Experiment

The M7.1 Darfield, New Zealand (NZ), earthquake triggered a complex earthquake cascade that provides a wealth of new scientific data to study earthquake triggering and the predictive skill of statistical and physics-based forecasting models. To this end, and in collaboration with CSEP New Zealand and the European FP7 project REAKT, CSEP is conducting a retrospective evaluation of a variety of short-term forecasting models during the 2010-12 Canterbury, New Zealand, earthquake sequence. The statistical model group includes variants of the Epidemic-Type Aftershock Sequence (ETAS) model, non-parametric kernel smoothing models, and the Short-Term Earthquake Probabilities (STEP) model. The physics-based model group includes variants of the Coulomb stress triggering hypothesis, which are embedded either in Dieterich's (1994) rate-state formulation or in statistical Omori-Utsu clustering formulations (hybrid models).

RESEARCH ACCOMPLISHMENTS

Initial results of 1-year forecasts beginning right after the Darfield event indicate that Coulomb/rate-state models that propagate the uncertainty of input parameters and data through to forecasts obtain the largest information gains (Figure 50), while a suite of ETAS models perform best when 1-year forecasts are updated after each of the largest earthquakes in the sequence.

VISES-funded Collaboration with CSEP Japan

With the aim of characterizing the influence of tectonic setting on the predictive skills of smoothed seismicity models, Werner et al. (in preparation) calibrated two forecasting models from the California testing region to Japanese seismicity. In collaboration with the Earthquake Research Institute (ERI), parameters of the two models were estimated for the three different CSEP-Japan testing regions to generate retrospective forecasts that will be compared to extent prospective models within CSEP-Japan. The two models were developed by Helmstetter & Werner (2012) and employ space-time kernels to smooth seismicity for time-independent forecasting. The models builds on the success of the Helmstetter (adaptive smoothing) model that performed well in the RELM experiment. The methods circumvent the need for declustering an earthquake catalog by estimating the distribution of rates with space-time kernels and choosing the median as the predictor of the future rate in each spatial cell. The models will be installed in the 3-month, 1-year and 3-year forecast groups of the Japan testing center for prospective evaluation. Figure 51 shows a 3-month forecast for the period including the M9 Tohoku earthquake sequence. The prospective predictive skills will be compared to Californian results to infer the extent to which skills are affected by local tectonic setting.

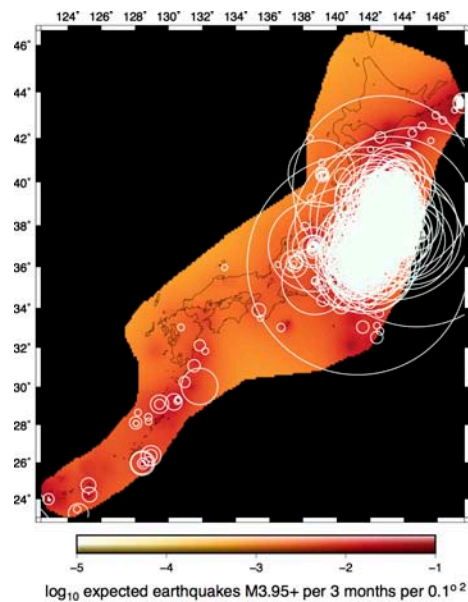


Figure 51. 3-month forecast for the AllJapan testing region of CSEP Japan along with observed earthquakes between February and April 2011, including the M9 Tohoku earthquake sequence. The forecast was generated with a space-time smoothed seismicity model, named Conan (Helmstetter & Werner, 2012), that is already under evaluation in California. Retrospective evaluations and comparisons against California will increase our understanding of the influence of tectonic setting on the model's forecasting skill.

Select Publications

- Mak, S., R. Clements, and D. Schorlemmer (2014), The Statistical Power of Testing Probabilistic Seismic-Hazard Assessments, *Seismol. Res. Lett.*, 85(4): 781-783, 10.1785/0220140012
- Mak, S., R. Clements, and D. Schorlemmer (in revision): Evaluating Intensity Prediction Equations for Italy, in revision
- Rhoades, D. A., M. C. Gerstenberger, A. Christophersen, J. D. Zechar, D. Schorlemmer, M. J. Werner, and T.H. Jordan (accepted), Regional Earthquake Likelihood Models: Information Gains of Multiplicative Hybrids, *Bull. Seismol. Soc. Am.*
- Schneider, M., R. Clements, D. Rhoades, and D. Schorlemmer (2014), Likelihood- and residual-based evaluation of medium-term earthquake forecast models for California, *Geophys. J. Int.*, 198 (3): 1307-1318, 10.1093/gji/ggu178
- Werner, M. J., W. Marzocchi, M. Taroni, J. D. Zechar, M. C. Gerstenberger, M. Liukis, D. Rhoades, C. Cattania, A. Christophersen, S. Hainzl, A. Helmstetter, A. Jimenez, S. Steacy and T. H. Jordan (2014, in preparation), Retrospective Evaluation of Earthquake Forecasts during the 2010-12 Canterbury, New Zealand, Earthquake Sequence, in preparation.
- Werner, M. J., H. Tsuruoka, S. Yokoi, A. Helmstetter, and N. Hirata (2014, in preparation), Influence of Tectonic Setting on the Predictive Skills of Space-Time Smoothed Seismicity Earthquake Forecasts in California and Japan, in preparation.
- Zechar, J. D., and J. Zhuang (2014), A parimutuel gambling perspective to compare probabilistic seismicity forecasts, *Geophys. J. Int.* (2014) 199, 60-68, doi: 10.1093/gji/ggu137

SCEC4 Science Milestones

Southern California Earthquake Center, September 2014

TABLE 1. SCEC4 FUNDAMENTAL PROBLEMS OF EARTHQUAKE PHYSICS

- I. Stress transfer from plate motion to crustal faults: long-term slip rates.
- II. Stress-mediated fault interactions and earthquake clustering: evaluation of mechanisms.
- III. Evolution of fault resistance during seismic slip: scale-appropriate laws for rupture modeling.
- IV. Structure and evolution of fault zones and systems: relation to earthquake physics.
- V. Causes and effects of transient deformations: slow slip events and tectonic tremor.
- VI. Seismic wave generation and scattering: prediction of strong ground motions.

Milestones

NSF has requested that we submit an annualized list of milestones as part of a revised SCEC4 plan for 2012-2017. According to NSF instructions, these milestones are based on the six fundamental problems in earthquake physics described in the SCEC4 proposal (see Table 1 of this supplement). Our response to the NSF request adopts the premise that milestones are to be used by SCEC and its sponsoring agencies as indicators of research progress along unknown conceptual pathways rather than, say, lists of working-group tasks, timelines for IT developments, or absolute measures of research volume from individual research groups.

We have therefore concentrated on targets for SCEC's interdisciplinary activities in earthquake system science, such as those related to the SCEC Community Models, which will include a new Community Geodetic Model (CGM) and a Community Stress Model (CSM); those related to a proposed new set of Special Fault Study Areas (SFSAs); and those coordinated through the Technical Activity Groups (TAGs), such as the newly established Ground Motion Simulation Validation TAG, which brings earthquake engineers together with ground motion modelers. Because SCEC interdisciplinary activities in some cases depend on ancillary support from special projects (e.g., IT developments, HPC resources), reaching some of the milestones will be contingent on receiving this ancillary support.

The milestones are organized by a numbered research topic or collaboration. The problems addressed by each numbered item are listed parenthetically at the end of each paragraph; e.g., [I-VI] indicates that the milestones for that topic or collaboration are relevant to all six problems. Owing to the unpredictable nature of basic research, the milestones for the first two years are more explicit than those for the out-years of the SCEC4 program.

Year 1 (2012-2013)

1. **Improved Observations.** Archive and make available at the SCEC waveforms, refined catalogs of earthquake locations and focal mechanisms for the period 1981-2011. Begin cataloging validation earthquakes and associated source descriptions and strong ground motion observations for California for use in ground motion simulation validation. Implement automated access to EarthScope GPS data for transient detections. Initiate planning with IRIS and UNAVCO to improve the scientific response capabilities to California earthquakes. [I-VI]
2. **Transient Geodetic Signals.** Develop data-processing algorithms that can automatically detect geodetic transients localized within Southern California using continuously recorded GPS data. Provide access to authoritative GPS data streams through CSEP. Implement at least two detection algorithms as continuously operating procedures within CSEP. [V]
3. **Community Modeling Environment.** Implement, refine, and release software tools for accessing the SCEC CVMs. Define reference calculations and evaluation criteria for 3D velocity models. Conduct comparative evaluations among different CFMs and CVMs. Deliver statewide versions of CFMs for use by WGCEP in UCERF3. Develop dynamic rupture verification exercises that incorporate effects of large-scale branching fault geometry on dynamic rupture and ground motions. [II, III, IV, VI]
4. **Community Geodetic Model.** Obtain input from the SCEC community via a workshop in order to define the conceptual and geographic scope of the CGM, including the time-independent and time-dependent model components, the data to be assimilated into the model, and the type and spatial distribution of model output. [I, II, V]
5. **Community Stress Model.** Develop a strategy for archiving and curating observational and model-based constraints on the tectonic stress field in Southern California. Based on this strategy, begin developing

SCEC4 SCIENCE MILESTONES

components of the database that will underlie the CSM. Organize a SCEC collaboration to contribute existing observational and model-based constraints to this database. [I, II]

6. **Special Fault Study Areas.** Identify requirements for SFSA Science Plans. Solicit SFSA projects from the SCEC community, notify community of projects and post Science Plan(s) for 2013 RFP on the website. Coordinate interdisciplinary activities, including workshops, to prototype at least one SFSA. [I-VI]
7. **Ground Motion Simulation Validation.** Develop a set of validation procedures suitable for the application of ground motion simulations in seismic hazard analysis and earthquake engineering. Identify a set of ground motions recorded in large California earthquakes to use for validation. Use codes available in the CME to simulate the ground motions. Compare these simulations with the observed recordings and other empirical models where they are well-constrained. [VI]
8. **Source Modeling.** Support WGCEP in the development and release of UCERF3. Reduce the updating interval of the short-term forecasting models being tested in CSEP. Improve methods for detecting, classifying, and analyzing various types of seismic clustering. [II, V]
9. **Time-Dependent Earthquake Forecasting.** Support WGCEP in the development and release of UCERF3. Reduce the updating interval of the short-term forecasting models being tested in CSEP. Improve methods for detecting, classifying, and analyzing various types of seismic clustering. [II, V]

Year 2 (2013-2014)

1. **Improved Observations.** Begin cataloging SCEC-supported geochronology analyses available for Southern California. Complete cataloging validation earthquakes and associated source descriptions and strong ground motion observations for California for use in ground motion simulation validation. Start comparing InSAR and GPS data to flag any suspect data as a first step to integrated use of GPS and InSAR in the CGM. Start developing plans for enhanced seismic instrument deployments in the SFSA and elsewhere in Southern California. Update coordination of earthquake response capabilities of the SCEC community with partner organizations, including USGS, IRIS, and UNAVCO. [I-VI]
2. **Transient Geodetic Signals.** Increase the number of geodetic transient detection algorithms automated within CSEP that continuously operate on authoritative GPS data streams. Assess and refine detection thresholds through the use of synthetic data for a range of earthquake sizes for all operating detectors. [V]
3. **Community Modeling Environment.** Improve CVMs by applying full-3D waveform tomography to data from hundreds of earthquakes. Perform reference calculations and apply goodness-of-fit measures to evaluate CVMs against earthquake waveform data. Improve stochastic kinematic rupture models that incorporate source complexity observed in dynamic rupture simulations, including supershear rupture. Provide access to the UCERF3 statewide hazard model via the OpenSHA software platform. Develop methodology for calculating an extended ERFs based on UCERF3. [II, III, IV, VI]
4. **Community Geodetic Model.** Start generating a unified GPS time series dataset for secular and transient deformation and compiling LOS velocity maps from available SAR catalogs. Establish strategy for estimating secular rate as well as temporally variable signals (e.g., seasonal, postseismic). Assess the feasibility and the potential benefits of incorporating additional datasets (e.g., strainmeter, LiDAR) into CGM. Specify the CGM output needed for input to the CSM and transient detection and begin providing preliminary datasets as available. [I, II, V]
5. **Community Stress Model.** Populate the CSM data system with existing observational and model-based constraints. Begin coordination efforts with developers of the CGM and earthquake models. Investigate the variations in directions and magnitudes of the stresses and stressing rates predicted by different existing models. [I, II, IV]
6. **Special Fault Study Areas.** Solicit SFSA Science Plan(s) from the SCEC community and post Science Plan(s) for 2014 RFP on the website. Re-examine requirements for SFSA Science Plans. Evaluate whether SCEC should increase the number of SFSA-oriented studies in the SCEC base program. [I-VI]
7. **Ground Motion Simulation Validation.** Develop a list of metrics identified by earthquake scientists and engineers as needed to validate ground motion predictions for application to seismic hazard analysis and earthquake engineering. Use the observed ground motions of well-recorded California earthquakes to evaluate existing ground motion simulation methods and recommend improvements. Establish the Broadband Simulation Platform as a high-performance cyberfacility for ground motion simulation by outside research communities, including earthquake engineers. [III, VI]
8. **Source Modeling.** Develop numerical methods that simultaneously resolve fault zone processes and large-scale rupture, including fault interaction, complex geometries, heterogeneities and multiple fault physics. Assess data available to distinguish source from path/site effects at high frequencies. Develop a methodology for uncertainty quantification in finite-fault source inversion and back-projection source imaging, tested on standardized data sets. [III, VI]
9. **Time-Dependent Earthquake Forecasting.** Assess the capabilities of UCERF3 for time-dependent forecasting through comparisons with earthquake catalogs or synthetic catalogs from earthquake models. Through CSEP and in collaboration with the USGS and CGS, test the suitability of deploying UCERF3 as an operational

earthquake forecast. Couple UCERF3 to the Cybershake simulation suite for the Los Angeles region to prototype a time-dependent urban seismic hazard model. [II, VI]

10. **Progress Report on SCEC4 Problems.** Report to the SCEC4 community and Advisory Council on the progress made so far in formulating and testing hypotheses that address the six fundamental problem areas of earthquake physics.

Year 3 (2014-2015)

1. **Improved Observations.** Archive and make available at the SCEC waveforms, refined catalogs of earthquake locations and focal mechanisms for the period 1981-2013. Continue cataloging SCEC-supported geochronology analyses available for Southern California. Submit a proposal to NSF/Earthscope that focuses on high-resolution imaging of SFSAs and elsewhere in Southern California. Begin developing catalogs of prehistoric surface rupturing events along major faults in the system. [I-VI]
2. **Transient Geodetic Signals.** Using the first two years of results from Southern California, assess the capability and consistency of the geodetic transient detection procedures. Develop ensemble-based detection procedures that combine the output of multiple detection algorithms. [II, V]
3. **Community Modeling Environment.** Incorporate stochastic descriptions of small-scale heterogeneities into the upper layers of the CVMs and evaluate the importance of these heterogeneities in ground motion models. Integrate and evaluate a statewide unified CVM suitable for 3D ground motion modeling. Incorporate new information on fault complexity from SFA projects into the CFM. [II, III, IV, VI]
4. **Community Geodetic Model.** Assemble existing InSAR LOS velocity models and compile GPS solutions from multiple sources. Conduct comparisons among InSAR velocity models, among GPS solutions, and between InSAR and GPS LOS velocities to highlight areas of disagreement and determine likely sources of disagreement. Continue test exercise to identify best practices for InSAR time series analysis. [I, II, V]
5. **Community Stress Model.** Quantitatively assess discrepancies between various stress models. Begin the process of identifying classes of alternative stress models or branches for the CSM. [I, II, IV]
6. **Special Fault Study Areas.** Continue to execute coordinated plans for disciplinary fieldwork and interdisciplinary synthesis in SFSAs. Finalize the set of SFSAs to be investigated in SCEC4. [I-VI]
7. **Ground Motion Simulation Validation.** Develop scientific and engineering criteria for appropriate use of deterministic and stochastic ground motion simulations. Based on the Year-2 evaluation, assess how future SCEC simulation efforts can best assist seismic hazard analysis, risk analysis, and earthquake engineering. Implement in the Broadband Platform the capability to use more than one planar fault to describe an earthquake source's fault geometry. Examine SCEC4 research on dynamic weakening and the effect of geometrical heterogeneity on faulting and discuss if it is a sufficiently mature pathway to improve estimates of high-frequency wave excitation by seismic sources. [III, VI]
8. **Source Modeling.** Verify numerical methods and assess physical formulations of fault geometries. Develop and calibrate parameterization of resistance mechanisms that are suitable for large scale models of dynamic ruptures, including interaction with fault roughness and damage-zone properties. Develop improved source inversion approaches with enhanced information extraction from high frequencies, including by integration with back-projection imaging. [III, VI]
9. **Time-Dependent Earthquake Forecasting.** Develop approaches for using computational earthquake-cycle simulation models in forecasting. Employ these models for studying the predictability of large events and constraining seismic cycle parameters (maximum magnitude, inter-event time, etc.). Conduct prospective forecasting experiments in CSEP that test the key hypotheses that underlie time-dependent forecasting methods. [II]
10. **Progress Report on SCEC4 Problems.** Report to the SCEC4 Community and Advisory Council on the progress made so far in formulating and testing hypotheses that address the six fundamental problem areas of earthquake physics and report to SCEC4 community.

Year 4 (2015-2016)

1. **Improved Observations.** Refine catalogs of prehistoric surface rupturing events along major faults in the system and, if needed, document more events, including paleo-magnitudes, with more robust uncertainty measurements. Initiate the use of GPS data to better constrain 3D motion observed by InSAR, especially in the North/South direction. [I-VI]
2. **Transient Geodetic Signals.** Incorporate the CGM into the transient detection procedures as the reference model for time-dependent geodetic signals. Using the data collected in Southern California and elsewhere on geodetic transients, assess the observational constraints on the spectrum of deformation transients that might be associated with earthquake processes in San Andreas Fault system. [II, IV, V]
3. **Community Modeling Environment.** Develop a prototype CyberShake hazard model for the Los Angeles region based on extensions of UCERF3 and large suites of ground motion simulations up to 1 Hz calculated from improved CVMs. Provide interactive access to this layered seismic hazard model. [II, III, IV, VI]

SCEC4 SCIENCE MILESTONES

4. **Community Geodetic Model.** Develop consensus approach for InSAR LOS time series analysis constrained by GPS data. Identify appropriate methods for characterizing noise in GPS time series, estimating derived quantities from GPS time series, and interpolating GPS-derived quantities for use in InSAR analysis. Apply these approaches to GPS time series product to provide necessary GPS constraints for InSAR component of CGM. [I, II, V]
5. **Community Stress Model.** Populate branches of the CSM that represent alternative approaches, assumptions, and data. Develop new models of stress and stressing rate in the southern California lithosphere to address identified gaps in the CSM. Validate CSM models using relevant data and physical constraints. Begin applying results to the problem of discriminating between competing models of fault system loading. [I, II]
6. **Special Fault Study Areas.** Through workshops and other collaborative mechanisms, begin to synthesize SFSA results for integration into SCEC products and activities and address SCEC science questions. [I-VI]
7. **Ground Motion Simulation Validation.** Extend validation studies to high-frequency ground motion simulations that incorporate improved representations of source physics, source complexity, attenuation, non-linear effects, and high-frequency scattering by small-scale heterogeneities. [VI]
8. **Source Modeling.** Validate implementation for more realistic models of fault resistance evolution through dynamic rupture code comparisons and work towards incorporating them into CFM-based simulations of earthquakes. Compare fault interaction patterns from dynamic rupture models to earthquake simulators. Generate a uniform database of kinematic source models of past earthquakes and extract constraints on mechanical fault properties. Develop fundamental insight into source inversion uncertainties. [III, VI]
9. **Time-Dependent Earthquake Forecasting.** Develop earthquake forecasting algorithms and evaluate their utility in deploying new versions of a Uniform California Earthquake Rupture Forecast. [II]
10. **Progress Report on SCEC4 Problems.** Report on the progress made so far by SCEC4 investigations of the six fundamental problem areas of earthquake physics. Synthesize the current state of interdisciplinary knowledge in each of these problem areas, and evaluate which among the alternate hypotheses described in the SCEC4 proposal are now favored by the observational data and model-based constraints. This report will be used as input to the SCEC5 proposal. [I-VI]

Year 5 (2016-2017)

1. **Improved Observations.** Archive and make available at the SCEC waveforms, refined catalogs of earthquake locations and focal mechanisms for the period 1981-2015. Document results from significant earthquakes that occurred during SCEC4. Continue refinement of the catalog of prehistoric surface rupturing events along major faults in the system including realistic uncertainty estimates. Initiate new project for archiving and making available InSAR datasets from Sentinel and ALOS2 acquisitions, which pertain to geological problems being studied by SCEC investigators. Complete comparing InSAR and GPS data to flag any suspect anomalies in GPS data as a first step to resolving discrepancies between GPS and InSAR strain rates. [I-VI]
2. **Transient Geodetic Signals.** Using the data collected in Southern California and elsewhere on geodetic transients during SCEC4, assess the validated and potential utility of geodetic data in time-dependent earthquake forecasting. [II, IV, V]
3. **Community Modeling Environment.** Perform reference calculations and apply goodness-of-fit measures to evaluate a SCEC California statewide CVMs using earthquake waveform data. Calculate statewide CyberShake hazard model based on extensions of UCERF3, the California statewide CVM, and large suites of ground motion simulations up to 1 Hz. Provide interactive and programmable access to this layered seismic hazard model. [II, III, IV, VI]
4. **Community Geodetic Model.** Generate GPS-constrained InSAR LOS velocity product for all areas of southern California that are not decorrelated, GPS time series product comprised of southern California continuous and campaign data, GPS-derived quantities (e.g., secular rates, seasonal terms), and GPS and InSAR LOS velocities interpolated to common geographic grid. Demonstrate time series analysis best practices by producing combined InSAR-GPS LOS time series for geographic region used in test exercise. Document best practices and a framework for incorporating future observations. [I, II, V]
5. **Community Stress Model.** Release the final SCEC4 version of the CSM and assess its implications for earthquake physics. Recommend guidelines for future data collection and modeling studies to improve resolution of the CSM. [I, II]
6. **Special Fault Study Areas.** Publish synthesis studies of the SCEC4 SFSA's. Assess the utility of these syntheses in improving seismic hazard models for California. [I-VI]
7. **Ground Motion Simulation Validation.** Complete an evaluation of the simulated ground motions produced by the current versions of the Broadband Platform and the statewide CyberShake model. [VI]
8. **Source Modeling.** Develop realistic broadband kinematic source models of well-recorded earthquake in California that are consistent with source inversion and dynamic rupture modeling. Work with USGS/Golden to migrate improvements in source inversion into operational methods. [III, VI]

9. ***Time-Dependent Earthquake Forecasting.*** Use earthquake models, the CFM and CSM, and other modeling tools to quantify how fault-system complexities govern the probabilities of large earthquakes and rupture sequences. **[II]**
10. ***Progress Report on SCEC4 Problems.*** Conduct a final assessment of SCEC4 investigations of the six fundamental problem areas of earthquake physics, and evaluate the utility of new knowledge in time-independent and time-dependent seismic hazard analysis. **[I-VI]**

Draft 2015 Science Plan

SCEC Planning Committee, September 2014

I. What's New This Year

The Collaboration Plan is not greatly changed from last year. There are a number of small changes and suggestions throughout the document. The most substantial changes are

1. The 2015 Collaboration Plan recognizes that we do not anticipate developing additional SFSAs in SCEC4.
2. An explicit call for simulations of ruptures such as those defined in UCERF3.
3. A more detailed description of collaboration with the engineering community in validation of ground motion simulations and physics-based probabilistic seismic hazard models.
4. InSAR-only and GPS-only geodetic models are now encouraged by the geodesy group, particularly if they include a plan for assessing whether their results are in agreement or conflict with other data types.
5. An explicit call for archiving geodetic data.
6. A pathway for inclusion of operational transient detection algorithms into a testing framework.
7. A call for new approaches for assimilating real-time high-rate GPS, seismic data, and other potential observations into rapid source characterization.
8. Explicit calls by the Computational Science group for requests for allocations of resources, where appropriate.
9. A call to incorporate new data (especially from the Salton Sea Imaging Project) into the CVMs with validation of improvements for ground-motion prediction.
10. In several places a call for attention to the problem of off-fault plasticity and its effect on rupture and wave propagation.
11. More emphasis on ground motion validation for engineering metrics at high frequencies, on basin effects, and on the potential impact of distributed ground motions on extended infrastructure.

For more specific guidance on each of these changes please see the relevant section of the Collaboration Plan.

II. Preamble

The Southern California Earthquake Center (SCEC) coordinates basic research in earthquake science using Southern California as its natural laboratory. SCEC emphasizes the connections between information gathering by networks of instruments, fieldwork, and laboratory experiments; knowledge formulation through physics-based, system-level modeling; improved understanding of seismic hazard; and actions to reduce earthquake risk and promote resilience. The Center is a consortium of institutions that coordinates earthquake system science within Southern California. SCEC's long-term goal is to understand how seismic hazards change across all time scales of scientific and societal interest, from millennia to seconds. The fourth phase of SCEC (SCEC4) moves earthquake science forward through highly integrated collaborations that are coordinated across scientific disciplines and research institutions and enabled by high-performance computing and advanced information technology. It focuses on six fundamental problems of earthquake physics:

1. Stress transfer from plate motion to crustal faults: long-term fault slip rates.
2. Stress-mediated fault interactions and earthquake clustering: evaluation of mechanisms.
3. Evolution of fault resistance during seismic slip: scale-appropriate laws for rupture modeling.
4. Structure and evolution of fault zones and systems: relation to earthquake physics.
5. Causes and effects of transient deformations: slow slip events and tectonic tremor.
6. Seismic wave generation and scattering: prediction of strong ground motions.

The six fundamental problems constitute the basic-research focus of SCEC. They are interrelated and require an interdisciplinary, multi-institutional approach. Interdisciplinary research initiatives focuses on special fault study areas, the development of a community geodetic model for Southern California, and a community stress model. The latter is a new platform where the various constraints on earthquake-producing stresses are integrated. Improvements are also being made to SCEC's unified structural representation and its statewide extensions.

Collaboration Plan. On February 1, 2012, the Southern California Earthquake Center (SCEC) transitioned from SCEC3 to SCEC4 under joint funding from NSF/EAR and the U.S. Geological Survey. SCEC4 is funded for the period February 2012 through January 2017. This document, referred to as the Collaboration Plan, solicits proposals from individuals and groups to participate in the fourth year of the SCEC4 research program.

III. Guidelines for Proposal Submission

- A. **Due Date.** Friday November 7, 2014, 5:00 pm PST. Late proposals will not be accepted. Note the different deadline for submitting annual progress reports below.
- B. **Delivery Instructions.** Proposals must be submitted through the SCEC Proposal Submission System, accessible at <http://www.scec.org/proposals>. See "Formatting Instructions" below for requirements and procedure for submitting proposals.
- C. **Formatting Instructions.**

Cover Page. The cover page should be headed with the words "2015 SCEC Proposal" and include the Project Title, Principal Investigator(s), Institutional Affiliation(s), Amount of Request per Investigator, Total Amount of Request, and Proposal Category (see Section IV). Collaborative proposals involving multiple investigators and/or institutions should list all Principal Investigators. Proposals do not need to be formally signed by institutional representatives, and should be for one year, with a start date of February 1, 2015. Also on the cover page, list - in order of priority - three SCEC science objectives (Section VII) that your proposal addresses (e.g. 1a, 3c and 4b). If your proposal includes undergraduate student funding, please be sure to note this on the cover page.

Technical Description. In five pages maximum (including figures), describe the technical details of the proposed project and how it relates to the short-term objectives outlined in the SCEC Research Priorities and Requirements (Section VII). If the proposed project is a continuation of a previously funded SCEC project, the technical description must also include a one-page summary of previous research results. This research summary is part of the five-page limit. References are not included in the five-page limit. See note below on submission of collaborative proposals.

Budget Page. Budgets and budget explanations should be constructed using NSF categories (http://www.nsf.gov/pubs/policydocs/pappguide/nsf11001/gpg_2.jsp). Under guidelines of the SCEC Cooperative Agreements and A-21 regulations, secretarial support and office supplies are not allowable as direct expenses.

Current Support. Statements of current support should be included for each Principal Investigator, following NSF guidelines (http://www.nsf.gov/pubs/policydocs/pappguide/nsf11001/gpg_2.jsp). Any proposal without a current and pending support statement will not be reviewed.

Labeling the Submitted PDF Proposal. Proposals must be submitted as PDF documents and follow the SCEC proposal naming convention. Investigators must label their proposals with their last name followed by 2015 (e.g. Beroza2015.pdf). If there is more than one proposal, then the file should be labeled as follows: Beroza2015_1.pdf (for the 1st proposal) and Beroza2015_2.pdf (for the 2nd proposal).

2014 Annual Progress Report. Scientists funded by SCEC in 2014 must submit a progress report by March 15, 2015 (5:00 pm PST). Submission of this report is critical to preparing the annual progress report to the funding agencies. **To receive 2015 SCEC funding, all prior SCEC-funded project reports must be submitted and up to date.** Reports should be a maximum of five pages (text and figures). Reports should include references to any SCEC publication during the past year (including papers submitted and in review), including their SCEC contribution number. Publications are assigned numbers when they are submitted to the SCEC publication database (via <http://www.scec.org/signin>).

Special Note on Workshop Reports. Reports on results and recommendations of workshops funded by SCEC in 2015 are to be submitted no later than 30 days following the completion of the workshop. The reports will be posted on the SCEC website as soon as possible after review by SCEC directors.

- D. **Principal Investigator Responsibilities.** Principal investigators are expected to interact with other SCEC scientists on a regular basis (e.g., by attending the annual meeting and presenting results of SCEC-funded research in the poster sessions, workshops and working group meetings) and to contribute data, analysis results, and/or models to the appropriate SCEC data center (e.g., Southern California Earthquake Data Center—SCEDC), database, or community model (e.g., Community Velocity Model—CVM). Publications resulting entirely or partially from SCEC funding must include a publication number (<http://www.scec.org/core/cis/pubsearch.php>). By submitting a proposal, investigators are agreeing to these conditions.
- E. **Eligibility.** Proposals can be submitted by eligible Principal Investigators from:

DRAFT 2015 SCIENCE PLAN

- U.S. academic institutions
 - U.S. private corporations
 - International institutions (funding will mainly be for travel to SCEC-sponsored meetings in the U.S.) Due to limited funding, requests for travel to the SCEC annual meeting must be cost shared by the international participants. Cost sharing **must** be described in the proposal.
- F. **Collaborative Proposals.** Collaborative proposals with investigators from the USGS are encouraged. USGS employees should submit their requests for support through USGS channels.
- Collaborative proposals involving multiple investigators and/or institutions are strongly encouraged. A collaborative proposal should be submitted only by the lead investigator. Information on all investigators (including budgets and current support statements) must be included in the proposal submission. Collaborative proposals may include one extra page per investigator to report results of previous research.
- G. **Budget Guidance.** Typical SCEC grants funded under this Science Plan fall in the range of \$10,000 to \$35,000. This is not intended to limit SCEC to a fixed award amount, nor to a specified number of awards, rather it is intended to calibrate expectations for proposals written by SCEC investigators. **Field research investigations outside southern California will not be supported.**
- H. **Award Procedures.** The Southern California Earthquake Center is funded by the National Science Foundation and the U.S. Geological Survey through a cooperative agreement with the University of Southern California. All awards will be funded by subcontract from the University of Southern California.

IV. SCEC Organization

- A. **Mission and Science Goal.** SCEC is an interdisciplinary, regionally focused organization with a mission to:
- Gather data on earthquakes in Southern California and other places where such data has direct relevance to southern California
 - Integrate information into a comprehensive, physics-based understanding of earthquake phenomena
 - Communicate understanding to the world at large as useful knowledge for reducing earthquake risk
- SCEC's primary science goal is to develop a comprehensive, physics-based understanding of earthquake phenomena in Southern California through integrative, multidisciplinary studies of plate-boundary tectonics, active fault systems, fault-zone processes, dynamics of fault ruptures, ground motions, and seismic hazard analysis.
- B. **Disciplinary Activities.** The Center sustains disciplinary science through standing committees in Seismology, Geodesy, Geology, and Computational Science. These committees are responsible for planning and coordinating disciplinary activities relevant to the SCEC Science Collaboration Plan, and they will make recommendations to the SCEC Planning Committee regarding support of disciplinary research and infrastructure. High-priority disciplinary activities are summarized in Section VIII.
- C. **Interdisciplinary Focus Areas.** Interdisciplinary research is organized into science focus areas: Unified Structural Representation (USR), Fault and Rupture Mechanics (FARM), Stress and Deformation Over Time (SDOT), Earthquake Forecasting and Predictability (EFP), Ground Motion Prediction (GMP), Southern San Andreas Fault Evaluation (SOSAFE), and Earthquake Engineering Implementation Interface (EII). High-priority activities are listed for each of these interdisciplinary focus areas in Section IX.
- D. **Technical Activity Groups.** Various groups of experts have formed Technical Activity Groups (TAGs) to verify the complex computer calculations needed for wave propagation and dynamic earthquake rupture simulations, to assess the accuracy and resolving power of source inversions, and to develop geodetic transient detectors and earthquake simulators. TAGs can be thought of as "mini-collaboratories" that pose well-defined "standard problems", encourage solution of these problems by different researchers using different algorithms or codes, develop a common cyberspace for comparing solutions, and facilitate meetings to discuss discrepancies and potential improvements.
- E. **Communication, Education, and Outreach.** The theme of the CEO program during SCEC4 is *Creating an Earthquake and Tsunami Resilient California*. CEO will continue to manage and expand a suite of successful activities along with new initiatives, within four CEO interconnected thrust areas:
- a. The *Implementation Interface* connects SCEC scientists with partners in earthquake engineering research, and communicates with and trains practicing engineers and other professionals.
 - b. The *Public Education and Preparedness* thrust area educates people of all ages about earthquakes, and motivates them to become prepared.

- c. The *K-14 Earthquake Education Initiative* seeks to improve earth science education and school earthquake safety.
- d. Finally, the *Experiential Learning and Career Advancement* program provides research opportunities, networking, and more to encourage and sustain careers in science and engineering.

Opportunities for participating in the CEO program are described in Section XII.

V. Proposal Categories

- A. **Data Gathering and Products.** SCEC coordinates an interdisciplinary and multi-institutional study of earthquakes in Southern California, which requires data and derived products pertinent to the region. Proposals in this category should address the collection, archiving and distribution of data, including the production of SCEC community models that are online, maintained, and documented resources for making data and data products available to the scientific community.
- B. **Integration and Theory.** SCEC supports and coordinates interpretive and theoretical investigations on earthquake problems related to the Center's mission. Proposals in this category should be for the integration of data or data products from Category A, or for general or theoretical studies. Proposals in Categories A and B should address one or more of the goals in Section VII, and may include a brief description (<200 words) as to how the proposed research and/or its results might be used in a special initiative (see Section X) or in education and/or outreach (see Section XII).
- C. **Special Fault Study Areas.** Special Fault Study Areas (SFSA) are integrated, multidisciplinary projects focused on areas of complex fault behavior within southern California. There are two primary goals of SFSA, as articulated in the SCEC4 proposal: (1) To understand how fault complexities affect the propagation of earthquake ruptures and the heterogeneity of stress in the crust, and (2) To investigate how tremor and microseismicity (including induced seismicity) affect the nucleation of large earthquakes. Tackling these problems will require the assembly of teams of researchers with diverse expertise. For example, research areas of fault complexity may seek to merge geological, seismological, and potential-field data to elucidate fault structure and paleoseismic history, integrate this information with geodetic data to derive fault loading and stressing rates, and apply dynamic rupture simulations to explore how earth structure and rupture history affect the potential sizes of future earthquakes. One of the anticipated advantages of SFSA is to leverage the impact of new and/or densified instrumentation. It is expected that collaborations built around SFSA will be open to the community, and generate open community data sets.

There are two SFSAs established in SCEC4: the San Geronio and Ventura Area SFSAs. We are approaching the midpoint of SCEC4 and received substantial budget cuts in the second year. All signs point to continued tight funding. Given this combination of factors, we do not anticipate developing additional SFSAs in SCEC4.

SFSA Science Plans: The SFSA Science Plans that describe the general structure and scientific questions to be addressed by the group. The two SFSAs have had workshops with Science Plans to be written by SCEC investigators as an outcome. These two-page science plans are due with the SCEC 2014 proposals and should detail:

- Identification of key questions and research targets that address fundamental problems in earthquake science with an interdisciplinary plan for achieving these goals within SCEC4
- Discussion of integrative activities and broader impacts
- Assessment of resources needed to achieve these goals and identification of outside resources that may be required
- Timeline identifying short and long term goals and completion date

SCEC Proposals associated with a SFSA: Each PI should submit a separate, standard 5 page SCEC proposal that clearly ties the investigator's work to the Science Plan, provides additional background and details on the data collection and/or analyses to be completed by that investigator, and a budget for that investigator. Each investigator's proposal will be evaluated separately through the standard SCEC proposal process (see Evaluation Process and Criteria). Workshop proposals for activities around the SFSA should be developed according to the standard workshop proposal process as outlined in the Collaboration Plan. The SFSA website (<http://www.scec.org/research/sfsa.html>) contains details about the SFSA process and structure, updates from proposed SFSA, and contact information.

- D. **Workshops.** SCEC participants who wish to host a workshop between February 1, 2014 and January 31, 2015 should submit a proposal for the workshop in response to this Collaboration Plan.

DRAFT 2015 SCIENCE PLAN

Please notify Tran Huynh (scecmeet@usc.edu) before submitting the proposal if you want to organize a workshop around the time of the SCEC Leadership Retreat (June) or SCEC Annual Meeting (September). Note that workshops scheduled in conjunction with the SCEC Annual Meeting are restricted to half-day session only.

Workshops in the following topics are particularly relevant:

- Organizing collaborative research efforts for the five-year SCEC program (2012-2017). In particular, interactive workshops that engage more than one focus and/or disciplinary group are strongly encouraged.
 - Engaging earthquake engineers and other partner and user groups in SCEC-sponsored research.
 - Participating in national initiatives such as EarthScope, the Advanced National Seismic System (ANSS), and the George E. Brown, Jr. Network for Earthquake Engineering Simulation (NEES).
- E. **Communication, Education, and Outreach.** SCEC has developed a long-range CEO plan and opportunities for participation are listed in Section XII. Investigators who are interested in participating in this program should contact Mark Benthien (213-740-0323; benthien@usc.edu) before submitting a proposal.
- F. **SCEC/SURE Intern Project.** Each year SCEC coordinates the Summer Undergraduate Research Experience (SCEC/SURE) Program, which supports undergraduate students working one-on-one with SCEC scientists on diverse research projects. Recruitment for SURE intern mentors begins in the fall. Potential research projects are published on the SCEC Internships website (<http://www.scec.org/internships>), where undergraduate students may apply and identify their preferred projects. Interested SCEC scientists are encouraged to include support for an undergraduate SURE intern in their SCEC proposals. SURE mentors are required to provide at least \$2500 of the \$5000 intern stipend. Mentor contributions can come from any source, including SCEC-funded research projects.

Questions about the SCEC/SURE Program should be referred to Robert de Groot (degroot@usc.edu).

If your proposal includes undergraduate student funding, please be sure to note this on the cover page.

- G. **SCEC Annual Meeting participation.** This category includes proposals by investigators requesting travel funding only for participation at the SCEC Annual Meeting. Investigators who are (a) already funded to study projects that would be of interest to the SCEC community, and/or (b) new to SCEC who would benefit from exposure to the SCEC Annual Meeting in order to fine-tune future proposals are encouraged to apply.

VI. Evaluation Process and Criteria

- A. Proposals should be responsive to the Collaboration Plan. A primary consideration in evaluating proposals will be how directly the proposal addresses the main objectives of SCEC. Important criteria include (not necessarily in order of priority):
1. Scientific merit of the proposed research,
 2. Competence and performance of the investigators, especially in regard to past SCEC-sponsored research,
 3. Priority of the proposed project for short-term SCEC objectives as stated in the Collaboration Plan,
 4. Promise of the proposed project for contributing to long-term SCEC goals,
 5. Commitment of the principal investigator and institution to the SCEC mission,
 6. Value of the proposed research relative to its cost,
 7. Ability to leverage the cost of the proposed research through other funding sources,
 8. Involvement of students and junior investigators,
 9. Involvement of women and underrepresented groups, and
 10. Innovative or "risky" ideas that have a reasonable chance of leading to new insights or advances in earthquake physics and/or seismic hazard analysis.
- B. Proposals may be strengthened by describing:
1. Collaboration
 - Within a disciplinary or focus group
 - Between disciplinary and/or focus groups
 - In modeling and/or data gathering activities
 - With engineers, government agencies, and others.
 2. Leveraging additional resources
 - From other agencies

- From your institution
 - By expanding collaborations
3. Development and delivery of products
 - Community research tools, software, models, and databases
 - Collaborative research reports
 - Papers in research journals
 - End-user tools and products
 - Workshop proceedings and CDs
 - Fact sheets, maps, posters, public awareness brochures, etc.
 - Educational curricula, resources, tools, etc.
 4. Educational opportunities
 - Graduate student research assistantships
 - Undergraduate summer and year-round internships (funded by the project)
 - K-12 educator and student activities
 - Presentations to schools near research locations
 - Participation in data collection
- C. The Science Planning Committee is chaired by the Deputy Director and comprises the chairs of the disciplinary committees, focus groups, and special projects. All research proposals will be evaluated by the appropriate disciplinary committees, focus groups, or special projects; the Science Planning Committee Chair; and the Center Director. CEO proposals will be evaluated by the CEO Associate Director and the Center Director.
 - D. The Science Planning Committee is responsible for recommending a balanced science budget to the Center Director. Its recommendations will be combined into an annual spending plan and forwarded to the SCEC Board of Directors for approval.
 - E. Final selection of research projects will be made by the Center Director, in consultation with the Board of Directors.
 - F. The 2015 SCEC science plan and budget requires final review and approval by the NSF and USGS.
 - G. The review process should be completed and applicants notified by March 2015.

VII. Coordination of Research between SCEC and USGS-EHRP

Earthquake research in Southern California is supported both by SCEC and by the USGS Earthquake Hazards Program (EHP). EHP's mission is to provide the scientific information and knowledge necessary to reduce deaths, injuries, and economic losses from earthquakes. Products of this program include timely notifications of earthquake locations, size, and potential damage, regional and national assessments of earthquake hazards, and increased understanding of the cause of earthquakes and their effects. EHP funds research via its External Research Program, as well as work by USGS staff in its Pasadena, Menlo Park, Vancouver (WA), Seattle, and Golden offices. The EHP also directly supports SCEC.

SCEC and EHP coordinate research activities through formal means, including USGS membership on the SCEC Board of Directors and a Joint Planning Committee, and through a variety of less formal means. Interested researchers are invited to contact Dr. Rob Graves, EHP coordinator for Southern California, or other SCEC and EHP staff to discuss opportunities for coordinated research.

The USGS EHP supports a competitive, peer-reviewed, external program of research grants that enlists the talents and expertise of the academic community, state and local governments, and the private sector. The investigations and activities supported through the external program are coordinated with and complement the internal USGS program efforts. This program is divided into six geographical/topical 'regions', including one specifically aimed at Southern California earthquake research and others aimed at earthquake physics and effects and at probabilistic seismic hazard assessment (PSHA). The Program invites proposals that assist in achieving EHP goals.

The EHP web page, <http://earthquake.usgs.gov/research/external/>, describes program priorities, projects currently funded, results from past work, and instructions for submitting proposals. The EHP external funding cycle is several months offset from SCEC's, with the RFP due out in February and proposals due in May. Interested PIs are encouraged to contact the USGS regional or topical coordinators for Southern California, Earthquake Physics and Effects, and/or National (PSHA) research, as listed under the "Contact Us" tab.

The USGS internal earthquake research program is summarized by topic at <http://earthquake.usgs.gov/research/topics.php>.

VIII. SCEC4 Fundamental Problems of Earthquake Physics: Research Priorities and Requirements

The six fundamental problems constitute the basic-research focus of SCEC4 and are listed in the preamble. They are interrelated and require an interdisciplinary, multi-institutional approach. Interdisciplinary research initiatives focus on special fault study areas, the development of a community geodetic model for Southern California, and a community stress model. The latter is a new platform where the various constraints on earthquake-producing stresses can begin to be integrated. In addition, improvements are to be made to SCEC's unified structural representation and its statewide extensions.

1. *Stress transfer from plate motion to crustal faults: long-term fault slip rates.*

Priorities and Requirements

1a. Mapping and studying faults in Southern California to determine slip rates for faults at multiple time scales and characterize fault zone properties for which brittle/ductile transitions have been exposed by detachment faulting or erosion.

1b. Focused laboratory, numerical, and geophysical studies of the character of the lower crust, its rheology, stress state, and expression in surface deformation. We will use surface-wave dispersion to improve depth resolution relative to teleseismic studies.

1c. Regional searches for seismic tremor at depth in Southern California to observe if (some) deformation occurs by slip on discrete structures at depth.

1d. Development of a Community Geodetic Model (CGM) for California, in collaboration with the UNAVCO community, to constrain long-term deformation and fault-slip models.

1e. Combined modeling/inversion studies to interpret GPS and InSAR geodetic results on postseismic transient deformation without traditional simplifying assumptions.

2. *Stress-mediated fault interactions and earthquake clustering: evaluation of mechanisms*

Priorities and Requirements

2a. Improvement of earthquake catalogs, including non-point-source source descriptions, over a range of scales. Traditional aftershock catalogs can be improved through better detection of early aftershocks. Long-term (2000-yr) earthquake chronologies, including slip-per-event data, for the San Andreas Fault system and other major faults are necessary to constrain long-term recurrence behavior.

2b. Improved descriptions of triggered earthquakes. While temporal earthquake clustering behavior (Omori's Law) is well known, the spatial and coupled temporal-spatial behavior of triggered earthquakes, potentially key diagnostics, are not well constrained.

2c. Lowered thresholds for detecting aseismic and infraseismic transients, and improved methods for separating triggering by aseismic transients from triggering by other earthquakes.

2d. Development of a Community Stress Model (CSM) for Southern California, based on merging information from borehole measurements, focal mechanisms, paleo-slip indicators, observations of damage, topographic loading, geodynamic and earthquake-cycle modeling, and induced seismicity. Use of seismicity to constrain CSM and investigate how stress may control earthquake clustering and triggering. Collaboration with other organizations in fault-drilling projects for in situ hypothesis testing of stress levels.

2e. Development of physics-based earthquake simulators that can unify short-term clustering statistics with long-term renewal statistics, including the quasi-static simulators that incorporate laboratory-based nucleation models.

2f. Development of a better understanding of induced seismicity, specifically induced by geothermal power production in the Salton Sea area, which warrant study as potential hazards.

3. *Evolution of fault resistance during seismic slip: scale-appropriate laws for rupture modeling*

Priorities and Requirements

3a. Analysis of laboratory experiments on fault materials under appropriate confining stresses, temperatures, and fluid contents/pressures through targeted experiments in collaboration with rock mechanics laboratories.

3b. Observations of geological, geochemical, paleo-temperature, microstructural, and hydrological indicators of specific resistance mechanisms that can be measured in the field. In particular, evidence of thermal decomposition in exhumed fault zones. Collaboration with other organizations involved in fault-drilling projects to measure observables for constraining coseismic resistance mechanisms, such as the temperature on faults before and after earthquakes.

3c. Formulation of theoretical and numerical models of specific fault resistance mechanisms for seismic radiation and rupture propagation, including interaction with fault roughness and damage-zone properties.

3d. Development of parameterized fault rheologies suitable for coarse-grained numerical modeling of rupture dynamics and for simulations of earthquake cycles on interacting fault systems. (Currently, the constitutive laws for co-seismic slip are often represented as complex coupled systems of partial differential equations, contain slip scales of the order of microns to millimeters, and hence allow detailed simulations of only small fault stretches.)

3e. Construction of computational simulations of dynamic earthquake ruptures to help constrain stress levels along major faults, to help explain the heat-flow paradox, and to help us understand extreme slip localization, the dynamics of self-healing ruptures, and the potential for repeated slip on faults during earthquakes.

3f. Development of computational earthquake-cycle simulators that can incorporate realistic models of fault-resistance evolution during earthquake cycles and the wave-propagation that occurs during seismic events.

4. *Structure and evolution of fault zones and systems: relation to earthquake physics*

Priorities and Requirements

4a. Detailed geologic, seismic, geodetic, and hydrologic investigations of fault complexities at Special Fault Study Areas and other important regions.

4b. Investigations of along-strike variations in fault roughness and complexity (including slip rate and geometry) as well as the degree of localization and damage perpendicular to the fault.

4c. Improvements to the CFM using better mapping, including LiDAR, and precise earthquake relocations. We will also extend the CFM to include spatial uncertainties and stochastic descriptions of fault heterogeneity.

4d. Use of special fault study areas to model stress heterogeneities both deterministically and stochastically. We will integrate the results of these special studies into the CSM.

4e. Use of earthquake simulators and other modeling tools, together with the CFM and CSM, to quantify how large-scale fault system complexities govern the probabilities of large earthquakes and rupture sequences.

5. *Causes and effects of transient deformations: slow slip events and tectonic tremor*

Priorities and Requirements

5a. Improvement of detection and mapping of the distribution of tremor across southern California by applying better instrumentation and signal-processing techniques to data collected in the special study areas, such as those outlined in the proposal.

5b. Application of geodetic detectors to the search for aseismic transients across southern California. We will use the CGM as the time-dependent geodetic reference frame for detecting geodetic anomalies.

5c. Collaboration with rock mechanics laboratories on laboratory experiments to understand the mechanisms of slow slip and tremor.

5d. Development of physics-based models of slow slip and tectonic tremor. We will constrain these models using features of tremor occurrence and its relationship to seismicity, geodetic deformation, and tectonic environment, as well as laboratory data.

5e. Use of physics-based models to understand how slow slip events and tremor activity affect earthquake probabilities in Southern California.

6. *Seismic wave generation and scattering: prediction of strong ground motions*

Priorities and Requirements

6a. Development of a statewide anelastic Community Velocity Model (CVM) that can be iteratively refined through 3D waveform tomography. Integration of new data (especially the Salton Sea Imaging Project) into the existing CVMs with validation of improvements in the CVMs. We will extend current methods of full-3D tomography to include ambient-noise data and to estimate seismic attenuation, and we will develop methods for estimating and representing CVM uncertainties.

6b. Modeling of ruptures that includes realistic dynamic weakening mechanisms, off-fault plastic deformation, and is constrained by source inversions. The priority is to produce physically consistent rupture models for broadband ground motion simulations of hazard-scale ruptures, such as the ruptures defined in UCERF3. An important issue is how to treat multiscale processes; specifically, does off-fault plasticity regularize the Lorentzian scale collapse associated with strong dynamic weakening? If not, how can adaptive meshing strategies be most effectively used to make full-physics simulations feasible?

6c. Development of stochastic representations of small-scale velocity and attenuation structure in the CVM for use in modeling high-frequency (> 1 Hz) ground motions. We will test the stochastic models with seismic and borehole logging data and evaluate their transportability to regions of comparable geology.

6d. Measurement of earthquakes with unprecedented station density using emerging sensor technologies (e.g., MEMS). The SCEC Portable Broadband Instrument Center will work with IRIS to make large portable arrays available for aftershock and flexible array studies.

6e. Measurement of earthquakes with unprecedented station density using emerging sensor technologies (e.g., MEMS). The SCEC Portable Broadband Instrument Center will work with IRIS to make large portable arrays available for aftershock and flexible array studies.

IX. Disciplinary Activities

The Center will sustain disciplinary science through standing committees in Seismology, Geodesy, Geology, and Computational Science. These committees will be responsible for planning and coordinating disciplinary activities relevant to the SCEC Science Collaboration Plan, and they will make recommendations to the SCEC Planning Committee regarding the support of disciplinary infrastructure. High-priority disciplinary objectives include the following tasks:

A. Seismology

Objectives

The objectives of the Seismology group are to gather data on the range of seismic phenomena observed in southern California and to integrate these data into physics-based models of fault slip. Of particular interest are proposals that foster innovations in network deployments, data collection, real-time research tools, and data processing. Proposals that provide community products that support one or more of the SCEC4 goals or those that include collaboration with network operators in Southern California are especially encouraged. Proposers should consider the SCEC resources available including the Southern California Earthquake Data Center (SCEDC) that provides extensive data on Southern California earthquakes as well as crustal and fault structure, the network of SCEC funded borehole instruments that record high quality reference ground motions, and the pool of portable instruments that is operated in support of targeted deployments or aftershock response.

Example Research Strategies

- Enhancement and continued operation of the SCEDC and other existing SCEC facilities particularly the near-real-time availability of earthquake data from SCEDC and automated access.
- Real-time processing of network data such as improving the estimation of source parameters in relation to faults, especially evaluation of the short-term evolution of earthquake sequences and real-time stress perturbations on major fault segments.
- Enhance or add new capabilities to existing earthquake early warning (EEW) systems or develop new EEW algorithms. Develop real-time finite source models constrained by seismic and GPS data to estimate evolution of rupture and potentially damaging ground shaking; develop strategies for robust uncertainty quantification in finite-fault rupture models.
- Advance innovative and practical strategies for densification of seismic instrumentation, including borehole instrumentation, in Southern California and develop innovative algorithms to utilize data from these networks. Develop metadata, archival and distribution models for these semi-mobile networks.
- Develop innovative methods to search for unusual signals using combined seismic, GPS, and borehole strainmeter data; collaborations with EarthScope or other network operators are encouraged.
- Investigate near-fault crustal properties, evaluate fault structural complexity, and develop constraints on crustal structure and state of stress.
- Collaborations, for instance with the ANSS and NEES projects, that would augment existing and planned network stations with downhole and surface instrumentation to assess site response, nonlinear effects, and the ground coupling of built structures.
- Preliminary design and data collection to seed future passive and active experiments such as dense array measurements of basin structure and large earthquake properties, OBS deployments, and deep basement borehole studies.
- Improve locations of important historical earthquakes.

Priorities for Seismology in 2015

1. **Tremor.** Tremor has been observed on several faults in California, yet it does not appear to be ubiquitous. We seek proposals that explore the distribution and source characteristics of tremor in California and those that explore the conditions necessary for the generation of seismically observable tremor.
2. **Low-cost seismic network data utilization and archiving.** Several groups are developing seismic networks that use low-cost MEMS accelerometers. We seek proposals that would address development of seismological algorithms to utilize data from these networks in innovative ways. We also seek proposals that would develop metadata and archiving models for these new semi-mobile networks, as well as archive and serve these data to the SCEC user community.
3. **Short-Term Earthquake Predictability.** We seek proposals that develop new methods in earthquake statistics or analyze seismicity catalogs to develop methods for determining short-term (hours to days) earthquake probability gain.
4. **Seismicity studies in the two SFSA; Ventura and San Geronio.** We seek proposals that use earthquake data to map the structure and seismotectonics of these regions as part of the SFSA community effort.

B. Tectonic Geodesy

Tectonic Geodesy activities in SCEC4 will focus on data collection and analysis that contribute to improved earthquake response and to a better understanding of fault loading and stress transfer, the causes and effects of transient deformation, and the structure and evolution of fault zones and systems. The following are research strategies aimed at meeting these broad objectives:

1. **Contribute to the development of a Community Geodetic Model (CGM).** The goal of this effort is to develop a time-dependent geodetic data product for southern California that leverages the complementary nature of GPS and InSAR time series data. The resulting product will consist of well-constrained, temporally and spatially dense horizontal and vertical displacement time series that can be used in meeting a variety of SCEC4 objectives. This will require development of optimal methods for combining GPS and InSAR data, characterizing seasonal/hydrologic/anthropogenic signals, incorporating new data, and accounting for earthquake effects as needed. Proposals should demonstrate coordination with the overall activities and timeline of the CGM project including group efforts to compile GPS data and compare InSAR analysis techniques. More information can be found here: <http://collaborate.scec.org/cgm>. InSAR-only and GPS-only models are also encouraged, particularly if they include a plan for assessing whether their results are in agreement or conflict with the data types not used to generate them.
2. **Analysis of geodetic data to address specific SCEC4 research targets.** Studies addressing geodetic/geologic slip rate discrepancies, assessing the role of lower crust/upper mantle processes in driving fault loading, developing more physically realistic deformation models, providing input to the development of Community Stress Models, and constraining physics-based models of slow slip and tremor are encouraged, as are studies that pursue integrated use of geodetic, geologic, seismic, and other observations targeting special fault study areas. Proposals that include collection of new data should explicitly motivate the need for such efforts. In compliance with SCEC's data policy, data collected with SCEC funding must be made publicly available upon collection by archiving at an appropriate data center such as UNAVCO; (contact *Jessica Murray* for further information on archiving options). Annual reports should include a description of archive activities.
3. **Improve our understanding of the processes underlying detected transient deformation signals and/or their seismic hazard implications through data collection and development of new analysis tools.** Work that advances methods for near-real-time transient detection and applies these algorithms within the SCEC transient detection testing framework to search for transient deformation in southern California is encouraged. Approaches that can be automated or semi-automated are the highest priority, as is their inclusion in the testing framework now in place at SCEC (contact *Rowena Lohman* for details on how to address this in the proposal). Extension of methods to include InSAR and strainmeter data and, when available, the CGM is also a priority. Work that develops means for incorporating the output of transient detection algorithms into time-dependent earthquake forecasting is encouraged.
4. **Develop and apply algorithms that use real-time high-rate GPS data in concert with seismic data for improved earthquake response.** We encourage proposals that explore new approaches for assimilating real-time high-rate GPS, seismic data, and other potential observations into efforts to rapidly characterize earthquake sources. Also of interest is the development and application of rigorous retrospective and prospective tests to evaluate algorithm performance.

C. Earthquake Geology

Objectives

The Earthquake Geology Disciplinary Committee promotes studies of the geologic record of the Southern California natural laboratory that advance SCEC science. Its primary focus is on the Late Quaternary record of faulting and ground motion, including data gathering in response to major earthquakes. Geologic observations provide important contributions, either directly or indirectly, to all six of the fundamental problems in earthquake physics identified in the SCEC4 proposal. Earthquake Geology also fosters research activities motivated by outstanding seismic hazard issues, understanding of the structural framework and earthquake history of special fault study areas (see Section VII, Problem 4), or will contribute significant information to the statewide Unified Structural Representation. Collaborative proposals that cut across disciplinary boundaries are encouraged.

Example Research Strategies

- Gathering well-constrained slip-rates on the southern California fault system, with emphasis on major structures (Problem 1).
- Mapping and analysis of fault-zone properties where the seismogenic zone or brittle-ductile transition has been exhumed (Problems 1a, 3b).
- Paleoseismic documentation of earthquake ages and displacements, with emphasis on long paleoseismic histories, slip-per-event, and slip-rate histories, including a coordinated effort to develop slip rates and slip-per-event history of southern San Andreas fault system (Problem 2a, in collaboration with the SoSAFE focus group).
- Improve understanding of the architecture and tectonic activity of the Ventura and San Geronio Pass special fault study areas (Problem 4a), such as using B4 and other lidar data sets to better define fault traces, fault activity, and geologic structure.
- Improve the statewide community fault model in areas of inadequate fault representations or where new data is available, such as using high-resolution topographic data sets to better define fault traces, spatial uncertainty, and stochastic heterogeneity of fault geometry (Problem 4c).
- Quantifying along-strike variations in fault roughness, complexity, strain localization, and damage in relation to the rupture propagation processes, including evaluation of the likelihood of multi-fault ruptures (Problem 4b).
- Validation of ground motion prediction through analysis and dating of precariously balanced rocks and other fragile geomorphic features (Problem 6).

Geochronology Infrastructure

The shared geochronology infrastructure supports C-14, optically stimulated luminescence (OSL), and cosmogenic dating for SCEC-sponsored research. The purpose of shared geochronology infrastructure is to allow flexibility in the number and type of dates applied to each SCEC-funded project as investigations proceed. Investigators requesting geochronology support should clearly state in their proposal an estimate of the number and type of dates required. For C-14 specify if sample preparation will take place at a location other than the designated laboratory. For cosmogenic dating, investigators are required to arrange for sample preparation. Sample preparation costs must be included in the proposal budget unless preparation has been pre-arranged with one of the laboratories listed. Investigators are strongly encouraged to contact the investigators at the collaborating laboratories prior to proposal submission. Currently, SCEC geochronology has established relationships with the following laboratories:

- C-14: University of California at Irvine (John Southon, jsouthon@uci.edu) and Lawrence Livermore National Laboratory (Tom Guilderson, tguilderson@llnl.gov),
- OSL: University of Cincinnati (Lewis Owen, lewis.owen@uc.edu) and Utah State University (Tammy Rittenour, tammy.rittenour@usu.edu), and
- Cosmogenic: Lawrence Livermore National Laboratory (Susan Zimmerman, zimmerman17@llnl.gov).

Investigators may alternatively request support for geochronology outside of the infrastructure proposal for methods not listed here or if justified on a cost-basis. These outside requests must be included in the individual proposal budget. Please direct questions regarding geochronology infrastructure to the Earthquake Geology group leader, Mike Oskin (meoskin@ucdavis.edu).

Data Reporting Requirements

Studies under Earthquake Geology gather diverse data that are at times challenging to consistently archive per NSF data reporting requirements. Under SCEC4, PIs will be required to provide full reporting of their geochronology samples, including raw data, interpreted age, and geographic/stratigraphic/geomorphic context (what was dated?). This reporting requirement

will be coordinated with the geochronology infrastructure program. A priority for SCEC4 is to define additional, achievable goals for geology data reporting to be followed by Earthquake Geology community.

Priorities for Earthquake Geology

- Support integrative research at the Ventura and San Geronio Pass special fault study areas. A specific need for this upcoming year is to analyze existing lidar data sets for these areas and assess whether new data are needed.
- Prioritize and coordinate research objectives with respect to SoSAFE focus group goals, targets for slip-rate studies, and mechanisms to achieve progress on exhumed fault-zone problems.
- Define consistent and achievable data reporting requirements for Earthquake Geology in SCEC4. Archive data from SCEC3.
- Improve understanding of the seismogenic faults along the coast and offshore.

D. Computational Science

Objectives

The Computational Science group promotes the use of advanced numerical modeling techniques and high performance computing (HPC) to address the emerging needs of SCEC users and application community on HPC platforms. The group works with SCEC scientists across a wide range of topics to take advantage of rapidly changing computer architectures and algorithms. It also engages and coordinates with national HPC labs/centers and vendors in crosscutting efforts enabling large-scale computing milestones. The group encourages research using national supercomputing resources, and supports students from both geoscience and computer science backgrounds to develop their skills in the area. Projects listing Computational Science as their primary area should involve significant software-based processing or high performance computing in some way; research utilizing standard desktop computing should list the most relevant non-Computational Science disciplinary or focus group as the primary area.

Computational Requirements

If your proposed research will require substantial SCEC computing resources or allocations, the Planning Committee requests that your SCEC proposal include a brief summary of computational requirements that includes the following information:

1. The scientific goal of your computational research
2. The scientific software you plan to use or develop
3. A list of computations you plan to run
4. The estimated computing time and/or storage space you believe will be required
5. The computer resources you plan to use to perform your simulations

Note that XSEDE startup allocations can be requested from NSF (<https://www.xsede.org/allocations>).

Example Research Strategies

1. Porting and optimization of HPC codes, required to reach SCEC research goals, and utilize hybrid programming models, combined with shared memory directives (e.g. OpenMP) and/or accelerator-programming APIs (e.g. OpenACC, pthreads) and languages (e.g. OpenCL, CUDA) to take advantage of advanced multi-core, many-core and/or next-generation heterogeneous architectures.
2. Novel algorithms for earthquake simulation, particularly those that either improve efficiency and accuracy or expand the class of problems that can be solved (e.g., adaptive mesh refinement).
3. Optimization of earthquake simulators that can resolve the faulting processes across the range of scales required to investigate stress-mediated fault interaction, including those caused by dynamic wave propagation, generate synthetic seismicity catalogs, and assess the viability of earthquake rupture forecasts.
4. Tools and algorithms for uncertainty quantification in large-scale inversion and forward-modeling studies, for managing I/O, data repositories, workflow and data analysis, fault tolerance, and advanced seismic data format.
5. Data-intensive computing tools, including but not limited to InSAR and geodesy, 3D tomography, cross-correlation algorithms used in ambient noise seismology, and other signal processing techniques used, for example, to search for tectonic tremor.

Key Problems in Computational Science

DRAFT 2015 SCIENCE PLAN

1. Seismic wave propagation
 - Validate SCEC community velocity models.
 - Develop high-frequency simulation methods and investigate the upper frequency limit of deterministic ground motions.
 - Extend existing simulation methodologies to a set of stochastic wavefield simulation codes that can extend the deterministic calculations to frequencies as high as 20 Hz, providing the capability to synthesize “broadband” seismograms.
 - Develop wave propagation codes incorporating more advanced physics, including inelastic material response and scattering by small-scale heterogeneities and topography.
2. Tomography
 - Assimilate regional waveform data into the SCEC community velocity models.
3. Rupture dynamics
 - Evaluate proposed fault weakening mechanisms in large-scale earthquake simulations, determine if small-scale physics is essential or irrelevant, and determine if friction law parameters can be artificially enhanced without compromising ground motion predictions.
 - Evaluate different representations of source complexity, including stress heterogeneity, variability in frictional properties, fault geometrical complexity, and dynamic rupture propagation in heterogeneous media.
4. Scenario earthquake modeling
 - Model a suite of scenario ruptures, incorporating material properties and fault geometries from the unified structural representation projects.
 - Isolate causes of enhanced ground motion using adjoint-based sensitivity methods.
5. Data-intensive computing
 - Develop computational tools for advanced signal processing algorithms, such as those used in ambient noise seismology and tomography, as well as InSAR and other forms of geodesy.
6. Engineering applications
 - Investigate the implications of ground motion simulation results by integrating observed and simulated ground motions with engineering-based building response models. Validate the results by comparison to observed building responses.
 - Facilitate the “rupture-to-rafters” modeling capability to transform earthquake risk management into a Cyber Science and Engineering discipline.

X. Interdisciplinary Focus Areas

Interdisciplinary research will be organized into seven science focus areas: Unified Structural Representation (USR), Fault and Rupture Mechanics (FARM), Stress and Deformation Over Time (SDOT), Earthquake Forecasting and Predictability (EFP), Ground Motion Prediction (GMP) Southern San Andreas Fault Evaluation (SOSAFE) and Earthquake Engineering Implementation Interface (EElI). Collaboration within and across focus areas is strongly encouraged.

A. Unified Structural Representation (USR)

The Unified Structural Representation group develops three-dimensional models of active faults and earth structure (velocity, density, attenuation, etc.) for use in fault-system analysis, ground-motion prediction, and hazard assessment. This year’s efforts will focus on (1) making improvements to existing community models (CVM, CFM) that will facilitate their uses in SCEC science, education, and post-earthquake response planning; (2) developing methods to represent smaller scale features, such as stochastic variations of seismic velocities and attenuation structure; and (3) improving IT tools that are used to deliver the USR components to the user community.

- **Community Velocity Model (CVM).** Improve the current SCEC CVMs, with emphasis on more accurate representations of V_p , V_s , density, attenuation, and basin structure. Incorporate new data (especially results from the Salton Sea Imaging Project) into the CVMs with validation of improvements for ground-motion prediction. Perform 3D waveform tomographic inversions and ambient noise analysis for evaluating and improving the CVMs. Develop and apply procedures (i.e., goodness-of-fit measures) for evaluating new models with data (e.g., waveforms, gravity) to distinguish alternative representations and quantify model uncertainties;

apply these methods for well-recorded earthquakes in southern California to delineate areas where CVM updates are needed. Develop databases, models, and model building tools that will help facilitate expansion of the CVMs to statewide and plate-boundary scale velocity representations. These efforts should be coordinated with the SCEC CME special project.

- **Community Fault Model (CFM).** Improve and evaluate the CFM and statewide CFM (SCFM), placing emphasis on defining the geometry of major faults that are incompletely, or inaccurately, represented in the current model, and on faults of particular concern, such as those that are located close to critical facilities. Refine representations of the linkages among major fault systems. Extend the CFM to include spatial uncertainties and stochastic descriptions of fault heterogeneity. Evaluate the new CFM version (5.0) with data (e.g., seismicity, seismic reflection profiles, geologic slip rates, and geodetic displacement fields) to distinguish alternative fault models. Update the CFM-R (rectilinear fault model) to reflect improvements in the CFM. Develop new tools and formats for making the CFM geometries and properties available to the user community. Work on the statewide CFM in regions outside the SCEC CFM should be coordinated with the appropriate agencies (e.g., USGS for central and northern CA).
- **Unified Structural Representation (USR).** Develop better IT mechanisms for delivering the USR, particularly the CVM parameters and information about the model's structural components, to the user community for use in generating and/or parameterizing numerical models. Generate maps of geologic surfaces compatible with the CFM that may serve as strain markers in crustal deformation modeling and/or property boundaries in future iterations of the USR.

B. Fault and Rupture Mechanics (FARM)

The primary mission of the Fault and Rupture Mechanics focus group in SCEC4 is to develop physics-based models of the nucleation, propagation, and arrest of dynamic earthquake rupture. We specifically solicit proposals that will contribute to the six fundamental problems in earthquake physics defined in the SCEC4 proposal and enhance understanding of fault system behavior through interdisciplinary investigation of the special fault study areas. We encourage researchers to address this mission through field, laboratory, and modeling efforts directed at characterizing and understanding the influence of material properties, geometric irregularities and heterogeneities in stress and strength over multiple length and time scales, and that will contribute to our understanding of earthquakes in the Southern California fault system.

Priorities for FARM in 2015

- Investigate the relative importance of different dynamic weakening and fault healing mechanisms, and the slip and time scales over which these mechanisms operate (3a, 3b, 3c, 3e).
- Determine the properties of fault cores and damage zones (1a, 1b, 3a, 3b, 4a, 4b) and characterize their variability with depth and along strike (1a, 1b, 4a, 4b) to constrain theoretical and laboratory studies, including width and particle composition of actively shearing zones, signatures of temperature variations, extent, origin and significance of on- and off-fault damage, healing, and poromechanical behavior.
- Determine the relative contribution of on- and off-fault damage to the total earthquake energy budget (3c, 4a, 4b), and the absolute levels of local and average stress (3e). Collaboration with the Community Stress Model (CSM) TAG is encouraged.
- Develop, test, and apply innovative source-inversion strategies to image the space-time rupture evolution of earthquakes reliably, propose source-inversion methods with minimal assumptions, and provide robust uncertainty quantification of inferred source parameters; collaboration with the Technical Activity Group (TAG) on Source Inversion Validation (SIV) is encouraged.
- Develop realistic descriptions of heterogeneity in fault geometry, rock properties, stresses and strains, and tractable ways to incorporate heterogeneity in numerical models of single dynamic rupture events and multiple earthquake cycles (3e, 3f, 4b, 4d, 6b). Test dynamic rupture modeling that incorporates these heterogeneities first by verifying the computational algorithms with benchmark exercises of the Dynamic Rupture Code Verification Technical Activity Group (TAG), then by comparing the results with geological and geophysical observations.
- Understand the significance of fault zone characteristics and processes for fault dynamics (3a, 3b, 3c) and formulate constitutive laws for use in dynamic rupture models (3d).
- Evaluate the relative importance of fault structure and branching, material properties, interseismic healing, fluid processes and prior seismic and aseismic slip to earthquake dynamics, in particular, to rupture initiation, propagation, and arrest, and the resulting ground motions (3c, 3d, 3f).
- Characterize earthquake rupture, fault loading, degree of localization, role of fluids and constitutive behavior at the base of and below the seismogenic zone (1a, 1b, 1e, 4a).

DRAFT 2015 SCIENCE PLAN

- Develop observations of slow slip events and non-volcanic tremors in southern California and understand their implications for constitutive properties of faults and overall seismic behavior (3a, 5a-5e).
- Assess the predictability of rupture direction and directivity of seismic radiation by collecting and analyzing field and laboratory data (4a, 4b), and conducting theoretical investigations to understand implications for strong ground motion.
- Develop physics-based models that can describe spatio-temporal patterns of seismicity and earthquake triggering (2e, 4e).
- Explore similarities between earthquakes and offshore landslide sources with the goal of better understanding their mechanics and the tsunami hazard from sources in southern California.

C. Stress and Deformation Over Time (SDOT)

The focus of the interdisciplinary focus group Stress and Deformation Over Time (SDOT) is to improve our understanding of how faults are loaded in the context of the wider lithospheric system evolution. SDOT studies these processes on timescales from 10s of Myr to 10s of yrs, using the structure, geological history, and physical state of the southern California lithosphere as a natural laboratory. The objective is to tie the present-day state of stress and deformation on crustal-scale faults and the lithosphere as a whole to the long-term, evolving lithospheric architecture, through 4D geodynamic modeling, constrained by the widest possible range of observables from disciplines including geodesy, geology, and geophysics.

One long-term goal is to contribute to the development of a physics-based, probabilistic seismic hazard analysis for southern California by developing and applying system-wide deformation models of lithospheric processes at time-scales down to the earthquake cycle. These deformation models require a better understanding of a range of fundamental questions such as the forces loading the lithosphere, the relevant rock rheology, fault constitutive laws, and the spatial distribution of absolute deviatoric stress. Tied in with this is a quest for better structural constraints, such as on density, Moho depths, thickness of the seismogenic layer, the geometry of lithosphere-asthenosphere boundary, as well as basin depths, rock type, temperature, water content, and seismic velocity and anisotropy.

Projects Solicited for SDOT

- Contributions to our understanding of geologic inheritance and evolution, and its relation to the three-dimensional structure and physical properties of present-day crust and lithosphere. Contributions to efforts of building a 4D model of lithospheric evolution over 10s of Myr for southern California.
- Seismological imaging of crust, lithosphere and upper mantle using interface and transmission methods with the goal of characterizing the 3D distribution of isotropic and anisotropic wave speed variations.
- Contributions to the development of a Community Stress Model (CSM), a set of spatio-temporal (4D) representations of the stress tensor in the southern California lithosphere. In particular, we seek compilations of diverse stress constraints (e.g. from borehole or anisotropy measurements), geodynamic models that explore the coupling of side, gravity, and basal loading to observed geodetic strain-rates and co-seismically imaged stress, and studies that explore regional, well-constrained settings as test cases for larger scale models.
- General geodynamic models of southern California dynamics to allow hypothesis testing on issues pertaining to post-seismic deformation, fault friction, rheology of the lithosphere, seismic efficiency, the heat flow paradox, stress and strain transients, fault system evolution, as tied in with stress and deformation measurements across scales.
- Development of models of interseismic and earthquake cycle deformation, including efforts to estimate slip rates on southern CA faults, fault geometries at depth, and spatial distribution of slip or moment deficits on faults. Assessments of potential discrepancies of models based on geodetic, geologic, and seismic data. Development of deformation models (fault slip rates and locking depths, off-fault deformation rates) in support of earthquake rupture forecasting.
- Research into averaging, simplification, and coarse-graining approaches across spatio-temporal scales, addressing questions such as the appropriate scale for capturing fault interactions, the adequate representation of frictional behavior and dynamic processes in long-term interaction models, fault roughness, structure, complexity and uncertainty. Modeling approaches may include analytical or semi-analytical methods, spectral approaches, boundary, finite, or distinct element methods, and a mix of these, and there are strong links with all other SCEC working groups, including FARM, Earthquake Simulators, and USR.

D. Earthquake Forecasting and Predictability (EFP)

The Earthquake Forecasting and Predictability (EFP) focus group coordinates five broad types of research projects: (1) the development of earthquake forecast methods, (2) the development of testing methodologies for evaluating the performance of earthquake forecasts, (3) expanding fundamental physical or statistical knowledge of earthquake behavior that may be

relevant for forecasting earthquakes, (4) the development and use of earthquake simulators to understand predictability in complex fault networks, and (5) fundamental understanding of the limits of earthquake predictability.

We seek proposals that will increase our understanding of how earthquakes might be forecast, to what extent and precision earthquakes are predictable, and what is a physical basis for earthquake predictability. Proposals of any type that can assist in this goal will be considered. In order to increase the amount of analyzed data, and so decrease the time required to learn about predictability, proposals are welcome that deal with global data sets and/or include international collaborations.

For research strategies that plan to utilize the Collaboratory for the Study of Predictability (CSEP), see Section 10.2 to learn of its capabilities. Successful investigators proposing to utilize CSEP would be funded via core SCEC funds to adapt their prediction methodologies to the CSEP framework, to transfer codes to the externally accessible CSEP computers, and to be sure they function there as intended. Subsequently, the codes would be moved to the identical externally inaccessible CSEP computers by CSEP staff who will conduct tests against a variety of data as outlined in the CSEP description.

Priorities for EFP in 2015

- Support the development of statistical or physics-based real-time earthquake forecasts.
- Utilize and/or evaluate the significance of earthquake simulator results. See sections on WGCEP and CSEP for more details.
- Study how to properly characterize and estimate various earthquake-related statistical relationships (including the magnitude distribution, Omori law, aftershock productivity, etc.).
- Focus on understanding patterns of seismicity in time and space, as long as they are aimed toward understanding the physical basis of earthquake predictability.
- Develop useful measurement/testing methodology that could be incorporated in the CSEP evaluations, including those that address how to deal with observational errors in data sets.
- Develop approaches to test the validity of the characteristic earthquake vs. Gutenberg-Richter earthquake models as they are used in seismic hazard analysis.

E. Ground-Motion Prediction (GMP)

The primary goal of the Ground-Motion Prediction focus group is to develop and implement physics-based simulation methodologies that can predict earthquake strong-motion waveforms over the frequency range 0-10 Hz. Source characterization plays a vital role in ground-motion prediction. At frequencies less than 1 Hz, the methodologies should deterministically predict the amplitude, phase and waveform of earthquake ground motions using fully three-dimensional representations of Earth structure, as well as dynamic or dynamically compatible kinematic representations of fault rupture. At higher frequencies (1-10 Hz), the methodologies should predict the main character of the amplitude, phase and waveform of the motions using a combination of deterministic and stochastic representations of fault rupture and wave propagation. *Note: the GMP focus group also shares interests with the GMSV TAG (Earthquake Engineering Implementation Interface, EEII) and CME (Special Project) - consult these sections for additional GMP-related research priorities.*

Research Topics in GMP

- Developing and/or refining physics-based simulation methodologies, with particular emphasis on high frequency (1-10 Hz and higher) approaches. This work could include implementation of simulation methodologies onto the Broadband Simulation Platform, or implementation of more efficient approaches in wave and rupture propagation schemes (in collaboration with CME), allowing accurate simulation of higher frequency ground motion in models with lower seismic wave speeds.
- Waveform modeling of past earthquakes to validate and/or refine the structure of the Community Velocity Model (CVM) (in collaboration with USR). This includes exploration and validation of the effects of statistical models of structural and velocity heterogeneities on the ground motion, the significance of the lowest (S-wave) velocities as frequencies increase, and development and validation of improved (possibly frequency-dependent) attenuation (intrinsic or scattering) models in physics-based simulations (in collaboration with USR).
- Develop and implement new models or implement existing models for frequency-dependent site effects into the SCEC BroadBand Platform (site effects module). Because site-specific profiles are rarely available for large scale simulations, the priority will be given to models that can work with generic site profiles or that use simplified site factors (e.g. empirical Vs30-based factors for example). Models that require a site profile as input will also be considered. The site effects models are to be applied so as to produce time series that include site effects.
- Incorporate off-fault plasticity into physics-based ground motion simulation methodologies and validate the effects.

DRAFT 2015 SCIENCE PLAN

- Development of more realistic implementations of dynamic or kinematic representations of fault rupture, including simulation of higher frequencies (up to 10+ Hz). Possible topics include simulation of dynamic rupture on nonplanar faults and studying the effects of fault roughness on the resulting synthetic ground motion, and development of kinematic representations based on statistical models constrained by observed and/or dynamic ruptures. This research could also include the examination of current source-inversion strategies and development of robust methods that allow imaging of kinematic and/or dynamic rupture parameters reliably and stably, along with a rigorous uncertainty assessment. Close collaboration with the Technical Activity Group (TAG) on Source Inversion Validation (SIV) is encouraged. Construct Equivalent Kinematic Source (EKS) models that approximate the effects of near-fault nonlinearities in a linear scheme and test the EKS model in CyberShake. Projects that involve dynamic earthquake rupture simulations should involve preliminary code testing using benchmarks developed by the Dynamic Rupture Code Verification Technical Activity Group (TAG).
- Investigate the importance of including 3D basin effects on ensemble averaged long-period ground motions on the BroadBand Platform, e.g., by comparing ensemble averages of long-period (<~1Hz) ground motions computed in 1D and 3D crustal models for events included in the GMSV.
- Verification (comparison against theoretical predictions) and validation (comparison against observations) of the simulation methodologies with the objective to develop robust and transparent simulation capabilities that incorporate consistent and accurate representations of the earthquake source and three-dimensional velocity structure. Comparison of synthetic ground motions from deterministic and stochastic approaches to data for overlapping bandwidths. Close collaboration with the Technical Activity Group (TAG) on Ground Motion Simulation Validation (GMSV).

It is expected that the products of the Ground-Motion Prediction group will have direct application to seismic hazard analysis, both in terms of characterizing expected ground-motion levels in future earthquakes, and in terms of directly interfacing with earthquake engineers in the analysis of built structures. Activities within the Ground-Motion Prediction group will be closely tied to several focus areas, including the GMSV TAG, with particular emphasis on addressing ground motion issues related to seismic hazard and risk (see EEII below).

F. Southern San Andreas Fault Evaluation (SoSAFE)

The SCEC Southern San Andreas Fault Evaluation (SoSAFE) Project aims to increase knowledge of slip rates, paleoearthquake ages, and slip distributions of past earthquakes, for the past two thousand years on the southern San Andreas fault system. From Parkfield to Bombay Beach, and including the San Jacinto fault, the objective is to obtain new data to clarify and refine relative hazard assessments for each potential source of a future 'Big One'.

Priorities for SoSAFE in 2015

- Lengthen existing paleoearthquake chronologies or start new sites in key locations along the fault system that will improve understanding of the last 2000 years of this fault system.
- Determine slip rates at many time scales, so that possible system-level interaction can be documented.
- Obtain the best possible measurements of geomorphic slip distributions from past earthquakes by developing field, LiDAR, or SfM datasets and validate the different measures or test uncertainties determined by each method.
- Explore chronometric, geomorphic, or statistical approaches to linking geomorphic offsets to dated paleoearthquakes.
- Use novel methods for estimating slip rates from geodetic data.
- Investigate methodologies for integrating paleoseismic (including geomorphic measures of slip) and geologic data into rupture histories. For example, studies may improve or inform interactions between SoSAFE results and scenario rupture modeling or rupture forecasts.

Requests for geochronology support (e.g., to date 12 radiocarbon samples) are encouraged and shall be coordinated with Earthquake Geology; a portion of SoSAFE funds will be contributed towards joint support for dating. We also welcome proposals that seek to add other data (such as climate variations) to earthquake chronologies, which may be used to improve age control, understanding of the formation of offset features, or site-to-site correlation of events.

Research by single or multi-investigator teams will be supported to meet priority scientific objectives related to the mission of the SoSAFE Interdisciplinary Focus Group. SoSAFE objectives also foster common longer-term research interests and facilitate future collaborations in the broader context of a decade-long series of interdisciplinary, integrated and complementary studies on the southern San Andreas Fault system such as those targeted by teams investigating Special Fault Study Areas.

G. Earthquake Engineering Implementation Interface (EEII)

The purpose of the Earthquake Engineering Implementation Interface is to create and maintain collaborations with research and practicing engineers, much as the Seismic Hazard and Risk Analysis focus group did during SCEC3. These activities may include ground motion simulation validation, rupture-to-rafter simulations of building response as well as the end-to-end analysis of large-scale, distributed risk (e.g., ShakeOut-type scenarios). Our goal of impacting engineering practice and large-scale risk assessments require even broader partnerships with the engineering and risk-modeling communities, which motivates the activities described next.

Technical Activity Group (TAG) on Ground Motion Simulation Validation (GMSV)

A TAG focused on validation of ground motion simulations for use in engineering applications is developing and implementing testing/rating methodologies, via collaboration between ground motion modelers and engineering users. The workshops and research of this TAG to date have identified the efforts below as potential priority activities in this area. See the Ground-Motion Prediction (GMP) and the Community Modeling Environment (CME) sections of the Collaboration Plan for related research priorities. Proposals on these topics will be reviewed with all other SCEC proposals in January of 2015. Interested researchers are invited to contact Dr. Nicolas Luco (nluco@usgs.gov) to discuss opportunities for coordinated research. Note that any PIs funded to work on GMSV-related projects will become members of the TAG and will be required to coordinate with each other, in part via participation in monthly conference calls and annual workshops/meetings.

- Develop validation methodologies that use relatively simple metrics (e.g., significant duration), and demonstrate them with existing simulated ground motions and their recorded counterparts. Such research must be coordinated with the Broadband Platform Validation Project.
- Develop validated and efficient methods for either i) adjusting ground motion time series simulated by the Broadband Platform to account for the local site conditions at historical earthquake stations; or ii) deconvolving recorded ground motion time series to a reference site condition corresponding to that for simulated ground motions.
- Develop and demonstrate validation methodologies that use common models of structures of interest (e.g. multi-degree-of-freedom nonlinear models of building or geotechnical systems) for particular engineering applications. Such research must be coordinated with the validation efforts of the Software Environment for Integrated Seismic Modeling (SEISM) project.
- Develop and demonstrate validation methodologies for the use of CyberShake ground motion simulations in developing probabilistic and deterministic hazard maps for building codes and other engineering applications. In particular, investigations of observed versus simulated region-specific path effects for small-magnitude earthquakes in Southern California are encouraged. Such research must be coordinated with the Committee for Utilization of Ground Motion Simulations (UGMS).
- Research important ground motion or structural (e.g. building or geotechnical system) response parameters and statistics that should be used in validation of simulations. Demonstrate similarities and differences between otherwise parallel validation tests/ratings using these ground motion or structural response parameters.
- Demonstrate validation methodologies with ground motions simulated with deterministic and stochastic methods above 1 Hz.

Improved Hazard Representation

- Develop improved hazard models that consider simulation-based earthquake source and wave propagation effects that are not already well reflected in observed data. These could include improved methods for incorporating rupture directivity effects, basin effects, and site effects in the USGS ground motion maps, for example. The improved models should be incorporated into OpenSHA.
- Use broadband strong motion simulations, possibly in conjunction with recorded ground motions, to develop ground motion prediction models (or attenuation relations). Broadband simulation methods must be verified (by comparison with simple test case results) and validated (against recorded strong ground motions) before use in model development. The verification, validation, and application of simulation methods must be done on the SCEC Broadband Simulation Platform. Such developments will contribute to the future NGA-H Project.
- Investigate bounds on the median and variability of ground motions for a given earthquake scenario.

Ground Motion Time History Simulation

- Develop acceptance criteria for simulated ground motion time histories to be used in structural response analyses for building code applications or risk analysis. This relates closely to the GMSV section above.

DRAFT 2015 SCIENCE PLAN

- Assess the advantages and disadvantages of using simulated time histories in place of recorded time histories as they relate to the selection, scaling and/or modification of ground motions for building code applications or risk analysis.
- Develop and validate modules for simulation of short period ground motions (< 1 sec) for incorporation in the Broadband Platform.
- Develop and validate modules for the broadband simulation of ground motion time histories close to large earthquakes, and for earthquakes in the central and eastern United States, for incorporation in the Broadband Platform.
- Develop and validate modules for nonlinear site response, including criteria for determining circumstances under which nonlinear modeling is required. Incorporate the modules into the Broadband Platform.
- Compare simulated versus recorded ground motions for different models of the regional geologic structure.

Collaboration in Engineering Analysis

- Infrastructure Systems. Assess the performance of distributed infrastructure systems (e.g., water, electrical and transportation) using simulated ground motions. Evaluate the potential impact of basin effects, rupture directivity, spatial distribution of ground motion, or other phenomena on risk to infrastructure systems.
- Tall Buildings and Other Long-Period Structures. Enhance the reliability of simulations of long period ground motions in the Los Angeles region using refinements in source characterization and seismic velocity models, and evaluate the impacts of these ground motions on tall buildings and other long-period structures (e.g., bridges, waterfront structures).
- End-to-End Simulation. Interactively identify the sensitivity of structural response to ground motion parameters and structural parameters through end-to-end simulation. Buildings of particular interest include non-ductile concrete frame buildings.
- Reference Buildings and Bridges. Participate with PEER investigators in the analysis of reference buildings and bridges using simulated broadband ground motion time histories. The ground motions of large, rare earthquakes, which are poorly represented in the NGA strong motion database, are of special interest. Coordination with PEER can be done through Yousef Bozorgnia (yousef@berkeley.edu).
- Earthquake Scenarios. Perform detailed assessments of the results of scenarios such as the ShakeOut exercise, and the scenarios for which ground motions were generated for the Tall Buildings Initiative (including events on the Puente Hills, Southern San Andreas, Northern San Andreas and Hayward faults) as they relate to the relationship between ground motion characteristics and structural response and damage.

Ground Deformation

- Investigate the relationship between input ground motion characteristics and local soil nonlinear response, liquefaction, lateral spreading, local soil failure, and landslides -- i.e., geotechnical hazards. Investigate hazards due to surface faulting and to surface deformation caused by subsurface faulting and folding.

Risk Analysis

- Develop improved site/facility-specific and portfolio/regional risk analysis (or loss estimation) techniques and tools, and incorporate them into the OpenRisk software.
- Use risk analysis software to identify earthquake source and ground motion characteristics that control damage estimates.

Other Topics

- Proposals for other innovative projects that would further implement SCEC information and techniques in seismic hazard, earthquake engineering, risk analysis, and ultimately loss mitigation, are encouraged.

XI. Special Projects and Initiatives

The following are special projects for which SCEC has obtained funding beyond the core program. This Collaboration Plan is not for those funds, which are committed; rather it is for SCEC core funding for research projects that are consonant with these special projects. This is consistent with SCEC policy that requires that special projects be aligned with core SCEC goals.

A. Working Group on California Earthquake Probabilities (WGCEP)

The following are special projects for which SCEC has obtained funding beyond the core program. This Collaboration Plan is not for those funds, which are committed; rather it is for SCEC core funding for research projects that are consonant with these special projects. This is consistent with SCEC policy that requires that special projects be aligned with core SCEC goals.

The following are examples of SCEC activities that could make direct contributions to WGCEP goals:

- Evaluate fault models in terms of the overall fault connectivity at depth (important for understanding the likelihood of multi-fault ruptures) and the extent to which faults represent a well-defined surface versus a proxy for a braided deformation zone.
- Evaluate existing deformation models, or develop new ones, in terms of applicability of GPS constraints, categorical slip-rate assignments (based on “similar” faults), applicability of back-slip methods, and other assumptions. Of particular interest is the extent to which slip rates taper at the ends of faults and at fault connections.
- Evaluate the UCERF3 implication that 30% to 60% of off-fault deformation is aseismic.
- Help determine the average along-strike slip distribution of large earthquakes, especially where multiple faults are involved (e.g., is there reduced slip at fault connections?).
- Help determine the average down-dip slip distribution of large earthquakes (the ultimate source of existing discrepancies in magnitude-area relationships). Are surface slip measurements biased with respect to slips at depth?
- Develop a better understanding of the distribution of creeping processes and their influence on both rupture dimension and seismogenic slip rate.
- Contribute to the compilation and interpretation of mean recurrence-interval constraints from paleoseismic data and/or develop site-specific models for the probability of events going undetected at a paleoseismic site.
- Develop ways to constrain the spatial distribution of maximum magnitude for background seismicity (for earthquakes occurring off of the explicitly modeled faults).
- Address the question of whether small volumes of space exhibit a Gutenberg Richter distribution of nucleations (even on faults).
- Develop improved estimates (including uncertainties) of the long-term rates of observed earthquakes for different sized volumes of space.
- Refine our magnitude completeness estimates (as a function of time, space, and magnitude). Develop such models for real-time applications (as will be needed in operational earthquake forecasting).
- Develop methods for quantifying elastic-rebound based probabilities in un-segmented fault models.
- Help quantify the amount of slip in the last event, and/or average slip over multiple events, on any major faults in California (including variations along strike).
- Develop models for fault-to-fault rupture probabilities, especially given uncertainties in fault endpoints.
- Determine the extent to which seismicity rates vary over the course of historical and instrumental observations (the so-called Empirical Model of previous WGCEPs), and the extent to which this is explained by aftershock statistics.
- Determine the applicability of higher-resolution smoothed-seismicity maps for predicting the location of larger, more damaging events.
- Explore the UCERF3 “Grand Inversion” with respect to: possible plausibility filters, relaxing the UCERF2 constraints, not over-fitting data, alternative equation-set weights, applying a characteristic-slip model, and applicability of the Gutenberg Richter hypothesis on faults (see report at www.WGCEP.org).
- Develop applicable methods for adding spatiotemporal clustering to forecast models (e.g., based on empirical models such as ETAS). Are sequence-specific parameters warranted?
- Is there a physical difference between a multi-fault rupture and a separate event that was triggered quickly?
- Develop more objective ways of setting logic-tree branch weights, especially where there are either known or unknown correlations between branches.

DRAFT 2015 SCIENCE PLAN

- Develop easily computable hazard or loss metrics that can be used to evaluate and perhaps trim logic-tree branches.
- Develop techniques for down-sampling event sets to enable more efficient hazard and loss calculations.
- Develop novel ways of testing UCERF3, especially ones that can be integrated with CSEP.
- Study the behavior of physics-based earthquake simulators, envisioning that they could become essential ingredients in future UCERF projects and a cornerstone of SCEC5. The goal is to develop the capability of simulators to be able to contribute meaningfully to hazard estimates. Examples of important tasks:
 - a. Study the sensitivity of simulator results to input details including fault-system geometry, stress-drop values, tapering of slip, methods of encouraging rupture jumps from fault to fault, cell size, etc.
 - b. Develop physically realistic ways of simulating off-fault seismicity.
 - c. Add additional physics into simulators, for example, the inclusion of high-speed frictional weakening and of off-fault viscoelastic and heterogeneous elastic properties.
 - d. Develop alternate methods of driving fault slip besides “back-slip”.
 - e. Make access to existing simulators easy for new users, including adequate documentation and version numbers, examples of input and output files for initial testing, and access to analysis tools. Publicize availability.
 - f. Develop new approaches to designing simulators and/or of making them more computationally efficient, including the use of better algorithms, point source Greens functions, and GPUs.
 - g. Develop validation tools for simulators, utilize existing UCERF data comparison tools with them, and develop capabilities for simulators to interact with UCERF infrastructure.
 - h. Develop the capability of simulators to deal with UCERF and SCEC CFM fault geometries, both for rectangular and triangular cell representations.
 - i. Create statewide synthetic earthquake catalogs spanning 100 My using as many different simulators as possible, in order to generate statistically significant behavior on even slow-slipping faults. Use small time-steps to permit evaluation of short-term clustering.
 - j. Use these catalogs as synthetic laboratories for CSEP testing as described under CSEP.
 - k. Data-mine these catalogs for statistically significant patterns of behavior. Evaluate whether much-shorter observed catalogs are statistically distinguishable from simulated catalogs. Consider and explore what revisions in simulators would make simulated catalogs indistinguishable from observed catalogs.
 - l. Develop and test a variety of statistical methods for determining the predictability of the of earthquakes in these simulated catalogs.
 - m. Compute other data types such as gravity changes, surface deformation, InSAR images, in order to allow additional comparisons with observations.

Further suggestions and details can be found at <http://www.WGCEP.org>, or by contacting the project leader (Ned Field: field@usgs.gov; (626) 644-6435).

B. Collaboratory for the Study of Earthquake Predictability (CSEP)

CSEP is developing a virtual, distributed laboratory—a collaboratory—that supports a wide range of scientific prediction experiments in multiple regional or global natural laboratories. This earthquake system science approach seeks to provide answers to the questions: (1) How should scientific prediction experiments be conducted and evaluated? and (2) What is the intrinsic predictability of the earthquake rupture process?

Priorities for 2015

- Canterbury experiment: finalizing the retrospective evaluation of physics-based and statistical forecasting models during the 2010-12 Canterbury, New Zealand, earthquake sequence by (i) using Bayesian approaches to construct optimal ensemble models, (ii) comparing against extent prospective models, (iii) transitioning models to prospective evaluation, including in other regions;
- Global CSEP experiments: developing and testing global models, including, but not limited to, those developed for the Global Earthquake Model (GEM);

- Strengthening testing and evaluation methods: developing computationally efficient performance metrics of forecasts and predictions that (i) account for aleatory variability and epistemic uncertainties, and (ii) facilitate comparisons between a variety of probability-based and alarm-based models (including reference models);
- Advancing Operational Earthquake Forecasting (OEF): (i) developing forecasting methods that explicitly address real-time data deficiencies, (ii) updating forecasts on an event basis and evaluating forecasts with overlapping time-windows or on an event basis, (iii) improving short-term forecasting models, (iv) developing prospective and retrospective experiments to evaluate OEF candidate models;
- Earthquake rupture simulators: developing experiments to evaluate the predictive skills of earthquake rupture simulators, against both synthetic (simulated) and observed data (see also the WGCEP section);
- External Forecasts and Predictions (EFP): developing and refining experiments to evaluate EFPs (generated outside of CSEP), including operational forecasts by official agencies and prediction algorithms based on seismic and electromagnetic data;
- Induced seismicity: developing models and experiments to evaluate hypotheses of induced seismicity, e.g. in the Salton Trough or in Oklahoma, including providing data access to injection/depletion rates and other potentially pertinent data;
- Hybrid/ensemble models: developing methods for forming optimal hybrid and ensemble models from a variety of existing probability-based or alarm-based forecasting models;
- Hazard models: developing experiments to evaluate seismic hazard models and their components (e.g., ground motion prediction equations);
- Coulomb stress: developing forecasting models based on the Coulomb stress hypothesis that can be tested retrospectively and prospectively within CSEP;
- Testing paleo-based forecasts: developing experiments to prospectively test the fault rupture and earthquake probabilities implied by paleoseismic investigations of California faults (e.g., testing probabilities of future ruptures at paleoseismic sites where numerous ruptures have been documented, the relative effectiveness of proposed fault segment boundaries at stopping ruptures, and the relative frequency of on-fault and off-fault ruptures in California) (see also the WGCEP and SoSafe sections).

General contributions may include:

- Establishing rigorous procedures in controlled environments (testing centers) for registering prediction procedures, which include the delivery and maintenance of versioned, documented code for making and evaluating predictions including intercomparisons to evaluate prediction skills;
- Constructing community-endorsed standards for testing and evaluating probability-based, alarm-based, fault-based, and event-based predictions;
- Developing hardware facilities and software support to allow individual researchers and groups to participate in prediction experiments;
- Designing and developing programmatic interfaces that provide access to earthquake forecasts and forecast evaluations.
- Providing prediction experiments with access to data sets and monitoring products, authorized by the agencies that produce them, for use in calibrating and testing algorithms;
- Characterizing limitations and uncertainties of such data sets (e.g., completeness magnitudes, source parameter and other data uncertainties) with respect to their influence on experiments;
- Expanding the range of physics-based models to test hypotheses that some aspects of earthquake triggering are dominated by dynamic rather than quasi-static stress changes and that slow slip event activity can be used to forecast large earthquakes;
- Working to develop testable fault-based forecasting models;
- Evaluating hypotheses critical to forecasting large earthquakes, including the characteristic earthquake hypothesis, the seismic gap hypothesis, and the maximum-magnitude hypothesis;
- Conducting workshops to facilitate international collaborations;

A major focus of CSEP is to develop international collaborations between the regional testing centers and to accommodate a wide-ranging set of prediction experiments involving geographically distributed fault systems in different tectonic environments.

C. Community Modeling Environment (CME)

The Community Modeling Environment is a SCEC special project that develops improved ground motion forecasts by integrating physics-based earthquake simulation software, observational data, and earth structural models using advanced computational techniques including high performance computing. CME projects often use results, and integrate work, from SCEC groups including Interdisciplinary Focus Groups Technical Activity Groups. The SCEC research community can contribute research activities to CME by providing scientific or computational capability that can improve ground motion forecasts.

Examples of CME research includes development of earth structural models, curation of data sets to support forecast validation, and development of scientific software that simulates physical processes in the earth including dynamic ruptures (such as those that are verified in the Dynamic Rupture Code Verification Technical Activity Group (TAG)), and wave propagation simulations. Proposals are encouraged that work towards improving the accuracy of the statewide community velocity model (SCVM).

CME computationally based research projects include three types of forecast evaluation and testing systems; transient detection and forecast evaluation, earthquake early warning earthquake parameter and ground motion forecast evaluation, and short-term earthquake forecast evaluation.

CME is developing ground motion simulations that produce broadband seismograms. These simulation tools include rupture generators, low frequency wave propagation models, high frequency stochastic models, non-linear site response modules, and validation capabilities including assembled observational strong motion data sets and waveform-matching goodness of fit algorithms and information displays. Proposals that enhance our ability to extend ground motion simulations to higher frequencies through high frequency source generation models, and stochastic models of source, propagation, and site effects are encouraged.

Ground motion simulation validation computational and organizational tools are needed to establish repeatable validation of ground motion simulations to engineering standards. Research in this area would contribute to the efforts under the ground motion simulation validation TAG.

CME is working to improve probabilistic seismic hazard calculations. CME physics-based PSHA research requires a high resolution 3D velocity model for California, a pseudo-dynamic rupture generator capable of generating an extended earthquake rupture forecast from UCERF3.0, highly efficient reciprocity-based seismogram calculations, and probabilistic hazard model information system providing access to calculation results. Proposals that develop improved pseudo-dynamic models, including parameterizations that include the possibility of super-shear rupture, are encouraged. Proposals that seek to use existing CyberShake simulations as a research database are encouraged.

D. Virtual Institute for the Study of Earthquake Systems (VISES)

NSF has funded a new effort within SCEC to broaden and deepen our collaborations with Japanese earthquake scientists. A particular emphasis will be to broaden the participation of early career scientists. Collaborative research funded through VISES should have relevance for research questions of concern to the SCEC core program. Examples of relevant research activities include testing earthquake forecast models, numerical simulation of earthquake ground motion to high frequencies, ground motion simulation using dense networks of high-dynamic range sensors, and geodynamical studies of fault interaction and deformation. Travel support to Japan for early career scientists developing collaborations with colleagues in Japan is a priority for funding under the VISES program.

Note: Funding for successful proposals for travel to Japan will be handled from the SCEC office. Your proposed budget should not include overhead.

E. National Partnerships through EarthScope

The NSF EarthScope project (<http://www.earthscope.org>) provides unique opportunities to learn about the structure and dynamics of North America. SCEC and the NSF EarthScope program encourage proposals that integrate the goals of the SCEC Science Plan with the many overlapping goals of the EarthScope Science Plan (<http://www.earthscope.org/ESSP>). Topics of interest include applying EarthScope observational resources to SCEC science and hazard problems; characterizing the crust and lithosphere of the natural laboratory of Southern California; exploring stress and deformation over time using EarthScope resources (including high resolution topography); testing hypothesis and enhancing models of earthquakes, faulting, and the rheology of the lithosphere; developing innovative contributions to identifying earthquake hazard and community response; and promoting Earth Science literacy in education and outreach in SCEC and EarthScope topic areas. These partnerships should seek to strengthen the connections across the organizations and leverage SCEC and EarthScope resources.

XII. Communication, Education, and Outreach

The theme of the CEO program during SCEC4 is *Creating an Earthquake and Tsunami Resilient California*. CEO will continue to manage and expand a suite of successful activities along with new initiatives, within four CEO interconnected thrust areas:

1. The *Implementation Interface* connects SCEC scientists with partners in earthquake engineering research, and communicates with and trains practicing engineers and other professionals.
2. The *Public Education and Preparedness* thrust area educates people of all ages about earthquakes, and motivates them to become prepared.
3. The *K-14 Earthquake Education Initiative* seeks to improve earth science education and school earthquake safety.
4. Finally, the *Experiential Learning and Career Advancement* program provides research opportunities, networking, and more to encourage and sustain careers in science and engineering.

These thrust areas present opportunities for members of the SCEC community to partner with CEO staff. Limited funding (typically no more than \$2000-\$5000) may be available as direct payments from SCEC (not subcontracts) for materials or activities and typically does not require a formal proposal. For larger activities, joint proposals with SCEC CEO to potential sources are the best approach. Those interested in partnering with SCEC CEO on activities, submitting a joint proposal, or in submitting a CEO proposal responding to this Collaboration Plan should first contact the Associate SCEC Director for CEO (Mark Benthien: benthien@usc.edu, 213-740-0323).

Saturday, September 6

- 08:00 - 18:00** **SCEC San Gorgonio Pass Special Fault Study Area Workshop**
(by application only)
Conveners: Michele Cooke, Doug Yule, David Oglesby
Location: Field Trip Offsite then return to Palm Canyon Room
- 08:00 Field Trip Group departs Hilton Lobby
- 08:30 Stop 1 – Mission Creek strand at Pushawalla Canyon (Blisniuk et al.)
- 09:45 Stop 2 – Banning strand west of Hwy 62 (Behr et al.)
- 11:00 Stop 3 – Mission Creek strand at Mission Creek Preserve (Kendrick et al.)
- 12:30 Field Trip Group returns to Hilton
- 13:00 Lunch in Horizon Ballroom 1
- 14:00 Summary of field trip discussion and outline of talks and goals (M. Cooke, D. Yule, D. Oglesby) in Palm Canyon Room
- 14:10 Fault activity in the San Gorgonio Pass (K. Kendrick, J. Matti)
- 14:30 Megatrench Results (D. Yule, K. Scharer, D. Heermance)
- 14:50 Observations of Activity of the Mill Creek Strand and Uplift of Yucaipa Ridge (A. Morelan, M. Oskin, J. Chester)
- 15:10 GPS Analysis (J. Spinler, R. Bennett)
- 15:30 Shallow 3D Structure in the San Gorgonio Pass (D. Oglesby)
- 15:50 Break
- 16:10 Assessing Fault Geometry from Seismicity (C. Nicholson)
- 16:30 Impact of Fault Geometry within the San Gorgonio Pass on Deformation (M. Cooke)
- 16:50 Stress Patterns from Seismicity (T. Goebel, E. Hauksson)
- 17:10 Dynamic Rupture Models along Irregular Faults (Z. Shi)
- 17:30 How does the San Gorgonio Pass fit into UCERF3? (T. Dawson)
- 17:50 Discussion of the Future of San Gorgonio Pass SFSA (All)
- 18:00 Adjourn
- 10:00 - 18:00** **SCEC CSEP/USGS/GEM Workshop: Next Steps for Testing Operational Earthquake Forecasts and Seismic Hazard Models**
(by invitation only)
Conveners: Max Werner, Danijel Schorlemmer, Tom Jordan, Andy Michael, Morgan Page
Location: Horizon Ballroom 2
- 10:00 Welcome, Introductions, Meeting Objectives (M. Werner / D. Schorlemmer)
Overview of OEF and CSEP
- 10:10 CSEP Overview and Status (M. Werner)
- 10:25 The Liaison between OEF and CSEP in Italy (W. Marzocchi)
- 10:35 OEF and CSEP in New Zealand (M. Gerstenberger)
- 10:50 OEF and CSEP in Japan (H. Tsuruoka / Y. Ogata)
- 11:05 Status and Requirements for OEF in US (M. Blanpied)
- 11:15 Evaluating UCERF2 and NSHMP (D. Schorlemmer)
- 11:25 OEF and CSEP in California (E. Field)
- 11:35 Discussion
- How adequate is CSEP's infrastructure for evaluating OEF models?

- 12:05 Immediate aftershock forecasting after a strong earthquake (T. Omi)
- 12:15 ComCat Overview and Real-Time Data (H. Benz)

Saturday, September 6

- 12:30 Panel Discussion
- How should real-time data uncertainties be handled in OEF models and their evaluation?
 - What products/features are/should be available in ComCat that help facilitate OEF and CSEP testing?
- 13:00 Lunch in Horizon Ballroom 1
- GEM, Global Experiments, and Ground Motion
- 14:00 Perspectives on Time-Dependent Earthquake Forecasting (T. Jordan)
- 14:10 GEM Overview and Perspectives on Testing and Evaluation (R. Stein)
- 14:30 GEM's GEAR Models (P. Bird)
- 14:40 Panel Discussion (D. Jackson / D. Rhoades / M. Werner)
- How should global experiments be conducted?
 - How can CSEP's testing methodology be improved?
- 15:10 Forecasting Focal Mechanisms and Evaluating Forecast Skill (Y. Kagan)
- 15:20 Testing Ground-Motion Models and Seismic Maps (S. Mak)
- 15:40 Discussion
- How should GEM and USGS ground motion forecasts be evaluated within CSEP and GEM's Testing and Evaluation group?
 - Is CSEP ready to evaluate hazard maps?
- 16:10 Break
- Retrospective Canterbury Experiment
- 16:20 Overview and Motivation of Experiment (M. Gerstenberger)
- 16:25 Overview of Coulomb-Based Models (C. Cattania)
- 16:30 Preliminary Results (W. Marzocchi)
- 16:45 Panel Discussion (C. Cattania / M. Gerstenberger / W. Marzocchi)
- How are physics-based models performing?
 - How should retrospective CSEP experiments be conducted to support OEF efforts?
 - How does real-time data affect forecasts?
- New Directions
- 17:00 Panel Discussion: CSEP and Induced Seismicity (E. Brodsky / B. Ellsworth / A. Llenos)
- 17:30 Panel Discussion: CSEP and Pale- and Simulator-Based Rupture (D. Jackson / E. Field)
- 18:00 Adjourn

Saturday, September 6

10:00 - 18:00 **SCEC Community Geodetic Model Workshop** (by invitation only)
Conveners: Jessica Murray, Rowena Lohman, David Sandwell
Location: Oasis Room II

Combined Session (GPS and InSAR Working Groups)

- 10:00 Introduction (J. Murray)
- CGM motivation, objectives
 - Charge to workshop participants
 - Workshop format
- 10:10 Transition to working group locations

GPS Working Group in Oasis Room II

- 10:15 Introduction and Overview (J. Murray)
Processing Software
- 10:25 GIPSY (S. Owen)
- 10:35 GAMUT (M. Murray)
Campaign GPS data
- 10:45 Summary of southern CA campaign data (G. Funning)
- 10:55 Campaign data compilation and reprocessing (Z.-K. Shen)
- 11:15 Discussion
- 11:30 Break

Continuous GPS Data

Available Solution and processing strategies:

- 11:40 PBO solutions (T. Herring)
- 11:50 USGS (J. Murray)
- 12:00 UNR (B. Hammond)
- 12:10 JPL, MEaSURES (S. Owen)
- 12:20 Comparison of time series solutions
- 12:50 Discussion
- What issues have come to light?
 - Are further comparisons needed? If so, which?

13:00 Lunch in Horizon Ballroom 1

14:00 Discussion (continued)

Strategy for combining CGPS solutions:

- 14:20 st_filter (Z. Liu)
- 14:30 Time series-based combination (T. Herring)
- 14:40 Discussion
- Other approaches to consider? Importance of open source?
 - Incorporation of SGPS data?
 - Reference frame adjustments

Time series analysis

- 15:00 Discussion
- Addressing steps in the data
 - Estimating rates, seasonal, coseismic, postseismic
 - Realistic uncertainty estimates with temporally correlated noise

Action Items

- 15:30 Discussion
- Campaign data reprocessing
 - Further comparisons among time series solutions?

Saturday, September 6

- Combining campaign and continuous solutions
 - Time series analysis to obtain derived products
 - Providing input to InSAR group
 - Group proposal for next year
- 15:50 Break and transition to combined group location in Oasis II
- InSAR Working Group*** in Whitewater Boardroom
- Data
- 10:15 Data used in exercise; data access/hosting (S. Baker)
- 10:30 Future missions, coverage over SoCal (D. Sandwell)
- 10:45 TBD (P. Agram)
- Status of ISCE Individual approaches
- 11:00 E. Tymofeyeva / Y. Fialko
- 11:15 G. Funning
- 11:30 Break
- 11:45 C. Johnson
- 12:00 Z. Liu
- 12:15 B. Riel
- 12:30 M. Shirzaei
- 12:45 X. Tong
- 13:00 Lunch in Horizon Ballroom 1
- Status of ISCE Individual approaches (continued)
- 14:00 Wrap-Up as Needed
- 14:15 Results of comparison (R. Lohman)
- Approach used for intra-InSAR and InSAR-GPS comparisons
 - Problems arising during comparison
 - Actual results
- 14:45 Discussion
- New strategies for intra-InSAR and InSAR-GPS comparisons
 - Appropriate spatial scale for the comparisons?
 - Impact of non-secular signals?
 - Other products would we like from the GPS community
- 15:00 Tinker Time
- Run own comparisons
 - Tweak Rowena's code
 - Look at posters
- 15:30 Wrap-Up
- 15:50 Break and transition to combined group location in Oasis II
- Combined Session (GPS and InSAR Working Groups)***
- Summary of GPS and InSAR comparison exercises
- 16:00 GPS (J. Murray)
- 16:15 InSAR (R. Lohman)
- 16:30 Merging InSAR and GPS
- 17:00 Group proposal(s)
- 17:25 SCEC4 milestones and CGM in SCEC5
- 17:45 Recap of action items
- 18:00 Adjourn

Sunday, September 7

08:00 - 18:00 **SCEC Annual Meeting Registration & Check-In** at Hilton Lobby

08:00 - 09:00 **Breakfast** at Hilton Poolside

09:00 - 20:00 **Poster Set-Up** in Plaza Ballroom

09:00 - 17:00 **SCEC Source Inversion Validation (SIV) Workshop**

Conveners: P. Martin Mai, Jean-Paul Ampuero, Danijel Schorlemmer, and Morgan Page

Location: Palm Canyon Room

09:00 Introduction and Current Status of SIV (M. Mai)

09:30 Methods and Approaches to Constrain Kinematic Source Parameters (T. Lay)

10:00 Source Inversion for the 2009 L'Aquila earthquake using SIV testing and Green's Function Including 3D Earth Structure (F. Gallovic)

10:30 Break

10:45 Bayesian Inversion for the 2011 Tohoku Earthquake and Green's Function Uncertainty (S. Minson)

11:00 Constraining Kinematic Source Models from Back-Projection (L. Meng)

11:15 The SIV Teleseismic Benchmark: Construction and First Results (O. Zielke)

11:30 Discussion

12:00 Lunch in Terrace Restaurant, Tapestry Room and Poolside

13:00 Discussion (continued)

13:30 Benchmark Results (M. Mai)

14:00 Short Talks on SIV Experiences (C. Ji, C. Twardzik, W. Fan, & others)

14:45 Discussion: Current SIV Status

15:15 Break

15:30 Future SIV Efforts

- How can we best understand/resolve differences among current SIV submissions?
- Future SIV Benchmarks & Deadlines
- Dividing the Labor
- SIV Funding
- How to increase participation?
- Future SIV workshops

17:00 Adjourn

09:00 - 17:00 **SCEC Workshop on Earthquake Ground Motion Simulation and Validation**

Conveners: Phil Maechling, Tom Jordan, Nico Luco, Sanaz Rezaeian (USGS)

Location: Horizon Ballroom 1

09:00 Overview of SCEC/CME Computational Research (P. Maechling)

09:15 Full 3D Tomography Development (P. Chen / E. Lee)

09:30 Hercules High Frequency Simulations (R. Taborda / J. Bielak)

09:45 AWP High Frequency Simulations (K. Olsen)

10:00 Discussion: Future Ground Motion Simulations (All)

10:30 Break

- 10:45 CyberShake Physics-based PSHA (T. Jordan)
- 11:00 Unified Community Velocity Model (UCVM) Software (D. Gill)
- 11:10 Broadband Platform (BBP) Software (F. Silva)

Sunday, September 7

- 11:20 High Performance Computing (HPC) Software (Y. Cui)
- 11:30 Discussion: Future Software Developments (All)
- 12:00 Lunch in Terrace Restaurant, Tapestry Room and Poolside
- 13:00 Overview of GMSV TAG and Related Efforts (S. Rezaeian)
- 13:15 Evaluation of SCEC Broadband Platform Phase 1 Ground Motion Simulation Results (C. Goulet)
- 13:35 Validation needs of the SCEC Committee for Utilization of Ground Motion Simulations (C.B. Crouse)
- 13:55 Discussion (All)
- 14:10 Validation of Ground Motion Simulations through Simple Proxies for the Response of Engineered Systems (J. Baker)
- 14:30 Validation of Simulated Ground Motions Based on Evolution of Intensity and Frequency Content (F. Zareian)
- 14:50 Discussion (All)
- 15:05 Use and Validation of Simulated Earthquakes for Nonlinear (G. Deierlein / N. Bijelic / T. Lin)
- 15:25 Validation of the Duration of Simulated Ground Motions to Be Used in Analysis of Geotechnical Systems (J. Stewart / K. Afshari)
- 15:45 Strawman GMSV TAG Plans for Next Year and SCEC5 (N. Luco)
- 16:00 Discussion: SCEC5 and Towards an Integrated Earthquake Ground Motion Simulation and Validation Program (All)
- 17:00 Adjourn

09:00 - 17:00 SCEC Workshop on Post-Earthquake Rapid Scientific Response

Conveners: Mike Oskin, Greg Beroza, Tran Huynh

Location: Horizon Ballroom 2

- 09:00 Introduction and Objectives (M. Oskin / G. Beroza)
- 09:15 Source Modeling (G. Funning / B. Aagaard)
- 09:45 Operational Earthquake Forecasting (M. Werner / T. Jordan)
- 10:15 Seismology (E. Cochran / J. Steidl)
- 10:45 Break
- 11:00 Geodesy (J. Murray / Y. Fialko)
- 11:30 Scientific Drilling (E. Brodsky / J. Chester)
- 12:00 Lunch in Terrace Restaurant, Tapestry Room and Poolside
- 13:00 Geology (K. Scharer / T. Rockwell)
- 13:30 Post-Event Imaging (M. Oskin / R. Lohman / K. Hudnut)
- 14:00 Response Coordination (T. Huynh / A. Rosinski)
- 14:30 Discussion of Overarching Response Goals and Framework (All)
- 15:00 Break
- 15:15 Discussion of Overarching Response Goals and Framework (continued) and Writing Assignments
- 17:00 Adjourn

MEETING AGENDA

- 17:00 - 18:00** **Welcome Social** in Hilton Lobby and Plaza Ballroom
- 18:00 - 19:00** **Distinguished Speaker Presentation** in Horizon Ballroom
Reducing Epistemic Uncertainty in Seismic Risk Estimation
(Norm Abrahamson)
- 19:00 - 20:30** **Welcome Dinner** at Hilton Poolside
- 19:00 - 21:00** **SCEC Advisory Council Meeting** in Tapestry Room
- 21:00 - 22:30** **Poster Session 1** in Plaza Ballroom

Monday, September 8

- 07:00 - 08:00** **SCEC Annual Meeting Registration & Check-In** at Hilton Lobby
- 07:00 - 08:00 Breakfast at Hilton Poolside
- 08:00 - 11:00** **The State of SCEC** in Horizon Ballroom
- 08:00 Welcome and State of the Center (Tom Jordan)
- 08:30 Report from the National Science Foundation (Greg Anderson)
- 08:45 Report from the U.S. Geological Survey (Bill Leith)
- 09:00 Communication, Education, & Outreach (Mark Benthien)
- 09:20 SCEC Science Accomplishments (Greg Beroza)
- 10:00 - 10:30 Break
- 10:30 - 10:45** **Briefing on the M6.0 South Napa Earthquake** in Horizon Ballroom
- 10:45 - 11:00** **Looking Forward to SCEC5** (Tom Jordan) in Horizon Ballroom
- 11:00 - 12:30** **Session 1: How do we deal with known unknowns and unknown unknowns?** Moderators: Glenn Biasi, Tom Herring
- 11:00 Reducing variability in earthquake stress drops to define secondary trends (Annemarie Baltay)
- 11:40 Theme Intro: Reducing Epistemic Uncertainty (Glenn Biasi)
- 11:45 Discussion: Looking Forward to SCEC5
- 12:30 - 14:00 Lunch at Hilton Restaurant, Tapestry Room, and Poolside
- 12:30 - 14:00** **SCEC Board of Directors Lunch Meeting** in Oasis Room III
- 14:00 - 16:00** **Session 2: What properties of the Earth and the faults within it are important for understanding system behavior?** in Horizon Ballroom
- Moderators: Yuri Fialko, Nadia Lapusta
- 14:00 Beyond Elasticity: New Directions in Earthquake Modeling (Eric Dunham)
- 14:40 Theme Intro: Beyond Elasticity (Yuri Fialko)
- 14:45 Discussion: Looking Forward to SCEC5
- 15:20 Theme Intro: Simulating Earthquake Processes (Nadia Lapusta)
- 15:25 Discussion: Looking Forward to SCEC5
- 16:00 - 17:30** **Poster Session 2** in Plaza Ballroom
- 19:00 - 21:00** **SCEC Honors Banquet** at Hilton Poolside

21:00 - 22:30 **Poster Session 3** in Plaza Ballroom

Tuesday, September 9

- 07:00 - 08:00 Breakfast at Hilton Poolside
- 08:00 - 10:00** **Session 3: How can the hazard from simulated earthquakes effectively reduce risk in the real world?** in Horizon Ballroom
Moderators: Kim Olsen, Jack Baker
- 08:00 Can We Rely on Linear Elasticity to Predict Long-Period Ground Motions? (Daniel Roten)
- 08:40 Theme Intro: Ground Motion Simulations (Kim Olsen)
- 08:45 Discussion: Looking Forward to SCEC5
- 09:20 Theme Intro: Infrastructure System Risk (Jack Baker)
- 09:25 Discussion: Looking Forward to SCEC5
- 10:00 - 10:30 Break
- 10:30 - 12:30** **Session 4: What aspects of earthquake behavior are predictable?** in Horizon Ballroom; Moderators: Emily Brodsky, Ned Field
- 10:30 Waste water injection induced seismicity in naturally-active, seismogenic regions in central California (Thomas Goebel)
- 11:10 Theme Intro: "Atectonic" or Triggered Seismicity (Emily Brodsky)
- 11:15 Discussion: Looking Forward to SCEC5
- 11:50 Theme Intro: Science of Operational Earthquake Forecasting (Ned Field)
- 11:55 Discussion: Looking Forward to SCEC5
- 12:30 - 14:00 Lunch at Hilton Restaurant, Tapestry Room, and Poolside
- 14:00 - 16:00** **Session 5: Here it comes! What just happened? How can SCEC better prepare to respond to future earthquakes?** in Horizon Ballroom; Moderators: Elizabeth Cochran, Mike Oskin
- 14:00 Differential LiDAR – a new tool for mapping coseismic fault-zone deformation (Ed Nissen)
- 14:40 Theme Intro: Earthquake Early Warning Research (Elizabeth Cochran)
- 14:45 Discussion: Looking Forward to SCEC5
- 15:20 Theme Intro: Post-Earthquake Rapid Response (Mike Oskin)
- 15:25 Discussion: Looking Forward to SCEC5
- 16:00 - 17:30** **Poster Session 4** in Plaza Ballroom
- 19:00 - 21:00 Dinner at Hilton Poolside
- 19:00 - 21:00** **SCEC Advisory Council Meeting** in Boardroom
- 21:00 - 22:30** **Poster Session 5** in Plaza Ballroom

Wednesday, September 10

- 07:00 - 08:00 Poster Removal from Plaza Ballroom
- 07:00 - 08:00 Breakfast at Poolside
- 08:00 - 08:30 Report from the Advisory Council** (Gail Atkinson) in Horizon Ballroom
- 08:30 - 10:00 Session 6: How can we communicate more effectively what we know and what we don't?** in Horizon Ballroom; Moderators: Mark Benthien, Dave Wald
- 08:30 The IDEA Model: A Practical Tool for Designing Effective Early Earthquake Warning Messages (Deanna Sellnow, Tim Sellnow)
- 09:10 Theme Intro: Risk Communication & New Technologies (Mark Benthien, Dave Wald)
- 09:15 Discussion: Looking Forward to SCEC5
- 10:00 - 10:30 Break
- 10:30 - 12:30 The Future of SCEC**
- 10:30 This Next Year: 2015 SCEC Science Collaboration (Greg Beroza)
- 11:30 Defining SCEC5 Priorities (Tom Jordan)
- 12:30 Adjourn
- 12:30 - 14:30 SCEC Planning Committee Lunch Meeting** in Palm Canyon Room
- 12:30 - 14:30 SCEC Board of Directors Lunch Meeting** in Tapestry Room

Distinguished Speaker Presentation

Sunday

Reducing Epistemic Uncertainty in Seismic Risk Estimation,*Norm Abrahamson (PG&E)*

Sunday, September 7, 2014 (18:00)

For most critical infrastructure, seismic safety is evaluated using standards-based seismic design criteria, but there is a move to also consider risk-informed regulation and risk-informed decision making as part of seismic safety. The residual risk of critical infrastructure that meet the standards-based criteria should be considered with a long-term goal of risk reduction over decades. A key impediment to risk-informed regulation is that the epistemic uncertainty in the current estimates of seismic risk is huge, making it difficult to determine if the risk is small enough or to distinguish between the risks for different facilities for prioritization of mitigation efforts. Of the three main parts of seismic risk (seismic hazard, structure capacity, and consequences of a failure), the largest source of epistemic uncertainty in the seismic risk is due to the uncertainty in the seismic hazard, and in particular, in the ground motion model for a given site and seismic source. The greatly expanded ground motion data sets available in the last decade have shown that the systematic site and path effects account for about 50% of the aleatory variance in typical global ground motion models that use the ergodic assumption and the region-specific source effects account for an additional 15-20%. While we know the aleatory variability in ergodic ground motion models is too large, using the reduced aleatory variability requires estimation of the site/source-specific effects on the median ground motions. Properly capturing these site/source-specific effects can drastically change the estimates of seismic risk for a particular structure. To be able to have useful seismic risk estimates, regulators and owners of critical infrastructure need improved site-specific seismic hazard models that capture the systematic source and path effects. Path effects can be estimated using analytical modeling of wave propagation in a 3-D crustal model, such as CyberShake, but before such models are used in engineering applications, they require adequate validation against recorded data. The current seismic instrumentation in California does not provide the density of stations required to adequately validate the analytical 3-D models for engineering applications. Greatly expanded seismic instrumentation in the regions around critical infrastructure will be needed in the next decade to support the move to risk-informed decision making and optimizing seismic risk reduction.



Dr. Abrahamson has been involved in strong motion seismology for 18 years. He has extensive experience in the practical application of seismology to the development of deterministic and probabilistic seismic criteria (response spectra, and/or time histories) for engineering design or analyses. He has been involved in developing design ground motions for hundreds of projects including dams, bridges, nuclear power plants, nuclear waste repositories, water and gas pipelines, rail lines, ports, landfills, hospitals, electric substations, and office buildings. About 3/4 of these projects have been in the Western US and the other 1/4 have been in the Eastern US or outside of the US.

At PG&E, Dr. Abrahamson is responsible for developing ground for seismic evaluations of PG&E facilities including nuclear power plants, nuclear waste storage, dams, penstocks, electric substations, office buildings, and gas pipelines. He is also responsible for the technical management of the PG&E seismic research program funded through the Pacific Engineering Research Center.

As a consultant, Dr. Abrahamson has been involved in the ground motion studies for several major engineering projects in California. Recent projects include the Caltrans major toll bridge retrofit projects, the CalFed project for the Sacramento Delta levee system, the BART seismic retrofit project, and the SFO expansion. He has been involved in developing ground motion for nuclear plants and dams in the United States and in other countries. He served as the leader of the ground motion characterization team for the proposed high level nuclear waste repository at Yucca Mountain.

Plenary Talk Presentations

Monday

Reducing variability in earthquake stress drops to define secondary trends, *Annemarie Baltay (USGS)*

Monday, September 8, 2014 (11:00)

Using a large set of stress drop estimates from a variety of methods and datasets, I identify several trends in earthquake stress drops, heretofore not rigorously investigated due to the considerable scatter in stress drop measurements. I find a dependence of stress drop on depth, as well as a decreased median stress drop for aftershocks when compared to mainshocks. Several approaches are used to estimate stress drop from different data sets, including the very large NGA-West2 database. These methods include both Brune stress drops from eGf deconvolution, and time-domain-based measures, i.e. aRMS stress drops. Applying the a-RMS methodology to the NGA-West2 database allows recovery of stress drops directly from the ground motion data, which compare well to inferred stress drops from ground motion prediction equations (GMPEs). I find that the Brune eGf-based stress drop estimates and the NGA-West2 a-RMS stress drops show a marked decrease in scatter, as compared to many other seismological studies.

The overall distribution of stress drops can be considered in two parts: aleatory variability, due to statistical or random variability, such as the natural variability of earthquake stress drops; and epistemic uncertainty, associated with things we don't currently know, but are knowable, such as whether earthquake stress drops depend on depth. We are often unable to separate the two, but the reduced scatter in our stress drop estimates allows us to ascertain deterministic secondary trends in the aleatory distribution, which I term epistemes.

Having identified a dependence of stress drop on depth and a decrease in median stress drops for on-fault aftershocks, as compared to mainshocks, we are able to account for their effects on estimates of stress drop. By identifying and removing these epistemes, we can actually reduce the observed aleatory variability in the stress drop distribution. While both the depth dependence and mainshock/aftershock offset are already included in some GMPEs, many previous seismological studies have been unable to conclusively uncover these trends because of their considerable scatter. Elucidating these effects in the context of understanding epistemic uncertainty and aleatory variability can help us to understand the true variability of the earthquake source, which may be due to the complex and diverse circumstances under which these earthquakes occur.

Beyond Elasticity: New Directions in Earthquake Modeling

Eric Dunham (Stanford)

Monday, September 8, 2014 (14:00)

Elasticity of Earth's crust gives rise to the cyclic accumulation and release of strain in earthquakes. Together with fault friction, elasticity determines the timing, location, and size of earthquakes, and provides the fundamental means for faults to interact with one another. Indeed, most modern earthquake models, in the form of either earthquake simulators or dynamic rupture simulations, are based solely on elasticity and friction. Despite the success of such models, future advances in earthquake science will require moving beyond elasticity; this talk explores several outstanding questions of interest to the SCEC community within this theme. The first is the classic problem of fault strength and the state of stress in Earth's crust. Here I will argue for the importance of fault geometric complexity and the inelastic response of material within fault damage zones, and present a possible explanation for why the San Andreas is weaker than most other faults. We will next examine simulated earthquake sequences on faults, like the Southern San Andreas and Imperial Valley faults, passing through sedimentary basins. One or more small events, confined beneath the basin, are followed by a much larger, surface-rupturing event that breaks through the basin. Do we expect this behavior in southern California and what would it imply for seismic hazard? Finally we will consider earthquakes on faults extending offshore, like the Ventura-Pitas Point thrust system, which could generate tsunamis in addition to seismic shaking. By adding an ocean layer and properly accounting for gravitational restoring forces, we can simultaneously model earthquake rupture dynamics, seismic and ocean acoustic waves, and tsunamis.

Plenary Talk Presentations

Tuesday

Can We Rely on Linear Elasticity to Predict Long-period Ground Motions?

Daniel Roten (SDSC), Kim B. Olsen (SDSU), Steven M. Day (SDSU), and Yifeng Cui (SDSC)

Tuesday, September 9, 2014 (08:00)

A major challenge in seismic hazard assessment consists in the prediction of near-source ground motions resulting from large, rare earthquakes, which are not well represented in observed data. In southern California a basis for assessing the economical and societal impact of a major ($M > 7.8$) earthquake rupturing the San Andreas fault has been provided by numerical simulations of various rupture scenarios. Simulations of SE-NW propagating sources (e.g., ShakeOut) have predicted strong long-period ($> 2s$) ground motions in the densely populated Los Angeles basin due to channeling of seismic waves through a series of contiguous sedimentary basins. Recently such a waveguide amplification effect has also been identified from virtual earthquakes based on Green's function derived from the ambient seismic field (Denolle et al., 2014).

Previous scenario simulations shared the assumption of a linear viscoelastic stress-strain relationship in crustal rocks, and methods that derive amplifications from ambient noise are also inherently assuming linear material behavior. Motivated by studies of dynamic rupture in nonelastic media, we simulate the wave propagation for selected San Andreas earthquake scenarios in a medium governed by Drucker-Prager elastoplasticity. For the ShakeOut earthquake scenario (based on the kinematic source description of Graves et al., 2008) plastic yielding in crustal rock reduces peak ground velocities in the Los Angeles basin between 30 and 70% as compared to viscoelastic solutions. Our simulations also show that the large strains induced by long-period surface waves in the San Gabriel and Los Angeles basins would trigger nonlinear behavior in cohesionless sediments, as suggested by theoretical studies (e.g., Sleep & Erickson, 2014). In the fault zone plasticity remains important even for conservative values of cohesions, suggesting that current simulations assuming a linear response of crustal rocks are overpredicting ground motions during future large earthquakes on the southern San Andreas fault. We analyze the sensitivity of ground motion levels to the choice of nonlinear material properties (cohesion, friction angle) and the initial stress field, and discuss how nonlinear material behavior may be included in future simulations of major earthquake scenarios and physics-based seismic hazard assessment.

Waste water injection induced seismicity in naturally-active, seismogenic regions in central California, *Thomas H. Goebel (Caltech), Egill Hauksson (Caltech), Jean-Paul Ampuero (Caltech), Fred Aminzadeh (USC), Frederic Cappa (Géoazur), and Jason B. Saleeby (Caltech)*

Tuesday, September 9, 2014 (10:30)

The lack of easily accessible hydrocarbon reservoirs requires increasingly invasive methods to unlock trapped oil and gas. As a consequence, large volumes of fluids are injected to stimulate reservoir production and to dispose of waste water. Concurrent with the increase in injection activity, there has been an increase in seismicity rates of events with $M > 3$ within the central US starting in ~2000. Similarly, the major oilfields in central California experienced a strong increase in injection rates, however, the seismogenic consequences are unknown or undocumented.

We analyzed seismicity in Kern county, the largest oil-producing county in California, where tectonically-driven earthquakes are frequent, potentially masking injection-induced events. Our study investigates parallels in waste-water injection parameters and geological conditions for wells with an increase in adjacent seismic activity. These wells are identified by simple criteria that highlight regions of strong spatio-temporal correlations between injection and seismic activity as well as seismicity-density changes due to injection. The method enables an objective analysis of large data-sets independent of background seismicity rates. Our results show that injection-induced seismic events are surprisingly rare at large scales although injection operations are extensive within the study area. We identified four likely induced sequences with some events above $M4$. These sequences exhibit different migration characteristics relative to the injection sites, suggesting fault creep and pore-pressure diffusion as possible triggering mechanisms. Diffusive processes may take advantage of pre-existing reservoir and fault structures which can lead to seismic activity at up to 10 km from the injecting well. Our results suggest that injection-related triggering processes are complex, and may occur with a significant time-delay. Pore-pressure diffusion may be more extensive in the presence of active faults and high-permeability damage zones thus altering the local seismic hazard in a non-linear fashion. Consequently, generic "best-practices" for fluid injections like a maximum distance from the nearest, active fault may not be sufficient to mitigate the increase in seismic hazard in tectonically-active regions. However, a synthesis of results from many different tectonic regions may help illuminate common geologic, reservoir and injection characteristics and thus also conditions likely to induce earthquakes.

Differential LiDAR – a new tool for mapping coseismic fault-zone

deformation, *Edwin Nissen (CSM), J Ramon Arrowsmith (ASU), Adrian Borsa (UCSD), Craig Glennie (Terrapoint), Alejandro Hinojosa-Corona (CICESE), Tadashi Maruyama (JAMSTEC), and Michael Oskin (UC Davis)*

Tuesday, September 9, 2014 (14:00)

The recent surge in airborne laser scanning along active faults in California and elsewhere provides high-resolution topographic baselines against which future, post-earthquake LiDAR datasets can be compared, equipping us with a powerful new tool for mapping coseismic rupture-zone deformation. Here, we showcase its rich potential using synthetic datasets derived from the southern California “B4” survey and real examples from earthquakes in Baja California and Japan to illustrate. Point-cloud differencing procedures based on the Iterative Closest Point algorithm or on cross-correlation techniques can determine the surface deformation field in 3 dimensions, complimenting conventional InSAR and pixel-tracking techniques which measure line-of-sight and horizontal displacement components only. A further advantage is that differential LiDAR retains coherence in the presence of steep displacement gradients, such as close to surface ruptures, and it is therefore well-suited for probing the slip distribution and mechanical properties of the shallow part of the fault zone. Challenges include the treatment of vegetation and the reliance on older, “legacy” LiDAR datasets – third party surveys which were not optimized for earthquake studies and for which important data acquisition and processing metrics may be unavailable. The 4 April 2010 El Mayor-Cucapah (Mexico) earthquake was the first complete rupture with both pre- and post-event LiDAR coverage, and its resultant 3-D displacement field is used to explore whether significant slip occurred on low-angle detachment faults, as has been postulated by some field geologists. The 11 April 2011 Fukushima-Hamadori (Japan) normal-faulting earthquake is the second such example, and was studied with support from the Virtual Institute for the Study of Earthquake Systems (VISES), a joint initiative between SCEC and the Earthquake Research Institute and Disaster Prevention Research Institute of Japan. Here, coherent differential LiDAR displacements within the interior part of the fault zone are used to help bridge a critical observational gap between surface faulting offsets (observed in the field) and slip occurring at depths of a few kilometers (inferred from InSAR modelling). Near-fault displacements and rotations are consistent with decreased primary fault slip at very shallow depths of a few 10s of meters, possibly accounting for the large, along-strike heterogeneity in field measurements of surface offset.

Plenary Talk Presentation

Wednesday

The IDEA Model: A Practical Tool for Designing Effective Early Earthquake Warning Messages, *Deanna Sellnow (U Kentucky) and Tim Sellnow (U Kentucky)*

Wednesday, September 10, 2014 (08:30)

The right message at the right time saves lives. These words are certainly true for early earthquake warnings. In this session, we will describe how we derived the IDEA model from the principles of effective risk and crisis communication, highlight some of the research we have done to inform our work, and explain how we are now using the model to design early earthquake warning messages to be delivered in 10 seconds or less on a smart phone app. We will also summarize the studies we have employed and conclusions drawn from them since beginning our work with the USGS SAFFR group July 2013. We will then engage in a Q&A discussion regarding next steps in research and development for rolling out the early earthquake warning app., as well as questions focusing on risk and crisis communication in general.

Poster Session Schedule

View full abstracts at www.scec.org/meetings/2014am

Sunday, September 7, 2014

21:00 – 22:30 Poster Session 1

Monday, September 8, 2014

16:00 – 17:30 Poster Session 2

21:00 – 22:30 Poster Session 3

Tuesday, September 9, 2014

16:00 – 17:30 Poster Session 4

21:00 – 22:30 Poster Session 5



Communication, Education, & Outreach

Posters 001-006

- 001 **Great ShakeOut Earthquake Drills**, *Mark L. Benthien and Jason E. Ballmann*
- 002 **Earthquake Country Alliance**, *Jason E. Ballmann and Mark L. Benthien*
- 003 **STEM Education Products and Programs from the SCEC Communication, Education, and Outreach (CEO) Program – 2014 Highlights**, *Robert M. de Groot, Mark L. Benthien, Kathleen Springer, Danielle Sumy, Cindy Pridmore, Bernadette Vargas, Mark Kline, Key McMurry, Alyssa Caudill, Elizabeth Cochran, Jesse Lawrence, Lilian Arevalo, Kevin Chan, Amelia Moura, David Bolen, Jonathan Ho, Benjamin Anderson, Michelle Vanegas, Luis Gomez, and Dylan Aldrich*
- 004 **Vital Signs of the Planet: A Professional Development Program for High School and Middle School Educators Provides Authentic Experiences In Scientific Inquiry and Encourages Instructional Improvement in Schools Through Lesson Study**, *Bernadette E. Vargas, William B. Banerdt, Erin Burkett, Elizabeth Cochran, Luis Cortez, Abigail Elvis, Robert M. de Groot, Demoree Deocales, Matthew P. Golombek, Luis J. Gomez, Troy L. Hudson, Jane Houston Jones, Thomas Jordan, Michael Hubenthal, Daniel Keck, Robert S. Kirkwood, Mark Kline, Hernan Lopez, Morris Martinez, James McClure, Sally McGill, Patrick McQuillan, Marc Moya, Lindsay Rosenbaum, Ricardo Ruiz, Joann Stock, Danielle Sumy, Ashitey Trebi-Ollennu, Margaret Vinci, Seth Wallace, Alice Wessen, Katherine Williams, and Rachel Zimmerman-Brachman*
- 005 **Visible Earthquakes: An open visualization and modeling platform for InSAR earthquake data**, *Rowan B. Cockett, Gareth J. Funning, and Beth Pratt-Sitaula*
- 006 **Applying Social and Behavioral Science to Broaden Use of the U.S. Geological Survey National Seismic Hazard Maps**, *Sue Perry and Mark Petersen*

Undergraduate Studies in Earthquake Information Technology (UseIT)

Posters 007-010

- 007 **UseIT: The Intern Odyssey**, *Sarah Vargas, Michael Francisco, Michael Gonzalez, Michael Matchen, LaTerrian Officer-McIntosh, Thomas Jordan, Robert de Groot, Nick Rousseau, Dave Smith, Jason Ballmann, Mark Romano, and Mark Benthien*
- 008 **UseIT 2014 Development Team**, *Greg Berger, Brandon Green, Mark Krant, Francisco Raygoza, Paulo Dos Santos, Ernest Scapini, Alicia Sellsted, Thomas Jordan, Robert de Groot, Nick Rousseau, Yao-Yi Chiang, Kevin Milner, Mark Benthien, Scott Callaghan, and Dave Smith*
- 009 **UseIT 2014 Analysis Team: Data Analysis with SCEC-VDO, Open SHA, GIS, and HAZUS for UseIT 2014 Grand Challenge**, *Sheila Bart, Georgina Campos, Thanh-Nhan Le, Rachel Hausmann, Elena Pierce, Krystel Rios, Thomas Jordan, Robert de Groot, Nick Rousseau, Yao-Yi Chiang, Kevin Milner, Mark Benthien, Scott Callaghan, Hope Seligson, and Dave Smith*
- 010 **UseIT 2014 Visualization Team: SCEC-VDO, GIS, OpenSHA, and HAZUS Implementations**, *Ryan Meier, Jaquelyn Felix, Krista McPherson, Rory Norman, Paulo Dos Santos, Thomas Jordan, Robert de Groot, Nick Rousseau, Yao-Yi Chiang, Kevin Milner, Mark Benthien, Scott Callaghan, and Dave Smith*

Working Group on California Earthquake Probabilities (WGCEP)

- 011 **UCERF3-ETAS: Including Spatiotemporal Clustering for a California Operational Earthquake Forecast**, *Edward H. Field and WGCEP 2014*
- 012 **Uncertainty in the 2014 USGS California hazard model**, *Peter M. Powers*
- 013 **Anomalous dearth of paleo-earthquakes in the last century**, *David D. Jackson*

Posters 011-014

- 014 **Regional Seismic Loss Assessment Applied Methodology – with a Case Study in Los Angeles County**, *Omid Esmaili*

Collaboratory for the Study of Earthquake Predictability (CSEP)

- 015 **Recent Developments within the Collaboratory for the Study of Earthquake Predictability**, *Maria Liukis, Maximilian Werner, Danijel Schorlemmer, John Yu, Philip Maechling, Jeremy Zechar, Thomas H. Jordan, and the CSEP Working Group*
- 016 **Aftershock triggering by postseismic stresses: a study based on Coulomb-Rate-and-State models**, *Camilla Cattania, Sebastian Hainzl, Lifeng Wang, Bogdan Enescu, and Frank Roth*
- 017 **Determination of 3D testing region for Kanto district in Japan**, *Sayoko Yokoi, Hiroshi Tsuruoka, and Naoshi Hirata*
- 018 **Prospective evaluation of 1-day testing class of the CSEP-Japan earthquake forecasts**, *Hiroshi Tsuruoka and Naoshi Hirata*
- 019 **Influence of Tectonic Setting on the Predictive Skills of Space-Time Smoothed Seismicity Earthquake Forecasts in California and Japan**, *Maximilian J. Werner, Hiroshi Tsuruoka, Sayoko Yokoi, Agnes Helmstetter, and Naoshi Hirata*

Posters 015-021

- 020 **Recent experiences in OEF in New Zealand**, *Matthew C. Gerstenberger, David Rhoades, Graeme McVerry, Annemarie Christophersen, Stephen Bannister, Bill Fry, and Sally Potter*
- 021 **Rate-and-State Southern California Earthquake Forecasts: Resolving Stress Singularities**, *Anne E. Strader and David D. Jackson*

Earthquake Forecasting & Predictability (EFP)

- 022 **Foreshock probability forecasting**, *Yosihiko Ogata*
- 023 **Bayesian forecasting of aftershocks by ETAS model**, *Takahiro Omi, Yosihiko Ogata, Yoshito Hirata, and Kazuyuki Aihara*
- 024 **Does aftershock triggering explain the information gains of medium-term forecasting models?**, *David A. Rhoades, Morgan T. Page, and Annemarie Christophersen*
- 025 **Dynamic Aftershock Triggering Correlated with Cyclic Loading in the Slip Direction**, *Jeanne L. Hardebeck*
- 026 **Bigger aftershocks happen farther away: non-separability of magnitude and spatial distributions of aftershocks**, *Nicholas J. van der Elst and Bruce E. Shaw*
- 027 **Predicting Offshore Swarm Rate Changes by Volumetric Strain Changes in Izu Peninsula, Japan**, *Takao Kumazawa, Yosihiko Ogata, Youichi Kimura, Kenji Maeda, and Akio Kobayashi*
- 028 **How predictable is background seismicity in Southern California?**, *Margarita Segou*
- 029 **Virtual California: Earthquake Statistics, Surface Deformation Patterns, Surface Gravity Changes and InSAR Interferograms for Arbitrary Fault Geometries**, *Kasey W. Schultz, Michael K. Sachs, Eric M. Heien, John B. Rundle, Jose Fernandez, Don L. Turcotte, and Andrea Donnellan*

Posters 022-034

- 030 **Towards a Unified Theory of Seismicity Rate Variation**, *Morgan T. Page and Karen Felzer*
- 031 **Operational earthquake forecasting in California: A prototype system combining UCERF3 and CyberShake**, *Kevin R. Milner, Thomas H. Jordan, and Edward H. Field*
- 032 **Space-time Renewal Model for Repeating Earthquakes and Slip-rate History in the Northeastern Japan Subduction Zone**, *Shunichi Nomura*
- 033 **Assessing magnitude Inter-dependency using global and local catalogs**, *Kevin Nichols, Devon Cook, and Jazmine Titular*
- 034 **Can we detect clustered megaquakes?**, *Eric G. Daub, Daniel T. Trugman, and Paul A. Johnson*

Earthquake Early Warning (EEW)

- 035 **Increasing Warning Times for the Onsite Earthquake Early Warning Algorithm**, *Elizabeth S. Cochran, Egill Hauksson, Maren Boese, and Claude Felizardo*
- 036 **Improvement of the single station algorithm for earthquake early warning**, *Shunta Noda, Shunroku Yamamoto, and Masahiro Korenaga*
- 037 **Status and Growth of the USGS Southern California GPS Network**, *Daniel N. Determan, Aris G. Aspiotes, Ken W. Hudnut, Nancy E. King, Keith F. Stark, and Derik T. Barseghian*
- 038 **Acquisition, Processing, and Modeling of Real-Time High-Rate GPS Data at USGS in Menlo Park for Improved Earthquake Early Warning**, *Deborah E. Smith, Jessica R. Murray, John O. Langbein, Christian Guillemot, and Sarah E. Minson*
- 039 **Crowd-Sourced Global Earthquake Early Warning**, *Sarah E. Minson, Benjamin A. Brooks, Craig L. Glennie, Jessica R. Murray, John O. Langbein, Susan E. Owen, Thomas H. Heaton, Robert A. Iannucci, and Darren L. Hauser*
- 040 **Next-Generation Model Averaging for Earthquake Early Warning**, *Thomas H. Heaton, Sarah E. Minson, Stephen Wu, James L. Beck, and Egill Hauksson*

Posters 035-043

- 041 **A Filter Bank Approach to Earthquake Early Warning**, *Men-Andrin Meier, Thomas Heaton, and John Clinton*
- 042 **Rapid kinematic slip inversion tsunami inundation modeling with regional geophysical data**, *Diego Melgar and Yehuda Bock*
- 043 **A real-time seismogeodetic network using MEMS accelerometers**, *Jennifer S. Haase, Jianghui Geng, Diego Melgar, Dara E. Goldberg, and Jessie K. Saunders*

Earthquake Engineering Implementation Interface (EII)

- 044 **Time-varying loss forecast for an earthquake scenario in Basel, Switzerland**, *Marcus Herrmann, Jeremy D. Zechar, and Stefan Wiemer*
- 045 **Shallow shear wave velocity characterization of the urban Christchurch, New Zealand region**, *Christopher McGann, Brendon Bradley, and Misko Cubrinovski*
- 046 **Parameterization of fling-step from ground motion recordings and simulations**, *Jack W. Baker and Lynne S. Burks*
- 047 **Ground motion selection for simulation-based seismic hazard analysis**, *Lynne S. Burks, Brendon A. Bradley, and Jack W. Baker*
- 048 **Characterization of dynamic soil properties and stratigraphy at Heathcote valley, New Zealand, for simulation of 3D valley effects**, *Seokho Jeong, Brendon A. Bradley, Christopher R. McGann, and Gregory P. De Pascale*
- 049 **Multiple Structure-Soil-Structure Interaction and Coupling Effects in Building Clusters**, *Yigit Isbiliroglu, Ricardo Tabora, and Jacobo Bielak*
- 050 **Creation of a standardized protocol for checking the applied seismic code or standard, by using the detected damages to buildings after an earthquake.**, *Jose Ferrandiz*
- 051 **Implications from observed drift of tall buildings during the March 11, 2011 M9.0 Tohoku Earthquake, Japan**, *Mehmet Celebi, Izuru Okawa, and Toshihide Kashima*
- 052 **Utilization of simulated ground motions for engineering performance assessment of tall buildings**, *Nenad Bijelic, Ting Lin, and Gregory Deierlein*
- 053 **Broadband Platform Ground Motion Simulations - Implementing New Validation Metrics and Exploring Aleatory Variability**, *Jeff Bayless, Andreas Skarlatoudis, and Paul Somerville*

Posters 044-057

- 054 **Development of Analytical Tools for Engineering Validation of Simulated Ground Motions**, *Peng Zhong*
- 055 **Sensitivity of Ground Motion Simulation Validation to Signal Processing and GOF Criteria**, *Naeem Khoshnevis and Ricardo Tabora*
- 056 **Validation approach for application of simulated ground motions to duration-sensitive systems**, *Kioumars Afshari and Jonathan Stewart*
- 057 **The Community Seismic Network**, *Monica D. Kohler, Robert W. Clayton, Anthony Massari, Thomas H. Heaton, Richard Guy, Mani Chandy, Julian Bunn, Leif Strand, and Santiago Arrangoiz*

Ground Motion Prediction (GMP)

- 058 **Validation of the SCEC Broadband Strong Ground Motion Simulation Platform: Ingredients and Methodology**, *Christine A. Goulet and the BBP Validation Working Group*
- 059 **The SCEC Broadband Platform: A Collaborative Open-Source Software Package for Strong Ground Motion Simulation and Validation**, *Fabio Silva, Philip Maechling, Christine Goulet, Paul Somerville, Thomas H. Jordan, and the Broadband Platform Working Group*
- 060 **GP14.3: Refinements to the Graves and Pitarka Broadband Simulation Method**, *Robert W. Graves and Arben Pitarka*
- 061 **The SDSU Broadband Ground Motion Generation Module Version 1.5**, *Kim B. Olsen and Rumi Takedatsu*
- 062 **Isolating Low Frequency Wave Propagation from High Frequency Wave Propagation in Broadband Ground Motions**, *Ralph J. Archuleta and Jorge G.F. Crempien*
- 063 **Are Current Fault Dimension Scaling Relationships Compatible with Eastern North America Earthquake Stress Drops?**, *Jorge G.F. Crempien and Ralph J. Archuleta*
- 064 **Adapting the Composite Source Model for the SCEC Broadband Platform**, *John G. Anderson*
- 065 **Validation Exercise for Two Southern California Earthquakes**, *William H. Savran and Kim B. Olsen*
- 066 **High-Complexity Deterministic Q(f) Simulation of the 1994 Northridge Mw 6.7 Earthquake**, *Kyle B. Withers, Kim B. Olsen, Zheqiang Shi, and Steve Day*
- 067 **Hazard Curve Results and a UCERF3-San Jacinto Fault Comparison From Precarious Rocks in Southern California**, *Glenn P. Biasi, James N. Brune, and John G. Anderson*
- 068 **Long-period ground-motion variability from scenario earthquakes on the Salt Lake City segment, Wasatch fault**, *Morgan P. Moschetti, Stephen Hartzell, Leonardo Ramirez-Guzman, Stephen Angster, and Arthur Frankel*
- 069 **Site response validation studies using KIK-net strong motion recordings**, *Dorniki Asimaki and Jian Shi*
- 070 **Low frequency ($f < 1\text{Hz}$) ground motion simulations of 10 events in the 2010-2011 Canterbury earthquake sequence**, *Brendon A. Bradley and Rob W. Graves*
- 071 **A 3D seismic velocity model of Canterbury, New Zealand for broadband ground motion simulation**, *Robin L. Lee, Brendon A. Bradley, Francesca C. Ghisetti, Jarg R. Pettinga, Matthew W. Hughes, and Ethan M. Thomson*

Posters 058-077

- 072 **Near source broadband ground-motion modelling of the Canterbury aftershocks and implications for assessing engineering metrics**, *Caroline Holden, Anna Kaiser, and Matt Gerstenberger*
- 073 **Frequency-dependent directivity effects from small earthquakes in Abruzzo region, Italy**, *Frantisek Gallovic, Francesca Pacor, Rodolfo Puglia, Lucia Luzi, and Maria D'Amico*
- 074 **Calibrating the composite source model for generating synthetic seismograms for Israel**, *Gony Yagoda-Biran and John G. Anderson*
- 075 **Strong Ground Motions Generated by Earthquakes on Creeping Faults**, *Ruth A. Harris and Norman A. Abrahamson*
- 076 **Virtual Topography – A New Strategy to Incorporate Surficial Irregularities into Earthquake Modeling**, *Doriam Restrepo and Jacobo Bielak*
- 077 **Statistics of Ground Motions in a Foam Rubber Model of a Strike-Slip Fault**, *Kevin M. McBean, John G. Anderson, and James N. Brune*

Community Modeling Environment (CME)

- 078 **Full-3D Tomography of the Crustal Structure in Southern California Using Earthquake Seismograms and Ambient-Noise Correlagrams**, *En-Jui Lee, Po Chen, Thomas H. Jordan, Philip J. Maechling, Marine Denolle, and Gregory C. Beroza*
- 079 **UCVM: Open Source Software for Understanding and Delivering 3D Velocity Models**, *David Gill, Patrick Small, Philip Maechling, Thomas H. Jordan, John Shaw, Andreas Plesch, Po Chen, En-Jui Lee, Ricardo Taborda, Kim Olsen, and Scott Callaghan*
- 080 **Evaluation of the Southern California Velocity Models through Simulation and Validation of Multiple Historical Events**, *Shima Azizzadehroodpish, Naeem Khoshnevis, and Ricardo Taborda*
- 081 **Optimizing CyberShake Seismic Hazard Workflows for Large HPC Resources**, *Scott Callaghan, Philip Maechling, Gideon Juve, Karan Vahi, Robert W. Graves, Kim B. Olsen, Kevin Milner, David Gill, and Thomas H. Jordan*

- 082 **A High Level Parallel IO Library for High-Performance Seismic Applications**, *Heming Xu, Efekan Poyraz, Daniel Roten, and Yifeng Cui*
- 083 **Exploring Distributed Physics-based Cellular Automata to Model Seismic Elastodynamics in OpenCL beyond GPGPU accelerators**, *Liwen Shih and Mark Garrett*
- 084 **Efficient Static and Dynamic Receiver Green's Tensor and Green's Function Computations for Large Scale Applications**, *Leonardo Ramirez-Guzman, Stephen Hartzell, Alan Juarez, and Jacobo Bielak*
- 085 **GPU Acceleration of Hercules**, *Patrick Small, Ricardo Taborda, Jacobo Bielak, and Thomas H. Jordan*
- 086 **IO Optimization Techniques for Distributed Heterogeneous Supercomputing Systems**, *Efekan Poyraz, Jun Zhou, and Yifeng Cui*
- 087 **Integration of a 3D Low-Frequency Simulation with the SCEC Broadband Platform**, *Ricardo Taborda, David Gill, Patrick Small, Fabio Silva, Philip J.*

- Maechling, Jacobo Bielak, and Thomas H. Jordan*
- 088 **Finite Element Simulation of Earthquakes with Coupling Tsunamis in Large Domains—A Case Study of the 2011 Tohoku-Oki Earthquake and Tsunami**, *Haydar Karaoglu and Jacobo Bielak*
- 089 **Tsunami hazard from the Ventura-Pitas fault and fold system**, *Hong Kie Thio, Wenwen Li, John Shaw, Judith Hubbard, Andreas Plesch, and Rick Wilson*
- 090 **GeoGateway as a Tool for Analyzing UAVSAR Observations from the El Mayor – Cucapah and La Habra earthquakes**, *Andrea Donnellan, Jay Parker, Parker Won, Lisa Grant Ludwig, Marlon Pierce, and Jun Wang*
- 091 **SCEC Community Modeling Environment SI2 and Geoinformatics Research Projects**, *Philip J. Maechling, Thomas H. Jordan, Jacobo Bielak, Yifeng Cui, Kim B. Olsen, and Jeroen Tromp*

Posters 078-091

Unified Structural Representation (USR)

- 092 **Geometry of the San Andreas Fault and Sedimentary Basin in the Northern Salton Trough**, *Gary S. Fuis, Klaus Bauer, Rufus D. Catchings, Mark Goldman, Trond Ryberg, Daniel S. Scheirer, Victoria E. Langenheim, Michael J. Rymer, Patricia Persaud, Joann M. Stock, and John A. Hole*
- 093 **The Distribution of Fault Slip Rates in the Ventura Fault System, CA**, *Scott T. Marshall, Gareth J. Funning, and Susan E. Owen*

- 094 **The geometry of the post-Miocene North Channel-Pitas Point Fault System including post-Miocene folding, Santa Barbara Channel, California**, *Christopher C. Sorlien, Craig Nicholson, Richard J. Behl, Marc J. Kamberling, Courtney J. Marshall, and James P. Kennett*
- 095 **Stochastic descriptions of small-scale, near-surface velocity variations in the Los Angeles basin**, *Xin Song, Thomas H. Jordan, Andreas Plesch, and John H. Shaw*

- 096 **SCEC Community Fault Model Version 5.0**, *Andreas Plesch, Craig Nicholson, Christopher Sorlien, John H. Shaw, and Egill Hauksson*

Posters 092-096

Stress & Deformation Over Time (SDOT)

- 097 **Constraining Moment Deficit Rate on Crustal Faults from Geodetic Data**, *Jeremy L. Maurer, Andrew Bradley, and Paul Segall*
- 098 **Kinematically Consistent Viscoelastic Block Models: Time Series Averaging and Accurate Plate Motions**, *Phoebe Robinson DeVries, Plamen G. Krastev, and Brendan J. Meade*
- 099 **Time-dependent model of aseismic slip on the Central San Andreas Fault from InSAR time series and repeating earthquakes**, *Mostafa Khoshmanesh, Manoochehr Shirzaei, and Robert Nadeau*
- 100 **A Southern California lithosphere deformation model for the SCEC CSM:**

- Status update and preliminary findings**, *Elizabeth H. Hearn*
- 101 **When the Rains Fail, the Mountains Rise: Drought-induced Uplift in the Western United States Observed by the PBO GPS network**, *Adrian A. Borsa, Duncan C. Agnew, and Daniel Cayan*
- 102 **Statistical analysis of GPS vertical uplift rates in southern California**, *Samuel M. Howell, Bridget Smith-Konter, Neil Frazer, Xiaopeng Tong, and David Sandwell*
- 103 **Seasonal stress loading and periodic seismicity in California**, *Christopher W. Johnson, Roland Burgmann, and Pierre Dutilleul*
- 104 **Stress equilibrium in southern California from Maxwell stress function models fit to**

- both earthquake data and a quasi-static dynamic simulation**, *Peter Bird*
- 105 **Mechanical insights into tectonic reorganization of the southern San Andreas fault system since ca. 1.5 Ma**, *Laura A. Fattaruso, Michele L. Cooke, Rebecca J. Dorsey, and Bernard A. Housen*
- 106 **Evolving strike-slip efficiency of restraining bends in wet kaolin analog experiments**, *Alex E. Hatem, Michele L. Cooke, and Elizabeth H. Madden*

Posters 097-106

Fault and Rupture Mechanics (FARM)

Posters 107-154

- 107 **Similarities between Vere-Jones' branching crack model and earthquake source process**, *Jiancang Zhuang, Dun Wan, and Mitsuhiro Matsuura*
- 108 **Micromechanics based permeability evolution model in brittle materials and implications for injection-induced earthquake nucleation**, *Thibaut Perol, Harsha S. Bhat, and Kurama Okubo*
- 109 **The role of gouge and temperature on flash heating and its hysteresis**, *John D. Platt, Brooks P. Proctor, Thomas M. Mitchell, Greg Hirth, David L. Goldsby, Giulio Di Toro, Nicholas M. Beeler, and Terry E. Tullis*
- 110 **Shear flow of angular grains: acoustic effects and non-monotonic rate dependence of volume**, *Charles K. Lieou, Ahmed E. Elbanna, James S. Langer, and Jean M. Carlson*
- 111 **Dynamic weakening of serpentinite gouges and bare-surfaces at seismic slip rates**, *Brooks P. Proctor, Tom M. Mitchell, Greg Hirth, David Goldsby, Federico Zorzi, John D. Platt, and Giulio Di Toro*
- 112 **The Effect of Mean Grain Size and Polydispersity on Auto-Acoustic Compaction**, *Stephanie E. Taylor and Emily E. Brodsky*
- 113 **Intersonic and Supersonic ruptures in a model of dynamic rupture in a layered medium**, *Xiao Ma and Ahmed Ettaf Elbanna*
- 114 **In-Situ Observations of Earthquake-Driven Fluid Pulses within the Japan Trench Plate Boundary Fault Zone**, *Patrick M. Fulton and Emily E. Brodsky*
- 115 **Using Fault-Zone Trapped Waves from Teleseismic Earthquakes to Document Deep Structure of the Calico Fault in Mojave Desert, California**, *Yong-Gang Li, Elizabeth S. Cochran, Po Chen, and En-Jui Lee*
- 116 **Metrics for Comparing Dynamic Earthquake Rupture Simulations**, *Michael Barall and Ruth A. Harris*
- 117 **A Multiscale Model for Shear flow of Granular Materials with Breakable Particles: Role of Force Chain Instabilities and Implications for Strain Localization, grain size evolution and energy partitioning.**, *Ahmed E. Elbanna, Charles Lieou, Rui Li, and Jean Carlson*
- 118 **Fault core and slip zone geometry, wear and evolution**, *Katherine A. Shervais and James Kirkpatrick*
- 119 **Determining Paleoseismicity using Biomarkers**, *Heather M. Savage, Pratigya J. Polissar, and Rachel Sheppard*
- 120 **Inversion for the physical parameters that control the source dynamics of the 2004 Parkfield earthquake**, *Cedric Twardzik, Raul Madariaga, and Shamita Das*
- 121 **Interaction of repeating earthquake sequences and its relation to fault friction properties**, *Ka Yan Semechah Lui and Nadia Lapusta*
- 122 **How energy efficiency and the potential for coseismic rupture change with strike-slip fault growth through releasing bends**, *Elizabeth H. Madden, Michele L. Cooke, and Jessica McBeck*
- 123 **Quantifying the temperature and age of seismic slip: Transition metal geothermometry and oxide (U-Th)/He chronology of exhumed fault surfaces**, *James P. Evans and Alexis Ault*
- 124 **Signatures of Fluid-Pressure Triggering, Natural and Induced: Comparing Migrating Earthquake Swarms in Long Valley Caldera, California and Azle, Texas**, *David R. Shelly, William L. Ellsworth, Emily K. Montgomery-Brown, David P. Hill, Stephanie G. Prejean, and Margaret T. Mangan*
- 125 **Seismogenic zone depth control on the likelihood of fault stepover jump**, *Kangchen Bai and Jean-Paul Ampuero*
- 126 **Dynamic Rupture Models of the Historic and Recent Paleoseismic Rupture Sequence of the Northern and Central San Jacinto Fault**, *Julian C. Lozos, Thomas K. Rockwell, and Nathan W. Onderdonk*
- 127 **Long-term fault behavior at the seismic-aseismic transition: space-time evolution of microseismicity and depth extent of earthquake rupture**, *Junle Jiang and Nadia Lapusta*
- 128 **An approach for calculating absolute stress from stressing rate**, *Aviel Stern and Michele L. Cooke*
- 129 **Slip Reactivation Model for the 2011 Mw9 Tohoku Earthquake: Dynamic Rupture and Strong Ground Simulations**, *Luis A. Dalguer and Percy Galvez*
- 130 **Large Earthquakes and Three Dimensional Strain on Interlocking Networks of Small Faults**, *John M. Fletcher, Michael E. Oskin, Orlando J. Teran, and Egill Hauksson*
- 131 **Towards Reconciling Magnitude-Invariant Stress Drops with Dynamic Weakening**, *Stephen M. Perry and Nadia Lapusta*
- 132 **Deterministic Model of Earthquake Clustering Shows Reduced Stress Drops for Nearby Aftershocks**, *Bruce E. Shaw, Keith Richards-Dinger, and James H. Dieterich*
- 133 **Dynamic earthquake rupture simulations on nonplanar faults embedded in 3D geometrically complex, heterogeneous Earth models**, *Kenneth Duru, Eric M. Dunham, and Sam A. Bydlon*
- 134 **The evolution of earthquake nucleating slip instabilities under spatially variable steady-state rate dependence of friction**, *Sohom Ray and Robert C. Viesca*
- 135 **Modeling Fragmentation, Acoustic Effects, and Flash Heating in Sheared Granular Materials: Implications of Geophysical Processes and Physical Constraints for Dynamic Friction**, *Jean M. Carlson, Charles Lieou, Ahmed Elbanna, and James Langer*
- 136 **Possible bias in ground motion and rupture simulations arising from forced nucleation locations that are inconsistent with heterogeneous stress conditions.**, *Jacquelyn J. Gilchrist, James H. Dieterich, David T. Oglesby, and Keith B. Richards-Dinger*
- 137 **Dynamic Compaction as a Simple Mechanism for Fault Zone Weakening**, *Evan T. Hirakawa and Shuo Ma*
- 138 **Late Quaternary displacement gradients along the Calico-Blackwater-Harper Lake fault systems, Eastern California**, *Jacob A. Selander and Michael E. Oskin*
- 139 **Do laboratory slide-hold-slide experiments really provide evidence for time-dependent healing in rock?**, *Pathikrit Bhattacharya, Allan M. Rubin, and Nicholas M. Beeler*
- 140 **Accelerated creep on the Hayward fault controlled by fluid pressure**, *Manoochehr Shirzaei*
- 141 **Scale dependency of fracture energy and estimates thereof via dynamic rupture solutions with strong thermal weakening**, *Robert C. Viesca and Dmitry I. Garagash*
- 142 **Array Waveform Coherency and Its Implication on Earthquake Source Properties**, *Ailin Zhang and Lingsen Meng*
- 143 **Influence of fluid pressure variations in earthquake swarms in the Salton Sea geothermal field?**, *Xiaowei Chen and Jeff McGuire*
- 144 **Permeability, porosity and pore geometry evolution of cohesive and incohesive sedimentary rocks**, *Keishi Okazaki, Hiroyuki Noda, Shin-ichi Uehara, and Toshihiko Shimamoto*
- 145 **Aseismic slow-slip and dynamic ruptures of the 2014 Iquique earthquake sequence**, *Lingsen Meng, Hui Huang, Roland Burgmann, Jean-Paul Ampuero, and Anne Strader*
- 146 **Modeling earthquake rupture on the Pitias Point fault: Implications for tsunami generation and propagation**, *Kenny J. Ryan, David D. Oglesby, and Eric L. Geist*
- 147 **Experimental Studies of Dynamic Fault Weakening Due to Thermal Pore-Fluid Pressurization**, *David L. Goldsby, Terry E. Tullis, Keishi Okazaki, John Platt, and Thomas Mitchell*

POSTER PRESENTATIONS

- 148 **Dynamic models of the 2010 Sierra El Mayor-Cucapah Earthquake**, *David D. Oglesby, Gareth J. Funning, and Christodoulos Kyriakopoulos*
- 149 **Earthquake Cycles in Heterogeneous Media: Sub-basin and Surface-rupturing Events on Faults Crossing a Sedimentary Basin**, *Kali L. Allison and Eric M. Dunham*
- 150 **Far-field seismic spectral response resulting from complex rupture behaviors**, *Yongfei Wang, Steven M. Day, and Peter M. Shearer*
- 151 **The Bimaterial Effect on the Earthquake Cycle**, *Brittany A. Erickson and Steven M. Day*
- 152 **Structural Self-similarity in Earthquake Swarms: Evidence from the 2008 West Reno, NV Earthquake Sequence**, *Christine J. Ruhl and Kenneth D. Smith*
- 153 **A New Creep Instability at Intermediate Homologous Temperatures with Application to Slow Earthquakes and Non-Volcanic Tremor**, *Marshall A. Rogers-Martinez, Rachel C. Lippoldt, and Charles G. Sammis*
- 154 **Geomechanical Seismicity-Based Reservoir Characterization**, *S. Mehran Hosseini and Fred Aminzadeh*

Seismology

- 155 **Products and Services Available from the Southern California Earthquake Data Center (SCEDC) and the Southern California Seismic Network (SCSN)**, *Ellen Yu, Prabha Acharya, Aparna Bhaskaran, Shang-Lin Chen, Faria Chowdhury, Kate Hutton, Doug Given, Egill Hauksson, and Rob Clayton*
- 156 **Summary of Caltech/USGS UASI Project Accomplishments: 2013-2014**, *Egill Hauksson and Valerie Thomas*
- 157 **IRIS's Large N initiative – enabling the recording of full seismic wavefields**, *Kent R. Anderson, John Hole, Robert Woodward, and Bruce Beauvain*
- 158 **Bridging Seismic Networks Across Time and Space**, *Roy D. Bowling, Marine Denolle, and Peter M. Shearer*
- 159 **An Automatic P-wave Onset Time Detector**, *Erol Kalkan*
- 160 **Automatic Earthquake Detection with Pseudo-Probabilities and Automatic Picking of P, S, and Fault Zone Head Waves**, *Zachary E. Ross and Yehuda Ben-Zion*
- 161 **Automatic identification of fault zone head waves and direct P waves and its application in the Parkfield section of the San Andreas Fault, California**, *Zhigang Peng and Zefeng Li*
- 162 **Computationally Efficient Search for Similar Seismic Signals in Continuous Waveform Data over the Northern California Seismic Network**, *Clara Yoon, Ossian O'Reilly, Karianne Bergen, and Gregory Beroza*
- 163 **Robust quantification of earthquake clustering: Overcoming the artifacts of catalog errors**, *Ilya Zaliapin and Yehuda Ben-Zion*
- 164 **Modeling seismic hazard and risk in Mexico: Effects of catalog declustering assumptions**, *Deborah L. Kane and Marleen Nyst*
- 165 **Exploring fault geometry uncertainties in finite-slip inversion with multiple moment tensor inversion**, *Wenyuan Fan, Peter M. Shearer, Guy Masters, and Chen Ji*
- 166 **Investigation of grid parameterization of earthquake source**, *Haoran Meng*
- 167 **Focal mechanisms and seismic tectonic features of the 2013 Laizhou MS=4.6 earthquake sequence**, *Jianchang Zheng, Dongmei Li, and Peng Wang*
- 168 **Uncertainties in estimates of earthquake dynamic source properties from body and surface waves**, *Marine A. Denolle and Peter M. Shearer*
- 169 **Improving spatial resolution of the moment rate function in regions of high slip determined from finite fault inversions**, *Mareike N. Adams, Chen Ji, and Ralph Archuleta*
- 170 **Finite-Source Modeling for Parkfield And Anza Earthquakes**, *Kathryn E. Wooddell, Taka'aki Taira, and Douglas Dreger*
- 171 **Path calibration and finite fault modeling of the 2014 Mw5.1 La Habra Earthquake**, *Shengji Wei, Junjie Yu, Kangchen Bai, and Don Helmberger*
- 172 **The 2011 Tohoku-oki Earthquake related to a strong velocity gradient within the Pacific plate**, *Makoto Matsubara and Kazushige Obara*
- 173 **The Mw=8.1 Pisagua Earthquake of 1 April 2014**, *Zacharie Duputel, Junle Jiang, Romain Jolivet, Mark Simons, Luis Rivera, Bryan Riel, Jean-Paul Ampuero, Sarah Minson, Hailiang Zhang, Nathalie Cotte, Eric J. Fielding, Juergen Klotz, Angelyn W. Moore, Edmundo O. Norabuena, Susan E. Owen, Sergey Samsonov and Anne Socquet*
- 174 **Analysis of the March 21, 2009 (M=4.7) Bombay Beach Earthquake Swarm**, *Gerry Simila and Geoffrey McStroul*
- 175 **Spatial Partitioning of Icequakes on Gornergletscher, Switzerland**, *Debi L. Kilb and Fabian Walter*
- 176 **A search for tremor-like precursors to earthquakes in southern California**, *Jessica C. Hawthorne and Jean-Paul Ampuero*
- 177 **Simulating high-frequency earthquake dynamic rupture scenarios on natural fault zones with SeisSol**, *Alice-Agnes Gabriel, Christian Pelties, Alexander Heinecke, Alexander Breuer, Sebastian Rettenberger, and Michael Bader*
- 178 **Modeling tsunami generation and propagation from an earthquake on the Pitas Point fault**, *Gabriel C. Lotto and Eric M. Dunham*
- 179 **Imaging the internal structure of the Earth with seismic noise recorded by accelerometers**, *Santiago Rabade and Leonardo Ramirez-Guzman*
- 180 **Empirical sensitivity kernels of noise correlations with respect to virtual sources**, *Pierre Boue, Laurent Stehly, Nori Nakata, and Gregory C. Beroza*
- 181 **Wave propagation between F-net and NECESSArray retrieved from ambient noise**, *Nori Nakata, Nishida Kiwamu, and Kawakatsu Hitoshi*
- 182 **Investigating inter-station attenuation retrieval from ambient seismic noise records on station triplets**, *Xin Liu, Yehuda Ben-Zion, and Dimitri Zigone*
- 183 **Imaging the internal structure of the San Jacinto Fault Zone with high Frequency noise**, *Dimitri Zigone, Yehuda Ben-Zion, Michel Campillo, Gregor Hillers, Philippe Roux, and Frank Vernon*
- 184 **Seismic Trapped Noise in the San Jacinto Fault Zone Southeast of Anza**, *Gregor Hillers, Yehuda Ben-Zion, Michel Campillo, Philippe Roux, and Frank L. Vernon*
- 185 **Multi-Scale Structure and Earthquake Properties in the San Jacinto Fault Zone Area**, *Yehuda Ben-Zion*
- 186 **Improved understanding of moderate-size earthquake sequences on the San Jacinto Fault and their relationship with deep creep**, *Xiaofeng Meng and Zhigang Peng*
- 187 **Variations of Seismic Anisotropy along the San Jacinto Fault Zone, Southern California**, *Zefeng Li, Zhigang Peng, Zachary Ross, Frank Vernon, and Yehuda Ben-Zion*
- 188 **Characterization of the San Jacinto Fault Zone northwest of the trifurcation area from dense linear array data**, *Pieter-Ewald Share, Yehuda Ben-Zion, Zachary Ross, Hongrui Qiu, and Frank Vernon*
- 189 **Internal structure of the San Jacinto fault zone at Jackass Flat from data recorded**

Posters 155-214

- 190 **Systematic search for non-volcanic tremor under the San Jacinto Fault,** *Hongrui Qiu, Yehuda Ben-Zion, Zachary E. Ross, Pieter-Ewald Share, and Frank Vernon*
- 191 **Revisiting tremor under the San Andreas Fault: an enhanced look through a mini seismic array near Parkfield,** *Abhijit Ghosh*
- 192 **Global Search of Triggered Tectonic Tremor,** *Hongfeng Yang, Zhigang Peng, Chastity Aiken, Abhey Ram Bansal, and Kevin Chao*
- 193 **Extracting Anisotropy with non-volcanic tremor (NVT) signals in the Cascadia Region in Northern Washington State,** *Eduardo Huesca-Perez and Abhijit Ghosh*
- 194 **Earthquake Triggering and Tremor: Detecting micro-seismic events in the Western U.S due to the 2010 El Mayor Cucapah Earthquake and the Mw6.8 Mendocino Triple Junction Earthquake in 2014,** *Rachel L. Hatch and Jascha Polet*
- 195 **A change point model to detect change and quantify seismicity rates from triggered seismicity,** *Abhineet Gupta and Jack W. Baker*
- 196 **A comparative study of the seismotectonics in the San Geronio and Ventura Special Fault Study Areas,** *Thomas H. Goebel, Egill Hauksson, Andreas Plesch, and John H. Shaw*
- 197 **LASSIE: A high-density short-duration broadband seismic survey of the Los Angeles Basin,** *Robert W. Clayton, Mitchell Barklage, Elizabeth Cochran, Dan Hollis, Paul Davis, Bill Erickson, Jascha Polet, Brady Barto, Catherine Cox, and Michael Padgett*
- 198 **Monitoring microseismicity in Long-beach, CA, using a dense seismic array,** *Asaf Inbal, Robert W. Clayton, and Jean-Paul Ampuero*
- 199 **Analysis of Micro-Earthquakes in the Sierra Madre-Cucamonga Fault Zone and the Greater Pomona Area as Recorded by a Temporary Seismic Deployment,** *Jonathan Levario, Celia Pazos, David Nget, and Jascha Polet*
- 200 **Preliminary Site Response Maps From H/V Spectral Ratio Analysis on Cal Poly Pomona Campus,** *King Yin Kennis Ho and Jascha Polet*
- 201 **Kappa (κ) estimates and origins: results from a downhole array,** *Olga-Joan Ktenidou, Stephane Drouet, Fabrice Cotton, and Norman Abrahamson*
- 202 **Systematic receiver function analysis of the Moho geometry in the southern California plate-boundary region ,** *Yaman Ozakin and Yehuda Ben-Zion*
- 203 **Reducing Uncertainties in the Velocities Determined by Inversion of Phase Velocity Dispersion Curves Using Synthetic Seismograms,** *Mehrdad Hosseini and Shahram Pezeshk*
- 204 **Continental shelf morphology and stratigraphy offshore San Onofre, CA: the interplay between eustasy and sediment supply ,** *Shannon A. Klotsko, Neal W. Driscoll, Graham M. Kent, and Daniel S. Brothers*
- 205 **Towards imaging the Isabella anomaly: Basin analysis, surface wave tomography, and receiver function analysis in central California,** *Sara L. Dougherty, Robert W. Clayton, Charles R. Hoots, and Brandon Schmandt*
- 206 **Geophysical Evidence for a Southwestward dipping Southern San**
- 207 **Preliminary simulations of the interaction between of pore fluids and seismicity with RSQSim,** *Kayla A. Kroll, James H. Dieterich, and Keith B. Richards-Dinger*
- 208 **Relationships between seismic velocity, metamorphism, seismic and aseismic fault slip in the Salton Sea Geothermal Field region,** *Jeffrey J. McGuire, Rowena B. Lohman, Rufus D. Catchings, Michael J. Rymer, and Mark R. Goldman*
- 209 **Swarm or induced: Comparing pre-production seismicity with current seismicity at the Coso geothermal field,** *Martin Schoenball, Nicholas C. Davatzes, and Jonathan M.G. Glen*
- 210 **Maximum magnitudes of earthquakes in geothermal fields?,** *Deborah A. Weiser, David D. Jackson, and Lucile M. Jones*
- 211 **Analyzing Induced Seismicity related to Water/Gas Injection/Production in California,** *Qingjun Meng and Emily Brodsky*
- 212 **Is the Recent Increase in Seismicity in southern Kansas Natural?,** *Justin L. Rubinstein, William L. Ellsworth, Andrea L. Llenos, and Steven Walter*
- 213 **Increased earthquake rates in the central and eastern US portend higher earthquake hazards,** *Andrea L. Llenos, Justin L. Rubinstein, William L. Ellsworth, Charles S. Mueller, Andrew J. Michael, Arthur McGarr, Mark D. Petersen, Matthew Weingarten, and Austin A. Holland*
- 214 **Investigation of Seismic Events associated with the Sinkhole at Napoleonville Salt Dome, Louisiana,** *Avinash Nayak and Douglas S. Dreger*

Tectonic Geodesy

- 215 **Plate Boundary Observatory Southwest Region Network Operations, Expansion and Communications Hardening,** *Christian Walls, Doerte Mann, Andre Basset, Ryan Turner, Karl Feaux, and Glen Mattioli*
- 216 **The Seamless SAR Archive (SSARA) Project and Other SAR Activities at UNAVCO,** *Scott Baker, Christopher J. Crosby, Charles M. Meertens, Eric J. Fielding, Gwendolyn Bryson, Brian Buechler, Jeremy Nicoll, and Chaitanya Baru*
- 217 **E-DECIDER Disaster Response and Decision Support Platform,** *Margaret T. Glasscoe, Jay W. Parker, Marlon E. Pierce, Jun Wang, Ronald T. Eguchi, Charles K. Huyck, ZhengHui Hu, ZhiQiang Chen, Mark R. Yoder, John B. Rundle, and Anne Rosinski*
- 218 **Long-term High-Quality Deformation Observations with Long-Base Strainmeters,** *Duncan C. Agnew and Frank K. Wyatt*
- 219 **The Community Geodetic Model: Current status of the GPS component,** *Jessica R. Murray*
- 220 **Improved imaging of Southern California crustal deformation using InSAR and GPS ,** *Zhen Liu, Paul Lundgren, and Zheng-Kang Shen*
- 221 **Mitigation of atmospheric phase delays in InSAR time series analysis, with application to the Eastern California Shear Zone,** *Ekaterina Tymofyeyeva and Yuri Fialko*

Posters 215-245

- 222 **Twenty-Two Years of Combined GPS Daily Coordinate Time Series and Derived Parameters (1992-2014): Implications for Maintaining a Geodetic Reference Frame,** *Yehuda Bock, Sharon Kedar, Angelyn W. Moore, Peng Fang, Zhen Liu, Susan E. Owen, and Melinda B. Squibb*
- 223 **A network approach of GPS velocity uncertainty estimation,** *Ksenia Dmitrieva and Paul Segall*
- 224 **Improving the density of GPS velocities in southern California by resurveying single occupation sites,** *Lisa Jose, Gareth Funning, John Conrad, and Michael Floyd*

POSTER PRESENTATIONS

- 225 **Vital Signs of the Planet: Southern California Educators Contribute to Crustal Deformation Studies Within San Bernardino and Riverside Counties**, *Mark Kline, Sally McGill, Luis Cortes, Demoree Deocales, Robert de Groot, Abigail Elvis, Luis Gomez, Dan Keck, Robert Kirkwood, Hernan Lopez, Morris Martinez, Marc Moya, Lindsay Rosenbaum, Bernadette Vargas, Seth Wallace, and Katherine Williams*
- 226 **One-dimensional modeling of fault slip rates using new geodetic velocities from a transect across the Pacific-North America plate boundary through the San Bernardino Mountains, California**, *Sally F. McGill, Joshua C. Spinler, John D. McGill, Richard A. Bennett, Michael Floyd, Joan E. Fryxell, and Gareth J. Funning*
- 227 **Geodetic constraints on shortening, uplift, and fault slip across the Ventura Basin**, *Kaj M. Johnson, William C. Hammond, and Reed Burgette*
- 228 **Measuring Ventura Area Uplift: A Four-Technique Geodetic Study of Vertical Tectonics Combining GPS, InSAR, Leveling and Tide Gauges**, *William C. Hammond, Reed Burgette, and Kaj Johnson*
- 229 **Quantizing the Complexity of the Western United States Fault System with Geodetically and Geologically Constrained Block Models**, *Eileen L. Evans and Brendan J. Meade*
- 230 **Rapid shortening at the eastern margin of the Tibetan plateau prior to the 2008 Mw=7.9 Wenchuan earthquake**, *T. Ben Thompson and Brendan J. Meade*
- 231 **Decadal-scale decoupling of the Japan Trench prior to the 2011 Tohoku-oki earthquake from geodetic and repeating-earthquake observations**, *Andreas P. Mavrommatis, Paul Segall, Naoki Uchida, and Kaj M. Johnson*
- 232 **Did the Stress Perturbation Caused by Fluid Extraction at the Cerro Prieto Geothermal Field Influence the El Mayor-Cucapah Rupture Sequence?**, *Daniel T. Trugman, Adrian Borsa, and David T. Sandwell*
- 233 **New observations of fault creep in the Imperial Valley from multi-look-angle InSAR and GPS**, *Eric O. Lindsey and Yuri Fialko*
- 234 **Mobile Laser Scanning Geodesy for Imaging Transient and Near-Field Fault Slip**, *Benjamin A. Brooks and Craig L. Glennie*
- 235 **Post-El Mayor Cucapah surface fracture deformation in UAVSAR images**, *Jay W. Parker and Andrea Donnellan*
- 236 **Factors controlling near-field coseismic deformation patterns: Quantifying distributed deformation of the 1992 Landers and 1999 Hector Mine earthquakes.**, *Chris W. Milliner, James Dolan, James Hollingsworth, Sebastien Leprince, Francois Ayoub, and Jean-Philippe Avouac*
- 237 **Refining the Magnitude of the Shallow Slip Deficit**, *Xiaohua Xu, Xiaopeng Tong, David T. Sandwell, and Christopher Milliner*
- 238 **An objective mechanical modelling approach for estimating the distribution of fault creep and locking from geodetic data**, *Gareth J. Funning and Roland Bürgmann*
- 239 **An integral method to estimate moment accumulation rate on the Creeping Section of the San Andreas Fault**, *Xiaopeng Tong, David Sandwell, and Bridget Smith-Konter*
- 240 **Faulting in anisotropic media: Elastic anisotropy biases estimates of fault depth**, *Brad P. Lipovsky and Paul Segall*
- 241 **An inverse modeling code for obtaining earthquake source parameters from InSAR data**, *Erika Noll and Gareth Funning*
- 242 **Development of a Simple Finite Element Based Inversion Framework: Application to Slow Slip Events Along the Hikurangi Subduction Margin, New Zealand**, *Charles A. Williams and Laura M. Wallace*
- 243 **Inverting for Shear Stress Rate on the Northern Cascadia Megathrust Using Geodetic Data**, *Lucile Bruhat, Paul Segall, and Andrew M. Bradley*
- 244 **Temporal Variation of A Large Slow Slip Event at the Southcentral Alaska Subduction Zone Between 2009-2013**, *Yuning Fu, Zhen Liu, Jeffrey Freymueller, Susan Owen, and Donald Argus*
- 245 **Interseismic Coupling Model of Nicoya Peninsula, Costa Rica by Joint Inversion of InSAR and GPS**, *Lian Xue, Susan Schwartz, and Zhen Liu*

Earthquake Geology

- 246 **Long-term uplift of the southern California coast between San Diego and Newport Beach resolved with new dGPS survey data: Testing blind thrust models in the offshore Borderlands**, *Erik C. Haaker, Thomas K. Rockwell, George L. Kennedy, Lisa B. Grant Ludwig, Justin A. Zumbro, and S. Thomas Freeman*
- 247 **Evidence of Coseismic Subsidence Along the Newport-Inglewood Fault Zone During the Late Holocene**, *Robert J. Leeper, Brady P. Rhodes, Matthew E. Kirby, Katherine M. Scharer, Scott W. Starratt, Eileen Hemphill-Haley, Nicole Bonuso, Behnaz Balmaki, Dylan J. Garcia, and Dliisa O. Creager*
- 248 **New High-Resolution 3D Imagery of Newport-Inglewood/Rose Canyon Fault Geometry and Deformation Offshore San Onofre, California**, *James J. Holmes, Jayne M. Bormann, Valerie J. Sahakian, Neal W. Driscoll, Graham M. Kent, Alistair J. Harding, and Steven G. Wesnousky*
- 249 **New Geophysical constraints on the Rose Canyon/Newport-Inglewood and Palos Verdes Fault Zones**, *Neal Driscoll, Valerie Sahakian, Jayne Bormann, Shannon Klotsko, James Holmes, Alistair Harding, Graham Kent, and Steven Wesnousky*
- 250 **Characterizing the recent behavior of the Ventura blind thrust fault: Preliminary results from the Brookshire Road, Ventura, study site**, *Jessica R. Grenader, James F. Dolan, Lee J. McAuliffe, Edward J. Rhodes, John H. Shaw, Thomas L. Pratt, and Judith Hubbard*
- 251 **Evidence of Subsidence Events along the Rincon Creek Fault in Carpinteria Marsh**, *Laura C. Reynolds, Alexander R. Simms, Thomas K. Rockwell, and Robert Peters*
- 252 **First radiometric ages for the Saugus Formation using cosmogenic isochron burial dating: Implications for fault slip rates in the Western Transverse Ranges**, *Duane E. DeVecchio and Dylan H. Rood*
- 253 **Geophysical and Geomorphic Constraints on the Location, Geometry and Kinematics of the Onshore Palos Verdes Fault Zone**, *Joshua Goodman, Phil Hogan, Dan O'Connell, Marco Ticci, Glen Adams, and James Turner*
- 254 **Neotectonics of the San Diego Trough and Coronado Bank fault systems, Inner California Borderlands**, *Jayne M. Bormann, Graham M. Kent, Neal W. Driscoll, Alistair J. Harding, James J. Holmes, Valerie J. Sahakian, and Steven G. Wesnousky*
- 255 **Other than tectonics, what other factors cause geographic variations in the elevations of marine terraces across the Pacific Coast of North America?**, *Alexander R. Simms, Kurt Lambeck, Helene Rouby, and Anthony Purcell*
- 256 **Qualitative Comparison of Offset Surfaces Between the Central and Eastern Garlock Fault**, *Thomas M. Crane and Sally F. McGill*

Posters 246-273

- 257 **Quaternary Off-Fault Uplift, Tilting, And Folding Within A Fault-Bounded Block Embedded In The Eastern California Shear Zone Near Twentynine Palms, Southern California**, *Christopher M. Menges, Jonathan C. Matti, and Stephanie L. Dudash*
- 258 **Field and LiDAR observations of the Hector Mine California 1999 surface rupture**, *Frank Sousa, Sinan Akciz, Janet Harvey, Kenneth Hudnut, David K. Lynch, Katherine Scharer, Joann Stock, Ryan Witkosky, Katherine Kendrick, and Crystal Wespestad*
- 259 **Using LiDAR to Evaluate Holocene Rupture Propagation Through Segment Boundaries, Central Wasatch Fault, Utah**, *Scott E.K. Bennett and Ryan D. Gold*
- 260 **Revised and Improved Fault Maps of Southwest Reno, Nevada using Light Detecting and Ranging (LiDAR) Imagery**, *Courtney M. Brailo, Graham M. Kent, Steven G. Wesnousky, Annie M. Kell, Ian Pierce, Christine J. Ruhl, and Kenneth D. Smith*
- 261 **Geologic and structural controls on rupture zone fabric: A field-based study of the 2010 Mw 7.2 El Mayor–Cucapah earthquake surface rupture**, *Orlando J. Teran, John M. Fletcher, Michael E. Oskin, Thomas K. Rockwell, Kenneth W. Hudnut, Ronald M. Spelz, Sinan O. Akciz, Ana P. Hernandez, and Alexander E. Morelan*
- 262 **Anatomy of a Fault Rupture: The 2013 Mw7.7 Balochistan Strike Slip Earthquake**, *William D. Barnhart, Nadine Reitman, Ryan Gold, and Richard Briggs*
- 263 **New Zealand's Alpine Fault: Insights into the San Andreas Fault System**, *Nicolas C. Barth*
- 264 **Geologic and geophysical maps and databases for Joshua Tree National Park, southern California**, *Robert E. Powell, Victoria E. Langenheim, Jonathan C. Matti, and Pamela M. Cossette*
- 265 **Symmetrical Bias in Reporting Slip Rates: Asymmetric Probability Density Functions are Inherent Outcomes of Accounting for Uncertainties in Displacement and Age**, *Nathan A. Toke*
- 266 **Combined hyperspectral and field mapping along the 1999 Hector Mine earthquake surface rupture**, *Ryan D. Witkosky, Sinan Akciz, Kerry Buckland, Janet Harvey, Ken Hudnut, Katherine Kendrick, Dave Lynch, Kate Scharer, Frank Sousa, Joann Stock, and David Tratt*
- 267 **Airborne Hyperspectral Infrared Imaging Survey of the San Andreas Fault in Southern California**, *David K. Lynch, David M. Tratt, Kerry N. Buckland, and Patrick D. Johnson*
- 268 **Spectral identification of offset fault features, with Mako hyperspectral data.**, *Janet C. Harvey and Joann Stock*
- 269 **Remotely Sensed Mineral Identifications at the Salton Sea Fumaroles**, *David M. Tratt, Paul M. Adams, David K. Lynch, Kerry N. Buckland, and Patrick D. Johnson*
- 270 **Characterization of subsurface faulting using ambient noise technology**, *John N. Louie, Aasha Pancha, and Satish Pullammanappallil*
- 271 **Using Global Arrays to Study Earthquake Rupture and Detect Earthquakes**, *Bo Li and Abhijit Ghosh*
- 272 **Single-grain post-infrared stimulated luminescence (pIR-pIRSL) dates for active faults in California and New Zealand**, *Christopher P. McGuire, Edward J. Rhodes, James F. Dolan, Sally McGill, Russ Van Dissen, Robert M. Langridge, Jessica R. Grenader, Robert Zinke, and Nathan Brown*
- 273 **Improving K-feldspar luminescence dating techniques**, *Jillian T.M. Daniels, Edward J. Rhodes, Michael J. Lawson, Christopher P. McGuire, and Nathan D. Brown*

Southern San Andreas Fault Evaluation (SoSAFE)

Posters 274-286

- 274 **Participation of the Parkfield segment in major San Andreas Fault events**, *Norman H. Sleep*
- 275 **Slip rate, slip history, and slip per event along the northern San Jacinto fault zone during the past 2000 years: a summary of work at the Mystic Lake and Quincy sites on the Claremont fault.**, *Nathan Onderdonk, Sally McGill, and Tom Rockwell*
- 276 **Active Dextral Slip on the Mill Creek fault through San Gorgonio Pass**, *Alexander Morelan, Michael Oskin, Judith Chester, and Daniel Elizondo*
- 277 **Holocene geologic slip rate for the Banning strand of the southern San Andreas Fault near San Gorgonio Pass**, *Peter O. Gold, Whitney M. Behr, Dylan Rood, Katherine Kendrick, Thomas K. Rockwell, and Warren D. Sharp*
- 278 **Vertical deformation along the Indio Hills, San Andreas Fault, California**, *Katherine M. Scharer, Kim Blisniuk, Warren Sharp, Pat Williams, and Kendra Johnson*
- 279 **Geochronology of surfaces within the San Gorgonio Pass from radiocarbon, in-situ cosmogenic nuclides, and pedogenesis: implications for climate and tectonics since the mid-late Pleistocene**, *Richard V. Heermance, Katherine J. Kendrick, Ian Dejarlais, Doug Yule, Paul McBurnett, and Shahid Ramzan*
- 280 **Using the B4 LiDAR dataset to constrain uplift across the San Gorgonio Pass Fault Zone**, *Kaitlyn L. Jones and Doug Yule*
- 281 **What can late Quaternary displacement on the San Andreas Fault in the greater San Gorgonio Pass region tell us about late Holocene to Recent strain patterns?**, *Jonathan C. Matti, Brett F. Cox, Douglas M. Morton, Robert E. Powell, and Stephanie L. Dudash*
- 282 **Reconciling contradicting trench and geomorphologic observations across the San Gorgonio Pass Fault Zone**, *Lisa R. Wolff, John D. Yule, Katherine M. Scharer, Ryan Witkosky, Shahid Ramzan, and Paul McBurnett*
- 283 **Late Pleistocene and Holocene Rates of Slip and Size of Prehistoric Earthquakes on the San Andreas Fault System in San Gorgonio Pass**, *Doug Yule, Dick Heermance, Ian Desjarlais, and Kerry Sieh*
- 284 **Investigation of San Andreas slip transfer east of Whitewater Canyon**, *Tarra Thompson, Lindsay Arvin, and Sally McGill*
- 285 **Filling the paleoseismic gap between Bidart and Frazier Mountain: Exploration of a promising sag pond site near the southeastern boundary of Carrizo National Monument**, *Sinan O. Akciz, Katherine M. Scharer, Kevin Coffey, Robert J. Leeper, Kyler Boyle-Pena, Crystal Wespestad, Lisa Grant Ludwig, and J Ramon Arrowsmith*
- 286 **The past 1500 years of paleoearthquakes at the Elizabeth Lake paleoseismic site, San Andreas fault, and tentative along-fault event correlations**, *Sean P. Bemis, Kate Scharer, James Dolan, Crystal Wespestad, Lucas Hatem, Joseph Lucas, Chris Milliner, and Jessica Grenader*

Meeting Abstracts

Reducing Epistemic Uncertainty in Seismic Risk Estimation, Norman A. Abrahamson (Invited Talk Sunday 18:00)

For most critical infrastructure, seismic safety is evaluated using standards-based seismic design criteria, but there is a move to also consider risk-informed regulation and risk-informed decision making as part of seismic safety. The residual risk of critical infrastructure that meet the standards-based criteria should be considered with a long term goal of risk reduction over decades. A key impediment to risk-informed regulation is that the epistemic uncertainty in the current estimates of seismic risk is huge, making it difficult to determine if the risk is small enough or to distinguish between the risks for different facilities for prioritization of mitigation efforts. Of the three main parts of seismic risk (seismic hazard, structure capacity, and consequences of a failure), the largest source of epistemic uncertainty in the seismic risk is due to the uncertainty in the seismic hazard, and in particular, in the ground motion model for a given site and seismic source. The greatly expanded ground motion data sets available in the last decade have shown that the systematic site and path effects account for about 50% of the aleatory variance in typical global ground motion models that use the ergodic assumption and the region-specific source effects account for an additional 15-20%. While we know the aleatory variability in ergodic ground motion models is too large, using the reduced aleatory variability requires estimation of the site/source-specific effects on the median ground motions. Properly capturing these site/source-specific effects can drastically change the estimates of seismic risk for a particular structure. To be able to have useful seismic risk estimates, regulators and owners of critical infrastructure need improved site-specific seismic hazard models that capture the systematic source and path effects. Path effects can be estimated using analytical modeling of wave propagation in a 3-D crustal model, such as cybershake, but before such models are used in engineering applications, they require adequate validation against recorded data. The current seismic instrumentation in California does not provide the density of stations required to adequately validate the analytical 3-D models for engineering applications. Greatly expanded seismic instrumentation in the regions around critical infrastructure will be needed in the next decade to support the move to risk-informed decision making and optimizing seismic risk reduction.

Improving spatial resolution of the moment rate function in regions of high slip determined from finite fault inversions, Mareike N. Adams, Chen Ji, and Ralph Archuleta (Poster 169)

Finite fault inversions attempt to resolve the spatial distribution of the moment rate function per unit area using seismic observations. However, the observational and synthetic limitations that exist due to the station distribution and frequency content of signals that can be modeled imply that various simplifications to the source representation are necessary to stabilize the inversions. These simplifications inevitably affect the final results, though it is largely unknown exactly how the regularization impacts the model parameters. Here, we explore the effects caused by a pre-assumed slip rate function using synthetic data from the Source Inversion Validation (SIV) produced by a crack-like spontaneous dynamic rupture embedded in a layered, elastic medium. Thus we have exact Green's functions, which allow us to consider only the effects of varying the slip rate function. We study the effect of three different inverted slip rate functions: i) asymmetric cosine functions; ii) modified Yoffe functions and iii) no negative functions within given time windows. The first approach has been used routinely in finite fault inversions and the second one is characteristic of dynamic simulations. We perform the inversions using the first two cases with a simulated annealing algorithm and attempt to answer whether the ideal synthetic data can differentiate between them. The first case has been thoroughly tested by changing the subfault size and removing various stations with mixed results. Currently, tests using the Yoffe function to represent the slip rate function are being studied and the third task will be examined in the near future. This last

case has the inverted slip rate function with the least a priori constraints but uses many more free parameters. It is inverted using the newly developed Projected Landweber (PL) method and we will explore its dependence on the choice of the initial model and the bandwidth of signals.

Validation approach for application of simulated ground motions to duration-sensitive systems, Kioumars Afshari and Jonathan Stewart (Poster 056)

This research is a part of the SEISM project, the goal of which is to validate ground motion time series produced by simulation routines implemented on the SCEC Broadband Platform. This research contributes to that effort by emphasizing validation relative to duration-related intensity measures (IMs), which are important for a number of geotechnical applications including seismic slope stability, soil liquefaction, and cyclic softening. A common approach used to validate IMs from simulations is to compare them to empirical ground motion prediction equations (GMPEs), which are presumed to represent the trends from empirical data. A difficulty in this case is the lack of a duration GMPE developed using modern databases, such as from the NGA-West 2 project. Accordingly, we begin by testing an older GMPE (from 2006) against durations from the NGA-West 2 database. We find significant bias, particularly at low magnitudes. We have developed a revised duration GMPE that better fits the data, especially at small magnitudes and large distances. This updated GMPE will be compared with simulated ground motion durations from the SCEC Broadband Platform. We will seek trends related to magnitude scaling, distance scaling, and standard deviation from the simulated motions. These results should be useful in better understanding potential biases in simulated ground motions, which in turn would be expected to affect the response of geotechnical systems evaluated using those motions.

The Broadband Platform has a large number of simulated events with different methods done by multiple research groups. With the new and more accurate GMPE ready, we will be able to run the GMPE for all simulated motions in order to study the performance of different ground motion simulation approaches. The bias and dispersion of the simulation results can be studied for different simulation methods, sites, and events.

Long-term High-Quality Deformation Observations with Long-Base Strainmeters, Duncan C. Agnew and Frank K. Wyatt (Poster 218)

Both to understand all phases of the seismic cycle and to monitor possible aseismic events, we have used long-base laser strainmeters to collect continuous deformation data at locations close to the two most active faults in Southern California. Pinyon Flat Observatory (PFO, operating since 1974) is 14 km from the Anza section of the San Jacinto fault (SJF: 2-3 m slip accumulated slip since the last large earthquake) and Salton City (SCS, since 2006) is within 15 km of the blind section of the SJF further SE. Two other sites (Cholame, or CHL, since 2008, and Durmid Hill, or DHL, since 1994) are within three km of the San Andreas fault (SAF): CHL, at the N end of the segment that ruptured in 1857, and DHL at the S end of the Coachella segment (4-6 m accumulated slip). Surface-mounted laser strainmeters (LSM's), 400 to 700 m long and anchored 25 m deep, provide long-term high-quality measurements of strain unmatched anywhere else: though in geological settings ranging from weathered granite to clay sediments, the LSM's record secular strain accumulation consistent with continuous GPS, something not otherwise possible. The LSM's record signals from 1 Hz to secular; at periods less than several months, they have a noise level far below that of fault-scale GPS networks.

Over periods of months and longer the LSM sites near the SAF show strain-rate fluctuations of up to 20 percent of the long-term rate. These sites have observed strain events unassociated with seismicity, lasting hours to days; at CHL these short-term signals have also been observed on borehole strainmeters (BSM's), and there and at DHL they appear to be

a few km deep. Aseismic signals observed at PFO are associated with local or regional earthquakes, and are nearer to seismogenic depths on the SJF. Further interpretation is hampered by not having similarly good measurements nearby.

LSM data have been used to rule out possible strain signals, often in ways relevant to short-term hazard, as at times of earthquake swarms close to DHL or following large regional events. The CHL data tightly limit aseismic strains at times of deep tremor. And the PFO data rule out large coseismic strains seen on nearby borehole strainmeters.

Operating these observatories shows that patience and persistence are needed to learn about the Earth: only a multiyear program captures interesting signals and properly characterizes the Earth's behavior. But this is difficult to do over geophysically useful timescales.

Filling the paleoseismic gap between Bidart and Frazier Mountain: Exploration of a promising sag pond site near the southeastern boundary of Carrizo National Monument, *Sinan O. Akciz, Katherine M. Scharer, Kevin Coffey, Robert J. Leeper, Kyler Boyle-Pena, Crystal Wespestad, Lisa Grant Ludwig, and J Ramon Arrowsmith* (Poster 285)

Differentiating between characteristic, uniform slip, and variable earthquake rupture models requires a string of proximal paleoseismic sites that provide tightly constrained age control, so that both the persistence of rupturing sections through time and the offset distribution along the fault can be evaluated. One of the most significant challenges in testing the variable slip hypothesis along the south-central San Andreas Fault is the distance between sites. Bidart Fan, Frazier Mountain, and Pallett Creek each provide a lengthy and robust rupture history for the Carrizo and Mojave sections, but ~100 km (the equivalent of a M7.3 earthquake) separates each site. Although existing earthquake ages permit some rupture correlation between sites, the distances between sites significantly limit our ability to infer how many prehistoric ruptures spanned the sites or the general spatial distribution of the inferred ruptures. In June 2014, to fill the gap between Bidart and Frazier Mountain, we excavated two exploration trenches, on both sides of a sag pond along the San Andreas Fault near the southern boundary of the Carrizo National Monument. Both trenches were ~ 2 m deep, 1 m wide and 30 m long. Coarse sand carried by nearby stream channels and clayey silt deposits interfinger with slope wash and colluvium deposits at the margin of the depression. No major bioturbation zones were observed. Using evidence such as filled fissures, angular unconformities, colluvial wedges, and fault-bounded deposits, we identified a minimum of three earthquakes on the walls of the northeastern trench (T1). The top-most stratigraphic layers, with abundant liquefaction evidence, are not cut by a fault and contain pieces of wooden planks, and thus likely indicate a post-1857 ground-shaking event. Organic material was abundant in T1, but so were deep roots that were completely charred in-situ. No peat or burn layers were identified, indicating that any future investigation will likely rely on the chronology from detrital charcoal samples and luminescence dating. Our southwestern exploration trench (T2) did not intersect any faults, though liquefaction features were abundant.

Earthquake Cycles in Heterogeneous Media: Sub-basin and Surface-rupturing Events on Faults Crossing a Sedimentary Basin, *Kali L. Allison and Eric M. Dunham* (Poster 149)

We have implemented a parallel code that simulates earthquake cycles on a strike-slip fault in two dimensions. The fault is governed by rate-and-state friction with depth-dependent parameters. The upper portion of the fault, above the seismogenic depth, is velocity-weakening, while the lower portion is velocity-strengthening. The method uses a spatial discretization that accommodates variable off-fault material properties. To simulate tectonic loading, the remote boundaries are driven at half the long-term slip rate.

Preliminary results suggest that material heterogeneity significantly affects system behavior in certain parts of parameter space. In a homogeneous half-space, events that rupture the full seismogenic depth occur periodically. In contrast, the presence of a sedimentary basin, represented by an elliptical region of decreased shear modulus and density, results in a more complex sequence of events. Two types of rupture emerge: sub-basin and surface-rupturing events. All ruptures nucleate at the seismogenic depth, but for the sub-basin events the rupture fails to

penetrate through the basin to the surface. Each sub-basin event leaves a stress concentration at the bottom of the basin, the presence of which enables the next event to rupture to the surface. For deeper and more compliant basins, the number of sub-basin events required before the occurrence of a surface-rupturing event increases. We have begun to explore this, focusing particularly on the effects of varying basin depth and shear modulus. We are also investigating the effects of incorporating a lithostatic normal stress gradient on the fault and velocity-strengthening within the basin. Additionally, previous work was limited to a state evolution distance D_c of 8-mm, several orders of magnitude greater than laboratory values. The parallel implementation allows us to investigate the effect of decreasing this value. Ultimately, this exploration will increase our understanding of how sedimentary basins affect the earthquake cycle.

Adapting the Composite Source Model for the SCEC Broadband Platform, *John G. Anderson* (Poster 064)

The composite source model is a kinematic source that, while stochastic in nature, can be described with a very small number of parameters. The source is a superposition of subevents (Brune pulses) distributed randomly on the fault, with sizes distributed according to a random realization of the Gutenberg-Richter distribution, and initiation time determined by the rupture velocity and distance from the hypocenter. Green's functions are calculated for a flat-layered structure using the method described by Luco and Apsel. The seismograms are found by combining the source and Green's functions using the representation theorem. While this model has been successful in reproducing the statistical characteristics of ground motions for several earthquakes, adaptation to the SCEC Broadband Platform requires implementation decisions and a systematic procedure for calibration of the model. The key parameters that must be adjusted are the velocity model, the Q model as a function of frequency and depth and the stress drop of the Brune subevents. The velocity model needs sufficient complexity to mimic the crustal waveguide. The site contribution to kappa is matched by adjusting the value of frequency-independent Q in layers shallower than 5 km, within observational limits, to obtain the target value. The distance dependence of kappa is initially approximated by setting the frequency-independent contribution to Q in layers below 5 km to maintain consistency with observed Q values obtained from regional wave propagation, but since Q and the geometrical spreading trade off and geometrical spreading in the selected velocity model is generally different from in the study that originally estimated Q, additional adjustments to Q are needed. The effect of frequency dependence in Q is reproduced by the approach to coda generation. Then an optimal subevent stress drop for each calibration event is determined, and trends with magnitude and faulting mechanism are used to find optimal values for modeling future events. A progress report on this ongoing calibration process will be given in the poster.

IRIS's Large N initiative – enabling the recording of full seismic wavefields, *Kent R. Anderson, John Hole, Robert Woodward, and Bruce Beaudoin* (Poster 157)

The concept of the IRIS "Large N" initiative is that well-sampled wavefields allow the application of wavefield imaging methods such as migration, full-waveform inversion, and wave equation adjoint imaging - methods that are impossible or severely limited with spatially aliased data. These methods can produce images of both sources and Earth structure at substantially improved spatial resolution and uniqueness, enabling improved understanding of Earth structure, composition, and active processes. The Incorporated Research Institutions for Seismology is beginning an initiative to enable new facility capabilities to better sample seismic wavefields with new instrumentation and enhanced installation and operations techniques.

Over the past decade, the EarthScope USArray Transportable Array has demonstrated several advantages of a large-aperture, densely sampled array to image large-scale Earth structure. Using a 70 km station spacing and a continental aperture, seismic wavefields at 101-102 s periods are well sampled, which enabled wavefield imaging at the 100 km scale of core and mantle structure, structures such as the lithosphere-asthenosphere boundary, and mega-thrust earthquakes in global subduction zones.

MEETING ABSTRACTS

Industry has a long history of recording over-sampled wavefields to image sedimentary basin structure. Using station spacings of 10's of meters, apertures of kilometers, and 101-102 Hz, seismic wavefield imaging methods are routinely used to image hydrocarbon reservoirs at the 10 m scale, and more recently hydrofracture microseismicity.

However, no facility exists to record well-sampled wavefields between 101 Hz and 101 s, corresponding to spatial scales between the reservoir and the lithosphere. IRIS's Large N initiative (where N=the number of sensors) has the goal of filling this gap. Dense spatial sampling in this frequency band will address several applications of societal interest, including earthquake hazards, hydrocarbon resources, induced seismicity, volcano processes, and explosion monitoring. In addition, we are looking at crossing gaps in spatial sampling with mixed-mode array designs that maximizes sampling over broad spatial scales, facilitating observations ranging from shallow soils to global structure. Evolving technologies will allow the deployment of seismic arrays capable of recording well-sampled wavefields, reducing or eliminating aliasing.

For more information www.iris.edu/hq/wavefields

Isolating Low Frequency Wave Propagation from High Frequency Wave Propagation in Broadband Ground Motions, *Ralph J. Archuleta and Jorge G.F. Crempien* (Poster 062)

Ground motion prediction equations for spectral acceleration in the western US have geometrical attenuation (GA) that is $\sim 1/R$ (Earthquake Spectra, 2008). However earthquakes simulated in 1D earth models have a larger GA for epicentral distances up to ~ 70 km (e.g., Burger et al., 1987). This difference is most likely caused by the 1D velocity structure's failure to represent the propagation of high frequency (HF) waves. Consider a finite fault representing the source embedded in a nearly homogeneous region of a 1D model. For epicentral distances greater than the source depth, upgoing rays will have a large angle of incidence when they impinge on the near-surface layers. These rays will then glance off the shallow structure and thus transmit insufficient energy to the surface. To overcome this effect in 1D models, we have modified the UCSB method for computing broadband synthetics (Liu et al, 2006; Schmedes et al., 2013). We use different velocity structures for HF and low-frequency (LF) propagation. The source remains the same. Liu et al. (2006) includes stitching of synthetics computed using a 1D velocity structure with those from a 3D velocity structure. Following this approach we compute ground motions up to a certain frequency using the full 1D model. We modify the full 1D model by replacing the medium above the Moho with a single elastic layer. Using the same source, we compute full waveform synthetics with the modified 1D model. We approximate the local amplification expected from the full 1D model by applying the quarter wavelength method (Boore & Joyner, 1997). We use wavelets to stitch the HF ground motion, computed with the modified 1D model and local amplification, to the LF ground motion, computed with the full 1D model. With these modifications we recomputed a set of validations used by SCEC. In particular we are interested in eliminating the bias (in the goodness of fit) that changed with distance.

Site response validation studies using KIK-net strong motion recordings, *Domniki Asimaki and Jian Shi* (Poster 069)

Earthquake simulations are nowadays producing realistic ground motion time-series in the range of engineering design applications. With the engineering community slowly adopting the use of simulated ground motions, site response models need to be re-evaluated in terms of their capabilities and limitations to 'translate' the simulated time-series from rock surface output to structural analyses input. We here study three widely used one-dimensional site response models: linear viscoelastic, equivalent linear and nonlinear. We evaluate the performance of the models by comparing predictions to observations at 30 downhole stations of the Japanese network KIK-Net that have recorded several strong events, including the 2011 Tohoku earthquake. Velocity profiles are used as the only input to all models, while additional parameters such as quality factor, density and nonlinear dynamic soil properties are estimated from empirical correlations. We quantify the differences of ground surface predictions and observations in terms of both seismological and engineering intensity measures, including bias ratios of peak ground response and visual comparisons of elastic spectra. In agreement with

recently published studies, we observe that measures of strain (here $PGV/V_s,30$) are better predictors of site nonlinearity than PGA, and that incremental nonlinear analyses are necessary to produce reliable estimates of high-frequency ground motion components at soft sites. We finally discuss the implications of our findings on the parameterization of nonlinear amplification factors in GMPEs, and on the extensive use of equivalent linear analyses in probabilistic seismic hazard procedures.

Evaluation of the Southern California Velocity Models through Simulation and Validation of Multiple Historical Events, *Shima Azizzadehroodpish, Naeem Khoshnevis, and Ricardo Taborda* (Poster 080)

We conduct a series of simulations for multiple historical moderate-magnitude earthquakes and validate our results against recorded data to evaluate the velocity models available for southern California. SCEC supports two main community velocity models for the region, namely CVM-S and CVM-H. Both models offer different possibilities or variations, which can be accessed via the SCEC UCVM Platform. CVM-S, for instance, can be queried in its original version (CVM-S4), or with modifications recently included after a 3D tomographic inversion study (CVM-S4.26). The information in CVM-H, on the other hand, can be alternatively used with a supplemental geotechnical model (GTL) or without it. One can therefore produce two different models, CVM-H+GTL (i.e., CVM-H with the GTL model) or CVM-H (i.e., without it). We performed multiple simulations of earthquakes with magnitudes varying between 3.5 and 5.5 using the four models just described (CVM-S4, CVM-S4.26, CVM-H, and CVM-H+GTL). The simulations were done for a maximum frequency of 1 Hz and a minimum shear wave velocity of 200 m/s using Hercules, an octree-based finite-element parallel earthquake ground motion simulator. The earthquake ruptures were modeled assuming a kinematic point-source (double-couple) representation. Synthetics on about 50 stations per event were compared with data recorded during the earthquakes and downloaded from the Southern California Earthquake Data Center. The seismograms were processed and compared with the synthetics in the range of 0.1-1.0 Hz using a modified version of the Anderson Goodness-of-Fit (GOF) method. This method combines various comparison criteria that are meaningful to both engineers and seismologists, and has been satisfactorily used in previous validation efforts. We compare the regional distribution of the GOF results for all the earthquakes and all the models and draw conclusions on the consistency observed in the results.

Seismogenic zone depth control on the likelihood of fault stepover jump, *Kangchen Bai and Jean-Paul Ampuero* (Poster 125)

Earthquakes can involve rupture of geometrically complex fault systems (e.g. 1992 Landers earthquake, 2012 Indian Ocean earthquake). One such complexity is the presence of fault stepovers, i.e. offsets in the fault trace or gaps between fault segments. Quantifying the likelihood of an earthquake to break multiple segments of a fault system is important to evaluate earthquake hazard. Empirical observations suggest that earthquakes rarely jump across stepovers that have a gap larger than about 5 km. Although the empirical data cannot distinguish between a random or a causal relation between gaps and rupture arrest, a maximum stepover distance for rupture jump has been previously shown to emerge in 2D dynamic rupture simulations and 2.5D earthquake cycle models. The mechanical origin of this critical stepover distance (R_c) is not fully understood yet. Here, we examine one possible mechanism that has not been explored extensively: the role of the finite seismogenic zone depth, which places a limit on the stress intensity factor and hence on how far off-fault large stresses can reach.

In this study we are using a 3D spectral element method coupled with a dynamic rupture solver to investigate the possibility of rupture jump across fault stepovers. We conduct spontaneous rupture simulations under slip-weakening friction incorporating the finite seismogenic zone depth (W) and we calculate the dynamic Coulomb stress perturbation surrounding the primary fault. Simulation results confirmed the depth (W) control over stress intensity factor while providing three new insights. (1) The normalized critical stepover distance R_c/W is determined by the ratio L_c/W (where $L_c=(\text{shear modulus})^*(\text{critical slip distance})/(\text{strength drop})$ is the characteristic size of the slip-weakening process zone), which controls the amplitude of the strong seismic phase radiated at the end point of the primary fault. (2) The stopping phase is more efficient at promoting rupture

across compressional stepovers than dilatational ones, which suggests the possibility of a larger R_c in compressional stepovers than in dilatational ones. (3) The Lorentz contraction at the front of a steady rupture substantially distorts the angular pattern of the Coulomb stress distribution, leading to an increase of Coulomb stress at a certain azimuth in the dilatational side.

Parameterization of fling-step from ground motion recordings and simulations, *Jack W. Baker and Lynne S. Burks* (Poster 046)

We identify potential data sources for fling-step and discuss their value, compile a dataset of simulated and recorded ground motions containing fling, extract fling pulses from these ground motions, and derive a predictive model for fling amplitude and period that is compared to existing empirical models. Fling is the result of permanent static offset of the ground during an earthquake, but is usually ignored because ground motion records from accelerometers contain errors that make it difficult to measure static offsets. But some data sources include fling, such as specially processed recordings, ground motion simulations, and high-rate global positioning systems (GPS). From this data, we extract fling pulses using the pattern search global optimization algorithm. The resulting displacement amplitudes and periods are used to create a new predictive equation for fling parameters, and are compared to existing empirical models for pulse period, fling amplitude, and surface displacement along the fault, and match reasonably well.

The Seamless SAR Archive (SSARA) Project and Other SAR Activities at UNAVCO, *Scott Baker, Christopher J. Crosby, Charles M. Meertens, Eric J. Fielding, Gwendolyn Bryson, Brian Buechler, Jeremy Nicoll, and Chaitanya Baru* (Poster 216)

The seamless synthetic aperture radar archive (SSARA) implements a seamless distributed access system for SAR data and derived data products (i.e. interferograms). SSARA provides a unified application programming interface (API) for SAR data search and results at the Alaska Satellite Facility and UNAVCO (WInSAR and EarthScope data archives) through the use of simple web services. A federated query service was developed using the unified APIs, providing users a single search interface for both archives. Interest from the international community has prompted an effort to incorporate ESA's Virtual Archive 4 Geohazard Super sites and Natural Laboratories (GSNL) collections and other archives into the federated query service. SSARA also provides Digital Elevation Model access for topographic correction via a simple web service through OpenTopography and tropospheric correction products through JPL's OSCAR service. Additionally, UNAVCO provides data storage capabilities for WInSAR PIs with approved TerraSAR-X and ALOS-2 proposals which allows easier distribution to US collaborators on associated proposals and facilitates data access through the SSARA web services. Further work is underway to incorporate federated data discovery for GSNL across SAR, GPS, and seismic datasets provided by web services from SSARA, GSAC, and COOPEUS.

Earthquake Country Alliance, *Jason E. Ballmann and Mark L. Benthien* (Poster 002)

The ECA is a public-private partnership of people, organizations, and regional alliances, each of which are committed to improving preparedness, mitigation, and resiliency. People, organizations, and regional alliances of the ECA collaborate in many ways: sharing resources; committing funds; and volunteering significant time towards common activities. ECA's mission is to support and coordinate efforts that improve earthquake and tsunami resilience. The Earthquake Country Alliance is now the primary SCEC mechanism for maintaining partnerships and developing new products and services for the general public. To participate, visit www.earthquakecountry.org/alliance.

SCEC created the Earthquake Country Alliance (ECA) in 2003 and continues to play a pivotal role in developing and sustaining this statewide (as of 2009) coalition with similar groups in the Bay Area and North Coast. Participants develop and disseminate common earthquake-related messages for the public, share or promote existing resources, and develop new activities and products. SCEC develops and maintains all ECA websites (www.earthquakecountry.org, www.shakeout.org, www.dropcoverholdon.org, and www.terremotos.org), has managed the

printing of the "Putting Down Roots" publication series throughout the state, SCEC Associate Director for CEO Mark Benthien serves as Executive Director of the ECA.

Feedback from selected ECA members collected through key informant interviews, indicate that the foundation and development of the ECA very much rests upon SCEC leadership and its credibility and reputation as a trusted science and research consortium. SCEC is viewed as a 'neutral' and trusted leader, who employs a collaborative model to organizing stakeholders around a common cause and event. SCEC's "culture of collaboration" has provided for a bottom-up rather than a top down approach to building the ECA community.

The Great California ShakeOut has been the primary collaborative activity so far, but additional activities are also managed or planned by the ECA. This planning builds on a California Emergency Management Agency earthquake communications plan developed in 2009 that emphasizes the value of a statewide collaboration.

Reducing variability in earthquake stress drops to define secondary trends, *Annemarie S. Baltay* (Invited Talk Monday11:00)

Using a large set of stress drop estimates from a variety of methods and datasets, I identify several trends in earthquake stress drops, heretofore not rigorously investigated due to the considerable scatter in stress drop measurements. I find a dependence of stress drop on depth, as well as a decreased median stress drop for aftershocks when compared to mainshocks. Several approaches are used to estimate stress drop from different data sets, including the very large NGA-West2 database. These methods include both Brune stress drops from eGf deconvolution, and time-domain-based measures, i.e. aRMS stress drops. Applying the a-RMS methodology to the NGA-West2 database allows recovery of stress drops directly from the ground motion data, which compare well to inferred stress drops from ground motion prediction equations (GMPEs). I find that the Brune eGf-based stress drop estimates and the NGA-West2 a-RMS stress drops show a marked decrease in scatter, as compared to many other seismological studies.

The overall distribution of stress drops can be considered in two parts: aleatory variability, due to statistical or random variability, such as the natural variability of earthquake stress drops; and epistemic uncertainty, associated with things we don't currently know, but are knowable, such as whether earthquake stress drops depend on depth. We are often unable to separate the two, but the reduced scatter in our stress drop estimates allows us to ascertain deterministic secondary trends in the aleatory distribution, which I term epistemes.

Having identified a dependence of stress drop on depth and a decrease in median stress drops for on-fault aftershocks, as compared to mainshocks, we are able to account for their effects on estimates of stress drop. By identifying and removing these epistemes, we can actually reduce the observed aleatory variability in the stress drop distribution. While both the depth dependence and mainshock/aftershock offset are already included in some GMPEs, many previous seismological studies have been unable to conclusively uncover these trends because of their considerable scatter. Elucidating these effects in the context of understanding epistemic uncertainty and aleatory variability can help us to understand the true variability of the earthquake source, which may be due to the complex and diverse circumstances under which these earthquakes occur.

Metrics for Comparing Dynamic Earthquake Rupture Simulations, *Michael Barall and Ruth A. Harris* (Poster 116)

One way to check the performance of a dynamic rupture computer code is to compare its results with the results of other codes running the same earthquake simulation. The SCEC/USGS Spontaneous Rupture Code Verification Project has published a series of computational dynamic rupture benchmark exercises suitable for performing such comparisons. On our website we have collected results, including both synthetic seismograms and rupture front time-contours, from several dozen modelers who have used more than 20 computer codes. Until recently, we compared the performance of these codes by displaying and visually inspecting the results that they produced. Here, we show how to compute a set of metrics for quantitative comparison of our dynamic rupture simulations. Designing metrics for our benchmarks is challenging due to

MEETING ABSTRACTS

the large size of our dataset, and the wide variety of modeling scenarios and numerical techniques. The metric computation is fully automated and obtains simulation results directly from our website database, making it possible to perform hundreds of thousands of comparisons. The results provided by each dynamic rupture computer code go through a series of preprocessing steps carefully designed to allow comparisons for many kinds of models and codes. For example, synthetic seismograms are filtered to remove spurious noise, time-shifted to compensate for differences in rupture propagation speed, and level-shifted to remove some DC components. For both synthetic seismograms and rupture contours, an effort is made to remove data that are influenced by the model boundaries, or are otherwise anomalous. Since codes report results at different points in time and space, we define interpolation procedures to convert the discrete modeling results into continuous functions. Then we can perform L2 comparisons of the preprocessed, continuous functions. For synthetic seismograms, most of the L2 comparisons are done using vector-valued data, to avoid comparing individual components that may be dominated by noise. Finally, the metric values are organized into a set of web pages that can be easily viewed in a web browser. The web pages are colored with a custom-designed coloring algorithm to help the viewer distinguish better from worse metric values. They can be viewed on our website at <http://scecddata.usc.edu/cvws/>. Publication: Barall, M., and R.A. Harris, Metrics for Comparing Dynamic Earthquake Rupture Simulations, SRL, accepted.

Anatomy of a Fault Rupture: The 2013 Mw7.7 Balochistan Strike Slip Earthquake, *William D. Barnhart, Nadine Reitman, Ryan Gold, and Richard Briggs* (Poster 262)

A vexing question in active tectonics and hazards analysis is how large co-seismic displacements translate to the geological record explored through paleoseismic studies. In particular, it is critical to identify how fault behavior may vary along strike, exhibiting slip indicators that may or may not constrain the behavior of a fault over multiple seismic cycles. The September 2013 Mw7.7 Balochistan earthquake in southern Pakistan ruptured ~200 km of the curved Hoshab reverse fault within the Makran accretionary prism – the active zone of convergence between the northward subducting Arabia plate and overriding Eurasia plate. This earthquake is odd in many ways, particularly with respect to sustained strike slip rupture in an environment and on a structure that otherwise would support thrust-type motion given the fault geometry and tectonic setting. In this study, we examine the detailed characteristics of the surface rupture of this event using high-resolution (0.5 m) pre- and post-event satellite imagery. We map the extent and complexity of the left-lateral motion through both manual inspection of imagery and automated image cross-correlation methods (e.g. pixel tracking). We find that the rupture propagated through several stepovers, and that the width of the surface rupture zone varies from <5 m to 2 km. Post event imagery reveals evidence for multiple strike-slip ruptures along portions of the Hoshab fault; however, there is no evidence for repeated events like the 2013 earthquake. Offsets inferred from geologic piercing points approach ~12 m, while pixel tracking results reveal displacements up to 16 m. Individual surface displacement measurements are inversely proportional to the width of the rupture zone. Further research will focus on the percentage of deformation accommodated at the fault versus at distances from the fault where paleoseismic studies would not capture the full magnitude of fault displacements and thus underestimate paleo magnitudes. These results will have implications for geologic fault slip-rate studies, paleoseismic studies that estimate earthquake magnitudes from geomorphic offsets, and comparisons of geodetic and geologic slip-rate data.

UseIT 2014 Analysis Team: Data Analysis with SCEC-VDO, Open SHA, GIS, and HAZUS for UseIT 2014 Grand Challenge, *Sheila Bart, Georgina Campos, Thanh-Nhan Le, Rachel Hausmann, Elena Pierce, Krystal Rios, Thomas Jordan, Robert de Groot, Nick Rousseau, Yao-Yi Chiang, Kevin Milner, Mark Benthien, Scott Callaghan, Hope Seligson, and Dave Smith* (Poster 009)

The 2014 Undergraduate Studies in Earthquake Information Technology (USEIT) Analysis Team studied and analyzed eighteen earthquake scenarios with similar magnitudes to the October 1989 magnitude 6.9 Loma Prieta Earthquake. This study included exploring the potential risk of substantial, typical, and minor aftershock sequences. Using graphical

interface systems that have access to a variety of GIS, geologic, and geodetic data, the Analysis Team collaborated with USGS to agree on a list of eighteen M6.9-7.1 earthquakes scenarios. These were analyzed to evaluate the damaging effects on population centers in California. Histograms, scatterplots, catalogs, and simulations were generated for each selected rupture to choose the substantial, typical, and minor aftershocks based on density and magnitude. With these datasets the Analysis Team, in collaboration with the USEIT Visualization Team, created ShakeMaps of corresponding shaking intensities. Through inputting ShakeMaps into HAZUS, a geographic information system that uses hazard loss estimation software, the Analysis Team found that specific areas in California are high density risk zones for earthquake damage. The goal of this work is to provide a broad array of stakeholders of the potential economic losses, injuries, and fatalities associated with Loma Prieta size earthquakes.

New Zealand's Alpine Fault: Insights into the San Andreas Fault System, *Nicolas C. Barth* (Poster 263)

The Alpine Fault (AF) is a ~900 km-long, dextral>reverse Pacific-Australian plate boundary structure, which currently accommodates up to 90% of 40 mm/yr plate boundary motion across the South Island of New Zealand. Compilations of new and existing work indicate remarkable seismotectonic similarities between the AF and the San Andreas Fault System (SAFS) including fault zone structure, friction/permeability/mineralogy of fault core materials, deformation style, and potential to generate large-great ($\geq M$ 8.0) earthquakes. Interesting contrasts exist in terms of geometric complexity, plate boundary partitioning, surface rupture styles, and interactions with other faults. Superb unweathered outcrops on the southern AF reveal fault zone materials and anatomy very similar to those encountered in the San Andreas Fault Observatory at Depth (SAFOD) borehole; relationships observed in these outcrops give insight into how seismic slip and fault creep (i.e., mixed-mode fault slip behavior) can occur on and within the same localized fault core. On the central AF, serial partitioning occurs as 1–6 km-long tears in the fault plane due to oblique motion, and the effects of topography and erosion. Structural contouring and geophysics indicate these structures merge into a single through-going fault zone at depths of ~1–3 km, while the paleoseismic record clearly indicates this extent of near-surface complexity does not halt the propagation of earthquakes through this region (which may be analogous to the unusual complexity of the SAFS at San Geronio Pass). In contrast to the SAFS, the AF has a relative lack of sub-parallel faults with similar kinematics, and consists of a single planar structure which has accommodated 460 km of dextral displacement. The relative geometric simplicity of the Alpine Fault overall, together with a long (8 kyr) quasi-regular paleoseismic record and temporally stable slip rates (for >3 Myr) indicate it is a mature plate boundary structure acting in isolation from subsidiary faults. This mature, isolated behavior makes the AF an ideal fault system to study and model to gain understanding of more complex systems like the SAFS. This poster will explore relevant similarities and contrasts between these two major Pacific Rim continental transform systems.

Broadband Platform Ground Motion Simulations - Implementing New Validation Metrics and Exploring Aleatory Variability, *Jeff Bayless, Andreas Skarlatoudis, and Paul Somerville* (Poster 053)

Two part project to (1) explore the aleatory variability of simulations on the SCEC BBP and (2) implement additional metrics for validation of median levels, in addition to adding both (1) and (2) to the standardized BBP process for validation events.

A major difficulty for (1) lies in comparing variability from global data sets (GMPEs) to that from individual rupture simulations. Nevertheless, to make progress on the topic, we calculate the between- and within-event dispersion of simulated ground motions created as part of the SCEC BBP Validation project, and compare them to empirical ground motion prediction models (NGA-West2). Residuals refer to the natural log ratio of the simulated spectral acceleration, to the recorded spectral acceleration. To categorize the variability of the simulations we will take the following steps first calculate a mean bias term, and then calculate between-event residuals using two distinct approaches, followed by the separation of within-event residuals. The standard deviations of the categorized residuals are compared with empirical models. Additionally, we make

direct comparisons of both components of the variability between the three various methods themselves to provide BBP developers with a currently unavailable perspective on the range of the match to the validation event set.

In (2) we apply the Anderson (2004) and Kristekova et al. (2009) GOF criteria for validating simulation waveforms to the existing validation simulations on the BBP, and incorporate these updates into the standardized SCEC BBP workflow in coordination with SCEC IT.

The past 1500 years of paleoearthquakes at the Elizabeth Lake paleoseismic site, San Andreas fault, and tentative along-fault event correlations, Sean P. Bemis, Kate Scharer, James Dolan, Crystal Wespestad, Alex E. Hatem, Joseph Lucas, Chris Milliner, and Jessica Grenader (Poster 286)

The extent of paleoruptures of the Mojave section of the San Andreas Fault has been hampered by a lack of paleoseismic sites on a 100 km stretch between the Frazier Mountain and Pallett Creek sites. We report on work conducted midway along this gap, at the Elizabeth Lake paleoseismic site, consisting of 10 trenches that cross a 40-m by 350-m fault-parallel depression containing a ~2000 year depositional record. Three trenches focused on the central portion of the site: EL5 and EL6 crossed the northeastern scarp and revealed active faulting along this margin since ca. 200 A.D. EL7 was excavated as a southward extension of EL5 to as a continuous exposure across the entire depression and demonstrated that recent surface ruptures do not disturb the southwest margin of the depression. Deposits in this central region are well stratified and not bioturbated but do not extend across the fault zone onto the bedrock scarp, leading to possible missing events, especially in the younger section. Four trenches (ERT, EL3, EL4, and EL9) were located at the eastern portion of the site where the active northeastern scarp projects across a north-flowing wash. These trenches reveal the thickest section of young stratigraphy found at the site and the widest fault zone. Faulting patterns here show that over the last ~800 years, a 3 m wide pop-up caused fluvial sand and gravel deposits and organic rich pond deposits to interfinger south of the fault while a thick organic-rich loam accumulated on the north side of the pop up. Faulting, fissures, and tilted blocks provide evidence for 4 to 5 paleoearthquakes since ca. 1250 A.D. The uncertain event is expressed on the north side of the pop up and cannot be stratigraphically correlated to the other earthquakes due to the thick organic unit. Radiocarbon dating established that the site has a significant component of detrital charcoal that can be 500 years older than other charcoal samples in the same layer, so extensive dating will be required to establish true layer ages. Preliminary dates suggest poor temporal correlation with neighboring paleoseismic sites, but additional radiocarbon dating is needed to refine event ages, and post-IR IRSL may help to establish contemporaneity of events on either side of the pop-up. Evidence for older earthquakes is expressed in the lower section of EL3 and the central portion of the site. The poster explores possible rupture extents on the San Andreas fault given these new dating constraints.

Multi-Scale Structure and Earthquake Properties in the San Jacinto Fault Zone Area, Yehuda Ben-Zion (Poster 185)

I review multi-scale multi-signal seismological results on structure and earthquake properties within and around the San Jacinto Fault Zone (SJFZ) in southern California. The results are based on data of the southern California and ANZA networks covering scales from a few km to over 100 km, additional near-fault seismometers and linear arrays with instrument spacing 25-50 m that cross the SJFZ at several locations, and a dense rectangular array with >1100 vertical-component nodes separated by 10-30 m centered on the fault. The structural studies utilize earthquake data to image the seismogenic sections and ambient noise to image the shallower structures. The earthquake studies use waveform inversions and additional time domain and spectral methods. We observe pronounced damage regions with low seismic velocities and anomalous Vp/Vs ratios around the fault, and clear velocity contrasts across various sections. The damage zones and velocity contrasts produce fault zone trapped and head waves at various locations, along with time delays, anisotropy and other signals. The damage zones follow a flower-shape with depth; in places with velocity contrast they are offset to the stiffer side at depth as expected for bimaterial ruptures with persistent

propagation direction. Analysis of PGV and PGA indicates clear persistent directivity at given fault sections and overall motion amplification within several km around the fault. Clear temporal changes of velocities, probably involving primarily the shallow material, are observed in response to seasonal, earthquake and other loadings. Full source tensor properties of M>4 earthquakes in the complex trifurcation area include statistically-robust small isotropic component, likely reflecting dynamic generation of rock damage in the source volumes. The dense fault zone instruments record seismic "noise" at frequencies up to 200 Hz that can be used for imaging and monitoring the shallow material with high space and time details, and numerous minute local earthquakes that contribute to the high frequency "noise".

Using LiDAR to Evaluate Holocene Rupture Propagation Through Segment Boundaries, Central Wasatch Fault, Utah, Scott E.K. Bennett and Ryan D. Gold (Poster 259)

Large (M_≥7.0) Holocene earthquakes on the segmented Wasatch fault (WF) are thought to produce single-segment surface ruptures that terminate at structural segment boundaries. However, uncertainties in earthquake timing from paleoseismic trenches constraining these single-segment scenarios also permit multi-segment rupture scenarios. Thus, the extent and frequency of fault ruptures that span segment boundaries remain poorly known, increasing uncertainty in seismic hazard models for this densely populated region of Utah. To improve our knowledge of the WF Holocene rupture history, we analyze newly acquired high-resolution (8 pts/m²) airborne LiDAR along the 350-km-long WF to (1) characterize previously unmapped Holocene fault traces; (2) use scarp morphology to estimate the extent of fault ruptures associated with most recent earthquakes (MREs); (3) map the 17 ka Lake Bonneville highstand shoreline and use it as a strain marker to quantify late Pleistocene vertical displacements and calculate slip rates; and (4) measure total mountain front exhumation. Within the Brigham City-Weber segment boundary, we identify fresh en-echelon graben scarps that may correspond with the MRE rupture that spanned this boundary, as suggested from nearby paleoseismic results. However, the Bonneville shoreline displays little to no offset here, suggesting that fault ruptures typically terminate at this boundary. Within the Provo-Nephi segment boundary, a 6-8 km-wide stepover, the Bonneville highstand shoreline is vertically offset ~25m across the Provo segment and ~27m across the Nephi segment. The resultant ~1.4-1.5 mm/yr vertical slip rate is similar to rates calculated from paleoseismic trenches and shoreline offsets within the central Provo segment, suggesting that the Holocene slip rate does not diminish at this segment boundary, which could be consistent with a pattern of repeated through-going ruptures. We also observe that total mountain front exhumation decreases towards several segment boundaries, supporting single-segment rupture histories, though locally contradicting relatively high slip rates from shoreline offsets. In summary, while paleoseismic evidence suggests that fault ruptures tend to terminate at segment boundaries, we present evidence for through-going ruptures along the WF. Ongoing LiDAR analysis of post-Bonneville, Holocene deposits will further quantify the spatial and temporal slip patterns near fault segment boundaries.

Great ShakeOut Earthquake Drills, Mark L. Benthien and Jason E. Ballmann (Poster 001)

Great ShakeOut Earthquake Drills began in southern California in 2008, to involve the general public in a large-scale emergency management exercise based on an earthquake on the San Andreas fault (the USGS "ShakeOut Scenario" developed by a team of more than 300 experts led by Dr. Lucy Jones). While no longer focused on the Southern California scenario, ShakeOut worldwide continues to communicate scientific and preparedness information based on 30 years of research about why people choose to get prepared. Its purpose is to motivate everyone, everywhere to practice earthquake safety ("Drop, Cover, and Hold On"), and to get prepared at work, school, and home.

SCEC has hosted the ShakeOut website (www.ShakeOut.org) since the beginning and created a registration system where participants could be counted in the overall total. In 2008 more than 5.4 million Californians participated. Though originally intended to be held only once, requests from ShakeOut participants prompted partners and state agencies to expand the event statewide as an annual ShakeOut drill on the third

MEETING ABSTRACTS

Thursday of October. This date is ideal for schools and follows National Preparedness Month in September, allowing for significant media exposure prior to the drill. While K-12 and college students and staff comprise the largest number of participants, the ShakeOut has also been successful at recruiting participation of businesses, non-profit organizations, government offices, neighborhoods, and individuals. Each year participants are encouraged to incorporate additional elements of their emergency plans into their ShakeOut drill. More than 9.6 million Californians participated in October, 2013.

In addition to its lead role in organizing the California ShakeOut, SCEC manages a growing network of ShakeOut Regions across the country (with support from FEMA) and around the world (see www.shakeout.org). In order to develop and maintain the ShakeOut brand and reduce potential confusion between the different drills, SCEC works with officials in these regions and for most hosts the website for their drill. This approach serves to standardize earthquake messaging nationally and internationally, and allow groups to share best practices for recruiting participation, such as the use of social networking sites. In total more than 24.9 million people registered to participate in 23 Official ShakeOut Regions in 2013. ShakeOut websites are now online in English, Spanish, French, Italian, and Japanese.

USEIT 2014 Development Team, *Greg Berger, Brandon Green, Mark Krant, Francisco Raygoza, Paulo Dos Santos, Ernest Scapini, Alicia Sellsted, Thomas Jordan, Robert de Groot, Nick Rousseau, Yao-Yi Chiang, Kevin Milner, Mark Benthien, Scott Callaghan, and Dave Smith* (Poster 008)

The 2014 Undergraduate Studies in Earthquake Information Technologies (USEIT) Development team was presented with the challenge of further developing SCEC-VDO to allow exploration and evaluation of aftershock hazards implied by the Uniform California Earthquake Rupture Forecast Version 3 (UCERF3). Upon receiving simulation files of Loma Prieta-like events (Earthquakes) and their aftershocks, the development team wrote Java code to rearrange the files in a more manageable way for the Analysis team. These simulation files are loaded into SCEC-VDO's UCERF3 Inversion Plugin and visualize aftershock sequences. Code was also written to filter out spontaneous earthquake data included in the simulations that were irrelevant to the Grand Challenge. A complete revamping of the scripting plugin was done. Utilizing SCEC-VDO's video-making capabilities is now a much more fluid process. Users can add specific features (ShakeMaps, Earthquake Animations, etc.) to their videos without pausing and can precisely specify how any features are laid out using Start and Stop Time parameters. These features can also be inserted easily at precise instances in videos using Start and Stop time parameters. Finally, the Hazus Events plugin was refactored so that new Hazus information can be easily added using XML files, making it far more manageable for future users.

Do laboratory slide-hold-slide experiments really provide evidence for time-dependent healing in rock? *Pathikrit Bhattacharya, Allan M. Rubin, and Nicholas M. Beeler* (Poster 139)

Over the last two decades, it has been widely held that the Aging law is better at explaining slide-hold-slide (SHS) tests on rock than the Slip law. The major laboratory evidence for this statement comes from a sequence of SHS tests on initially bare granite by Beeler et al. (1994), wherein the observed peak stress after the reslide was found to increase logarithmically with hold time across the sequence of holds with a slope independent of machine stiffness, a feature shared by the Aging law but not by the Slip law. This conclusion was based on using the peak stress upon reslide as a proxy for the amount of frictional healing during the holds, an approximation which is valid only if there is negligible state evolution across the hold. Because some experiments suggest that this condition is not met [e.g., Dieterich and Kilgore, 1994], we re-examine the data of Beeler et al. (1994) focussing on the stress relaxation during the holds. We show through rigorous parameter inversion and a series of analytical results that for such velocity-weakening materials, the Aging law cannot explain the continual weakening (i.e., sliding) observed during the hold portion of the test; time-dependent healing makes the interface too strong. In particular, when forced to fit only the stress relaxation, the only possible Aging law solution is velocity strengthening and it drastically overestimates the stress peaks upon reload. A velocity weakening Slip law produces a much better fit to the stress relaxation but underestimates the

peaks upon reload and mispredicts their time evolution. A recently proposed stressing rate dependent state evolution law (Nagata et al. (2012)) produced the best fit to both the stress relaxation and peak stresses after reslides, but failed to reproduce some robust features of the long term time evolution of the peak stresses. We conclude that 1) None of the laws examined in this study (including the hybrid law of Kato and Tullis (2003)) can explain all the robust features of the SHS data from Beeler et al. (1994); 2) Given that the Aging law also fails to fit large velocity step data from laboratory experiments, there is little experimental support from rock friction experiments that the Aging law should be the state evolution law of choice for numerical simulations of the earthquake cycle.

Hazard Curve Results and a UCERF3-San Jacinto Fault Comparison From Precarious Rocks in Southern California, *Glenn P. Biasi, James N. Brune, and John G. Anderson* (Poster 067)

We improved the quantity and quality of ground motion constraints in the precarious rock database at UNR using 2D estimates from photographs. SCEC and NEHRP support were instrumental in this progress. New work linked locations for over 1000 rocks to static toppling acceleration estimates from 2D, and sparse 3D photographic methods. This greatly improved resolution of ground motion bounds from precarious rock evidence. Rock survival as a function of distance from active faults provides an empirical ground motion prediction relation. PBR survival resolves a clear empirical ground motion prediction bound as a function of distance from the San Andreas fault (SAF). Within 5 km of active faults, rocks that would topple at 0.35g become rare, while at 20 km, this threshold decreases to about 0.25 g. Distance from the SAF controls PBR survival to a greater degree than distance from most nearer active faults. This is apparently because earthquakes occur more frequently on the SAF than on other active faults near PBRs. The toppling levels and their distance dependence are similar to what would be expected for hard rock sites and median ground motion predictions. For instance, over multiple earthquake cycles ground accelerations have not exceeded 120-130% of median AS08 NGA values. Interpreted purely in terms of the event-to-event contribution to ground motion sigma, this bound would translate to a sigma of ~0.18 for San Andreas fault earthquakes. If the median ground motion is overestimated somehow for the largest SAF events, sigma could be closer to GMPE estimates.

We have evaluated rock survival for event predictions of UCERF3 on the San Jacinto fault. Subsection earthquake participation rates indicate that earthquakes of $M \geq 7.4$ should be expected at recurrence times much less than 1000 years. Events of this size would topple precarious rocks near the fault stepover onto the Claremont strand (see also Lozos et al, this meeting). At the same time, the net seismic hazard (2% in 50-year estimates) has not changed much between the 2008 and 2014. The simplest reconciliation suggested by the PBRs would be that UCERF3 has partitioned moment out of smaller events consistent with the rocks and into larger, less frequent earthquakes.

Utilization of simulated ground motions for engineering performance assessment of tall buildings, *Nenad Bijelic, Ting Lin, and Gregory Deierlein* (Poster 052)

This work focuses on utilization of simulated ground motions for nonlinear structural response estimation of tall buildings. Structural building response is first estimated using conventional methods (multiple stripe analysis, incremental dynamic analysis), where recorded and simulated (broadband) ground motions are selected and scaled based on consistent hazard targets that consider spectral shape and duration. Performance demand parameters of a twenty-story building are examined at different ground motion intensity levels up to collapse to determine whether statistically significant differences exist between the responses to simulated and recorded ground motions. Amplitude scaling of both simulated and recorded ground motions is used in these analyses, following conventional approaches used in earthquake engineering. These comparisons revealed insignificant differences between the recorded and simulated ground motions, when scaled to match consistent hazard parameters. In a second on-going phase of the study, structural response is evaluated using unscaled, large-amplitude simulated ground motions generated as part of SCEC's CyberShake project. Differences in response

to simulated and recorded ground motions are contrasted and opportunities and challenges for using simulated ground motions in structural performance assessment are discussed.

Stress equilibrium in southern California from Maxwell stress function models fit to both earthquake data and a quasi-static dynamic simulation, Peter Bird (Poster 104)

The lithospheric stress field is divided into 3 components: a standardized pressure curve, a topographic stress anomaly, and a tectonic stress anomaly. The topographic stress anomaly is computed by numerical convolution of density anomalies with 3 tensor Green's functions provided by Bousinesq, Cerruti, and Mindlin. By assuming either a seismically-estimated or isostatic Moho depth, and by using Poisson ratio of either 0.25 or 0.5, I obtain 4 alternative topographic stress models. The tectonic stress field, which satisfies the homogeneous quasi-static momentum equation, is obtained from particular second-derivatives of Maxwell vector potential fields which are weighted sums of basis functions representing constant stress components, stress components varying linearly along 3 spatial axes, and stress components varying harmonically in 1-D, 2-D, and 3-D. Boundary conditions include zero traction due to tectonic stress at sea level, and zero traction due to total stress anomaly on model boundaries at asthenospheric depths. The total stress anomaly is fit by least-squares to both 449 World Stress Map data and a previous faulted-lithosphere, realistic-rheology dynamic model of the region computed with Shells. Constraints of computer memory, execution time, and ill-conditioning of the linear system (which requires damping) limit spatially-oscillating stress to no more than 5 cycles per axis of the model. No conflict is seen between the two target datasets, and the best-fitting model (using an isostatic Moho and Poisson ratio 0.5) gives minimum directional misfits relative to both targets. Peak shear stresses in this preferred model are 130 MPa, and peak vertically-integrated shear stresses are 3.4×10^{12} N/m. Channeling of deviatoric stress along the strong Peninsular Ranges and Great Valley lithosphere is evident. A comparison calculation using the 178152 focal mechanisms of Yang et al. [2012, BSSA] (instead of WSM data) gives very similar results, but larger residual misfit measures.

Twenty-Two Years of Combined GPS Daily Coordinate Time Series and Derived Parameters (1992-2014): Implications for Maintaining a Geodetic Reference Frame, Yehuda Bock, Sharon Kedar, Angelyn W. Moore, Peng Fang, Zhen Liu, Susan E. Owen, and Melinda B. Squibb (Poster 222)

The NASA-funded "Solid Earth Science ESDR System (SESES)" MEASUREs project publishes long-term Earth Science Data Records (ESDRs), the result of a combined solution of independent daily JPL (GIPSY-OASIS software) and SIO (GAMIT software) GPS analyses, using a common source of metadata from the SOPAC database. The project has now produced up to twenty-two years of consistent, calibrated and validated ESDR products for over 3200 GPS stations from Western North America, other plate boundaries, and global networks made available through the GPS Explorer data portal and NASA's CDDIS archive. The combined solution of daily coordinate time series uses SOPAC h-files and JPL STACOV files as input to the *st_filter* software. The combined time series are then fit with the *analyze_tseri* software for daily positions/displacements, secular velocities, coseismic and postseismic displacements, as well as annual and semi-annual signatures and non-coseismic offsets due primarily to equipment (antenna) changes. Published uncertainties for the estimated parameters take into account temporal noise in the daily coordinate time series. The resulting residual coordinate time series with typical daily RMS values of 1.5-4.0 mm in the horizontal and 4.0-8.0 mm in the vertical can then be mined for other signals such as transient deformation associated with earthquake tremor and slip (ETS) and hydrological effects. As part of this process we have catalogued and characterized coseismic displacements due to more than 80 earthquakes (including 28 in western North America since 1992) affecting over hundreds of regional and global stations, as well as significant postseismic deformation for the larger events. The larger events can affect stations 1000's of km from the earthquake epicenters and thus significantly affect the positions of stations used in defining the reference frame. We discuss the implications and contributions of our ongoing analysis to the long-term maintenance of a geodetic reference frame, and present a combined velocity field for the western U.S.

Neotectonics of the San Diego Trough and Coronado Bank fault systems, Inner California Borderlands, Jayne M. Bormann, Graham M. Kent, Neal W. Driscoll, Alistair J. Harding, James J. Holmes, Valerie J. Sahakian, and Steven G. Wesnousky (Poster 254)

Geodetic data indicate that faults offshore of Southern California currently accommodate 6-8 mm/yr of dextral Pacific-North American relative plate motion. In the Inner California Borderlands (ICB), modern strike-slip deformation overprints a prominent system of basins and ridges that formed during plate boundary reorganization 30-15 Ma. Despite its proximity to densely populated Southern California, the hazard posed by faults in the ICB remains poorly understood due to unknown fault geometry and loosely constrained slip rates.

The San Diego Trough fault and Coronado Bank fault systems are northwest striking, sub-parallel, right-lateral faults within the ICB system. We use reprocessed legacy 2D multichannel seismic (MCS) reflection data, newly acquired high-resolution 2D MCS reflection data, and multibeam bathymetry to constrain the architecture and evolution of these faults. We interpret the MCS data using a sequence stratigraphic approach to establish a chronostratigraphy and determine the relative recency of slip for the San Diego Trough and Coronado Bank fault systems.

Our new data refine assumptions about fault geometry and slip rates made in previous models of ICB deformation. Linear troughs that cut bathymetric highs along the trace of the Coronado Bank fault are geomorphic indicators that the fault has accommodated right-lateral strike slip deformation in the past. However, the MCS data show that younger, undeformed marine sediments onlap the bathymetric highs, which suggests that slip on the Coronado Bank fault has decreased over time. Additionally, a thick package of undeformed Late Pliocene sediments overlies the northern extent of the Coronado Bank fault; therefore, slip rate estimates based on kinematic linkage with the Holocene active Palos Verdes fault are unwarranted. To the west of the Coronado Bank fault, the San Diego Trough fault offsets young sediments between the US/Mexico border and the eastern margin of Avalon Knoll, where the fault is spatially coincident with the mapped trace of the San Pedro Basin fault. The length, linearity, and simplicity of the San Diego Trough fault trace suggest that this fault may accommodate a significant portion of modern ICB dextral deformation. Possible kinematic linkage between the San Diego Trough and San Pedro Basin faults increases the potential rupture length for earthquakes on either fault and may allow events nucleating on the San Diego Trough fault to propagate much closer to the LA Basin.

When the Rains Fail, the Mountains Rise: Drought-induced Uplift in the Western United States Observed by the PBO GPS network, Adrian A. Borsa, Duncan C. Agnew, and Daniel Cayan (Poster 101)

The western United States has been experiencing severe drought since 2013. The solid earth response to the accompanying loss of surface and near-surface water mass should be a broad region of uplift. We use seasonally-adjusted time series from continuously operating GPS stations in the Plate Boundary Observatory to measure this uplift, which reaches 15 mm in the California Coastal Ranges and Sierra Nevada and has a median value of 4 mm over the entire region. The pattern of mass loss due to the drought, which we recover from an inversion of uplift observations, ranges up to 50 cm of water equivalent and is consistent with observed decreases in precipitation and streamflow. Coulomb stresses on the San Andreas Fault have increased 100-200 Pa due to the unloading, which is approximately the same as a week of tectonic strain accumulation and is unlikely to affect seismicity. Modeling and removing the large displacement signals from hydrological sources (both seasonal and interannual) is an important step for improving the recovery of tectonic signals from GPS.

Empirical sensitivity kernels of noise correlations with respect to virtual sources, Pierre Boue, Laurent Stehly, Nori Nakata, and Gregory C. Beroza (Poster 180)

Cross-correlation of time-series, or interferometry, applied to the ambient seismic field is an established method to observe the propagation of waves between pairs of sensors without involving transient sources. These reconstructed waves are routinely used to develop high-resolution

MEETING ABSTRACTS

images of the crust and upper mantle, or in mapping the time-dependent velocity changes associated with tectonic events. Using similar methods, recent work have highlighted more challenging observations, such as higher mode surface wave propagation and body wave reconstruction at various scales of the Earth: from the industrial surveys at the reservoir scale to the global scale. Furthermore, the reconstruction of the correct amplitude information can be used to image the anelastic attenuation of the medium and has led to a new type of ground motion prediction using virtual earthquakes method. The dependability of such amplitude retrieval had been debated and represents a difficult challenge due to uneven source distribution. In this study, we discuss the possibility to use the correlation of ambient noise correlation (similar to C3 method) to map the contribution of different source locations for Rayleigh wave reconstruction between receiver pairs. These maps constructed in terms of traveltime or amplitude perturbations of the Green's function, can be considered as empirical sensitivity kernels with respect to the contribution of each virtual source. We propose for the first time to map these kernels using a dataset of continuous records from a dense array of about 2600 sensors deployed at the local-scale in Long Beach (CA, USA). Finally, these maps are used to analyze the impact of the original ambient noise directivity on the recovered Green's functions and discuss the effects of the velocity lateral heterogeneity within the array. We aim at understanding, and thereby reducing, the bias in ambient field measurements.

Bridging Seismic Networks Across Time and Space, Roy D. Bowling, Marine Denolle, and Peter M. Shearer (Poster 158)

The threat of future large earthquakes compels the seismological community to better understand the likely ground motion that will result from earthquakes. A key factor in predicting accurate ground motion is to understand how seismic waves propagate in a complex 3D crustal structure. Seismologists traditionally extract wave speed information between earthquake sources and receivers. Scientists also use Green's functions constructed from simultaneous ambient field recordings to gain wave speed information between virtual sources and receivers. The use of ambient noise Green's functions normally requires synchronous recordings of the ambient field. However, Ma and Beroza (2012) show that one can bypass this condition of simultaneity using higher-order correlations. We aim to link three asynchronous deployments in the Sierra Nevada (SNEP), Mendocino (FAME), and High Lava Plains (HLP) areas by using the continuously recording USArray and regional permanent stations as references. We take advantage of the flash-based memory of the Gordon supercomputer at the San Diego Super Computing Center to compute all synchronous correlations. Then using the first-order Green's functions as scattered wave sources, we compute higher-order correlations between all station pairs, including those deployed asynchronously. We show that higher-order correlations improve ray path coverage over synchronous correlations, and asynchronous Green's functions allow for measurement of seismic properties along ray paths that are not possible with first-order correlations. The spatiotemporal bridging of seismic networks therefore brings new opportunities to overcome sparsity of data.

Low frequency ($f < 1\text{Hz}$) ground motion simulations of 10 events in the 2010-2011 Canterbury earthquake sequence, Brendon A. Bradley and Rob W. Graves (Poster 070)

This poster presents initial results from low frequency ($f < 1\text{Hz}$) ground motion simulations of the 2010-2011 Canterbury, New Zealand earthquakes. The 10 most significant earthquake events in the sequence, based on magnitude ($M_w 4.7-7.1$) and proximity to the Christchurch urban area were considered. The four largest events (4 Sept 2010, 22 Feb 2011, 13 June 2011 2:20pm, 23 Dec 2011 2:18pm) use source geometry informed from the source inversion studies of Beavan et al. (2010, 2012), while the remaining six events ($M_w 4.7-5.8$) use source geometry based on magnitude-geometry scaling relationships (as well as being alternatively modeled as point sources). The kinematic rupture description of the finite sources is based on an updated version of the Graves and Pitarka (2010) rupture generator. The crustal structure in the Canterbury region was initially considered via a 1D velocity model comprising prior tomography models and a generalized representation of the shallow velocity structure in the Canterbury sedimentary basin. Finite difference wave propagation simulations (4th order spatial and 2nd order temporal accuracy) were

performed using 2048 cores on the University of Canterbury IBM BlueGene supercomputer. Calculations were obtained for a minimum velocity, $V_s = 500\text{m/s}$, and for frequencies, $f \leq 1\text{Hz}$. Shallow site response corrections based on V_s30 were performed using the method of Campbell and Bozorgnia (2008). The simulations provide a reasonable representation of observed seismograms during body wave arrivals, but underestimate the amplitude of surface waves, particularly in the Christchurch urban area. Simulations with a 3D velocity structure are beginning to commence with prototype versions of a model under development (Lee et al. 2014).

Revised and Improved Fault Maps of Southwest Reno, Nevada using Light Detecting and Ranging (LiDAR) Imagery, Courtney M. Brailo, Graham M. Kent, Steven G. Wesnousky, Annie M. Kell, Ian Pierce, Christine J. Ruhl, and Kenneth D. Smith (Poster 260)

A new Light Detection and Ranging (LiDAR) survey images the fault network of the Truckee Meadows region of western Nevada, including the Reno-Sparks metropolitan area in Washoe County. The airborne LiDAR imagery (1485 sq. km) is being used to create high-quality bare-earth digital elevation models that were previously unattainable in vegetated, populated or alpine terrain. LiDAR gives us an opportunity to improve fault maps that may be outdated or incomplete in the area. Faulting on the Mt. Rose pediment is highlighted here, where LiDAR imagery confirms the presence of previously mapped faults, introduces previously unmapped faults and clarifies areas where mapping of faults has been difficult in the past.

Conflicting stress regimes, with strike-slip regions overlapping extensional domains in the Walker Lane Deformation Belt, complicate regional tectonics of Washoe County. In this region, east of the Sierra Nevada batholith, approximately 20-25% of Pacific-North American plate motion (mostly right-lateral shear) is accommodated along the Walker Lane. There is ample evidence of Magnitude 6-7 earthquakes in or surrounding the Truckee Meadows region as recently as the late 1800s and it is possible that earthquakes of this size may occur here in the near future. Accurate mapping of faults and associated earthquake hazards in populated areas is critically important for earthquake mitigation and preparedness, and furthers our understanding of regional tectonics. Current and future research will also focus on dating of glacial outwash terraces and alluvial fans, particularly on the Mt. Rose pediment. Coupled with comprehensive fault maps and displacement measurements improved by this new LiDAR dataset, these data may allow researchers to get more accurate slip rate estimates on faults in this region, and may support the hypothesis that some faults in the Washoe County region are more active than previously reported.

Mobile Laser Scanning Geodesy for Imaging Transient and Near-Field Fault Slip, Benjamin A. Brooks and Craig L. Glennie (Poster 234)

Transient fault slip, ranging from slow, quasi-continuous fault creep to rapid, post-earthquake, afterslip is one of the more important processes to study as we strive for an understanding of earthquake physics and the space- and time-dependent hazards they pose to human society. For instance, ground motion simulations for earthquake rupture scenarios on creeping faults differ dramatically depending on the amount of fault creep permitted to occur. Earthquake afterslip can produce surface displacements on the order of coseismic displacements and a signal that decays sharply within hours to days of an event, but this has proven to be difficult to document. Mobile Laser Scanning (MLS) is an emerging tool that permits autonomous and rapid high-resolution imaging of the surface expression of fault slip. Here, we test two manners of performing MLS geodesy: (1) MLS data referenced to legacy Airborne Laser Scanning (ALS) data sets and (2) MLS data referenced to other MLS data sets collected from a moving automobile. From 2012 to 2014, we collected multiple MLS data sets from a creeping section of Northern California's Hayward fault near Fremont, CA; the area was also imaged in the 2007 EarthScope regional ALS survey. The study area is a residential neighborhood and we utilize the stability and geometric regularity of built structures as virtual control points in the geodetic analysis. For the ALS-MLS technique this presents a complication because ALS data (few points / m^2) image mostly house roofs whereas MLS data (thousands pts / m^2) image a combination of roofs and vertical walls. We derive estimated fault

offset by a least squares rigid body transformation of planar surfaces from structural features common to each data set and typically within ~ 300 m of the fault trace. We find that both ALS-MLS and MLS-MLS techniques have relative accuracy capability of measuring surface fault slip at the ~1cm/yr level. Furthermore, we find good agreement between independently measured creep and the ALS-MLS derived measurement of ~6 cm over 6 years.

Inverting for Shear Stress Rate on the Northern Cascadia Megathrust Using Geodetic Data, Lucile Bruhat, Paul Segall, and Andrew M. Bradley (Poster 243)

Past physics-based models of slow slip events (SSE) have shown that, when averaged over many SSE cycles, the shear stress within the SSE zone remains roughly constant. Stress accumulates between SSE, and then is released during slow slip events. However, the predicted long-term deformation rates from such models, assuming the plate boundary is locked to the top of the ETS zone, do not fit well GPS velocities and uplift rates determined from leveling and tide-gauge data. These physics-based models particularly misfit the vertical rates. At the same time, previous kinematic inversions display a gap between the down-dip limit of the locked region and the top of the ETS zone.

Our inversions of geodetic data for fault slip rates exhibit a steeper slip-rate profile at the top of the ETS zone, relative to the constant shear stress model, as well as creep up dip of the ETS zone. We explore physics-based models with velocity-strengthening regions of different length up dip the ETS zone, i.e. within the "gap" identified in kinematic inversions. However, this still does not match the observations well. We therefore try a new approach: we invert for shear stress rates on the megathrust that best fit the data. We show that a small decrease in shear stress within the top of the ETS zone, reaching 5 kPa/year at a depth of ~ 30 km, is required to fit the data. Possible explanations for this include a slow decrease in normal stress with time, possibly due to an increase in pore pressure, or a reduction in fault friction. We explore these hypotheses, using 2D quasi-dynamic simulations with rate-and-state friction and isothermal v-cutoff models for generating slow slip events. The potential for creep above the top of the ETS zone has important implications for the mechanical relationship between deep slow slip and dynamic events in the locked region.

Ground motion selection for simulation-based seismic hazard analysis, Lynne S. Burks, Brendon A. Bradley, and Jack W. Baker (Poster 047)

Ground motion selection is a critical link between seismic hazard analysis and seismic response analysis, as a small number of time series are used to represent our knowledge of the seismic hazard. This work describes how that process, which is traditionally done using empirical ground motion prediction equations and recorded ground motions, can be adopted for use with simulation-based hazard calculations such as Cybershake. A selection process is still needed in this case to extract a small number of time series from the much larger set developed as part of the hazard calculation. Four methods are proposed for doing this selection, and pros and cons of each are discussed. All four methods are implemented and used to predict seismic response of a simple nonlinear structural model; a benchmark result (using all simulated ground motions) is also provided to show the consistency of the selection methods. Through the comparison of these methods, the logic of advanced empirical approaches for selecting ground motions is also illustrated; in the case of recorded ground motions there is no benchmark answer available, but in the case of simulations where there is a benchmark, the ability of those methods to reproduce the benchmark provides further empirical confirmation of their effectiveness.

Optimizing CyberShake Seismic Hazard Workflows for Large HPC Resources, Scott Callaghan, Philip Maechling, Gideon Juve, Karan Vahi, Robert W. Graves, Kim B. Olsen, Kevin Milner, David Gill, and Thomas H. Jordan (Poster 081)

The CyberShake computational platform is a well-integrated collection of scientific software and middleware that calculates 3D simulation-based probabilistic seismic hazard curves and hazard maps for the Los Angeles region. Currently each CyberShake model comprises about 235 million synthetic seismograms from about 415,000 rupture variations computed

at 286 sites. CyberShake integrates large-scale parallel and high-throughput serial seismological research codes into a processing framework in which early stages produce files used as inputs by later stages. Scientific workflow tools are used to manage the jobs, data, and metadata. The Southern California Earthquake Center (SCEC) developed the CyberShake platform using USC High Performance Computing and Communications systems and open-science NSF resources.

CyberShake calculations were migrated to the NSF Track 1 system NCSA Blue Waters when it became operational in 2013, via an interdisciplinary team approach including domain scientists, computer scientists, and middleware developers. Due to the excellent performance of Blue Waters and CyberShake software optimizations, we reduced the makespan (a measure of wallclock time-to-solution) of a CyberShake study from 1467 to 342 hours. This improvement enabled the calculation of hazard maps for 4 models, including the new community velocity model CVM-S4.26. We will describe the technical enhancements behind this improvement, including judicious introduction of new GPU software, improved scientific software components, increased workflow-based automation, and Blue Waters-specific workflow optimizations.

Our CyberShake performance improvements highlight the benefits of scientific workflow tools. The CyberShake workflow software stack includes the Pegasus Workflow Management System (Pegasus-WMS), which includes Condor DAGMan, HTCondor, and Globus GRAM, with Pegasus-mpi-cluster managing the high-throughput tasks on the HPC resources. The workflow tools handle data management, automatically transferring about 13 TB back to SCEC storage.

We will present performance metrics from the most recent CyberShake study, executed on Blue Waters. We will compare the performance of CPU and GPU versions of our large-scale parallel wave propagation code, AWP-ODC-SGT. Finally, we will discuss how these enhancements have enabled SCEC to move forward with plans to increase the CyberShake simulation frequency to 1.0 Hz.

Modeling Fragmentation, Acoustic Effects, and Flash Heating in Sheared Granular Materials: Implications of Geophysical Processes and Physical Constraints for Dynamic Friction, Jean M. Carlson, Charles Lieou, Ahmed Elbanna, and James Langer (Poster 135)

Incomplete understanding of friction, deformation, and failure is a primary limiting factor in forecasting seismic hazards. We report recent progress on a physics-based framework for constitutive laws. Our methods are rooted in the underlying statistical thermodynamics of amorphous materials, and bridge the gaps between microscopic dynamics, laboratory experiments, and dynamic rupture.

We expand Shear-Transformation-Zone theory, describing frictional response of sheared gouge layers over a wide range of velocities and normal stresses, to account for geophysically relevant processes such as breakage and thermal heating, as well as grain shapes. We combine theoretical advances with quantitative fits to experimental data obtained within the fault and rock mechanics community.

Fragmentation is described by a constitutive equation for grain size reduction involving the applied work rate and pressure, constrained by energy balance. We show that grain breakage is a potential weakening mechanism at high strain rates. It promotes strain localization and may explain long-term persistence of shear bands in natural faults.

Shape effects are modeled by an orientational bias that describes grain interlocking and geometric frustration. We interpret inter-particle friction as an additional source of acoustic noise. We obtain quantitative agreement between experimental measurements and theoretical predictions for both internally generated acoustic noise and externally applied vibrations.

Frictionally generated thermal heating is incorporated using a contact strength model that accounts for local increases in temperature at grain contacts during sliding. The magnitude of this effect depends on grain size and porosity of the granular layer. Our model predicts logarithmic rate dependence of steady state shear stress in the quasi-static regime. In the dense flow regime frictional strength decreases rapidly with increasing slip rate due to thermal softening at granular interfaces. The transient response following a step in strain rate includes a direct effect and

MEETING ABSTRACTS

subsequent evolution effect, both depending on the magnitude and direction of the velocity step.

We anticipate using dynamic rupture simulations to extrapolate our results to geophysically relevant regimes that are beyond reach of laboratory experiments. Our work offers experimentalists and field workers insights for interpreting data, identifying features to target in future work, and estimating seismic hazards.

Aftershock triggering by postseismic stresses: a study based on Coulomb-Rate-and-State models, *Camilla Cattania, Sebastian Hainzl, Lifeng Wang, Bogdan Enescu, and Frank Roth* (Poster 016)

The spatio-temporal clustering of earthquakes is a feature of medium and short term seismicity, indicating that earthquakes interact. However, controversy exists about the physical mechanism behind aftershock triggering: static and dynamic stress transfer, as well as reloading by postseismic processes, have been proposed as explanations. Assessing the relative importance of these processes would not only advance scientific understanding, but could also lead to improved medium term forecasts.

We use a Coulomb Rate-and-State model to assess the relative impact of coseismic and postseismic stress changes on aftershocks. We focus on two processes: creep on the mainshock fault plane (afterslip), and secondary aftershock triggering by previous aftershocks. We model the seismic response to Coulomb stress changes using the Dieterich constitutive law, and focus on two events: the Parkfield, Mw=6.0 earthquake; and the Tohoku, Mw=9.0 megathrust.

We find that modeling secondary triggering systematically improves the maximum log-likelihood fit of the sequences. The effect of afterslip is more subtle, and difficult to assess for near-fault events, where model errors are largest. More robust conclusions can be drawn for off-fault aftershocks: following the Tohoku earthquake, afterslip promotes shallow crustal seismicity in the Fukushima region. Simple geometrical considerations indicate that afterslip-induced stress changes may have been significant on trench parallel crustal fault systems following several of the largest recorded subduction earthquakes. Moreover, the time dependence of afterslip strongly enhances its triggering potential, underlining the importance of employing a time-dependent treatment.

Implications from observed drift of tall buildings during the March 11, 2011 M9.0 Tohoku Earthquake, Japan, *Mehmet Celebi, Izuru Okawa, and Toshihide Kashima* (Poster 051)

One of the most significant effects of the M9.0 Tohoku, Japan earthquake of March 11, 2011 is the now well-known long duration (>10 minutes) shaking of buildings in Japan – particularly those in Tokyo (~ 350-375 km from the epicenter) and in places as far as Osaka (~770 km from the epicenter). Although none collapsed, the strong shaking caused many tall buildings to be non-functional for days and weeks. Here, the recorded behavior and computed performance of four tall buildings, considered to be representative of most tall buildings in Tokyo and Osaka are discussed. The average drift ratio for one of the buildings, in Osaka, reached 0.5%, which is significant considering that the ground-level input motion was only ~3% g. What might have happened during an event with input level motions with similar low frequency content and in 10-20% g range merits further consideration. This particular building also has significant site effects that contributed to resonance. The other three buildings are in Tokyo. For example, based on records obtained from a 54-story Tokyo building retrofitted with 288 oil dampers distributed on 24 floors, computations show that average drift ratio reached ~0.3%, and the maximum drift ratio likely was higher. For comparison, the maximum drift ratio allowed by Japanese practice for buildings taller than 60 m and for collapse protection (level 2) motions is 1% (The Building Center of Japan, 2001). However, Kubo et al. (2011) state that if the drift ratio is over 1%, then moderate to severe damage can occur, and if it is within the range of 0.5% to 1%, then minor damage can occur. Average drift ratios of the two other tall buildings in Tokyo were 0.3 and 0.5%.

Performances of tall buildings in many seismically active regions of the world or those affected by long-period motions from distant sources (e.g. Chile, Turkey, Abu Dhabi, Dubai and the US) are of interest to the earthquake engineering community. Currently the standards for drift ratio

limits differ among countries. Chile, for example, imposes a 0.2 % inter-story drift ratio limit for elastic design, while the USA and Turkey impose a 2% drift limit. Such wide variations of drift limits in design practices deserve discussion in light of the impact of the 2011 Tohoku event on the functionality and performance of tall buildings.

Influence of fluid pressure variations in earthquake swarms in the Salton Sea geothermal field?, *Xiaowei Chen and Jeff McGuire* (Poster 143)

The Salton Sea geothermal field (SSGF) occurs on top of a plate boundary fault system and has one of the highest rates of microseismicity in Southern California. The “ladder-like” seismicity rate increase with time mimics the “ladder-like” increase of injection activities from west to east since 1981. Chen and Shearer, [2011] analyzed earthquakes from 1981-2009 using an empirical-Green’s function analysis of all earthquakes in the Salton Sea region. They found that earthquake stress drop increases with distance away from injection wells within the SSGF. Both seismicity clustering and source spectra suggest a significant role of fluid in the earthquake generation process [Chen and Shearer, 2011]. We analyze the space-time patterns of seismicity from 2009 to 2013 and found diffusive migration during the beginning stage of the 2010 earthquake swarm, and a diversity of migration directions within the east sub-cluster of seismicity. We are conducting detailed analysis of source spectra using the borehole recordings available since 2008, in order to better understand the detailed correlation between injection operation parameters and earthquake source parameters. Additionally, we estimate temporal changes in the average shear-wave velocity using the S-wave coda for selected earthquake clusters at stations close to the main fault-zone within the SSGF. Preliminary results indicate drops in the shear-wave velocity of a percent during earthquake swarms. The combination of source spectra, earthquake clustering and velocity changes studies will hopefully provide a detailed understanding of the role of fluid pressure variations in modulating earthquake swarms.

LASSIE: A high-density short-duration broadband seismic survey of the Los Angeles Basin, *Robert W. Clayton, Mitchell Barklage, Elizabeth Cochran, Dan Hollis, Paul Davis, Bill Erickson, Jascha Polet, Brady Barto, Catherine Cox, and Michael Padgett* (Poster 197)

LASSIE (Los Angeles Syncline Seismic Interferometry Experiment) is a collaborative experiment between industry and academia to operate a high-density short-duration broadband seismic survey across the Los Angeles Basin. The survey will consist of a linear array of broadband seismic stations that will transect an area from the Long Beach harbor to the foothills north of Whittier with a high-density 3D array of instruments in the Long Beach area. The industry objective of this survey is to derive seismic velocity information from ambient-noise surface waves, and use it to improve subsurface reflection images of the Long Beach oil field. The academic interest is to see if we can image the Los Angeles Basin with receiver functions and seismic interferometry. Approximately 60 broadband instruments will be used in the deployment, which will occur Sept 27, 2014 to Nov 1, 2014. The instruments will include 40 sets (Guralp 3Ts and Refteks) from the PASSCAL Instrument Center and a number of sets from the academic institutions. The specific station design for this survey will be streamlined to minimize the impact on private property and landowners in the urban environment of the LA Basin. The data will be archived at the IRIS Data Management Center and will be open access after the standard two-year waiting period.

Increasing Warning Times for the Onsite Earthquake Early Warning Algorithm, *Elizabeth S. Cochran, Egill Hauksson, Maren Boese, and Claude Felizardo* (Poster 035)

A significant source of alert latency in earthquake early warning (EEW) algorithms, which can possibly be reduced, is the duration of the time window used to estimate EEW parameters following a P wave detection. We investigate whether the detection time for the τ -Pd Onsite algorithm can be reduced by estimating EEW parameters using shorter waveform windows. The Onsite algorithm is currently one of three EEW algorithms implemented in ShakeAlert, the earthquake early warning system being developed for the west coast of the United States. Onsite uses the ground-motion period parameter (τ) and peak initial displacement parameter (Pd) to estimate the magnitude and expected ground shaking

of an ongoing earthquake. The current implementation of Onsite requires a 3 second window of the P waveform before issuing magnitude estimates. We use a large suite of waveform records of local earthquakes ($M > 3$) recorded in southern California to examine the performance for a range of window lengths between 1-5 s. We examine source-to-station distances up to 300 km and focus on the results for distances less than 100 km. We find that Pd shows a stronger correlation with magnitude than is observed for τ_c , for all tested window lengths. τ_c does not correlate with magnitude for earthquakes with $M < 4$; however, we do not apply any quality metrics to remove bad or noisy records (e.g. Böse et al., 2012). The broadband waveforms give more reliable Pd and tc measurements than strong motion waveforms, at least for moderate sized earthquakes, likely because of higher signal to noise ratios. However, these results may be biased since the dataset does not include many waveforms for earthquakes with $M > 6$. Overall, preliminary results suggest that it may be feasible to use shorter window lengths (1 sec) without significantly degrading the magnitude estimate in the Onsite algorithm. We will determine the optimal waveform window that provides both fast and reliable estimates of τ_c and Pd for use in the Onsite algorithm, and will work with spatially varying station density. Further, we will investigate if sliding window lengths can be used to improve the τ_c and Pd estimates continuously.

Visible Earthquakes: An open visualization and modeling platform for InSAR earthquake data, Rowan B. Cockett, Gareth J. Funning, and Beth Pratt-Sitaula (Poster 005)

Interferometric synthetic aperture radar (InSAR) is widely used in research of earthquake source parameters, however, the method is only taught in a handful of university campuses across the country. This reflects, we believe, a lack of accessibility to software and data for nonspecialists. Here we present a web-based interactive tool for comparing real InSAR data from earthquakes with simple elastic models, designed with accessibility in mind. This tool is intended for use in education and outreach settings, and may also facilitate the sharing and interpretation of data following significant earthquakes, thus potentially playing a useful role in earthquake response.

The tool, named 'Visible Earthquakes', uses web-based technologies to instantly render the displacement field that would be observable using InSAR for a given fault location, geometry, orientation, and slip. The user can adjust these source parameters using a simple graphical interface and see how these affect the resulting model interferogram. By visually matching the model interferogram to a real earthquake interferogram, users can produce their own estimates of the earthquake's source parameters. The difference between the observational data and the user's modeled data is calculated and shown to the user to help assess how well the proposed model fits the data. Once satisfied with the fit of their models, users submit their results and see how they compare with the distribution of all other contributed earthquake models.

All the data produced by people using the tool is shown to the user once they have modeled a certain earthquake. This includes the modeled earthquake parameters, as well as metadata such as time taken and the modeler's confidence in their results. The spread of different results for each individual earthquake allows the teaching of concepts such as model uncertainty and non-uniqueness when modeling real scientific data. In addition to familiarizing students and the public with InSAR and elastic deformation modeling, Visible Earthquakes enables participation in scientific modeling and classification of real earthquake data.

Qualitative Comparison of Offset Surfaces Between the Central and Eastern Garlock Fault, Thomas M. Crane and Sally F. McGill (Poster 256)

The Garlock fault consists of three distinct segments, known as western, central and eastern, together reaching approximately 260 km from the San Andreas fault to the southern end of Death Valley. Although published slip rates are available along the Western and Central Garlock fault, little is currently known of the Garlock fault earthquake history or slip rate farther east. Using LiDAR and satellite imagery, the Central (CGF) and Eastern Garlock fault (EGF) were analyzed for visibly offset features that may potentially be used for estimating slip rate. Qualitative methods of assessing preserved alluvial surface maturity were adapted and used to establish unit age categories. Qualitative comparisons of surfaces

considered to be similar ages reveal that the total offset at sites along the EGF is less than half that of sites of comparable age along the CGF, suggesting a significant reduction in slip rate across the intersection of the Brown Mountain, Owl Lake, and Garlock faults. Digitally-measured offsets and their age groups were plotted in order to achieve preliminary slip-rate estimates. The resulting plot confirms an eastward decrease in late Pleistocene-Holocene slip rate at sites along the CGF and EGF. The CGF slip-rate estimate taken from Slate Range West (SRW) and Slate Range East (SRE) sites in Pilot Knob Valley was approximately 4.19 mm/yr, within error of previously published rates. The slip-rate estimate from the Quail Mountains site (QMTNS), at the easternmost extent of the CGF, was approximately 2.52 mm/yr. The slip-rate estimate from the Avawatz (AVA) section of the EGF was approximately 1.01 mm/yr.

Are Current Fault Dimension Scaling Relationships Compatible with Eastern North America Earthquake Stress Drops? Jorge G.F. Crempien and Ralph J. Archuleta (Poster 063)

Given a seismic moment, earthquake fault dimension is an important parameter that will control stress drop and therefore the intensity of ground shaking. Leonard (BSSA, 2010) proposed a self-consistent relationship in which the static stress drop of stable continental regions such as Eastern North America (ENA) is always 5.8 MPa. As an example, the 2011 Mineral Virginia Earthquake had a reported seismic moment of $M_0 = 4.96 \times 10^{17}$ Nm (GCMT). Using Leonard's Scaling Rules (LSR), the fault area would be ~ 35 km², and if we consider a rectangular fault, the length and width would predict ~ 7 and ~ 5 km respectively. However, based on the previous results of Shao et al. (AGU, 2011), we performed a finite fault kinematic inversion for this earthquake, and we see a length of ~ 5 and a width of ~ 4 km for the ruptured portion of the fault. We also computed a Brune stress drop of ~ 23 MPa using 4 near-field strong ground motion stations. Our static stress change from the kinematic finite fault inversion exceeds 23 MPa for the ruptured portion on the fault. Our average slip exceeds the ~ 43 cm predicted by LSR with several subfaults exceeding 100 cm of slip. In conclusion, we see that there is an inconsistency between LSR and the finite fault source parameters of the Mineral Virginia and other major earthquakes in ENA, specifically earthquakes with $M_w > 5.8$.

To illustrate the effects a constant stress drop scaling rule will have on predicted ground motions, we performed over 20 synthetic ground motion simulations of the 2011 Mineral Virginia Earthquake using the method of Crempien and Archuleta (SSA, 2014). We used a fault compatible with LSR and a proposed a scaling rule that takes into account variable static stress drop and seismic moment. We compare these values with recorded RotD50 at different sites where ground motions were recorded. We repeat the same procedure for the 2005 Riviere du Loup and 1988 Saguenay earthquakes.

We observe systematic under-prediction of LSR with respect to the observed recorded ground motion intensities for all three earthquakes we analyzed. Preliminary results show no systematic bias in RotD50 for the proposed scaling dimensional parameters.

Slip Reactivation Model for the 2011 Mw9 Tohoku Earthquake: Dynamic Rupture and Strong Ground Simulations, Luis A. Dalguer and Percy Galvez (Poster 129)

The 2011 Mw9 Tohoku earthquake has been recorded with a vast GPS and seismic network given unprecedented chance to seismologists to unveil complex rupture processes in a mega-thrust event. In fact more than one thousand near field strong-motion stations across Japan (K-Net and Kik-Net) revealed complex ground motion patterns attributed to the source effects, allowing to capture detailed information of the rupture process.

The seismic stations surrounding the Miyagi regions (MYGH013) show two clear distinct waveforms separated by 40 seconds. This observation is consistent with the kinematic source model obtained from the inversion of strong motion data performed by Lee's et al (2011). In this model two rupture fronts separated by 40 seconds emanate close to the hypocenter and propagate towards the trench. This feature is clearly observed by stacking the slip-rate snapshots on fault points aligned in the EW direction passing through the hypocenter (Gabriel et al, 2012), suggesting slip

MEETING ABSTRACTS

reactivation during the main event. A repeating slip on large earthquakes may occur due to frictional melting and thermal fluid pressurization effects. Kanamori & Heaton (2002) argued that during faulting of large earthquakes the temperature rises high enough creating melting and further reduction of friction coefficient.

We created a 3D dynamic rupture model to reproduce this slip reactivation pattern using SPEC3D (Galvez et al, 2014) based on a slip-weakening friction with sudden two sequential stress drops. Our model starts like a M7-8 earthquake breaking dimly the trench, then after 40 seconds a second rupture emerges close to the trench producing additional slip capable to fully break the trench and transforming the earthquake into a megathrust event. Using this model we could reproduce roughly the three seismic wave fronts observed from the seismograms located along the Japanese coast. We argue that dynamic rupture model with slip reactivation can explain near source ground motion patterns observed in this earthquake.

Improving K-feldspar luminescence dating techniques, *Jillian T.M. Daniels, Edward J. Rhodes, Michael J. Lawson, Christopher P. McGuire, and Nathan D. Brown* (Poster 273)

Infra-red stimulated luminescence (IRSL) is a technique that can be used for dating fault rupture events. This K-feldspar based method is preferred in southern California over optically stimulated luminescence (OSL) of quartz, as quartz grains in tectonically active areas tend to have poor characteristics for dating. However, the origin of IRSL signals in feldspars is still not fully understood. We are investigating the effect of major composition, trace elements, aluminum-silicon order-disorder, and microstructures such as exsolution lamellae on the IRSL behavior of a wide range of feldspars. Measurement methods such as post-IR IRSL, grain selection techniques such as the Super-K method and a new visual representation of acceptable contamination (the "Grid of Concern") are also discussed.

Can we detect clustered megaquakes? *Eric G. Daub, Daniel T. Trugman, and Paul A. Johnson* (Poster 034)

We study the ability of statistical tests to identify nonrandom features of synthetic global earthquake records. We construct a series of four synthetic catalogs containing various types of clustering, with each catalog containing 10000 events over 100 years with magnitudes above $M = 6$. We apply a suite of statistical tests used in the literature to each catalog in order to evaluate the ability of each test to identify the catalog as nonrandom. Our results show that detection ability is dependent on the quantity of data, the nature of the type of clustering in the catalog, and the specific signal used in the statistical test. Catalogs that exhibit a stronger time variation in the seismicity rate are generally easier to identify as nonrandom for a given background rate. We also show that in some cases, a test that fails to identify a catalog as nonrandom can have predictive power to bound the range of possible clustering strengths of a certain type. Our results help in the interpretation of the results of statistical tests on the global earthquake record since 1900.

STEM Education Products, Partnerships, and Programs from the SCEC Communication, Education, and Outreach (CEO) Program – 2014 Highlights, *Robert M. de Groot, Mark L. Benthien, Kathleen Springer, Danielle Sumy, Cindy Pridmore, Bernadette Vargas, Mark Kline, Key McMurry, Alyssa Caudill, Elizabeth Cochran, Jesse Lawrence, Lilian Arevalo, Kevin Chan, Amelia Moura, David Bolen, Jonathan Ho, Benjamin Anderson, Michelle Vanegas, Luis Gomez, Hernan Lopez, and Dylan Aldrich* (Poster 003)

The SCEC CEO program collaborates with a broad array of educators and institutions to develop STEM products and programs that improve the teaching and learning about earthquakes and tsunamis. This poster provides highlights and successes in 2014 including expansion and development of the Earthquake Country Alliance - Earthquake Education Public Information Center (ECA-EPIcenter) Network, the Quake Catcher Network, and other projects that engage K-12 science educators and students. Also featured will be very exciting and productive efforts with EarthScope, NASA-JPL, UNAVCO, CGS, and IRIS. SCEC CEO has expanded its participation in tsunami education through working with the Cascadia EarthScope Earthquake and Tsunami Education Program

(CEETEP) and the California Geological Survey. Ranging from designed spaces to everyday activities, informal learning environments account for the majority of lifelong learning of STEM topics. Founded with the San Bernardino County Museum in 2008, the ECA-EPIcenter Network currently consists of over 60 informal learning institutions throughout California with prospects of expansion to other regions such as the Pacific Northwest and the Central US. The Quake-Catcher Network (QCN) uses low-cost seismic sensors to record data in real-time on volunteer computers and engages participants in authentic science. As of fall 2014 there have been over 100 QCN sensors installed in California, the Pacific Northwest, and Alaska.

Uncertainties in estimates of earthquake dynamic source properties from body and surface waves, *Marine A. Denolle and Peter M. Shearer* (Poster 168)

The energy released during an earthquake partitions between seismic radiated energy ER, friction energy EF, which include heat dissipation, and fracture energy EG, which includes inelastic cracking. The relative sizes of ER and EG determine the radiation efficiency, which is an important parameter in rupture mechanics. However, uncertainties in our measurements of ER and dynamic stress drop directly affect our estimates of EG and radiation efficiency, and ultimately may bias our understanding of earthquake mechanics.

We explore the contribution of surface waves to the total estimate of ER for shallow events in the cases of point sources and of dynamic ruptures.

For energy estimates derived from body-wave spectra, we find that uncertainties in the corner frequency are the dominant contributor to uncertainties in the scaled radiated energy ER/M0, while uncertainties in high-frequency fall-off rates and the theoretical model used to compute stress drop from corner frequency have a large effect on estimates of radiation efficiency. In general, higher fall-off rates yield lower values of radiation efficiency and larger theoretical stress drop estimates for the same corner frequency yield higher values of radiation efficiency. In addition, even assuming radiation pattern differences in observed amplitudes are correctly computed, directivity will have a strong biasing effect on energy estimates unless the focal sphere is completely sampled.

We investigate all of these factors, as well as additional uncertainties that arise from commonly used approaches to remove path effects from velocity seismograms, i.e., empirical corrections for radiation pattern differences on amplitude and empirical Green's functions (eGf) to calibrate spectra. We show preliminary results on evaluating ER/M0 and its uncertainties for recent large M8.5+ megathrust earthquakes.

Status and Growth of the USGS Southern California GPS Network, *Daniel N. Determan, Aris G. Aspiotes, Ken W. Hudnut, Nancy E. King, Keith F. Stark, and Derik T. Barseghian* (Poster 037)

The USGS Pasadena field office is currently expanding its permanent, continuously-operating GPS network in Southern California through the Urban Area Security Initiative (UASI) project led by Egill Hauksson of Caltech. The project purchased 41 new Trimble NetR9 GPS receivers with Zephyr Geodetic II antennas. The new Trimble equipment includes GLONASS tracking, like the newer Topcon Net-G3A receivers purchased through the American Recovery and Reinvestment Act (ARRA) in 2010, and also has the recently developed on-board RTX software option that allows for Precise Point Positioning with Ambiguity Resolution (PPP-AR) at the receiver. This new capability will be most advantageous for supporting the West Coast Earthquake Early Warning (WC-EEW) system at sites located close to the fault. We therefore used most of the new Trimble NetR9 receivers with RTX (PPP-AR) to upgrade the existing "zipper array" sites and other existing stations located close to the San Andreas Fault (SAF) to achieve faster displacements after a large event. In addition to the existing stations along the SAF, there are seven new UASI sites where the new Trimble NetR9 equipment has been installed with seismic instrumentation. Some of these sites are located near other critical faults, including the San Jacinto and Elsinore. USGS Pasadena is currently working to re-install the Topcon equipment, removed from "zipper array" and other sites, at new UASI stations. Before the UASI project, our SoCal GPS network consisted of 104 permanent, continuously operating GPS stations for which 95 had real time telemetry and 26 were co-located with seismic equipment. After UASI and re-installations of the Topcon

equipment, our network will increase to 144+ GPS stations for which 135 will include real time telemetry and 64 will be co-located with seismic equipment. This larger network will utilize three types of geodetic grade GPS receivers; 12 stations will remain with Trimble NetRS receivers; 63 stations will contain Topcon NetG3A receivers; and 41 stations will utilize the new Trimble NetR9 receivers with RTX (PPPAR). We are also collaborating with our other WC-EEW stakeholders, such as the Los Angeles Department of Water and Power (LADWP) and the Metropolitan Water District (MWD), to install seismic and GPS monitoring equipment at critical infrastructure locations where major Los Angeles water and/or power supply lines cross the most potentially hazardous faults.

Kinematically Consistent Viscoelastic Block Models: Time Series Averaging and Accurate Plate Motions, Phoebe Robinson DeVries, Plamen G. Krastev, and Brendan J. Meade (Poster 098)

Quasi-static elastic block models have become a widely applied technique for interpreting and decomposing nominally interseismic geodetic velocity fields. These models include a first-order approximation of earthquake cycle processes. However, they typically neglect the effects of long-term and temporally variable viscoelastic processes. Integrating viscoelastic deformation into kinematically consistent block models is non-trivial. Here we introduce a kinematically consistent viscoelastic block model framework where viscoelastic velocity contributions are treated as perturbations around the time-independent elastic solution. This approach guarantees kinematic consistency and accurate representations of plate motions at the (computational) cost of requiring the calculation of the average viscoelastic perturbation throughout an entire earthquake cycle. Here we provide: 1) exact mathematical expressions, 2) examples with two-dimensional models, and 3) computational considerations for three-dimensional problems. This approach establishes a foundation for kinematically consistent viscoelastic block models of southern California and beyond.

First radiometric ages for the Saugus Formation using cosmogenic isochron burial dating: Implications for fault slip rates in the Western Transverse Ranges, Duane E. DeVecchio and Dylan H. Rood (Poster 252)

We successfully produced the first radiometric ages for the Quaternary Saugus Formation using cosmogenic isochron burial dating. Developing the chronology of the Saugus Formation is important to quantifying the tectonic evolution of the Western Transverse Ranges, as it is variably deformed across numerous major structures including the San Gabriel, Santa Susana, Northridge, Oak Ridge, Simi, San Cayetano, and Ventura faults. Four sites were sampled during our first season, with the focus of our initial endeavor being aimed at constraining the fault-slip rate on the Oak Ridge fault, where current estimates of the slip rate are extremely high and uncertain, ranging between 5.9 mm/yr and 12.5 mm/yr. Existing rates are based on the inferred age of the Saugus Formation, with the 2-fold range in the rate reflecting the uncertainty in the upper age of the Saugus. We produced two new ages for the lower and upper Saugus Formation. The base of the Saugus Formation exposed south of Fillmore, CA in the hangingwall anticline of the Oak Ridge fault yields a high-precision ^{26}Al - ^{10}Be isochron burial age of $1.01 \pm 0.16/-0.14$ Ma (1-sigma, $n=4$). Samples from the upper Saugus near Santa Clarita, CA give an isochron burial age of $0.35 \pm 0.71/-0.53$ Ma (1-sigma, $n=4$). Although the age on the upper Saugus near Santa Clarita is highly uncertain because of the youthfulness of the strata and temporal limitations of ^{26}Al - ^{10}Be isochron burial dating, these results are in general agreement with a previous age estimate of ~ 0.4 Ma. Moreover, samples from the modern San Gabriel River, have ^{26}Al - ^{10}Be ratios that are indistinguishable from the surface production ratio, suggesting that our burial ages are robust. Geologic mapping and structural data were combined with subsurface data to construct a cross-section across the Oak Ridge fault and hangingwall anticline, and quantify the magnitude of deformation. Preliminary estimates from this section suggest ~ 1550 m of south-side-up displacement of the top of the Saugus Formation across the Oak Ridge fault. At present, numerical ages for the upper Saugus Formation sampled on the back limb of the Oak Ridge anticline are not yet complete, and therefore slip rates estimates are not assessed.

A network approach of GPS velocity uncertainty estimation, Ksenia Dmitrieva and Paul Segall (Poster 223)

Some current estimates of GPS velocity uncertainties for continuous stations with more than a decade of data can be very low, < 0.1 mm per year. Yet, velocities with respect to rigid plates can be an order of magnitude larger, even in nominally stable plate interiors. This could be caused by underestimating low frequency, time-dependent noise, such as random walk. Traditional estimators, based on individual time series, are insensitive to low amplitude random walk, yet such noise significantly increases GPS velocity uncertainties. This is important in Southern California, where formal velocity uncertainties are often inflated to fit the data, because they are unrealistically small otherwise.

We develop a new approach to estimating noise in GPS time series, focusing on areas where the signal in the data is well characterized. We analyze data from the seismically inactive parts of central US. The data is decomposed into signal, plate rotation and Glacial Isostatic Adjustment (GIA), and various noise components. Our method processes multiple stations simultaneously with a Kalman Filter, and estimates average noise components for the network by maximum likelihood. Currently, we model white noise, flicker noise and random walk. Synthetic tests show that this approach correctly estimates the velocity uncertainty by determining a good estimate of random walk variance, even when it is too small to be correctly estimated by traditional approaches.

We present preliminary results from a network of 15 GPS stations in the central USA. The data is in a North America fixed reference frame, we subtract seasonal components and GIA displacements used in the SNARF model. Hence, all data in this reference frame is treated as noise. We estimate random walk of $0.82 \text{ mm/yr}^{0.5}$, flicker noise of $3.96 \text{ mm/yr}^{0.25}$ and white noise of 1.05 mm. From these noise parameters the estimated velocity uncertainty is 0.29 mm/yr for 10 years of daily data. This uncertainty is significantly greater than estimated by the traditional methods, at 0.12 mm/yr. The estimated uncertainty is still less than the median residual velocity in the North America fixed reference frame, which could indicate that the true uncertainties are even larger.

Additionally we estimated noise parameters and velocity uncertainties for the vertical component and for the data with common-mode signal removed. We are planning to extend this work by processing larger networks.

GeoGateway as a Tool for Analyzing UAVSAR Observations from the El Mayor – Cucapah and La Habra earthquakes, Andrea Donnellan, Jay Parker, Parker Won, Lisa Grant Ludwig, Marlon Pierce, and Jun Wang (Poster 090)

The north end of the 2010 M 7.2 El Mayor – Cucapah earthquake and the 2014 M 5.1 La Habra earthquake were both observed with UAVSAR. East-west flight lines were flown 6 and 2 months before the earthquakes respectively and within a week following the events. Both earthquakes show detectible deformation in the interferograms or repeat pass interferometry (RPI) products with a substantial amount of deformation on structures away from the main rupture. Online tools were used to analyze and model the data. The tools were developed under NASA's QuakeSim project and are being transitioned to a new interface called GeoGateway. The tools allow the user to extract line of sight profiles from the RPI products, which are displayed in a map interface. Modeling tools include forward and inverse multi-fault elastic deformation models that are used to analyze surface deformation for both Global Positioning System (GPS) and UAVSAR observations.

Towards imaging the Isabella anomaly: Basin analysis, surface wave tomography, and receiver function analysis in central California, Sara L. Dougherty, Robert W. Clayton, Charles R. Hoots, and Brandon Schmandt (Poster 205)

The tectonic origin of the Isabella high-velocity anomaly in the upper mantle of California's southern Great Valley is indistinct based on previous low-resolution seismic imaging studies of the region. The two dominant hypotheses attribute the Isabella anomaly to a fossil slab or the foundered lithospheric root of the Sierra Nevada batholith. The Central California Seismic Experiment (CCSE) is designed to distinguish between these hypotheses. We present preliminary results from the CCSE, which

MEETING ABSTRACTS

consists of 44 broadband seismometers in a quasi-linear array spanning from the Pacific coast, across the Great Valley, to the Sierra Nevada foothills, at an approximate latitude of 36°N. This array was deployed starting in December 2013 and will continue to collect data until summer 2015. Forward modeling of the 2D structure of the crust using local earthquakes recorded by the CCSE and a finite-difference algorithm is performed to provide constraints on the geometry and velocity of the seismic structure of the Great Valley. A well-constrained basin structure will be important in correcting the tomography and receiver function images. Preliminary surface wave tomography results using empirical interstation Green's functions derived from ambient seismic noise recorded by more than 500 stations that currently or previously surround the CCSE array are presented. Initial Ps receiver function images from common conversion point stacking are also presented. In addition to the CCSE array, a dense array of 116 short-period, vertical component geophones was also deployed temporarily in the Peachtree Valley, where the CCSE crosses the San Andreas Fault (SAF). This small high-resolution array will be used to determine the location and level of microseismicity along a creeping section of the SAF.

New Geophysical constraints on the Rose Canyon/Newport-Inglewood and Palos Verdes Fault Zones, Neal Driscoll, Valerie Sahakian, Jayne Bormann, Shannon Klotsko, James Holmes, Alistair Harding, Graham Kent, and Steven Wesnousky (Poster 249)

The Rose Canyon/Newport-Inglewood (RC/NI) and Palos Verdes (PV) fault zones are the eastern-most components of the Inner Continental Borderlands fault system. Collectively, between La Jolla and Newport Beach, they accommodate approximately 1-3 mm/yr of Pacific/North American plate motion offshore (as suggested by onshore trenching), and pose a hazard to the populated coastal regions. We will present high-resolution bathymetry offshore Southern California, as well as several Multi-Channel Seismic (MCS) datasets - two reprocessed datasets from 1979 and 2006, and a newly acquired dataset from August and December 2013. The data acquisition is designed to elucidate the interactions and structure of these two fault zones with the ultimate aim of better quantifying the seismic hazard they pose. Here, we will present our interpretations of these two fault zones, and how their structure varies along-strike. The age of the most recent deformation on these faults varies from La Jolla to Newport Beach, as well as the their fault architecture. The data are providing a 3-d picture of several restraining and releasing bends that may play a role in limiting the extent of future earthquake ruptures.

Beyond Elasticity: New Directions in Earthquake Modeling, Eric M. Dunham (Invited Talk Monday 14:00)

Elasticity of Earth's crust gives rise to the cyclic accumulation and release of strain in earthquakes. Together with fault friction, elasticity determines the timing, location, and size of earthquakes, and provides the fundamental means for faults to interact with one another. Indeed, most modern earthquake models, in the form of either earthquake simulators or dynamic rupture simulations, are based solely on elasticity and friction. Despite the success of such models, future advances in earthquake science will require moving beyond elasticity; this talk explores several outstanding questions of interest to the SCEC community within this theme. The first is the classic problem of fault strength and the state of stress in Earth's crust. Here I will argue for the importance of fault geometric complexity and the inelastic response of material within fault damage zones, and present a possible explanation for why the San Andreas is weaker than most other faults. We will next examine simulated earthquake sequences on faults, like the Southern San Andreas and Imperial Valley faults, passing through sedimentary basins. One or more small events, confined beneath the basin, are followed by a much larger, surface-rupturing event that breaks through the basin. Do we expect this behavior in southern California and what would it imply for seismic hazard? Finally we will consider earthquakes on faults extending offshore, like the Ventura-Pitas Point thrust system, which could generate tsunamis in addition to seismic shaking. By adding an ocean layer and properly accounting for gravitational restoring forces, we can simultaneously model earthquake rupture dynamics, seismic and ocean acoustic waves, and tsunamis.

The Mw=8.1 Pisagua Earthquake of 1 April 2014, Zacharie Duputel, Junle Jiang, Romain Jolivet, Mark Simons, Luis Rivera, Bryan Riel, Jean-Paul Ampuero, Sarah Minson, Hailiang Zhang, Nathalie Cotte, Eric J. Fielding, Juergen Klotz, Angelyn W. Moore, Edmundo O. Norabuena, Susan E. Owen, Sergey Samsonov and Anne Socquet (Poster 173)

We investigate the rupture process of the 2014 Mw=8.1 Pisagua earthquake using ALTAR: an innovative Bayesian algorithm that is now implemented to run on GPU and allows sampling of posterior PDFs for high-dimensional problems. Our observations include InSAR, GPS and Tsunami data. We include a full data covariance matrix to account for measurement and prediction uncertainties. This covariance model provides a physical rationale for the relative weighting between available datasets and provides more realistic estimates of uncertainty on the inferred parameters. Our results indicate a relatively compact slip zone located down dip of the hypocenter. The absence of shallow rupture is mainly controlled by tsunami observations. In the same way, the 1995 Antofagasta and the 2001 Arequipa earthquakes did not involve any slip near the trench. Using land-based geodetic data, it is fundamentally difficult to know if shallow portions of the north Chilean subduction zone are seismogenic or not. Therefore the occurrence of a major event rupturing the southern portion of the seismic gap and driving slip at shallow depth is plausible. However, the possibility of multiple smaller events that would progressively release the accumulated strain cannot be ruled out.

Dynamic earthquake rupture simulations on nonplanar faults embedded in 3D geometrically complex, heterogeneous Earth models, Kenneth Duru, Eric M. Dunham, and Sam A. Bydlon (Poster 133)

Dynamic propagation of shear ruptures on a frictional interface is a useful idealization of a natural earthquake.

The conditions relating slip rate and fault shear strength are often expressed as nonlinear friction laws.

The corresponding initial boundary value problems are both numerically and computationally challenging.

In addition, seismic waves generated by earthquake ruptures must be propagated, far away from fault zones, to seismic stations and remote areas.

Therefore, reliable and efficient numerical simulations require both provably stable and high order accurate numerical methods.

We present a numerical method for:

- a) enforcing nonlinear friction laws, in a consistent and provably stable manner, suitable for efficient explicit time integration;
- b) dynamic propagation of earthquake ruptures along rough faults;
- c) accurate propagation of seismic waves in heterogeneous media with free surface topography.

We solve the first order form of the 3D elastic wave equation on a boundary-conforming curvilinear mesh, in terms of particle velocities and stresses that are collocated in space and time, using summation-by-parts finite differences in space.

The finite difference stencils are 6th order accurate in the interior and 3rd order accurate close to the boundaries. Boundary and interface conditions are imposed weakly using penalties. By deriving semi-discrete energy estimates analogous to the continuous energy estimates we prove numerical stability. Time stepping is performed with a 4th order accurate explicit low storage Runge-Kutta scheme.

We have performed extensive numerical experiments using a slip-weakening friction law on nonplanar faults, including recent SCEC benchmark problems. We also show simulations on fractal faults revealing the complexity of rupture dynamics on rough faults. We are presently extending our method to rate-and-state friction laws and off-fault plasticity.

*The studies have been done in collaboration with Frank Vernon, Amir Allam, Dimitri Zigone, Zach Ross, Hongrui Qiu, Pieter-Ewald Share, Yaman Ozakin, Xin Liu, Gregor Hillers, Ittai Kurzon, Michel Campillo, Philippe Roux, Lupei Zhu, Dan Hollis, Mitchell Barklage and others.

A Multiscale Model for Shear flow of Granular Materials with Breakable Particles: Role of Force Chain Instabilities and Implications for Strain Localization, grain size evolution and energy partitioning, *Ahmed E. Elbanna, Charles Lieou, Rui Li, and Jean Carlson* (Poster 117)

Deformation and failure of fault gouge play an important role in earthquake mechanics. One of the fundamental mechanisms controlling shear strength of fault zones is gouge particles comminution. Here, we describe our recent work on developing a constitutive model for sheared granular materials with breakable particles that integrates principles of non-equilibrium statistical thermodynamics and force chain instabilities. Our primary theoretical tool is the Shear Transformation Zone theory (STZ) which is capable modeling irreversible plastic deformations in the gouge due to local rearrangements of the particles. To model grain breakage, an energy balance approach is used which augments the STZ theory with an equation for the grain size reduction as a function of the applied work rate and pressure.

Previous numerical and experimental work on grain breakage was inconclusive regarding whether grain breakage was a softening or a hardening mechanism. The outcome depends on the competition between evolving grain angularity and reduced particle size with both processes affecting force chain dynamics. To account for local force chain instabilities, we develop a small scale model for force chain buckling that is integrated within the STZ formulation through variations of the minimum flow stress of the system. We idealize a typical force chain as an array of particles with both translational and rotational degrees of freedom. The relative motion between the particles is resisted by sliding and rolling friction. The sliding friction is provided by a rigid-plastic element. The rolling resistance is modeled by a torsional spring. The deflection of the force chain is resisted by an array of lateral springs representing the effective confinement provided by the rest of the granular medium.

Our results suggest that there exist a critical grain size below which the buckling stress for the force chain, and hence the flow stress, decreases linearly with the decrease of the particle size. Furthermore, we show that grain breakage is a potential weakening mechanism at high pressures and at strain rates high enough to reduce the grain size below the aforementioned critical limit. Grain breakage also promotes strain localization, particularly in compact layers, and may explain the long term persistence of shear bands in natural faults due to the permanent change in the layer fabric resulting from comminution. We discuss the implications of these findings on the fault zone evolution and earthquake energy budget.

The Bimaterial Effect on the Earthquake Cycle, *Brittany A. Erickson and Steven M. Day* (Poster 151)

Both laboratory studies and dynamic rupture simulations on a bimaterial fault interface show that the material contrast can cause the rupture to take a "preferred" direction, where the rupture propagates in the direction of particle motion of the side with slower shear wave velocity. In addition, dynamic ruptures on bimaterial faults have lead to such phenomena as asymmetric rupture features, a preferred aftershock triggering, and asymmetric off-fault damage. However, many of these conclusions drawn from dynamic rupture simulations depend on the artificial initial conditions necessary to nucleate rupture. We have developed a computational method for studying how the bimaterial effect plays out over multiple earthquake cycles that develop spontaneously. The method is developed for the classical plane-strain equations capable of incorporating non-planar fault geometries and material heterogeneities. As a first step we consider the bimaterial problem on planar, vertical strike slip fault governed by rate-and-state friction. The system is loaded at the remote boundaries at the slow, tectonic plate rate. During the long interseismic period we solve the equations for static-equilibrium. Quasi-dynamic events nucleate spontaneously on the fault. We find that the preferred nucleation site migrates in the preferred direction. Ruptures propagate with asymmetric properties, the strength of which increases with greater material mismatch. We are currently studying the long term behavior of the earthquake cycle and under what conditions rupture in the non-preferred direction (periodically observed on natural faults) is possible.

Regional Seismic Loss Assessment Applied Methodology – with a Case Study in Los Angeles County, *Omid Esmaili* (Poster 014)

This study is devoted to the formulation and construction of an integrated regional earthquake loss assessment method for buildings in seismic regions. Regional Seismic Loss Assessment (RSLA) of buildings is an important issue of concern to practicing engineers working in city planning, risk management, and the insurance industry. In contrast to previous research in this field, the RSLA framework presented herein is hazard-based and utilizes a regional rapid seismic hazard deaggregation tool by which RSLA can be done faster with less computational effort. This paper presents and discusses a general approach to RSLA framework, through using it over four-story reinforced concrete moment-resisting frame (RC-SMRF) buildings in Los Angeles County, a region with high seismic hazard, at 475-yrs ground motion return period.

Quantizing the Complexity of the Western United States Fault System with Geodetically and Geologically Constrained Block Models, *Eileen L. Evans and Brendan J. Meade* (Poster 229)

Geodetic observations of interseismic deformation provide constraints on microplate rotations, earthquake cycle processes, slip partitioning, and the geometric complexity of the Pacific-North America plate boundary. Paleoseismological observations in the western United States provide a complimentary dataset of Quaternary fault slip rate estimates. These measurements may be integrated and interpreted using block models, in which the upper crust is divided into microplates bounded by mapped faults, with slip rates defined by the differential relative motions of adjacent microplates, integrating the motion of tectonic plates with a first-order approximation earthquake cycle processes. The number and geometry of microplates are typically defined with boundaries representing a limited sub-set of the large number of potentially seismogenic faults. An alternative approach is to include large number of potentially active faults in a dense array of microplates, and then deterministically estimate the boundaries at which strain is localized, while simultaneously satisfying interseismic geodetic and geologic observations. This approach is possible through the application of total variation regularization (TVR), which simultaneously minimizes the L_2 norm of data residuals and L_1 norm of the variation in the estimated state vector. Applied to three-dimensional spherical block models, TVR reduces the total variation between estimated rotation vectors, creating groups of microplates that rotate together as larger blocks, and localizing fault slip on the boundaries of these larger blocks. Here we consider a suite of block models containing 3-137 microplates, where active block boundaries have been determined by TVR optimization constrained by both interseismic GPS velocities and geologic slip rate estimates.

Quantifying the temperature and age of seismic slip: Transition metal geothermometry and oxide (U-Th)/He chronology of exhumed fault surfaces, *James P. Evans and Alexis Ault* (Poster 123)

Establishing the peak temperatures resulting from seismic slip on faults is important for deciphering the physics of slip, and determining the absolute age of slip is critical for examining fault evolution. We (Evans et al., 2014) examine mm-thick, high gloss exhumed slip surfaces from the Wasatch fault, Utah, where Fe-coated slip surfaces exhibit Fe alteration that we hypothesize is a function of temperature. Slip surfaces are extremely thin, display multiple, variably oriented slip striae, are comprised of comminuted, crystalline hematite, exhibit local variations in magnetism, and display round to elliptical zones of iridescence. Iron in the hematite-coated surfaces (Fe³⁺) is locally reduced to Fe²⁺ in the iridescent zones that we interpret to be sites of rapid slip at geometric asperities. Temperature-induced reduction in other first row transition elements (V, Cr, Mn, and Co) may occur on other oxide coated fault surfaces and may be a paleothermometer that we can use to estimate temperatures at slip.

We use hematite (U-Th)/He dating of aliquots extracted from the slip surface to constrain slip events. Pliocene hematite (U-Th)/He dates overlap published and new apatite (U-Th)/He and apatite fission-track data from several locations in the host rock. Texturally identical comminuted hematite from five samples separated by ~5-10 cm on a single fault surface yield internally consistent but significantly different hematite He dates from sample to sample. This is inconsistent with an interpretation of the dates as conventional thermochronologic ambient

MEETING ABSTRACTS

cooling ages. We suggest these hematite (U-Th)/He dates reflect extremely rapid cooling from heating during multiple, localized events on a single fault surface. The highly reflective faults studied to date slipped at $T \geq 300^\circ \text{C}$, at depths of 2-4 km, and developed on small faults 10 cm² to 10 m² in area, reflecting seismicity of $-3 \leq M \leq 0$ in a region that would have experienced aftershocks related to slip on the main fault. We use white-light interferometry and laser-scanning metrology to define the surface roughness associated with zones of heating.

We aim to test these methods in a range of faults in southern California. Together these new methods may yield insight into the thermal history of fault slip. Preliminary work suggests that highly localized seismic slip that produces high temperatures, may occur on extremely small faults, thus supporting the concept of picoseismicity with micron-scale.

Exploring fault geometry uncertainties in finite-slip inversion with multiple moment tensor inversion, Wenyuan Fan, Peter M. Shearer, Guy Masters, and Chen Ji (Poster 165)

Finite-fault source inversions are often performed with an assumed fault geometry. Green's functions calculated using a fixed strike, dip and rake can introduce hard-to-quantify errors in the inversions if the true fault geometry deviates from the model assumptions. For mega-earthquakes with large rupture areas, it is important to consider fault curvature and other non-planar fault effects. To accommodate uncertainties in the fault geometry, we propose to parameterize the fault as multiple moment-tensor sources within a 3D grid of possible source locations. The grid is defined with respect to an assumed initial fault plane, spanning the likely 2D rupture extent and a small range in the direction to normal to the fault to accommodate errors in assumed fault location or orientation. Instead of determining the slip-rate history, a moment-rate function is solved. There are six unknowns per point at a given frequency and the best-fitting double-couple (i.e., strike and dip) can be extracted from the results. If we assume the earthquake occurs within a few fault planes, the unknowns to be solved should be spatially sparse. Recently emerging tools such as compressive sensing (CS) can be used to deal with the problem. For a case study, we will analyze the 2013 Okhotsk Mw 8.3 earthquake and hope to understand the uncertainty limits caused by fault geometry in the finite fault modeling.

Mechanical insights into tectonic reorganization of the southern San Andreas fault system since ca. 1.5 Ma, Laura A. Fattaruso, Michele L. Cooke, Rebecca J. Dorsey, and Bernard A. Housen (Poster 105)

Between ~1.5 -1.1 Ma, the southern San Andreas fault system underwent a major reorganization that included initiation of the San Jacinto fault and termination of slip on the extensional West Salton detachment fault during a local change from transtension to transpression, with no known change in relative plate motion. The southern San Andreas fault itself has also evolved since this time, with several changes to the active trace of the fault within San Geronio Pass. While the geologic record reveals these changes, mechanisms that controlled abandonment of active faults, initiation of new strands, and shifting loci of uplift are incompletely understood. We use three-dimensional mechanical Boundary Element Method models to investigate these changes to the fault network.

A series of snapshot models of the succession of active fault geometries explore the role of fault interaction and tectonic loading in abandonment of the West Salton detachment fault, initiation of the San Jacinto fault, and changes to the trace of San Andreas fault. We assess the viability of our models by comparison with uplift patterns inferred from the stratigraphic record. Interpreted changes to uplift patterns are well matched by models, and affirm ideas about the role of the San Jacinto fault in changing uplift rates. Results for vertical axis rotation are compared to data from paleomagnetism studies. We explore mechanical efficiency at each step in the evolution using calculations of tectonic work. Strain energy density patterns are used to identify regions of incipient faulting, supporting north-to-south propagation of the San Jacinto fault.

Creation of a standardized protocol for checking the applied seismic code or standard, by using the detected damages to buildings after an earthquake, Jose Ferrandiz (Poster 050)

After every earthquake all the codes and standards are analyzed and modified. This poster will introduce a new protocol that will relate the

detected damages to buildings after an earthquake with the code used to design them.

The new protocol will use a multi-option analysis that will include, General design Building Concepts, Damage type, Foundations, Soil problems, Structural type used, Non-structural elements, Joints and Design concepts that modifies the damping and Stiffness of the building.

With this tool we will be able to understand why the damage had happened and the factors which triggered.

This would give us the opportunity to focus our efforts on the analysis of the problem and its implementation in the standard.

UCERF3-ETAS: Including Spatiotemporal Clustering for a California Operational Earthquake Forecast, Edward H. Field and WGCEP 2014 (Poster 011)

The Working Group on California Earthquake Probabilities (WGCEP) has been developing the third Uniform California Earthquake Rupture Forecast (UCERF3). With the time-independent model published, which relaxes segmentation and includes multi-fault ruptures, and the long-term time-dependent model in review, which incorporates elastic rebound, we have now turned our attention to including spatiotemporal clustering. In recognition that triggered events can be large and damaging, the ultimate goal is to deploy an Operational Earthquake Forecast (OEF) for California, now listed as one of the USGS's strategic-action priorities (<http://pubs.usgs.gov/of/2012/1088>; page 32). Our poster will demonstrate progress thus far, where we have added an Epidemic Type Aftershock Sequence (ETAS) component to UCERF3 (UCERF3-ETAS or "U3ETAS" for short). Our model represents a merging of ETAS with finite-fault based forecasts, and the inclusion of elastic rebound, both firsts as far as we are aware. In fact, inclusion of elastic-rebound is critical in terms of getting spatiotemporal clustering statistics correct, otherwise ~85% of large triggered events simply re-rupture the same fault, which we don't see in nature. Our poster will also outline additional steps needed for taking U3ETAS operational.

Large Earthquakes and Three Dimensional Strain on Interlocking Networks of Small Faults, John M. Fletcher, Michael E. Oskin, Orlando J. Teran, and Egill Hauksson (Poster 130)

Tectonic plate boundary shear zones commonly initiate along preexisting weaknesses oriented oblique to the direction of relative motion. Slip on multiple fault sets with diverse orientations and slip directions is required to accommodate the three dimensional strain of such plate margins. However, little is known about how this is accomplished by faults that rupture in individual earthquakes and specifically whether permutations in stress state are required to drive slip on multiple fault sets. The 2010 Mw 7.2 El Mayor-Cucapah (EMC) earthquake ruptured a complex network of high- and low-angle faults that record systematic changes in kinematics with fault orientation. Here we show that stress inversions of coseismic surface rupture and aftershock focal mechanisms define two coaxial, but permuted stress states. The maximum and intermediate principal stresses are close in magnitude, but switch orientations due to topography- and density-controlled gradients in lithostatic load. Both states of nearly uniaxial stress permitted diverse fault orientations to slip at once, accomplishing three-dimensional strain in a single earthquake sequence. If the normal fault on which rupture initiated was critically stressed, all other activated faults had sections that were supercritically stressed with apparent friction well exceeding experimentally determined limits. This demonstrates the interlocking nature of the complex fault network and explains the spontaneous rupture of multiple faults after failure of the keystone normal fault. We conclude that oblique plate boundary shear zones contain high-stress regions associated with knotted interlocking fault networks that have longer recurrence intervals and generate earthquakes significantly larger than expected from any one constituent fault. High stress and dynamic weakening expands the range of faults prone to slip including the low-angle normal faults of the EMC rupture.

Temporal Variation of A Large Slow Slip Event at the Southcentral Alaska Subduction Zone Between 2009-2013, Yuning Fu, Zhen Liu, Jeffrey Freymueller, Susan Owen, and Donald Argus (Poster 244)

We identify and study a Slow Slip Event (SSE) in the southcentral Alaska subduction zone during 2009-2013 using continuous GPS measurements.

This is the second large SSE in this region since modern geodetic measurements became available in 1993. This SSE occurs downdip of the main asperity that ruptured in the 1964 Alaska earthquake, on the same part of the subduction interface as the earlier 1998–2001 SSE. The average slip rate of this SSE is ~4–5 cm/yr, with a cumulative moment magnitude of Mw 7.5. As an initial study [Fu and Freymueller, 2013], we divide this SSE into two phases according to their transient displacement time evolution; their slip distributions are similar to each other but slip rates are slightly different. The time and space dependence of the GPS displacements suggest that the slip area remained nearly the same during Phase I, while the slip rate increased with time. The SSEs occur on a transitional section of the subduction plate interface between the fully locked updip part and the freely slipping deeper part. During the 1964 earthquake, slip on the region of the SSE was much lower than slip in the updip region. Based on this observation and the repeated SSEs, we conclude that this part of the interface slips repeatedly in SSEs throughout the interseismic period and does not build up a large slip deficit to be released through large slip in earthquakes. We also adopt TDEFNODE to conduct time-dependent inversion to investigate the whole picture of this event. Our results indicate the slip area did not change substantially, and the slip rate was increasing with time.

Geometry of the San Andreas Fault and Sedimentary Basin in the Northern Salton Trough, Gary S. Fuis, Klaus Bauer, Rufus D. Catchings, Mark Goldman, Trond Ryberg, Daniel S. Scheirer, Victoria E. Langenheim, Michael J. Rymer, Patricia Persaud, Joann M. Stock, and John A. Hole (Poster 092)

The Salton Seismic Imaging Project (SSIP) was undertaken, in part, to provide more accurate information on the plate-boundary faults and basin geometry in the Salton Trough region. One of these faults, the southernmost San Andreas Fault (SAF) zone in the northern Salton Trough (Coachella Valley), is considered by many to be likely to produce a large-magnitude earthquake in the near future. We report here on the geometry of the SAF and the adjacent sedimentary basin beneath the Coachella Valley.

We interpret two seismic profiles in the northern Salton Trough that are orthogonal to the axis of the Coachella Valley. Seismic imaging, potential-field studies, and (or) earthquake hypocentral relocations along these profiles indicate that the active strand of the SAF dips NE. On a southern profile, through the Mecca Hills, we obtain a reflection image of the SAF zone in the depth range of 6–12 km that coincides with the microearthquake pattern reported by Hauksson et al. (2012), dipping ~ 60° NE. Steeply dipping reflectors above 6 km emerge at the surface at mapped secondary fault traces in the Mecca Hills, clearly defining a “flower structure” for the upper SAF. On the second profile, from Palm Springs to Landers, two alternative interpretations of SAF structure are possible. By one interpretation, which is based on earthquakes alone, the Banning and Garnet Hill Faults are two closely spaced faults, dipping ~ 60° NNE that pass through two aftershock clusters of the 1986 M 5.9 North Palm Springs earthquake. By the second interpretation, which is based on our reflection imaging on this line, the Banning and Garnet Hill faults converge at 10-km depth; below that depth, a single SAF dips ~ 60° NNE. In the second interpretation, the faults above 10 km resemble the flower structure interpreted beneath the Mecca Hills on our southern profile. The deeper fault in the second interpretation is subparallel to the closely spaced faults of the first interpretation but a few km deeper.

Sedimentary basin depth ($V_p < 5.5$ km/s, estimated) ranges from 3–4 km in the northern Coachella Valley to a maximum of 5 km in the southern Coachella Valley. Because of the generally flat magnetic field, basement beneath the Coachella Valley southwest of the SAF is interpreted to be similar to that in the Peninsular Ranges.

In-Situ Observations of Earthquake-Driven Fluid Pulses within the Japan Trench Plate Boundary Fault Zone, Patrick M. Fulton and Emily E. Brodsky (Poster 114)

Fault valving and transient fluid flow has long been suspected to be an important process in the earthquake cycle, but has not previously been captured by direct measurements during an episode. In particular, earthquakes are thought to drive fluids in fault zones, but again, evidence has been limited to the geologic record. Here we report on the signature

of fluid pumping events inside the Tohoku Fault associated with individual earthquakes. As part of the Japan Trench Fast Drilling Project (JFAST), a sub-seafloor temperature observatory was installed across the plate boundary fault zone that ruptured during the 2011 Mw 9.0 Tohoku-oki earthquake. The observatory consisted of 55 autonomous temperature sensing dataloggers extending up to 820 m below sea floor at a water depth of ~7 km. The temporary deployment recorded data from July 2012 through April 2013. In addition to measuring the frictional heat signal from the megathrust earthquake, the high-resolution temperature time series data reveal spatially coherent temperature transients following regional earthquakes. Temperature increases vertically upwards from a fracture zone and decreases downwards, which is consistent with the expected signature of a pulse entering the annulus from the fracture zone. The anomalies are a few hundredths of degree Celsius and occur repeatedly at depths that are independently interpreted to have higher fracture permeability. High-pass filtered data are spatially correlated in areas disturbed by transient fluid advection. Fluid pulses occur in response to over a dozen local earthquakes, including a Mw 5.4 on 14 October 2012, a Mw 5.5 on 11 November 2012, and a doublet of two very local Mw 7.2 intraplate earthquakes on 7 December 2012, along with its associated aftershocks. There does not appear to be a response to large far-field earthquakes such as the 28 October 2012 Mw 7.8 Haida Gwaii or 6 February 2013 Mw 8.0 Santa Cruz Islands earthquakes.

These measurements provide the first in situ documentation of seismic pumping at fractured regions of the fault damage zone. Near fault measurements such as these may provide insight into drivers of earthquake occurrence. The redistribution of fluid pressures within fault zones, such as observed here in response to earthquakes, is a potential mechanism that may be involved in earthquake triggering.

An objective mechanical modelling approach for estimating the distribution of fault creep and locking from geodetic data, Gareth J. Funning and Roland Bürgmann (Poster 238)

We present a Markov Chain Monte Carlo method that can be used to find the extents of creeping fault areas, an important input to seismic hazard models, from mechanical boundary element modelling of geodetic data. In our scheme, the surface of a partially-creeping fault is represented as a mesh of triangular elements, each of which is modelled as either locked or creeping (freely-slipping) using the boundary element code poly3d. Slip on the creeping elements of our fault mesh, and therefore elastic deformation of the surface, is driven by stresses imparted by semi-infinite faults beneath the base of the mesh (and any other surface faults) that slip at the geodetic slip rate of the faults. Starting from a random distribution of locked and unlocked patches, a modified Metropolis algorithm is used to propose changes to the locking state (i.e. from locked to creeping, or vice-versa) of randomly selected elements, retaining or discarding these based on a geodetic data misfit criterion; the succession of accepted models forms a Markov chain of model states. After a “burn-in” period of a few hundred samples, these Markov chains sample a region of parameter space close to the minimum misfit configuration. By running multiple Markov chains, we can realise multiple such well-fitting models, and look for robustly resolved features (i.e. features common to a majority of the models, and/or present in the mean of those models).

We apply this method to a combination of persistent scatterer InSAR and GPS data covering the Hayward fault in northern California. Preliminary results show strong agreement between all models on the presence of regions of creep across the full down-dip extent of the fault at its northwest and southeast ends. The central portion of the fault, thought to be the source of the M~7 1868 Hayward earthquake, shows less consistent patterns. Most elements in this area are locked in around half of the models, with only a few locked in all models, indicating that the fault is likely partially locked here, and that multiple possible configurations of locked and creeping elements can fit the data approximately equally well. Additional observations, e.g. from surface creep measurements or characteristic repeating earthquakes, will be used to further refine these results in future.

MEETING ABSTRACTS

Simulating high-frequency earthquake dynamic rupture scenarios on natural fault zones with SeisSol, Alice-Agnes Gabriel, Christian Pelties, Alexander Heinecke, Alexander Breuer, Sebastian Rettenberger, and Michael Bader (Poster 177)

In this presentation we highlight the benefits of using modern numerical methods for physics-based ground motion modelling and expanding the current state of knowledge of earthquake physics. To this end, SeisSol, an arbitrary high-order derivative Discontinuous Galerkin (ADER-DG) scheme, is utilized to solve the spontaneous earthquake rupture problem with high-order accuracy in space and time on three-dimensional unstructured tetrahedral meshes. SeisSol has been verified using numerous advanced SCEC test cases, including branching and dipping fault systems, heterogeneous background stresses, bi-material faults and rate-and-state friction constitutive formulations.

SeisSol obtains peta-flop performance on heterogeneous supercomputers through optimization of parallel I/O, hardware-aware kernels, an offload scheme to address multi-physics calculations and hybrid MPI+OpenMP parallelization and is nominated as Gordon Bell Prize Finalist Application 2014.

Here we study three-dimensional dynamic rupture processes and emanated high-frequency wave fields on complex fault systems. The discrete representation of these fault systems have been constrained using a range geological and geophysical data including; high-resolution topography, 3D velocity models and fault geometries. Specifically I will present large scale earthquake dynamic rupture scenarios based on the 1992 Landers strike-slip event and the 1994 Northridge blind thrust event in Southern California in which we observed high-detail dynamic rupture evolution and ground motion frequencies up to 10 Hz.

Our results imply that natural rupture dynamics depends heavily on the local background stress state concurrently with fault geometry, as the simultaneous failure of several discrete large Landers fault segments and the pulse-like rupture behavior favored by the curved Northridge fault geometry. We observe in the Landers scenario rupture transfers between principal faults in terms of jumps and branching as well as back slip in the vicinity of fault branches. High-frequency signals are caused by rupture complexity and the non-linear interaction of earthquake dynamics and seismic wave propagation with the fault system, free surface and regional topography, without stochastic model ingredients. Despite the complexity, the kinematics in terms of rupture speed, magnitude, and slip distribution are reasonably well reproduced.

Frequency-dependent directivity effects from small earthquakes in Abruzzo region, Italy, Frantisek Gallovic, Francesca Pacor, Rodolfo Puglia, Lucia Luzi, and Maria D'Amico (Poster 073)

Significant directivity-induced amplification effects on earthquake ground motions, related to the rupture propagation along a fault, have been well recognized at low frequencies ($f < 1$ Hz) and for large magnitude events. On the contrary, directivity effects at high frequencies and for small-to-moderate-magnitude earthquakes have not been widely inferred from recorded data yet. Although it is of utmost importance to correctly take into account the directivity in seismic hazard assessment and earthquake engineering applications, there is a long standing controversy on its frequency and azimuthal dependence, both from theoretical and observational viewpoints. Observations of strongly directive large earthquakes are sparse and, moreover, often characterized by a poor azimuthal coverage, thus hiding its azimuthal dependence. To overcome the lack of data, analysis of more abundant small events, densely recorded, can be an appealing alternative. However, contribution of the source rupture propagation is masked by wave propagation phenomena due to complex path and site effects.

In this paper we present clear observations of directivity effects for small events (magnitudes 3-5) using ~ 250 aftershocks of the Mw6.3 2009 L'Aquila earthquake (central Italy). The source spectrum properties of these events are recovered by means of removing path and site effects using standard Generalized Inversion Technique, GIT (Andrews, 1986; Castro et al., 1990, Shearer et al., 2006; Prieto et al., 2004). At selected frequencies we evaluate residuals defined as differences between the mean and the apparent source spectra (i.e. the source spectra as seen by the individual stations). We then investigate azimuthal and frequency

dependence of these residuals. Considering only 10 strongly directive events with very good azimuthal coverage, we observe a remarkable decrease of the directivity amplification at high frequencies (in particular at frequencies greater than ~5 times the corner frequency of the respective event). We demonstrate that the decay of the directivity with increasing frequency is controlled by the earthquake source, since it is observed at sites located both close and far from the epicenters.

Recent experiences in OEF in New Zealand, Matthew C. Gerstenberger, David Rhoades, Graeme McVerry, Annemarie Christophersen, Stephen Bannister, Bill Fry, and Sally Potter (Poster 020)

In the last few years GNS Science has gained significant experience in various aspects of OEF and in aftershock hazard and forecasting. First was the Canterbury sequence of events which began in 2010 and included the destructive Christchurch earthquake of February, 2011. In response to this, we developed a time-dependent model that combined short-term (STEP & ETAS) and longer-term (EEPAS) clustering model components with time-independent model components. We used this model to produce a forecast of the expected ground-motion for the next 50 years which has been used to revise building design standards for the region and has contributed to planning the rebuilding of Christchurch. An important contribution to this model comes from medium-term clustering. EEPAS is based on three empirical regressions that relate the magnitudes, occurrence times, and locations of major earthquakes to regional precursory scale increases in the magnitude and rate of occurrence of minor earthquakes. Also important is the rate to which seismicity is expected to return in 50-years. With little historical seismicity in the region, the model learning period and whether-or-not a declustered catalog is used becomes critical in estimating the long-term rate. This model uncertainty was allowed for by using forecasts from both declustered and non-declustered catalogs. With two recent moderate sequences in the Wellington region, we have continued to refine our forecasting techniques. An important addition has been scenarios based on the aftershock forecasts. These provide examples of how the sequence might eventuate, including the understanding of nearby faults and the Hikurangi megathrust. They have been developed with input from social scientists and have been provided to the public and government officials; they have proven useful in aiding the interpretation of the aftershock probabilities.

Revisiting tremor under the San Andreas Fault: an enhanced look through a mini seismic array near Parkfield, Abhijit Ghosh (Poster 191)

I designed and installed a mini seismic array to image the San Andreas Fault (SAF) near Parkfield. The array is continuously scanning the fault about 100 km alongstrike that includes the patch that breaks quasi-periodically to produce damaging M6 earthquakes, and its southeastern and northwestern boundaries that witness tremor activity at depth. I collected more than a year worth of continuous seismic data so far, and the array is still fully operational. I apply a beam backprojection technique [Ghosh et al., 2012] to the array data to detect and locate seismicity, including tremor under the SAF. In spite of having a high-quality, dense seismic network in this area, the array alone is able to detect about 5 times more duration of tremor activity compared to the existing network [Nadeau and Guilhem, 2009]. More interestingly, it detects comparable amount of tremor activity near both sides of the Parkfield patch. This is in contrast to the tremor observations using the existing seismic network, which indicates the southeastern boundary near Cholame being by far the most tremor-active area. In addition, I observe rapidly propagating tremor streaks that appear to be a prevalent feature of tremor activity near Cholame. The solo mini seismic array is providing an enhanced look at the tremor activity under the SAF.

Possible bias in ground motion and rupture simulations arising from forced nucleation locations that are inconsistent with heterogeneous stress conditions, Jacquelyn J. Gilchrist, James H. Dieterich, David D. Oglesby, and Keith B. Richards-Dinger (Poster 136)

Initial conditions used for dynamic models, particularly the pattern of initial stresses, play a primary role in controlling rupture characteristics and resulting ground motions. We find that the location of forced rupture nucleation in models with heterogeneous initial stresses can strongly affect rupture propagation and ground motions. We use the earthquake

simulator RSQSim, which is a 3D boundary element code that incorporates rate-state fault friction, to simulate long sequences of earthquakes (typically >100,000 events). We generate suites of heterogeneous initial conditions for large rupture events. In these simulations, earthquakes nucleate spontaneously — hence, each observed rupture has a set of initial stress conditions and an associated observed nucleation location that is not set a priori or forced. One important aspect of the simulations, and presumably natural fault systems, is that repeated small events (prior to a large, through-going event) test the ability of a rupture to propagate through the system at different locations, and through this process the system finds a near optimal nucleation location that enables ruptures to propagate at minimal stress conditions. Forcing nucleation at non-optimal locations for a given stress condition requires system-wide increases in shear stress to produce through-going ruptures. Compared to ruptures with heterogeneous initial stresses and arbitrary forced nucleation locations, the spontaneous RSQSim events are able to propagate at lower average initial stresses and thus have lower stress drops and lower rupture propagation speeds. Forced nucleation at other locations requires an additional 1.4 MPa of shear stress, on average, to produce a through-going rupture, but some nucleation locations require up to 3.7 MPa of additional stress. Such assumptions lead to stress drops that are, on average, 5.6 MPa, which is over 50% higher than the 3.1 MPa stress drop of the original, spontaneous event. Because the stress drops of events with forced nucleation are roughly 50% higher than the events with nucleation locations tied to the stress conditions, we expect comparable differences in the ground motions. Dynamic rupture simulations, using the finite element code FaultMod, are in progress to test this hypothesis.

UCVM: Open Source Software for Understanding and Delivering 3D Velocity Models, *David Gill, Patrick Small, Philip Maechling, Thomas H. Jordan, John Shaw, Andreas Plesch, Po Chen, En-Jui Lee, Ricardo Tabora, Kim Olsen, and Scott Callaghan* (Poster 079)

Physics-based ground motion simulations can calculate the propagation of earthquake waves through 3D velocity models of the Earth. The Southern California Earthquake Center (SCEC) has developed the Unified Community Velocity Model (UCVM) framework to help researchers build structured or unstructured velocity meshes from 3D velocity models for use in wave propagation simulations.

The UCVM software framework makes it easy to extract P and S wave propagation speeds and other material properties from 3D velocity models by providing a common interface through which researchers can query earth models for a given location and depth. Currently, the platform supports multiple California models, including SCEC CVM-S4 and CVM-H 11.9.1, and has been designed to support models from any region on earth. UCVM is currently being used to generate velocity meshes for many SCEC wave propagation codes, including AWP-ODC-SGT and Hercules.

In this presentation, we describe improvements to the UCVM software. The current version, UCVM 14.3.0, released in March of 2014, supports the newest Southern California velocity model, CVM-S4.26, which was derived from 26 full-3D tomographic iterations using CVM-S4 as the starting model (Lee et al., this meeting), and the Broadband 1D velocity model used in the CyberShake 14.2 study. We have ported UCVM to multiple Linux distributions and OS X.

Also included in this release is the ability to add small-scale stochastic heterogeneities to extract Cartesian meshes for use in high-frequency ground motion simulations. This tool was built using the C language open-source FFT library, FFTW. The stochastic parameters (Hurst exponent, correlation length, and the horizontal/vertical aspect ratio) can be customized by the user.

UCVM v14.3.0 also provides visualization scripts for constructing cross-sections, horizontal slices, basin depths, and Vs30 maps. The interface allows researchers to visually review velocity models. Also, UCVM v14.3.0 can extract isosurfaces of shear-wave velocities equal to 1 km/s (Z1.0) and 2.5 km/s (Z2.5) for any of the registered velocity models. We have also improved our open source distribution by including a user's guide, an advanced user's guide, and a developer's guide so that users of all levels can get started using and extending the UCVM platform.

E-DECIDER Disaster Response and Decision Support Platform, *Margaret T. Glasscoe, Jay W. Parker, Marlon E. Pierce, Jun Wang, Ronald T. Eguchi, Charles K. Huyck, ZhengHui Hu, ZhiQiang Chen, Mark R. Yoder, John B. Rundle, and Anne Rosinski* (Poster 217)

Getting the right information to the right people at the right time is critical during a natural disaster. E-DECIDER (Emergency Data Enhanced Cyber-Infrastructure for Disaster Evaluation and Response) is a NASA decision support system providing rapid delivery of advanced situational awareness data products that are relevant to the emergency preparedness and response communities and serves as a gateway to enable the delivery of NASA decision support products to these communities.

The E-DECIDER decision support system produces remote sensing and hazard data, model-based map products, information from simulations, loss estimation, damage detection, and crowdsourcing that are integrated into a single geospatial view. This is delivered through a service-oriented architecture for improved decision-making and then directly to mobile devices of responders. By adopting a Service Oriented Architecture based on Open Geospatial Consortium standards, the system provides an extensible, comprehensive framework for geospatial data processing and distribution on Cloud platforms and other distributed environments.

The E-DECIDER tools, services, and products have been used to support end-user exercises in partnership with the California Earthquake Clearinghouse since 2012. E-DECIDER's underlying service architecture allows the system to facilitate delivery of NASA decision support products to the Clearinghouse through XchangeCore Web Service Data Orchestration that allows trusted information exchange among partner agencies. This in turn allows Clearinghouse partners to visualize data products produced by E-DECIDER and other NASA projects through incident command software such as SpotOnResponse or ArcGIS Online.

While the Clearinghouse and its partners are not first responders, they do support the emergency response community by providing information about the damaging effects of earthquakes. It is critical for decision makers to maintain a situational awareness that is knowledgeable of potential and current conditions, possible impacts on populations and infrastructure, and other key information. E-DECIDER and the Clearinghouse have worked together to address many of these issues and challenges to deliver interoperable, authoritative decision support products.

Waste water injection induced seismicity in naturally-active, seismogenic regions in central California, *Thomas H. Goebel, Egill Hauksson, Jean-Paul Ampuero, Fred Aminzadeh, Frederic Cappa, and Jason B. Saleeby* (Invited Talk Tuesday10:30)

The lack of easily accessible hydrocarbon reservoirs requires increasingly invasive methods to unlock trapped oil and gas. As a consequence, large volumes of fluids are injected to stimulate reservoir production and to dispose of waste water. Concurrent with the increase in injection activity, there has been an increase in seismicity rates of events with $M > 3$ within the central US starting in ~2000. Similarly, the major oilfields in central California experienced a strong increase in injection rates, however, the seismogenic consequences are unknown or undocumented.

We analyzed seismicity in Kern county, the largest oil-producing county in California, where tectonically-driven earthquakes are frequent, potentially masking injection-induced events. Our study investigates parallels in waste-water injection parameters and geological conditions for wells with an increase in adjacent seismic activity. These wells are identified by simple criteria that highlight regions of strong spatio-temporal correlations between injection and seismic activity as well as seismicity-density changes due to injection. The method enables an objective analysis of large data-sets independent of background seismicity rates. Our results show that injection-induced seismic events are surprisingly rare at large scales although injection operations are extensive within the study area. We identified four likely induced sequences with some events above $M4$. These sequences exhibit different migration characteristics relative to the injection sites, suggesting fault creep and pore-pressure diffusion as possible triggering mechanisms. Diffusive processes may take advantage of pre-existing reservoir and fault structures which can lead to seismic activity at up to 10 km from the injecting well. Our results suggest that

MEETING ABSTRACTS

injection-related triggering processes are complex, and may occur with a significant time-delay. Pore-pressure diffusion may be more extensive in the presence of active faults and high-permeability damage zones thus altering the local seismic hazard in a non-linear fashion. Consequently, generic “best-practices” for fluid injections like a maximum distance from the nearest, active fault may not be sufficient to mitigate the increase in seismic hazard in tectonically-active regions. However, a synthesis of results from many different tectonic regions may help illuminate common geologic, reservoir and injection characteristics and thus also conditions likely to induce earthquakes.

A comparative study of the seismo-tectonics in the San Gorgonio and Ventura Special Fault Study Areas, Thomas H. Goebel, Egill Hauksson, Andreas Plesch, and John H. Shaw (Poster 196)

The SCEC Special Fault Study Areas (SFSAs) are regions of complex deformation involving series of strike-slip and blind-thrust faults close to densely-populated, urban areas. A better understanding of fault and seismic activity requires an integrated analysis of geologic and seismic data within the SFSAs.

We show results from a comparative study between the two regions, focusing on differences in fault zone structures, stress regimes, stress-drops, and geologic slip rates. The Ventura region is characterized by highly variable seismic activity that extends to depths of ~20 km, and contains a series of strike-slip, blind-thrust and reverse faults. The rapid convergence rates across the basin suggest that several of these faults slip at high rates and are capable of producing large-magnitude earthquakes. San Gorgonio pass, on the other hand, marks the location of a structural knot and low geologic slip rates within the San Andreas fault system. The region exhibits diffuse deformation and seismicity distributions with focal depths of up to ~20 km. The base of the seismicity becomes shallower to the north, beneath the San Bernardino mountains. In the proximity of this seismicity-step, we observed anomalously high stress drops (>20 MPa) in a small region between the traces of the San Gorgonio and Mission Creek segments of the San Andreas fault. The estimated stress drops also increase below depths of ~10 km and along the San Andreas fault segments, both from the north and south, towards San Gorgonio Pass, showing a negative correlation with geologic slip rates. We identified crustal conditions and fault properties that contribute to local variations in stress drops including changes in geologic slip rates, mineralogical composition, as well as the hypocentral depths of seismic events.

The Ventura region shows significantly lower stress-drops than the San Gorgonio area, possibly connected to the large seismic activity within the deep basin. We observed a slight increase in stress-drops with depth which can be explained by a continuous increase in rupture velocities. We performed a detailed analysis of seismic velocities to document possible differences in fluid content. An increase in fluid content and pore-pressure may explain the relatively low stress-drops within the Ventura basin. The present study may help advance our understanding of the complex fault geometries within the SFSAs and the potential for large-magnitude earthquakes.

Holocene geologic slip rate for the Banning strand of the southern San Andreas Fault near San Gorgonio Pass, Peter O. Gold, Whitney M. Behr, Dylan Rood, Katherine Kendrick, Thomas K. Rockwell, and Warren D. Sharp (Poster 277)

We present the first Holocene geologic slip rate for the Banning strand of the southern San Andreas Fault in southern California. Our new slip rate measurement, critically located at the northwestern end of the Banning strand, overlaps within errors with the published rate for the southern San Andreas Fault measured to the south at Biskra Palms Oasis. This indicates that the majority of southern San Andreas Fault displacement transfers from the southeastern Mission Creek strand northwest to the Banning strand and into San Gorgonio Pass. Our result corroborates the UCERF3 hazard model, and is consistent with most previous interpretations of how slip is partitioned between the Banning and Mission Creek fault strands. To measure this slip rate, we used B4 airborne LiDAR to identify the apex of an alluvial fan offset laterally 30 ± 5 m from its source. We calculated the depositional age of the fan using in-situ Be-10 cosmogenic exposure dating of 5 cobbles and a depth profile. We calculated a most probable

fan age of 4.0 ± 2.0 -1.6 ka (1σ) by combining the inheritance-corrected cobble ages assuming Gaussian uncertainty. However, the probability density function yielded a multi-peaked distribution, which we attribute to variable ^{10}Be inheritance in the cobbles, so we favor the depth profile age of 2.2-3.6 ka. Combined, these measurements yield a late Holocene slip rate for the Banning strand of the southern San Andreas Fault of 11.1 ± 3.1 -3.3 mm/yr. This slip rate does not preclude possibility that some slip transfers north along the Mission Creek strand and the Garnet Hill fault, but it does confirm that the Banning strand has been the most probable rupture path for earthquakes nucleated on the southern San Andreas Fault over the past few thousand years, and is likely to remain so in the near future. This clarification of slip partitioning within the northwest Coachella Valley is timely given that the southern San Andreas Fault is considered overdue for a large earthquake.

Experimental Studies of Dynamic Fault Weakening Due to Thermal Pore-Fluid Pressurization, David L. Goldsby, Terry E. Tullis, Keishi Okazaka, John Platt, and Thomas Mitchell (Poster 147)

Thermal pressurization is a co-seismic weakening mechanism driven by the thermal expansion of native pore fluids, which leads to elevated pore pressures and significant co-seismic weakening. While thermal pressurization has been studied theoretically for many decades, and has been invoked in recent earthquake simulations, its activation in laboratory experiments has remained elusive. Several high-speed friction experiments yield indirect evidence for thermal pressurization, yet none have directly linked with existing theoretical models or the relevant physical parameters -- such as permeability, slip, and slip rate -- that control the weakening rate.

We are conducting thermal pressurization experiments on fluid-saturated, low-permeability rocks (primarily Fredrick diabase; also SAFOD gouge) at slip rates up to ~5 mm/s, with constant confining pressures in the range 21–149 MPa and initial pore pressures in the range 10–25 MPa. The impractically low permeability of the diabase, $\sim 10^{(-23)}$ m², is increased prior to the friction test by thermally cracking the samples, yielding measured permeabilities in the range $1.3 \times 10^{(-18)}$ to $6.1 \times 10^{(-19)}$ m². These permeabilities are high enough to allow sample saturation over one to several days, but also low enough to confine pore pressure rises during rapid sliding and allow thermal pressurization to occur. In recent experiments we also embed a thermocouple ~1–2 mm from the sliding surface, and use the resulting data to calibrate a finite element model that calculates the sliding surface temperature.

One experiment revealed a rapid decay of shear stress by ~25% following a step-change in velocity from 10 $\mu\text{m/s}$ to 4.8 mm/s. For the first 28 mm of slip the experimentally measured shear stress agrees closely with the theoretical solution for slip on a plane (Rice [2006]) with an inferred slip weakening distance of ~500 mm, which is in the range predicted by inserting laboratory determined rock and fluid properties into the formula for L^* from Rice [2006]. Deviations from the theoretical prediction occur at larger displacements since the experimental sample is not a semi-infinite half space, as assumed in the theoretical model, and heat is lost to the high-conductivity steel of the sample assembly. To our knowledge this is the best experimental validation of thermal pressurization to date.

Geophysical and Geomorphic Constraints on the Location, Geometry and Kinematics of the Onshore Palos Verdes Fault Zone, Joshua Goodman, Phil Hogan, Dan O'Connell, Marco Ticci, Glen Adams, and James Turner (Poster 253)

New high-resolution 2-D seismic reflection data were collected for the Sanitation Districts of Los Angeles County's proposed Joint Water Pollution Control Plant Effluent Outfall Tunnel across the Holocene-active Palos Verdes fault zone (PVFZ) in the eastern Palos Verdes Peninsula (PVP). These data were used in conjunction with digital renderings of early 20th-century topography and borehole data to refine the location, geometry and kinematics of shallow (< 6,000 feet) faulting and folding along one of the highest-slip-rate structures in the greater metropolitan Los Angeles area. The onshore PVFZ is approximately 6,000 feet wide and consists of three principal strands, referred to herein as the northern, middle and southern splays (PFVN, PVFM and PVFS, respectively). PVFN bounds the northeastern range front of the PVP, and is interpreted as a 75-degree, southwest-dipping blind reverse fault. The location of the fault

tipline is well constrained at an elevation of approximately -1,500 feet by an unfaulted angular unconformity near the top of the Pliocene Fernando Formation. The unconformity and adjacent reflectors are folded into a prominent synclinal hinge, and form the common limb with a hangingwall anticline involving the Miocene Monterey Formation and Quaternary San Pedro Sand. The axial surface bisecting the syncline projects upwards to a well-defined topographic break-in-slope, which we interpret as a fold scarp. PVFM is interpreted as an 80- to 85-degree, southwest-dipping, right-reverse-oblique fault. Integration of the reflection data with subsurface constraints from nearby oil and gas wells shows that the Monterey Formation thickens in the hangingwall of the PVFM. Based on an attenuated to absent section of equivalent strata in the footwall, PVFM likely initiated as a Miocene extensional fault and was subsequently inverted in transpression; PVFN may be a footwall-breakout off of this fault. PVFS is interpreted as a vertical strike-slip fault based on the down-dip trajectory of reflection terminations, an abrupt juxtaposition of contrasting reflection sequences and, as visible in the early 20th-century topographic data, aligned linear drainages, slope breaks and channel deflections. This study provides robust constraints on the location and geometry of what was previously a poorly located section of the fault zone.

Validation of the SCEC Broadband Strong Ground Motion Simulation Platform: Ingredients and Methodology, *Christine A. Goulet and the BBP Validation Working Group* (Poster 058)

The SCEC Broadband ground motion simulation platform (BBP) is an open-source, multi-module software package developed to simulate broadband earthquake ground motions. Before codes such as those on the BBP are used in practical applications, it is necessary to validate them to ensure they produce realistic ground motions. To this effect, a large-scale validation exercise of the SCEC BBP was initiated in early 2012. This validation exercise is a multi-year project involving many stakeholders and the participating seismologists, engineers, programmers and users are referred to as the BBP Validation Working Group. While most of the BBP methods produce time series, the current focus of evaluation is geared toward engineering-based metrics such as aggregate goodness-of-fit for average horizontal component pseudo-spectral acceleration (PSA). The validation is completed through two complementary approaches: in Part A, the simulated ground motions are compared to recordings from past earthquakes while in Part B they are compared to medians from ground motion prediction equations (GMPEs). Additional statistical and visualization tools have been integrated into the BBP to provide uniform results for the evaluation, which determines distance and frequency ranges for which each method is considered to be reliable. The BBP is in constant evolution with improvements affecting the seismological computations themselves, the software computational efficiency and the post-processing tools. At set times, a new version of the platform is officially released and validated. Subsets of the validation exercise are also completed through the BBP development. This approach allows the validation results to inform improvements of the BBP as much as it provides a formal assessment of its products. Two rounds of validation (for releases 13.6 and 14.3) have now been completed for a subset of simulated events, for several simulation methodologies.

GP14.3: Refinements to the Graves and Pitarka Broadband Simulation Method, *Robert W. Graves and Arben Pitarka* (Poster 060)

Goulet et al. (2014) have examined the performance of several ground motion simulation methods currently implemented on the SCEC Broadband Simulation Platform (BBP). The analysis utilizes two complementary validation approaches: one comparing simulated ground motions with recordings from past earthquakes and the other comparing median ground motion prediction equation results for hypothetical earthquakes with predictions from the BBP methods. Here we describe refinements to the Graves and Pitarka (2010) simulation method (GP2010 hereafter) that have been implemented in version 14.3 of the BBP. The updated version of our method is referred to as GP14.3. One refinement involves the addition of a deep weak zone to the rupture characterization, analogous to the shallow weak zone introduced by GP2010. The deep zone begins at 15 km and is characterized by a two-fold linear increase in the average rise time down to a fault depth of 18 km. Below 18 km, a constant factor of two increase applies. This is accompanied by a

reduction in the width of slip tapering along the fault edges. These modifications reduce the radiation of strong motion energy from the deep fault while still allowing large fault displacement to occur in this zone. The result is to reduce the tendency of the simulations to over-predict observed ground motion levels in the period range of 1 to 5 sec, particularly for larger magnitude ruptures ($M_w > 6.5$). A second refinement in GP14.3 is to add perturbations to the correlation structure for rise time and rupture speed parameterization. The original approach in GP2010 directly correlated variations of rise time and rupture speed with variations in local fault slip. In GP14.3 the correlation structure is relaxed such that the variations are randomly selected from a log-normal distribution having a median value that follows the specified correlation with local slip. The effect is to reduce the coherency of radiated motions around 1 to 2 sec period and provide a smoother transition into the stochastic approach used at shorter periods.

Characterizing the recent behavior of the Ventura blind thrust fault: Preliminary results from the Brookshire Road, Ventura, study site, *Jessica R. Grenader, James F. Dolan, Lee J. McAuliffe, Edward J. Rhodes, John H. Shaw, Thomas L. Pratt, and Judith Hubbard* (Poster 250)

Analysis of three new continuously cored boreholes and six new cone-penetrometer tests (CPTs) from strata folded above the tipline of the eastern Ventura fault, together with a high-resolution seismic reflection profile acquired August 2010 along the same transect, reveal the geometry of these deposits and provide information on incremental displacements during latest Pleistocene-Holocene on this major blind thrust fault. These structural and stratigraphic observations, in combination with ongoing luminescence and radiocarbon dating of samples from the boreholes provide incremental fault slip rates as well as the timing and displacement in recent Ventura fault earthquakes. Preliminary analysis reveals a minimum of 30 m of structural relief across the fold in the 35 m depth interval sampled in our boreholes. These results add to a growing body of paleoseismic and structural information along the Ventura fault that is changing our view of the hazard posed by this structure. In particular, evidence for large-displacement ($5\text{-} > 10$ m), a rapid fault slip rate, and structural analyses documenting the interconnectivity of major reverse faults of the western Transverse Ranges demonstrate that the Ventura fault has the potential to generate very large-magnitude ($M_w 7.5\text{-}8$) earthquakes involving multiple faults in the western and central Transverse Ranges. The occurrence of such large magnitude earthquakes has important implications for seismic risk in the densely populated southern California region.

A change point model to detect change and quantify seismicity rates from triggered seismicity, *Abhineet Gupta and Jack W. Baker* (Poster 195)

The authors employ Bayesian inference to detect changes in seismicity rates from induced seismicity and determine the probability distributions of these rates utilizing real-time data. There has been a dramatic increase in seismicity in Central and Eastern United States (CEUS) in recent years (Ellsworth 2013). For example, the number of magnitude ≥ 3 earthquakes in Oklahoma has increased from about 2 per year prior to year 2000, to 238 in the first six months of year 2014. There is a possibility that this increased seismicity in CEUS is caused by fluid injection processes and hence it is referred to as induced or triggered seismicity. The earthquakes are a nuisance for people and some larger magnitude earthquakes have also caused structural damage.

This study utilizes earthquake occurrence data to update seismic hazard when a change in seismicity rates is observed, and detects a change in rates quickly using real-time data to facilitate decision making. The authors implement Change Point detection using Bayesian analysis (Raftery and Akman 1986) to assess whether earthquake occurrence data observed in real-time indicates that a change in seismicity rates has occurred. This model also provides the probability distributions of seismicity rates before and after the change. Information about seismicity rates is utilized to update seismic hazard at a site. Information about occurrence of change can serve as a decision support tool to inform decisions on whether to continue, monitor or pause operations linked to induced seismicity.

MEETING ABSTRACTS

Long-term uplift of the southern California coast between San Diego and Newport Beach resolved with new dGPS survey data: Testing blind thrust models in the offshore Borderlands, Erik C. Haaker, Thomas K. Rockwell, George L. Kennedy, Lisa B. Grant Ludwig, Justin A. Zumbro, and S. Thomas Freeman (Poster 246)

Marine terrace shorelines provide information on vertical tectonic motions, thereby yielding constraints on rates and styles of deformation for underlying structures, such as blind thrust faults. In coastal southern California, the Oceanside Blind Thrust (OBT) has been inferred from offshore seismic reflection data, and its intersection with the coast has been inferred to be the source of uplift of the San Joaquin Hills (SJH). The OBT has been interpreted to be the result of a tectonically inverted Miocene detachment fault, and has been hypothesized as a late Quaternary seismic source underlying coastal San Diego and southern Orange counties. Late Quaternary motion on the OBT should deform and uplift Quaternary marine terraces. To test OBT seismic source models, we collected over 3000 high-resolution GPS elevation data points for flights of Pleistocene marine terraces spanning the southern California coastal zone from central San Diego County through the city of Newport Beach in Orange County. We mapped the terraces by geomorphically tracing out and correlating individual shoreline exposures. In addition, we compiled subsurface geotechnical borehole data that supplemented our survey data where urban development had obscured or obliterated the original geomorphic relationships. From these new data, the shorelines for terraces below 140 m elevation are observed to remain at nearly constant elevation from San Diego northward through Camp Pendleton. The lowest two terraces that date to MIS 5.1 and 5.5 show minor variation in San Clemente, and then gently decrease a few meters in elevation towards the north in the vicinity of Newport Bay, consistent with the observation that terraces below about 60 m elevation show no significant variation along the coast from San Diego into Newport Beach. These observations do not appear to support late Quaternary activity of the OBT, and raise questions about how to reconcile recent seismicity in the SJH with published models of an underlying blind thrust.

A real-time seismogeodetic network using MEMS accelerometers, Jennifer S. Haase, Jianghui Geng, Diego Melgar, Dara E. Goldberg, and Jessie K. Saunders (Poster 043)

The seismogeodetic combination of high-rate GPS observables and seismic acceleration captures the broadband on-scale recording of large earthquake ground motions. The use of these data for determining rapid centroid moment tensor solutions ("fastCMT") has been demonstrated in the post-analysis of the 2010 Mw 7.2 El Mayor-Cucapah earthquake. This seismogeodetic combination will improve real-time source inversions for future earthquakes, but large-scale accelerometer deployment at the many available permanent GPS stations is limited by the cost of traditional observatory-grade accelerometers. We expand the number of collocated sites by installing Scripps Institution of Oceanography (SIO) Geodetic Modules and low-cost MEMS accelerometers at 17 GPS stations in southern California near the San Andreas, San Jacinto, and Elsinore faults, transmitting data in real time to produce seismic velocity and displacement waveforms. We examine the performance of our seismogeodetic subnetwork using the El Mayor-Cucapah earthquake as our focus. We show the differences between seismic, geodetic, and seismogeodetic time series for the subset of collocated stations in existence at the time of the event. We also compare the amplitude of synthetic ground displacements at the new sites equipped with the SIO geodetic module and MEMS accelerometers with the noise levels at these stations to describe the practical level of detectability for such an event. The MEMS accelerometer has higher noise than the typical observatory grade accelerometer. We quantify the effect this has on the seismogeodetic solution using strong motion recordings from a series of experiments conducted at the University of California San Diego Large High Performance Outdoor Shake Table. Results provide confidence in the use of the MEMS accelerometer for a large-scale upgrade of the permanent GPS network to support seismogeodesy.

Measuring Ventura Area Uplift: A Four-Technique Geodetic Study of Vertical Tectonics Combining GPS, InSAR, Leveling and Tide Gauges, William C. Hammond, Reed Burgette, and Kaj Johnson (Poster 228)

The western Transverse Ranges is the topic of the SCEC Ventura Special Fault Study Area (SFSA) that promotes interdisciplinary science to better understand this large multi-segment system of thrust and left lateral faults. Strain and rotation in the crust can be seen in the topography of the ranges, uplift and deformation of marine terraces, earthquake focal mechanisms, and vertical axis spin and north-south contraction in the crust as seen in GPS geodesy. While geodetic measurements strive to place limits on the budgets of slip across complex fault systems, they suffer from various uncertainties and incomplete coverage that depend on the method used. Measurements of vertical motion place complementary constraints on the rate and localization of elastic strain accumulation in the crust, and are especially valuable in regions of high rates of contraction where thrusting results in uplift. Vertical geodetic rates are becoming more precise and accessible given the increased length of GPS time series, availability of InSAR data, and potential for integration with terrestrial techniques such as leveling and tide gauges. Each technique is individually capable of measuring vertical tectonic motion at the level of 1 mm/yr or better and could resolve the signals of active Ventura area structures.

Here we combine these four geodetic techniques to place new constraints on the elastic strain accumulation in the crust in the SFSA. We align the vertical rates from the four techniques into the International Terrestrial Reference Frame using ties from collocated or near-collocated stations. This framework allows us to assess the agreement, uncertainties and applicability of each technique. The data show a change in sign of the vertical rate across the Mission Ridge/Santa Ynez fault systems from near 2 mm/yr downward around the Ventura Basin to between 1 and 2 upward between the Santa Ynez fault and San Andreas fault to the north. Upward rates in the Transverse Ranges in this area may be influenced by groundwater unloading in the southern Great Valley, so we account for this effect by using an elastic half-space model to estimate and remove this signal from the GPS time series. We explore the implications that these measurements have for estimates of fault slip rates in a separate presentation (see Johnson et al., SCEC 2014 abstract).

Dynamic Aftershock Triggering Correlated with Cyclic Loading in the Slip Direction, Jeanne L. Hardebeck (Poster 025)

Dynamic stress changes have been shown to contribute to aftershock triggering, but the physical triggering mechanisms are not fully understood. Some proposed mechanisms are based on dynamic stress loading of the target fault in a direction that encourages earthquake slip (e.g. dynamic Coulomb stress triggering), while other mechanisms are based on fault weakening due to shaking. If dynamic stress loading in the fault slip direction plays a role in aftershock triggering, we would expect to see a relationship between the dynamic stress orientations and the aftershock focal mechanisms. Alternatively, if dynamic stress change triggering functions only through a fault weakening mechanism that is independent of the slip direction of the target fault, no such relationship is expected. I study aftershock sequences of 4 $M \geq 6.7$ mainshocks in southern California, and find a small but significant relationship between modeled dynamic stress direction and aftershock focal mechanisms. The mainshock dynamic stress changes have two observed impacts: changing the focal mechanisms in a given location to favor those aligned with the dynamic stress change, and changing the spatial distribution of seismicity to favor locations where the dynamic stress change aligns with the background stress. The aftershock focal mechanisms are significantly more aligned with the dynamic stress changes than the preshock mechanisms for only the first 0.5-1 year following most mainshocks, although for at least 10 years following Hector Mine. Dynamic stress effects on focal mechanisms are best observed at long periods (30-60 sec). Dynamic stress effects are only observed when using metrics based on repeated stress cycling in the same direction, for example considering the dominant stress orientation over the full time series, and not for the peak dynamic stress. These results imply that dynamic aftershock triggering operates at least in part through cyclic loading in the direction of fault slip, although non-directional fault weakening may be important as well. This suggests that the orientation of the dynamic stresses, as well as

their amplitude, should be considered in the development of physics-based aftershock forecasting models.

Strong Ground Motions Generated by Earthquakes on Creeping Faults, *Ruth A. Harris and Norman A. Abrahamson* (Poster 075)

We investigate the peak ground motions from the largest well-recorded earthquakes on creeping strike-slip faults in active-tectonic continental regions. Our goal is to evaluate if the strong ground motions from earthquakes on creeping faults are smaller than the strong ground motions from earthquakes on locked faults. Smaller ground motions might be expected from earthquakes on creeping faults if the fault sections that strongly radiate energy are surrounded by patches of fault that predominantly absorb energy. For our study we used the ground motion data available in the PEER NGA-West2 database, and the ground motion prediction equations that were developed from the PEER NGA-West2 dataset. We analyzed data for the eleven largest well-recorded creeping-fault earthquakes, that ranged in magnitude from M5.0-6.5. Our findings are that these earthquakes produced peak ground motions that are statistically indistinguishable from the peak ground motions produced by similar-magnitude earthquakes on locked faults. These findings may be implemented in earthquake hazard estimates for moderate-size earthquakes in creeping-fault regions. Further investigation is necessary to determine if this result will also apply to larger earthquakes on creeping faults.

Please also see:

Harris, R.A., and N.A. Abrahamson (2014), Strong ground motions generated by earthquakes on creeping faults, *Geophysical Research Letters*, vol. 41, doi:10.1002/2014GL060228.

Spectral identification of offset fault features, with Mako hyperspectral data., *Janet C. Harvey and Joann Stock* (Poster 268)

In 2013 the Aerospace Corporation flew the Mako sensor over the high slip zone from the 1999 Hector Mine earthquake (Mw 7.1) on the Lavic Lake fault, Bullion Mountains, in order to provide surface composition data to facilitate updated geologic mapping in an area of limited access due to the restrictions of the active training ranges of the Marine Corps Air Ground Combat Center (MCAGCC). Data was additionally acquired in a flight over the South Bristol Mountains (SBM) where geologic mapping of the basement rocks had been previously completed by Dave Miller (USGS) at ~ 1:62,500, and recent of mapping of basement, volcanic and sedimentary rocks adjacent to the South Bristol Mountains fault zone (SBMFZ) conducted at 1:10,000. The SBM and the Bullion Mountains are composed of similar Neogene volcanic rock sequences floored by Proterozoic through Mesozoic basement rocks and thus the SBM flight was intended to serve as a well constrained comparison for the Bullion Mountains data for which limited ground truth is available. The high spatial resolution (~2 meter pixels) and the ~5km wide swathe width of this Mako flight configuration with the high spectral resolution (0.044 μm per channel) of Mako, allows for a high frequency sampling of surface composition that could only be replicated on the ground by highly detailed mapping in rough terrain with closely spaced sampling and clast counting in the clastic units, yielding benefits for geologic mapping even in areas without access restrictions.

Reconstructing multiple opposing basement spectral signatures in the MAKO data along the southern section of the SBFZ confirms the finding of ~6km of total offset between porphyritic granites previously determined by Dave Miller. Additionally, by correlating the spectral signatures of active drainages and sequentially inset alluvial terraces to their basement source drainages across the southwest range front fault zone, Quaternary alluvial units Qaa through Qia show no significant displacement, although in the field they host high angle faults parallel to the main strand of the SBFZ. A series of undated, deeply incised, tilted or isolated conglomerates, mapped only as a Quaternary-Tertiary fanglomerate by Dibblee (1967), Miller and subsequent mapping, can be shown to be offset dextrally from a basement source area with a similar spectral signature, providing the relative timing of slip cessation along the SBFZ.

Earthquake Triggering and Tremor: Detecting micro-seismic events in the Western U.S due to the 2010 El Mayor Cucapah Earthquake and the Mw6.8 Mendocino Triple Junction Earthquake in 2014, *Rachel L. Hatch and Jascha Polet* (Poster 194)

Recent studies indicate that the passage of seismic waves from large earthquakes is able to trigger small earthquakes and tremor at regional distances. These small events may be detected by applying a high-pass filter to seismograms to remove the much larger ground motion amplitudes from the large distant earthquake. Our interests are in examining the local triggering of earthquakes and tremor throughout the West Coast of North America from the magnitude 7.2 El Mayor-Cucapah 2010 earthquake and the magnitude 6.8 Northern California March 10, 2014 earthquake, just north of the Mendocino Triple Junction. We will present the results of the analysis of waveform data from hundreds of seismometers throughout Southern California, Northern California, Oregon, Washington, as well as some stations bordering these states. Our preliminary results suggest that triggering of local earthquakes and tremor occurred for both earthquakes. In the case of the records of the Southern California stations for the El Mayor Cucapah 2010 earthquake, 27 stations showed triggering near the seismic station. 13 of these stations are located in or near known geothermal areas, while others were located along active faults and one offshore. While conducting this study, we detected an instrumental noise signal present in 63 of the Southern California seismograms for the El Mayor-Cucapah earthquake. Initially, the signal looked like a typical triggered event, yet with further investigation we found its likely cause to be instrumental noise. We plan to relate our observations of triggered seismicity and tremor to the tectonic environment to test the hypothesis that triggering and tremor most commonly occurs in volcanic and geothermal areas.

Evolving strike-slip efficiency of restraining bends in wet kaolin analog experiments, *Alex E. Hatem, Michele L. Cooke, and Elizabeth H. Madden* (Poster 106)

Restraining bends between discrete strike-slip faults are known to migrate and evolve over time by propagation of new faults and abandonment of fault segments. Such processes are poorly constrained in space and time, leaving open questions about how strike-slip faults interact over geologic time. Scaled analog modeling using wet kaolin allows our team to make qualitative observations and quantitative analyses about restraining bend evolution. We document fault initiation, propagation, linkage and abandonment to see how restraining bends overcome initial mechanical inefficiencies. Deformation is analyzed using Particle Image Velocimetry (PIV), which tracks pixels between successive images. Restraining bends within the claybox grow new oblique-slip faults outboard of the initial restraining segment on one (low angle bends) or both sides (high angle bends) of the restraining bend. These new faults often link with the initial faults. We quantify the evolving mechanical efficiency of the fault systems using strike-slip efficiency, a ratio of measured fault slip rate to applied plate velocity. At the start of fault slip, the strike-slip efficiency correlates to restraining bend angle; shallower restraining bends have greater initial strike-slip efficiency. Restraining bends with higher angles begin with low incremental strike-slip efficiency, but their efficiency increases as new faults form and link with the existing faults. Regardless of angle, all restraining bends have roughly equal strike-slip efficiency (~85%) after 55 mm applied displacement. All restraining bends propagate a primary oblique-slip fault after a threshold level of accumulated convergence, suggesting that convergence within a strike-slip system controls the timing of new fault propagation. Quantifying bend topography provides insights into its dependence on restraining bend angle. These analog models provide insight into the evolution of crustal restraining bends, including those along the Denali, Dead Sea and San Andreas faults.

Summary of Caltech/USGS UASI Project Accomplishments: 2013-2014, *Egill Hauksson and Valerie Thomas* (Poster 156)

From April 2013 to August 2014, the City of Los Angeles and Long Beach Urban Areas Security Initiative (UASI) region provided UASI-09 and UASI-12 Department of Homeland Security (DHS) funds to upgrade the infrastructure of the Caltech/USGS Southern California Seismic Network (SCSN) and the Southern California Earthquake Data Center (SCEDC). This upgrade was needed to catch up on maintenance of infrastructure,

MEETING ABSTRACTS

and to enable the network to support earthquake early warning (EEW) in the future.

The UASI funding provided the following items:

- 1) Infrastructure upgrades at Caltech/USGS in Pasadena, including new uninterruptible power system, 5 years worth of data storage facilities, and computer servers
- 2) Upgrades of 43 existing seismic stations with new sensors or dataloggers
- 3) Rebuild and instrumentation of 36 very old style (analog) seismic stations with modern digital sensors and dataloggers
- 4) A total of 46 new digital seismic stations were added to the seismic network
- 5) A total of 41 high precision GPS receivers were installed to upgrade existing USGS operated permanent GPS sites

These new stations will provide more detailed data for use in EEW, earthquake reporting, and ground motion studies, including ShakeMap, than was available in the past. In particular, the increased station density along major faults such as the San Jacinto and Elsinore faults will increase warning times for future major earthquakes that will occur along these faults. Similarly, these stations will provide much needed near-field ground motion records.

In summary, 125 (SCSN) seismic stations were upgraded or installed, and most were equipped with modern cell-modem or digital radio data communications. Although, the UASI funding provided important improvements, much work still needs to be done to accomplish optimal station density and telemetry reliability for EEW.

A search for tremor-like precursors to earthquakes in southern California, *Jessica C. Hawthorne and Jean-Paul Ampuero* (Poster 176)

We conduct a search for tremor-like precursors to $M > 3$ earthquakes in southern California. We use a frequency-domain phase coherence technique to examine the seismograms in the minutes to seconds before each of about 5000 earthquakes. This approach allows us to identify signals coming from the same location as the earthquake. It uses recordings at multiple stations to identify coherence even when the source-time functions are complicated. If the signals recorded just before an earthquake have the same Green's functions as the earthquake, they should have a high phase coherence with the earthquake records. They should also have high phase coherence with the records of nearby earthquakes. We usually compare potential precursors with nearby earthquakes because temporally persistent noise sources create a bias when we compare the potential precursor with the mainshock.

This method successfully detects previously identified foreshocks. However, among the 5000 earthquakes examined so far, we see no evidence for additional precursory signals. For more than half of these earthquakes, error estimates suggest that we should be able to detect signals with durations of 5 seconds and energy equivalent to a $M1$ earthquake. We are continuing to examine more earthquakes and to consider the uncertainty introduced by using nearby earthquakes as templates.

A Southern California lithosphere deformation model for the SCEC CSM: Status update and preliminary findings, *Elizabeth H. Hearn* (Poster 100)

Although several dynamic models of current southern California lithosphere deformation have been developed, few (if any) incorporate all of the major active faults, as well as three-dimensional geometry and heterogeneous material properties. I am developing a finite-element (FE) deformation model of the southern California lithosphere which incorporates these properties to estimate current-day lithosphere stresses and stressing rates for the SCEC Community Stress Model. Deformation is driven by far-field velocity boundary conditions (so far); and upper crust plasticity, viscous shear zone creep and viscoelastic relaxation of the lower lithosphere and asthenosphere are represented. The complete model will be calibrated to (1) a version of the SCEC CMM 4.0 velocity field corrected for viscoelastic perturbations, (2) a strain energy minimization criterion, and (3) stress axis orientations and slip rates from the SCEC CSM and the UCERF3 slip rate compilation.

Preliminary forward models suggest that the San Andreas Fault (SAF) slip rates decrease in the Big Bend region, as expected, though details depend on how geometric irregularities and plasticity are handled. A version of the model incorporating earthquake cycles along the 1857 and 1906 SAF rupture segments and low shear stresses along the crustal root of the SAF gives current-day, near-field offset rates along the SAF creeping section that are about 20% lower than the relative offset rates of points tens of km from the fault trace, consistent with the findings of Titus et al. (2006). Hence, viscoelastic earthquake-cycle effects (rather than partial locking of the creeping section or activity of unmapped faults within 35 km of the SAF) could be responsible for the apparent discrepancy.

Next-Generation Model Averaging for Earthquake Early Warning, *Thomas H. Heaton, Sarah E. Minson, Stephen Wu, James L. Beck, and Egill Hauksson* (Poster 040)

The earthquake early warning (EEW) system currently under development in the western U.S. is built on the principle of operating multiple EEW algorithms independently and then averaging these results into a single real-time estimate of earthquake source properties. This model averaging mechanism is referred to as the decision module. We will present a performance review of the currently operating EEW algorithms and decision module estimates. We then suggest potential improvements to the decision module to both improve performance with the existing EEW algorithms and to prepare for new EEW algorithms that are starting to come online. This next generation decision module would weight the contribution of different algorithms in different earthquake scenarios based on their performance in the past using Bayesian model class selection with a new likelihood model for combining the different algorithms' results.

Geochronology of surfaces within the San Geronio Pass from radiocarbon, in-situ cosmogenic nuclides, and pedogenesis: implications for climate and tectonics since the mid-late Pleistocene, *Richard V. Heermance, Katherine J. Kendrick, Ian Dejarlais, Doug Yule, Paul McBurnett, and Shahid Ramzan* (Poster 279)

Accurate age control on geomorphic surfaces is critical to understanding past climatic conditions and uplift rates across fault systems. In the San Geronio Pass near Palms Springs, CA, dextral slip on strands of the San Andreas Fault zone is transferred onto right-lateral reverse slip faults of the San Geronio Pass Fault Zone that have formed fault scarps across the alluvial-fan terraces. We have identified at least five abandoned alluvial fan surfaces and associated deposits in Millard Canyon (Holocene Fan surfaces (Qf) 1-4, and the Pleistocene Heights Fanglomerate) and provide new age constraints based on radiocarbon, in-situ cosmogenic radionuclides (^{10}Be and ^{26}Al), and soil stratigraphy. Qf-1 (~ 5 m above the active channel) is 890 ± 300 calibrated y.b.p. based on seven detrital charcoal ages from the uppermost strata below the surface. Qf-2 (~6 m above the active channel) has an age of 1270 ± 80 calibrated y.b.p. based on the minimum radiocarbon ages from the population ($n=14$) of charcoal fragments within the uppermost strata beneath the surface. New ^{10}Be cosmogenic exposure ages for Qf-3 (~10 m above the active channel) are pending, but soil development suggests a surface age of ~ 5-9.5 ka, based on quantitative indices of profile development and rubification, as compared to dated soil chronosequences elsewhere in the region. Qf-4 (~12 m above the active channel) has a surface-abandonment age of 7700 ± 1500 y.b.p. based on ^{10}Be cosmogenic exposure ages from four surface boulders and a depth profile ($n=4$). Soil development associated with Qf-4 is similar to that of Qf-3, ~5-9.5 ka. The highest and oldest surface exposed in Millard Canyon is the Heights Fanglomerate, which sits 80-150 m above the active channel, depending on location. Erosion of this surface limits our ability to apply surface exposure dating and quantitative soil analysis to this surface, but new cosmogenic $^{26}\text{Al}/^{10}\text{Be}$ burial ages from four deeply buried (~25 m) cobbles below this surface provide a maximum age of ~680,000 y.b.p. This age, combined with new minimum ages for a correlative surface near Whitewater Wash of ~65,000 y.b.p. (Owen et al., 2014), limit the age range of this surface to mid-late Pleistocene. Overall, our compilation of new and previously collected data provides a framework from which to evaluate Holocene climate and determine long-term slip-rates on faults that offset these terraces.

Time-varying loss forecast for an earthquake scenario in Basel, Switzerland, *Marcus Herrmann, Jeremy D. Zechar, and Stefan Wiemer* (Poster 044)

When an unexpected earthquake occurs, people suddenly want advice on how to cope with the situation. The 2009 L'Aquila quake highlighted the importance of public communication and pushed the usage of scientific methods to drive alternative risk mitigation strategies. For instance, van Stiphout et al. (2010) suggested a new approach for objective short-term evacuation decisions: probabilistic risk forecasting combined with cost-benefit analysis. In the present work, we apply this approach to a scenario earthquake sequence that simulated a repeat of the 1356 Basel earthquake, one of the most damaging events in central Europe. Probabilistic aftershock forecasts are a relatively recent development intended to benefit society in case of a large, damaging earthquake. But seismic risk delivers a more direct expression of the socioeconomic impact. To forecast the short-term seismic risk, we translate aftershock probabilities to time-varying seismic hazard and combine this with time-invariant loss estimation. Compared with van Stiphout et al. (2010), we use an advanced aftershock forecasting model and more detailed settlement data to allow us spatial forecasts and district-wise decision-making. We quantify the risk forecast in terms of human loss. For instance one minute after the M6.6 mainshock, the probability for an individual to die within the next 24 hours is 4 orders of magnitude higher than the long-term average; but the absolute value remains far below one per mille. The final cost-benefit analysis adds value beyond making probabilistic forecasts: it provides objective statements that may justify evacuations. To deliver supportive information in a simple form, we propose a warning approach in terms of alarm levels. Our results do not justify evacuations prior to the M6.6 mainshock, but in certain districts afterwards. The ability to forecast the short-term seismic risk at any time—and with sufficient data anywhere—is the first step of personal decision-making and raising risk awareness among the public.

References:

Van Stiphout, T., S. Wiemer, and W. Marzocchi (2010). "Are short-term evacuations warranted? Case of the 2009 L'Aquila earthquake". In: *Geophysical Research Letters* 37.6, url: <http://onlinelibrary.wiley.com/doi/10.1029/2009GL042352/abstract>

Seismic Trapped Noise in the San Jacinto Fault Zone Southeast of Anza, *Gregor Hillers, Yehuda Ben-Zion, Michel Campillo, Philippe Roux, and Frank L. Vernon* (Poster 184)

Systematic velocity contrasts across and within fault zones can produce head and trapped waves that provide direct information on structural units that are important for many aspects of earthquake and fault mechanics. Hillers et al. (JGR, 2014) showed that conditions controlling the emergence of seismic fault zone trapped noise have less limitations compared to trapped ballistic waves. Here we construct trapped waves from the scattered seismic wave field recorded by a dense rectangular array with >1100 vertical-component nodes separated by 10-30 m centered on the Clark segment of the San Jacinto fault zone southeast of Anza.

The frequency dependent interaction between the ambient wave field and the fault zone environment is studied using properties of the noise correlation field. A critical frequency defines a threshold above which the in-fault scattered wave field has increased isotropy and coherency compared to the ambient noise. The increased randomization of in-fault propagation directions produces a wave field that is trapped in a waveguide/cavity-like structure associated with the low velocity damage zone.

The dense rectangular sampling allows the reconstruction of a 2-D near field focal spot, which emerges from the superposition of a collapsing, time-reversed wave front. The shape of the focal spot depends on local medium properties, and a focal spot-based distribution of wave speeds indicates a velocity reduction that can be compared to results from a more standard far field travel time inversion. Preliminary imaging results will be presented in the meeting.

Dynamic Compaction as a Simple Mechanism for Fault Zone Weakening, *Evan T. Hirakawa and Shuo Ma* (Poster 137)

Elevated pore fluid pressures have long been thought to contribute to the apparent weakness of large plate bounding faults such as the San Andreas Fault. Sleep and Blanpied (1992) propose a mechanism in which compaction during interseismic creep reduces available pore space and hence increases fluid pressure. Assuming that the fault zone is not fully compacted during the interseismic period, we invoke a similar concept in this study, however in this case the compaction process occurs dynamically via the stresses associated with earthquake rupture. Microstructural analysis of fault zone rocks reveals intragranular fragmentation that is developed dynamically (e.g. Rempel et al., 2009) and is consistent with the style of fracture observed in individual quartz grains during bulk compaction (Chester et al., 2004), which thus lends some justification to our proposed mechanism.

We incorporate undrained compaction into a dynamic rupture model of a strike-slip fault by using an end-cap failure criterion (e.g. Wong et al., 1997). We show that dynamic stresses associated with rupture propagation cause the fault zone to compact, leading to elevated pore pressure in the undrained fault zone and low effective shear stress on the fault, consistent with the heat-flow constraints. An important result is that radiated S-waves propagating ahead of the rupture front can cause compactant failure and consequently lower the static friction as well as the dynamic friction, leading to a low strength drop on the fault. This may present a possible advantage over other dynamic weakening mechanisms such as thermal pressurization, which involves large strength drops accompanying rupture propagation.

Preliminary Site Response Maps From H/V Spectral Ratio Analysis on Cal Poly Pomona Campus, *King Yin Kennis Ho and Jascha Polet* (Poster 200)

Site characteristics are an important factor in earthquake hazard assessment. To better understand site response differences on a small scale, as well as the seismic hazard of the area, we develop site response parameter maps of Cal Poly Pomona campus. Cal Poly Pomona is located in southern California about 40 km east of Los Angeles, within 50 km of San Andreas Fault. The campus is situated on top of the San Jose Fault. With about twenty two thousand students on campus, it is important to know the site response in this area.

To this end, we apply the Horizontal-to-Vertical (H/V) spectral ratio technique, which is an empirical method that can be used in an urban environment with no environmental impact. This well-established method is based on the computation of the ratio of vertical ambient noise ground motion over horizontal ambient noise ground motion as a function of frequency. By applying the spectral ratio method and the criteria from Site Effects Assessment Using Ambient Excitations (SESAME) guidelines, we can determine fundamental frequency and a minimum site amplification factor. We installed broadband seismometers throughout the Cal Poly Pomona campus, with an initial number of about 15 sites. The sites are approximately 50 to 150 meters apart and about two hours of waveforms were recorded at each site. We used the Geopsy software to make measurements of the peak frequency and the amplitude of the main peak from the spectral ratio. These two parameters have been determined to be estimates of fundamental frequency and a minimum site amplification factor, respectively. Based on the geological map from the U.S. Geological Survey (USGS) and our data collected from Cal Poly Pomona campus, our preliminary results suggest that the area of campus that is covered by alluvial fan material tends to have a single significant spectral peak with a fundamental frequency of ~1Hz and a minimum amplification factor of ~3.7. The minimum depth of the surface layer is about 56 meters, as determined from the peak frequency and an estimate of the local shear wave velocity. We will present two preliminary site response parameter maps: one for fundamental frequency and one for minimum site amplification factor.

Near source broadband ground-motion modelling of the Canterbury aftershocks and implications for assessing engineering metrics, *Caroline Holden, Anna Kaiser, and Matt Gerstenberger* (Poster 072)

We produced broadband synthetic seismograms for the largest M5.9+ aftershocks of the 2010-2011 Canterbury earthquake sequence at sites of interest for slope failure studies (Massey et al., 2013). These synthetic

MEETING ABSTRACTS

seismograms are used as rock input motions for detailed modelling of slope responses. We employ a stochastic approach to compute the seismograms (Motazedian and Atkinson, 2005) that is not only controlled by detailed source models but also by regional parameters derived using spectral inversion of the extensive Canterbury strong motion dataset (Oth & Kaiser in press; Kaiser et al. 2013). We validate the method by comparing and obtaining good agreement between recorded seismograms and synthetic seismograms computed at strong motion sites within 20 km of the earthquake sources.

Our results show that using appropriate stress drop value and site-specific amplification functions helps greatly to reproduce key engineering parameters such as Peak Ground Acceleration (PGA) and response spectra. The technique is particularly efficient for “moderate shaking” events such as the local Mw 5.3 April 16th event and the distant Mw 5.9 December 23rd event. For larger events such as the February 22nd and the June 13th events, key parameters are also fairly reproduced for sites exhibiting linear response behaviour. However for sites behaving non-linearly, adding a site-specific amplification function results as expected in over-predicting ground shaking (by factors of 2 to 4 times PGA) and respective response spectra. These sites require detailed non-linear soil-response analyses. These results support the method we have chosen to produce rock ground-motion time histories and characteristics at sites of interest in slope-response analysis.

New High-Resolution 3D Imagery of Newport-Inglewood/Rose Canyon Fault Geometry and Deformation Offshore San Onofre, California, James J. Holmes, Jayne M. Bormann, Valerie J. Sahakian, Neal W. Driscoll, Graham M. Kent, Alistair J. Harding, and Steven G. Wesnousky (Poster 248)

The Inner California Borderlands (ICB) is situated off the coast of southern California and northern Baja. The structural and geomorphic characteristics of the area record a middle Oligocene transition from subduction to microplate capture along the California coast. Marine stratigraphic evidence shows large-scale extension and rotation overprinted by modern strike-slip deformation. Geodetic and geologic observations reported by others indicate that approximately 6-8 mm/yr of Pacific-North American relative plate motion is currently accommodated by offshore strike-slip faulting in the ICB. The farthest inshore fault system, the Newport-Inglewood/Rose Canyon (NI/RC) fault complex is a dextral strike-slip system that extends primarily offshore approximately 120 km from San Diego to the San Joaquin Hills near Newport Beach, California. The NI/RC fault system Holocene slip rate is 1.5-2.0 mm/yr to the south and 0.5 mm/yr along its northern extent based on onshore trenching. An earthquake rupturing the entire length of the system can be expected to produce an event of Mw 7.0+. In late 2013, we completed the first high-resolution 3D seismic surveys (3.125 m bins) of the NI/RC fault system offshore of San Onofre as part of the Southern California Regional Fault Mapping project aboard R/V New Horizon. Two separate data volumes were acquired using a “P-Cable” system consisting of fourteen 50 m long streamers, spaced 6.25 m apart, with 8 embedded hydrophones each. The first survey was an ~45 sq. km area collected over the continental slope (230-700 m depths) using a single “sparker” seismic source (6.25 m shot interval) with a 2000 ms record length and 0.5 ms sample rate. The second survey was an ~54 sq. km grid acquired on the continental shelf (50-100 m depths) using a single “boomer” seismic source (3.125 m shot interval) with a 800 ms record length and 0.25 ms sample rate. Both data volumes were stacked and processed to remove multiples. Migration calculations were then made using the Kirchhoff algorithm. Velocity estimation was completed using RMS smoothed velocity models created with 2D data acquired in the same survey locations by R/V New Horizon in 2013. It is anticipated that analysis of both data volumes will lead to new constraints on fault geometry and segmentation of the fault system, with the potential of updated slip-rate estimates if suitable targets are located/dated.

Geomechanical Seismicity-Based Reservoir Characterization, S. Mehran Hosseini and Fred Aminzadeh (Poster 154)

Permeability defined as the ability of porous medium to transport fluids through it, is one of the important crust properties. The nature of this property is scale dependent and there are several different methods for permeability estimation and measurement corresponding to different

scales. Large-scale permeability estimation can be inferred from seismicity. Such methods are referred to Seismicity-Based Reservoir Characterization (SBRC) methods, used in hydrological and petroleum reservoir studies. Most of previous SBRC methods assume that reservoir is critically stressed and a minimum pore pressure increase can cause failure in pre-existing faults and create seismicity or microseismicity. Geomechanical Seismicity-Based Reservoir Characterization (GSBRC) relaxes the assumption of minimum pore pressure increase required for shear failure and calculates the pore pressure increase required for shear failure as a function of reservoir geomechanical state and fault properties; hence GSBRC might give a more comprehensive solution than SBRC. GSBRC is used with seismicity data from the German Continental Deep Drilling Project (KTB) to estimate large-scale permeability. KTB’s estimated permeability using GSBRC ranges between 10–17 to 10–16 m², which matches the reported permeability in the literature for KTB.

Reducing Uncertainties in the Velocities Determined by Inversion of Phase Velocity Dispersion Curves Using Synthetic Seismograms, Mehrdad Hosseini and Shahram Pezeshk (Poster 203)

Characterizing the near-surface shear-wave velocity structure using Rayleigh-wave phase velocity dispersion curves is widespread in the context of reservoir characterization, exploration seismology, earthquake engineering, and geotechnical engineering. This surface seismic approach provides a feasible and low-cost alternative to the borehole measurements. Phase velocity dispersion curves from Rayleigh surface waves are inverted to yield the vertical shear-wave velocity profile. A significant problem with the surface wave inversion is its intrinsic non-uniqueness, and although this problem is widely recognized, there have not been systematic efforts to develop approaches to reduce the pervasive uncertainty that affects the velocity profiles determined by the inversion. Non-uniqueness cannot be easily studied in a nonlinear inverse problem such as Rayleigh-wave inversion and the only way to understand its nature is by numerical investigation which can get computationally expensive and inevitably time consuming. Regarding the variety of the parameters affecting the surface wave inversion and possible non-uniqueness induced by them, a technique should be established which is not controlled by the non-uniqueness that is already affecting the surface wave inversion. An efficient and repeatable technique is proposed and tested to overcome the non-uniqueness problem; multiple inverted shear-wave velocity profiles are used in a wavenumber integration technique to generate synthetic time series resembling the geophone recordings. The similarity between synthetic and observed time series is used as an additional tool along with the similarity between the theoretical and experimental dispersion curves. The proposed method is proven to be effective through synthetic and real world examples. In these examples, the nature of the non-uniqueness is discussed and its existence is shown. Using the proposed technique, inverted velocity profiles are estimated and effectiveness of this technique is evaluated; in the synthetic example, final inverted velocity profile is compared with the initial target velocity model, and in the real world example, final inverted shear-wave velocity profile is compared with the velocity model from independent measurements in a nearby borehole. Real world example shows that it is possible to overcome the non-uniqueness and distinguish the representative velocity profile for the site that also matches well with the borehole measurements.

Statistical analysis of GPS vertical uplift rates in southern California, Samuel M. Howell, Bridget Smith-Konter, Neil Frazer, Xiaopeng Tong, and David Sandwell (Poster 102)

Variations in crustal surface velocities obtained from GPS stations provide key constraints on physical models that predict surface deformation in response to earthquake cycle loading processes. Vertical GPS velocities, however, are highly susceptible to short scale (<10’s km) variations in both magnitude and direction induced by local changes in water-storage, pore pressure, precipitation, and water runoff. These short-wavelength spatial variations both dominate and contaminate vertical GPS velocity measurements, and often mask coherent long-wavelength deformation signals. Because of these complications, vertical GPS velocities, like those provided by the Southern California Earthquake Center (SCEC) and EarthScope’s Plate Boundary Observatory (PBO), have traditionally been

omitted from crustal deformation models. Here we attempt to overcome these obstacles by first eliminating GPS velocities influenced by non-tectonic deformation sources based on high-resolution InSAR data. Second, we employ model selection, a statistical technique that provides an objective and robust estimate of the velocity field that best describes the regional signal without overfitting the highly variable short-wavelength noise. Spline-based interpolation techniques are also used to corroborate these models. We compare these results to published physical models that simulate 3D viscoelastic earthquake cycle deformation in Southern California and find that the statistical SCEC-based and PBO-based vertical velocity models are in good agreement with physical models, yielding 0.59 mm/yr and 0.96 mm/yr residuals, respectively. We also utilize sources of disagreement as a tool for improving our physical model and to further inspect non-tectonic sources of deformation. Moreover, these results suggest that vertical GPS velocities can be used as additional physical model constraints, leading to a better understanding of faulting parameters that are critical to seismic hazard analyses.

Extracting Anisotropy with non-volcanic tremor (NVT) signals in the Cascadia Region in Northern Washington State, *Eduardo Huesca-Perez and Abhijit Ghosh* (Poster 193)

The Cascadia region experiences tectonic/Non-Volcanic Tremor (NVT) that is thought to occur at the top plate interface of the subducted Juan de Fuca plate in the transition zone [e. g. Ghosh et al., 2012]. So far, NVT related studies have primarily focused on understanding the relationship between tremor [Obara, 2002] and slow slip [Dragert et al., 2001; Rogers and Dragert, 2003] and their implications for hazard analysis of megathrust earthquakes. Due to the high reverberatory nature of the source excitation, less attention has been directed to the use of tremor to investigate earth structure since it is more difficult to identify discrete arrivals. In Vancouver Island, Bostock and Christensen (2012) successfully extracted anisotropic parameters from NVT signal, and show that Cascadian crust is noticeably anisotropic. Cascadia has low levels of crustal and Wadati – Benioff seismicity and therefore NVT provides a unique opportunity to study anisotropy in this area. Polarization and splitting analyses [e. g. Silver and Chan, 1991] of one-minute-long time windows of NVT at 3-component broadband stations provide evidence for anisotropy of the crustal part of the North American plate beneath northern Washington State. Tremor energy is predominant in the horizontal components and inferred to manifest a wave field composed of S-waves. Under this assumption, estimates of incidence angle and back azimuth can be calculated from the orientation of the smallest principal direction of motion from the covariance matrix. Results show that the NVT signal poses systematic fast polarization directions and splitting times. Fast polarization directions in general have east-west orientations that parallel the east-plunging anticline. Tremor is providing us important structural information that is currently unknown in Cascadia.

Systematic search for non-volcanic tremor under the San Jacinto Fault, *Alexandra A. Hutchison and Abhijit Ghosh* (Poster 190)

In this exploratory study, we use seismic array data and Plate Boundary Observatory (PBO) borehole broadband seismic data to search for ambient tremor in the San Jacinto Fault (SJF) and the southern San Andreas Fault (SAF). We are particularly interested in the region surrounding the Anza Gap, an aseismic segment of the SJF that has been accumulating stress as the rest of the fault segments have undergone MW ~6+ earthquakes for the last hundred years or so (Thatcher et al., 1975; Sanders and Kanamori, 1984), likely posing a major seismic hazard to the surrounding region. During the time period for which there is array data available, March – July, 2011, we apply a beamforming algorithm (Ghosh et al., 2009) to automatically scan for ambient tremor in the region. We compare the location of the beam in the slowness space relative to the center of the array to determine the signal's origin. Should the origin match the slowness parameters of tremor originating in the SJF or the southern SAF, we apply a set of criteria to eliminate all other possibilities, such as, regular earthquakes, noise etc. In addition, we visually check the data for a tremor-like signal and eliminate any possible artifacts. Our preliminary analyses found some interesting tremor-like signals that require further investigation.

Monitoring microseismicity in Long-beach, CA, using a dense seismic array, *Asaf Inbal, Robert W. Clayton, and Jean-Paul Ampuero* (Poster 198)

Monitoring microseismicity is important for illuminating active faults and for improving our understanding earthquake physics. This task is difficult in urban areas where the signal-to-noise ratio (SNR) is poor, and the level of background seismicity is low. One example is the Newport-Inglewood fault (NIF), an active fault that traverses the city of Long-Beach (LB). The catalog magnitude of completeness within this area is $M=2$, about one unit larger than along other, less instrumented faults in southern California. Since earthquakes obey a power-law distribution according to which for each unit drop in magnitude the number of events increases by a factor of ten, reducing the magnitude of completeness in LB should significantly decrease the time needed for effective monitoring. During 2011, over 5000 seismometers were deployed for exploration purposes in a 70 km² area covering LB, and recorded continuously for a period of six months. This experiment provides a unique opportunity for studying seismicity along the NIF. The recordings are dominated by anthropogenic noise sources such as the local airport, highways, and pumping in the LB oil field. We utilize array processing techniques to enhance the SNR. The recorded wave field is downward continued to a depth of a few kilometers, which allows us to detect signals whose amplitude is a few percent of the average surface noise. The migrated wave field is back-projected onto a volume beneath the city to search for seismic events. We identified several seismic swarms that lasted for a few weeks and exhibited complex spatial distribution. During the activity coherent energy was continuously emitted from segments whose length is a few hundred meters, and that are located at depths of 10-15 kilometers. We present a calibration scheme used to determine the magnitude of the events, and find that it is considerably smaller than the magnitude of completeness of the local catalog.

Multiple Structure-Soil-Structure Interaction and Coupling Effects in Building Clusters, *Yigit Isbilloglu, Ricardo Taborda, and Jacobo Bielak* (Poster 049)

We study the presence of multiple structure-soil-structure interaction effects in idealized building clusters during earthquakes, their effect on the ground motion, and how individual buildings interact with the soil and with each other. We seek to characterize, through a parametric approach, the coupling effects between the soil, the foundation, and the structural response of the buildings, including torsion, in the presence of surrounding structures. We simulate the ground motion of a historical earthquake and focus on the response of simplified symmetric and asymmetric building models located on soft soil. We use as reference the response of isolated symmetric and asymmetric building models, which allows us to separate the different contributing factors and distinguish between individual soil-structure and coupled structure-soil-structure interaction effects. Numerical results show that coupling effects vary with the number and dynamic properties of the buildings, their separation, and their impedance with respect to the soil. Our results indicate that the effects of torsion are also relevant. Interaction effects appear as an increased spatial variability of the ground motion, and significant reductions in the buildings' base motion at frequencies above the natural frequencies of the building-foundation systems.

Anomalous dearth of paleo-earthquakes in the last century, *David D. Jackson* (Poster 013)

The third Uniform California Earthquake Rupture Forecast (UCERF3), relies on reported dates of observed paleo-seismic displacements at 31 sites on 13 named faults in California. However, there is a problem: recorded paleo-seismic events ceased at about the beginning of the instrumental seismic era.

The reported event rates for the ensemble of 31 sites sums to about 0.1 per year. Allowing generously for occurrences of earthquakes that rupture multiple sites simultaneously, the event rate is on the order of 0.04 per year. Yet the most recent paleo-event date is 1910. Such a long open interval would be extremely unlikely for a Poisson process with that rate. Quasi-periodic behavior for the whole ensemble would make the discrepancy worse, as would quasi-period behavior at individual sites using the parameters in the report.

MEETING ABSTRACTS

Possible explanations for the discrepancy include (1) extreme luck, (2) unexplained regional interaction amongst faults, or (3) mistaken identification of near-surface displacements as evidence of large earthquakes. The first can be rejected with 99% confidence. There is no evidence for the second in the pre-1910 paleo-seismic history nor in any theoretical models yet published. The third could explain the observed quiescence because mistaken identity would be prevented by instrumental seismic data.

Characterization of dynamic soil properties and stratigraphy at Heathcote valley, New Zealand, for simulation of 3D valley effects, Seokho Jeong, Brendon A. Bradley, Christopher R. McGann, and Gregory P. De Pascale (Poster 048)

This poster presents a summary of our ongoing effort in developing a 3D representation of the stratigraphy—including volcanic rock interface—and dynamic soil properties at Heathcote valley, a suburb of Christchurch, New Zealand, where we suspect basin-diffracted Rayleigh waves played a significant role in amplifying the ground motion intensity during the 2010-2011 Canterbury earthquake sequence. The strong motion station at Heathcote Valley School (HVSC) recorded extremely high peak ground accelerations (2.21g vertical and 1.41g horizontal) during the February 2011 Christchurch earthquake; ground motions recorded at HVSC in numerous other events also exhibit consistently higher intensities compared with nearby strong motion stations.

We have developed a complete representation of the soil stratigraphy and constitutive characteristics of Heathcote valley necessary for detailed 3D site response simulation, synthesizing data obtained from seismic cone penetration tests (sCPT), active source multichannel analyses of surface wave (MASW), and seismic refraction tomography, performed in numerous locations within the valley. We also used our knowledge of local geology for estimating constraints on inversion parameters and velocities of bedrock. Our model provides shear and compressional wave velocity and density of colluvium sediments across the valley as function of position vector; we plan to approximate the inelastic constitutive behavior of soils based on its elastic properties, obtained from seismic testings, and shear strength estimated from CPT resistance readings. We also delineated the boundary of the rock outcrop utilizing digital elevation models and satellite imagery, while the bedrock topography beneath colluvium sediments is approximated from CPT refusal depths and MASW results. While velocities of bedrock are largely estimated based on the knowledge of local geology, the velocities of shallow weathered rocks are partly resolved with MASW results.

We have planned a series of 2D and 3D site response simulations, utilizing our model at Heathcote valley. We expect comparison of simulated ground motions with recorded ground motions will offer a valuable case study, which elucidates the causes of high intensity ground motions observed at HVSC during the 2010-2011 Canterbury earthquake sequence.

Long-term fault behavior at the seismic-aseismic transition: space-time evolution of microseismicity and depth extent of earthquake rupture, Junle Jiang and Nadia Lapusta (Poster 127)

What controls the fault behavior at the seismic-aseismic transition? Natural faults feature depth-dependent frictional, hydraulic, and structural properties and local heterogeneities. Observationally, faults are separated into seismogenic layers (SL) and deeper creeping extensions based on either microseismicity or inferred locking depth. Slip in large earthquakes is often assumed to be limited to the SL. Physically, this separation can be explained by transition, at slow slip rates, from rate-weakening (RW) to rate-strengthening (RS) behavior. However, as revealed in experimental and theoretical studies, enhanced weakening during rapid earthquake slip - e.g., due to thermal pressurization (TP) of pore fluids - may be critical to rupture propagation. The extent of such weakening need not coincide with the SL.

Using observations of microseismicity and several recent major earthquakes, we show that different behaviors are observed for the space-time evolution of microseismicity and the depth extent of mainshock coseismic slip: (1) depth of microseismicity unaffected by mainshock (2004 Parkfield); (2) sudden increase and gradual decrease of aftershock depth with overlapping mainshock slip (1989 Loma Prieta); (3) elimination

of microseismicity at the bottom of the SL with deeper coseismic slip (1999 Izmit and 2002 Denali).

To understand the physical reasons behind such differences, we use 3D fault models governed by rate-and-state friction with temperature and pore pressure evolution to study the long-term behavior of faults with realistic depth-dependent permeability and shear-zone width. Competition between the two properties determines the depth dependence of coseismic weakening due to TP. We find that earthquake ruptures can penetrate below the traditionally defined SL due to TP. Microseismicity patterns at the bottom of the SL change in response to the depth extent of earthquake penetration. Our models can explain the observed relation between microseismicity patterns and coseismic slip, potentially allowing for identification of deeper penetration in recent events. Based on fault properties, the rate of change in locking depth in the post- and inter-seismic period could be predicted, placing constraints on the depth limit of the previous deeper events. The behavior of large ruptures, including their depth extent, varies along strike, even though the fault properties are uniform along strike, leading to complexities in the earthquake sequences.

Seasonal stress loading and periodic seismicity in California, Christopher W. Johnson, Roland Burgmann, and Pierre Dutilleul (Poster 103)

Seasonal modulations in California seismicity rates have been shown to correlate with low amplitude stress perturbations (<5kPa) attributed to changes in atmosphere pressure or hydrospheric surface loading. We examine earthquake catalog data encompassing the San Andreas Fault (SAF) section near Parkfield and the Sierra Nevada - Eastern California shear zone (SN-ECSZ) for significant periodicities using a multi-frequency periodogram analysis. The analysis is performed using original and declustered data sets. The declustering is done with a nearest neighbor algorithm and a stochastic ETAS algorithm. Both methods are utilized so we can resolve the influence of each algorithm with respect to the resolved periodicities. We find annual periods in the SAF data that agree with previous studies, which indicates a hydrologic forcing is responsible for this periodicity. The SN-ECSZ seismicity indicates a significant period of 14 months and may suggest an Earth pole-tide mechanism. In order to further test the significance of these observed periodicities we are exploring mechanical models to resolve changes in the stress field from periodic surface loads. We are testing the loading models in the Lake Shasta region which experiences a seasonal loading effect modulated by changes in lake level. Data is obtained from PBO operated GPS solutions, daily tide gauge measurements of lake level, and the ANSS catalog. We compute the surface displacements and subsurface stress resulting from the seasonal lake level variations and compare these models with the GPS time series and seismicity levels in the region. Analysis for our Lake Shasta case study allows us to assess if seismicity varies in phase with a periodic subsurface stress change on active faults.

Geodetic constraints on shortening, uplift, and fault slip across the Ventura Basin, Kaj M. Johnson, William C. Hammond, and Reed Burgette (Poster 227)

The Ventura Special Fault Study Area (SFA) project seeks a multidisciplinary approach to explore the potential for large, multi-segment ruptures on thrust faults in the Ventura Basin. The far-field, regional loading rate constrained by geodetic data is a critical component to this multidisciplinary study. In a separate presentation (see Hammond et al., 2014 SCEC abstract), we combine four geodetic measurements (GPS, InSAR, leveling, tide gauge) to generate a vertical velocity field for the Ventura Basin region. Here, this vertical field is combined with the previously published horizontal GPS-derived velocity field (UCERF3, CMM4) to constrain regional kinematic models of present-day deformation rates. We model the present-day horizontal and vertical fields, and the long-term, geologic surface uplift rates using a plate model in which faults are forced to slip in an elastic plate under gravitational restoring forces. Fault slip rates are constrained by published geologic slip rates as well as the UCERF3 geologic slip model. Monte Carlo inversions are conducted to produce ranges of slip rates consistent with data. Near Ventura, the sum of reverse slip across the Mission Ridge, Oak Ridge, Red Mountain and Ventura faults must be at least 12 mm/yr to match the ~8 mm/yr of observed horizontal shortening across the Ventura Basin. This fault slip produces up to several mm/yr of present-day subsidence in the Ventura Basin and 1-3 mm/yr of present-day uplift of the Santa Ynez

Mountains, generally consistent with geodetic observations. The model predicts 1-2 mm/yr of long-term surface uplift (integrated over multiple earthquake cycles) that can be compared with rates determined from uplifted marine terraces.

Using the B4 LiDAR dataset to constrain uplift across the San Gorgonio Pass Fault Zone, Kaitlyn L. Jones and Doug Yule (Poster 280)

The San Andreas Fault system appears to lose about 50% of its slip rate as it enters the San Gorgonio Pass. For example, strike-slip sections outside of the pass region move at ~15 mm/yr (McGill et al., 2012; Behr et al., 2010) whereas thrust-dominated sections in the pass move at ~7 mm/yr in (Yule et al., this meeting) Understanding how slip varies along fault strike could help clarify how slip is transferred through the structural complexity at San Gorgonio Pass. To address this topic, we have begun to study the B4 LiDAR data in San Gorgonio Pass to measure scarp heights across entire strike length of the San Gorgonio Pass Fault zone (SGFPZ) from near Calimesa on the west to Whitewater Canyon on the east. Using QT Modeler and Google Earth we have begun to measure and estimate the vertical separations of a variety of late Pleistocene and Holocene alluvial terraces across SGFPZ splays. Preliminary results of the study show that vertical displacements across the faults fall into several "bins" that range in offset. Small scale offsets range from 3 to 20 meters. Large-scale offsets are 100 meters and above and middle scale offsets range from 30 to 80 meters. These offsets clearly document significant slip over the last ~150,000 yrs and could constrain slip rates across the zone if ages can be determined for the terraces. Age dating and field mapping combined with the data from the B4 LiDAR can help answer the questions about slip transfer and rates through San Gorgonio Pass.

Improving the density of GPS velocities in southern California by resurveying single occupation sites, Lisa Jose, Gareth Funning, John Conrad, and Michael Floyd (Poster 224)

While the density of continuous GPS stations in southern California has greatly improved in the past decade, several areas of interest are lacking GPS coverage. We identified three such areas – the Ventura basin, the northern Elsinore fault, and the northern Mojave Desert – as areas where many campaign sites have as few as one previous survey measurement available in publicly available GPS archives. Revisiting these sites and obtaining new GPS data would thus allow us to obtain new velocity measurements and potentially improve our understanding of the deformation occurring in these areas of interest.

Before starting each survey campaign, we determined the stability and ease of access for each target site using NGS data sheets and reported site descriptions and photographs from geocachers. These online resources also provided us with adequate information about the location of each benchmark to make the process of finding the benchmarks more efficient. Of the 54 sites we looked for, we found 32 and occupied 21. An additional 5 benchmarks that were unknown to us were found and 2 of those found were measured. Each site was measured using survey-grade GPS equipment for a minimum of eight hours each. Some previously unmeasured sites were also selected in order for future campaigns in these areas to have denser GPS coverage, as well as an increased number of velocity measurements.

Precise site positions in the ITRF 2008 reference frame were obtained for both new and existing data using the GAMIT processing software. Velocities for these sites were estimated, and rotated into a fixed North America reference frame using the GLOBK software. In total, 9 new velocity estimates were produced, and velocity estimates were updated at 5 existing sites. These data are being prepared for archiving in the UNAVCO Campaign Data archive, so that they may be incorporated in the SCEC Community Geodetic Model in the future.

An Automatic P-wave Onset Time Detector, Erol Kalkan (Poster 159)

Since the 1980s, numerous techniques have been proposed for detecting and picking arrivals of different seismic waves. The conventional picking algorithm computes a running-window energy ratio of the short-term average to the long-term average (STA/LTA) of the seismic data. This technique also requires predefined or dynamically identified threshold settings. For the common case of a low signal-to-noise ratio (SNR), the conventional method is not sufficiently effective at identifying P-wave

onset. Recent techniques based on the cross-correlation of the energy ratios computed by the conventional method promise superior detection and pick accuracy. Presented here is a new technique for automated detection of P-wave onset in single-component ground motion acceleration or broadband velocity records without requiring any site-specific or magnitude dependent threshold settings. This algorithm ("PWDETECTOR" henceforth) transfers the signal into a response domain of a linear-elastic fixed-base single-degree-of-freedom (SDF) system with viscous damping, and then tracks the rate of change (power) of dissipated damping energy. The SDF system has a very short natural period and a correspondingly high resonant frequency, which is higher than most frequencies in a seismic wave. It also has a high damping ratio (or fraction of critical damping) $\zeta = 0.6$ similar to the short period seismometer, which are particularly used to study body waves. The period and damping parameters selected return this SDF system to the equilibrium position quickly without free vibration. In this way, the input energy imparted to the system is dissipated in a greater amount by hysteretic response and viscous damping. The damping energy yields a smooth dissipation function over time. It is zero in the beginning of the signal, near zero before the P-wave arrival, and builds up rapidly following the P-wave arrival. Thus, it is a convenient metric to track and detect the P-wave onset even in signals with low SNR. The PWDETECTOR detects P-wave onset time within seconds. Its performance is compared with the picking technique of Lomax et al. (2012) based on STA/LTA, and the picking method of Maeda (1985) that finds first P-wave arrival using the Akaike Information Criterion. A large set of ground motion records with various intensities obtained by a number of strong motion observation networks is used for testing.

Modeling seismic hazard and risk in Mexico: Effects of catalog declustering assumptions, Deborah L. Kane and Marleen Nyst (Poster 164)

Earthquake hazard and risk models often assume that earthquake rates can be represented by a stationary Poisson process, and that aftershocks observed in historical seismicity catalogs represent a deviation from stationarity that must be corrected before earthquake rates are estimated. Algorithms for classifying individual earthquakes as independent mainshocks or as aftershocks vary widely, and analysis of a single catalog can produce considerably different earthquake rates depending on the declustering method implemented. As these rates are propagated through hazard and risk models, the modeled results will vary due to the assumptions implied by these choices.

In Mexico, approximately 70% of the modeled average annual loss is attributed to subduction zone sources where rates are primarily derived from large magnitude historical earthquakes. Most of the remaining ~30% of average annual loss is due to country-wide modeled background seismicity. These rates are derived using a historical catalog spanning a wider range of magnitudes and the choice of declustering approach plays a much greater role than for the subduction zone sources. We use an earthquake catalog from Mexico (1577 – 2013, Mw > 3.5) to explore and quantify the subsequent effects on hazard and risk introduced by these model assumptions.

Finite Element Simulation of Earthquakes with Coupling Tsunamis in Large Domains—A Case Study of the 2011 Tohoku-Oki Earthquake and Tsunami, Haydar Karaoglu and Jacobo Bielak (Poster 088)

Seaquakes and tsunamis are usually coupled in nature. This is especially evident around the subduction zones where most of the top ten strongest earthquakes have been recorded in the last century.

Addressing the coupled nature of the two phenomena requires concurrent simulations. Accordingly, this study deals with the simulation of strongly-coupled subduction zone earthquakes, with a focus on the generation of tsunami waves.

We present an application to the 2011 Tohoku-Oki earthquake and tsunami employing a multi-system finite element method for the elastoacoustic problem. In the past, we have reported on the simulation capabilities of Hercules, our finite element tool, for earthquake scenarios such as ShakeOut and Chino-Hills using ideal anelastic material models with kinematic faulting. With the latest improvements we have introduced

MEETING ABSTRACTS

into Hercules, we can now incorporate oceans and the attendant gravity waves into our three-dimensional simulations.

We examine the relationship between the fault rupture, the generation of the tsunami, and the ocean's effects on the propagation of seismic waves through the solid and acoustic media. Additionally, we clarify the validity of common assumptions made for the tsunami generation mechanism with classical tsunami simulation methods. While our focus is on the physical interpretation of the results and its comparison with observations, we also report on the current understanding of the geologic structure of the Japan Trench, computing resources, and the numerical method.

Time-dependent model of aseismic slip on the Central San Andreas Fault from InSAR time series and repeating earthquakes, *Mostafa Khoshmanesh, Manoochehr Shirzaei, and Robert Nadeau* (Poster 099)

The Central segment of the San Andreas Fault (CSAF) is characterized by a nearly continuous right-lateral aseismic slip. Geodetic observations of surface deformation along CSAF indicate an interseismic strain accumulation with a rate of about 10 mm/yr. The creep rates obtained using Characteristic Repeating Earthquakes (CREs) show pulses of creep, affecting most of the CSAF, suggesting spatiotemporal variability of seismic hazard. Therefore, a high resolution time-dependent model of creep on the CSAF can greatly enhance the knowledge of aseismic and seismic faulting processes as well as the seismic hazard estimates.

We used InSAR surface deformation time series in conjunction with observations of fault creep obtained from CREs. The SAR data set includes C-band scenes acquired by the ERS-2 and Envisat satellites during period 2003-2011, comprising 46 images, resulted in about 150 interferograms. Within the same observation period, the CRE data set includes more than 630 repeating sequences, with an average of 8 events per each set. Understanding the spatiotemporal distribution of creep, we implement a time-dependent modeling scheme, allowing us to jointly invert the surface deformation time series and CRE estimates of the fault creep.

The distribution of the obtained creep rate on the CSAF includes features similar to that reported in earlier works. The map of long-term slip rate reveals that fastest creep rate occurs at the central part of CSAF with an average rate of 27 mm/yr, which is less than the long-term shearing rate. Moving northwestward, the slip rate gradually drops to less than half of its long-term rate. The spatiotemporal map of the creep includes unique features such as afterslip due to the 2004 Parkfield earthquake affecting the southeastern part of the CSAF and the clear evidence of creep pulsing along the strike and depth of the CSAF with a period of 1.5 to 2 years. Considering 34.5 mm/yr as the long-term shearing rate, the zone of afterslip is characterized by relaxation time of about 16.35 years. The moment accumulation rate due to slip deficit is between 4.34×10^{17} and 4.51×10^{17} Nm/yr, which is equivalent to a magnitude 5.6-5.7 earthquake. Considering the contribution of afterslip due to the 2004 Parkfield earthquake in releasing the geodetic moment on the CSAF, the moment deficit drops to between 3.62×10^{17} and 3.82×10^{17} Nm/yr, which is equivalent to a magnitude 5.6 earthquake.

Sensitivity of Ground Motion Simulation Validation to Signal Processing and GOF Criteria, *Naeem Khoshnevis and Ricardo Taborda* (Poster 055)

The validation of ground motion synthetics has received increased attention over the last few years due to advances in physics-based deterministic and hybrid simulation methods. Validation of synthetics is necessary in order to determine whether the available simulation methods and models are capable of faithfully reproducing the characteristics of ground motions from past earthquakes. Since a major use of synthetically generated seismograms is in areas of engineering, some validation methods are based on metrics that are oriented towards satisfying specific characteristics of use in engineering such as response spectrum, duration, peak values, and intensity. Other alternative methods are based on the time-frequency characteristics of the signals themselves. Some of these methods require significant amount of signal processing, which involves filtering of signals in order to assess the quality of the fit between synthetics and data at different frequency bands. This allows one to weight the contribution of different wavelengths in a physically intuitive way, where the low frequencies are given more weight than the higher frequencies. Two particular methods of interest are the goodness-of-fit

(GOF) criteria introduced by Anderson (2004) and Kristekova et al. (2006, 2009). In Anderson's method a suit of ten different metrics are combined for different frequency bands and ground motion components to obtain a final score. In Kristekova et al.'s approach, a wavelet-based analysis is used to quantify the quality of the fit based on amplitude and phase characteristics. We investigate the level of agreement between these two methods for the purpose of validation, and the sensitivity of Anderson's method to the manipulation of the signals. We discuss the implications that the choice of different filtering parameters has on the results for a simulation of the 2008 Chino Hills earthquake, for which we have comparisons between synthetics and data in more than 300 stations. Our analysis shows that different methods and metrics can lead to different interpretations of the results, which can vary significantly.

Spatial Partitioning of Icequakes on Gornergletscher, Switzerland, *Debi L. Kilb and Fabian Walter* (Poster 175)

We examine the temporal and spatial signature of surface icequake activity (several thousand a day) on Gornergletscher, Switzerland, in relation to drainages of a nearby glacier-dammed lake in the summers of 2004, 2006 and 2007. We observed three different kinds of lake drainages: rapid subglacial (2004), slow supraglacial (2006) and a combination supraglacial, subglacial and englacial (2007). The occurrence of three different drainage mechanisms provides a unique opportunity to study the interaction between glacier hydraulics and seismicity. We monitored glacier seismicity with high-density arrays of surface seismometers (apertures of approximately 300-400m, 8-24 3-component sensors). Using a Rayleigh wave coherence surface icequake location technique [Roux et al., 2010] we locate ~20-40% of the icequake catalog. Of the over ~3000 icequakes that locate within the footprint of the network each summer, a large majority constitute fractures and crevasses opening near the glacier surface. Within each summer season we track the spatial and temporal behavior of icequakes and assess what features repeat season to season. Surprisingly, only the 2004 data show a strong increase in icequake productivity coincident with lake drainage. For the other years (2006 and 2007) there is no correlation between lake drainage and icequake productivity. One pattern that remains consistent through each summer recording period is a tendency for icequakes to occur in the northeast (southwest) portion of our study region in the daytime (nighttime). The absence of a strong correlation between rupture time-of-day and waveform amplitude suggests these results are not artifacts of detectability. We also established that this dichotomy is sustainable and not dominated by individual bursts of activity that last only a few days.

Vital Signs of the Planet: Southern California Educators Contribute to Crustal Deformation Studies Within San Bernardino and Riverside Counties, *Mark Kline, Sally McGill, Luis Cortes, Demoree Deocales, Robert de Groot, Abigail Elvis, Luis Gomez, Dan Keck, Robert Kirkwood, Hernan Lopez, Morris Martinez, Marc Moya, Lindsay Rosenbaum, Bernadette Vargas, Seth Wallace, and Katherine Williams* (Poster 225)

In conjunction with California State University, San Bernardino, Inland Empire high school teachers used GPS to monitor movement along the San Andreas and San Jacinto faults within the Inland Empire, San Bernardino Mountains and high desert regions of Southern California since 2002. Stations observed in 2014 were selected from those that previously had relatively poorly constrained time series, so as to contribute useful new velocity constraints for use by the SCEC community and others. Procedures for the study included setting up a tripod (or spike mount), antenna and receiver over existing survey monuments for a 10 hour period each day for 4 days. GPS data were processed at the University of Arizona and benchmark positions were compared to those in previous years. Time series graphs were used to estimate the north, east and vertical velocities of each site.

Velocities for our sites were combined with velocities from SCEC's Crustal Motion Model version 4 (Shen et al. 2011) and with velocities from continuous GPS stations archived at the Plate Boundary Observatory. One-dimensional elastic modeling of the combined data set was used to infer fault slip rates within a transect across the plate boundary through the San Bernardino Mountains.

Results indicate that the combined slip rate of the 15 faults within our transect is 44.7-46 mm/yr. The San Andreas (SAF) and San Jacinto (SJF)

faults have the highest rate of movement with a combined slip rate of 16-20 mm/yr. This is substantially less than the published 35 mm/yr slip rate of the SAF alone in central California. Nonetheless our inferred slip rates for the SAF and SJF are consistent with previously published slip rates for these faults in southern California over late Quaternary time scales. The two faults are so close together within our transect that their slip rates are strongly inversely related. Our best-fitting model apportioned slip of 14 mm/yr for the SJF and 6 mm/yr for the SAF, but models with SAF slipping 0-12 mm/yr and SJF slipping 4-20 mm/yr also fit the observed site velocities relatively well.

Continental shelf morphology and stratigraphy offshore San Onofre, CA: the interplay between eustasy and sediment supply, Shannon A. Klotsko, Neal W. Driscoll, Graham M. Kent, and Daniel S. Brothers (Poster 204)

New high-resolution CHIRP seismic data acquired offshore San Onofre, southern California reveal that shelf sediment distribution and thickness are primarily controlled by eustatic sea level rise and sediment supply. Throughout the majority of the study region, a highly defined abrasion platform and associated shoreline cutoff are observed from ~72 to 53 m depth. These appear to be formed between Melt Water Pulse 1A and Melt Water Pulse 1B, when the rate of sea-level rise was lower. There are three distinct sediment units observed in the seismic data: an infilling lag deposit, a midshelf lag deposit, and modern deposition. The deepest unit infills the abrasion platform formed by wave-base erosion and pinches out landward against the shore-line cutoff. The midshelf unit is material eroded from a shallower abrasion platform that thins seaward by downlap and landward by onlap. The youngest unit is acoustically transparent and records modern deposition. Faults in the study area do not appear to offset the transgressive surface. The Newport Inglewood-Rose Canyon fault system is active in other regions to the south (e.g., La Jolla) and offsets the transgressive surface and creates seafloor relief. Several shoals observed along the transgressive surface could record minor deformation in the study area. Nevertheless, our preferred interpretation is the shoals are regions more resistant to erosion. The Crisitanitos fault zone also causes a shoaling of the transgressive surface. This is also likely from resistant antecedent topography due to compression on the fault. The Cristianitos fault zone was previously defined as a down-to-the-north normal fault, but the folding and faulting architecture imaged in the CHIRP data are more consistent with a strike-slip fault with a down to the northwest dip-slip component. A third area of shoaling is observed off of San Mateo and San Onofre creeks. This shoaling has a constructional component interpreted to be a relic beach or spit structure. Legacy USGS mini sparker data were used to map transgressive surface regionally and to define the deeper shelf structure.

The Community Seismic Network, Monica D. Kohler, Robert W. Clayton, Anthony Massari, Thomas H. Heaton, Richard Guy, Mani Chandry, Julian Bunn, Leif Strand, and Santiago Arrangoiz (Poster 057)

The Community Seismic Network (CSN) involves participants from communities at large to install low-cost accelerometers in houses and office buildings for assessment of shaking intensity due to earthquakes. The CSN is now in its third year of operation and has expanded to 400 stations in the Los Angeles region. Elements of CSN include: i) Distributed computing – the sensors themselves are smart sensors that perform the basic detection and size estimation in the onboard computers and send the results immediately (without packetization latency) to the central facility; ii) Cloud computing – the central facility is housed in the cloud, which means it is more robust than a local site. It has expandable computing resources available so that it can operate with minimal resources during quiet times but still be able to exploit a very large computing facility during an earthquake; iii) Low-cost/low-maintenance sensors – the MEMS sensors are capable of staying on-scale to $\pm 2g$, and can measure events in the Los Angeles Basin as low as magnitude 3. We have also instrumented a number of buildings with the goal of determining the state of health of these structures before and after they have been shaken. Linear-elastic motion is computed for every floor of tall buildings using only earthquake records from a single floor and an analytical dynamic model for each building. Visualization models that map the instrumented buildings' responses have been constructed using Google SketchUp and an associated plug-in to Matlab with recorded shaking data. In one instrumented, 15-story, steel, moment-frame building, the

sensors distributed two per floor show body waves propagating in the building during the 1/15/14 M4.4 Fontana, 2/8/14 M3.0 Hollywood, 3/17/14 M4.4 Encino, and 3/29/14 M5.1 La Habra CA earthquakes. Sensors in a 52-story, steel, moment-and-brace frame building, which we plan to instrument with two sensors per floor, show the modes of the building down to the fundamental mode at 5.5 s due to shaking from the La Habra, CA earthquake. The CSN uses a number of technologies that will likely be important in building future, dense, low-cost networks.

Preliminary simulations of the interaction between of pore fluids and seismicity with RSQSim, Kayla A. Kroll, James H. Dieterich, and Keith B. Richards-Dinger (Poster 207)

A new tool has been developed to model seismic events resulting from increases in pore pressure related to the injection of fluids. We have coupled the 3D, physics-based earthquake simulator, RSQSim, to a reservoir model that calculates pressure changes that reduce effective stress and drive the occurrence of earthquakes. RSQSim is a computer code that generates long catalogs of seismicity based on stress changes due to fault interaction. The rate- and state- constitutive laws that govern the deterministic fault behavior in RSQSim have been shown to reproduce the spatio-temporal clustering of seismicity that is observed in foreshock and aftershock sequences. The computational efficiency of RSQSim allows for multiple simulations to systematically explore the parameters that control induced seismicity. Additionally, the simulations can contribute to the formalization of optimal injection parameters designed to minimize seismic hazard, provide physics-based statistical data from which stop-light procedures can be developed, and aid in hazard assessments of a given site under specified injection locations, rates, and volumes.

Here, we present preliminary results from simulations of seismicity resulting from effective stress histories due to injection. The simulations incorporate optimally oriented, single isolated faults and simple fault systems. Several scenarios are modeled which include variable injection rates, well locations, and background stressing rates. Additionally, the sensitivity of induced seismicity to initial stress conditions is investigated by initiating injection at different time periods in the system's earthquake cycle (i.e. at varying time intervals before the next full-fault rupture). From these simulations, we determine the maximum magnitude given the specified injection parameters, the effect of injection rates on Gutenberg-Richter b-values, and changes in injection induced seismicity rate compared to that of tectonic seismicity. We also investigate the spatial and temporal distribution of seismicity after injection ceases to determine the seismicity decay rate and the likelihood of a larger earthquake occurring, as has been observed at some industrial injection localities.

Kappa (κ) estimates and origins: results from a downhole array, Olga-Joan Ktenidou, Stephane Drouet, Fabrice Cotton, and Norman Abrahamson (Poster 201)

At high frequencies, the acceleration spectral amplitude decreases rapidly. Anderson and Hough (BSSA,1984) modeled this with the spectral decay factor, κ , whose site component, κ_0 , is used widely today in ground motion prediction and simulation. In this study we estimate κ for the EUROSEISTEST valley, a test site with a strong motion array of 14 surface and 6 downhole stations. Site conditions range from $V_{s30}=190-1900$ m/s. Our goal is three-fold. First, we use two different approaches: the acceleration spectrum (AS), and the transfer function (TF) approach. For the AS approach, we separate the site and path (regional Q attenuation) components of κ . We then compare results from the two approaches. κ_0 results are similar and the differences between the methods provide an estimate of epistemic uncertainty on κ_0 . The regional Q results are also similar, and in agreement with independent crustal attenuation studies. Second, we use our knowledge of the geological profile and material properties to examine the correlation of κ_0 with various site characterization parameters. κ_0 correlates to V_{s30} as expected, though the scatter is large. It also correlates with the resonant frequency and depth to bedrock, indicating a relation to the geological structure down to 400 m. Thus, correlations with the entire soil column may complement the usual correlations of κ_0 with the first 30 m. Third, we use results to improve our understanding of κ and propose two new notions regarding its physics. On the one hand, and contrary to existing correlations, we observe that κ_0 stabilizes for high V_s values. This may indicate the

MEETING ABSTRACTS

existence of regional minima for rock κ_0 . If so, we propose that borehole measurements (almost never used up to now) may be useful in determining them. On the other hand, we find that material damping, as expressed through travel times, may not suffice to account for the total κ_0 measured at the surface. The uncertainty in the damping does not justify this discrepancy, because our values are well constrained from both lab and in situ tests. We propose that additional attenuation may be due to scattering from small-scale variability in the profile. If this is so, geotechnical damping measurements may not suffice to infer the overall crustal attenuation under a site, but starting with a borehole value and adding soil damping could define a lower bound for site-specific κ_0 . More precise estimation necessitates site instrumentation.

Predicting Offshore Swarm Rate Changes by Volumetric Strain Changes in Izu Peninsula, Japan, Takao Kumazawa, Yosihiko Ogata, Youichi Kimura, Kenji Maeda, and Akio Kobayashi (Poster Q27)

The eastern offshore of Izu peninsula is one of the well known volcanic active regions in Japan, where magma intrusions have been observed several times since 1980s monitored by strain-meters located nearby. Major swarm activities have been synchronously associated with coseismic and preseismic significant sizes of a volumetric strain changes (Earthquake Research Committee, 2010). We investigated the background seismicity changes during these earthquake swarms using the nonstationary ETAS model (Kumazawa and Ogata, 2013), and have found the followings. The modified volumetric strain change data by removing the effect of earth tides and precipitation as well as removing coseismic jumps have much higher cross-correlations to the background rates of the ETAS model than to the whole seismicity rate change of the ETAS, and further the strain changes precede the background seismicity by lag of about a day. This relation suggests an enhanced prediction of earthquakes in this region using volumetric strain measurements. Thus we propose an extended ETAS model where the background seismicity rate is predicted by the time series of preceding volumetric strain changes. Our numerical results for Izu region show consistent outcomes throughout the major swarms in this region.

References

Earthquake Research Committee (2010). Report on "Prediction of seismic activity in the Izu Eastern Region" (in Japanese), <http://www.jishin.go.jp/main/yosoku/izu/index.htm>

Kumazawa, T. and Ogata, Y. (2013). Quantitative description of induced seismic activity before and after the 2011 Tohoku-Oki earthquake by nonstationary ETAS model, *J Geophys. Res.* 118, 6165-6182.

Full-3D Tomography of the Crustal Structure in Southern California Using Earthquake Seismograms and Ambient-Noise Correlagrams, En-Jui Lee, Po Chen, Thomas H. Jordan, Philip J. Maechling, Marine Denolle, and Gregory C. Beroza (Poster 078)

We have constructed a high-resolution model for the Southern California crust, CVM-S4.26, by inverting more than half-a-million waveform-misfit measurements from about 38,000 earthquake seismograms and 12,000 ambient-noise correlagrams. The inversion was initiated with the Southern California Earthquake Center's Community Velocity Model, CVM-S4, and seismograms were simulated using K. Olsen's staggered-grid finite-difference code, AWP-ODC, which was highly optimized for massively parallel computation on supercomputers by Y. Cui et al. We navigated the tomography through 26 iterations, alternating the inversion sequences between the adjoint-wavefield (AW) method and the more rapidly converging, but more data-intensive, scattering-integral (SI) method. Earthquake source errors were reduced at various stages of the tomographic navigation by inverting the waveform data for the earthquake centroid-moment tensors. All inversions were done on the Mira supercomputer of the Argonne Leadership Computing Facility. The resulting model, CVM-S4.26, is consistent with independent observations, such as high-resolution 2D refraction surveys and Bouguer gravity data. Many of the high-contrast features of CVM-S4.26 conform to known fault structures and other geological constraints not applied in the inversions. We have conducted several other validation experiments, including checking the model against a large number (>28,000) of seismograms not used in the inversions. We illustrate this consistency with the excellent fits at low frequencies (≤ 0.2 Hz) to three-component seismograms recorded

throughout Southern California from the 17 Mar 2014 Encino (MW4.4) and 29 Mar 2014 La Habra (MW5.1) earthquakes, and we show these fits to be much better than those obtained by two community velocity models in current use, CVM-S4 and CVM-H11.9. We conclude by describing some of the novel features of the CVM-S4.26 model, which include unusual velocity reversals in some regions of the mid-crust.

A 3D seismic velocity model of Canterbury, New Zealand for broadband ground motion simulation, Robin L. Lee, Brendon A. Bradley, Francesca C. Ghisetti, Jarg R. Pettinga, Matthew W. Hughes, and Ethan M. Thomson (Poster 071)

This poster presents the on-going development of a new 3D seismic velocity model of Canterbury, New Zealand. The intention of the model is to provide the 3D crustal structure in the region at multiple length scales for seismic wave propagation simulations, such as broadband ground motion and shallow site response analyses related to understanding the ground motions and site responses during the 2010-2011 Canterbury earthquakes. Basement rock properties are controlled by 3D regional tomographic data. Basement depth and shallower sedimentary and volcanic rock horizons are calculated based on the reinterpretation of a relatively comprehensive network of seismic reflection surveys from seven different campaigns over the past 50 years, as well as point constraints across an array of petroleum industry drill holes. Particular attention is also given to the representation of shallow ($z < 250$ m) stratigraphy in the model. Seismic velocities are obtained from seismic reflection processing (for Vp) and also recently performed active and passive surface analyses (for Vs). Over 1,700 water wells in the region are used to constrain the complex inter-bedded stratigraphy (gravels, sands, silts, organics etc) near the coastline, including beneath urban Christchurch, which has resulted from fluvial deposition and marine regression and transgression in the Quaternary. For the near-surface Springston and Christchurch Formations in the Christchurch urban area ($z < 50$ m), high-spatial resolution seismic velocities (including Vs30) were obtained from over 15,000 cone penetration tests combined with a recently developed CPT-Vs correlation.

Evidence of Coseismic Subsidence Along the Newport-Inglewood Fault Zone During the Late Holocene, Robert J. Leeper, Brady P. Rhodes, Matthew E. Kirby, Katherine M. Scharer, Scott W. Starratt, Eileen Hemphill-Haley, Nicole Bonuso, Behnaz Balmaki, Dylan J. Garcia, and Dliisa O. Creager (Poster 247)

The Seal Beach wetlands (SBW) are located along strike of the Newport-Inglewood fault zone (NIFZ), where fault geometry is poorly understood. However, the fault steps to the right in the SBW, and oil well and seismological studies indicate that the northeast segment of the fault is down-dropped as a result of oblique-normal slip. The location is significant because coseismic subsidence could alter tidal and/or fluvial processes within the SBW. Such a change should be recorded in the stratigraphy by sudden changes in grain size, magnetic susceptibility, and/or diatom assemblages. Based on field observations of 48 reconnaissance gouge cores and multi-proxy analyses of three vibracores and one piston core, we identify four stratigraphic units in the SBW: (1) very fine to fine sand from 426-350 cm; (2) organic-rich mud from 350-225 cm; (3) fine to coarse silt and clay from 225-100 cm; and (4) organic-rich mud with interbedded mud laminae from 100-0 cm. We interpret unit 2 to represent a relic marsh surface that subsided coseismically and was preserved under unit 3. We analyzed 38 sediment samples for diatoms from vibracore SB002VC to test this idea and characterize the depositional environment of stratigraphic units 4, 3, and 2. The diatom data suggest unit 4 is an intertidal deposit, unit 3 is a fresh/slightly brackish water deposit, and unit 2 is an intertidal deposit. Units 2 and 3 are separated by a sharp, irregular contact. Thus, the diatom data and depositional contact from vibracore SB002VC are consistent with a relic marsh surface subsiding abruptly during an earthquake on the NIFZ. As a result of the earthquake, the intertidal environment abruptly changed to an environment dominated by fresh to slightly brackish water. We hypothesize that the earthquake did not result in flooding by seawater because coseismic uplift of the southwest segment of the NIFZ temporarily isolated the SBW from tidal influence. Radiocarbon dates constrain this event to no more than 1957 cal yr BP. Future work will include Cs-137/Pb-210 dating of unit 4 and pollen analysis in units 3 and

2, additional radiocarbon dating and completing grain size analysis of vibracore SB002VC.

Analysis of Micro-Earthquakes in the Sierra Madre-Cucamonga Fault Zone and the Greater Pomona Area as Recorded by a Temporary Seismic Deployment, Jonathan Levario, Celia Pazos, David Nget, and Jascha Polet (Poster 199)

From July to September 2013, we conducted a micro-seismic survey of the Sierra Madre-Cucamonga fault zone and the greater Pomona area. Nine Guralp CMG-6TD seismometers were deployed in the foothills of the San Gabriel Mountains. At the end of the deployment period, our network had detected nearly 400 local earthquakes. Included in this catalog are two M3.7 earthquakes that occurred in the Pomona area. This strike-slip faulting doublet is part of a sequence of tens of events that may connect to the Upland earthquakes along the San Jose fault, which is thought to continue through Cal Poly Pomona campus. To better capture this sequence we moved one of our seismometers to a location directly above the doublet.

The waveform data recorded by our network, together with data from the Southern California Seismic Network (SCSN), was processed in order to (better) locate these earthquakes. We made measurements of P and S wave arrival times and combined these measurements with SCSN arrival time picks. We then used the Hypoinverse software to relocate events already published in the SCSN catalog and to determine the locations for those events not in the SCSN catalog.

Of the 382 events, we did not locate any events on the Sierra Madre-Cucamonga fault transition. However, cross sections of seismicity across the Cucamonga fault indicate that several events may have occurred on this fault. We recorded and located 52 events as part of the Pomona sequence. Other than indirectly by an offset of the water table, the San Jose fault has not previously been observed in this area. Our spatial analysis of the Pomona sequence indicates that these events occurred on a northeast striking and northwest dipping fault, consistent with the San Jose fault.

Using Global Arrays to Study Earthquake Rupture and Detect Earthquakes, Bo Li and Abhijit Ghosh (Poster 271)

The earthquake rupture process is fundamental for our understanding of fault systems and earthquake hazards. It can provide us information about the source properties, fault mechanism, rupture directivity, earth structures, aftershocks, disaster prediction and relief, and more. The back-projection technique is first successfully applied by Ishii et al. (2005) to study earthquake rupture and propagation for the 2004 Sumatra-Andaman earthquake. Thus far, it has been successfully applied to study the rupture process of some large and moderate earthquakes. Compared to the detection by standard location method, higher resolution may also allow the detection of earthquakes. Our preliminary results using the US array for the Apr. 1st 2014 Mw8.2 Iquique earthquake show that the rupture propagated to the northeast of the epicenter and then changed to the northwest. And within the first hour after the mainshock, we detected fifteen aftershocks.

Using Fault-Zone Trapped Waves from Teleseismic Earthquakes to Document Deep Structure of the Calico Fault in Mojave Desert, California, Yong-Gang Li, Elizabeth S. Cochran, Po Chen, and En-Jui Lee (Poster 115)

Fault-zone trapped waves (FZTWs) are observed at a square seismic array consisting of 40 intermediate-period stations deployed in a 1.5 km by 5.5 km grid adjacent to the Calico Fault (CF) in the Mojave Desert, California for teleseismic earthquakes and used to characterize the deep structure of the fault damage zone. In a previous study, inversion of travel times, FZTWs generated by explosions and local earthquakes, and InSAR observations were used to document the seismic velocity structure of the CF zone (Cochran et al., 2009). They found that velocities are reduced to a maximum of ~40% in the center of a 1.5-km-wide compliant zone along the fault strike and extend to at least 5-6 km depth at the array site. To further investigate the deep portion of the CF, we use FZTWs from teleseismic earthquakes recorded by the seismic array, which have great promise to provide unprecedented constraints on the depth extension of fault-zone damage structure. We examine data from 72 M_≥6 teleseismic

earthquakes recorded at the Calico array. We identify FZTWs by their characteristic dominant frequencies, larger amplitudes, and longer wavetrains that start ~5-s after the first-arrivals for stations located within the 1-1.5 km wide compliant zone along the CF strike. FZTWs are prominently observed for teleseismic events with greater source depths and are more difficult to identify in seismograms recorded for shallow source teleseismic events because strong surface waves, pervasive at all stations, dominate the wavetrain. We suggest that the observed FZTWs are formed by P- to S- converted phases that encounter the bottom of the low-velocity compliant zone on the CF at the Moho (~30-km depth beneath Mojave Desert). The FZTWs from teleseismic earthquakes consistently show longer wavetrains (~12-s duration) than those (3-8-s duration) recorded at the same stations for local earthquakes at shallow depths, indicating that the low-velocity compliant zone along the CF likely extends throughout much of the seismogenic zone. FZTWs are likely formed by cracking and yielding of rocks during individual ruptures as part of the development of long-lived fault systems. We use the shallow fault damage structure obtained in the previous study (Cochran et al., 2009) to simulate observed FZTWs for teleseismic events as plane waves from Moho depths incident to the bottom of the CF using a waveguide model. We are able to achieve improved constraints on the depth extension of the low-velocity damage zones along the CF.

Variations of Seismic Anisotropy along the San Jacinto Fault Zone, Southern California, Zefeng Li, Zhigang Peng, Zachary Ross, Frank Vernon, and Yehuda Ben-Zion (Poster 187)

Shear waves splitting (SWS) occurs when polarized shear waves enter an anisotropic medium, and hence provide useful information about the polarization directions and anisotropic intensity. In this study we examine crustal anisotropy in the San Jacinto Fault Zone (SJFZ), using seismic data recorded by five small-aperture linear arrays (BB, RA, SGB, DW and JF). Each array contains 7-12 stations with a length at 180-450 m, straddling different segments of the SJFZ, including the Anza seismic gap. We compute delay times and fast directions using the MFAST code (Savage et al., 2010), which is based on the method of Silver and Chan (1991) and cluster analysis (Teanby et al, 2004). Due to the large volume of the data set, we adopt an iterative predict-and-search scheme to pick S waves automatically. Preliminary results from the 2012-2013 data on five linear arrays show that the fast directions are generally around the north, indicating that the regional stress is likely the dominant mechanism for the anisotropy in the study area. However, we observe systematic variations of fast directions across the SJFZ on the RA, DW, JF, SGB array. For example, from the RA01 on the SW to the RA11 on the NE, the fast directions change from NNE to NNW. Given the small array apertures, such variations likely result from shallow fault structures beneath the arrays, e.g., spatial changes of crack density and preferential alignment. In comparison, the BB array shows strong scattering of the fast direction patterns, which might be resulted from the complex subsurface structure and/or stress state. To fully explore the anisotropy patterns in the SJFZ, we plan to expand the SWS analysis to all available seismic data. Updated results will be presented in the meeting.

Shear flow of angular grains: acoustic effects and non-monotonic rate dependence of volume, Charles K. Lieou, Ahmed E. Elbanna, James S. Langer, and Jean M. Carlson (Poster 110)

Naturally-occurring granular materials often consist of angular particles whose shape and frictional characteristics may have important implications on macroscopic flow rheology. In this paper, we provide a theoretical account for the peculiar phenomenon of auto-acoustic compaction -- non-monotonic variation of shear band volume with shear rate in angular particles -- recently observed in experiments. Our approach is based on the notion that noise sources in a driven granular material couple its various degrees of freedom and the environment, causing the flow of entropy between them. The grain-scale dynamics is described by the shear-transformation-zone (STZ) theory of granular flow, which accounts for irreversible plastic deformation in terms of localized flow defects whose density is governed by the state of configurational disorder. To model the effects of grain shape and frictional characteristics, we propose an Ising-like internal variable to account for nearest-neighbor grain interlocking and geometric frustration, and interpret the effect of friction as an acoustic noise strength. We show quantitative agreement

MEETING ABSTRACTS

between experimental measurements and theoretical predictions, and propose additional experiments that provide stringent tests on the new theoretical elements.

New observations of fault creep in the Imperial Valley from multi-angle InSAR and GPS, Eric O. Lindsey and Yuri Fialko (Poster 233)

We present new observations of the pattern of fault creep and interseismic deformation in the Imperial Valley, California using a combination of multiple InSAR viewing geometries and survey-mode GPS. We combine more than 100 survey-mode GPS velocities (Crowell et al., 2013) with Envisat InSAR observations from descending tracks 84 and 356 and ascending tracks 77 and 306 (149 total acquisitions), processed using the Stanford Method for Persistent Scatterers (StaMPS) package (Hooper et al., 2007). The result is a dense map of surface velocities across the Imperial fault and surrounding areas. The data suggest that a previously little-known extension of the Superstition Hills fault through the town of El Centro may accommodate a significant portion of the slip previously attributed to the Imperial Fault. We investigate a suite of possible models for the transfer of this slip to the Imperial and Cerro Prieto faults to the south, yielding a range of plausible hazard scenarios. Finally, we compare the geodetic data to models of earthquake cycles with rate- and state-dependent friction to assess the implications for creep depth, moment accumulation rate, and recurrence interval of large events on these faults.

Faulting in anisotropic media: Elastic anisotropy biases estimates of fault depth, Brad P. Lipovsky and Paul Segall (Poster 240)

Measurements of Earth surface deformation near active faults are routinely used to estimate the motion of slip surfaces. The role of elastic anisotropy in such estimates has not previously been quantified. We find that anisotropy introduces a skewing of length scales in the depth direction. This finding may help explain some discrepancies between seismic and geodetic estimates of faulting depth. We present analytical expressions for the displacements in homogeneous and layered anisotropic media. We demonstrate our findings by modeling data from the Imperial Fault, California.

Investigating inter-station attenuation retrieval from ambient seismic noise records on station triplets, Xin Liu, Yehuda Ben-Zion, and Dimitri Zigone (Poster 182)

We study inter-station attenuation from ambient noise cross-correlation functions on linear arrays. Based on derivations on the amplitude decay of ensemble averaged cross-correlation due to attenuation, we form linear least-square inversions for inter-station Q values applied to linear arrays of three stations (triplets). With this method, the background attenuation can be canceled and the site amplification factor is approximated as constant in narrow frequency bands of interest. Synthetic tests are performed to evaluate the effectiveness of the inversion at different scales. Synthetic noise cross-correlation data are generated by a ray-theory-based simulation with heterogeneous attenuation and homogeneous velocity structure. Phase velocity dispersion curves and inter-station attenuation are inverted from synthetic data. This method is applied to triplets from regional arrays and dense linear arrays in the San Jacinto Fault zone, where initial results show attenuation variations across the fault.

Improved imaging of Southern California crustal deformation using InSAR and GPS, Zhen Liu, Paul Lundgren, and Zheng-Kang Shen (Poster 220)

Differential interferometric synthetic aperture radar (InSAR) provides the capability to image surface deformation of plate boundary zones at fine spatial resolution with coarse temporal sampling. More than 18 years of extensive SAR data collection over southern California makes it now possible to generate a long time interval InSAR-based LOS velocity map to examine the resolution of both steady-state and transient deformation processes. As of date, we have performed systematic InSAR time series analysis of crustal deformation in southern California using ~18 yrs ERS-1/2 and Envisat data from all ascending and descending tracks since 1992. For the Envisat data, our results show a new source of temporally correlated ramp drifting error across the range that can significantly affect the resultant time series and mean line-of-sight (LOS) velocity map. Such error source was recently discovered and attributed to long term local

oscillator (LO) frequency drift of Envisat ASAR sensor [Marinkovic & Larsen, 2013]. Correction of such error source, along with other noise sources, proves important to generate accurate InSAR deformation map. We adopt an empirical approach to correct such noise and show that such correction achieves comparable result as the approach that base on a priori GPS model. The RMS misfit between corrected InSAR LOS velocity and CMM4 GPS velocity is less than a few mm/yr. We present the results of the improved analysis to all ascending Envisat tracks. We also revisit our previous observation of long-term transient across Eastern California Shear Zone by combining ERS-1&2 and corrected Envisat SAR data and show such transient are still present in broad spatial extent even after taking into account such time-dependent ramp drifting error.

Recent Developments within the Collaboratory for the Study of Earthquake Predictability, Maria Liukis, Maximilian Werner, Danijel Schorlemmer, John Yu, Philip Maechling, Jeremy Zechar, Thomas H. Jordan, and the CSEP Working Group (Poster 015)

The Collaboratory for the Study of Earthquake Predictability (CSEP) supports a global program to conduct prospective earthquake forecast experiments. There are now CSEP testing centers in California, New Zealand, Japan, and Europe, with 430 models under evaluation.

In this presentation, we describe how the Southern California Earthquake Center (SCEC) testing center has evolved to meet CSEP objectives and we share our experiences in operating the center. The SCEC testing center has been operational since September 1, 2007, and currently hosts 30-minute, 1-day, 3-month, 1-year and 5-year forecasts, both alarm-based and probabilistic, for California, the Western Pacific, and a global testing region. We have reduced testing latency, implemented prototype evaluation of M8 forecasts and currently develop procedures to evaluate externally-hosted forecasts and predictions. These efforts are related to CSEP support of the USGS program in operational earthquake forecasting and a Department of Homeland Security project to register and test external forecast procedures from experts outside seismology. Retrospective experiment for the 2010 Darfield earthquake sequence formed an important addition to the CSEP activities where the predictive skills of physics-based and statistical forecasting models are compared.

We describe the open-source CSEP software that is available to researchers as they develop their forecast models (<http://northridge.usc.edu/trac/csep/wiki/MiniCSEP>). We also discuss applications of CSEP infrastructure to geodetic transient detection and the evaluation of ShakeAlert system for earthquake early warning (EEW), and how CSEP procedures are being adopted for intensity prediction and ground motion prediction experiments.

Increased earthquake rates in the central and eastern US portend higher earthquake hazards, Andrea L. Llenos, Justin L. Rubinstein, William L. Ellsworth, Charles S. Mueller, Andrew J. Michael, Arthur McGarr, Mark D. Petersen, Matthew Weingarten, and Austin A. Holland (Poster 213)

Since 2009 the central and eastern United States has experienced an unprecedented increase in the rate of $M \geq 3$ earthquakes that is unlikely to be due to natural variation. Where the rates have increased so has the seismic hazard, making it important to understand these changes. Areas with significant seismicity increases are limited to areas where oil and gas production take place. By far the largest contributor to the seismicity increase is Oklahoma, where recent studies suggest that these rate changes may be due to fluid injection (e.g., Keranen et al., *Geology*, 2013; *Science*, 2014). Moreover, the area of increased seismicity in northern Oklahoma that began in 2013 coincides with the Mississippi Lime play, where well completions greatly increased the year before the seismicity increase. This suggests a link to oil and gas production either directly or from the disposal of significant amounts of produced water within the play.

For the purpose of assessing the hazard due to these earthquakes, should they be treated differently from natural earthquakes? Previous studies suggest that induced seismicity may differ from natural seismicity in clustering characteristics or frequency-magnitude distributions (e.g., Bachmann et al., *GJI*, 2011; Llenos and Michael, *BSSA*, 2013). These differences could affect time-independent hazard computations, which typically assume that clustering and size distribution remain constant. In Oklahoma, as well as other areas of suspected induced seismicity, we find

that earthquakes since 2009 tend to be considerably more clustered in space and time than before 2009. However differences between various regional and national catalogs leave unclear whether there are significant changes in magnitude distribution.

Whether they are due to natural or industrial causes, the increased earthquake rates in these areas could increase the hazard in ways that are not accounted for in current hazard assessment practice. Clearly the possibility of induced earthquakes needs to be considered in seismic hazard assessments.

Modeling tsunami generation and propagation from an earthquake on the Pitas Point fault, Gabriel C. Lotto and Eric M. Dunham (Poster 178)

The Pitas Point fault is a steeply dipping thrust fault approximately 10 km from the California coastline in the Santa Barbara Channel. It is connected to the Ventura fault on land and likely linked at depth to other regional faults, including the San Cayetano and Red Mountain faults. Geologic evidence suggests that the entire fault system rises in discrete events with 5-10 m of uplift every 400-2400 years, with the most recent event occurring ~800 years ago. Rupture of this magnitude on the Pitas Point fault could generate a strong tsunami that would pose a serious threat to the regional coastline. To better understand the hazard caused by an earthquake on the Pitas Point fault and the subsequent tsunami, we are using a provably stable and accurate high-order finite difference method that can model the full seismic, ocean acoustic, and tsunami wavefield generated by subduction zone earthquakes in two dimensions. Our numerical method uses summation-by-parts (SBP) finite difference operators and weak enforcement of boundary conditions via the simultaneous approximation term (SAT) method. The method rigorously couples the elastodynamic response of the solid Earth with that of a compressible ocean, in the presence of gravity. We can model surface gravity waves using a linearized traction-free boundary condition on the perturbed free surface of an ocean initially in hydrostatic balance. To model an earthquake on the Pitas Point fault, we approximate the geometry of the Santa Barbara Channel with a very shallow, flat, compressible ocean layer overlying a thick layer of Earth, in which is embedded a steeply dipping thrust fault.

Characterization of subsurface faulting using ambient noise technology, John N. Louie, Aasha Pancha, and Satish Pullammanappallil (Poster 270)

We present independent studies demonstrating that 2D ambient noise imaging is a valuable tool for the identification and characterization of faulting within urban environments. This method can cost-effectively identify faults in urban settings and under deep basins, and provide initial reconnaissance of potential trenching sites to constrain fault-trace locations. The case studies confirm microtremor technology can effectively locate unknown or buried faults where traditional refraction and reflection seismology become impractical or cost prohibitive. To characterize lateral changes in shear-wave velocity at depth, we perform a series of 1-D velocity soundings along a seismic array by applying the Refraction Microtremor method across consecutive subsets of instruments. In essence, the 2D image is composed from a moving array of microtremor recordings. Recent investigations on the flanks of Mt. Hood determined buried fault-offset locations to within a spatial accuracy of 40 m. This test recorded microtremor data along 376-m-long arrays across fault traces approximately located by geomorphic observations. Resulting shear velocity cross-sections, to approximately 100 m depth, effectively constrained fault locations to within 10 to 40 m, where the arrays were perpendicular to strike. Extrapolation of this technology to image structure to depths exceeding 1 km has been successfully tested and vetted by agreement with gravity studies. Data acquired within the Reno-area basin using arrays 3 km and 6 km long, with 100 m and 200 m instrument spacing, enabled velocity resolution of basement. A dramatic 400 m to 500 m vertical offset in basement elevation, restricted to a lateral distance of 350 m, coincides with the location of a suspected Quaternary fault. Air photos, topography, and mapped geological contacts showed no evidence supporting the existence of this fault, and it had therefore been dismissed. However, the 2D velocity shows that sediment thicknesses on either side of the offset are not equivalent and taper, indicative of overlapping of sediments towards the south. The observations could therefore be interpreted as an expression of the paleotopography, but also support progressive episodic vertical movement along the proposed fault. While

routinely used in industry, these results reinforce the prospects that subsurface velocity imaging using ambient noise has great potential for characterizing seismic hazard.

Dynamic Rupture Models of the Historic and Recent Paleoseismic Rupture Sequence of the Northern and Central San Jacinto Fault, Julian C. Lozos, Thomas K. Rockwell, and Nathan W. Onderdonk (Poster 126)

We use the 3D finite element method to conduct dynamic rupture models on the Claremont, Casa Loma, and Clark strands of the San Jacinto Fault, in order replicate rupture extents and slip distributions for historic and recent paleoseismic earthquakes. The recent historic behavior of the northern and central San Jacinto Fault has been limited to moderate events, but paleoseismic data indicates that all three strands have experienced multiple large ruptures, with an average of 2.5 to 3 m slip on the Claremont (Onderdonk et al., 2014) and 3 to 3.5 m slip on the Clark (Rockwell et al., 2014). We vary initial stresses on the fault to see which conditions are necessary to replicate these larger events, as well as which changes to those conditions are required to also accommodate smaller historic earthquakes.

A wide range of initial stress conditions produces many ruptures that span the entire Claremont strand, with an average surface slip of ~2.5 m, regardless of where we nucleate along strike. These Claremont ruptures continue through the extensional stepover at Mystic Lake, but produce lower slip on the adjacent Casa Loma strand; this may imply incomplete stress drop on the Casa Loma even in a large rupture, leaving some stored stress for a smaller event, such as the ~M6.4 1899 earthquake that caused damage in this area. Our model does produce 1899-like events when we use a lower stress drop. These same initial conditions also produce ruptures similar to the ~M6.9 1918 earthquake centered on the Clark strand near Anza.

We find that the major barrier to rupture on the northern San Jacinto Fault is the compressional stepover between the Casa Loma and Clark strands at Park Hill. The persistence of this barrier suggests that early-1800s paleoseismic records of high-slip events on both the Claremont and Clark may represent separate earthquakes, rather than a single rupture. If the 22 November 1800 earthquake noted at Missions San Diego and San Juan Capistrano occurred on the Clark (Salisbury et al., 2012), then the Claremont may have participated in the 8 December 1812 earthquake, which is traditionally interpreted as a San Andreas-only rupture. We also find that a lower fault strength and a higher stress drop are required to produce a rupture of the full Clark strand than of the full Claremont. This suggests that the 1800 event, if it did rupture the Clark, must have been a very energetic rupture, which is consistent with observations of significant damage at large distances from the fault.

Interaction of repeating earthquake sequences and its relation to fault friction properties, Ka Yan Semechah Lui and Nadia Lapusta (Poster 121)

It is widely known that earthquakes can trigger each other. Most explanations attribute this interaction to either static or dynamic stress changes caused by coseismic slip, although other mechanisms of interaction exist. With the interactive behavior of small repeating earthquake sequences (RES) on the creeping section of the San Andreas Fault as our motivation, we study, through numerical modeling of rate- and state faults, how clustered small seismogenic zones embedded into creeping fault areas trigger seismic events on one another.

Our work has shown that, for a wide range of laboratory-motivated fault properties, static stress changes due to postseismic slip is more important in triggering seismic events than the coseismic stress changes. Such finding is based on the comparison of the time advance of triggered earthquakes in our simulations and in fault failure models which only account for the stress increase at where earthquakes are triggered due to coseismic slip elsewhere. The interaction of RES extends much farther than would be predicted based on static stress changes from coseismic slip alone.

In this study, we investigate how the interaction of the repeating sequences depends on the properties of the creeping segment. Our results indicate that more velocity-strengthening faults, i.e. faults with larger values of (a-b), suppress propagating creep fronts and reduce interaction. Further, triggering time is determined by the propagation

MEETING ABSTRACTS

speed of postseismic creep, which depends on the frictional properties and the coseismic stress increase on the creeping area. The latter parameter is related to stress drop of the seismic event and can be estimated from coseismic slip. So with known stress drops and triggering times, it is possible to infer the frictional properties of the creeping region.

Our models also show that interaction of seismogenic patches of different sizes leads to significant irregularity in the recurrence time and magnitude of the resulting seismic events, even though each patch would produce a perfect repeating sequence on its own. Such irregularity is observed for natural repeating sequences. While spatial and/or temporal variability in fault properties may be responsible for such behavior, our simulations show that the irregularity may be at least in part due to the interaction.

Airborne Hyperspectral Infrared Imaging Survey of the San Andreas Fault in Southern California, David K. Lynch, David M. Tratt, Kerry N. Buckland, and Patrick D. Johnson (Poster 267)

Mako is a wide-swath, three-axis-stabilized, whiskbroom airborne hyperspectral imager that operates across the wavelength range 7.6-13.2 μm in the longwave-infrared (LWIR) spectral region. Designed and built by The Aerospace Corporation, its innovative spectrometer design enables low-noise performance ($\text{NE}\Delta\text{T} \lesssim 0.1 \text{ K @ } 10 \mu\text{m}$) at small pixel IFOV (0.55 mrad) and high frame rates, making possible $\pm 42^\circ$ nadir angles that provide for an area-coverage rate of 20 km^2 per minute at 2-m GSD from 12,500 ft (3.8 km) AGL. Mako has been used in numerous studies involving other earthquake fault systems, mapping of surface geology, geothermal activity studies, urban surveys, and the detection, quantification, and tracking of natural and anthropogenic gaseous emission plumes. The strand of the San Andreas Fault (SAF) between Desert Hot Springs and Bombay Beach in southern California has been surveyed along its 145-km (90-mile) length the Mako airborne imager. The data were acquired with a 4-km swath width centered approximately on the SAF, so that many offset features associated with the fault are present in the imagery and can be studied in context with the faultline. Spectral analysis keying on diagnostic LWIR spectral features of the lithological horizons occurring along the SAF precisely locates the rupture zone and provides a means for independently assessing slip over time.

Mako is available to participate in airborne field studies. For more information please contact David Tratt: dtratt@aero.org 310-336-2876

Intersonic and Supersonic ruptures in a model of dynamic rupture in a layered medium, Xiao Ma and Ahmed Ettaf Elbanna (Poster 113)

The velocity structure in the lithosphere is quite complex and is rarely homogeneous. Wave reflection, transmission, and diffraction from the boundaries of the different layers and inclusions are expected to lead to a rich dynamic response and significantly affect rupture propagation on embedded faults. Here, we report our work on modeling dynamic rupture in an elastic domain with an embedded soft (stiff) layer as a first step towards modeling rupture propagation in realistic velocity structures.

We use the Finite Element method (Pylith) to simulate rupture on a 2D in-plane fault embedded in an elastic full space. The simulated domain is 30 km wide and 100km long. Absorbing boundary conditions are used around the edges of the domain to simulate an infinite extension in all directions. The fault operates under linear slip-weakening friction law. We initiate the rupture by artificially overstressing a localized region near the left edge of the fault. We consider embedded soft/stiff layers with 20% to 60% reduction/increase of wave velocity respectively. The embedded layers are placed at different distances from the fault surface.

We observed that the existence of a soft layer significantly shortens the transition length to supershear propagation through the Burridge-Andrews mechanism. The higher the material contrast, the shorter the transition length to supershear propagation becomes. We also observe that supershear rupture could be generated at prestress values that are lower than what is theoretically predicted for a homogeneous medium. We find that the distance from the lower boundary of the soft layer to the fault surface has a stronger influence on the supershear transition length as opposed to the thickness of the soft layer.

In the existence of an embedded stiffer layer we found that rupture could propagate faster than the fault zone P-wave speed. In this case, the

propagating rupture generate two Mach cones; one is associated with the shear wave, and the other is associated with the local P-wave speed. This is a signature of supersonic crack tips. We also noted a smooth transition into supershear, with the rupture speed increasing continuously through the so-called 'energetically forbidden zone' (between Rayleigh wave speed and shear wave speed) corresponding to the wave speeds of the background medium.

Our investigation will enable us to predict implications of intersonic and supersonic rupture propagation on ground motion in layered media. In future work, rate and state friction and more realistic velocity structures will be implemented.

How energy efficiency and the potential for coseismic rupture change with strike-slip fault growth through releasing bends, Elizabeth H. Madden, Michele L. Cooke, and Jessica McBeck (Poster 122)

Strike-slip fault segments link over multiple earthquake cycles to form through-going structures, as demonstrated by the more continuous nature of the mature San Andreas Fault relative to the younger, segmented San Jacinto Fault nearby. However, despite its relative immaturity, the San Jacinto Fault supports one third to one half of the relative motion of the Pacific and North American plates. This suggests that its segmented structure efficiently accommodates applied plate motion. We test the effect of segmentation on efficiency using the algorithm GROW (Growth by Optimization of Work), which assumes that fault systems evolve toward higher efficiency. GROW simulates fault interactions and honors tensile and frictional failure criteria along pre-existing faults and at fault tips, but selects the orientation of fault growth as that which minimizes the energy of the system. We model the growth pattern and changing efficiency of systems of two right-lateral, strike-slip fault segments with varying amounts of overlap separated by releasing steps with varying widths. In general, efficiency increases rapidly as fault segments grow toward one another initially, and then plateaus, even if the segments continue to propagate. Fault growth after this point appears to occur in order to maintain efficiency. Certain models with faults that do not hard-link reach similar levels of efficiency as models with faults that do hard-link. To study how segmentation and efficiency relate to seismic hazard, we test the ability of an earthquake to rupture through these releasing steps at three different stages of fault growth: (1) an inefficient stage from early in each GROW model; (2) a more efficient stage from later in each GROW model; and (3) the final stage of each GROW model, after the fault segments have stopped growing. Should higher efficiency correspond to a higher potential for a single earthquake to rupture both faults, this approach has utility for assessing the seismic hazard associated with segmented fault systems.

SCEC Community Modeling Environment S12 and Geoinformatics Research Projects, Philip J. Maechling, Thomas H. Jordan, Jacobo Bielak, Yifeng Cui, Kim B. Olsen, and Jeroen Tromp (Poster 091)

The SCEC Community Modeling Environment (SCEC/CME) collaboration performs a broad range of computational research with support from NSF awards S12-SSI: A Sustainable Community Software Framework for Petascale Earthquake Modeling (SEISM) (OCI-1148493), and Geoinformatics: Community Computational Platforms for Developing Three Dimensional Models of Earth Structure (EAR-1226343). On the SEISM project, SCEC researchers are integrating high-level and middle-level scientific software elements (SSEs) into a Software Environment for Integrated Seismic Modeling (SEISM), a sustainable software ecosystem for physics-based seismic hazard analysis. The SCEC SEISM software supports the use of petascale computers by earthquake scientists to generate and manage the large suites of earthquake simulations needed for physics-based PSHA, and advances basic research on rupture dynamics, an elastic wave scattering, and Earth structure. The SEISM software framework includes high-level SSEs for developing and managing unified community velocity models, codes for dynamic and pseudo-dynamic rupture generation, deterministic and stochastic earthquake simulation engines, and the applications necessary to employ forward simulations in two types of inverse problems: seismic source imaging and full-3D tomography. On the Geoinformatics project, SCEC researchers have established an interoperable set of community computational platforms that allow investigators to employ the techniques

of full-3D tomography to refine Earth structures. Two tomographic platforms have been built on highly scalable codes for solving the forward problem: the AWP-ODC 4th-order, staggered-grid, finite-difference code, which has been widely used for regional earthquake simulation and physics-based seismic hazard analysis and the SPEC3D spectral element code, which is capable of modeling wave propagation through aspherical structures of essentially arbitrary complexity on scales ranging from local to global. A third platform, based on the Unified Community Velocity Model (UCVM) software developed by the Southern California Earthquake Center (SCEC), provides a common framework for comparing and synthesizing Earth models and delivering model products to a wide community of geoscientists.

The Distribution of Fault Slip Rates in the Ventura Fault System, CA, Scott T. Marshall, Gareth J. Funning, and Susan E. Owen (Poster 093)

The recognition of the greater Ventura region as a Special Fault Study Area (SFSA) has largely been driven by recent work suggesting a local source for ~M8 earthquakes in the past. Such large magnitude events are difficult to reconcile with the discontinuous fault geometry present in the SCEC Community Fault Model version 4.0 (CFM4.0) for the Ventura region. As part of the Ventura SFSA, two competing and updated regional fault geometries were proposed. We test these two fault geometries, update several other faults that require revision, and compare results to the CFM4.0 geometry for the region. We also update several faults in the Ventura region to better fit the current data, most notably the Oak Ridge fault, which we have meshed as a contiguous surface onshore and offshore. In total approximately 20 faults have required modification to incorporate the new SFSA geometries.

Using a mechanical model driven by geodetically-calculated strain rates, we calculate the full three-dimensional slip distributions along the faults of the greater Ventura region for all three geometries tested. Preliminary model results predict that the overall average slip rates of most faults in the region are not greatly different in the three models. For example, the overall average reverse slip rate of the Ventura fault only changes from 2.3 mm/yr in the CFM4.0 model to 2.7 mm/yr in the model with the significantly larger and through-going Ventura fault. Analysis of the full three-dimensional model-predicted slip distributions indicates that while the maximum slip rates at the surface of the Earth are approximately 4-4.5 mm/yr, more than 7 mm/yr of slip may occur at depth below the flat ramp section of the Ventura fault. Despite these seemingly fast slip rates, the ramp geometry actually makes the fault surface mechanically inefficient at accommodating slip and slows reverse slip rates dramatically, locally in the flat ramp section. The net result is that the average slip rate of the Ventura fault appears only marginally faster than the CFM4.0 representation. This is, perhaps, misleading because near surface sections of the updated Ventura fault representation are predicted to slip much faster than this average value. Additionally, the model predicted maximum slip rate for the Ventura fault at the surface of the Earth (4.4 mm/yr) is located near the sites of Rockwell [in review], where large coseismic uplifts and fast slip rates were interpreted from the geologic record.

The 2011 Tohoku-oki Earthquake related to a strong velocity gradient within the Pacific plate, Makoto Matsubara and Kazushige Obara (Poster 172)

We conduct seismic tomography using arrival time data picked by NIED Hi-net, including earthquakes off the coast, outside the seismic network. For these offshore events, we use the focal depth estimated from CMT analysis by NIED F-net since the centroid depth determined using seismic waveform has little uncertainties.

The target region, 20-48N and 120-148E, covers the Japanese Islands from Hokkaido to Okinawa. We used 46622346 P- and 3062846 S-wave arrival time data from 100733 events detected at 1212 seismic stations operated by NIED, JMA, universities, and other institutes observed from October 2000 to September 2009. We selected one event with the largest number of pick data within the 1-km block.

We determined the upper boundary of the Pacific plate with tomogram. We consider the low-velocity oceanic crust at the uppermost part of the subducting Pacific plate, the thrust type seismicity at the plate boundary, and the upper side of the double seismic zone.

We can analyze the seismic velocity structure within the Pacific plate rather than structure within the overriding plate since the ray paths take off downward from the hypocenter and reach the seismic stations. We discuss the velocity structure within the subducting Pacific slab 10-km beneath the plate boundary.

We detect two rows of low-velocity (low-V) zones in the uppermost part of the subducting Pacific slab off the Tohoku coast. The landward long NNE-SSW low-V zone corresponds to the western edge of the coseismic slip zone of the 2011 Tohoku-oki Earthquake. Large high-V zone on the east side the long low-V zone is consistent with the coseismic slip region of the Tohoku-oki Earthquake. The initial break point (hypocenter) is associated with the edge of a slightly low-V and low-Vp/Vs zone within the high-V zone. This trenchward low-V and low-Vp/Vs zone extending southwestward from the hypocenter may indicate the existence of a subducted seamount. This low-V anomalous zone within the high-V zone is the unstable heterogeneous structure and might have acted as the initial break point of the 2011 Tohoku-oki Earthquake. The high-V zone and low-Vp/Vs zone might have accumulated the strain and the rupture of whole high-V zone lead to the huge 2011 Tohoku-oki Earthquake.

Reference: Matsubara, M. and K. Obara, The 2011 off the Pacific coast of Tohoku Earthquake related to a strong velocity gradient with the Pacific plate, *Earth Planets Space*, 63, 663-667, 2011.

What can late Quaternary displacement on the San Andreas Fault in the greater San Gorgonio Pass region tell us about late Holocene to Recent strain patterns? Jonathan C. Matti, Brett F. Cox, Douglas M. Morton, Robert E. Powell, and Stephanie L. Dudash (Poster 281)

In the San Gorgonio Pass (SGP) region, geologic evidence suggests that for the last few hundred thousand years dextral slip has entered SGP from Coachella Valley via the Banning and Garnet Hill strands of the San Andreas Fault (SAF), worked its way through the contractional SGP Fault zone, and exited northwest out of SGP via the SAF's San Bernardino strand (SBS). Total dextral slip appears to be as great as 5 km:

- (1) In easternmost SGP, the SAF Banning strand displaces very old alluvial deposits as much as 4.6 km from Whitewater River Canyon;
- (2) In E-central SGP, several major N-S drainages are incised into late Cenozoic sedimentary rocks uplifted by south-vergent thrusts of the SGP Fault zone (SGPFZ). Their size indicates the drainages were sculpted by high-discharge streamflows that could have been generated only by Stubbe and Cottonwood Canyons 3-5 km to the east. The drainages were displaced by a dextral fault now overprinted by a thrust of the SGPFZ;
- (3) In western SGP, restoring ~ 5 km of dextral slip on the SBS positions northern tributaries of Hathaway Creek downstream from Wood Canyon, suggesting that the two drainages formed an integrated network prior to disruption by late Quaternary slip on the SBS;
- (4) In the Forest Falls quad the SBS has displaced an old landslide mass in the Pine Bench area 3.8 to 4.6 km from a cross-fault counterpart near Burro Flats;
- (5) W of San Gorgonio River, the large canyons of Little SG River and Noble Creek are truncated on the N by the SBS; the canyons have been displaced 4.6 and 2.6 km, respectively, from the headwaters of SG River;
- (6) In the Yucaipa quad the SBS has displaced very old Pleistocene gravels as much as 5 km from the canyon mouth of Mill Creek.

This long-term history provides a baseline for evaluating latest Holocene strain budgets in SGP. Here, strain patterns are difficult to interpret because (1) slip rates estimated for the contractional SGPFZ do not translate in any obvious way to rates estimated for strands of the SAF that enter and exit SGP, and (2) the SBS in SGP and farther NW has 5 discrete segments (Potrero Canyon, Burro Flats, Oak Glen, Yucaipa, and Plunge Creek), each having its own tectonogeomorphic expression, structural complexity, and average azimuthal trend. Nonetheless, modern strands of the SAF in SGP display significant slip during late Q time, with implications for the entire SAF system. How real-time strain exploits the SGP tectonic matrix, though, remains a mystery.

MEETING ABSTRACTS

Constraining Moment Deficit Rate on Crustal Faults from Geodetic Data, *Jeremy L. Maurer, Andrew Bradley, and Paul Segall (Poster 097)*

Constraining moment deficit rates on crustal faults using geodetic data is currently an under-utilized but powerful method for estimating the potential seismic hazard presented by crustal faults. Two previous approaches to moment-bounding, bootstrapping and Metropolis-Hastings sampling, can both fail (even catastrophically) when estimating the probability distribution of moment given data, $p(Mo|d)$. Straightforward application of traditional Metropolis-Hastings sampling with uniform prior probabilities on slip rate leads to a mesh-dependent estimate of moment rate with a variance inversely related to the number of model elements. Moment rate thus estimated exhibits an "effective prior" on $p(Mo)$ that tends toward a delta function halfway between the implied bounds as the fault discretization becomes finer! Thus, it is incorrect to estimate the uncertainty in moment directly from the uncertainty in slip rate. Bootstrapping also sometimes fails as it can produce optimistic bounds that exclude the true value in synthetic tests. A third approach is functional moment bounding (FMB), which obtains bounds on moment by minimizing the data misfit for all possible values of Mo and accepting only those values with a total misfit less than some threshold (Johnson et al., 1987). The difficulty with this approach is that the weighted residual norm does not follow a simple statistic (e.g. Chi-squared) when the bounds on slip rate are active. We present a modified FMB method that creates a probability distribution function on Mo from the misfit and uses this pdf to obtain confidence bounds. This approach can be viewed as an approximation method that produces conservative results and does not exhibit mesh dependencies. We compare the results from FMB to those obtained from other methods and assess the results.

Decadal-scale decoupling of the Japan Trench prior to the 2011 Tohoku-oki earthquake from geodetic and repeating-earthquake observations, *Andreas P. Mavrommatis, Paul Segall, Naoki Uchida, and Kaj M. Johnson (Poster 231)*

We report geodetic evidence for decadal-scale decoupling of the Japan Trench prior to the 2011 M9 Tohoku earthquake, with supporting evidence from repeating earthquakes. We build on the results of Mavrommatis et al. (2014, GRL), where we investigated GPS time series for 15 years before the M9 event, correcting for the copious postseismic deformation following numerous $M \sim 6.5+$ earthquakes between 2003 and 2011. We modeled interseismic deformation as linear trends plus constant accelerations and corrected for coseismic and postseismic effects of $M 6.3+$ quakes during the period 1996 to 2011. We find spatially coherent and statistically significant accelerations throughout northern Honshu.

While the accelerations in northern Tohoku can be explained by decaying postseismic deformation following the 1994 M7.7 Sanriku quake, the accelerations in south-central Tohoku cannot be explained simply by postseismic effects. Time series in south-central Tohoku reveal an approximately continuous transient spanning the period 1996 to 2011, without any obvious onset. The transient is consistent with a decrease in the average shear strain rate by $\sim 1/3$ in 15 years, and can be explained by increasing average slip rate and/or updip migration of the locked-to-creeping transition depth. MCMC inversions of instantaneous velocities in 1996 and 2011 imply a shallowing of the transition depth by 13.5 ± 9.5 km and an increase in the average slip rate in the depth range from 22 km to the transition depth by 48.5 ± 10.5 mm/yr.

To test these predictions and to provide additional constraints on the changes in slip rate, we use independent observations of repeating earthquakes during the same period. We find that several sequences of repeaters offshore south-central Tohoku exhibit decreasing recurrence intervals, possibly implying increasing slip rate, while sequences offshore Sanriku exhibit increasing recurrence intervals, consistent with decaying afterslip from the 1994 M7.7 Sanriku event. This along-strike dichotomy is consistent with an inversion of the GPS accelerations and suggests that some change in slip rate in depths shallower than ~ 60 km is required by the data. Further analysis of the repeating earthquakes will provide additional constraints to discriminate between such models.

Statistics of Ground Motions in a Foam Rubber Model of a Strike-Slip Fault, *Kevin M. McBean, John G. Anderson, and James N. Brune (Poster 077)*

The peak acceleration and velocity from 6862 ruptures of a foam rubber stick-slip model are not distributed according to a lognormal probability distribution function. PGA and PGV values are decomposed into residuals using the method of Anderson and Uchiyama (2011), which is similar to the averaging-based factorization of Wang and Jordan (2014). The statistically significant deviations from the lognormal distribution occur near the peak of the probability distribution. In some cases, the high-amplitude tails differ by a much greater ratio, but the statistical significance of this effect is low. This result is true of both raw data and data adjusted for site and magnitude. Event terms are also not lognormal, but they can be modeled as a sum of a small number of lognormal subdistributions, which possibly represent different preferred rupture initiation points, rather than a uniform distribution of initiation points. The event term subdistributions with the highest median values have small standard deviations, so if shapes of this nature were to be used in ground motion prediction equations (GMPEs) during a probabilistic seismic hazard analysis (PSHA), the effect of the long tail of the lognormal distribution in controlling the hazard would be weakened considerably. Unlike the NGAW2 GMPEs or CyberShake in Wang and Jordan (2014), residual variances for the foam rubber model are dominated by variability in the source slip function, rather than the path and site effects. This difference in the variance budget results from the way in which the source and site residuals are defined in this study; the source uncertainty includes variation in the rupture size (magnitude) and location, along with deviations in distance and path. We do not know if these results apply to earthquakes, of course, but we do think tests such as these on repeating stick-slip events in a physical system are one possible way to expand the set of credible hypotheses regarding possible behavior modes of earthquake faults.

Shallow shear wave velocity characterization of the urban Christchurch, New Zealand region, *Christopher McGann, Brendon Bradley, and Misko Cubrinovski (Poster 045)*

This poster provides a summary of the development of a 3D shallow ($z < 40$ m) shear wave velocity (V_s) model for the urban Christchurch, New Zealand region. The model is based on a recently developed Christchurch-specific empirical correlation between V_s and cone penetration test (CPT) data (McGann et al. 2014a,b) and the large high-density database of CPT logs in the greater Christchurch urban area ($> 15,000$ logs as of 01/01/2014). In particular, the 3D model provides shear wave velocities for the surficial Springston Formation, Christchurch Formation, and Riccarton gravel layers which generally comprise the upper 40m in the Christchurch urban area. Point-estimates are provided on a 200m-by-200m grid from which interpolation to other locations can be performed. This model has applications for future site characterization and numerical modeling efforts via maps of time averaged V_s over specific depths (e.g. V_{s30} , V_{s10}) and via the identification of typical V_s profiles for different regions and soil behaviour types within Christchurch. In addition, the V_s model can be used to constrain the near-surface velocities for the 3D seismic velocity model of the Canterbury basin (Lee et al. 2014) currently being developed for the purpose of broadband ground motion simulation.

One-dimensional modeling of fault slip rates using new geodetic velocities from a transect across the Pacific-North America plate boundary through the San Bernardino Mountains, California, *Sally F. McGill, Joshua C. Spinler, John D. McGill, Richard A. Bennett, Michael Floyd, Joan E. Fryxell, and Gareth J. Funning (Poster 226)*

Campaign GPS data collected from in and around the San Bernardino Mountains over an 11-year period from 2002-2013 result in 41 new site velocities from the San Bernardino Mountains and valley areas to the southwest, which are now available for incorporation into the Community Geodetic Model. We combined these velocities with those from continuous GPS stations and with published campaign velocities and modeled the deformation along a 40-km-wide, 300-km-long transect across the Pacific-North American plate boundary passing through the San Bernardino Mountains, southern California. The profile of site

velocities displays two prominent velocity gradients, one beneath the San Andreas (SAF) and San Jacinto faults (SJF), which are located only 12-22 km apart in our transect, and the other beneath the vicinity of the 1992 Landers and 1999 Hector Mine earthquakes. A pronounced flattening of the velocity profile beneath the Helendale and Lenwood faults separates these two distinct shear zones.

In our modeling, we used 14 parallel screw dislocations and 1 obliquely oriented screw dislocation (representing the San Bernardino strand of the SAF) within an elastic half-space. We conducted a non-linear least-squares fit to solve for slip rates and locking depths simultaneously, with locking depths constrained to be between the 90th and 98th percentiles of hypocentral depths along the transect. The modeled slip rate for the northern SJF (16.0 ± 2.0 mm/yr) is in good agreement with published Holocene and Late Pleistocene slip rates. The modeled slip rate for the San Bernardino strand of the SAF (5.7 ± 2.3 mm/yr), however, is somewhat slower than published Holocene and Late Pleistocene slip rates, and the modeled slip rates for the two faults combined is slower than geologic slip-rate estimates for the SAF north of their juncture. Our modeled rate for all faults of the Eastern California shear zone (ECSZ) combined (14.2 ± 3.7 mm/yr) is faster than the sum of Late Pleistocene rates for these faults, even when an estimate of permanent, off-fault deformation is included. These results suggest that in the present-day strain regime, a somewhat greater amount of slip is being transferred from the southernmost SAF into the ECSZ than has been the case for most of the period since the Late Pleistocene. Present-day deformation across the Newport-Inglewood fault is occurring at a rate (6.7 ± 3.5 mm/yr) that is about four-times faster than expected from geologic studies.

Single-grain post-infrared stimulated luminescence (pIR-pIRSL) dates for active faults in California and New Zealand, *Christopher P. McGuire, Edward J. Rhodes, James F. Dolan, Sally McGill, Russ Van Disen, Robert M. Langridge, Jessica R. Grenader, Robert Zinke, and Nathan Brown* (Poster 272)

We present dates and preliminary slip-rates using a post-Infrared Stimulated Luminescence (pIR-IRSL) procedure for K-feldspar sand grains in faulted Pleistocene and Holocene sedimentary deposits from California and New Zealand. The pIR-IRSL method has proven effective in a wide variety of fluvial and alluvial environments due to improvements in laboratory procedures and single-grain data analysis. Super-K (SuK) mineral separation by heavy liquid (2.565 g.cm^{-3}) increases single-grain yield by isolating the target mineral, K-feldspar, from other feldspars and denser minerals. A two-step pIR-IRSL measurement protocol has been adopted, with IR stimulation at 50 C followed by IR stimulation at 225 C. The higher temperature signal (pIR-IRSL₂₂₅) is more stable than lower temperature IRSL measurements and results in minor (~10 - 15%) or, in some cases, no age correction for anomalous fading. Single-grain data analysis techniques provide higher precision dates by isolation of the well-bleached single-grain population (i.e., the grains for which the IRSL signal has been reset at time of deposition) in conjunction with a stratigraphic Bayesian age model. Procedural and analytic improvements for the single-grain pIR-IRSL technique broaden opportunities to date active faulting using sand from alluvial and fluvial deposits in trenched faults and from fluvial terraces.

Relationships between seismic velocity, metamorphism, seismic and aseismic fault slip in the Salton Sea Geothermal Field region, *Jeffrey J. McGuire, Rowena B. Lohman, Rufus D. Catchings, Michael J. Rymer, and Mark R. Goldman* (Poster 208)

The Salton Sea Geothermal Field is one of the most seismically active areas in California and presents an opportunity to study the effects of high-temperature metamorphism on the properties of seismogenic faults. The area includes numerous faults that have recently been imaged with active-source seismic reflection and refraction surveys. The reflection surveys show dense faulting near geothermal extraction operations along a main central fault (MCF; Hulen et al., 2003), with less-dense faulting extending at least several kilometers outward. We also utilized the active-source surveys, along with the abundant microseismicity data from a dense borehole seismic network, to image the 3D variations in seismic velocity in the upper 5 km of the crust. We observe strong velocity

variations, up to ~30%, that correlate spatially with the distribution of shallow heat-flow patterns. The combination of hydrothermal circulation and high-temperature contact metamorphism have significantly altered the shallow clastic sedimentary layers within the geothermal field to denser rock with higher P-wave velocity, as is also seen in the numerous exploration wells within the field. This alteration appears to have a first-order effect on the frictional stability of shallow faults, as we infer from seismicity and geodetic measurements. In 2005, a large earthquake swarm and an aseismic deformation event occurred. Analysis of InSAR data, earthquake relocations, and field studies indicate that the shallow aseismic fault creep that occurred in 2005 was localized on the Kalin Fault (M.J. Rymer and K. Hudnut, pers. comm. 2005), which lies just outside the region of high-temperature metamorphism. In contrast, the earthquake swarm, which includes all M>4 earthquakes that have occurred within the SSGF in the last 15 years, ruptured the MCF locally in the heart of the geothermal anomaly. Microseismicity induced by the geothermal operations is also concentrated in the high-temperature regions within the vicinity of operational wells. However, whereas the microseismicity occurs over a few-km-scale region, much of it is localized near the MCF and clusters in earthquake swarms that last from hours to a few days.

Hulen, J., D. Norton, D. Kaspereit, L. Murry, T. van de Putte, and M. Wright (2003), *Geology and a working conceptual model of the Obsidian Butte (Unit 6) sector of the Salton Sea Geothermal Field, California*, Geothermal Resources Council Transactions, 27, October 12-14.

A Filter Bank Approach to Earthquake Early Warning, *Men-Andrin Meier, Thomas Heaton, and John Clinton* (Poster 041)

Earthquake Early Warning (EEW) is a race against time. The longer it takes to detect and characterize an ongoing event, the larger is the blind zone - the region where a warning arrives only after the most damaging ground motion has occurred. The problem is most acute during medium size earthquakes, which can cause severe damage but where the damaging ground motion is confined to a small zone around the epicenter. An ideal EEW algorithm which is fast enough to provide relevant alerts for such scenario events would have to produce reliable event characterization based on observations of very short snippets of data recorded at only very few stations. For such a scheme to work, without significant numbers of false alarms (which continue to hamper both single-station and network based approaches today), the real-time information that is available for an earthquake has to be exploited in a more optimal way than what is currently done.

Our approach is to fully mine the broadband frequency content of incoming real-time waveforms. We propose a filter bank approach with minimum phase delay filters which allows us to use frequency information from each frequency band at each triggered station at the earliest possible time. We have compiled and processed an extensive dataset of near-field earthquake waveforms. In an empirical maximum likelihood scheme, we use the filter bank output from the first seconds after the P-wave onset of each waveform to estimate the most likely magnitude and epicentral distance to have caused this waveform. We show how our single station approach can be integrated into an evolutionary and fully probabilistic network EEW system. We demonstrate that our method can allow sufficiently accurate characterization of an ongoing event with two stations, with consistent characterization of the evolving uncertainty of the location and magnitude.

USEIT 2014 Visualization Team: SCEC-VDO, GIS, OpenSHA, and HAZUS Implementations, *Ryan Meier, Jaquelyn Felix, Krista McPherson, Rory Norman, Paulo Dos Santos, Thomas Jordan, Robert de Groot, Nick Rousseau, Yao-Yi Chiang, Kevin Milner, Mark Benthien, Scott Callaghan, and Dave Smith* (Poster 010)

The 2014 Undergraduate Studies in Earthquake Information Technology (USEIT) Visualization Team at the Southern California Earthquake Center (SCEC) created visualizations using the Southern California Earthquake Center Virtual Display of Objects (SCEC-VDO), an object-oriented, open source, visualization software for demonstrating complex earthquake science concepts. The Visualization Team created and produced twenty-three visualizations of seismic events between a magnitude of 6.9 and 7.1 throughout California in order to mimic the 1989 magnitude 6.9 Loma Prieta earthquake. In addition, the team demonstrated the capabilities of

MEETING ABSTRACTS

aftershock sequences of these events for the visualizations, with an aim to aid in current seismic research, and to educate the general public about the hazards of these events and the risks associated with them. These visualizations were created using the Uniform California Earthquake Rupture Forecast, Version 3 (UCERF3) fault model. For the selected earthquake scenarios, the team computed ShakeMaps displaying peak ground acceleration (PGA) utilizing the Open Source Seismic Hazard Analysis (OpenSHA), an earthquake software application Scenario ShakeMap, and displayed them in SCEC-VDO. This provided insight as to which faults posed the greatest hazard in particular regions. Earthquake scenario data from ShakeMap was then implemented into Hazard United States (HAZUS), which allowed the generation of population and building exposure models. These results were displayed in videos to help educate the public throughout areas in Northern California.

Rapid kinematic slip inversion tsunami inundation modeling with regional geophysical data, Diego Melgar and Yehuda Bock (Poster 042)

Rapid kinematic slip inversions immediately following earthquake rupture is traditionally limited to teleseismic data and delayed many hours after large events. Regional data such as strong motion is difficult to incorporate quickly into images of the source process because baseline offsets render the long period portion of the recording unreliable. Recently it's been demonstrated that high rate GPS can potentially produce rapid slip inversions for large events but is limited to very long periods. With an example of the 2011 M9 Tohoku-oki event we will demonstrate that the optimal on-the-fly combination of GPS and strong motion through a seismogeodetic Kalman filter produces reliable, broadband strong motion displacement and velocity waveforms that can be used for kinematic inversion. Through joint inversion of displacement and velocity waveforms we will show that it is possible to obtain a broadband image of the source. Furthermore, we will also show that it is possible to include offshore geophysical observables such as sea surface measurements of tsunami propagation from GPS buoys and ocean bottom pressure sensors into the kinematic inversion. These data better constrain the shallowest part of rupture. We will use the time-dependent deformation of bathymetry predicted from the inversion results as an initial condition for tsunami propagation and inundation modeling. Through a comparison to post-event survey observations we will demonstrate that it is possible to reproduce the inundation pattern along the coastline in great detail and argue that detailed site-specific forecast of tsunami intensity is achievable with current methods and instrumentation.

Investigation of grid parameterization of earthquake source, Haoran Meng (Poster 166)

Cell parameterization has been applied in the modeling of earthquake source, which is constrained by the limitation that minimum wavelength must far outweigh the size of cell. As a result, relatively high frequency records are abandoned during source inversion when the length of cell is large. In this paper, we develop the grid parameterization of earthquake source to interpolate the source time function and Green's function. We then intergrate the convolution of the interpolated functions to get the displacement. In this way, every single point on the fault plane has been considered and thus the limitation that the wavelength must far outweigh the size of cell can be removed.

Aseismic slow-slip and dynamic ruptures of the 2014 Iquique earthquake sequence, Lingsen Meng, Hui Huang, Roland Burgmann, Jean-Paul Ampuero, and Anne Strader (Poster 145)

The transition between seismic rupture and aseismic creep is of central interest to better understand the mechanics of subduction processes. A M 8.2 earthquake occurred on April 1st, 2014 in the Iquique seismic gap of northern Chile. This event was preceded by a long foreshock sequence including a 2-week-long migrating swarm initiated by a M 6.7 earthquake. Repeating earthquakes are found among the foreshock sequence that migrated towards the mainshock hypocenter, suggesting a large scale slow-slip event on the megathrust preceding the mainshock. The variations of the recurrence times of the repeating earthquakes highlight the diverse seismic and aseismic slip behaviors on different megathrust segments. The repeaters that were active only before the mainshock recurred more often and were distributed in areas of substantial coseismic

slip, while repeaters occurred both before and after the mainshock in the area complementary to the mainshock rupture. The spatial and temporal distribution of the repeating earthquakes illustrate the essential role of propagating aseismic slip leading up to the mainshock and illuminate the distribution of postseismic afterslip. Various finite fault models indicate that the largest coseismic slip generally occurred down-dip from the foreshock activity and the mainshock hypocenter. Source imaging by teleseismic back-projection indicates an initial down-dip propagation stage followed by a rupture-expansion stage. In the first stage, the finite fault models show an emergent onset of moment rate at low frequency (< 0.1 Hz), while back-projection shows a steady increase of high frequency power (> 0.5 Hz). This indicates frequency-dependent manifestations of seismic radiation in the low-stress foreshock region. In the second stage, the high-frequency rupture remains within an area of low gravity anomaly, suggesting the presence of upper-crustal structures that promote high-frequency generation. Back-projection also shows an episode of reverse rupture propagation which suggests a delayed failure of asperities in the foreshock area. Our results highlight the complexity of the interactions between large-scale aseismic slow-slip and dynamic ruptures of megathrust earthquakes.

Analyzing Induced Seismicity related to Water/Gas Injection/Production in California, Qingjun Meng and Emily Brodsky (Poster 211)

Oil, gas and geothermal power are major sources of energy, however pumping water and gas into or out of a reservoir can increase the local seismicity rate. Oil and gas high production states in central United States, like Arkansas, Texas, Ohio and Oklahoma, now face sharply rising numbers of earthquakes, warning us the potential hazard caused by fluid and gas injection and production. The exact relationship between gas/fluid volume and subsequent activity is seldom well-defined and the problem of clarifying seismicity caused by human activity or by tectonic loading is still very challenging. California, with its excellent seismometers, huge amount of earthquakes and big number of oil, gas and geothermal plants, provides us a good experimental field to address these problems. We will use ETAS as aftershock-corrected method to derive background seismicity in several oil or geothermal fields, such as Salton Sea, Los Angeles and Geysers in California.

Improved understanding of moderate-size earthquake sequences on the San Jacinto Fault and their relationship with deep creep, Xiaofeng Meng and Zhigang Peng (Poster 186)

Since 1950, several M6-7 earthquakes occurred along the San Jacinto Fault (SJF), all of which were in the top 10 km and likely only ruptured the shallow part of the seismogenic zone. Wdowinski [2009] hypothesized that the deeper part of the seismogenic zone (i.e. 10-17 km) beneath the SJF marks a transition zone between a locked shallow part and a ductile crust, where the stored elastic strain is released both seismically (e.g. tremors, small to moderate earthquakes) and aseismically (e.g. creeping), instead of by large earthquakes. Moreover, it is suggested that the moderate-size earthquakes along the SJF may be accompanied by the deep creep process [Agnew and Wyatt, 2005; Wdowinski, 2009; Hodgkinson, 2013]. Since 2001 a total of 5 earthquakes with M4.5-5.5 occurred near the Anza gap along the SJF (i.e. 2001 M5.1, 2005 M5.2, 2010 M4.9, 2010 M5.4, and 2013 M4.7). The evolution of their aftershock sequences may shed new light on the deep creep process along the SJF. Most previous studies [e.g., Wdowinski, 2009] used standard SCSN or relocated catalog [Hauksson et al., 2012] to investigate the relationship between deep creep and microearthquakes. However, Kilb et al. [2007] have shown that a significant fraction of early aftershocks was missing following the 2001 M5.1 Anza earthquake. The same problem may occur to other sequences as well. To obtain complete aftershock sequences, we apply a recently developed matched filter technique to all 5 moderate-size earthquake sequences. Using thousands of templates, we detect ~10 times more aftershocks than existing local catalogs for each sequence. We then compare the aftershock areas among 5 sequences. The 3 events that initiated in the deeper part (> 13 km) of the seismogenic zone (i.e. 2001 M5.1, 2005 M5.2 and 2010 M5.4) all have an elongated aftershock area along the SJF (i.e. ~15 km long). The 2013 M4.7 event, which is ~10 km in depth, has a much smaller aftershock area (i.e. ~5 km long). The shallowest event (~ 8 km), 2010 M4.9 event, has the smallest aftershock area of ~2 km along strike. The positive association between focal depth

and aftershock area supports the hypothesis that deep creep process along the SJF may drive the aftershock sequence and hence cause a much larger aftershock area for deep events. Next, we plan to relocate all detected events and examine the spatio-temporal migration pattern for each sequence, which will further help us understand the relationship between aftershocks and deep creep.

Quaternary Off-Fault Uplift, Tilting, And Folding Within A Fault-Bounded Block Embedded In The Eastern California Shear Zone Near Twentynine Palms, Southern California, *Christopher M. Menges, Jonathan C. Matti, and Stephanie L. Dudash* (Poster 257)

We present geomorphic, stratigraphic, and structural evidence for mid-late Quaternary uplift, tilting, and internal folding of an intrafault block within the Eastern California Shear Zone near Twentynine Palms, southern California. The EW-trending sinistral Pinto Mountain fault bounds the southern 8-km-wide side of a triangle-shaped alluvial piedmont block. The W and NE borders of the block are defined by two converging NW-striking dextral faults (Canyon Road, CRF, and Mesquite Lake, MLF) that meet 16 km to the NNW at the block apex. The block is capped by a thin alluvial gravel deposit that is uplifted along a W-facing escarpment of the CRF on the W border, and tectonically tilted downwards toward a closed depression along the MLF on the NE boundary. This uplift and tilting has induced variable incision along an E-draining transverse canyon that decreases in depth from 30 m to 0 m to the E across the block. Timing of block uplift and tilting is constrained by the mid-Pleistocene age of the capping gravel deposit and a stairstepped set of 3 to 4 convergent younger mid- and late Pleistocene terraces inset within canyon walls. The capping surface of the block is internally disrupted by a discontinuous series of subparallel N-striking elongate ridge systems. In plan, individual ridges commonly overlap, branch, and converge with one another with minor westward convexity. The ridges in cross-section display crest heights of 2 to 30 m with asymmetric short steeper (6- 9°) W slopes, and longer, less steep (3-5°) E slopes. Ridgecrest heights commonly plunge and terminate to either end beneath intervening younger alluvium or deflected incised drainages. The flanks and crests of the ridges are underlain by the same gravel deposit that caps the main fault block, which can be traced continuously across the ridge axis with distinct slope reversals. Growth of the ridges is indicated by (a) the inclusion of younger alluvial deposits along the flanks of sideslopes and noses, and (b) variations in crest height and degree of internal dissection. We interpret the ridges as the expression of an actively growing set of W-vergent, asymmetric, gentle to open anticlines likely associated with an underlying imbricate set of blind thrust faults. The composite deformation indicates off-fault intra-block strain transfer that is related to transpressive contraction and possibly horizontal rotation induced by the right-bending convergence of the dextral boundary faults.

Factors controlling near-field coseismic deformation patterns: Quantifying distributed deformation of the 1992 Landers and 1999 Hector Mine earthquakes, *Chris W. Milliner, James Dolan, James Hollingsworth, Sebastien Leprince, Francois Ayoub, and Jean-Philippe Avouac* (Poster 236)

Coseismic surface deformation is typically measured in the field by geologists and by a range of geophysical methods such as InSAR, LiDAR and GPS. Current methods, however, either fail to capture the near-field coseismic surface deformation pattern where vital information is needed, or lack pre-event data. There is also little understanding of the behavior of off-fault deformation and the parameters that control it. We develop a standardized and reproducible methodology to fully constrain the surface, near-field, coseismic deformation pattern in high resolution using aerial photography. We apply our methodology using the program COSI-corr to cross-correlate pairs of aerial, optical imagery before and after the 1992, Mw 7.3 Landers and 1999 Mw 7.1 Hector Mine earthquakes. This technique allows measurement of the surface deformation pattern with sub-pixel precision and can be applied to recent and historic earthquakes in a cost-effective manner. COSI-corr offers the advantage of measuring displacement across the entire fault zone and over a far wider aperture than that available to field geologists. For both earthquakes we find our displacement measurements derived from cross-correlation are systematically larger than the field displacement measurements, indicating

the presence of off-fault deformation. Here we show the Landers and Hector Mine earthquake accommodated 46% and 38% of displacement away from the main primary rupture as off-fault deformation, over a mean deformation shear width of 183 m and 133 m, respectively. The magnitude and width of off-fault deformation across these structurally immature faults are observed to be primarily controlled by the macroscopic structural complexity with a weak correlation with the near-surface materials and is largest in stepovers, bends and terminations of the surface ruptures. We also utilize synthetic tests robustly constrain the measurement precision and accuracy when subjectively estimating the displacement and width of deformation. Knowledge of the behavior of distributed deformation gives important insight into mechanics and kinematics of fault zones, and has implications for the use of both fault slip rates and paleo-earthquake magnitudes that are derived from surface offset measurements for probabilistic seismic hazard analysis.

Operational earthquake forecasting in California: A prototype system combining UCERF3 and CyberShake, *Kevin R. Milner, Thomas H. Jordan, and Edward H. Field* (Poster 031)

Operational earthquake forecasting (OEF) is the dissemination of authoritative information about time-dependent earthquake probabilities to help communities prepare for potentially destructive earthquakes. The goal of OEF is to inform the decisions that people and organizations must continually make to mitigate seismic risk and prepare for potentially destructive earthquakes on time scales from days to decades. To attain this goal, OEF must provide a complete description of the seismic hazard—ground motion exceedance probabilities as well as short-term rupture probabilities—in concert with the long-term forecasts of probabilistic seismic hazard analysis. We have combined the Third Uniform California Earthquake Rupture Forecast (UCERF3) of the Working Group on California Earthquake Probabilities (Field et al., 2014) with the CyberShake ground-motion model of the Southern California Earthquake Center (Graves et al., 2011; Callaghan et al., this meeting) into a prototype OEF system for generating time-dependent hazard maps. UCERF3 represents future earthquake activity in terms of fault-rupture probabilities, incorporating both Reid-type renewal models and Omori-type clustering models. The current CyberShake model comprises approximately 415,000 earthquake rupture variations to represent the conditional probability of future shaking at 285 geographic sites in the Los Angeles region (~236 million horizontal-component seismograms). This combination provides significant probability gains relative to OEF models based on empirical ground-motion prediction equations (GMPEs), primarily because the physics-based CyberShake simulations account for the rupture directivity, basin effects, and directivity-basin coupling that are not represented by the GMPEs.

Crowd-Sourced Global Earthquake Early Warning, *Sarah E. Minson, Benjamin A. Brooks, Craig L. Glennie, Jessica R. Murray, John O. Langbein, Susan E. Owen, Thomas H. Heaton, Robert A. Iannucci, and Darren L. Hauser* (Poster 039)

Although earthquake early warning (EEW) has shown great promise for reducing loss of life and property, it has only been implemented in a few regions due, in part, to the prohibitive cost of building the required dense seismic and geodetic networks. However, many cars and consumer smartphones, tablets, laptops, and similar devices contain low-cost versions of the same sensors used for earthquake monitoring. If a workable EEW system could be implemented based on either crowd-sourced observations from consumer devices or very inexpensive networks of instruments built from consumer-quality sensors, EEW coverage could potentially be expanded worldwide. Controlled tests of several accelerometers and global navigation satellite system (GNSS) receivers typically found in consumer devices show that, while they are significantly noisier than scientific-grade instruments, they are still accurate enough to capture displacements from moderate and large magnitude earthquakes. The accuracy of these sensors varies greatly depending on the type of data collected. Raw coarse acquisition (C/A) code GPS data are relatively noisy. These observations have a surface displacement detection threshold approaching ~1 m and would thus only be useful in large Mw 8+ earthquakes. However, incorporating either satellite-based differential corrections or using a Kalman filter to combine the raw GNSS data with low-cost acceleration data (such as from a

MEETING ABSTRACTS

smartphone) decreases the noise dramatically. These approaches allow detection thresholds as low as 5 cm, potentially enabling accurate warnings for earthquakes as small as Mw 6.5. Simulated performance tests show that, with data contributed from only a very small fraction of the population, a crowd-sourced EEW system would be capable of warning San Francisco and San Jose of a Mw 7 rupture on California's Hayward fault and could have accurately issued both earthquake and tsunami warnings for the 2011 Mw 9 Tohoku-oki, Japan earthquake.

Active Dextral Slip on the Mill Creek fault through San Gorgonio Pass, *Alexander Morelan, Michael Oskin, Judith Chester, and Daniel Elizondo* (Poster 276)

We present preliminary results that the Mill Creek fault, also known as the northern strand of the San Andreas fault, is active with dextral slip through San Gorgonio Pass. Newly acquired airborne LiDAR from San Bernardino County illuminates previously unidentified, discontinuous scarps along the Mill Creek fault on the north side of Yucaipa Ridge, and between Mill Creek and the Santa Ana River. We find evidence that the fault displaces the alluvium-bedrock contact and overlying gravel deposits at the Mill Creek jump off and Raywood Flat. The displaced sediments are undated, but are locally sourced and appear to be late Pleistocene in age. Further southeast, right-deflection of the entrenched East Fork Whitewater River along the trace of the Mill Creek fault presents a possible slip-rate site. Fault orientation and kinematic data suggest that some slip on the Mill Creek fault is transferred across the eastern end of Yucaipa Ridge to the Mission Creek fault by distributed shear along a network of large, oblique-slip secondary faults within a broad, highly fractured damage zone. This slip transfer is accompanied by rapid uplift of Yucaipa Ridge. A tilted alluvial deposit mantling its north-facing slope shows that folding of basement is an important component of this uplift. Slip on the active Mill Creek fault and its distributed transfer to the active Mission Creek fault provide an alternative pathway for earthquake ruptures through San Gorgonio Pass that bypasses the San Gorgonio Pass thrust and Banning strand. Determining the rates of slip of the Mill Creek and Mission Creek faults, the magnitude of slip transfer between the faults, and the nature of their connection to the San Bernardino strand of the San Andreas fault are critical to better assess this hypothesis.

Long-period ground-motion variability from scenario earthquakes on the Salt Lake City segment, Wasatch fault, *Morgan P. Moschetti, Stephen Hartzell, Leonardo Ramirez-Guzman, Stephen Angster, and Arthur Frankel* (Poster 068)

We construct a set of ninety-six earthquake rupture models for M7 scenario earthquakes on the Salt Lake City segment of the Wasatch fault, Utah, and perform 3-D simulations to investigate the variability of long-period ($T \geq 1$ s) earthquake ground motions arising from natural variations in earthquake ruptures. Our work focuses on the sensitivity of long-period ground motions to five parameters used in constructing the kinematic rupture models: the realization and the correlation length of the slip field, hypocenter location, average rupture velocity and the slip velocity, which controls the rise time of each sub-event. We select values for these rupture parameters that are appropriate for M7 normal-faulting earthquakes and that span the observed or inferred range for each variable. Rupture models are constructed with the method of Frankel et al. (2013), which uses a magnitude-invariant dynamic stress drop and produces ground motions consistent with the observations in the NGA-W database. Ruptures are modeled on a 3-D geometric representation of the fault constrained by surficial mapping, previously calculated surface dips, analogous structural models, and basement contact. We model 3-D seismic wave propagation using the Hercules finite element tool-chain and the Wasatch community velocity model.

We focus our examination of ground motion variability on the influence of the rupture parameters as a function of distance. Ground-motion results are examined for peak ground velocity and for 5-percent-damped response spectral accelerations at 3.5 and 7 s natural periods. We construct a reference empirical model of ground motion attenuation with distance from all measurements for comparison with the ground motions from models constructed with common rupture parameters (e.g., common average rupture velocity). On average, hypocenter location, average rupture velocity and slip velocity or rise time have the greatest effect on strong ground-motions; the realization of the stochastic random field and

its correlation length have much smaller average effects. We observe strong spatial variation in the ground motions and apparent correlations with local geologic structure, which will be the subject of future investigations.

The Community Geodetic Model: Current status of the GPS component, *Jessica R. Murray* (Poster 219)

The goal of the Community Geodetic Model (CGM) project is to produce spatially and temporally dense time series of ongoing deformation for southern California utilizing the complementary features of GPS and InSAR data. The CGM will provide observations central to several SCEC core initiatives and science targets. Examples include quantifying slip rates and strain rates, investigating the physical processes that give rise to transient deformation, characterizing non-tectonic time-varying signals, constraining lithospheric rheology and evaluating its role in the earthquake cycle, and providing input to develop or refine stressing rate models. The continued expansion of GPS coverage, launch of new SAR satellites, recent innovations in InSAR time series analysis, and ongoing advances in noise assessment and mitigation can now be leveraged in order to develop methodology for generating a state-of-the-art data set that records the spatio-temporal patterns of crustal motion.

The CGM will encompass three components: one drawing on GPS data from temporary and permanent deployments, one based on InSAR, and a combined GPS-InSAR product. This approach will allow further data type-specific technique development, thorough assessment of the individual data types' noise characteristics, and comparison of time-varying crustal motion recorded by GPS and InSAR prior to integration into the combined CGM. The CGM will provide raw position time series (east, north, and vertical for GPS and line of sight for InSAR) on a nonuniform spatial grid and estimates of derived quantities such as outliers, offsets, noise parameters, common mode error, seasonal signals, velocities, coseismic displacements, and postseismic decay.

This poster summarizes ongoing activities pertaining to GPS data; a companion poster presents a similar summary for the InSAR data. The current focus of the GPS-related effort is 1) compilation of a comprehensive southern California campaign GPS data set and reprocessing using self-consistent methodology, 2) comparisons among several continuous GPS time series solutions produced by different analysis centers, 3) and identifying the best strategies for combining multiple GPS solutions and estimating derived quantities (e.g., secular rates) with realistic uncertainties that account for temporally-correlated noise and non-secular signals. These topics will be discussed in detail in a one-day workshop September 6, 2014 and the follow-on workshop report.

Wave propagation between F-net and NECESSArray retrieved from ambient noise, *Nori Nakata, Nishida Kiwamu, and Kawakatsu Hitoshi* (Poster 181)

We apply cross-correlation techniques to ambient noise to retrieve propagating waves between F-net in Japan and NECESSArray in China. Both F-net and NECESSArray are continuous-recording broadband-seismometer networks and consist of about 80 and 120 receivers, respectively. NECESSArray was deployed in the northeast China during September 2009 and August 2011. The receiver spacing is about 80 km, and the size of the entire array is roughly 1500 km (east-west) by 650 km (north-south). Based on the shape of the arrays, with F-net and NECESSArray, we can create a large network that surrounds the sea of Japan and extract wavefields traveling through the sea by applying seismic interferometry to ambient noise. In the period of 50–100 s, the retrieved wavefields propagate about 4 km/s and 7 km/s, which corresponds to Rayleigh and P wave velocities, respectively. Because of the data quality or excitation, the crosscorrelation of vertical-vertical components has better signal-to-noise ratio than other combinations. The extracted wavefields can be used for imaging of velocity structure, time-lapse studies, or analyses of seismic anisotropy. In this study, we propose the image the velocity structure at the sea of Japan as an application to use the wavefields. Another potential of the large network is to extract global reflections from ambient noise because the sensors are all broadband. We are grateful to NIED and the people involved in the NECESSArray project for providing the data.

Investigation of Seismic Events associated with the Sinkhole at Napoleonville Salt Dome, Louisiana, Avinash Nayak and Douglas S. Dreger (Poster 214)

This study describes the ongoing efforts in analysis of the intense sequence of complex seismic events associated with the formation of a large sinkhole at Napoleonville Salt Dome, Assumption Parish, Louisiana in August 2012. We investigate source mechanisms of these events, represented by a general 2nd order point source centroid seismic moment tensor (MT) using data from a temporary network of broadband stations established by the United States Geological Survey. We have implemented a grid-search technique to detect and compute the centroid hypocenter and MT solution of events using low frequency (0.1-0.3 Hz) 25-second duration displacement waveforms and 1D velocity models for the salt dome and the surrounding sediment sequence. We present preliminary results of application of this technique to data extending up to 17 days before and after the appearance of the sinkhole that yields a catalog of > 1200 events. We describe the evolution of the seismicity in time with respect to hypocenters, source-types, and magnitudes. Since fewer stations were operational during the time period preceding the appearance of the sinkhole, we perform various sensitivity tests to examine the effects of decrease in station coverage from a 5-station network to a 3-station network on location, source-type and magnitude uncertainties.

Assessing magnitude Inter-dependency using global and local catalogs , Kevin Nichols, Devon Cook, and Jazmine Titular (Poster 033)

Statistically, earthquakes can either be identified as main shocks, caused naturally, or as aftershocks, resulting from a previously occurring earthquake. Until recently, statistically differentiating between main shocks and aftershocks has been difficult. Through new stochastic de-clustering algorithms it is possible now to probabilistically assign earthquakes as main shocks or as aftershocks and in the cases of aftershocks to determine which previously occurring earthquake triggered the aftershock. Through a modification of model independent stochastic de-clustering (Marsan and Lengline 2008) and a global Centroid Moment Tensor catalog as well as a localized catalog provided by the Southern California Earthquake Data Center (SCEDC), it is now possible to directly assess levels of correlation between earthquakes and the aftershocks they trigger. Results indicate that the positive correlation observed between larger earthquakes in the gCMT catalog and their aftershocks is also evident in the relationship between the magnitudes of earthquakes in the SCEDC data and their aftershocks. However, with the lower minimum magnitude of completeness found in the SCEDC catalog and with short periods of extreme earthquake activity evident within the data, the statistical power of the stochastic de-clustering algorithms to distinguish between mainshocks and aftershocks is diminished for the localized catalog. Once incorporated into epidemic type aftershock models, conditional distributions for the magnitudes of new earthquakes can be implemented to improve the forecasting capabilities of this class of model.

Differential LiDAR – a new tool for mapping coseismic fault-zone deformation, Edwin Nissen, J Ramon Arrowsmith, Adrian Borsa, Craig Glennie, Alejandro Hinojosa-Corona, Tadashi Maruyama, and Michael Oskin (Invited Talk Tuesday14:00)

The recent surge in airborne laser scanning along active faults in California and elsewhere provides high-resolution topographic baselines against which future, post-earthquake LiDAR datasets can be compared, equipping us with a powerful new tool for mapping coseismic rupture-zone deformation. Here, we showcase its rich potential using synthetic datasets derived from the southern California "B4" survey and real examples from earthquakes in Baja California and Japan to illustrate. Point-cloud differencing procedures based on the Iterative Closest Point algorithm or on cross-correlation techniques can determine the surface deformation field in 3 dimensions, complementing conventional InSAR and pixel-tracking techniques which measure line-of-sight and horizontal displacement components only. A further advantage is that differential LiDAR retains coherence in the presence of steep displacement gradients, such as close to surface ruptures, and it is therefore well-suited for probing the slip distribution and mechanical properties of the shallow part of the fault zone. Challenges include the treatment of vegetation and the

reliance on older, "legacy" LiDAR datasets – third party surveys which were not optimized for earthquake studies and for which important data acquisition and processing metrics may be unavailable. The 4 April 2010 El Mayor-Cucapah (Mexico) earthquake was the first complete rupture with both pre- and post-event LiDAR coverage, and its resultant 3-D displacement field is used to explore whether significant slip occurred on low-angle detachment faults, as has been postulated by some field geologists. The 11 April 2011 Fukushima-Hamadori (Japan) normal-faulting earthquake is the second such example, and was studied with support from the Virtual Institute for the Study of Earthquake Systems (VISES), a joint initiative between SCEC and the Earthquake Research Institute and Disaster Prevention Research Institute of Japan. Here, coherent differential LiDAR displacements within the interior part of the fault zone are used to help bridge a critical observational gap between surface faulting offsets (observed in the field) and slip occurring at depths of a few kilometers (inferred from InSAR modelling). Near-fault displacements and rotations are consistent with decreased primary fault slip at very shallow depths of a few 10s of meters, possibly accounting for the large, along-strike heterogeneity in field measurements of surface offset.

Improvement of the single station algorithm for earthquake early warning, Shunta Noda, Shunroku Yamamoto, and Masahiro Korenaga (Poster 036)

Estimation of epicenters (or hypocenters) is one of the key observables needed in order to issue a regional Earthquake Early Warning (EEW). The B- Δ method [Odaka et al., 2003] and Principle Component Analysis (PCA) [Meteorological Research Institute, 1985] are used to determine the epicentral distance and back-azimuth, respectively, in the single station algorithm in operation at the JMA- and Shinkansen-EEW systems in Japan. In this study, we propose new techniques to improve the speed and the accuracy of epicentral determination.

To estimate the epicentral distance, we propose a new method, the C- Δ method, instead of the B- Δ method. The proposed method has two important characteristics; first, a simpler equation $y=C*t$, compared with $y=B*t*\exp\{-A*t\}$ in the B- Δ method, is used as a fitting function for the initial envelope of the high frequency (10-20Hz) P-wave acceleration; second, a shorter length (0.5 seconds from the P-arrival) for the time window is used for the estimation, compared with the conventional one (2 seconds). We consider the proposed technique to be more appropriate for the estimation than the conventional one, because our analysis shows that the amplitude growth of the initial P-wave for about 0.5 seconds from the onset is almost independent of magnitude. We also introduce an anelastic attenuation term ($Y*\Delta$) into the relation equation between C and Δ in addition to the geometrical spreading term ($\beta*\log\Delta$). The modified relation equation is expressed as $\log C = \alpha + \beta*\log\Delta + Y*\Delta$, whereas the conventional one is $\log C = \alpha + \beta*\log\Delta$. Using these modifications, the accuracy and the speed of estimations of epicentral distance are improved by about 19% and 75%, respectively, compared with the conventional method.

In order to improve the performance of the back-azimuth estimation with PCA, we introduce the variable-length time window technique, instead of a conventional fixed-length time window (1.1 second from the P-arrival). The proposed method utilizes the time from the P-arrival to the first zero-crossing of the band passed (1-2Hz) displacement for the analysis. We consider that this suggested technique reduces the influence of the P-coda. Consequently, it is found that the accuracy and the rapidness of estimations of back-azimuth are improved by about 28% and 36%, respectively, compared with the conventional method.

An inverse modeling code for obtaining earthquake source parameters from InSAR data, Erika Noll and Gareth Funning (Poster 241)

The data for theories of earthquake mechanics and for models of fault activity often come from catalogs of source parameters from earlier earthquakes. Most of these source parameters come from inversions of seismic data, but for over a decade, InSAR has provided another source of data. Inversions of InSAR data use a variety of codes, all using smoothing algorithms, and as a result, may find different results for the same earthquake. A better understanding of the uncertainty inherent in the data and the ability to quantify the model-based uncertainty might ameliorate this issue. This project aims to do both by creating a code to invert InSAR data using discrete nesting slip patches to represent the

MEETING ABSTRACTS

fault, removing the need for a smoothing algorithm and allowing direct calculation of the model-based uncertainty. The code is MATLAB-based and uses the `fmincon` function to optimize fault geometry and slip, as well as a vectorized version of the Okada (1992) formulas to forward model displacement. In addition to allowing calculation of model-based uncertainty, use of a variable number of discrete parameters - by controlling the number of slip patches - allows the user to explore the effects of increased detail in a model and find the level of complexity in the model that is justified by the data. Adding a second slip patch has decreased the WRSS misfit by half in the case of both a synthetic interferogram and the 2003 Bam, Iran earthquake, and further exploration is planned.

Space-time Renewal Model for Repeating Earthquakes and Slip-rate History in the Northeastern Japan Subduction Zone, Shunichi Nomura (Poster 032)

We propose a non-stationary stochastic model for repeating earthquakes to estimate spatio-temporal variation in slip rate. Repeating earthquake sequences on the plate subduction zone represent the slip-rate histories around their fault patches. So they are useful resources for monitoring aseismic slow slip on plate boundaries. Repeating earthquakes are often modeled by renewal processes, point processes whose recurrence intervals are independent and identically distributed. However, their repeating intervals are greatly influenced by larger seismic events or aseismic slow slip, and hence we need to model such non-stationary behavior of repeating earthquakes. Then the proposed model can estimate spatio-temporal variation in slip rate with smoothness restriction adjusted to optimize its Bayesian likelihood. We used the empirical relation between magnitudes and slip sizes of repeating earthquakes by Nadeau and Johnson (1998) to estimate the slip-rate histories in repeating sequences. The Proposed model can estimate slip rate at depth where GPS system can not measure directly. Although it is difficult to estimate coseismic slip of large earthquakes from repeating earthquakes, this model may be useful to monitor the transition of stress field or interplate coupling on plate boundaries. We apply the proposed model to the large catalog of repeating earthquakes on subduction zone of Pacific Plate in the northwestern Japan from 1993 to 2011 and estimate slip-rate history of the plate boundary.

Foreshock probability forecasting, Yosihiko Ogata (Poster 022)

We are concerned with whether currently occurring earthquakes will be "foreshocks" of a significantly larger earthquake or not. When plural earthquakes occur in a region, I attempt to statistically discriminate foreshocks from a swarm or the mainshock-aftershock sequence. The forecast needs identification of an earthquake cluster using the single-link algorithm; and then the probability is calculated based on the clustering strength and magnitude correlations. The probability forecast model were estimated from the JMA hypocenter data of earthquakes of $M \geq 4$ in the period 1926-1993 (Ogata et al., 1996).

Then we presented the performance and validation of the forecasts during 1994 - 2010 by using the same model (Ogata and Katsura, 2012). The forecasts perform significantly better than the unconditional (average) foreshock probability throughout Japan region. The frequency of the actual foreshocks is consistent with the forecasted probabilities. In my poster, I would like to discuss details of the outcomes in the forecasting and evaluations. Furthermore, I would like to apply the forecasting in California and global catalogs to show some universality in the forecasting procedure.

Reference:

[1] Ogata, Y., Utsu, T. and Katsura, K. (1996). Statistical discrimination of foreshocks from other earthquake clusters, *Geophys. J. Int.* 127, 17-30.

[2] Ogata, Y. and Katsura, K. (2012). Prospective foreshock forecast experiment during the last 17 years, *Geophys. J. Int.*, 191, 1237-1244.

Dynamic models of the 2010 Sierra El Mayor-Cucapah Earthquake, David D. Oglesby, Gareth J. Funning, and Christodoulos Kyriakopoulos (Poster 148)

The M 7.2 2010 Sierra El Mayor-Cucapah Earthquake took place on a complex system of oblique normal/right-lateral faults separated by apparent stepovers and gaps as large as 5 km wide and 11 km long. We

use the 3D dynamic finite element method and fault geometry motivated by both LIDAR and InSAR imagery to investigate the physical causes of the complex rupture behavior in this event, and the apparent long-range jump in particular. We find that for rupture to jump the largest stepover (in the Accommodation Zone between the two largest fault segments), some sort of previously-unmapped slip structure(s), such as an intermediate fault or extensions of the neighboring sections, must exist in the intervening space, either at depth or intersecting the surface. The ground motion from this geometrically complex fault system is also quite complex, with a bias toward higher ground motion on the hanging wall sides of the dipping fault segments, and with local heterogeneity caused by the nonplanarity and discontinuity of the fault segments. The results help to explain not just the physics of this event, but to foreshadow the behavior of suites of small fault segments in potential complex earthquakes in the future.

Permeability, porosity and pore geometry evolution of cohesive and incohesive sedimentary rocks, Keishi Okazaki, Hiroyuki Noda, Shin-ichi Uehara, and Toshihiko Shimamoto (Poster 144)

Permeability k is expressed as a product of the hydraulic radius R_h (= pore volume V_p / sample surface area S) squared, porosity ϕ , and a nondimensional geometrical factors $1/G$. G is often assumed constant depending on the model, partly because its measurement is difficult. Estimating the geometrical factor G and its changes by measuring permeability, porosity and surface area will be a useful tool particularly for studying fluid flow for fine-grained rocks for which observations of pore microstructures are difficult. Fluid flow in impermeable fine-grained rocks is important in many problems such as fluid flow in the Earth, hydrocarbon accumulation, waste isolation and CCS. Moreover, incohesive fault rocks such as fault gouge and fault breccia will have similar pore structures to those of sediments and porous sedimentary rocks. But predominant fluid flow will be along fractures in cohesive fault rocks such as cataclases.

We propose a method to measure G without assuming any microstructural model, and present its evolution during compaction of sedimentary rocks that are too fine-grained to observe and quantify microstructures. We measured S , k , V_p , and grain volume V_g during compaction with confining pressure up to 100 MPa of diatomaceous mudstone from Koetoi Formation (K_{dm} , $\phi = 0.53-0.64$) and siliceous mudstone from Wakkanai Formation (W_{sm} , $\phi = 0.28-0.33$), Horonobe, Japan. They are similar sedimentary rocks, but are different in the grade of diagenesis. V_p and S yield R_h , and thus we can estimate G . G for K_{dm} remains nearly constant during compaction and varies from 1.3 to 6, whereas G for some samples from less porous W_{sm} increases irreversibly with compaction from about 0.1 to 10. The increase in G by 2 orders of magnitude probably indicates the change in the dominant fluid conduit from concentrated flow along fractures to pervasive flow.

The SDSU Broadband Ground Motion Generation Module Version 1.5, Kim B. Olsen and Rumi Takedatsu (Poster 061)

SCEC has completed Phase 1 of its Broadband Platform (BBP) ground motion simulation results, evaluating the potential applications for engineering of the resulting PSAs generated by 5 different methods. The evaluation included part A, where the methods were evaluated based on the bias of simulation results to observations for 7 well-recorded historical earthquakes with source-station distances between 1 and 193 km, and part B, where simulation results for Mw 6.2 and Mw 6.6 strike-slip and reverse-slip scenarios were evaluated at 20 km and 50 km from the fault. The methods were assessed based on the bias of the median PSA for the 7 events in part A, and on a specified acceptance criterion compared to NGA-West2 GMPEs in part B. One of the 5 methods evaluated was BBtoolbox, a hybrid method combining deterministic low-frequency (LF) synthetics with high-frequency (HF) scattergrams (Mai et al., 2010; Mena et al., 2010; V1.4). In the validation exercise, the LFs are generated using 1-D Green's Functions and 50 source realizations from the kinematic source generator module by Graves and Pitarka (2010, 'GP'). However, the results from BBtoolbox V1.4 did not pass the SCEC validation phase 1. In order to obtain more accurate BB synthetics, we generated BBtoolbox V1.5 which scales the HFs to a theoretical spectral level at the merging frequency (GP, Eq. 10) fixed at 1Hz, rather than the level of the LFs in V1.4. This modification has generated much improved spectral levels at higher frequencies, while we have seen little evidence of artifacts

from this technique. In addition, V1.5 introduced a new source time function with rise-time scaled as a function of moment. With these modifications, BBtoolbox V.15 became one of three methods passing the SCEC validation exercise Phase I. Here, we describe the details of BBtoolbox V1.5, and show comparisons between BBtoolbox V1.5 synthetics and observations from the validation exercise.

Bayesian forecasting of aftershocks by ETAS model, Takahiro Omi, Yoshihiko Ogata, Yoshito Hirata, and Kazuyuki Aihara (Poster 023)

Operational forecasting of aftershocks has been conducted to reduce seismic risks after a large earthquake. Here we investigate the impact of the estimation uncertainty of a forecasting model on the performances of the aftershock forecasting. The epidemic-type aftershock sequence (ETAS) model that can reproduce potentially complex aftershock activity is employed for the forecasting. We usually use only an optimal set of parameter values such as the maximum likelihood estimates or the maximum a posteriori estimates to prepare forecasting (plug-in forecasting). On the other hand, if the estimation uncertainty is large, which occurs especially in using the early and incomplete aftershock data, such forecasting that relies on a single set of parameter values may severely miss other part of the actual observations. Alternatively we present a Bayesian forecasting method that considers the estimation uncertainty. Specifically, we combine the forecasts from the ETAS model with various probable parameter values, which are sampled from the posterior probability distribution given the learning data by using the MCMC method. We analyze many aftershock sequences in Japan, and show that the Bayesian forecasting method generally performs better than the plug-in forecasting, demonstrating the importance of considering the estimation uncertainty of forecasting models.

Slip rate, slip history, and slip per event along the northern San Jacinto fault zone during the past 2000 years: a summary of work at the Mystic Lake and Quincy sites on the Claremont fault. Nathan Onderdonk, Sally McGill, and Tom Rockwell (Poster 275)

The main objective of the SCEC Southern San Andreas Fault Evaluation project was to “increase our understanding of the slip rate, paleo-earthquake chronology, and slip distribution in recent earthquakes on the southern San Andreas fault system during the past 2000 years”. Work along the Claremont strand of the San Jacinto fault zone during the past 6 years has done this and we summarize the results here. Four field seasons of paleoseismic trenching at the Mystic Lake site have produced a record of 15 ground-rupturing earthquakes in the past 3500 years. During the last 2000 years there were 12 earthquakes, with the most recent occurring around AD 1800. The average recurrence interval is 175 ± 20 years, and the 200+ years since the most recent event is longer than any gap in the past 2000 years. Trenching and dating of offset streams and one buried channel at a second site (the Quincy site) has resulted in four independent calculations of slip rate and average slip per event. The slip rate for the last 2000 years is 12 to 19 mm/yr and the average slip per event is 2.3 m. Short-term slip rates calculated from an offset stream and the buried channel, which were offset in the past three events, are higher by about 10 mm/yr due to a cluster of earthquakes on the fault between AD 1400 and AD 1800 and higher than average displacements of 2.7 to 3 m in one or more of these earthquakes. This spurt of activity may explain the longer than normal time between earthquakes that we are now experiencing. Comparison of the Mystic Lake earthquake history with the Hog Lake paleoseismic record on the Clark fault to the south, and the Wrightwood paleoseismic record on the Mojave segment of the San Andreas fault to the north, shows overlaps in the timing of some events. Five possible correlations between the Mystic Lake record and the Hog Lake record, and another five possible correlations between Mystic Lake and Wrightwood suggest that some events may have ruptured through the step-overs at the ends of the Claremont fault or that events on one fault trigger closely-timed events on the adjacent fault. None of the events in the past 2000 years overlap at all three sites, indicating that an earthquake rupturing the San Andreas fault all the way to the central San Jacinto fault (or vice-versa) is unlikely.

Systematic receiver function analysis of the Moho geometry in the southern California plate-boundary region, Yaman Ozakin and Yehuda Ben-Zion (Poster 202)

We investigate the geometry of the Moho interface in the southern California region including the San Andreas fault (SAF), San Jacinto fault zone (SJFZ), Elsinore fault (EF) and Eastern California Shear Zone with systematic analysis of receiver functions. The data set consists of 145 teleseismic events recorded at 188 broadband stations throughout the region. The analysis utilizes a 3D velocity model associated with detailed double-difference tomographic results for the seismogenic depth section around the SAF, SJFZ and EF combined with a larger scale community model. A 3D ray tracing algorithm is used to produce effective 1D velocity models along each source-receiver teleseismic ray. Common Conversion Point (CCP) stacks are calculated using the set of velocity models extracted for each ray. The CCP stacks are analyzed with volumetric plots, maps of maximum CCP stack values, and projections along profiles that cross major faults and other features of interest. The results indicate that the Moho geometry in the study area is very complex and characterized by large prominent undulations along the NE-SW direction. A zone of relatively deep Moho (~35-40 km) with overall N-S direction crosses the SAF, SJFZ and EF. A section of very shallow Moho (~10 km) below and to the SE of the Salton Trough, likely associated with young oceanic crust, produces large Moho offsets at its margins. Locations with significant changes of Moho depth appear to be correlated with fault complexity in the brittle crust. The observations also show vertical Moho offsets of ~8 km across the SAF and the SJFZ close to Cajon pass, and sections with no clear Moho phase underneath Cajon pass and adjacent to the SJFZ likely produced by complex local velocity structures in the brittle upper crust. These features are robust with respect to various parameters of the analysis procedure.

Towards a Unified Theory of Seismicity Rate Variation, Morgan T. Page and Karen Felzer (Poster 030)

A necessary ingredient for a moment-balanced hazard model is the total seismicity rate. Typical catalogs, however, will often underestimate the true long-term seismicity rate. Seismicity rate variation also plays an important role in the debate over whether earthquakes on faults follow a characteristic or Gutenberg-Richter (G-R) magnitude distribution; that is, if faults are G-R, substantial rate variability must exist.

How far off from the true, long-term seismicity rate can a catalog of finite duration be? We attack this problem from multiple fronts. We evaluate historically observed rate changes in locations with long seismic histories such as Turkey, the Dead Sea, and China. We compare this variability to shorter-term variability in well-instrumented regions. We also use Epidemic-Type Aftershock Sequence (ETAS) modeling to determine whether the level of seismicity rate variability is beyond what would be expected from aftershock-driven clustering. We find that catalog variability can be described with a Poisson component and a clustering component (perhaps only partially due to aftershock clustering), is inversely proportional to both the strain rate and catalog duration, and is magnitude dependent.

Post-El Mayor Cucupah surface fracture deformation in UAVSAR images, Jay W. Parker and Andrea Donnellan (Poster 235)

By the end of 2010 the NASA UAVSAR program had released separate interferograms of the 20 km wide strip just north of the California-Mexico border for times spanning the April 4, 2010 El Mayor Cucupah (EMC) Earthquake in Mexico (October 21, 2009 to April 13, 2010) and for two post-seismic intervals, April 13, 2010 to July 10, 2010, and from that date to December 1, 2010, the first of which showed substantial deformation features associated with a June 14, 2010 M5.7 aftershock near Ocotillo, California. Recently released interferograms spanning dates October 21, 2009 to September 28, 2010 (coseismic plus early post seismic), and April 12, 2010 to February 11, 2014 (long-term post seismic deformation) have remarkably good coherence despite the long time intervals, probably due to dry desert conditions. These interferograms provide vivid deformation images from the coseismic and postseismic EMC including many aftershocks, exposing a network of mutually near-perpendicular faults filling the conceptual gap between the Laguna Salada and related faults in Mexico, and the Superstition Hills and Imperial faults in California. These

MEETING ABSTRACTS

observations support a plate boundary framework where transitional regions between the ends of long strike-slip and oblique faults have less detectable short faults often bounding rotating blocks that fill in the gaps and accommodate a significant portion of the plate to plate shear.

Automatic identification of fault zone head waves and direct P waves and its application in the Parkfield section of the San Andreas Fault, California, Zhigang Peng and Zefeng Li (Poster 161)

Fault zone head waves (FZHWs) are observed along major strike-slip faults, and can provide high-resolution imaging of fault interface properties at seismogenic depth. In this paper we present a new method to automatically detect FZHW and pick direct P waves secondary arrivals (DSWAs). The algorithm identifies FZHWs by computing the amplitude ratios between the potential FZHWs and DSWAs. The polarity, polarization and characteristic period of FZHWs and DSWAs are then used to refine the picks or evaluate the pick quality. We apply the method to the Parkfield section of the San Andreas Fault where FZHWs have been identified before by manual picks. We compare results from automatically and manually picked arrivals and find general agreement between them. The obtained velocity contrast at Parkfield is generally 5%-10% near Middle Mountain while it decreases below 5% near Gold Hill. However, we find many FZHWs recorded by the stations within 1 km of the background seismicity (i.e., the Southwest Fracture Zone) that has not been reported before. This could be explained by a relatively wide low velocity zone sandwiched between the fast Salinian block on the southwest side and the slow Franciscan Melange on the northeast side. Station FROB on the southwest (fast) side on the also recorded a small portion of FZHWs, which could be related to the reversal of velocity contrast at depth between Middle Mountain and Gold Hill.

Micromechanics based permeability evolution model in brittle materials and implications for injection-induced earthquake nucleation, Thibaut Perol, Harsha S. Bhat, and Kurama Okubo (Poster 108)

We investigate the role of off-fault damage, and damage-enhanced off-fault permeability, on earthquake nucleation. This aims to mimic a situation in which wastewater, injected into a reservoir, diffuses towards an active/inactive fault close by. First, we develop a micro-mechanics based permeability evolution model for micro-crack dominated brittle materials that are strain rate sensitive. We extend the micromechanical model developed by Bhat et al. (2012) in which the constitutive description of a brittle material is governed by micro-cracks and appropriate crack growth laws. This allows us to evaluate the micro-crack geometry and its evolution for fluid migration. With an assumed law for evolution of the connectivity of the crack network we then use the model developed by Gueguen and Dienes (1989) to compute permeability evolution. Computed permeability evolution shares reasonable characteristics with experimental results.

Additionally, we explore the role of frozen off-fault permeability structure (measured in the Horse Canyon Segment of the San Jacinto fault by Mitchell et al. 2012) on pore pressure evolution on a hypothetical fault 200 m away from an injection well. This pore pressure evolution was supplied to a Quasi-Dynamic earthquake simulator with rate and state friction law and aging state evolution law to study the role of off-fault damage zone on earthquake nucleation. Preliminary results show injection-induced pore pressure changes on the fault have a considerable impact on earthquake nucleation, triggering earthquakes on normally inactive faults. The frozen permeability structure significantly affects the timing of earthquake nucleation. Therefore, it seems necessary to quantify the dynamic changes of off-fault permeability due to dynamic earthquake rupture to understand injection-induced earthquake nucleation. We thus plan to incorporate the earthquake damage-induced permeability evolution model presented in this study into earthquake cycle models to better quantify induced seismicity.

Towards Reconciling Magnitude-Invariant Stress Drops with Dynamic Weakening, Stephen M. Perry and Nadia Lapusta (Poster 131)

The energy budget of earthquakes is a question of significant fundamental and practical interest. Using rate-and-state fault models that produce earthquake sequences, we focus on exploring the breakdown energy portion G of this budget and its relation to stress drop in events over a

range of magnitudes. We focus on understanding which models can reproduce the observation that breakdown energy increases with increasing magnitude, but stress drop appears to be magnitude-invariant.

We begin with simulations with pure rate-and-state friction and study how breakdown energy changes with characteristic slip distance L of rate-and-state friction, a parameter often selected based on numerical tractability. We explore values of L ranging two orders of magnitude and calculate breakdown energy G for events with various amounts of slip. The values of G in our simulations are similar to those of natural earthquakes. However, we find nearly-constant values of G across a range of slips for a given L , as well as decreasing G with smaller values of L , as expected based on prior studies. Hence simulations with laboratory-like values of L (0.01-0.1 mm), necessary for producing microseismicity, would result in breakdown energies too small for large events, compared with observations.

We then proceed to a model utilizing dynamic weakening due to thermal pressurization of pore fluid within the fault core. Co-seismic weakening through mechanisms such as thermal pressurization can explain the trend of increasing breakdown energy with magnitude as shown by Rice (JGR, 2006) in a simplified slip model. Our goal is to explore this result in fully dynamic simulations that produce a series of seismic events of different sizes, and investigate whether it can be reconciled with the magnitude-invariant stress drop. We find that our sequences are able to capture the trend of increasing breakdown energy with increasing magnitude while also displaying roughly magnitude-invariant stress drops for a range of the smaller magnitude events. Our current work is directed towards studying the stress drops for the largest, model-spanning events, which can be smaller, larger, or similar depending on the model assumptions.

Applying Social and Behavioral Science to Broaden Use of the U.S. Geological Survey National Seismic Hazard Maps, Sue Perry and Mark Petersen (Poster 006)

The National Seismic Hazard Maps (NSHM) are a flagship product of the U.S. Geological Survey (USGS). Because they go into the seismic provisions of building codes, they help to save lives. In addition, NSHM affect insurance rates and risk assessments. All told, NSHM influence trillions of dollars of business decisions annually. Currently, NSHM serve very specialized expertise, which restricts usage and increases misuse. However, NSHM - and the data that go into them - could benefit many other groups. Thus, the USGS has launched a campaign to develop new NSHM products for new users, beginning with local officials and the general public.

To start, a recent USGS workshop united experts from 18 disciplines. There, earthquake scientists and engineers described NSHM, then attendees from behavioral and social sciences, public health, marketing, communication, and design shared risk perception and communication concepts - and offered remarkably consistent guidelines to develop successful products:

1. Define your goals. What information do you want to communicate, to whom? What do you want the audience to do with your information? To what benefit? How will you define success?
2. Know your audience. Understand user concerns, worries, goals, needs, levels of literacy and science understanding, experience, expectations, plus demographic and cultural influences.
3. Meet people where they are. Work with your users throughout product development. Do not tell them what they need, or expect them to change in order to understand you. Build from their understanding and viewpoint - not yours. Use plain language.
4. Employ design thinking. Be inclusive, open to new ideas, collaborative; avoid pre-conceptions and focus on the user.
5. Test early and often. Begin product assessment when a project starts. The assessment process will help you to achieve the other guidelines.
6. Iterate.

The workshop provided numerous "ah ha!" moments, including these:
+ Risk perception is subjective and personal; risk communication is never "one size fits all".

+ While the USGS carefully distinguishes earthquake hazard from risk, to most of the non-USGS attendees - and the general population - these two words are synonyms. When the USGS says "hazard" most people hear - and interpret based on - "risk".

The attendees also brainstormed strawman products to propose to target users. We welcome your input about NSHM, the strawman products on this poster, and this process to serve new users.

The role of gouge and temperature on flash heating and its hysteresis, *John D. Platt, Brooks P. Proctor, Thomas M. Mitchell, Greg Hirth, David L. Goldsby, Giulio Di Toro, Nicholas M. Beeler, and Terry E. Tullis* (Poster 109)

Geophysical observations and high-velocity friction experiments suggest that mature faults weaken significantly during earthquakes. One mechanism used to explain this weakening is the breakdown of frictional contacts at a critical weakening temperature, a process known as flash heating. For bare surface sliding Rice [2006] showed that heat generation at highly stressed frictional contacts triggers flash heating above a critical weakening velocity V_w of ~ 0.1 m/s. However, all faults generate a gouge layer at least a few millimeters wide, and the efficiency of flash heating in sheared gouge is still unknown.

Building on Beeler et al. [2008] we model flash heating in gouge by assuming that the total slip rate applied across the deforming zone is shared between multiple frictional contacts. Solving for the contact temperature we show that flash heating occurs when the strain rate exceeds a critical weakening strain rate controlled by the gouge properties. For a deforming zone 100 μm wide the equivalent V_w is ~ 4 m/s, making flash heating much less efficient in gouge than for bare surfaces.

The lower contact slip rate associated with distributed shear leads to longer contact lifetimes, increasing the thickness of the thermal boundary layer at a slipping contact W . We show that W can become comparable to the expected spacing between slipping contacts D . Accounting for this in a new model for contact temperature we show that when $W \approx D$ flash heating begins at much lower slip rates, and friction decreases slowly as the slip rate increases.

Finally we study the hysteresis commonly seen in bare surface experiments, with higher friction observed during acceleration than deceleration. We show that accounting for the sensitive dependence of V_w on sliding surface temperature T_f allows us to match at least some experimental data for both acceleration and deceleration over a wide range of slip rates. Building on this we discuss how flash heating may operate near the trailing edge of a rupture where temperatures are high and slip is decelerating.

SCEC Community Fault Model Version 5.0, *Andreas Plesch, Craig Nicholson, Christopher Sorlien, John H. Shaw, and Egill Hauksson* (Poster 096)

We present a new release of the SCEC Community Fault Model (CFM) for southern California. CFM version 5.0 includes a number of major improvements, including refinement and additions of new 3D fault surfaces using the USGS Quaternary Fault (Qfault) traces and relocated seismicity (Yang et al., 2012; Hauksson et al., 2012), as well as an updated naming system. The previous version of CFM (4.0) offered a fully populated database of fault properties including a hierarchical naming and numbering system, average fault dip, associated Qfault ID, and a quality factor average. Version 4.0 underwent a formal evaluation process with fault rankings that were used to comprise a preferred fault set for CFM. CFM 5.0 builds on these enhancements by providing a comprehensive suite of improved 3D fault representations in southern California. The new fault representations are more precise, and often more highly segmented than in previous CFM versions. CFM 5.0 also includes many new faults that were not represented in previous model versions. In the onshore Santa Maria basin, these include blind and emergent structures such as the Orcutt, Lompoc, Zaca, Los Alamos, Pezzoni-Casmania, and Santa Ynez Valley faults. In the Ventura-Santa Barbara area, new models include a substantially revised set of alternative representations for the Ventura, Pitas Point, Red Mountain, Mission Ridge, Santa Ynez, San Cayetano,

Oak Ridge and Simi-Santa Rosa faults, all in support of the Ventura Special Fault Study Area (SFSA). In the offshore Borderland, new or updated faults include the Santa Cruz-Catalina Ridge, East Santa Cruz basin, Coronado Bank fault and detachment, Ferrello, San Clemente, San Mateo-Carlsbad, San Diego Trough and San Pedro Basin faults. In the Eastern Transverse Ranges, 3D fault models for the Cleghorn, Pinto Mountain and North Frontal Thrust faults were substantially updated. In the Mojave area, updated faults include the Lenwood-Lockhart, Helendale-South Lockhart and faults involved in the Landers and Hector Mine ruptures, among many others. In the San Geronio Pass area, the Crafton Hills fault zone and other cross faults were added. Finally, we attempted to define several detachment surfaces at mid and deep crustal levels beneath both the San Jacinto and San Bernardino Mountains, as part of the San Geronio Pass SFSA. CFM 5.0 is provided as a series of fault tsurfs with coordinates in the WGS-84 reference ellipsoid, and is available through the SCEC CME website.

Geologic and geophysical maps and databases for Joshua Tree National Park, southern California, *Robert E. Powell, Victoria E. Langenheim, Jonathan C. Matti, and Pamela M. Cossette* (Poster 264)

Joshua Tree National Park lies within the eastern part of the Transverse Ranges province and straddles the transition between the Mojave and Sonoran deserts. Mountain ranges and basins in the Park exhibit an E-W physiographic grain controlled by left-lateral fault zones that form a sinistral domain within the broad zone of dextral shear along the transform boundary between the North American and Pacific plates. The sinistral faults connect the Mojave Desert dextral faults of the Eastern California Shear Zone to the N and E with the Coachella Valley strands of the southern San Andreas Fault Zone (SAFZ) to the W.

The geologically diverse terrain that underlies the Park evolved over a span of nearly 2 Ga. Proterozoic plutonic and metamorphic rocks constitute an inlier of the North American craton within the Mesozoic Cordilleran magmatic arc. In the Park, the arc forms a composite batholith of Triassic through Late Cretaceous plutons arrayed in NW-trending lithodemic belts. Subordinate Jurassic and Cretaceous volcanic and meta-sedimentary rocks occur in the Pinto and Coxcomb Mts.

The Park's present landscape began to form as crystalline basement was exhumed during the Paleogene and early Neogene and underwent differential deep weathering beneath a low-relief erosion surface. The deepest weathering profiles formed on quartz-rich, biotite-bearing granitoid rocks. Late Miocene fluvio-lacustrine deposits and basalt flows locally overlapped the erosion surface and sinistral faulting began subsequently, perhaps as early as ca 7 Ma, but no later than ca 5 Ma. Syn-faulting uplift of the mountain blocks led to erosional stripping of the weathered quartz-rich granitoids to form etchplains dotted by bouldery tors—the iconic landscape of the Park. The erosional debris filled basins that developed along the E-W fault zones, chiefly during the Pliocene and Quaternary.

Geologic and potential-field geophysical data yield measurements of varying left-lateral displacement on the Blue Cut (5-10 km), Smoke Tree Wash-Victory Pass, Porcupine Wash-Substation fault zones (1-3 km), Pinto Mountain (16-20 km), and Chiriaco (8-11 km) fault zones. The data indicate left steps along the fault zones where gravity data define 1- to 2-km-deep sub-basins. Along the eastern margin of the sinistral domain, deep (>2-km) triangular basins lie at the intersections of the E-W faults with the NW-trending Sheep Hole Fault. Such basins are absent to the W where the E-W faults intersect the SAFZ.

Uncertainty in the 2014 USGS California hazard model, *Peter M. Powers* (Poster 012)

The recently updated 2014 National Seismic Hazard Model (NSHM; Petersen et al., 2014) and associated maps provide a time-independent ground motion forecast for use in building codes and other applications. The California component of the model is based on the third version Uniform California Earthquake Rupture Forecast (UCERF3; Field et al., 2013). The 2014 NSHM includes both aleatory and epistemic uncertainty, with epistemic uncertainty in seismic source and ground motion models represented primarily by logic trees and associated branch weights. Logic-trees ideally span the full range of possible models and, although they typically grow in size as models increase in complexity over time (e.g.

MEETING ABSTRACTS

480 branches in 2007 UCERF2 model versus 1440 branches in the 2013 UCERF3), the published NSHM maps only show the result of collapsing all branches with their associated weights to mean hazard. Such collapsing is often motivated by a desire for greater computational efficiency. Each release of the maps naturally raises numerous questions about what has led to changes in mean forecast ground motions. While the changes always stem from specific model changes (e.g. new faults, model methodologies, ground motion models, or logic-tree branch weights), little context is provided for understanding how such variation stacks up against the uncertainty in the model. For several sites in California, I calculate a full set of hazard curves defined by the NSHM logic tree for peak ground acceleration, and 5Hz and 1Hz spectral accelerations, and derive histograms of ground motions that show the uncertainty in the mean ground motions reported in the 2014 NSHM. The curves at sites in close proximity to active faults show that ground motion models are the primary contributor to uncertainty, whereas away from active faults, uncertainty is commonly driven by the choice of smoothed seismicity model. These analyses show that in many cases where changes in mean forecast ground motions between 2008 and 2014 are high, there is actually significant overlap in the range of possible ground motions suggesting that large changes should be taken with a grain of salt.

IO Optimization Techniques for Distributed Heterogeneous Supercomputing Systems, Efecan Poyraz, Jun Zhou, and Yifeng Cui (Poster 086)

Significant challenges have emerged in run-time IO when scaling large-scale earthquake applications on heterogeneous systems. We introduce a variety of IO optimization techniques implemented in two versions of AWP, one to calculate ground motions at many sites and the other to calculate ground motions from many single-site ruptures. These techniques help improve the IO performance for running simulations at extreme scale. Reading or writing large number of small files can stretch the file system quite a bit, in particular when using more than tens of thousands of processor cores. We introduce an optimal file system striping approach for large files, and achieve high efficiency through writing less interleaved larger contiguous blocks of data.

We have developed a two-layer IO model to allow a tradeoff between IO and communication costs. The large and highly interleaved media input data is read by a subset of MPI tasks in large contiguous chunks. Then the data is distributed to corresponding MPI tasks using asynchronous point-to-point communications. We compare the collective MPI-IO performance to the two-layer model, and demonstrate that the chosen approach is more efficient since it allows a more detailed control over the access to the data in the file system. Our goal is to reduce the number of file system accesses and improve overall IO performance.

When designing low-level MPI-IO output format, we choose two flexible formats that can be switched at run-time between fast-space (or fast-x) and fast-time (or fast-t). The fast-t format, with two consecutive values belonging to the same variable's different values in time, produces less interleaved and larger chunks of output data, since the entire time dimension is computed in the same MPI task. On the other hand, the fast-x format is favored for visualization operations, which require plane/volume data at specific time instances.

On GPU-based systems, we use an application programming interface API, which utilizes small and light weight pthread modules to post-process the intermediate results in-situ while the main solver is accelerated on GPUs. That way we minimize the total amount of output for improved IO performance and reduced time-to-solution.

The IO tuning methods implemented result in nearly perfect scalability of our target code on petascale hybrid systems. The techniques introduced are applicable to other seismic applications facing similar IO challenges.

Dynamic weakening of serpentinite gouges and bare-surfaces at seismic slip rates, Brooks P. Proctor, Tom M. Mitchell, Greg Hirth, David Goldsby, Federico Zorzi, John D. Platt, and Giulio Di Toro (Poster 111)

Serpentinite is a common rock type in oceanic transform faults. Our ability to understand and predict seismicity generated along these faults depends on models for the frictional behavior of serpentinite at conditions spanning the seismogenic zone. To investigate differences in the frictional

behavior between serpentinite bare-rock surfaces and powdered serpentinite ('gouge') at sub-seismic to seismic-slip rates, we conducted rotary shear experiments on an antigorite-rich and lizardite-rich serpentinite at slip rates (V) from 0.003 m/s to 6.5 m/s, sliding displacements up to 1.6 m, and normal stresses (σ_n) up to 22 MPa for gouge and 97 MPa for bare surfaces. Nominal steady-state friction values (μ_{ss}) in gouge at $V=1$ m/s are larger than in bare surfaces for all on tested and demonstrate a strong σ_n dependence; μ_{ss} decreased from 0.51 at 4.0 MPa to 0.39 at 22.4 MPa. Conversely, μ_{ss} values for bare surfaces remained ~ 0.1 with increasing σ_n and V . Additionally, the velocity at the onset of frictional weakening and the amount of slip prior to weakening were orders of magnitude larger in gouge than in bare surfaces. Extrapolation of the normal stress dependence for μ_{ss} suggests that the behavior of antigorite gouge approaches that of bare surfaces at $\sigma_n \geq 60$ MPa. X-ray diffraction revealed dehydration reaction products in samples that frictionally weakened. Microstructural analysis revealed highly localized slip zones with melt-like textures in some cases gouge experiments and in all bare-surfaces experiments for $V \geq 1$ m/s. 1-D thermal modeling indicates that flash heating is the primary process causing initial weakening in bare surfaces. Flash heating also occurs in gouge, however because strain is more distributed, dynamic weakening occurs at higher velocities and after larger displacements. Our findings suggest that at shallower depths (<5 km) the frictional behavior of faults will be strongly affected by the presence of unconsolidated gouge.

Internal structure of the San Jacinto fault zone at Jackass Flat from data recorded by a dense linear array, Hongrui Qiu, Yehuda Ben-Zion, Zachary E. Ross, Pieter-Ewald Share, and Frank Vernon (Poster 189)

We analyze seismograms recorded in the San Jacinto Fault Zone at Jackass Flat (JF), southeast of the trifurcation area, by a dense linear array oriented normal to the fault (southwest to northeast) with ~ 20 - 30 m spacing between instruments. A set of events with $M > 1.0$ recorded in 2012-2013 are used to search for fault zone head and trapped waves. Time delays between seismograms generated by 800 earthquakes are utilized to estimate the velocity structure across the array. We use automatic P picks for each source-receiver pair to calculate the ratio of each station pick to the array-wide average pick. The results based on statistical analysis of all events indicate an initial increase followed by flattening of relative slowness from SW to NE, suggesting that all stations of the JF array are inside the fault damage zone. The largest observed difference is $\sim 2\%$. We perform systematic search for fault zone head waves using an automatic detection algorithm. By visually inspecting the candidate head waves, we find a cluster of events that shows a clear moveout between these phases and direct P with the JF array; the moveout increases from SW to NE. However, data generated by different events and observed at a given station show no moveout with increasing source-receiver distance, implying that the head waves are generated by a local interface (perhaps edge of the damage zone or basin) rather than a deep fault interface. Fault zone trapped waves are identified with a simple automatic detection scheme that combines an automatic S-picking with measures of peak energy ratio, and corresponding time delay relative to the pick. Records with measurements above a minimum threshold are flagged. A number of stations on the SW part of the JF array have candidate trapped waves with weak S arrivals and large amplitude energy delayed ~ 0.5 - 1 s behind the S arrival. These characteristics are generated by events located on the southwestern side of the fault, and they are not observed at the stations on the NE part of the array. Sets of waveforms recorded across the entire array, with candidate trapped waves at the stations to the SW, are inverted with a genetic inversion algorithm for fault zone parameters. The results indicate a trapping structure with depth of 3-5 km, width of 100-200 m and velocity reduction of 40-50% from the host rock.

Imaging the internal structure of the Earth with seismic noise recorded by accelerometers, Santiago Rabade and Leonardo Ramirez-Guzman (Poster 179)

Low-cost accelerometric seismic arrays are widely deployed around the world to obtain reliable strong ground motion records. Today, numerous networks store the information gathered in the field continuously, providing an opportunity to explore the use of noise recorded in diverse applications. In this research, we explore the applicability of the

tomography based on noise cross-correlations using the aforementioned data. We lay out the procedure used to correct accelerometric recordings and compare the cross-correlations obtained against those computed with broadband velocity sensors. The data used comprise one year of continuous recordings. Preliminary results for central Mexico lead us to conclude and highlight that the use of widely deployed accelerographs to conduct regional studies using ambient noise tomography is feasible.

Efficient Static and Dynamic Receiver Green's Tensor and Green's Function Computations for Large Scale Applications, *Leonardo Ramirez-Guzman, Stephen Hartzell, Alan Juarez, and Jacobo Bielak* (Poster 084)

Highly efficient algorithms to compute Static and Dynamic Receiver Green's Tensors in complex velocity models are presented and analyzed. Following Lee et al. (2011), Receiver Green's Tensor (RGT) calculations were computed using the octree-based finite element tool-chain Hercules (Tu et al., 2006). The computations were carried out for each RGT by three static or wave propagation simulations with orthogonal loads at the receiver location. The field gradients at the desired source locations were stored and processed to obtain the tensors separately. Synthetic seismograms are then obtained by applying spatial reciprocity for ruptures at point sources and fault planes. We present comparisons for a one-dimensional model and two complex 3D structures against forward simulations (Wenchuan and Central Mexico regions), with satisfactory results. Additionally, we study the convergence of the method in order to establish efficiency, the computational demands, and lay the groundwork for future improvements.

This project is partially supported by DGAPA-PAPIIT project TB100313-RR170313.

The evolution of earthquake nucleating slip instabilities under spatially variable steady-state rate dependence of friction, *Sohom Ray and Robert C. Viesca* (Poster 134)

Following laboratory rock friction experiments, fault strength under sub-seismic slip speeds is thought to depend on a slip rate- and state-dependent friction. Laboratory-measured temperature dependence of the frictional properties and their implied variation with depth form the basis for current models of the seismic cycle. However, scant attention has been paid to the role such heterogeneity has on determining the location and manner in which an earthquake nucleating slip instability develops. Slip instability on a fault with rate-and-state friction (in which state evolution follows the aging law) occurs as the attraction of a dynamical system towards a fixed point (Viesca, in prep). Based on this development, we find that the location of that fixed point may be determined if a heterogeneous distribution of the relative rate-weakening parameter a/b is known. (Rate-weakening occurs for $0 < a/b < 1$, and rate-strengthening for $a/b > 1$). That this arises can be deduced considering that (i) the problem that determines the fixed points is equivalent to finding the equilibrium solution for a linearly slip-weakening crack, and (ii) heterogeneities in the parameter a/b have analogy in the equivalent problem to heterogeneities in the background stress. Physically, instability develops where rate-weakening is strongest. We examined the influence such a heterogeneity has on the fixed-point attractor (and hence on the instability development) by considering the scenario of a rate-weakening patch embedded within a rate-strengthening region. Specifically, we solve for fixed points under a rate-weakening heterogeneity within $|x| < H$ of the simple form $a(x)/b = (a/b)_m + (1 - (a/b)_m) * |x|/H$ and rate-strengthening behavior outside. For analytical simplicity, we focus here on the elastic configuration of in- or anti-plane slip below and parallel to a free surface. Analogous results are found for slip between two half spaces. A linear stability analysis reveals the effect of heterogeneity on the stability of the fixed points of the dynamical system. The heterogeneity parameters $(a/b)_m$ and H enter as bifurcation parameters indicating a transition in the classification of the fixed point from asymptotically stable to unstable at critical values of $(a/b)_m$ and H . The results are verified by numerical simulation of slip-acceleration and state-evolution including the heterogeneity and are also compared with the fixed-point solutions under homogeneous frictional properties.

Virtual Topography – A New Strategy to Incorporate Surficial Irregularities into Earthquake Modeling, *Doriam Restrepo and Jacobo Bielak* (Poster 076)

The earth's surface imposes a material discontinuity capable of generating strong wave mode conversion and severe structural damage. From a computational viewpoint, surface topography makes the practical incorporation of irregularities into conventional domain discretization schemes a challenge. Here, we develop a modeling scheme based on a fictitious domain framework aimed at including realistic topographies into numerical models of earthquake-induced ground motion. We provide evidence that by adopting a non-conforming octree-based meshing scheme associated with a fictitious-domain representation of the topography, we can obtain accurate representations of ground motion for mountainous regions. Our methodology preserves the salient features of multi-resolution cubic-shaped finite elements for wave propagation applications. We implemented the non-conforming meshing scheme for the treatment of topography into Hercules, the octree-based finite-element earthquake simulator developed by the Quake Group at Carnegie Mellon University. We tested the strategy by benchmarking its results against reference examples, and by means of numerical error estimate analyses. Our qualitative and quantitative comparisons showed a close agreement with the benchmark results. They also show that nearly optimum convergence is almost preserved. Moreover, the numerical results provide evidence that our strategy can produce accurate results using the same mesh resolution as in traditional flat free-surface earthquake simulations.

Evidence of Subsidence Events along the Rincon Creek Fault in Carpinteria Marsh, *Laura C. Reynolds, Alexander R. Simms, Thomas K. Rockwell, and Robert Peters* (Poster 251)

Recent marine terrace work indicates that the Ventura Avenue Anticline (VAA) and associated Pitas Point thrust fault have produced at least four Holocene uplift events between Ventura and Carpinteria, with a maximum uplift of 7-8m each, implying a significant earthquake and tsunami risk for the southern California coast. Previous work has also suggested that Carpinteria Marsh, located on the northern, downgoing side of the Rincon Creek Fault (RCF), has subsided nearly 1 km during the Quaternary. What is less clear is whether the nature of this subsidence is slow and steady or episodic, and to what degree the RCF is linked to motion on the VAA and Pitas Point thrust. A comparison between 10 new radiocarbon dates obtained from Carpinteria Marsh and regional records of Holocene relative sea level indicates that Carpinteria Marsh has experienced ~1m/ky of subsidence over the past 7ky. A preliminary stratigraphy based on 39 vibracores that are up to 4m in length, and 7 Geoprobe cores that are up to 13m in length, shows three candidate surfaces for subsidence events at 4m, 5.5m and 8m bmsl, respectively. The candidate event at 4m is characterized by a marsh surface that is sharply overlain by marine-influenced estuarine sand that correlates across the front of the marsh. The two other candidate surfaces are characterized by sharp-based marsh surface deposits overlying fluvial deposits, also possibly indicating a change in the elevation of the marsh surface at times when mean sea level was lower. Natural marsh processes, such as changes in sediment supply or mouth closure are other explanations for these candidate surfaces, although some degree of subsidence is likely required to produce the observed relationships. Future work will focus on using microfossil analysis to address whether the candidate surfaces represent abrupt elevation changes, as well as improving the chronology to test whether marsh surfaces are synchronous with the uplifted Holocene marine terraces.

Does aftershock triggering explain the information gains of medium-term forecasting models? *David A. Rhoades, Morgan T. Page, and Annemarie Christophersen* (Poster 024)

It has been suggested that aftershock triggering, with power-law decay of triggered events in time and space, is sufficient to explain precursory seismicity patterns on all temporal and spatial scales. We use synthetic earthquake catalogs for California generated by the Epidemic Type Aftershock (ETAS) model to test the hypothesis that aftershock triggering can explain the patterns of medium-term precursory seismicity as modelled by the Every Earthquake a Precursor According to Scale

MEETING ABSTRACTS

(EEPAS) model. We compare information gains of the EEPAS model on the synthetic catalogs to those on the actual ANSS catalogue. The EEPAS model has characteristic scales for precursor time, magnitude and area. It views every earthquake as a possible precursor of larger earthquakes to follow it in the medium term. It is based on the precursory scale increase phenomenon and incorporates the associated precursory scaling relations for magnitude, precursor time and precursor area, which depend on the magnitude of the precursory earthquake. The ETAS model views every earthquake as a main shock with its own aftershock sequence conforming to the Omori-Utsu law, the Gutenberg-Richter law and a spatial distribution with a power-law tail shape.

A 10,000-year synthetic ETAS catalogue for California with a lower magnitude threshold of $M 2.95$ was split into 40 sub-catalogs. For each sub-catalog, we first measured the information gain of two versions of the EEPAS model (with equal weights and aftershocks down-weighted, respectively, as submitted for CSEP testing in California) over the Stationary Uniform Poisson (SUP) model and the Proximity to Past Earthquakes (PPE) smoothed seismicity model. Secondly we fitted the PPE and EEPAS models to a 10-year period of each synthetic catalog and measured the information gain on the 10-year period immediately following, and then did the same for the real catalogue. In each case the information gains per earthquake using the real catalog were much higher than the average over the synthetic catalogs and at levels rarely seen in the synthetic catalogs. We conclude that epidemic-type aftershock triggering does not fully explain the information gains of the EEPAS model.

A New Creep Instability at Intermediate Homologous Temperatures with Application to Slow Earthquakes and Non-Volcanic Tremor, Marshall A. Rogers-Martinez, Rachel C. Lippoldt, and Charles G. Sammis (Poster 153)

Recent high-pressure torsion (HPT) experiments have revealed a mechanism that produces unstable creep at intermediate homologous temperatures in the range of those at the base of the seismogenic zone. In these experiments, a thin disc or ring is first subjected to a normal stress of 1-6 GPa and then to a simple shear deformation by rotating one of the loading pistons. The high normal stress suppresses fracture allowing ductile flow at intermediate values of T/T_m . A decrease in the flow stress was observed to be associated with dynamic recrystallization and the growth of larger grains with lower dislocation densities. This new mechanism is especially promising for slow earthquakes because, unlike runaway thermal weakening, the strain weakening associated with recrystallization is not catastrophic. The observed recrystallization extends over a large strain, producing a long effective slip-weakening displacement that leads to slow earthquakes. Although this weakening mechanism was observed in Al, Mg, Zn and wet NaCl, it was not observed in Cu. Two possible explanations are: 1) Al, Mg, Zn, and NaCl are being deformed at a significantly higher homologous temperature and 2) the stacking fault energies (SFE) of Al, Mg, Zn, and NaCl are significantly higher than Cu. A high SFE means that the separation between partial dislocations is very small. This promotes easy cross-slip of the dislocations, which facilitates recrystallization. In Cu, the separation between partial dislocations is on the order of 12 times the atomic spacing. Although there are no robust observations of stacking faults in olivine, it is expected to be very high because the separation between the partial dislocations is very small ($l < 40 \text{ \AA}$). The implication is that shear weakening via dynamic recrystallization is likely in olivine at or near the brittle-ductile transition.

We present here new HPT experimental results for an alloy (Al-6061) that show strain weakening, which indicate that the phenomenon is not limited to high-purity materials. An analytic slip pulse model was used to show that very slow propagation is possible for reasonable values of shear zone width and slip pulse dimensions. A 2D viscoelastic finite element model (FEM) was used to simulate the nucleation and propagation of slow events in a layer having strain weakening corresponding to the experimental results. The FEM produced events with a slow stable propagation velocity.

Automatic Earthquake Detection with Pseudo-Probabilities and Automatic Picking of P, S, and Fault Zone Head Waves, Zachary E. Ross and Yehuda Ben-Zion (Poster 160)

We develop an automatic earthquake detection algorithm combining information from numerous indicator variables in a non-parametric

framework. The method is shown to perform well with multiple ratios of moving short- and long-time averages having ranges of time intervals and frequency bands. The results from each indicator are transformed to a pseudo-probability time-series (PPTS) in the range $[0, 1]$. The various PPTS of the different indicators are multiplied to form a single joint PPTS that is used for detections. Since all information is combined, redundancy among the different indicators produces robust peaks in the output. This allows the trigger threshold applied to the joint PPTS to be significantly lower than for any one detector, leading to substantially more detected earthquakes.

We also develop a set of algorithms for automatic detection and picking of direct P and S waves, as well as fault zone head waves (FZHW) generated by earthquakes on faults that separate different lithologies and recorded by local seismic networks. The S-wave picks are performed using polarization analysis and related filters to remove P-wave energy from the seismograms, and utilize STA/LTA and kurtosis detectors in tandem to lock on the phase arrival. The early portions of P waveforms are processed with STA/LTA, kurtosis and skewness detectors for possible first-arriving FZHW. Identification and picking of direct P and FZHW is performed by a multistage algorithm that accounts for basic characteristics (motion polarities, time difference, sharpness and amplitudes) of the two phases. The automatic earthquake detection and phase picking algorithms were tested and perform well on data of the San Jacinto fault zone, San Andreas fault at Parkfield and the Hayward fault.

Can We Rely on Linear Elasticity to Predict Long-period Ground Motions?

Daniel Roten, Kim B. Olsen, Steven M. Day, and Yifeng Cui (Invited Talk Tuesday08:00)

A major challenge in seismic hazard assessment consists in the prediction of near-source ground motions resulting from large, rare earthquakes, which are not well represented in observed data. In southern California a basis for assessing the economical and societal impact of a major ($M > 7.8$) earthquake rupturing the San Andreas fault has been provided by numerical simulations of various rupture scenarios. Simulations of SE-NW propagating sources (e.g., ShakeOut) have predicted strong long-period ($> 2s$) ground motions in the densely populated Los Angeles basin due to channeling of seismic waves through a series of contiguous sedimentary basins. Recently such a waveguide amplification effect has also been identified from virtual earthquakes based on Green's function derived from the ambient seismic field (Denolle et al., 2014).

Previous scenario simulations shared the assumption of a linear viscoelastic stress-strain relationship in crustal rocks, and methods that derive amplifications from ambient noise are also inherently assuming linear material behavior. Motivated by studies of dynamic rupture in nonelastic media, we simulate the wave propagation for selected San Andreas earthquake scenarios in a medium governed by Drucker-Prager elastoplasticity. For the ShakeOut earthquake scenario (based on the kinematic source description of Graves et al., 2008) plastic yielding in crustal rock reduces peak ground velocities in the Los Angeles basin between 30 and 70% as compared to viscoelastic solutions. Our simulations also show that the large strains induced by long-period surface waves in the San Gabriel and Los Angeles basins would trigger nonlinear behavior in cohesionless sediments, as suggested by theoretical studies (e.g., Sleep & Erickson, 2014). In the fault zone plasticity remains important even for conservative values of cohesions, suggesting that current simulations assuming a linear response of crustal rocks are overpredicting ground motions during future large earthquakes on the southern San Andreas fault. We analyze the sensitivity of ground motion levels to the choice of nonlinear material properties (cohesion, friction angle) and the initial stress field, and discuss how nonlinear material behavior may be included in future simulations of major earthquake scenarios and physics-based seismic hazard assessment.

Is the Recent Increase in Seismicity in southern Kansas Natural? Justin L. Rubinstein, William L. Ellsworth, Andrea L. Llenos, and Steven Walter (Poster 212)

Earthquakes in southern Kansas were nearly unheard of until September 2013, when two $M2$ earthquakes occurred. Since then, the earthquake rate has risen dramatically. Between December 2013 and July 28, 2014, 14 $M \geq 3$ earthquakes were recorded in Harper and Sumner counties, the

largest being a M3.8 earthquake in December 2013. Residents of the towns of Caldwell and Anthony have reported feeling even more earthquakes. In response to the surge in earthquakes, the USGS deployed a 10-station seismic network to monitor earthquakes in southeastern Harper and southwestern Sumner counties. We have identified over 200 earthquakes that occurred from mid-June to late-July, 2014. The locations of these earthquakes cluster within or near the seismic array, ranging in magnitude from 0.5 to 3.5.

The earthquakes we identified are occurring within the Mississippian Lime Play, an area of rapidly expanding oil and gas development stretching from central Oklahoma to northwestern Kansas. In Kansas, new development of the play is largely in the adjoining areas of Harper and Sumner counties. Even with the new development, production in Sumner County has largely remained constant. However, in Harper County, where production was fairly stable from 1995-2010, it began increasing rapidly in 2011. In 2013 the highest yearly production volumes to date were approximately five times larger than those in 2010.

The spatial and temporal correlation of the oil and gas development and seismicity in southern Kansas suggests a potential relationship between the two; some of the earthquake clusters lie within 1-2 kilometers of recent development. We examine the possibility that the earthquakes in southern Kansas are induced by wastewater injection and/or hydraulic fracturing. This involves using a refined earthquake catalog built upon cross-correlation detections and high-precision earthquake relocation techniques. We also compute first-motion focal mechanisms and compare them to the regional stress field.

Structural Self-similarity in Earthquake Swarms: Evidence from the 2008 West Reno, NV Earthquake Sequence, *Christine J. Ruhl and Kenneth D. Smith* (Poster 152)

High-quality relocations coupled with over 400 focal mechanisms reveal complex spatiotemporal evolution of the 2008 west Reno, NV earthquake sequence (WRES) consistent with a model of earthquake swarms proposed by Hill (1977) on two observable scales. Most prevalent and most studied, volcanic earthquake swarms have been modeled as systematically organized normal and shear fractures due to extension above a magma intrusion and/or fluid injection. The model consists of a dense network of tensional dikes opening in the direction of σ_3 with the long direction aligned with σ_1 , while obliquely oriented shear failures propagate to connect the crack tips in a swarm-like fashion. Weaver and Hill (1978) used this model to explain the occurrence of tectonic earthquake swarms in dextral offsets (5-10 km) along the San Andreas fault through local crustal spreading between overlapping fault strands, similar to offset spreading centers observed at mid-ocean ridges. The energetic WRES extended for a 6-month period beginning in late February 2008 with 8 weeks of foreshock activity prior to the Mw5.0 'mainshock' (April 26, 2008). It occurred in an 80-km wide highly fractured shear-zone between the Sierra Nevada range-front normal faults and dextral faults of the Northern Walker Lane. We interpret the WRES to be a two-fold manifestation of the extensional process described by Hill (1977). Treated as one seismic entity, the sequence transfers NW-oriented dextral shear between N-striking normal faults analogous to shear failures between volcanic dikes. At small scale, the sequence itself is comprised of a network of interacting fractures including at least 3 dextral offsets in the ~6 km-long NW-oriented dextral structure ranging in length from 0.2 – 0.5 km. This apparent scale-invariance in the generation of earthquake swarms suggests self-similarity. Weaver and Hill (1978) found the length of offset to be proportional to the depth of seismicity for continental swarms in CA, although offset lengths well exceed seismic depths at mid-ocean ridges. When viewed as a single entity, the proportional relationship is consistent with CA swarms and the unusual shallowness of the sequence could be explained by the swarm-like nature and offset length relations. At finer scale, however, seismic depths are much greater than the length of step-overs observed. Despite this proportional discrepancy, we suggest self-similarity of faulting observed within this long-duration sequence.

Modeling earthquake rupture on the Pitas Point fault: Implications for tsunami generation and propagation, *Kenny J. Ryan, David D. Oglesby, and Eric L. Geist* (Poster 146)

The Ventura Basin in southern California is becoming increasingly recognized for seismic and tsunami hazards. Within the region is a network of dip-slip faults, potentially producing earthquakes of Mw 7 or greater. As part of the Ventura Anticline and Thrust System Special Fault Study Area (SFSA) effort, we are constructing 3D dynamic models of earthquakes on the Pitas Point fault, with a goal of elucidating the seismic and tsunami hazard in this area. These models can be used to produce ground motion, which can in turn be used as a time-dependent boundary condition within tsunami propagation codes. Using structural information obtained by other groups studying this SFSA (e.g., fault geometry and evidence for past slip events) as constraints, we are investigating the effects of different prestress and frictional regimes on rupture dynamics, with implications for tsunami formation and local propagation. Additionally, we look at first order differences in the tsunami wavefield for both static and time-dependent seafloor uplift. Results from these modeling efforts can also be used to pinpoint areas that require more data to better constrain source properties.

Geophysical Evidence for a Southwestward dipping Southern San Andreas Fault, *Valerie J. Sahakian, Annie Kell, Alistair J. Harding, Neal Driscoll, and Graham Kent* (Poster 206)

The Southern San Andreas Fault (SSAF) accommodates a significant (19-25 mm/yr) amount of strain in the Pacific-North American plate boundary, and as such, poses a large hazard to the populated regions of Southern California. This fault has had no historic rupture, and is considered to be towards the end of its interseismic cycle. In order to understand better the hazard associated with rupture on the SSAF, we conducted an active-source seismic investigation in 2010 and 2011 in the Salton Sea to study the structure of the SSAF. This dataset was collected as a component of the Salton Seismic Imaging Project (SSIP) and includes several Multi-channel seismic (MCS) lines as well as a coincident refraction dataset from Ocean Bottom Seismometers (OBS). The seismic reflection lines do not intersect the SSAF, though the main seismic refraction line we present includes both land and marine shots recorded on the OBS and thus crosses over the SSAF. These data place important constraints on stratal geometry and velocity structure of the terminus of the SSAF and the Salton pull-apart basin. The terminus of the SSAF appears to be dipping to the southwest, and accommodates an extensional component with down-to-the-southwest motion in addition to dextral strike-slip motion, though this is in disagreement with past interpretations from GPS and microseismicity data. These results would suggest that the internal structure and geometry of this releasing bend (formed by a step between the SSAF and the Imperial Fault (IF) system to the South) could alter how we interpret communication of rupture and earthquake triggering in the region between the SSAF and IF. Here we will present the results and conclusions of this investigation.

Determining Paleoseismicity using Biomarkers, *Heather M. Savage, Pratigya J. Polissar, and Rachel Sheppard* (Poster 119)

The rock record is rich in fault structural detail, but independent identification of earthquakes is essential to relate these observations to earthquake processes. One of the only ways to identify earthquakes in outcrop is to measure the frictional heating on faults relative to the surrounding rock. Here we utilize the thermal maturity of extractable organic material (biomarkers) to estimate the maximum frictional heating experienced by several faults during earthquake slip, including the Punchbowl fault, California.

The organic thermal maturity indicators most prevalent in the Punchbowl fault and other faults exhumed from shallow depths are methylphenanthrenes. Using experimentally-determined kinetic reaction rates for methylphenanthrenes at high temperature and short time scales relevant to earthquake heating, we determine that the minimum temperature rise during an earthquake needed for methylphenanthrene reaction is 600°C. We also consider tradeoffs between total slip, slip rate, and slip localization that modulate temperature rise and help constrain the maximum event possible along the fault.

MEETING ABSTRACTS

Validation Exercise for Two Southern California Earthquakes, William H. Savran and Kim B. Olsen (Poster 065)

We are in the process of a comprehensive validation exercise constraining parameters describing $Q(f)$ and statistical models of small-scale heterogeneities for finite-difference earthquake simulations in Los Angeles basin. The parameters for our model of shallow crustal heterogeneities are constrained by inverting 38 deep borehole logs in Los Angeles basin (Hurst number 0.0-0.1, correlation length 50-150 m, $\sim 5\% \sigma$), which are superimposed onto the SCEC CVM-SI 4.26. We simulate viscoelastic waves for the 2008 Mw 5.4 Chino Hills Event (0-2.5 Hz, modified finite fault source from Shao et al., 2012) and the 2014 Mw 5.1 La Habra event (0-1 Hz, point source), and compare our simulations to strong-motion records. The optimal linear Q_s - V_s relation derived from our results is $Q_s = 0.1V_s f^{0.6}$ (V_s in m/s). We find excellent goodness-of-fit (GOF) scores for $f < 1.0$ Hz, in particular at deep-basin sites, that degrade when frequencies increase to 2.5 Hz, suggesting an inadequate description of the finite-fault source for $f > 1$ Hz. Poor fits (under prediction of metrics) are often found at hard-rock sites even for $f < 1$ Hz, likely due to too large values of the shallow V_s in the CVM. The statistical distributions of small-scale heterogeneities generate localized 2x amplifications and de-amplifications, and tend to improve GOF scores by 5-10%. Our simulations suggest that the majority of the scattering recorded in ground motions originates as a path effect as waves propagate through the basins, while local site-specific scattering in the immediate vicinity of a station at the earth's surface tends to play a smaller role. We find almost equal contributions from scattering in the sedimentary basins and deeper parts of the shallow crust.

Our modeling demonstrates unique amplification patterns caused by scattering due to the heterogeneous structure of the shallow crust. In particular, we find that shallow sources located on the boundary to a sedimentary basin generate bands of strong amplification aligned in the direction of the ray paths. The nature of these bands depends strongly on the incidence angle of the waves into the sediments. Moreover, this banded amplification pattern is absent for sources deeper than 1-2 km. Our results imply that surface rupture on a range-bound fault (e.g. the San Andreas fault by the San Bernardino Basin) may generate a different patterns of ground motion shaking along lines parallel to the fault as compared to profiles perpendicular to the fault.

Vertical deformation along the Indio Hills, San Andreas Fault, California, Katherine M. Scharer, Kim Blisniuk, Warren Sharp, Pat Williams, and Kendra Johnson (Poster 278)

Halfway between the Salton Sea and San Geronio Pass, the southernmost San Andreas Fault (SAF) bifurcates into the Mission Creek and Banning strands. These strands bound the Indio Hills (IH), and mark the first of a series of left-stepping branches that define the transpressional, southern Big Bend of the SAF. Between the fault strands, the Quaternary Ocotillo Formation is deformed with fold axis orientations consistent with dextral shear; structurally the IH are synclinal in the east, transitioning to a complex antiform with increased uplift suggested by exhumation of Tertiary units in the west. We report new long- and short-term erosion rates across the IH and uplift rates on the Banning strand, and we evaluate these measurements in terms of slip rates across the fault system and structural deformation within the IH. Two methods of catchment-averaged erosion rates provide minimum rates yield similar results, (0.08 to 0.34 mm/yr) across 6 catchments. The long-term rates are calculated from eroded volumes estimated from a 10-m DEM surface enveloping the Indio Hills and assume that all folding and uplift initiated ca. 500ka (the 750 ka Bishop ash is uplifted and warped within the IH). The short-term rates, determined from ^{10}Be concentrations of fluvial sand, increase gradually to the northwest. Similarity of the rates suggests steady state uplift over the history of the fold; ongoing structural analysis and dating needed to constrain the maximum rates will test this possibility. The new uplift rate for the Banning strand at the east end of the IH is determined from a 60 pts/m² DEM produced by structure from motion photogrammetry and U-series ages and cosmogenic dates that provide an age range of 18-76ka for a fan vertically offset by ~ 2.5 m. The resulting uplift rate on the fault (0.03-0.13 mm/yr) overlaps with the short-term catchment-averaged erosion rate for this location (0.08 mm/yr). Consequently, we interpret that vertical strain is partitioned onto both the

Banning fault and in uplift and folding of the IH. The uplift rates increase westward along the IH, possibly indicating increased activity on the Banning strand to the west. This pattern will be considered in the context of paleoseismic and horizontal slip rate studies in the region, and implications for rupture directivity on this hazardous fault system.

Swarm or induced: Comparing pre-production seismicity with current seismicity at the Coso geothermal field, Martin Schoenball, Nicholas C. Davatzes, and Jonathan M.G. Glen (Poster 209)

The increased levels of seismicity induced by forced fluid circulation in the sub-surface in connection to hydrocarbon production, wastewater disposal and geothermal power production created a demand for methods to distinguish induced from natural seismicity. The discrimination is especially difficult in areas that have a high activity of natural seismicity, such as the geothermal fields at Salton Sea and Coso. Furthermore, both areas show swarm-like sequences that may have spatio-temporal patterns that resemble sequences of induced seismicity.

Here we analyze a two-year microseismic survey of the Coso geothermal field that was acquired before exploration in the area started (Walter & Weaver, 1980) to compare it with current levels of seismic activity. We perform a cluster analysis on the earthquake catalog to identify notable event sequences as either aftershock sequences of earthquake swarms. Using this method 10 earthquake swarms comprised of 20 to more than 200 events that occurred in an area that is now used for extensive geothermal power production could be identified. The SCSN catalog is used to define a consistent baseline for earthquake magnitudes covering the period 1975-2014 to compare the levels of seismicity from the pre-production period to the current state. This enables us to compare the baseline survey with the current level of the seismic activity, which is perturbed by fluid production from and reinjection into more than 100 wells.

Virtual California: Earthquake Statistics, Surface Deformation Patterns, Surface Gravity Changes and InSAR Interferograms for Arbitrary Fault Geometries, Kasey W. Schultz, Michael K. Sachs, Eric M. Heien, John B. Rundle, Jose Fernandez, Don L. Turcotte, and Andrea Donnellan (Poster 029)

Just as hurricane forecasts are derived from the consensus among multiple atmospheric models, earthquake forecasts cannot be derived from a single comprehensive model. Here we present the utility of Virtual California, a numerical simulator that can generate earthquake statistics and forecasts, surface deformations, surface gravity changes, and InSAR interferograms.

Virtual California is a boundary element code designed to explore the seismicity of today's fault systems. For arbitrary input fault geometry, Virtual California can output simulated seismic histories of up to 100,000 years or more. Using the times between successive earthquakes we generate probability distributions and earthquake forecasts. Furthermore, using co-seismic slip distributions from the output data, we model the distribution of surface deformation and surface gravity changes as well as simulated InSAR interferograms.

Virtual California is now supported by the Computational Infrastructure for Geodynamics. The source code is available for download and it comes with a users' manual. The manual includes instructions on how to generate fault models from scratch, how to deploy the simulator in a parallel computing environment, etc.

How predictable is background seismicity in Southern California? Margarita Segou (Poster 028)

A critical question in physics-based earthquake forecasts is the representation of the background rate, corresponding to the initial conditions of our natural system. Usually, in the rate/state implementation, few years of seismicity play the role of reference seismicity model but the question that persists is "How representative of California seismicity are the few years that we selected? Do we need a time-dependent formulation for improving our background rate representation?" To answer these questions efficiently we need an improved determination of the background seismicity and to achieve that we combine statistical ETAS modeling and static stress changes estimation considering important sources of uncertainty. Stochastic declustering of the high-accuracy

earthquake catalog (Hauksson et al., 2012) reveals that background seismicity has significant non-Poissonian behavior. We model background seismicity, comprised by events having greater than 50 and 95% background probability, using varying minimum magnitude thresholds ($2.7 < M < 3.5$) and time intervals (2, 4 and 6 months). For events with background probability greater than 95%, the probability our catalog (modeled within 6 months interval) being adequately described by a Poisson process (Pp) equals 0.3, 3, and 45 % for $M_{min}2.8$, $M_{min}3.0$ and $M_{min}3.5$, respectively. A possible reason for this non-Poissonian behavior is the existence of static stress effects, induced by major earthquakes inside our study area. Therefore, we consider the stress changes following 11 major earthquakes within the time period 1979-2012 for which we have available source models. Analytically, we estimate inside a 3D spatial grid with 2-km spacing the stress changes for different slip distributions and friction coefficients ($0 < \mu < 0.8$) at optimally-oriented for failure receiver faults. We find a very low Pp (= 2%) for events above $M3.0$, with background probability greater than 95% when modeling seismicity rates within 6-months time intervals. Fault specific calculations above $M3.0$, within the aforementioned time interval, reveal Pp=0.1 for San Jacinto Fault Zone and non-Poissonian behavior of background seismicity for San Andreas and Elsinore faults.

Late Quaternary displacement gradients along the Calico-Blackwater-Harper Lake fault systems, Eastern California, *Jacob A. Selander and Michael E. Oskin* (Poster 138)

Displacement gradients must exist along faults to prevent unreasonable strains at fault tips. These strains may be accommodated via transfer of slip to intersecting structures or off-fault distributed deformation in the crustal volume surrounding a fault tip. Within the Mojave segment of the East California Shear Zone (ECSZ), slip-transfer at fault intersections, uplift along concealed thrust ramps, and along-strike changes in displacement may contribute to the discrepancy between geologic and geodetic fault slip rates. Here, we focus on the Calico- Blackwater- Harper Lake fault system to test for late Quaternary displacement-rate gradients and explore the role of fault connectivity to accommodate along-strike variations in long-term displacement. Slip along the northern Calico fault is transferred to the Harper Lake- Gravel Hills fault and the Blackwater fault via blind thrust ramps underlying the Mitchell Range and Mud Hills, respectively. Field mapping and ^{10}Be exposure-age geochronology at five new slip-rate sites along the Calico, Mud Hills, and Harper Lake- Gravel Hills faults will quantify the effects of these connections. Reconstructions of late Quaternary offsets show $50 \pm 10\text{ m}$ of dextral displacement of Q2b fans along the southern Calico fault, and $100 \pm 20\text{ m}$ of uplift along the Mud Hills thrust. Along the northernmost Harper Lake-Gravel Hills fault, we identify a displacement-rate gradient from offset of correlative Q2c alluvial fans from $40 \pm 10\text{ m}$ decreasing to $12 \pm 4\text{ m}$. Well-preserved fan surfaces at each of these sites were sampled for exposure-age dating using the ^{10}Be depth profile approach. Sample analysis is pending. Displacement data from the Harper Lake- Gravel Hills fault shows a 75% decrease in slip in the final 10 km of fault length. This sharp decrease in late Quaternary displacement coincides with a region of widely distributed deformation at the fault tip, illustrating how this mechanism absorbs fault tip-line strain.

The IDEA Model: A Practical Tool for Designing Effective Early Earthquake Warning Messages, *Deanna Sellnow and Tim Sellnow* (Invited Talk Wednesday08:30)

The right message at the right time saves lives. These words are certainly true for early earthquake warnings. In this session, we will describe how we derived the the IDEA model from the principles of effective risk and crisis communication, highlight some of the research we have done to inform our work, and explain how we are now using the model to design early earthquake warning messages to be delivered in 10 seconds or less on a smart phone app. We will also summarize the studies we have employed and conclusions drawn from them since beginning our work with the USGS SAFFR group July 2013. We will then engage in a Q&A discussion regarding next steps in research and development for rolling out the early earthquake warning app., as well as questions focusing on risk and crisis communication in general.

Characterization of the San Jacinto Fault Zone northwest of the trifurcation area from dense linear array data, *Pieter-Ewald Share, Yehuda Ben-Zion, Zachary Ross, Hongrui Qiu, and Frank Vernon* (Poster 188)

Data from a linear seismic array at Blackburn saddle NW of the trifurcation area, crossing the Clark section of the San Jacinto Fault Zone, are used to study the internal structure of the fault in the area. The linear array (BB) is 250 m in length and comprises 7 broadband three-component seismometers. Characteristics including the existence and location of a fault associated damage zone, velocity contrast and trapping structure(s) are studied. Statistical analyses of the P body wave travel times of 508 events, within a 120 by 10 km window centered along the length of the fault, show a 0.6-0.8 % gradual increase in slowness from the southwest most (BB01) to the northeast most (BB07) stations. The increase in slowness is corroborated by a general increase in the P to S differential travel times from BB01 to BB07. This result suggests BB07 overlies a zone of greater damage or is located on top of a trapping structure. Sharp velocity contrasts across the fault are mainly studied using the presence of fault zone head waves. The P head waves are distinguished from P body phases using an automatic detection algorithm that exploits differences in arrival times, kurtosis and skewness characteristics between the two phases. In total, 53 anomalous events (within the same 120 by 10 km window) with head wave characteristics are identified. Further analyses of the candidate events show head waves originating as far as approximately 32 km and 56 km northwest and southeast along the fault from the linear array, respectively. Preliminary calculations suggest an average velocity contrast across the fault over the top 16 km of 3-4 %, with the southwest block being slower (the contrast is likely double in the top 8 km). We also detect S trapped waves from a number of events at stations BB06 and BB07 (the two northern most stations). Waveform modeling results will be presented in the meeting.

Deterministic Model of Earthquake Clustering Shows Reduced Stress Drops for Nearby Aftershocks, *Bruce E. Shaw, Keith Richards-Dinger, and James H. Dieterich* (Poster 132)

The clustering of earthquakes in space and time is a well established phenomena.

A number of viable physical mechanisms have been offered to explain the temporal $1/t$ Omori law decay of aftershocks following a mainshock. In contrast, the spatial clustering of aftershocks have posed a challenge for physical models, in particular the intense productivity of aftershocks very near the area which ruptured in the mainshock. Here we present a new deterministic physical model capable of reproducing both the spatial and temporal clustering seen in earthquakes. We apply this new model to a very puzzling question raised by recent Ground Motion Prediction Equation (GMPE) empirical regressions of recorded seismograms, wherein a number of prominent GMPEs suggest nearby aftershocks show reduced median ground motions. Examining sequences of events in the model, we find a physical basis for these observations in reduced median stress drops for nearby aftershocks compared with similar magnitude mainshocks.

Signatures of Fluid-Pressure Triggering, Natural and Induced: Comparing Migrating Earthquake Swarms in Long Valley Caldera, California and Azle, Texas, *David R. Shelly, William L. Ellsworth, Emily K. Montgomery-Brown, David P. Hill, Stephanie G. Prejean, and Margaret T. Mangan* (Poster 124)

Earthquake swarms are common in volcanic regions where fluids exsolved from magma bodies may trigger a sequence of earthquakes as they episodically transit from ductile surroundings into the neighboring brittle crust. Such swarms do not fit mainshock-aftershock patterns commonly seen with tectonic seismicity. Similar swarms are increasingly being observed in association with industrial fluid injection. Here, we investigate and compare earthquake swarms at Long Valley Caldera (a volcanic center) and Azle, Texas (near active industrial production and wastewater-disposal wells). We perform waveform-correlation-based event detection coupled with double-difference relative location, using catalog events as waveform templates to examine their space-time evolution. This greatly enhances the earthquake catalog, providing locations for ~4 times as many events as in the routine catalog, with location precision often better than 10 m. Despite differences in depth, fluid chemistry, and tectonic

MEETING ABSTRACTS

environment, we find pronounced spatiotemporal migration of earthquake hypocenters in both of these swarms.

Both swarms occurred on well-defined fault structures. The Long Valley south moat swarm followed an inactive, steeply dipping fault zone. Earthquakes began ~7.5 km beneath the surface on 7 July 2014, propagated dominantly upward and northward ~600 m in the first 12 hours, and continued sporadically into late July 2014. The Azle swarm of 28-29 January 2014 activated an ancient normal fault at shallow depths of ~3 km, just below the injection and extraction horizon, and propagated ~400 m northeastward along strike and bilaterally along dip over ~12 hours. For both swarms, we hypothesize that the migration of hypocenters reflects corresponding diffusion of a fluid pressure front within pre-existing fault zones. In some cases we observe larger earthquakes followed by rapid (but not instantaneous) propagation of events into previously inactive zones, perhaps reflecting enhanced permeability and accelerated fluid pressure diffusion via the newly ruptured fault patch. By integrating observations from natural and induced earthquake swarms, we aim to understand factors controlling the combined physics of faulting and fluid pressure diffusion in the crust.

Fault core and slip zone geometry, wear and evolution, *Katherine A. Shervais and James Kirkpatrick* (Poster 118)

Both the static strength and dynamic shear resistance of seismic faults are dependent on characteristics such as composition, shape, spatial variability, and distribution of asperities on fault surfaces. To characterize these qualities in a paleoseismic fault, we studied the Boyd Fault, a Laramide thrust exposed south of Palm Desert, CA. High resolution digital elevation models of outcrops were rectified with fault strike and dip and used to map the fault core in the field at three exposures. This totaled 62 m of exposed fault over 175 m along strike. The fault core exhibits stratified layers of fault gouge of varying thicknesses with crosscutting relationships and discontinuous layers. One layer is interpreted as the most recent slip event because it crosscuts all the others and has injection veins branching into both the footwall and hanging wall. Microstructures and the presence of gouge injections indicate fluidization of the gouge throughout the fault slip zone during seismic slip. We compared the geometry of the most recent slip event to the fault core as a whole to constrain how the characteristics of the fault evolve with displacement. We found four “thresholds”: a. the length scales at which the variance of 1. total fault core thickness and 2. the most recent gouge layer thickness do not fluctuate and remain stable, via experimental semivariograms; b. the length scale at which wear is scale dependent, via power spectral density (PSD) calculations from cross sections through the most recent layer and the fault core; and c. the scale at which fault wear transitions from inelastic to elastic, via the maximum length of hanging wall asperity clasts in the fault gouge. By comparing the most recent event with the core as a whole, these results indicate that faults smooth with displacement, but clast compositions provide evidence of preferential wear due to wall rock composition differences. In addition, slip zone thickness decreases and becomes less variable. We suggest the correlation length scale in the slip zone thickness defines the length scale of an asperity on the fault surface. Overall, our results indicate an evolution of the size and distribution of asperities, implying dynamic shear strength and the static strength of the fault also vary with increasing displacement.

Exploring Distributed Physics-based Cellular Automata to Model Seismic Elastodynamics in OpenCL beyond GPGPU accelerators, *Liwen Shih and Mark Garrett* (Poster 083)

With M8 simulation being selected as the sole 2010's global representative on HPC scientific analysis achievement at SC13 25th year silver anniversary in Denver, CyberShake is a flagship project developed by the Southern California Earthquake Center (SCEC) to create a physics-based probabilistic seismic hazard analysis (PSHA) which is intended to provide a spatial map identifying hazardous zones where seismic activity is most probable. CyberShake produces the hazard curves by generating synthetic seismograms using an estimated rupture forecast. Generating the hazard curves in increased frequency, accuracy, and coverage is extremely computational demanding due to the complexity of the physics-based computations. As supercomputing progresses beyond petascale many-core GPGPU accelerators toward exascale, the simpler physics-

based cellular automata (CA) implementation is proposed here to model seismic elastodynamics, which has been shown to be equivalent to the centered-difference finite-difference (FD) method. The project is to develop and profile distributed CA simulations of seismic elastodynamics using OpenCL on GPGPU accelerators and beyond with the intent of exposing any performance improvement in execution times, memory accesses, data movements, scalability and power saving over traditional FD method.

Accelerated creep on the Hayward fault controlled by fluid pressure, *Manoochehr Shirzaei* (Poster 140)

Constraining the size, location and recurrence time of large earthquakes requires detailed knowledge of the distribution of the fault locked asperities. It is also shown for several large earthquakes (such as the Tohoku 2011 event) that the seismic event is preceded by accelerated creep occurring near its hypocenter. Linked to the interseismic fault coupling, the accelerated creeps are attributed to variations in fluid content at the fault interface.

Here we use geodetic and seismic data to explore the relation between pore fluid pressure and observations of accelerated creep on the Hayward fault. Time-dependent model of creep on the Hayward fault obtained from inversion of a 19-year InSAR surface deformation time series includes zones of accelerated creep, compared with the long term creep rates. Applying a rate and state friction model, the variations of the creep rate are linked to the temporally variable normal stress on the fault. Moreover, high-resolution three-dimensional seismic tomography reveals variations in the ratio of seismic P- to S-wave velocities (V_p/V_s) along this fault. Using a laboratory-driven physical model relating pore pressure to P- to S-wave velocities, we show that these zones of accelerated creep are characterized by elevated pore fluid pressure. In contrast, low V_p/V_s domains are associated with zones of lower pore fluid pressure, and correlate with locked parts of the plate interface, where unstable slip and earthquakes occur. We conclude that variable pore fluid pressure at the fault interface control the spatiotemporal variation of interseismic coupling, allowing accelerated creep, which may be followed by large earthquakes.

The SCEC Broadband Platform: A Collaborative Open-Source Software Package for Strong Ground Motion Simulation and Validation, *Fabio Silva, Philip Maechling, Christine Goulet, Paul Somerville, Thomas H. Jordan, and the Broadband Platform Working Group* (Poster 059)

The Southern California Earthquake Center (SCEC) Broadband Platform is a collaborative software development project involving geoscientists, earthquake engineers, graduate students, and the SCEC Community Modeling Environment. The SCEC Broadband Platform (BBP) is open-source scientific software that can generate broadband (0-100Hz) ground motions for earthquakes, integrating complex scientific modules that implement rupture generation, low and high frequency seismogram synthesis, non-linear site effects calculation, and visualization into a software system that supports easy on-demand computation of seismograms.

The Broadband Platform operates in two primary modes: validation simulations and scenario simulations. In validation mode, the Platform runs earthquake rupture and wave propagation modeling software to calculate seismograms for a well-observed historical earthquake. Then, the BBP calculates a number of goodness of fit measurements that quantify how well the model-based broadband seismograms match the observed seismograms for a certain event. Based on these results, the Platform can be used to tune and validate different numerical modeling techniques.

In scenario mode, the Broadband Platform can run simulations for hypothetical (scenario) earthquakes. In this mode, users input an earthquake description, a list of station names and locations, and a 1D velocity model for their region of interest, and the Broadband Platform software then calculates ground motions for the specified stations.

Working in close collaboration with scientists and research engineers, the SCEC software development group continues to add new capabilities to the Broadband Platform and to release new versions as open-source scientific software distributions that can be compiled and run on many Linux computer systems. Our latest release includes 5 simulation

methods, 7 simulation regions covering California, Japan, and Eastern North America, the ability to compare simulation results against GMPEs, and several new data products, such as map and distance-based goodness of fit plots. As the number and complexity of scenarios simulated using the Broadband Platform increases, we have added batching utilities to substantially improve support for running large-scale simulations on computing clusters.

Analysis of the March 21, 2009 (M=4.7) Bombay Beach Earthquake Swarm, *Gerry Simila and Geoffrey McStroul* (Poster 174)

From March 21, 2009 through April 9, 2009, an earthquake swarm occurred near Bombay Beach, which is located on the eastern side of the Salton Sea near the southern end of the San Andreas Fault. During this period, over 460 earthquakes were recorded, and the largest of which had a magnitude of 4.7. The M4.7 moment tensor solution showed left-lateral, strike-slip motion with a preferred nodal plane strike of N57E which is consistent with faults orthogonal to the San Andreas fault in this area. The 2009 swarm events were relocated using hypoDD and the SCEC CVM. The seismicity consisted of two swarms, both striking about N57E, with dimensions of 4-6 km in length and 1 km in width, and the depth range was 2-8 km. Potential causes include the extension of the Extra Fault Zone (EFZ) from the western region of the Salton Sea to Bombay Beach. In addition, published seismic reflection data in the Salton Sea area near Bombay Beach show NE trending, near-vertical dipping faults possibly resulting from a young pull-apart basin.

Other than tectonics, what other factors cause geographic variations in the elevations of marine terraces across the Pacific Coast of North America? *Alexander R. Simms, Kurt Lambeck, Helene Rouby, and Anthony Purcell* (Poster 255)

The elevations of marine terraces have long been used to determine past sea levels and as a datum in which to calculate rates of tectonic motion across the Pacific Coast of North America. The elevation of marine terraces formed during marine isotope stages (MIS) 5a (~84 ka) and 5c (~105 ka) along the central Pacific Coast of North America generally decrease with higher latitudes. Because sea level itself varies through time due to glacio-hydro-isostatic processes (GIA), we examine here whether this process makes a significant contribution to the observed variations in marine terrace elevations. Our GIA results are generally consistent with the observed trends in the elevations of MIS5a and MIS5c marine terraces. GIA results in up to 6 m of variation in local sea levels across the Pacific Coast of North America during MIS5e (120 ka), 25 m during MIS5c and MIS5a, 30 m during MIS3 (50 ka), and up to 50 m during the Last Glacial Maximum (LGM) at 20 ka. Our results show that applying paleo-sea level records derived from the well-dated marine terraces of southern California to locations north of San Simeon (California) or south of Meluge (Mexico) for MIS5c, MIS5a, MIS3, or the LGM may introduce large errors to uplift estimates.

Participation of the Parkfield segment in major San Andreas Fault events, *Norman H. Sleep* (Poster 274)

The Parkfield segment is inferred to have occasionally participated in major events $M > 7.5$ on the San Andreas with a few meters of local seismic displacement. Failure of fragile geological features indicates that past peak ground velocities (PGV) of ~2 m s⁻¹ at the Pilot Hole for infrequent (few 1000 yr recurrence) events. An analytical method represents near-field velocity pulses of San Andreas events as horizontal motion where dynamic strain varies slowly with depth. Then peak dynamic strain is particle velocity PGV divided by the phase velocity c of the pulse. Dynamic stress is dynamic strain times the shear modulus G , which is a function of depth. Rock failure occurs when dynamic stress exceeds frictional strength, which (for simplicity) increases linearly with depth. PGV for failure is then $c * (\text{rock density} - \text{water density}) * (\text{coef of friction}) * \text{gravity} * \text{depth} / G$, where G is the product of shear wave velocity squared and density. (1) Repeated frictional failure from strong seismic waves tends to locally relax shallow ambient tectonic stresses providing a potential fragile geological feature. Relaxation of the regional fault-normal compression appears to have occurred within granite from 768 m down to ~1000-1600 depth at the Pilot Hole. Subsequent movements on the main fault have imposed strike-slip stress within the relaxed region. (2) The

ambient rock itself is a fragile feature. Intact stiff rock fails under the imposed strain; repeated failure events lead to pervasively cracked rocks. For given maximum PGV, G at failure is $c * (\text{rock density} - \text{water density}) * (\text{coef of friction}) * \text{gravity} * \text{depth} / \text{PGV}$. The shear modulus of the damaged shallow subsurface self organizes to linearly with depth, so that typical dynamic strains barely produce frictional failure and the crack concentration comes to steady state. Measurements of the S-wave velocity indicate that this situation (low-cycle fatigue approximately prevails at the Pilot Hole within sandstone and granite. Numerical models of realistic velocity pulses and realistic 3-D structure would provide more precise estimates of PGV to damage the rock by frictional failure.

GPU Acceleration of Hercules, *Patrick Small, Ricardo Taborda, Jacobo Bielak, and Thomas H. Jordan* (Poster 085)

This work describes one of the recent SCEC efforts to advance the use of general-purpose graphics processing units (GPGPU) in physics-based earthquake simulation software. In particular, we report on performance improvements achieved using GPGPU-oriented coding on Hercules, a SCEC-supported 3D earthquake ground motion simulator originally developed by the Quake Group at Carnegie Mellon University and currently part of the SEISM Project's High-F Simulation Platform. Hercules is a parallel simulation code written in the standard C programming language. It uses the Message Passing Interface (MPI) libraries to manage inter-processor communications and an octree-based backbone to manage unstructured finite-element meshes. In its original form, Hercules has been thoroughly tested in multiple high-performance computing systems including Kraken (NICS, now decommissioned) and Blue Waters (NCSA), where it has shown near-excellent scalability. Hercules has also been used in multiple verification and validation simulations led by SCEC, including the TeraShake and ShakeOut scenarios, and other historical events such as the 1994 Northridge and the 2008 Chino Hills earthquakes. Utilizing CUDA, a parallel computing platform and programming model designed to work with NVIDIA graphics processing units, several computationally intensive physics calculations within Hercules have been moved to the GPGPU, resulting in greatly improved runtime performance. This implementation has been tested on multiple systems with hybrid CPU-GPU architectures, including USC's HPCC system, NCSA's Blue Waters, and OLCF's Titan, one of the fastest supercomputers in the world, housed at Oak Ridge National Laboratory. The latest tests executed on Titan, in particular, correspond to simulations of the 2008 Chino Hills and the 2014 La Habra earthquakes. Our results for Chino Hills are consistent with previous simulations done using the CPU-only version of Hercules. Results for La Habra were used for a recent verification and validation effort still underway. Computationally speaking, the implementation of the GPU modules on Hercules shows performance improvements of the order of 2.5x on the overall solver execution time, and of higher factors on individual computing modules. These improvements are important because they will allow us to tackle larger and more detailed problems in the future.

Acquisition, Processing, and Modeling of Real-Time High-Rate GPS Data at USGS in Menlo Park for Improved Earthquake Early Warning, *Deborah E. Smith, Jessica R. Murray, John O. Langbein, Christian Guillemot, and Sarah E. Minson* (Poster 038)

Currently implemented Earthquake Early Warning (EEW) algorithms based on seismic data alone should provide the most robust warnings for $M < 6$ earthquakes, since real-time GPS positions are too noisy to aid in EEW. However, for larger events, which generate larger surface offsets, GPS data can provide a direct measurement of displacement that stays on scale and has sufficient precision. In such situations, the GPS observations may enable more accurate estimation of magnitude and rupture extent than seismic data.

The USGS Earthquake Science Center (ESC) in Menlo Park obtains real-time data from approximately 100 GNSS stations in Northern California. Current real-time GPS efforts for EEW are concentrated in: 1) development of software tools for monitoring and trouble-shooting data, 2) evaluating the latency and precision of position estimates obtained through real time processing, and 3) implementation of the BEFORES algorithm (Minson et al, 2014) for real-time finite fault inversion.

MEETING ABSTRACTS

We conduct centralized real-time processing of raw, 1 Hz data in Menlo Park to obtain position estimates for each station using two software packages, TrackRT and RTNet. We have developed web-based software for monitoring a variety of state-of-health, data quality, and latency metrics as well as for real-time and static plotting of processed station positions.

For EEW applications, real-time GPS positions must have low latency and good short-term repeatability. We process data in two modes: differential (requiring a reference station) and Precise Point Positioning (PPP) which provides absolute positions. The differential and PPP solutions have similar robust precision but different latency characteristics. Differential solutions typically have latencies of less than 5 seconds whereas PPP often has latencies exceeding 50 seconds; although new technology may yield acceptably low PPP latencies for EEW.

We are now implementing the BEFORES algorithm (Minson et al., 2014) which uses Bayesian analysis to determine the best-fitting fault orientation and finite fault slip distribution in real-time. We are focusing on: 1) receiving real-time earthquake locations from seismic EEW algorithms, 2) synchronization and quality control of real-time GPS streams from TCP/IP connections, and 3) optimizing the computation of elastic Green's functions. These tasks plus additional tests using simulated data will prepare the algorithm for implementation in the West Coast EEW system.

Stochastic descriptions of small-scale, near-surface velocity variations in the Los Angeles basin, *Xin Song, Thomas H. Jordan, Andreas Plesch, and John H. Shaw* (Poster 095)

Simulations of earthquake ground motions at high frequencies (> 1 Hz) require high-resolution velocity models to quantify the effects of wave scattering, attenuation, and anisotropy. Valuable information about the statistical variations of the velocity structure in the upper few kilometers of the crust can be obtained from well logs. We apply geostatistical methods to characterize the one-point and two-point statistics of velocity variations observed at vertical scale lengths less than 200 m in an ensemble of vertical sonic logs from the central Los Angeles basin. The stochastic variability at these scales can be separated into two components, one with a correlation length of about 10-60 m and a second with a correlation length of about 1-4 m. The one-point statistics of both components are distinctly non-Gaussian, with those of the first skewed to low velocities and those of the second skewed to high velocities. Assuming that the horizontal correlation lengths are much greater than the vertical correlation lengths, we then obtain a long-wavelength polarization anisotropy of around 6-8% from up-scaling method of the profiles. We also investigate the magnitude of wave scattering caused by the small-scale heterogeneity and speculate on its role in explaining the anomalous near-surface attenuation of high-frequency seismic waves.

The geometry of the post-Miocene North Channel-Pitas Point Fault System including post-Miocene folding, Santa Barbara Channel, California, *Christopher C. Sorlien, Craig Nicholson, Richard J. Behl, Marc J. Kamerling, Courtney J. Marshall, and James P. Kennett* (Poster 094)

The active N-dipping North Channel-Pitas Point fault system (NC-PP) has been mapped ~120 km from the onshore Ventura area to west of Point Conception. Data include dense grids of industry multichannel seismic reflection (MCS) data, local grids of high-resolution MCS data, and several 3D MCS surveys. We use precisely-dated post-~1 Ma stratigraphy, and compare the MCS data to a series of published cross sections through wells (Redin et al., 2005). The Pitas Point fault strands (=Ventura fault onshore) can be traced ~80 km west, to ~120° 13' W. There, they die out, at least in the imaged upper few km, below a backthrust and N-verging Hondo anticline. The broader S-directed fault system continues across a 6-km right stepover to another blind (oblique) thrust. Although probably not directly continuous with North Channel fault strands mapped farther east, it has historically been called the North Channel fault. It continues for another 40 km to west of Point Conception.

The NC-PP strands are variably blind along strike, with their upper tips in places below the 1-Ma horizon and in other locations cutting up to higher levels. The blind slip is absorbed by a progressively tilting, S-dipping forelimb almost everywhere. Forelimb dips and structural relief, although variable, are not systematically greater in the east than in the west between Carpinteria and the UCSB campus at 119° 50' W. Farther west,

the rate of tilting, and probably the rate of offshore shortening, decreases steadily through the western 40 km to the end of the system beyond Point Conception. This trend mirrors the decrease in elevation and structural relief of the Santa Ynez Mountains above the deep fault. There is no evidence of a major change in tilt rate at any one location through the last 1 Myr along the offshore fault system. The MCS data image the progressively steeper dips until imaging is lost. The Redin et al. (2005) cross sections indicate that the forelimb dips reach near vertical to overturned in early Quaternary rocks east of UCSB. Progressive tilts to at least moderate dips above the western fault affect Pliocene strata. These observations suggest that the entire fault system has been active in contraction since at least early Pliocene time rather than propagating westward.

Redin, T., J. Forman and M.J. Kamerling, 2005, Santa Barbara Channel structure and correlation sections, Pacific Section AAPG CS-32 through CS-42, Bakersfield, CA.

Field and LiDAR observations of the Hector Mine California 1999 surface rupture, *Frank Sousa, Sinan Akciz, Janet Harvey, Kenneth Hudnut, David K. Lynch, Katherine Scharer, Joann Stock, Ryan Witkosky, Katherine Kendrick, and Crystal Wespestad* (Poster 258)

We report new field- and computer-based investigations of the surface rupture of the October 16, 1999 Hector Mine Earthquake. Since May 2012, in cooperation with the United States Marine Corps Air Ground Combat Center (MCAGCC) at Twentynine Palms, CA, our team has been allowed ground and aerial access to the entire surface rupture. We have focused our new field-based research and imagery analysis along the ~10 kilometer-long maximum slip zone (MSZ) which roughly corresponds to the zone of >4 meter dextral offset. New data include: 1) a 1 km wide aerial LiDAR survey along the entire surface rupture (@ 10 shots/m², May 2012, www.opentopography.org); 2) terrestrial LiDAR surveys at 5 sites within the MSZ (@ >1000 shots/m², April 2014); 3) low altitude aerial photography and ground based photography of the entire MSZ; 4) a ground-truthed database of 87 out of the 94 imagery-based offset measurements made within the MSZ; and 5) a database of 50 new field-based offset measurements made within the MSZ by our team on the ground, 31 of which have also been made on the computer (Ladicaoz) with both the 2000 LiDAR data (@ 0.5 m DEM resolution; Chen et al, in review) and 2012 LiDAR data (@ 35 cm DEM resolution; our team).

New results to date include 1) significant variability (> 2 m) in horizontal offsets measured along short distances of the surface rupture (~100 m) within segments of the surface rupture that are localized to a single fault strand; 2) strong dependence of decadal scale fault scarp preservation on local lithology (bedrock vs. alluvial fan vs. fine sediment) and geomorphology (uphill vs. downhill facing scarp); 3) newly observed offset features which were never measured during the post-event field response; 4) newly observed offset features too small to be resolved in airborne LiDAR data (< 1 m); 5) nearly 25% of LiDAR imagery-based measurements that were later ground-truthed were judged by our team to warrant removal from the database due to incorrect feature reconstruction; and 6) significant variability in both accuracy of LiDAR offset measurements (relative to field-based measurements) and reported uncertainty between workers, mostly based on differing interpretations of geomorphic complexity.

An approach for calculating absolute stress from stressing rate, *Aviel Stern and Michele L. Cooke* (Poster 128)

Crustal deformation yield stressing rate information that provides critical information about fault interaction but cannot produce the absolute stress distribution needed for dynamic rupture models. We use the stressing rates from a forward deformation model of the San Geronio Pass region along information about recurrence intervals and time since last event to estimate absolute stress. From a 3D Boundary Element Method model that simulates interseismic deformation of the region, we calculate the distribution normal and shear stressing rates along the San Bernardino Segment, San Geronio Pass Thrust, Banning strand, Garnet Hill strand, Mission Creek strand and Coachella segment of the San Andreas fault. Tectonic loading is prescribed as velocities at the outside of the model while leaving the rest of the system freely slipping. Uncertainties in the tectonic loading are considered by testing a range of velocities.

We calculate the absolute stress from the stressing rates by assuming regular earthquake rupture intervals and complete stress drop during these events. The stress drop is governed by the drop in friction coefficient from static to sliding values. We use the four equations for 1) stress at onset of sliding, 2) stress at end of sliding, 3) normal and 4) shear stress accumulation between events to solve for shear and normal stress. In this approach we consider only large ground rupturing events that are likely to be preserved in the paleoseismic record. The absolute stress depends on stressing-rates as well as recurrence intervals and time since last event. The tectonic loading will affect the freely slipping faults and cause the faults to deform due to the interaction of faults and its geometry. We use log-normal probability distributions for recurrence intervals from the UCERF3 compilation by Biasi (2013) and the compiled time since last event. For the San Geronio Pass thrust, Banning strand, and Garnet Hill Strand of the SAF we use data from the Cabazon and Millard Canyon sites (Yule and Sieh, 2003). The resulting shear stress ranges are consistent with those used as initial conditions in dynamic rupture models but differ in distribution because our approach considers the effect of fault interaction.

Rate-and-State Southern California Earthquake Forecasts: Resolving Stress Singularities, Anne E. Strader and David D. Jackson (Poster 021)

In previous studies, we pseudo-prospectively evaluated time-dependent Coulomb stress earthquake forecasts, based on rate-and-state friction (Toda and Enescu, 2011 and Dieterich, 1996), against an ETAS null hypothesis (Zhuang et al., 2002). At the 95% confidence interval, we found that the stress-based forecast failed to outperform the ETAS forecast during the first eight weeks following the 10/16/1999 Hector Mine earthquake, in both earthquake number and spatial distribution. The rate-and-state forecast was most effective in forecasting far-field events (earthquakes occurring at least 50km away from modeled active faults). Near active faults, where most aftershocks occurred, stress singularities arising from modeled fault section boundaries obscured the Coulomb stress field. In addition to yielding physically unrealistic stress quantities, the stress singularities arising from the slip model often failed to indicate potential fault asperity locations inferred from aftershock distributions. Here, we test the effects of these stress singularities on the rate-and-state forecast's effectiveness, as well as mitigate stress uncertainties near active faults. We decrease the area significantly impacted by stress singularities by increasing the number of fault patches and introducing tapered slip at fault section boundaries, representing displacement as a high-resolution step function.

Integration of a 3D Low-Frequency Simulation with the SCEC Broadband Platform, Ricardo Tabora, David Gill, Patrick Small, Fabio Silva, Philip J. Maechling, Jacobo Bielak, and Thomas H. Jordan (Poster 087)

We have recently worked on a pilot integration of a three-dimensional (3D) physics-based code with the SCEC Broadband Platform for earthquake ground motion simulations. The Broadband Platform is a collaborative software development project involving SCEC researchers, research engineers, and the SCEC/CME software development group. It is designed to generate broadband (0-100 Hz) ground motions for earthquakes, which integrates different simulation codes that have been contributed by various SCEC simulation groups. The different modules include rupture generation, low- and high-frequency seismogram synthesis, site effects, visualization, and validation with data and with ground motion prediction equations. The low-frequency ground motion simulators in the platform have, however, been limited to one-dimensional (1D) layered models. The main reason behind this is the desire to keep the Broadband Platform highly portable and accessible to most users at a low computational cost. We are interested in exploring the capabilities of the Broadband Platform if it is combined, despite the additional cost, with 3D simulations that can improve the prediction of the ground motion at low frequencies. We present results of an initial integration scheme that combines the power of Hercules---a 3D octree-based finite element parallel earthquake ground motion simulator---with the Broadband Platform. We use the 2008 Chino Hills earthquake as a testbed event and simulate ground motions using the Broadband Platform with two simulation modules and a 1D model (for reference), the Broadband Platform with Hercules using the same 1D model for the low frequencies (for verification purposes), and the Broadband Platform with Hercules

using a 3D model (CVM-S4.26) to investigate the improvements drawn from using a 3D model in comparison to the 1D-model simulations. Our initial results indicate that the use of 3D models notably improves the validation of simulation results obtained with the Broadband Platform. Some aspects of the integration, however, still require additional work. These include the appropriate definition of the threshold minimum shear wave velocity and the treatment of site effects in light of the available data for validation recorded both on soil and rock sites. The integration, nonetheless, looks very promising.

The Effect of Mean Grain Size and Polydispersity on Auto-Acoustic Compaction, Stephanie E. Taylor and Emily E. Brodsky (Poster 112)

The behavior of granular flows is strongly dependent on shear rate. At relatively slow shear velocities, a granular flow will support stresses elastically through force chains in what is recognized as the quasi-static regime. At relatively high shear velocities, it will support stresses by transferring momentum in higher velocity grain collisions in the grain-inertial regime, which results in dilation of the flow. Recent experiments conducted using a commercial torsional rheometer (TA AR-2000ex) found that at intermediate shear velocities, force chain collapse in angular sand samples produces sound waves capable of vibrating the shear zone enough to cause compaction. To expand on the characterization of this newly identified rheological regime, the auto-acoustic regime, we used the same experimental set up to observe how volumetric and acoustic response to shear stress changes with grain size mean and range. Stepped velocity ramp experiments were conducted first on four separate logarithmically sized grain size bins, and then on three mixtures of varying polydispersity. Smaller mean grain sizes exhibited more pronounced compaction resulting from the auto-acoustic regime, and the largest mean grain sizes showed no compaction, implying a grain size threshold for auto-acoustic compaction. In mixtures of different grain size bins, the response of the flow to intermediate shear velocities was consistent with the response of the smallest grain size bin included in the mixture, while the response of the flow to high shear velocities was most dependent on the largest grain sizes present in the mixture. The results imply that the auto-acoustic behavior could potentially be predicted from the extremum of a grain size distribution.

Geologic and structural controls on rupture zone fabric: A field-based study of the 2010 Mw 7.2 El Mayor-Cucapah earthquake surface rupture, Orlando J. Teran, John M. Fletcher, Michael E. Oskin, Thomas K. Rockwell, Kenneth W. Hudnut, Ronald M. Spelz, Sinan O. Akciz, Ana P. Hernandez, and Alexander E. Morelan (Poster 261)

We systematically mapped (scales >1:500) the surface rupture of the 4 April 2010 Mw 7.2 El Mayor-Cucapah earthquake through Sierra Cucapah to understand how faults with similar structural and lithologic characteristics control rupture zone fabric, which is here defined by the thickness, distribution and internal configuration of shearing in a rupture zone. Fault zone architecture and master fault dip showed the strongest controls on rupture zone fabric. Highly localized slip was observed along simple narrow fault cores (<20 m), whereas wide cores (>50 m) composed of multiple zones of high shear strain had wider and more complex rupture zones that generally lacked principal-displacement scarps. Rupture zone thickness also increases systematically with decreasing fault zone dip. We observed that coseismic slip along faults that dip >40° was mostly confined to the fault core, whereas faults that dip as low as 20° had surface rupture entirely developed entirely outside of the fault zone. The lack of large off-fault strain along faults dipping >40° is contrary to predictions by dynamic stress modeling (e.g., Ma, 2009). We show that static tectonic loading, which varies significantly with fault orientation, has a significant effect not only on rupture zone fabric but also on the evolution of fault zone architecture in this transtensional setting.

Rupture zones in undeformed alluvium are dominated by secondary fractures associated with fault-tip propagation, and arrays of fault scarps become wider and more complex with oblique slip compared to pure normal dip-slip or pure strike-slip. Field relations show that as magnitude of coseismic slip increases from 0 to 60 cm, the linkages between kinematically distinct fracture sets increases systematically to the point of forming a through going principal scarp, which is contrary to many analogue models (e.g., Tchalencko, 1970; Naylor et al., 1995). Our data indicate that secondary faults and penetrative off-fault strain continue to

MEETING ABSTRACTS

accommodate the oblique kinematics of coseismic slip after the formation of a through going principal scarp.

Tsunami hazard from the Ventura-Pitas fault and fold system, Hong Kie Thio, Wenwen Li, John Shaw, Judith Hubbard, Andreas Plesch, and Rick Wilson (Poster 089)

The Ventura fold and thrust complex consists of the rapidly growing Ventura Avenue anticline underlain by a Ventura-Pitas Point fault. Although the offset on the fault decreases towards the surface, consistent with a fault-propagation fold, there is 5-10 of uplift recorded along the local coast for the last event, which occurred 800 years ago (Rockwell, 2011). Given the recurrence rates of less than 2500 yrs for even the largest potential event, this structure may constitute a significant source for tsunami hazard in southern California.

We are currently in the process of developing probabilistic tsunami hazard maps for the state of California, with return periods between 100 to 2500 years. In our present model, the hazard in southern California is dominated by distant sources in Alaska and Chile. The purpose of this study is to evaluate the hazard posed by the Ventura-Pitas Point fault to local communities in southern California, how it compares to the distant tsunami sources, and thus whether it is necessary to include this structure in the state-wide tsunami hazard maps.

Because the structure is a fault-propagation fold, the slip on the fault and the uplift that occurs during an event is strongly dependent on details of the kinematic model of the fault system. In this preliminary study, we will present tsunami hazard calculations for some simple slip models.

The results of this study may also help in the identification of potential areas for paleo-tsunami field studies that can be used to constrain the rupture history of the Ventura Pitas-Point fault system.

Investigation of San Andreas slip transfer east of Whitewater Canyon, Tarra Thompson, Lindsay Arvin, and Sally McGill (Poster 284)

Slip on the San Andreas fault zone in Coachella Valley is partitioned onto 3 fault strands. Near Indio the northeasternmost strand, the Mission Creek fault, appears to carry most of the slip since late Pleistocene time, yet the more southerly strands appear to carry most of the late Quaternary slip west of Whitewater. Our objective is to investigate how and where slip may transfer from the Mission Creek strand to the more southerly strands. The abrupt westward transition from the flat floor of Coachella Valley to uplifted Miocene to Pleistocene sedimentary rocks and alluvial fans in the hills east of Whitewater Canyon represents a potential locus of slip transfer. We attempt to constrain the amount of shortening in this vicinity through mapping and surveying of geologic structures that have deformed units of three different ages. (1) The geometry of faulting beneath the Rainbow anticline in the Coachella fan is poorly constrained, but our preferred fault-bend fold model suggests a thrust ramp dipping about 24 degrees WNW and WNW-ESE shortening of at least 4 km. This suggests a minimum shortening rate of 0.4 mm/yr, if shortening began soon after deposition of the Coachella fan, or of > 1 mm/yr if shortening began after 4 Ma, as a result of deformation of the Mission Creek fault by the Pinto Mountain fault. (2) The Cabezon fan east of Whitewater Canyon sits ~ 200 m above the modern drainages. Given a published age estimate of 70-200 ka based on soil development, uplift of this unit may be occurring at a rate of 1-2 mm/yr with a shortening rate larger than that, depending on fault dip. (3) Near the mouth of Mission Creek, we surveyed two profiles across a well-defined, northeast-striking fault scarp within a Late Pleistocene alluvial fan with a published Be-10 age of 66 ± 13 ka. The southwestern profile has a vertical surface offset of 8.9 m, and the northeastern profile has a vertical surface offset of 6.5 m. The two profiles are separated by a subtle terrace riser, suggesting that the southwestern profile may record one more earthquake than the northeastern profile. A fault dip of 17 degrees (34 degrees maximum) was estimated from potential overlap of a soil horizon that is poorly exposed in a gully wall. Using the southwestern profile, this suggests a shortening rate between 0.43 and 0.19 mm/yr, depending on fault dip. These preliminary data suggest that only a minor amount of slip transfer is occurring in this region.

Rapid shortening at the eastern margin of the Tibetan plateau prior to the 2008 Mw=7.9 Wenchuan earthquake, T. Ben Thompson and Brendan J. Meade (Poster 230)

The Longmen Shan is the steepest topographic front of the India-Asia collision and was the site of the Mw=7.9 Wenchuan earthquake. Shortening estimates across the Longmen Shan provide strain accumulation rates and clarify the eastward extrusion of the Tibetan plateau. Here, to explain the interseismic GPS velocities across the greater Longmen Shan region, we develop a boundary element model including earthquake cycle effects, topography, the westward dipping Beichuan fault, and a ~20 km deep, shallowly dipping, detachment. The detachment is inferred from observations of postseismic afterslip following the Wenchuan earthquake and from structural considerations. In contrast to analyses which neglect the detachment and earthquake cycle effects, we find that interseismic GPS data are consistent with a shortening rate of 6 ± 1 mm/yr. These results suggest that the Longmen Shan is an active fold-and-thrust belt with Wenchuan style earthquake recurrence intervals of <500 years.

Symmetrical Bias in Reporting Slip Rates: Asymmetric Probability Density Functions are Inherent Outcomes of Accounting for Uncertainties in Displacement and Age, Nathan A. Toke (Poster 265)

Constraining the slip rate of an active fault requires estimation of both displacement and age of an offset Quaternary deposit or landform. Estimating displacement requires knowledge of fault structure, kinematics, and the initial morphology of the displaced feature. Estimating the age of the feature requires the use of geochronology to bracket the timing of deposition or sculpting of a landform. All of these estimates include uncertainty. Over the past decade the earthquake geology community has been improving the quantification of our uncertainties in reporting geologic slip rates. A major improvement has been the use of probability density functions (PDFs) that graphically present the full range of slip rate probability values and provide a rigorous way to quantify the most likely slip rate for an active fault. One outcome from the PDF approach is the realization that nearly all slip rate PDFs are asymmetric with the most probable rate skewed toward the lower end of the range. This can be illustrated with a hypothetical example of a right-laterally displaced channel such as those found along the San Andreas Fault: geologists might estimate a displacement of 50.0 m with a symmetrical uncertainty of plus or minus 3.0 m and geochronology could yield age constraints of 1500 years BP plus or minus 100 years. If both of these input PDFs are symmetric, the convolution of their probabilities will result in an asymmetric slip rate PDF. Consider the range from the minimum estimate of 29.4 mm/y (47m/1600yBP) to the maximum estimate of 37.9 mm/y (53 m/1400yBP). This range has a median of 33.65 mm/y. A publication might therefore report the slip rate as 33.65 ± 4.25 mm/y. However, the most probable displacement (median = 50 m) divided by the most probable age (median = 1500 y) yields a slip rate of 33.3 mm/y. In this example, the most probable slip rate is skewed 3.8 percent toward the lower end of the slip rate range. While this is not an astounding percentage of asymmetry, it is inherent in all geologic slip rate calculations and such asymmetries can be more significant for less well-constrained rates measured across young landforms. In this hypothetical case it would have been better to report the slip rate as $33.3 +4.6/-3.9$ mm/y. We must continue to improve our accounting for uncertainty in slip rate estimations, especially as we aim to compare rates across complex fault systems over both geodetic and geologic time scales.

An integral method to estimate moment accumulation rate on the Creeping Section of the San Andreas Fault, Xiaopeng Tong, David Sandwell, and Bridget Smith-Konter (Poster 239)

Moment accumulation rate is a fundamental quantity for evaluating seismic hazard. The conventional approach for evaluating moment accumulation rate of creeping faults is to invert for the slip distribution from geodetic measurements, although even with perfect data these slip-rate inversions are non-unique. In this study we show that the slip-rate inversion is not needed because moment accumulation rate can be estimated directly from surface geodetic data. We propose an integral approach that uses dense geodetic observations from Interferometric Synthetic Aperture Radar (InSAR) and GPS to constrain the moment

accumulation rate. The moment is related to the integral of the product of the along-strike velocity and the distance from the fault. We demonstrate our method by studying the Creeping Section of the San Andreas fault observed by GPS and radar interferometry onboard the ERS and ALOS satellites. Along-strike moment rate variation is derived in order to investigate the degree of partial locking of the creeping segment. The central creeping segment has a moment accumulation rate of $\sim 3.1 \times 10^{15}$ Nm/yr/km while the fully locked fault, e.g. Cholame-Carrizo segment, has a typical moment accumulation rate of $\sim 12.2 \times 10^{15}$ Nm/yr/km. The upper and lower bounds of the moment accumulation rate are derived based on the statistics of the noise. Finally we compare the results from this simple integral method with the results obtained by the moment-bounding inverse method.

Remotely Sensed Mineral Identifications at the Salton Sea Fumaroles, *David M. Tratt, Paul M. Adams, David K. Lynch, Kerry N. Buckland, and Patrick D. Johnson* (Poster 269)

The Salton Sea Geothermal field and associated volcanic necks are testament to the earthquake potential in the active plate margin and complex spreading center of the Salton Trough. One kilometer southeast of the northernmost volcano (Mullet Island) lie several fumarole fields that were recently exposed (~ 2006) by recession of the Salton Sea. These boiling-hot vents harbor a complex assemblage of evaporite minerals, many of an ammoniated composition. This area has been a target for a number of infrared hyperspectral studies, which have been used to produce mineral occurrence maps for mascagnite, gypsum, bloedite, thenardite, nitratine, and others. Based on infrared hyperspectral aerial surveys using Mako and SEBASS, many of these minerals showed a tendency to occur in ring and arcuate patterns roughly concentric with the major vents. They are also highly variable with time.

Given the ephemeral nature of many of the minerals present at the fumarole field, a campaign was mounted to specifically conduct simultaneous airborne and ground truth measurements, the former using Mako, an infrared hyperspectral remote sensing system. Shortly after the fumarole overflights, the aircraft landed to hand off the geolocated mineral maps to the field team, who then returned to the fumaroles and gathered samples from locations of interest indicated by the aerial surveys. An Exoscan portable FTIR spectrometer was used to acquire in situ mineral spectra along specific radial lines transecting the rings and arcs to provide real time feedback for the collection of samples for subsequent laboratory X-ray diffraction identification. The results of this study attest to the ability of high spectrospatial resolution infrared imaging to remotely identify and discriminate complex mineral assemblages.

Did the Stress Perturbation Caused by Fluid Extraction at the Cerro Prieto Geothermal Field Influence the El Mayor-Cucapah Rupture Sequence? *Daniel T. Trugman, Adrian Borsa, and David T. Sandwell* (Poster 232)

The 2010 Mw 7.2 El Mayor-Cucapah (EMC) earthquake ruptured a complex fault system that was previously considered inactive. The Cerro Prieto Geothermal Field (CPGF), the world's second-largest geothermal field, is located approximately 15 km to the east of the EMC hypocenter. In this work, we study the substantial anthropogenic subsidence caused by fluid extraction and recharge at the CPGF, and assess whether this extraction causes a significant perturbation to the stress field in the EMC rupture zone. We use InSAR data acquired from ALOS satellite tracks in the three years preceding the El Mayor-Cucapah earthquake to constrain the magnitude of the subsidence rate (~ 15 cm/yr), and its spatial extent near the CPGF. LIDAR data acquired from 1995-2006 suggests that this mean subsidence rate has been relatively consistent over the past 20 years. We model the spatial complexity of fluid extraction and recharge at the CPGF as a grid of Mogi-source spherical pressure cavities, using the observed InSAR surface deformation to perform an L1-inversion for the source pressure intensities. We apply this model to estimate the anthropogenic perturbation to the stress field near the EMC hypocenter. Subsidence at the CPGF generates positive Coulomb stress changes of order 15 KPa/year near the EMC hypocenter. Further, stressing rates of order 25 KPa/year are induced at the juncture of the initial fault plane with the secondary fault planes that allowed for sustained rupture. Although we cannot definitively conclude that production at the CPGF triggered the EMC earthquake or helped sustain its rupture, its influence on the local

stress field is substantial, and should not be neglected in local seismic hazard assessments.

Prospective evaluation of 1-day testing class of the CSEP-Japan earthquake forecasts, *Hiroshi Tsuruoka and Naoshi Hirata* (Poster 018)

Laboratory for the Study of Earthquake Predictability (CSEP) is a global project of earthquake predictability research. The primary purpose of the CSEP is to develop a virtual, distributed laboratory. The final goal of this project is to investigate the intrinsic predictability of earthquake rupture process.

One major focus of the Japanese earthquake prediction research program 2009-2013 is to develop testable earthquake forecast models. So, the Earthquake Research Institute (ERI) joined the CSEP and installed an international collaboration a testing center in ERI as CSEP-Japan for rigorous evaluation of earthquake forecast models.

CSEP-Japan has conducted prospective experiments since 1 November 2009. Over 160 models have been submitted to CSEP-Japan from all over the world. The models are currently under test in 12 categories, with 3 testing regions and 4 testing classes of different time spans (1 day, 3 month, 1 year and 3 years). We evaluate the performance of the models in the official suite of tests defined by the CSEP (L, M, N, S, CL, T and W tests) against the authorized catalogue compiled by Japan Meteorological Agency, the unified JMA catalogue.

CSEP-Japan testing center has conducted over 600 trials of tests for 1-day testing classes including the 2011 Tohoku-oki earthquake. We will discuss these results of evaluation test of the prospective experiments, and checked the performance of the earthquake models.

Inversion for the physical parameters that control the source dynamics of the 2004 Parkfield earthquake, *Cedric Twardzik, Raul Madariaga, and Shamita Das* (Poster 120)

A fully dynamic inversion for the earthquake source process in which the geometry of the rupture area, the stress conditions and frictional properties on the fault are obtained, is carried out by inverting displacement records for the 2004 Mw6.0 Parkfield, California earthquake. The rupture area of the earthquake is modelled using elliptical patches, and seismograms from 10 near-field digital stations are used. Synthetic tests to investigate the performance of the inversion in retrieving the rupture process demonstrate that we can reliably recover the large scale features of the spatio-temporal distribution of slip. To investigate the stress conditions and frictional properties of the fault under which we produce a rupture model that fits the observed data, we explore the parameter space using a Monte-Carlo method and find an optimal region where the source models fit the data well. The best fitting rupture process is shown to occur mainly within one horizontal elliptical region, 22 km long along strike and 4 km wide along depth. The seismic moment is 1.2×10^{18} Nm, and the stress drop over the ellipse is ~ 4 MPa. The rupture speed, nearly constant during the entire rupture process, is ~ 2.9 km/s. The dimensionless quantity κ (roughly the strain energy change per unit fault surface divided by the energy release rate), which includes information on the stress and frictional properties on the fault, is found to be ~ 1.4 for the ellipse, and strongly controls the rupture process along with the size of the initial circular patch that initiates the earthquake.

Mitigation of atmospheric phase delays in InSAR time series analysis, with application to the Eastern California Shear Zone, *Ekaterina Tymofeyeva and Yuri Fialko* (Poster 221)

Atmospheric propagation effects are the dominant source of noise in radar interferograms, and the most significant limiting factor in applying Interferometric Synthetic Aperture Radar (InSAR) data to the study of low-amplitude (sub-cm) deformation signals. We present a method for estimating radar phase delays due to propagation effects based on the averaging of redundant interferograms that share a common scene. Estimated atmospheric contributions can then be subtracted from the radar interferograms to improve measurements of surface deformation. Inversions using synthetic data demonstrate that this procedure can considerably reduce scatter in the timeseries of the line-of-sight displacements. We demonstrate the feasibility of this method by comparing the InSAR time series derived from ERS-1/2 and ENVISAT data to continuous Global Positioning System (GPS) data from Eastern

MEETING ABSTRACTS

California. We also present results from several sites in the Eastern California Shear Zone where anomalous deformation has been reported by previous studies, including the Blackwater Fault, the Hunter Mountain Fault, and the Coso geothermal plant. In particular, we find that subsidence around the Coso geothermal plant (the second largest geothermal production site in the US) is persisting at a nearly constant rate over the period of observations (1992-2010). The average subsidence rate at Coso is about 2 cm/yr. We find a localized LOS velocity gradient across the Blackwater Fault over 3-5 km using data from tracks 170 and 399, consistent with findings of Peltzer et al. (2001), who used data spanning the eight-year period between 1992-2000. A time series analysis reveals that the deformation signal across the fault is transient, leveling out after 2001. This result is also consistent with the previous study, which suggested that the deformation across the fault was due to a transient postseismic process resulting from the large earthquakes that have occurred on some of the neighboring faults. Finally, we investigate the deformation across the Hunter Mountain Fault, where a secular anomaly had been inferred from InSAR data from track 442, and attributed to interseismic slip rate of 5 mm/yr and an anomalously shallow locking depth of 2 km (Gourmelen et al. 2011). Our analysis of data from the same track, as well as the overlapping track 170, does not reveal a step in secular LOS velocity across the Hunter Mountain Fault.

Bigger aftershocks happen farther away: non-separability of magnitude and spatial distributions of aftershocks, Nicholas J. van der Elst and Bruce E. Shaw (Poster 026)

Earthquakes set off cascading sequences of aftershocks in the surrounding region, some of which can be as large or larger than the initial mainshock. Aftershocks may be driven by stress concentrations due to heterogeneous slip in the main rupture, or by elastic stress transfer along the fault and onto neighboring strands. Physical intuition suggests that the aftershocks that relax stress concentrations on the main rupture should be limited in size, because the typical length scale of the slip-induced stress heterogeneities should be smaller than the length scale of the primary rupture. On the other hand, aftershocks that occur on adjacent fault segments should have no such size limitation. Hence, aftershocks that occur near the margins of the original rupture should have a higher likelihood of propagating onward to become as large or larger than the original main shock. This elastic rebound model for aftershock triggering is consistent with observations that aftershocks tend to cluster at the margins of slip patches. From the standpoint of probabilistic aftershock forecasting, the elastic rebound model predicts that the magnitude and spatial distributions of aftershocks should be non-separable. We examine high-precision Double-Difference relocated earthquake catalogs in California for evidence that the spatial distribution of aftershocks depends on aftershock magnitude. We measure the location of aftershocks with respect to the centroid location of all previous activity in the aftershock sequence, which we assume represents the mainshock rupture centroid. We find that aftershocks that are as large or larger than the mainshock tend to occur farther away than smaller aftershocks. Nearly half of the aftershocks equal to or larger than their mainshock occur in the outer quarter of the aftershock zone. At a magnitude difference of 0.5 units, the fraction of aftershocks in the outer quarter rises to two-thirds. At a magnitude difference of 1.0, 5 out of 5 of the observed aftershocks occur in the outer quarter. These observations are significant at 99.8%. The patterns cannot be reproduced using simulated Epidemic-Type Aftershock Sequence catalogs with standard magnitude and distance kernels. We conclude that the signature of elastic rebound is found in the spatial distribution of large aftershocks. Probabilistic forecasting of societally relevant large aftershocks may be much improved by incorporating magnitude-dependence into the spatial prediction kernels.

Vital Signs of the Planet: A Professional Development Program for High School and Middle School Educators Provides Authentic Experiences In Scientific Inquiry and Encourages Instructional Improvement in Schools Through Lesson Study, Bernadette E. Vargas, William B. Banerdt, Erin Burkett, Elizabeth Cochran, Luis Cortez, Abigail Elvis, Robert M. de Groot, Demoree Deocales, Matthew P. Golombek, Luis J. Gomez, Troy L. Hudson, Jane Houston Jones, Thomas Jordan, Michael Hubenthal, Daniel Keck, Robert S. Kirkwood, Mark Kline, Hernan Lopez, Morris Martinez, James McClure, Sally McGill, Patrick McQuillan, Marc Moya, Lindsay

Rosenbaum, Ricardo Ruiz, Joann Stock, Danielle Sumy, Ashitey Trebi-Ollennu, Margaret Vinci, Seth Wallace, Alice Wessen, Katherine Williams, and Rachel Zimmerman-Brachman (Poster 004)

The JPL InSight E/PO team and SCEC along with California State University San Bernardino (CSUSB), and USGS engaged science educators in the Vital Signs of the Planet Professional Development Program, a standards-based middle school and high school research experience and curriculum development program offering strong connections to STEM research.

The program fellows interacted with scientists at Caltech, JPL, and USGS. They were briefed on topics including seismic hazards, the Quake Catcher Network, Earthquake Early Warning Systems, GPS, and earthquake information technology at Caltech and USGS. While at JPL, they met with researchers in their labs and were briefed on the InSight (Interior Exploration Using Seismic Investigations and Heat Transport) mission to Mars by the mission Principal Investigator.

An important aspect of this experience was participation in a 5-day Field research component, wherein these fellows contributed to ongoing research on tectonic deformation along the San Andreas fault lead by Sally McGill of CSUSB. They plotted data collected through GPS and utilized modeling programs for analysis of slip rate around the fault.

The combination of these experiences lead to the development and eventual classroom implementation of Vive lessons in Earth science and physics.

Using the Lesson Study approach, a professional development process where teachers systematically examine their practice, participants identified where their students encounter learning challenges. Taking into careful consideration the Next Generation Science Standards, the program fellows collaborated to develop lessons that focused on what teachers want students to learn rather than on what teachers plan to teach.

UseIT: The Intern Odyssey, Sarah Vargas, Michael Francisco, Michael Gonzalez, Michael Matchen, LaTerrian Officer-McIntosh, Thomas Jordan, Robert de Groot, Nick Rousseau, Dave Smith, Jason Ballmann, Mark Romano, and Mark Benthien (Poster 007)

The 2014 Undergraduate Studies in Earthquake Information Technology (UseIT) interns represent a diverse range of academic backgrounds such as Earth science, computer science, engineering, and cinematic arts. The interns collaborated to complete the Grand Challenge. The duty of the Media Team is to chronicle this process and produce a short documentary about the UseIT intern experience. This documentary is a media project that not only serves as a testimony to the hard work of the UseIT interns. It also serves as a demonstration of how the UseIT program benefits the Southern California Earthquake Center, the greater scientific community, and the general public. The process of making this documentary is fast-paced, educational, and dynamic, and begins by learning the basics of earthquake science while understanding the current developments made in earthquake research. After the Grand Challenge is given, the Media Team works on developing a concept that is interesting, informative, and unique for a documentary. Filming interviews with interns, mentors, and scientists, the Media Team pieces together a visual outline in Adobe Premiere, a proprietary editing software. This becomes the foundation around which the documentary is built, and a final product that is made demonstrates the experience of the UseIT internship as well as the important achievements the interns make during the summer.

Scale dependency of fracture energy and estimates thereof via dynamic rupture solutions with strong thermal weakening, Robert C. Viesca and Dmitry I. Garagash (Poster 141)

Seismological estimates of fracture energy show scaling with the total slip of an earthquake [e.g., Abercrombie and Rice, 2005]. Potential sources for scale dependency are continued coseismic fault strength reductions with increasing slip or an increasing amount of off-fault inelastic deformation with dynamic rupture propagation [e.g., Andrews, 2005; Rice, 2006]. We investigate the first by solving for the slip dependence of fracture energy at the crack tip of a dynamically propagating rupture in which weakening occurs by strong reductions of friction via flash heating of asperity

contacts and thermal pressurization of pore fluid leading to reductions in effective normal stress.

Laboratory measurements of small characteristic slip evolution distances for friction [e.g., Marone and Kilgore, 1993; Kohli et al., 2011] imply that flash weakening of friction occurs at small slips before any significant thermal pressurization (TP) and may thus have a negligible contribution to the total fracture energy [Brantut and Rice, 2011; Garagash, 2011]. The subsequent manner of weakening under TP (the dominant contributor to fracture energy) spans a range of behavior from the deformation of a finite-thickness shear zone in which diffusion is negligible (i.e., undrained-adiabatic) to that in which large-scale diffusion obscures the existence of a thin shear zone (i.e., resembling slip on a plane). The dynamic rupture solutions reduce to a problem with a single parameter: the ratio of the characteristic slip-weakening distances for these limiting regimes (Δ_c , L^*). However, for any value of the parameter, there are two end-member scalings of the fracture energy: for small slip, $G \sim \Delta_c^2$, and for large slip we find that $G \sim \Delta_c^{2/3}$.

We compile fracture energy estimates of both continental and subduction zone earthquakes. In doing so, we incorporate independent estimates of fault prestress to distinguish fracture energy G from the parameter G' defined by Abercrombie and Rice [2005]. We find that the dynamic rupture solutions (which account for the variable manner of thermal pressurization and result in a self-consistent slip rate history) allow for a close match of the estimated fracture energy over several orders of total event slip, further supporting the proposed explanation that fracture energy scaling may largely be attributed to a fault strength that weakens gradually with slip, and additionally, the potential prevalence of thermal pressurization.

Plate Boundary Observatory Southwest Region Network Operations, Expansion and Communications Hardening, *Christian Walls, Doerte Mann, Andre Basset, Ryan Turner, Karl Feaux, and Glen Mattioli* (Poster 215)

The Southwest Region of the Plate Boundary Observatory manages 480 continuously operating GPS stations located principally along the transform system of the San Andreas fault, Eastern California Shear Zone and the northern Baja peninsula. In the past year, network uptime averaged 98% with greater than 99% data acquisition.

In an effort to modernize the network, we have started to replace Trimble NETRS receivers with GNSS capable NETR9 receivers. Currently, we have 432 NetRS receivers deployed in the region, and 48 NetR9 receivers. In addition, 82 stations (17%) stream 1 Hz data over the VRS3Net typically with <0.5 second latency and an average completeness of >92%. Based on their typical data download rates, approximately 252 (53%) of all stations are capable of streaming 1 Hz, but have not yet been added to the real time network because of lack of resources. Following the M8.2 Chile earthquake in April 2014, high rate data downloads from the entire SW network had a success rate of 95% and 71% for 1 Hz and 5 Hz data downloads, respectively.

We have continued to upgrade critical radio networks, including the San Francisco Bay Area, Anza Borrego, and Santa Barbara networks. These efforts are ongoing, but they have already significantly improved data download rates and dependability. We are also converting cell modem to radio communications whenever possible for increased reliability and cost savings.

In December 2013 the 13-station Edison network expansion was completed through cost recovery contracts. These stations span coastal southern California in Orange, San Diego and Los Angeles counties including a hybrid site on the Elly oil platform. The primary purpose of the stations is to aid in the seismic source characterization of the San Onofre Nuclear Generating Station and assess the strain field associated with the Oceanside Blind Thrust and Newport Inglewood fault. The new stations fill a gap between those of SCIGN and PBO. Three sites have WXT520 Vaisala metpacks and twelve stations stream 1Hz data via VRS3Net.

UNAVCO and SCRIPPS are working in collaboration to augment a subset of stations with low-cost strong-motion sensors along the San Andreas and San Jacinto faults. To date twelve PBO stations have been upgraded with MEMS accelerometer packages.

Far-field seismic spectral response resulting from complex rupture behaviors, *Yongfei Wang, Steven M. Day, and Peter M. Shearer* (Poster 150)

Many earthquake physical properties, such as seismic moment, rupture extent and stress drop, can be estimated from far-field seismic wave spectra. Corner frequency and the high-frequency fall-off rate of the spectra are often measured in order to make an assessment of dynamic stress drop and other source parameters such as radiated energy. Based on specific theoretic models, some quantitative relations have been established between far-field spectra and source properties. The most widely accepted model is described in Madariaga (1976), who performed a finite-difference simulation of a circular crack model. An important relation is $f_c = k\beta/a$, where f_c is azimuthally averaged corner frequency, β is S-wave speed, a is circular radius and k is an empirical constant with different values for P and S wave spectra. Many other models have been proposed, including the recent dynamically realistic rupture simulations of Kaneko and Shearer (2014), all of which have yielded a variety of different values for k . However, models to date have been for relatively simple ruptures and the effect of rupture complexity, including heterogeneous stress and slip, on stress drop and scaled energy estimates has not been fully explored. Here, we consider complicated ruptures, which include fault roughness and complex pre-stress distributions, and compute the spectra that would be recorded by realistic distributions of surface stations. We then process the synthetic data using methods commonly applied to real data and attempt to quantify which fault properties can be reliably estimated from the observations and the most likely sources of errors in the analysis.

Path calibration and finite fault modeling of the 2014 Mw5.1 La Habra Earthquake, *Shengji Wei, Junjie Yu, Kangchen Bai, and Don Helmberger* (Poster 171)

The 2014 Mw5.1 La Habra earthquake is the largest event occurred in the LA basin following the 2008 Mw5.4 Chino Hills earthquake which is located about 10km away but at a much deeper depth (14.5km). Both seismic and geodetic data indicated a centroid depth of ~5.0km for the La Habra earthquake which has produced much stronger ground shaking, with recorded PGA up to 0.713g, than the Chino Hills earthquake. The La Habra earthquake was well recorded by the dense strong motion and broadband seismic stations, but due to its limited magnitude, high frequency (up to 3Hz) waveform modeling is required to invert the finite rupture process of the earthquake. However, the existing 3D velocity models are not good enough to resolve the waveform at such frequency range, e.g., the CVMS4.0 model has a 1.0km thick sediment layer on the top of the nearby mountain. In addition, the earthquake is located on the edge of the sediment basin which brings in extra complexity to waveform modeling. Here we use the Mw3.6 aftershock with much simpler source time function to establish path calibration of the 1D and 2D velocity models near the source. We found that the calibrated velocity structure on the nearby mountains is much faster (>25%) than that in the 3D velocity models (CVMS4.0 and CVMH) at the shallow (<4km) depth. These velocity models are verified by the aftershock from the 2008 Chino Hills sequence. We selected the stations within 10km that have been calibrated by the aftershock to conduct finite fault modeling of the mainshock. Our preliminary results indicate that the earthquake ruptured multiple asperities (at least three) at the depth around 5km with total duration longer than 2.0s which is an extraordinary large value compared with its size. The finite fault model shows some rupture directivity towards northeast along the strike which explained the large PGV observed in this direction. However, refined 2D (3D) velocity models are required to model some of the complicated waveform which will be left for the future work.

Maximum magnitudes of earthquakes in geothermal fields? *Deborah A. Weiser, David D. Jackson, and Lucile M. Jones* (Poster 210)

We examine California geothermal fields to determine if historical earthquakes may yield evidence of a maximum magnitude limit for future events. An earthquake catalog presents a limited past sample of a population of earthquake magnitudes, whose properties can be extrapolated. For a catalog of events at each geothermal field, we postulate a limiting maximum magnitude, and ask if it is consistent with the data. If enough earthquakes near the limit should have occurred but

MEETING ABSTRACTS

did not, we reject the suggested magnitude limit with confidence. For a Poisson process, we are unable to reject a limiting magnitude unless the expected number of events is >3 and the number observed is zero.

Our search has begun for an earthquake catalog with a finite magnitude limit, based on real earthquake data. McGarr (2014) suggests that maximum magnitudes for injection-induced earthquakes are constrained by volume of fluid injected, and that future induced earthquake magnitudes may be limited by this relationship. For appropriate catalogs, we evaluate whether McGarr's hypothesis may be explained by an insufficient number of events. When catalogs do not provide for a maximum magnitude limit, we will extrapolate current magnitude-frequency distributions to obtain future probabilities of occurrence for specific magnitudes over a given time period.

Influence of Tectonic Setting on the Predictive Skills of Space-Time Smoothed Seismicity Earthquake Forecasts in California and Japan,

Maximilian J. Werner, Hiroshi Tsuruoka, Sayoko Yokoi, Agnes Helmstetter, and Naoshi Hirata (Poster 019)

The Collaboratory for the Study of Earthquake Predictability (CSEP) conducts blind and prospective evaluations of earthquake forecasts in a variety of regions around the globe to assess the influence of tectonic setting on the predictability of earthquake occurrence. Helmstetter & Werner (2012) used Californian data to calibrate a new time-independent earthquake forecasting model, CONAN, that employs adaptive space-time kernels to smooth seismicity. Their method circumvents the need for declustering an earthquake catalog by estimating the distribution of rates with space-time kernels and choosing the median as the predictor of the future rate in each spatial cell. Here, we calibrate the model to the CSEP testing regions in Japan and compare the model's predictive skill in Japan with the skill in California. We retrospectively evaluate the model and compare its performance against existing models installed within the CSEP Japan testing center. A calibrated model will be installed in the 3-month, 1-year and 3-year forecast groups of the Japan testing center for blind prospective evaluation.

Development of a Simple Finite Element Based Inversion Framework: Application to Slow Slip Events Along the Hikurangi Subduction Margin, New Zealand,

Charles A. Williams and Laura M. Wallace (Poster 242)

We are developing a simple inversion framework to allow the use of the finite element method (FEM) for geodetic slip inversions. Using FEM-based inversions allows us to take into account material inhomogeneities as well as topographic effects, which are not accounted for in traditional inversions based on elastic half-space solutions (e.g., Okada, 1985; 1992). As a first step, we have developed a workflow that allows us to generate Green's functions using the PyLith finite element code (Aagaard et al., 2013) for use with the DEFNODE geodetic inversion code (McCaffrey, 1995; 2002). This workflow has been applied to slow slip events (SSEs) along the Hikurangi subduction margin, where we make use of a New-Zealand-wide seismic velocity model (Eberhart-Phillips et al., 2010), as well as an improved interface geometry (Williams et al., 2013). In our initial results, we find that inversions that make use of the seismic velocity model reduce the predicted amount of slip by approximately one third, when compared to models assuming a uniform elastic half-space. This emphasizes the importance of accounting for material property variations in our slip inversions, since this can greatly impact the estimated slip budget accommodated by SSEs at subduction zones, as well as the equivalent moment magnitude of SSEs.

In addition to the PyLith-DEFNODE workflow, we are developing a separate inversion framework to allow the usage of FEM-based Green's functions for coseismic (or SSE) geodetic inversions of fault slip. This inversion framework is meant to be a starting point for scientists interested in performing FEM-based inversions; however, it is designed to be extensible, and should thus allow the solution of fairly complex problems. We compare the DEFNODE-based inversions with those using the new framework to determine the sensitivity of the results to the inversion method. We are thus able to estimate the sensitivity of our results to the assumed interface geometry, as well as the assumed elastic structure and inversion technique. By quantifying the sensitivity of our

solution to these effects, we should be able to provide much more robust slip estimates for the Hikurangi Margin and elsewhere.

High-Complexity Deterministic Q(f) Simulation of the 1994 Northridge Mw 6.7 Earthquake,

Kyle B. Withers, Kim B. Olsen, Zheqiang Shi, and Steve Day (Poster 066)

With the recent addition of realistic fault topography in 3D simulations of earthquake source models, ground motion can be deterministically generated more accurately up to higher frequencies. The synthetic ground motions have been shown to match the characteristics of real data, having a flat power spectrum up to some cutoff frequency (Shi and Day, 2013). However, the earthquake source is not the only source of complexity in the high-frequency ground motion; there are also scattering effects caused by small-scale velocity and density heterogeneities in the medium that can affect the ground motion intensity. Here, we dynamically model the source of the 1994 Mw 6.7 Northridge earthquake using the Support Operator Rupture Dynamics (SOR) code up to 8 Hz. Our fault model was input into a layered velocity structure characteristic of the southern California region characterized by self-similar roughness from scales of 80 m up to the total length of the fault. We extend the ground motion to further distances by converting the output from SOR to a kinematic source for the finite difference anelastic wave propagation code AWP-ODC. This code incorporates frequency-dependent attenuation via a power law above a reference frequency in the form $Q0fn$.

We model the region surrounding the fault with and without small-scale medium complexity, with varying statistical parameters. Furthermore, we analyze the effect of varying both the power-law exponent of the attenuation relation (n) and the reference $Q(Q0)$ (assumed to be proportional to the S-wave velocity), and compare our synthetic ground motions with several Ground Motion Prediction Equations (GMPEs) as well as observed accelerograms. We find that the spectral acceleration at various periods from our models are within 1 interevent standard deviation from the median GMPEs and compare well with that of recordings from strong ground motion stations at both short and long periods. At periods below 1 second, $Q(f)$ is needed to match the decay of spectral acceleration seen in the GMPEs as a function of distance from the fault ($n=0.6-0.8$). We find when binning stations with a common distance metric (such as Joyner-Boore or r_{rup}) that the effect of media heterogeneity is canceled out, however, the similarity between the intra-event variability of our simulations and observations increases when small-scale heterogeneity is included.

Combined hyperspectral and field mapping along the 1999 Hector Mine earthquake surface rupture,

Ryan D. Witkosky, Sinan Akciz, Kerry Buckland, Janet Harvey, Ken Hudnut, Katherine Kendrick, Dave Lynch, Kate Scharer, Frank Sousa, Joann Stock, and David Tratt (Poster 266)

We explore the use of infrared hyperspectral remote sensing techniques combined with field observations to perform geologic mapping along the 1999 Hector Mine earthquake surface rupture. Existing geologic maps of this region are based on field studies completed more than four decades ago. Field access to the location of the surface rupture is highly restricted, but in April 2014 we were granted limited access to collect geologic ground-truth data. We mapped a ~ 4500 m² area of well-exposed volcanic bedrock, digitized and georeferenced the geological unit contacts from this map, and compared this to a swath of hyperspectral data from Mako, an airborne spectrometer built by The Aerospace Corporation. The Mako airborne imagery provides 2-m pixel resolution along a 1.8 km-wide swath centered on the Lavic Lake fault, the site of 1999 earthquake maximum slip zone. Mako captures 128 bands in the thermal infrared covering 7.8 to 13.4 microns. Mako's high spatial and spectral resolution, along with the lack of a significant vegetation cover in the study area, makes it possible to distinguish distinct small bedrock outcrops and geomorphic surfaces proximal to the fault. With the geologic unit contacts superimposed on the hyperspectral imagery, pixels with ground-truthed lithology were chosen from the Mako data to train a supervised classification of the same ~ 4500 m² area. The resulting map from the supervised classification was then compared with the ground-truthed field map to assess the user accuracy of a remotely-produced product. Preliminary results show that for a small area, a Mako-based geologic map can be produced with a user accuracy of $\sim 50\%$, based on an error matrix. Further refinements to our technique

will improve the data processing sequence and increase the signal-to-noise ratio. These improvements will likely result in geologic maps that have a greater areal extent and higher user accuracy, and should be useful for initial mapping in restricted areas or remote terrain.

Reconciling contradicting trench and geomorphologic observations across the San Gorgonio Pass Fault Zone, *Lisa R. Wolff, John D. Yule, Katherine M. Scharer, Ryan Witkosky, Shahid Ramzan, and Paul McBurnett* (Poster 282)

Along the San Gorgonio Pass Fault Zone (SGPFZ), paleoseismic data tell a story of low slip rates with infrequent and small earthquakes. However, it is likely that paleoseismic trenches are not capturing the full deformation history in the Pass. We excavated a 'mega' trench near Cabazon in 2013 with the intent of capturing an extended paleoseismic record. Exposures in the trench date back to ~6000 yrs BP with four events at 630-590, 1220-1097, 2345-1905, and ~5500 yrs BP. The quakes ruptured on two thrust splays with <1 m vertical offset/event, resulting in a slip rate of 2 +/- 1 mm/yr. Two observations from the mega trench suggest an incomplete record. First, gaps in charcoal C14 ages from 2000-2400, 2700-3200, and 3700-4900 yrs BP suggest that >2000 yrs of sediment record is absent, indicating non deposition and no record of events during those times. Second, we uncovered late Pleistocene Cabazon Fonglomerate in the footwall at the bottom of the trench. This requires another thrust fault somewhere south of the trench and indicates that the mega trench does not cover the full zone of deformation. In comparing the mega trench with previous trenches, the number of fault splays changes. Trenches 1-4 showed three fault splays while there was one fault splay in trench 5, no faults in trench 6 and two fault splays in trench 7 and the mega trench. A likely explanation is that trenches are too short to capture the whole width of the rupture zone and the missing uplift is due to off-fault folding and/or rotation of clasts in unconsolidated gravel. In contrast to paleoseismic data, geomorphic terrace offsets support higher slip rates and infrequent but large ruptures and support the hypothesis that the paleoseismic data are incomplete. For example, Yule et al. (this meeting) interpret the most recent earthquake to have offset a terrace surface in Millard Canyon by a combined ~3 m on two fault splays and late Pleistocene slip rates of 6 +/- 3 mm/yr, roughly 3 times the rate from trenches. Though the Cabazon mega trench uncovered a lengthy record, it is likely incomplete and underestimates slip and rupture history in the Pass. If the geomorphic data at Millard Canyon are more representative of slip the SGPFZ experiences large (>4 m) once-per-millennia events.

Finite-Source Modeling for Parkfield And Anza Earthquakes, *Kathryn E. Wooddell, Taka'aki Taira, and Douglas Dreger* (Poster 170)

Repeating earthquakes occur in the vicinity of creeping sections along the Parkfield section of the San Andreas fault (Nadeau et al., 1995) and the Anza section of the San Jacinto fault (Taira, 2013). Utilizing an empirical Green's function (eGF) approach for both the Parkfield and Anza events, we are able to conduct a comparative study of the resulting slip distributions and source parameters to examine differences in the scaling of fault dimension, average slip, and peak-slip with magnitude. Following the approach of Dreger et al. (2007), moment rate functions (MRFs) are obtained at each station for both Parkfield and Anza earthquakes using a spectral domain deconvolution approach where the complex spectrum of the eGF is divided out of the complex spectrum of the target event. Spatial distributions of fault slip are derived by inverting the MRFs, and the coseismic stress change is computed following the method of Ripperger and Mai (2004). Initial results are based on the analysis of several Parkfield target events ranging in magnitude from Mw1.8 to 6.0 (Dreger et al., 2011) and a Mw4.7 Anza event. Parkfield peak slips are consistent with the Nadeau and Johnson (1998) tectonic loading model, while average slips tend to scale self-similarly. Results for the Anza event show very high peak and average slips, in exceedance of 50 cm and 10 cm respectively. Directivity for this event is in the northwest direction, and preliminary sensitivity analyses suggest that the rupture velocity is near the shear wave velocity and the rise time is short (~0.03 sec). Multiple eGFs for the Anza event have been evaluated and the results appear robust. Finite fault modeling will be conducted for additional Anza M4+ earthquakes to evaluate the variability in stress drop between events in this region.

A High Level Parallel IO Library for High- Performance Seismic Applications, *Heming Xu, Efekan Poyraz, Daniel Roten, and Yifeng Cui* (Poster 082)

In the last years numerical simulations of dynamic rupture and wave propagation have been scaled up to run on petascale supercomputers, enabling researchers to simulate the wavefield during large earthquakes for frequencies up to 5 Hz. With grid dimensions of several 100 billion mesh points, the performance of input and output (IO) operations during such computations has always represented a major concern, and significant effort has been expended to optimize and tune the IO performance of parallel wave propagation codes. Many HPC applications based on structured meshes used within SCEC share similar requirement in terms of IO operations (e.g., AWP-ODC, SORD, or Hercules). Examples of such operations include initialization of the geophysical properties in the computational mesh, the input of the moment-rate time histories for a kinematic source, output of velocity time series at selected sites or saving of stresses for the computational volume.

In order to minimize duplicate investments in the handling of IO for each application, we introduce a modular IO library, called SEISM-IO, which is developed in the framework of SEISM (Software Environment for Integrated Seismic Modeling). SEISM-IO implements optimized high-performance IO operations in a software layer between the high-level application and the file system. It aims to simplify the programming of parallel IO for code developers by hiding some of the more complicated aspects from the user (i.e., dealing with output on a partitioned grid or buffering of outputs for improved performance). SEISM-IO provides both a C and Fortran interface to structured mesh applications. It follows the SEISM data standards and provides a wide range of internal file choices, from low-level direct IO, partitioned IO, collective MPI-IO, to high-level HDF5 IO, ADIOS IO, etc., allowing users to choose the most appropriate file formats and IO models for managing their data. SEISM-IO also includes comprehensive service tools for the HPC environment, including binary conversion, mesh and source generation, data transfer, management and analysis techniques.

The library has successfully been tested in the AWP-ODC code, and will be released to code developers in the near future.

Refining the Magnitude of the Shallow Slip Deficit, *Xiaohua Xu, Xiaopeng Tong, David T. Sandwell, and Christopher Milliner* (Poster 237)

Geodetic inversions for slip versus depth for several major (Mw > 7) strike-slip earthquakes (e.g. 1992 Landers, 1999 Hector Mine, 2010 El_Mayor-Cucapah) show a 10% to 40% reduction in slip near surface (depth < 2 km) compared to the slip at deeper depths (5 to 8 km). This has been called the shallow slip deficit (SSD). The large magnitude of this deficit has been an enigma since it cannot be explained by shallow creep during the interseismic period or by triggered slip from nearby earthquakes.

One potential explanation for the SSD is that the previous geodetic inversions used incomplete data that do not go close to fault so the shallow portions of the slip models were poorly resolved and generally underestimated. In this study we improve the geodetic inversion, especially at shallow depth by: 1) refining the InSAR processing with non-boxcar phase filtering, model-dependent range corrections, more complete phase unwrapping by SNAPHU using a correlation mask and allowing a phase discontinuity along the rupture; 2) including near-fault offset data from optical imagery and SAR azimuth offsets; 3) using more detailed fault geometry; 4) and using additional campaign GPS data.

With these improved observations, the slip inversion has significantly increased resolution at shallow depth. For the Landers rupture the SSD is reduced from 45% to 16%. Similarly for the Hector Mine rupture the SSD is reduced from 15% to 5%. We are assembling all the relevant co-seismic data for the El Major-Cucapah earthquake and will report the inversion result with its SSD at the meeting.

Interseismic Coupling Model of Nicoya Peninsula, Costa Rica by Joint Inversion of InSAR and GPS, *Lian Xue, Susan Schwartz, and Zhen Liu* (Poster 245)

Accurate measurements of interseismic deformation at subduction zones are critical for identifying regions accumulating strain and likely to fail in future large earthquakes. The unique location of the Nicoya Peninsula

MEETING ABSTRACTS

directly above the seismogenic zone, the presence of a dense continuously operating GPS and seismic network, and the recent occurrence of a gap-filling earthquake make it a prime region to attempt to obtain a high-resolution model of interseismic strain accumulation. Here we present an interseismic coupling model of the plate interface at Nicoya Peninsula, Costa Rica, determined by integrating both GPS and InSAR. The GPS data are from both campaign and continuous measurements between 1996 and 2010 and the InSAR data are from the Advanced Land Observing Satellite (ALOS) ascending acquisitions between 2007 and 2011. The resulting coupling model is very similar to that obtained with GPS alone (Feng et al., 2012), demonstrating that even in regions of very wet troposphere, InSAR can be used to extract interseismic deformation when GPS data are also available. Our model of interseismic locking reveals two strongly coupled regions. One under the middle portion of the Nicoya Peninsula centered at ~ 22 km depth, which coincides very well with the rupture pattern of the Costa Rica 2012 MW 7.6 earthquake. The other one locates offshore, nearly parallel to the first but centered at ~15 km depth. This patch had very little slip during the 2012 Costa Rica earthquake. Most slow slip, tremors and very low frequency earthquakes locate in regions adjacent to the strong coupling.

Calibrating the composite source model for generating synthetic seismograms for Israel, Gony Yagoda-Biran and John G. Anderson (Poster 074)

The region of Israel, and the entire Levant, has suffered several destructive earthquakes during its long history. The major earthquake source in the region is the active Dead Sea left-lateral transform Fault system (DSFS), 1000 km long, stretching from the Red Sea rift in the south to the Taurus-Zagros collision zone in the north. Recurrence intervals for earthquakes on the Israeli section of the DSFS are of the order of 10^2 years for magnitude 6, and 10^3 years for magnitude 7 earthquakes. The Israeli seismic network has yet to record very strong ground motions, but estimating realistic ground motions for higher magnitude events in the DSFS is a priority. In this research we calibrate the composite source model (CSM), a finite fault model for generating synthetic ground motions, with the strongest available earthquake that occurred in the region in the last decades, the February 11, 2004, ML 5.2 earthquake, with epicenter at the northeast Dead Sea, for which we have records from 19 stations.

The CSM computes synthetic strong ground motions, using synthetic Green's functions convolved with a set of circular sub-events that follow a Gutenberg-Richter size distribution, are randomly distributed on the fault, and radiate energy in the form of a Brune pulse. The synthetic Green's functions are computed for a flat-layered velocity structure with attenuation. Our calibration process started with constraining the focal mechanism by comparing the S-wave displacement patterns to the ones generated by a synthetic point source. We then continued with developing a velocity model based on recent research, assigning reasonable density values, and adjusting a recent Q model to approximately match the distance dependence of Fourier spectral amplitudes at a subset of hard rock sites. The Q adjustment is essential because Q depends strongly on the assumed geometrical spreading, and geometrical spreading in our Green's functions is controlled by the layered velocity model and earthquake source depth. This was followed by fine adjustments of magnitude (to 5.22) and subevent stress drop (to 175 bars) to minimize the average spectral residuals at the hard rock sites. The resulting waveforms and spectral amplitudes are comparable to the data at the hard sites, and Fourier spectral amplifications relative to our model are somewhat correlated to available, independent estimates of site amplification. Once more site response data is available, the calibration can be fine-tuned.

Global Search of Triggered Tectonic Tremor, Hongfeng Yang, Zhigang Peng, Chastity Aiken, Abhey Ram Bansal, and Kevin Chao (Poster 192)

Large earthquakes are capable of triggering shallow microearthquakes and deep tectonic tremor at long-range distances. At Parkfield-Cholame section of the San Andreas Fault, numerous large-distant earthquakes have triggered tremor in this region. However, so far only the 2002 Mw7.9 Denali Fault and the 2011 Mw9.1 Tohoku-Oki earthquakes have triggered tremor along the Anza segment of the San Jacinto Fault in Southern California, and the resulting tremor signals are much weaker than at the Parkfield-Cholame region. To better understand the cause of such difference, we conduct a systematic search of triggered tremor around the

world, focusing on regions where tremor has not been reported before. These include Central and South America, Eastern Africa, Indian subcontinent, Himalaya mountain belts, and Sumatra and Java subduction zones. In each region, we first select distant events that have produced reasonable dynamic stresses (>0.5 kPa), then apply a 5-Hz high-pass filter to identify triggered tremor as long-duration, non-impulsive signals that are modulated by the passing long-period surface waves. So far we have found tremor along the Oriente and Enriquillo-Plantain Garden Faults in the Caribbean, the Queen Charlotte-Fairweather fault system, the Denali fault in the western Canada and Alaska, the Chile and the Java subduction zones, and large strike-slip faults around South Sandwich and Indonesia Islands. In general, triggered tremor is found at relatively young subduction zones and mature strike-slip faults at transpressional tectonic settings. In comparison, we mostly find triggered shallow microearthquakes at transextensional environments. Such a difference could be simply due to the build-up of overpressure at compressive environments, which is found to be one necessary condition for tremor generation.

Determination of 3D testing region for Kanto district in Japan, Sayoko Yokoi, Hiroshi Tsuruoka, and Naoshi Hirata (Poster 017)

We are attempting to construct a 3-dimensional (3D) earthquake forecasting model to study the effect of earthquake depth distribution for the Kanto district in Japan. Because the seismicity in this area ranges from shallow depth to over 100 km due to subduction of the Philippine Sea plate and the Pacific plate. We already confirmed that the RI model (Nanjo, 2011) shows better performance in the 3D forecasting area with $0.1^\circ \times 0.1^\circ \times 10$ km grid size and depth than 2D area with $0.1^\circ \times 0.1^\circ$ grid size and a non-divided depth column from 0 km to 100 km. In the next, we tried to optimize the spatial resolution of the 3D forecasting area using the RI model with several smoothing radii (from 2.5 to 100km) for 1 day, 3 months, 1 year and 3 years forecasting periods. We prepare 5 datasets of different grid size and depth interval for 3D forecasting area which are $0.025^\circ \times 0.025^\circ \times 2.5$ km, $0.05^\circ \times 0.05^\circ \times 5$ km, $0.1^\circ \times 0.1^\circ \times 10$ km, $0.25^\circ \times 0.25^\circ \times 25$ km and $0.5^\circ \times 0.5^\circ \times 50$ km. RI models for each forecasting period forecast earthquake rate using JMA catalog after 1998 retrospectively. Performance of RI models was evaluated in terms of information gain based on a uniform model. We considered as an optimized grid size that RI model shows the best information gain. After searching combination, RI models with 5 to 10 km smoothing radius, at $0.05^\circ \times 0.05^\circ \times 5$ km in depth, show better information gain for 1 day, 3 months, 1 year and 3 years for forecasting periods. Therefore, we determine that a $0.05^\circ \times 0.05^\circ$ horizontal grid with 5 km depth is spatial resolution of 3D forecasting area for Kanto region. In this presentation, we present the results of all combination of grid size of above 5 datasets for RI model. The authors thank the Japan Meteorological Agency for the earthquake catalog. This work is sponsored by the Special Project for Reducing Vulnerability for Urban Mega Earthquake Disasters from Ministry of Education, Culture, Sports and Technology of Japan.

Computationally Efficient Search for Similar Seismic Signals in Continuous Waveform Data over the Northern California Seismic Network, Clara Yoon, Ossian O'Reilly, Karianne Bergen, and Gregory Beroza (Poster 162)

Cross-correlating continuous seismic data streams with waveform templates has proven to be a sensitive, discriminating detector of repeating seismic signals; however, template matching requires a priori knowledge of the signals we wish to detect. Detection of unknown sources is possible with autocorrelation, which searches for similar waveforms within all pairs of short overlapping windows from continuous data. Unfortunately, naïve application of autocorrelation scales quadratically with time, which limits its use to short duration time series.

We previously developed an efficient, correlation-based approach to find similar seismic waveforms, with the help of techniques traditionally used in data mining and computer science. We avoid comparing most non-similar signals by first developing compact, discriminative "fingerprints" of waveforms, and then assigning signals to sub-groups (buckets) using locality-sensitive hash functions (LSH). The probability that two signals enter the same bucket increases monotonically with similarity. LSH trades space for speed, requiring near-linear storage, yet yielding near-constant

query time, and avoiding nearly all of the unproductive pair-wise computation of autocorrelation.

Our method previously detected uncataloged earthquakes 40 times faster than autocorrelation when applied to 24 hours of single-channel continuous data from one station near the Calaveras Fault in the Northern California Seismic Network (NCSN). Here we extend our method to incorporate multiple channels of continuous data from the distributed network of NCSN stations. We find additional uncataloged earthquakes after several minutes of processing time – much faster than an analogous autocorrelation application. This method has considerable potential to detect low-magnitude earthquakes that are otherwise difficult to find in continuous data over a seismic network.

Products and Services Available from the Southern California Earthquake Data Center (SCEDC) and the Southern California Seismic Network (SCSN), *Ellen Yu, Prabha Acharya, Aparna Bhaskaran, Shang-Lin Chen, Faria Chowdhury, Kate Hutton, Doug Given, Egill Hauksson, and Rob Clayton (Poster 155)*

The SCEDC archives continuous data from 8063 data channels and 480 SCSN recorded stations. To date in 2014 SCEDC has triggered event waveforms from 776 stations. The SCEDC processes and archives an average of 17,000 earthquakes each year and provides public access to these earthquake parametric and waveform data through its website www.data.scec.org and through client applications such as STP and web services. This poster will describe the most significant developments at the SCEDC in the past year.

New data holdings:

- In addition to the real time GPS displacement waveforms now archived at SCEDC, the SCEDC will be archiving seismogeodetic waveforms displacement and velocity waveforms produced by the California Real Time Network (CRTN <http://sopac.ucsd.edu/projects/realtime>). These waveforms are computed by combining the 1 sps real time GPS solutions with 100 Hz accelerometer data. They are archived at regular intervals and converted into miniseed format by SCEDC. This project was funded by the NASA Advanced Information System Technologies program.
- A searchable focal mechanism catalog from 1981 to present will be available at www.data.scec.org. The focal mechanisms are derived by the HASH method. Historical data was loaded from the Yang, Hauksson, Shearer 2011 data set.
- The SCEDC will make relocated event locations from 1981-2011 using double difference techniques available via STP. The source of the catalog is based on Hauksson, Yang, Shearer, 2011.

New distribution methods:

- The SCEDC is developing a new version of its stationXML web service which serves out FDSNStationXML format. Users can either use the form or call the service programmatically via curl or wget. Users can query for station metadata by network, station, channel, location, time and other search criteria and request results at multiple levels (network, station, channel, response).

New infrastructure:

- www.data.scec.org is moving to the Cloud. The SCEDC is in the progress of moving its Recent Earthquake Map and static web pages into Amazon Web Services. This will enable the web site to serve large number of users without competing for resources needed by SCSN/SCEDC mission critical operations.
- The Data Center has begun implementation the Continuous Wave Buffer (CWB) to manage its waveform archive. This software was developed and currently in use at NEIC. Implementation will make continuous data available within minutes of real time.

Late Pleistocene and Holocene Rates of Slip and Size of Prehistoric Earthquakes on the San Andreas Fault System in San Geronio Pass, *Doug Yule, Dick Heermance, Ian Desjarlais, and Kerry Sieh (Poster 283)*

Two active thrust splays of the San Andreas Fault system cross Millard Canyon in San Geronio Pass (SGP) where they deform Quaternary surfaces. The northern splay is a reactivated portion of the Banning fault (F1), and the southern splay is part of the San Geronio Pass Fault Zone (F2). Age constraints (years before present (yr BP)) are: 890 ± 300 for Qf1;

1270 ± 80 for Qf2; 7700 ± 1500 for Qf4; and 65,000 to 680,000 for Qh (see Heermance et al., this meeting, for details on ages). For Qh we use a plausible surface age of $150,000 \pm 50,000$ yr BP based on the premise that the surface was abandoned after the initiation of faulting and uplift in this region at this time (Matti et al., 1993). We use the Qf2 and Qf4 ages to bracket the age of Qf3 at $5,000 \pm 2,000$ yr BP. 282082

Here we estimate the amount of fault slip on F1 and F2 using offsets of the Qf3, Qf4, and Qh surfaces. One way to estimate slip is to resolve the relative uplift across scarps onto the fault plane. To do this we assume that slip occurred parallel to the geodetic slip vector (N45°W) on fault planes observed to strike E-W and dip 45° N (F1) and 30° N (F2). Thus fault slip here must be accommodated by oblique thrust motion. We also use the offset buttress unconformity beneath Qh at F1 to define the slip vector there. For slip on F1: the buttress unconformity defines a piercing line oriented ~N50°W and a displacement of 400 ± 75 m (140 ± 15 horizontally, and 375 ± 75 m laterally); the Qf3 scarp is 5.2 ± 0.7 m high and resolves to 10.4 ± 1.4 m of fault slip. Using the above age data, these F1 slip values give Holocene and late Pleistocene slip rates of 2.5 ± 1.4 mm/yr and 3.2 ± 1.6 mm/yr. For F2: the Qh surface is uplifted by 125 ± 25 m and resolves to 350 ± 70 m of fault slip; the Qf4 scarp is 12.6 ± 0.7 m high and resolves to 36 ± 2.0 m of fault slip. Using the above age data, these F2 slip values give Holocene and late Pleistocene slip rates of 4.9 ± 1.2 mm/yr and 2.8 ± 1.4 mm/yr.

Summing rates across the two faults gives Holocene and late Pleistocene rates of 7.4 ± 2.6 mm/yr and 6.0 ± 3.0 mm/yr, respectively. Uplift across the youngest scarps in Millard Canyon (cutting Qf1 and Qf2) records 6.7 ± 1.0 m of oblique thrust slip (slip resolved from scarp heights) during the most recent earthquake 590-630 yr BP (see Wolff et al., this meeting). Slip of this magnitude supports a model for SGP where elastic strain accumulates at ~ 7 mm/yr and is released by large, once-per-millennia earthquakes.

Robust quantification of earthquake clustering: Overcoming the artifacts of catalog errors, *Ilya Zaliapin and Yehuda Ben-Zion (Poster 163)*

Quantitative characterization of earthquake clustering in space and time in relation to different event sizes and physical properties of the lithosphere are fundamental problems of statistical seismology. Recently, we approached these problems by taking advantage of the new statistical results, improved empirical constraints, and relatively uniform high-quality earthquake catalogs available for southern California and other selected regions. This led to identification and classification of statistically significant earthquake clusters in southern California, relating cluster characteristics to effective viscosity of the crust, and documenting some robust properties of observed earthquakes not simulated by the Epidemic Type Aftershock Sequence (ETAS) model. Extending these results to other seismically active areas and lower magnitude ranges, however, is impeded by inferior data quality. Most available catalogs are based on non-uniform recordings/analyses that lead to non-uniform (in space, time, magnitude) location errors, varying magnitude of completeness, and other problems. These non-uniformities may (and do) produce artificial patterns in the space-time-magnitude clusters of seismicity detected by our, as well as other, methods. In the present work we document the effects of catalog errors on inferred cluster properties, and report some striking patterns that emerge as artifacts of those errors. This includes apparent magnitude dependence, fluctuations in the proportion of singles (clusters consisting of individual events), space-dependent distance to the likely parents of events, and other effects. We also discuss additional differences between the ETAS model and observed seismicity. Finally, we propose a generalization of our method that involves assigning multiple possible parents to each event, and discuss some graph-theoretic techniques that may provide results that are more robust to location errors and other catalog deficiencies.

Array Waveform Coherency and Its Implication on Earthquake Source Properties, *Ailin Zhang and Lingsen Meng (Poster 142)*

Numerous contributions have been made to develop refined structural models of the Earth's interior ever since the deployment of large regional seismic arrays (e.g. USArray). However earthquake source studies don't take full advantage of the dataset except for back-projections of large earthquakes. Waveform coherence across a seismic array is crucial for

MEETING ABSTRACTS

back-projection earthquake source imaging. While previous studies indicate waveform coherency decays dramatically with distance and frequency, their adoption of time windows with fixed duration may naturally degrade the coherence at high frequency. In this study, we measure the correlation coefficients of teleseismic waveforms recorded by USArray using window lengths proportional to $1/\text{frequency}$.

We test deep and intermediate earthquakes with depths of over 150km. Preliminary results show that the coherency is high across the USArray over inter-station distances >10 wavelengths and up to 5 Hz. The coherence of large/shallow earthquakes decays faster with distance than small/deep earthquakes. For the same earthquake, coherence falls slower along the ray-path than across it. One possible explanation for such patterns is finite source effect including scattering near the source. Synthetic test can support the interpretation. We seek to establish a waveform coherence pattern with respect to different variables (e.g. inter-station distance, frequency). With the help of waveform coherency, we will have a better understanding of earthquake source properties.

Focal mechanisms and seismic tectonic features of the 2013 Laizhou MS=4.6 earthquake sequence, Jianchang Zheng, Dongmei Li, and Peng Wang (Poster 167)

Local time at noon on Nov. 23, 2013, an MS=4.6 earthquake occurs at Laizhou, Shandong province, China. This earthquake is the largest event since Sep. 20, 1995 Cangshan MS=5.2 earthquake in Shandong area, and shakes the whole Shandong Peninsula.

We investigate the faulting process of the Laizhou MS=4.6 earthquake sequence by combining relocated hypocenters and focal mechanisms. CAP method and additional bootstrap technique are employed to stably invert the moment tensor solution and to estimate its uncertainties. All available stations are chosen at equal probabilities and assembled as a new dataset to make a repeated moment tensor inversion. After 1000 times inversion, we get an average faulting parameter as: A. strike=239.6°, dip=75.0°, rake=174.4°; B. strike=331.1°, dip=84.6°, rake=15.0°, and error range of P, T axes is about 20°.

We use HASH method to find the focal mechanism solutions for 12 small events ($M_L \geq 3.0$) in the sequence, and adopt double difference method to analysis precise aftershock distribution.

Relocation images show that, except 3 small shocks away from swarm, the concentrated area of Laizhou sequence presents a NE-oriented major axis, and the sources distribution indicates a NW dipping fault, with a dipping angle about 70°, which is according with solutions for small events retrieved by HASH method.

Finally, a discussion on the structure features of seismic tectonic and faulting process is made by using of all the results and relative geological data, and several opinions are concluded blow.

1. There has an ordered fracture at the earlier stage of Laizhou sequence. At the very beginning, fracture spreads towards NE. After the MS4.6 mainshock taken place, fracture of aftershocks became disordered, sources distribution became more stochastic.
2. Small events before the mainshock scattered around the main fracture area; the occurrence of MS4.6 event filled in the gap.
3. Strike slipping is the dominant faulting type in earlier stage of the sequence. Two foreshocks right before the mainshock display some thrust component. This maybe implicates the strengthen process of regional stress relative to the mainshock.
4. Slipping vectors of the fault are in accord with accurate location result, and reveals the dynamics of faulting process.

Development of Analytical Tools for Engineering Validation of Simulated Ground Motions, Peng Zhong (Poster 054)

This project is part of a concerted effort in Ground Motion Simulation Validation (GMSV) Technical Activity Group (TAG) in which simulated ground motions are vetted for engineering applications. In particular, this presentation summarizes the authors' efforts in validating simulated ground motions for implementation in building-code type Ground Motion Selection Scaling (GMSM) aiming at assessing nonlinear response of structures at a target ground motion hazard level. This validation technique looks into similarity between building response obtained from

suites of simulated and recorded ground motions conditioned that these suits of ground motions are selected according to ASCE 7-10 GMSM technique rather than similarity of seismic event and recording station.

We provide a validation method to verify whether simulated ground motions can solely be used for code application purposes; this validation method is tested on two steel moment-resisting frame structures—a 4-story and an 8-story—both designed according to latest design codes. We focus on maximum interstory drift ratio and maximum floor acceleration as engineering demand parameter of building response. The difference between demands from simulated and recorded motion sets are compared using statistical tests to show if these differences are statistically meaningful. Preliminary results show that the structural behavior resulting from recorded ground motions and simulated ground motions are different. Overestimation of structural response is observed once simulated motions are used. This is mainly due to existence of higher number of pulse like ground motions in simulated ground motion database.

Similarities between Vere-Jones' branching crack model and earthquake source process, Jiancang Zhuang, Dun Wan, and Mitsuhiro Matsuura (Poster 107)

Vere-Jones' branching crack model was developed in 1970s. In this model, the earthquake source is regarded as the result from the total population of crack elements in a critical or near-critical branching process, where the crack propagates through a series of steps. At each step, each crack element simply terminates or generates several other crack elements nearby. Regarding the total number of steps (generations) as the duration time and the total number of crack elements as the total energy released, the following similarities are found between earthquake sources and this model:

1. The distribution of energies is asymptotically a Pareto distribution (power law) for the critical case, or a tapered Pareto distribution (tapered power law, Kagan distribution) for the subcritical case.
2. The number of crack elements at each generation (time step) show similar patterns of earthquake source time functions. The stochastic property of VJ's branching crack model explains why the EQ magnitude cannot be determined or predicted before the whole earthquake source process is completed.
3. The branching crack model explains why the variance of duration times is relatively large for small magnitudes. But it gives a different scaling law for duration times.

Imaging the internal structure of the San Jacinto Fault Zone with high Frequency noise, Dimitri Zigone, Yehuda Ben-Zion, Michel Campillo, Gregor Hillers, Philippe Roux, and Frank Vernon (Poster 183)

Regional tomography studies in the San Jacinto Fault Zone (SJFZ) area gives detailed images up to the top 500 meters or so of the crust (Zigone et al., 2014; Allam et al., 2014). To obtain additional high resolution information on local structures at the shallower crust, we use cross correlation of ambient seismic noise between 10 Hz and 70 Hz recorded by several linear arrays that cross the Clark strand of the SJFZ with typical inter-station distances around 40 m. Pre-processing techniques involving earthquakes removal and whitening on 15 minutes time windows are used to obtained the 9-component correlation tensors associated with all station pairs. The obtained cross correlations exhibit coherent waves up to 30-40 Hz that travel between the station pairs. Polarization and dispersion analysis show that both body and surface waves are reconstructed with Rayleigh group velocity around 400-500 m/s. The results likely include also body waves and trapped fault zone signals. After rejecting paths without sufficient signal to noise ratios, we invert the Rayleigh group velocity measurements using the Barmin et al. (2001) approach on a 20m grid size. The obtained group velocity maps reveal complex structures with very low velocity damage zones around the surface traces of the SJFZ. The group velocities are inverted to 3D images of shear wave speeds using the linear inversion method of Hermann & Ammon (2002). The results show local flower-type damage structures in the top 200m, with Vs values at 30m depths around 250-300 m/s in agreement with the available Vs30 values in the literature. Updated results will be presented in the meeting.

Meeting Participants

AAGAARD Brad, USGS
ABOLFATHIAN Niloufar, USC
ABRAHAMSON Norman, PG&E 075, 201, Sun1800
ACHARYA Prabha, Caltech 155
ADAMS Paul, Aerospace Corporation 269
ADAMS Glen, Geotechnology Inc 253
ADAMS Mareike, UCSB 169
AFSHARI Kioumars, UCLA 056
AGNEW James, CA DWR
AGNEW Duncan, IGPP/SIO/UCSD 101, 218
AIHARA Kazuyuki, Tokyo 023
AIKEN Chastity, Georgia Tech 192
AKCIZ Sinan, UCLA 258, 261, 266, 285
ALDRICH Dylan, SCEC 003
ALLEGRE Vincent, UCSC
ALLISON Kali, Stanford 149
AMINZADEH Fred, USC 154
AMPUERO Jean-Paul, Caltech 125, 145, 173, 176, 198
ANDERSON Kent, IRIS 157
ANDERSON Greg, NSF
ANDERSON John, UNR 064, 067, 074, 077
ANDERSON Benjamin, USC 003
ANDREWS Dudley, retired
ANGSTER Stephen, USGS 068
APPEL Vikki, USGS
ARCHULETA Ralph, UCSB 062, 063, 169
AREVALO Lilian, SCEC 003
ARGUS Donald, JPL 244
ARRANGOIZ Santiago, Caltech 057
ARROWSMITH J Ramon, ASU 285
ARVIN Lindsay, USC 284
ASIMAKI Domniki, Caltech 069
ASPIOTES Aris, USGS 037
ATKINSON Gail, Western Univ
AULT Alexis, Arizona 123
AVOUAC Jean-Phillippe, Caltech 236
AYOUB Francois, Caltech 236
AZIZZADEHROODPISH Shima, Memphis 080
BACA Austin, CalPoly Pomona
BADER Michael, TU München 177
BAI Kangchen, Caltech 125, 171
BAKER Jack, Stanford 046, 047, 195
BAKER Scott, UNAVCO 216
BALLMANN Jason, SCEC 001, 002, 007
BALMAKI Behnaz, UNR 247
BALTAY Annemarie, USGS Mon1100
BANERDT William, NASA/JPL 004
BANNISTER Stephen, GNS Science 020
BANSAL Abhey, NGRI 192
BARALL Michael, Invisible Software 116
BARKLAGE Mitchell, NodalSeismic 197
BARNHART William, USGS/NEIC 262
BARRETT Sarah, Stanford
BARSEGHIAN Derik, USGS 037
BART Sheila, Old Dominion 009
BARTH Nicolas, UCR 263
BARTO Brady, Signal Hill Petrol 197
BARU Chaitanya, SDSC 216
BASLER-REEDER Kyle, UNR
BASSET Andre, UNAVCO 215
BAUER Klaus, GFZ Potsdam 092
BAUTISTA Jennifer, Pierce College
BAYLESS Jeff, URS Corp 053
BEAUDOIN Bruce, IRIS PASSCAL 157
BECK James, Caltech 040
BECKER Thorsten, USC
BEELER Nicholas, USGS 109, 139
BEHL Richard, CSULB 094
BEHR Whitney, UT Austin 277
BEMIS Sean, Kentucky 286
BEN-ZION Yehuda, USC 160, 163, 182, 183, 184, 185, 187, 188, 189, 202
BENNETT Richard, Arizona 226
BENNETT Scott, USGS 259
BENOIT Maggie, NSF
BENTHIEN Mark, SCEC/USC 001, 002, 003, 007, 008, 009, 010
BENTZ John, UCSB
BERELSON William, USC
BERGEN Karianne, Stanford 162
BERGER Greg, USC 008
BEROZA Gregory, Stanford 078, 162, 180
BHASKARAN Aparna, Caltech 155
BHAT Harsha, Harvard 108
BHATTACHARYA Pathikrit, Princeton 139
BIASI Glenn, UNR 067
BIELAK Jacobo, CMU 049, 076, 084, 085, 087, 088, 091
BIJELIC Nenad, Stanford 052
BILHAM Roger, UC Boulder
BIRD Peter, UCLA 104
BLANPIED Michael, USGS
BLISNIUK Kimberly, UC Berkeley 278
BOCK Yehuda, UCSD 042, 222
BOESE Maren, Caltech 035
BOLEN David, USC 003
BONUSO Nicole, CSUF 247
BORMANN Jayne, UNR 248, 249, 254
BORSA Adrian, UCSD/SIO 101, 232
BOUE Pierre, Stanford 180
BOWLING Roy, CSM 158
BOYLE-PENA Kyler, 285
BRADLEY Andrew, Stanford 097, 243
BRADLEY Brendon, Univ Canterbury 045, 047, 048, 070, 071
BRAILO Courtney, UNR 260
BREUER Alexander, TU München 177
BRIGGS Richard, USGS Golden 262
BRIGHAM Kelly, CalPoly Pomona
BROCHER Thomas, USGS
BRODSKY Emily, UCSC 112, 114, 211
BROOKS Benjamin, USGS 039, 234
BROTHERS Daniel, UCSD 204
BROWN Justin, James Madison Univ
BROWN Nathan, UCLA 272, 273
BROWN Kevin, UCSD
BRUHAT Lucile, Stanford 243
BRUNE James, UNR 067, 077
BRYSON Gwendolyn, ASF 216
BUCKLAND Kerry, Aerospace Corp 266, 267, 269
BUECHLER Brian, Alaska Fairbanks 216
BUNN Julian, Caltech 057
BURGETTE Reed, NMSU 227, 228
BÜRGMANN Roland, UC Berkeley 103, 145, 238
BURKETT Erin, USGS 004
BURKS Lynne, Stanford 046, 047
BYDLON Samuel, Stanford 133
CALAIS-HAASE Gwenaelle, UCLA
CALLAGHAN Scott, SCEC 008, 009, 010, 079, 081
CAMPILLO Michel, UJF 183, 184
CAMPOS Georgina, ELAC 009
CAPPA Frederic, Géoazur
CARDONA Jose, CSUN
CARLSON Jean, UCSB 110, 117, 135
CATCHINGS Rufus, USGS 092, 208
CATTANIA Camilla, GFZ Potsdam 016
CAUDILL Alyssa, South Bend HS 003
CAYAN Daniel, SIO 101
CELEBI Mehmet, USGS 051
CHAN Kevin, USC 003
CHANDY Kaniyantra, Caltech 057
CHAO Kevin, Georgia Tech 192
CHE Shi, CEA (China)
CHEN Shang-Lin, Caltech 155
CHEN ZhiQiang, UMKC 217
CHEN Po, U Wyoming 078, 079, 115
CHEN Xiaowei, WHOI 143
CHESTER Judith, Texas A&M 276
CHIANG Yao-Yi, USC 008, 009, 010
CHIOU Ray, NAVFAC EXWC
CHOWDHURY Faria, Caltech 155
CHRISTOPHERSEN Annemarie, GNS Science 020, 024
CLAYTON Robert, Caltech 057, 155, 197, 198, 205
CLINTON John, Caltech 041
CLUFF Lloyd, PG&E
COCHRAN Elizabeth, USGS 003, 004, 035, 115, 197
COCKETT Rowan, 3point Science 005
COFFEY Kevin, UCLA 285
COLELLA Harmony, ASU/SESE
CONRAD John, UCR 224
COOK Devon, CSUF 033
COOKE Michele, UMass 105, 106, 122, 128
CORTES Luis, Etiwanda HS 225
CORTEZ Luis, Etiwanda HS 004
COSSETTE Pamela, USGS 264
COTTE Nathalie, UJF 173
COTTON Fabrice, UJF 201
COX Catherine, Signal Hill Petrol 197
COX Brett, USGS 281
CRANE Thomas, CSUSB 256
CREAGER D'lisa, CSUF 247
CREMPIEN Jorge, UCSB 062, 063
CROSBY Christopher, ASU 216
CROUSE C.B., URS Corp
CUBRINOVSKI Misko, Univ Canterbury 045
CUI Yifeng, SDSC 082, 086, 091
CURRY Brittany, CalPoly Pomona
D'AMICO Maria, INGV 073
DAI Junwu, IEM CEA
DAK HAZIRBABA Yildiz, SIUC
DALGUER Luis, swissnuclear 129
DANIELS Jillian, UCLA 273
DAS Shamita, Oxford 120
DAUB Eric, Memphis 034
DAVATZES Nicholas, Temple 209
DAVIS Paul, UCLA 197
DAWSON Timothy, CGS
DAY Steven, SDSU 066, 150, 151

MEETING PARTICIPANTS

DE GROOT Robert, SCEC/USC 003, 004, 007, 008, 009, 010, 225
DE PASCALE Gregory, Univ Canterbury 048
DEIERLEIN Gregory, Stanford 052
DEJARLAIS Ian, CSUN 279
DEL ANGEL-PEARSON Jozi, Chevron
DEL VECCHIO Joanmarie, Pomona College
DENOLLE Marine, IGPP/SIO 078, 158, 168
DEOCALES Demoree, Chaffey HS 004, 225
DESJARLAIS Ian, CSUN 283
DETERMAN Daniel, USGS 037
DETRICK Robert, IRIS
DEVECCHIO Duane, ASU/SESE 252
DI TORO Giulio, INGV 109, 111
DIERKHISING Joseph, UNR
DIETERICH James, UCR 132, 136, 207
DMITRIEVA Ksenia, Stanford 223
DOLAN James, USC 236, 250, 272, 286
DONNELLAN Andrea, JPL 029, 090, 235
DORSEY Rebecca, Oregon 105
DOS SANTOS Paulo, UC Boulder 008, 010
DOUGHERTY Sara, Caltech 205
DREGER Douglas, UC Berkeley 170, 214
DRISCOLL Neal, SIO 204, 206, 248, 249, 254
DROUET Stephane, Observatorio Nacional 201
DUDASH Stephanie, USGS 257, 281
DUNBAR Sean, DWR
DUNHAM Eric, Stanford 133, 149, 178, Mon1400
DUPUTEL Zacharie, Caltech 173
DURU Kenneth, Stanford 133
DUTILLEUL Pierre, McGill 103
EBERHART-PHILLIPS Donna, UC Davis
EBRAHIMIAN Hamed, UCSD
EGUCHI Ronald, ImageCat Inc 217
ELBANNA Ahmed, UIUC 110, 113, 117, 135
ELIZONDO Daniel, Texas A&M 276
ELLSWORTH William, USGS 124, 212, 213
ELVIS Abigail, Etiwanda HS 004, 225
ENESCU Bogdan, NEID 016
ERICKSON Bill, NodalSeismic 197
ERICKSON Brittany, Portland State 151
ESMAILI Omid, UC Irvine 014
ESPLIN Emily, UVU
EVANS Eileen, Harvard 229
EVANS James, USU 123
EYMOULD William, USC
FAN Wenyuan, SIO/UCSD 165
FANG Peng, UCSD 222
FATTARUSO Laura, Umass Amherst 105
FEAUX Karl, UNAVCO 215
FELIX Jaquelyn, CSUN 010
FELIZARDO Claude, Caltech 035
FELZER Karen, USGS 030
FENG Helen, MIT/WHOI
FERNANDEZ Jose, IGEO 029
FERRANDIZ Jose, UAEU 050
FIALCO Yuri, UCSD 221, 233
FIELD Edward, USGS 011, 031
FIELDING Eric, JPL 173, 216
FLETCHER John, CICESE 130, 261
FLOYD Michael, MIT 224, 226
FOSDICK Julie, Indiana
FRANCISCO Michael, USC 007
FRANKEL Arthur, USGS 068
FRAZER Neil, U Hawaii at Manoa 102
FREDRICKSON Shelby, UCSB
FREEMAN Stephen, GeoPentech 246
FREYMUELLER Jeffrey, Alaska 244
FRY Bill, GNS Science 020
FRYXELL Joan, CSUSB 226
FU Yuning, JPL/Caltech 244
FUIS Gary, USGS 092
FULTON Patrick, UCSC 114
FUNNING Gareth, UCR 005, 093, 148, 224, 226, 238, 241
GABRIEL Alice-Agnes, LMU Munich 177
GALLOVIC Frantisek, Charles Univ in Prague 073
GALVEZ Percy, Caltech 129
GAO Mengtan, CEA (China)
GARAGASH Dmitry, Dalhousie 141
GARCIA Andrew, CalPoly Pomona
GARCIA Dylan, CSUF 247
GARCIA-REYES Jose, Caltech
GARRETT Mark, 083
GEIST Eric, USGS 146
GENG Jianghui, UCSD 043
GERSTENBERGER Matthew, GNS Science 020, 072
GERSTOFT Peter, UCSD
GHISSETTI Francesca, Univ Canterbury 071
GHOSH Abhijit, UCR 190, 191, 193, 271
GILCHRIST Jacquelyn, UCR 136
GILL David, SCEC/USC 079, 081, 087
GIVEN Doug, USGS 155
GLASSCOE Margaret, NASA JPL 217
GLEN Jonathan, USGS 209
GLENNIE Craig, Terrapoint 039, 234
GOEBEL Thomas, Caltech 196, Tue1030
GOLD Ryan, USGS 259, 262
GOLD Peter, UT Austin 277
GOLDBERG Dara, SIO 043
GOLDMAN Mark, USGS 092, 208
GOLDSBY David, Penn 109, 111, 147
GOLOMBEK Matthew, NASA JPL 004
GOMEZ Luis, Chaffey College 003, 004, 225
GONZALEZ Michael, SMU 007
GONZÁLEZ-GARCÍA Jose Javier, CICESE
GONZÁLEZ-ORTEGA Javier, IGPP/SIO
GOODING Margaret, LSA Associates Inc
GOODMAN Joshua, Fugro 253
GORI Marcello, Caltech
GORMLEY Deborah, SCEC/USC
GOULET Christine, PEER/UC Berkeley 058, 059
GRANT LUDWIG Lisa, UC Irvine 090, 246, 285
GRAVES Robert, USGS 060, 070, 081
GREEN Brandon, PCC 008
GRENERER Jessica, USC 250, 272, 286
GUILLEMOT Christian, USGS 038
GUPTA Abhineet, Stanford 195
GUY Richard, Caltech 057
HAAKER Erik, SDSU 246
HAASE Jennifer, UCSD/SIO 043
HADDADI Hamid, CGS
HADDON Elizabeth, WWU
HAGOS Lijam, CGS/SMIP
HAINZL Sebastian, GFZ Potsdam 016
HAMMOND William, Nevada Geod Lab 227, 228
HARDEBECK Jeanne, USGS 025
HARDING Alistair, UCSD 206, 248, 249, 254
HARRIS Ruth, USGS 075, 116
HARTE David, GNS Science
HARTZELL Stephen, USGS 068, 084
HARVEY Janet, Caltech 258, 266, 268
HATCH Rachel, CalPoly Pomona 194
HATEM Alexandra, USC 106
HATEM Lucas, 286
HATFIELD Billy, UCSD/SIO
HAUKSSON Egill, Caltech 035, 040, 096, 130, 155, 156, 196
HAUSER Darren, Houston 039
HAUSMANN Rachel, SCEC 009
HAWTHORNE Jessica, Caltech 176
HEARN Elizabeth, 100
HEATON Thomas, Caltech 039, 040, 041, 057
HEERMANCE Richard, CSUN 279, 283
HEIEN Eric, UC Davis 029
HEINECKE Alexander, TU München 177
HELMBERGER Donald, Caltech 171
HELMSTETTER Agnes, Grenoble 019
HEMPHILL-HALEY Eileen, Humboldt State 247
HENRY Pamela, Screenwriter
HERNANDEZ Deborah, CalPoly Pomona
HERNANDEZ Janis, CGS
HERNANDEZ Ana, CICESE 261
HERRING Thomas, MIT
HERRMAN Mike, CalPoly Pomona
HERRMANN Marcus, ETH Zürich 044
HILL David, USGS 124
HILLERS Gregor, UJF/ISTerre Grenoble 183, 184
HINOJOSA-CORONA Alejandro, CICESE
HIRAKAWA Evan, SDSU 137
HIRATA Naoshi, Tokyo 017, 018, 019
HIRATA Yoshito, Tokyo 023
HIRTH Greg, Brown 109, 111
HISLOP Ann, Kentucky
HITOSHI Kawakatsu, Tokyo 181
HO King Yin Kennis, CalPoly Pomona 200
HO Jonathan, USC 003
HOGAN Phillip, Fugro 253
HOIRUP Don, CA DWR
HOLDEN Caroline, GNS Science 072
HOLE John, Virginia Tech 092, 157
HOLLAND Austin, OGS 213
HOLLENBACK Justin, PEER
HOLLINGSWORTH James, USC 236
HOLLIS Daniel, NodalSeismic 197
HOLMES James, SIO/UCSD 248, 249, 254
HOLT William, SUNY-Stony Brook
HOOTS Charles, UNM 205
HOSSEINI Mehrdad, URS 203
HOSSEINI S. Mehran, USC 154
HOUSEN Bernard, WWU 105
HOWELL Samuel, U Hawaii at Manoa 102
HU Chunfeng, CEA (China)
HU ZhengHui, 217
HUANG Yihe, SCITS (Stanford)
HUANG Hui, 145
HUBBARD Judith, EOS 089, 250
HUBENTHAL Michael, IRIS 004
HUDNUT Kenneth, USGS 037, 258, 261, 266
HUDSON Troy, NASA/JPL 004
HUERTA Brittany, CSUN
HUESCA-PEREZ Eduardo, UCR 193
HUGHES Matthew, Univ Canterbury 071
HUTCHISON Alexandra, UCR 190
HUTTON Kate, Caltech 155
HUYCK Charles, ImageCat Inc 217
HUYNH Tran, SCEC/USC
IANNUCCI Robert, CMU Silicon Valley 039
INBAL Asaf, Caltech 198
ISBILIROGLU Yigit, CMU 049
JACKSON David, UCLA 013, 021, 210
JANECKE Susanne, USU
JEONG Seokho, Univ Canterbury 048
JERRETT Andrew, SDSU
JI Kang Hyeun, Alabama

JI Chen, UCSB 165, 169
JIANG Junle, Caltech 127, 173
JINWEI Ren, CEA (China)
JOHNSON Patrick, Aerospace Corp 267, 269
JOHNSON Kendra, CSM 278
JOHNSON Kaj, Indiana 227, 228, 231
JOHNSON Paul, LANL 034
JOHNSON Leonard, NSF
JOHNSON Marilyn, PCC
JOHNSON Christopher, UC Berkeley 103
JOLIVET Romain, Caltech 173
JONES Kaitlyn, CSUN 280
JONES Jane, NASA JPL 004
JONES Lucile, USGS 210
JORDAN Thomas, USC 004, 007, 008, 009, 010, 015, 031, 059, 078, 079, 081, 085, 087, 091, 095
JORDAN, JR. Frank, DOGGR
JOSE Lisa, U Maryland, Baltimore Co 224
JUAREZ Alan, UNAM 084
JUVE Gideon, USC/ISI 081
KAGAN Yan, UCLA
KAISER Anna, GNS Science 072
KALKAN Erol, USGS 159
KAMERLING Marc, UCSB 094
KANE Deborah, RMS Inc 164
KARAOGU Haydar, CMU 088
KASHIMA Toshihide, 051
KECK Daniel, Etivanda HS 004, 225
KEDAR Sharon, JPL 222
KELL Annie, UNR 206, 260
KELLER Edward, UCSB
KENDRICK Katherine, USGS 258, 266, 277, 279
KENNEDY George, Brian F Smith & Assoc 246
KENNETT James, UCSB 094
KENT Graham, UNR 204, 206, 248, 249, 254, 260
KHOSHMANESH Mostafa, ASU 099
KHOSHNEVIS Naem, Memphis 055, 080
KILB Debi, UCSD 175
KIMURA Youichi, MRI Japan 027
KING Nancy, USGS 037
KIRBY Matthew, CSUF 247
KIRKPATRICK James, CSU 118
KIRKWOOD Robert, RUSD 004, 225
KIWAMU Nishida, Tokyo 181
KLEBER Emily, ASU
KLINE Mark, Banning HS 003, 004, 225
KLOTSKO Shannon, UCSD/SIO 204, 249
KLOTZ Juergen, GFZ Potsdam 173
KNUDSEN Keith, USGS
KOBAYASHI Akio, JMA 027
KOHLER Monica, Caltech 057
KORENAGA Masahiro, DPRI 036
KRANT Mark, USC 008
KRASTEV Plamen, Harvard 098
KROLL Kayla, UCR 207
KTENIDOU Olga-Joan, ISTERre, Grenoble 201
KUMAZAWA Takao, ISM Japan 027
KYRIAKOPOULOS Christodoulos, UCR 148
LAMBECK Kurt, ANU 255
LAMONTAGNE Anne, UCSB
LANGBEIN John, USGS 038, 039
LANGENHEIM Victoria, USGS 092, 264
LANGER James, UCSB 110, 135
LANGRIDGE Robert, USGS 272
LAPUSTA Nadia, Caltech 121, 127, 131
LAWRENCE Jesse, Stanford 003
LAWSON Michael, UCLA 273
LAY Thorne, UCSC
LE Thanh-Nhan, PCC 009
LEE En-Jui, SCEC 078, 079, 115
LEE Robin, Univ Canterbury 071
LEEPER Robert, USGS 247, 285
LEGG Mark, Legg Geophysical
LEITH William, USGS
LEIVA Frances-Juliana, CalPoly Pomona
LEPRINCE Sebastien, Caltech 236
LEVARIO Jonathan, CalPoly Pomona 199
LEVY Yuval, SDSU
LI Zefeng, Georgia Tech 161, 187
LI Bo, UCR 271
LI Rui, UIUC 117
LI Wenwen, URS 089
LI Yong-Gang, USC 115
LI Dongmei, 167
LIEOU Charles, UCSB 110, 117, 135
LIN Ting, Marquette 052
LINDSEY Eric, SIO/UCSD 233
LIPOVSKY Brad, Stanford 240
LIPPOLDT Rachel, USC 153
LIU Zhen, UCLA 220, 222, 244, 245
LIU Xin, USC 182
LIUKIS Maria, SCEC 015
LLENOS Andrea, USGS 212, 213
LOHMAN Rowena, Cornell 208
LONG Kate, Cal OES
LOPEZ Hernan, CalPoly Pomona 004, 225
LOTTO Gabriel, Stanford 178
LOUIE John, UNR 270
LOZOS Julian, Stanford/USGS 126
LUCAS Joseph, 286
LUCO Nicolas, USGS
LUI Ka Yan Semechah, Caltech 121
LUNA Eloy, LAFD
LUNDGREN Paul, JPL 220
LUZI Lucia, INGV 073
LYNCH David, USGS 258, 266, 267, 269
MA Shengli, CEA (China)
MA Shuo, SDSU 137
MA Xiao, UIUC 113
MADARIAGA Raul, IGP/Paris 120
MADDEN Elizabeth, Umass Amherst 106, 122
MAECHLING Philip, SCEC/USC 015, 059, 078, 079, 081, 087, 091
MAEDA Kenji, MRI Japan 027
MAI Paul, KAUST
MAK Sum, GFZ-Potsdam
MANGAN Margaret, USGS 124
MANN Doerte, UNAVCO 215
MARAFI Nasser, Washington
MARLIYANI Gayatri, ASU
MARQUIS John, SCEC
MARSHALL Scott, Appalachian State 093
MARSHALL Courtney, CSULB 094
MARTINEZ Morris, Morongo School 004, 225
MARUYAMA Tadashi, JAMSTEC
MARZOCCHI Warner, INGV
MASSARI Anthony, Caltech 057
MASTERS Guy, SIO/IGPP 165
MATCHES Michael, USC 007
MATHESON Ephram, UVU
MATSUBARA Nanae, Arakawaoki PS
MATSUBARA Makoto, NIED 172
MATSUURA Mitsuhiro, Tokyo 107
MATTI Jonathan, USGS 257, 264, 281
MATTIOLI Glen, UNAVCO 215
MAURER Jeremy, Stanford 097
MAVROMMATIS Andreas, Stanford 231
MCAULIFFE Lee, USC 250
MCBEAN Alexa, UNR
MCBEAN Kevin, UNR 077
MCBECK Jessica, UMass 122
MCBURNETT Paul, CSUN 279, 282
MCCAFFREY Robert, Portland State
MCCLURE James, NASA/JPL 004
MCCLURE Mark, UT Austin
MCCRINK Timothy, CGS
MCGANN Christopher, Univ Canterbury 045, 048
MCGARR Arthur, USGS 213
MCGILL John, CSUSB 226
MCGILL Sally, CSUSB 004, 225, 226, 256, 272, 275, 284
MCGUIRE Christopher, UCLA 272, 273
MCGUIRE Jeffrey, WHOI 143, 208
MCMURRY Key, Key Environ Solutions 003
MCPHERSON Krista, USC 010
MCQUILLAN Patrick, IRIS 004
MCRANEY John, SCEC/USC
MCSTROUL Geoffrey, NAVAIR 174
MCVERRY Graeme, GNS Science 020
MEADE Brendan, Harvard 098, 229, 230
MEERTENS Charles, UNAVCO 216
MEIER Men-Andrin, ETH Zürich 041
MEIER Ryan, USC 010
MELGAR Diego, UCSD/SIO 042, 043
MELTZNER Aron, EOS
MENG Xiaofeng, Georgia Tech 186
MENG Lingsen, UCLA 142, 145
MENG Qingjun, UCSC 211
MENG Haoran, USC 166
MENGES Christopher, USGS 257
MICHAEL Andrew, USGS 213
MILLER M. Meghan, UNAVCO
MILLINER Christopher, USC 236, 237, 286
MILNER Kevin, SCEC 008, 009, 010, 031, 081
MINSON Sarah, Caltech 038, 039, 040, 173
MITCHELL Thomas, Univ College London 109, 111, 147
MONTGOMERY-BROWN Emily, Wisconsin 124
MOORE Angelyn, JPL 173, 222
MORELAN Alexander, UC Davis 261, 276
MORTON Douglas, UCR 281
MOSCHETTI Morgan, USGS 068
MOSER Amy, USU
MOURA Amelia, SCEC 003
MOYA Marc, C/JUHS 004, 225
MUELLER Charles, USGS 213
MURRAY Lyndon, Anza-Borrego Desert SP
MURRAY Mark, New Mexico Tech
MURRAY Jessica, USGS 038, 039, 219
NADEAU Robert, UC Berkeley 099
NAKATA Nori, Stanford 180, 181
NAYAK Avinash, UC Berkeley 214
NEIGHBORS Corrie, UCR
NEWMAN Susan, SSA
NG Raymond, CalPoly Pomona
NGET David, CalPoly Pomona 199
NGUYEN Rosa, CalPoly Pomona
NICHOLS Kevin, CSUF 033
NICHOLSON Craig, UCSB 094, 096
NICOLL Jeremy, ASF 216
NISSEN Edwin, CSM Tue1400
NODA Hiroyuki, Caltech 144
NODA Shunta, RTRI 036
NOLL Erika, UCR 241
NOMURA Shunichi, ISM Japan 032
NORABUENA Edmundo, IGP 173

MEETING PARTICIPANTS

NORMAN Rory, *Glendale College* 010
NYST Marleen, *RMS Inc* 164
O'CONNELL Daniel, *William Lettis & Assoc* 253
O'REILLY Ossian, *Stanford* 162
OBARA Kazushige, *ERI Tokyo* 172
OFFICER-MCINTOSH LaTerrian, *USC* 007
OGATA Yoshiko, *ISM Japan* 022, 023, 027
OGLESBY David, *UCR* 136, 146, 148
OKAWA Izuru, 051
OKAZAKA Keishi, *Brown* 147
OKAZAKI Keishi, *Brown* 144
OKUBO Kurama, *Kyoto* 108
OKUMURA Koji, *Hiroshima*
OLLER Brian, *UCSD/SIO*
OLSEN Kim, *SDSU* 061, 065, 066, 079, 081, 091
OLSON Brian, *CGS*
OMI Takahiro, *Tokyo* 023
ONDERDONK Nathan, *CSULB* 126, 275
ORTEGA Gustavo, *CALTRANS-LA*
ORTIZ Maggie, *EERI*
ORTON Alice, *Kentucky*
OSKIN Michael, *UC Davis* 130, 138, 261, 276
OWEN Susan, *JPL* 039, 093, 173, 222, 244
OZAKIN Yaman, *USC* 202
PACE Alan, *Petra Geotechnical*
PACOR Francesca, *INGV* 073
PADGETT Michael, *Signal Hill Petrol* 197
PAGE Morgan, *USGS Pasadena* 024, 030
PANCHA Aasha, *Victoria Univ Wellington* 270
PARKER Jay, *JPL* 090, 217, 235
PAULSON Elizabeth, *USC*
PAZOS Celia, *CalPoly Pomona* 199
PELTIES Christian, *LMU Munich* 177
PENG Zhigang, *Georgia Tech* 161, 186, 187, 192
PEREZ Velveth, *Pierce College*
PEROL Thibaut, *Harvard* 108
PERRY Stephen, *Caltech* 131
PERRY Suzanne, *USGS* 006
PERSAUD Patricia, *Caltech* 092
PETERS Robert, *SDSU* 251
PETERSEN Mark, *USGS* 006, 213
PETTINGA Jarg, *Univ Canterbury* 071
PEZESHK Shahram, *Memphis* 203
PIERCE Marlon, *NASA JPL* 090, 217
PIERCE Elena, *PCC* 009
PIERCE Ian, *UNR* 260
PITARKA Arben, *LLNL* 060
PLATT John, *Harvard* 109, 111
PLATT John, *USC* 147
PLESCH Andreas, *Harvard* 079, 089, 095, 096, 196
POLET Jascha, *CalPoly Pomona* 194, 197, 199, 200
POLISSAR Pratiyga, *LDEO* 119
POTTER Kate, *ASU*
POTTER Sally, *GNS Science* 020
POWELL Robert, *USGS* 264, 281
POWERS Peter, *USGS* 012
POYRAZ Efekan, *SDSC* 082, 086
PRATT Thomas, *USGS* 250
PRATT-SITAUOLA Beth, *CWU* 005
PREJEAN Stephanie, *USGS* 124
PRIDMORE Cynthia, *CGS* 003
PROCTOR Brooks, *Brown* 109, 111
PRUSH Veronica, *UC Davis*
PUGLIA Rodolfo, *INGV* 073
PULLAMMANAPPALLIL Satish, *Optim* 270
PURASINGHE Rupa, *CSULA*
PURASINGHE Ruwanka, *LADWP*
PURCELL Anthony, *ANU* 255
QIU Hongrui, *USC* 188, 189
QUIMPO Stephen, *CalPoly Pomona*
RABADE GARCIA Santiago, *UNAM* 179
RAINS Christine, *CSUN*
RAMIREZ Lina, *Pierce College*
RAMIREZ-GUZMAN Leonardo, *UNAM* 068, 084, 179
RAMZAN Shahid, *CSUN* 279, 282
RAY Sohom, *Tufts* 134
RAYGOZA Francisco, *PCC* 008
REITMAN Nadine, *USGS* 262
RESTREPO Doriam, *CMU* 076
RETTENBERGER Sebastian, *TU München* 177
REYNOLDS Laura, *UCSB* 251
REZAEIAN Sanaz, *USGS*
RHOADES David, *GNS Science* 020, 024
RHODES Brady, *CSUF* 247
RHODES Edward, *UCLA* 250, 272, 273
RIAHI Nima, *UCSD*
RICE James, *Harvard*
RICHARDS-DINGER Keith, *UCR* 132, 136, 207
RIEGEL Hannah, *CSUN*
RIEL Bryan, *Caltech* 173
RIOS Krystel, *ELAC* 009
RIVERA Luis, *IPGS* 173
ROBINSON DEVRIES Phoebe, *Harvard* 098
ROCKWELL Thomas, *SDSU* 126, 246, 251, 261, 275, 277
ROGERS-MARTINEZ Marshall, *USC* 153
ROLLINS John, *Caltech*
ROMANO Mark, *Video Production* 007
ROOD Dylan, *SUERC* 252, 277
ROSENBAUM Lindsay, *Morongo School* 004, 225
ROSINSKI Anne, *CGS* 217
ROSS Zachary, *USC* 160, 187, 188, 189
ROTEN Daniel, *SDSC* 082, Tue0800
ROTH Frank, *GFZ Potsdam* 016
ROUBY Helene, *ENS* 255
ROUSSEAU Nick, *SCEC* 007, 008, 009, 010
ROUX Philippe, *UJF/IPGP* 183, 184
ROWSHANDEL Badie, *CEA/CGS*
RUBIN Allan, *Princeton* 139
RUBINSTEIN Justin, *USGS* 212, 213
RUDDY Braden, *CalPoly Pomona*
RUHL Christine, *UNR* 152, 260
RUIZ Ricardo, *Chaffey HS* 004
RUNDLE John, *UC Davis* 029, 217
RYAN Kenny, *UCR* 146
RYBERG Trond, *GFZ Potsdam* 092
RYMER Michael, *USGS* 092, 208
SACHS Michael, *UC Davis* 029
SAHAKIAN Valerie, *SIO* 206, 248, 249, 254
SALEEBY Jason, *Caltech*
SALISBURY James, *ASU*
SAMMIS Charles, *USC* 153
SAMSONOV Sergey, *Western Ontario* 173
SANDWELL David, *UCSD* 102, 232, 237, 239
SAUNDERS Jessie, *SIO* 043
SAVAGE Heather, *LDEO* 119
SAVRAN William, *UCSD/SDSU* 065
SCAPINI Ernest, *PCC* 008
SCHARER Katherine, *USGS* 247, 258, 266, 278, 282, 285, 286
SCHIEIRER Daniel, *USGS* 092
SCHMANDT Brandon, *UNM* 205
SCHOENBALL Martin, *USGS/Temple* 209
SCHORLEMMER Danijel, *USC* 015
SCHROEDER Sean, *CalPoly Pomona*
SCHULTZ Kasey, *UC Davis* 029
SCHWARTZ Susan, *UCSC* 245
SCHWARTZ David, *USGS*
SEGALL Paul, *Stanford* 097, 223, 231, 240, 243
SEGOU Margarita, *CNRS* 028
SEITZ Gordon, *CGS*
SELANDER Jacob, *UC Davis* 138
SELIGSON Hope, *MMI Engineering* 009
SELLNOW Deanna, *Kentucky* Wed0830
SELLNOW Timothy, *Kentucky*
SELLSTED Alicia, *WSU* 008
SHAKIBAY SENOBARI Nader, *UCR*
SHARE Pieter-Ewald, *USC* 188, 189
SHARP Warren, *BGC* 277, 278
SHAW John, *Harvard* 079, 089, 095, 096, 196, 250
SHAW Bruce, *LDEO* 026, 132
SHEARER Peter, *UCSD* 150, 158, 165, 168
SHELLY David, *USGS* 124
SHEN Zheng-Kang, *NSF* 220
SHEPPARD Rachel, *LDEO* 119
SHERVAIS Katherine, *CSU* 118
SHI Jian, *Caltech* 069
SHI Zheqiang, *SDSU* 066
SHIH Liwen, *Univ Houston-Clear Lake* 083
SHIMAMOTO Toshihiko, *Hiroshima* 144
SHIRZAEI Manoochehr, *ASU* 099, 140
SIEH Kerry, *NTU/EOS* 283
SILVA Fabio, *SCEC/USC* 059, 087
SIMILA Gerry, *CSUN* 174
SIMMS Alexander, *UCSB* 251, 255
SIMONS Mark, *Caltech* 173
SKARLATOUDIS Andreas, *URS Corp* 053
SLEEP Norman, *Stanford* 274
SMALL Patrick, *SCEC* 079, 085, 087
SMITH Kenneth, *UNR* 152, 260
SMITH Dave, *USC* 007, 008, 009, 010
SMITH Deborah, *USGS Menlo Park* 038
SMITH Karissa, *WVU*
SMITH-KONTER Bridget, *UTEP* 102, 239
SOCQUET Anne, *ISTerre* 173
SOMERVILLE Paul, *URS* 053, 059
SONG Xin, *USC* 095
SORLIEN Christopher, *UCSB* 094, 096
SOUSA Frank, *Caltech* 258, 266
SPELZ Ronald, *UABC* 261
SPINLER Joshua, *Arizona* 226
SPRINGER Kathleen, *SBCM* 003
SQUIBB Melinda, *UCSB* 222
STARK Keith, *SCIGN* 037
STARRATT Scott, *USGS* 247
STEHLY Laurent, *UC Berkeley* 180
STEIDL Jamison, *UCSB*
STEIN Ross, *USGS*
STEMBERK Jakob, *USMH*
STEPANCIKOVA Petra, *IRSM*
STERN Aviel, *UMass* 128
STEWART Jonathan, *UCLA* 056
STOCK Joann, *Caltech* 004, 092, 258, 266, 268
STRADER Anne, *UCLA* 021, 145
STRAND Leif, *Caltech* 057
SUMY Danielle, *USGS* 003, 004
TABORDA Ricardo, *CERI* 049, 055, 079, 080, 085, 087
TAIRA Taka'aki, *UC Berkeley* 170
TAKEDATSU Rumi, *SDSU* 061
TAYLOR Stephanie, *UCSC* 112
TENG Ta-liang, *USC*

MEETING PARTICIPANTS

TERAN Orlando, CICESE 130, 261
THATCHER Wayne, USGS
THIO Hong Kie, URS 089
THOMAS Valerie, USGS 156
THOMPSON Tarra, CSULA 284
THOMPSON Thomas, Harvard 230
THOMSON Ethan, Univ Canterbury 071
THURBER Clifford, UW-Madison
TICCI Marco, Fugro 253
TITULAR Jazmine, CSUF 033
TODA Shinji, Tohoku
TOKE Nathan, UVU 265
TONG Xiaopeng, Washington 102, 237, 239
TRATT David, Aerospace Corp 266, 267, 269
TREBI-OLLENNU Ashitey, NASA/JPL 004
TREIMAN Jerome, CGS
TREMAYNE Heidi, EERI
TROMP Jeroen, Princeton 091
TRUGMAN Daniel, SIO 034, 232
TSANG Stephanie, UCSB
TSUDA Kenichi, Osaki Research Inst
TSURUOKA Hiroshi, Tokyo 017, 018, 019
TULLIS Terry, Brown 109, 147
TURCOTTE Donald, UC Davis 029
TURINGAN Maria, IGPP/SIO
TURNER James, Fugro 253
TURNER Ryan, UNAVCO 215
TWARDZIK Cedric, UCSB 120
TYMOFYEYEVA Ekaterina, SIO 221
UCHIDA Naoki, Tohoku 231
UEHARA Shin-ichi, Toho 144
VADMAN Michael, CalPoly Pomona
VAHI Karan, USC/ISI 081
VAN DER ELST Nicholas, LDEO 026
VAN DISSEN Russ, GNS Science 272
VANEGAS Michelle, CSULA 003
VARGAS Sarah, Chaffey College 007
VARGAS Bernadette, Etiwanda HS 003, 004, 225
VERNON Frank, UCSD 183, 184, 187, 188, 189
VIDALE John, U of Washington
VIESCA Robert, Tufts 134, 141
VINCI Margaret, Caltech 004
VINE Michael, Cambridge
WALD David, USGS
WALLACE Seth, GTHS 004, 225
WALLACE Laura, UTIG 242
WALLS Christian, UNAVCO 215
WALTER Fabian, SIO 175
WALTER Steven, USGS 212
WAN Dun, 107
WANG Weitao, CEA (China)
WANG Lifeng, GFZ Potsdam 016
WANG Jun, Indiana 090, 217
WANG Kang, SIO/UCSD
WANG Yongfei, UCSD/SDSU 150
WANG Peng, 167
WARD Brandie, RMC Research
WEI Shengji, Caltech 171
WEI Kaibo, CEA (China)
WEIDMAN Luke, SDSU
WEINGARTEN Matthew, USGS 213
WEISER Deborah, USGS/UCLA 210
WERNER Maximilian, Bristol 015, 019
WERSAN Louis, Indiana
WESNOUSKY Steven, UNR 248, 249, 254, 260
WESPESTAD Crystal, Wisconsin 258, 285, 286
WESSEL Kaitlin, SDSU
WESSEN Alice, NASA JPL 004
WHITCOMB James, NSF
WIEMER Stefan, ETH Zürich 044
WILLIAMS Katherine, Colton MS 004, 225
WILLIAMS Charles, GNS Science 242
WILLIAMS Patrick, SDSU 278
WILLS Chris, CGS
WILSON Rick, CGS 089
WITHERS Kyle, SDSU/UCSD 066
WITKOSKY Ryan, Caltech 258, 266, 282
WOLFF Lisa, CSUN 282
WON Parker, Caltech 090
WOODDELL Kathryn, PG&E 170
WOODWARD Robert, USGS/ASL 157
WU Francis, USC/SUNY-Binghamton
WU Stephen, 040
WYATT Frank, UCSD 218
WYMAN Dana, Stanford
XIE Furen, ICD CEA
XU Xiaohua, IGPP/SIO 237
XU Heming, SDSC/UCSD 082
XUE Lian, UCSC 245
YAGODA-BIRAN Gony, UNR 074
YAMAMOTO Shunroku, NIED 036
YANG Hongfeng, Georgia Tech 192
YILDIRIM Battalgazi, Stanford
YODER Mark, UC Davis 217
YOKOI Sayoko, ERI Tokyo 017, 019
YONG Alan, USGS
YOON Clara, Stanford 162
YOUNG Karen, USC
YU Junjie, Caltech 171
YU Ellen, Caltech 155
YU John, USC 015
YUAN Zhang, CEA (China)
YULE Doug, CSUN 279, 280, 282, 283
YUN Sang-Ho, NASA JPL
ZALIAPIN Ilya, UNR 163
ZAREIAN Farzin, UC Irvine
ZECHAR Jeremy, ETH Zürich 015, 044
ZEIDAN Tina, SDSU
ZENG Yuehua, USGS
ZHANG Dandan, CalPoly Pomona
ZHANG Hailiang, Caltech 173
ZHANG Ailin, UCLA 142
ZHENG Jianchang, CEA (China) 167
ZHONG Peng, PBEE-UCI 054
ZHOU Jun, SDSC 086
ZHUANG Jiancang, ISM Japan 107
ZIELKE Olaf, KAUST
ZIGONE Dimitri, USC 182, 183
ZIMMERMAN-BRACHMAN Rachel, NASA JPL 004
ZINKE Robert, USC 272
ZORZI Federico, Università di Padova 111
ZUMBRO Justin, GeoPentech 246

MEETING NOTES

The Southern California Earthquake Center (SCEC) is an institutionally based organization that recognizes both **core institutions**, which make a major, sustained commitment to SCEC objectives, and a larger number of **participating institutions**, which are self-nominated through the involvement of individual scientists or groups in SCEC activities and confirmed by the Board of Directors. Membership continues to evolve because SCEC is an open consortium, available to any individual or institution seeking to collaborate on earthquake science in Southern California.

Core Institutions and Representatives

USC, Lead Tom Jordan	Harvard Jim Rice	UC Los Angeles Peter Bird	UC Santa Cruz Emily Brodsky	USGS Pasadena Rob Graves
Caltech Nadia Lapusta	MIT Tom Herring	UC Riverside David Oglesby	UNR Glenn Biasi	
CGS Chris Wills	SDSU Steve Day	UC San Diego Yuri Fialko	USGS Golden Jill McCarthy	
Columbia Bruce Shaw	Stanford Paul Segall	UC Santa Barbara Ralph Archuleta	USGS Menlo Park Ruth Harris	

Core institutions are designated academic and government research organizations with major research programs in earthquake science. Each core institution is expected to contribute a significant level of effort (both in personnel and activities) to SCEC programs, as well as a yearly minimum of \$35K of institutional resources (spent in-house on SCEC activities) as matching funds to Center activities. Each core institution appoints an **Institutional Director** to the Board of Directors.

SCEC membership is open to participating institutions upon application. Eligible institutions may include any organization (including profit, non-profit, domestic, or foreign) involved in a Center-related research, education, or outreach activity. As of August 2014, the following institutions have applied for and approved by the SCEC Board of Directors as participating institutions for SCEC4.

Domestic Participating Institutions and Representatives

Appalachian State Scott Marshall	Carnegie Mellon Jacob Bielak	Oregon State Andrew Meigs	UC Davis Michael Oskin	U Oregon Ray Weldon
Arizona State J Ramon Arrowsmith	Colorado Sch. Mines Edwin Nissen	Penn State Eric Kirby	UC Irvine Lisa Grant Ludwig	U Texas El Paso Bridget Smith-Konter
Brown Terry Tullis	Cornell Rowena Lohman	Purdue Andrew Freed	U Cincinnati Lewis Owen	U Texas Austin Whitney Behr
CalPoly Pomona Jascha Polet	Georgia Tech Zhigang Peng	Smith John Loveless	U Illinois Karin Dahmen	U Wisconsin Madison Clifford Thurber
CSU Fullerton David Bowman	Indiana Kaj Johnson	SUNY at Stony Brook William Holt	U Kentucky Sean Bemis	URS Corporation Paul Somerville
CSU Long Beach Nate Onderdonk	JPL Andrea Donnellan	Texas A&M Judith Chester	U Massachusetts Michele Cooke	Utah State Susanne Janecke
CSU Northridge Doug Yule	LLNL Arben Pitarka	U Alaska Fairbanks Carl Tape	U Michigan Ann Arbor Eric Hetland	Utah Valley Nathan Toke
CSU San Bernardino Sally McGill	Marquette U Ting Lin	UC Berkeley Roland Bürgmann	U New Hampshire Margaret Boettcher	WHOI Jeff McGuire

Participating institutions do not necessarily receive direct support from the Center. Each participating institution (through an appropriate official) appoints a qualified **Institutional Representative** to facilitate communication with the Center. The interests of the participating institutions are represented on the Board of Directors by two Directors At-Large.

International Participating Institutions

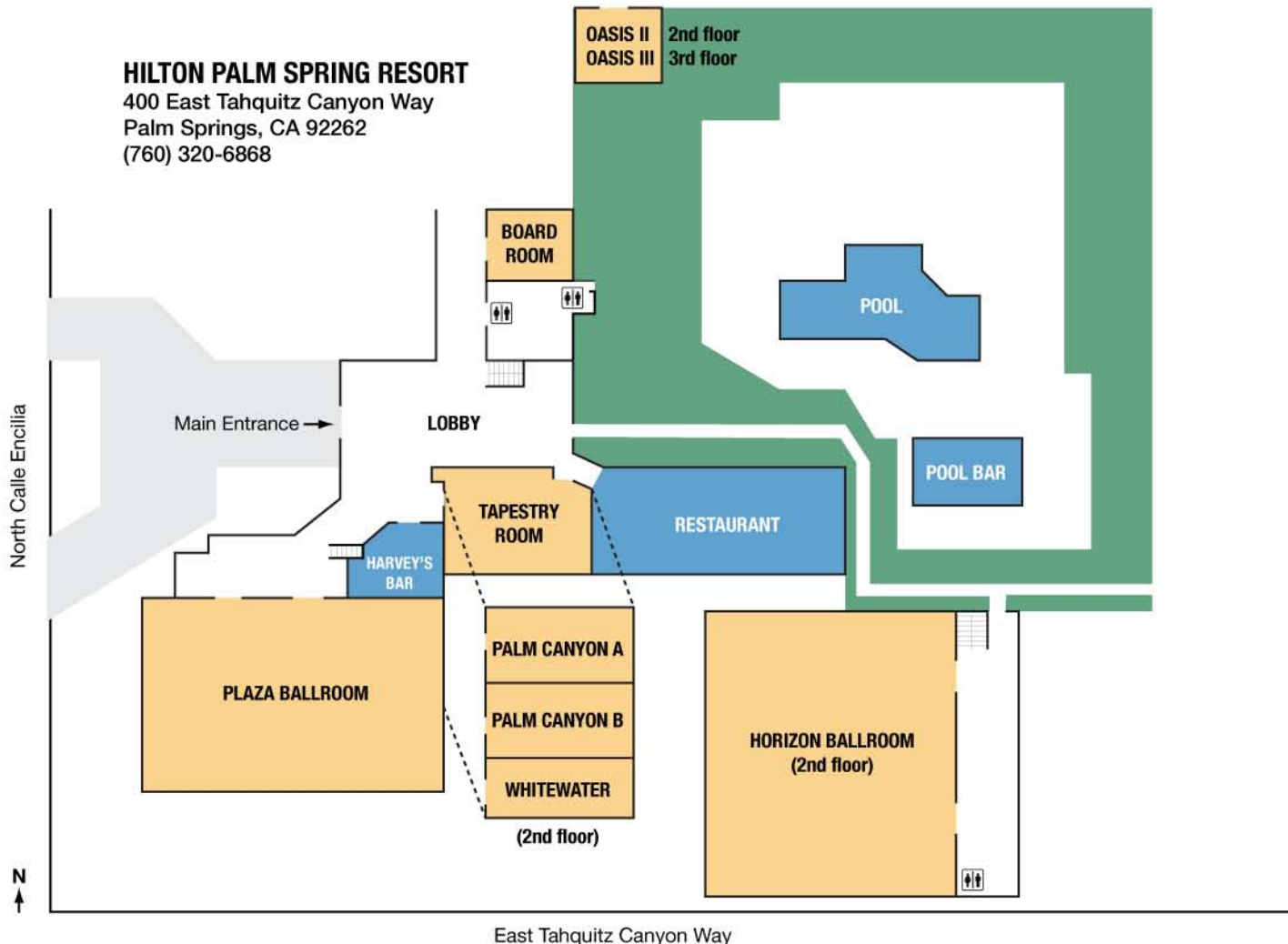
Academia Sinica (Taiwan)	ERI Tokyo (Japan)	Nat'l Central U (Taiwan)	U Western Ontario (Canada)
CICESE (Mexico)	ETH Zürich (Switzerland)	Nat'l Chung Cheng (Taiwan)	
DPRI Kyoto (Japan)	IGNS (New Zealand)	Nat'l Taiwan U (Taiwan)	

Apply as a Participating Institution

E-mail application to John McRaney [mcraney@usc.edu]. The application should come from an appropriate official (e.g. department chair or division head) and include a list of interested faculty and a short statement on earthquake science research at your institution. Applications must be approved by a majority vote of the SCEC Board of

HILTON PALM SPRING RESORT

400 East Tahquitz Canyon Way
Palm Springs, CA 92262
(760) 320-6868



SATURDAY, September 6

- 08:00-18:00 Workshop: San Gorgonio Pass (depart from Lobby)
- 10:00-18:00 Workshop: CSEP/USGS/GEM (Horizon 2)
- 10:00-18:00 Workshop: Community Geodetic Model (Oasis II)

SUNDAY, September 7

- 08:00-18:00 Registration and Check-In (Lobby)
- 08:00-09:00 Breakfast (Poolside)
- 09:00-20:00 Poster Set-Up (Plaza)
- 09:00-17:00 Workshop: EQ Ground Motion Simulation & Validation (Horizon I)
- Workshop: Post-EQ Rapid Scientific Response (Horizon II)
- Workshop: Source Inversion Validation (Palm Canyon)
- 12:00-13:00 Lunch (Restaurant and Poolside)
- 17:00-18:00 Annual Meeting Ice-Breaker (Lobby, Harvey's, Plaza)
- 18:00-19:00 Distinguished Speaker Presentation (Horizon)
- 19:00-20:30 Welcome Dinner (Poolside)
- 19:00-21:00 SCEC Advisory Council Dinner Meeting (Tapestry)
- 21:00-22:30 Poster Session (Plaza)

MONDAY, September 8

- 07:00-08:00 Registration and Check-In (Lobby)
- 07:00-08:00 Breakfast (Poolside)
- 08:00-10:00 Session: The State of SCEC (Horizon)
- 10:30-10:45 Briefing on M6.0 South Napa Earthquake (Horizon)
- 10:45-11:00 Looking Forward to SCEC5 (Horizon)
- 11:00-13:00 Session: How do we deal with known unknowns & unknown unknowns? (Horizon)
- 12:30-14:00 Lunch (Restaurant, Tapestry, Poolside)
- 12:30-14:00 SCEC Board Lunch Meeting (Oasis III)
- 14:00-16:00 Session: What properties of the Earth & the faults within it are important for understanding system behavior? (Horizon)

MONDAY, September 8 (continued)

- 16:00-17:30 Poster Session (Plaza)
- 19:00-21:00 SCEC Honors Banquet (Poolside)
- 21:00-22:30 Poster Session (Plaza)

TUESDAY, September 9

- 07:00-08:00 Breakfast (Poolside)
- 08:00-10:00 Session: How can the hazard from simulated earthquakes effectively reduce risk in the real world? (Horizon)
- 10:30-12:30 Session: What aspects of earthquake behavior are predictable? (Horizon)
- 11:30-13:00 Session: Causes & Effects of Transient Deformations: Slow Slip Events and Tectonic Tremor (Horizon)
- 12:30-14:00 Lunch (Restaurant, Tapestry, Poolside)
- 14:00-16:00 Session: Here it comes! What just happened? How can SCEC better prepare to respond to future EQs? (Horizon)
- 16:00-17:30 Poster Session (Plaza)
- 19:00-21:00 Dinner (Poolside)
- 19:00-21:00 SCEC Advisory Council Dinner Meeting (Boardroom)
- 21:00-22:30 Poster Session (Plaza)

WEDNESDAY, September 10

- 07:00-08:00 Poster Removal (Plaza)
- 07:00-08:00 Breakfast (Poolside)
- 08:00-08:30 Report from the Advisory Council (Horizon)
- 08:30-10:00 Session: How can we communicate more effectively what we know and what we don't? (Horizon)
- 10:30-12:30 Session: The Future of SCEC (Horizon)
- 12:30 Adjourn 2013 SCEC Annual Meeting
- 12:30-14:30 SCEC PC Lunch Meeting (Palm Canyon)
- SCEC Board Lunch Meeting (Tapestry)